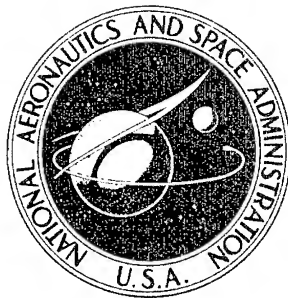


NASA CONTRACTOR
REPORT

NASA CR-1205(1)



NASA CR-1205(1)

Reproduced From
Best Available Copy

COMPENDIUM OF HUMAN RESPONSES
TO THE AEROSPACE ENVIRONMENT

Volume I

Sections 1 - 6

20000920 201

Prepared by

LOVELACE FOUNDATION FOR MEDICAL EDUCATION AND RESEARCH
Albuquerque, N. Mex.

for

NATIONAL AERONAUTICS AND SPACE ADMINISTRATION • WASHINGTON, D. C. • NOVEMBER 1968

DISTRIBUTION STATEMENT A

Approved for Public Release
Distribution Unlimited

**COMPENDIUM OF HUMAN RESPONSES TO THE
AEROSPACE ENVIRONMENT**

Volume I

Sections 1 - 6

Edited by Emanuel M. Roth, M.D.

Distribution of this report is provided in the interest of information exchange. Responsibility for the contents resides in the author or organization that prepared it.

Fred B. Benjamin, D.M.D., Ph. D.
NASA Project Manager

Prepared under Contract No. NASr-115 by
LOVELACE FOUNDATION FOR MEDICAL EDUCATION AND RESEARCH
Albuquerque, N. Mex.

for

NATIONAL AERONAUTICS AND SPACE ADMINISTRATION

For sale by the Clearinghouse for Federal Scientific and Technical Information
Springfield, Virginia 22151 - ~~CFSTI~~ price \$3.00

FOREWORD

The Office of Space Medicine, NASA Headquarters, at the request of the Apollo Program Office conducted a review of the existing qualitative and quantitative human data available for engineers and life scientists to develop design and operational planning criteria for manned spacecraft systems and operations.

This study was conducted with five major goals in mind:

1. To review existing Apollo documents, to extract information on human factors and related design standards, and to evaluate this information.
2. To provide a comprehensive source of human factors data applicable to the Apollo missions which can serve as a source document and as a reference for all future manned space system requirements.
3. To assure a systematic coverage of the whole field which makes it possible to identify areas where available information is deficient.
4. To produce a system for easy storage and retrieval of human factors information.
5. To ultimately provide for every critical environmental parameter a statement regarding (a) the range of normal function, (b) the range above and below normal where performance is impaired, and (c) the tolerance limits.

This effort was conducted by an integrated working group consisting of:

Lovelace Foundation, Albuquerque, New Mexico

A. H. Schwichtenberg
E. M. Roth (Editor of Compendium)
S. Finkelstein
G. W. Hoover (Consultant)

Harvard School of Public Health, Boston, Mass.

R. A. McFarland
W. H. Teichner
R. L. Craig

Bellcomm, Inc., Washington, D. C.

P. R. Knaff
A. N. Chambers
T. A. Bottomley

Office of Space Medicine, NASA Headquarters, Washington, D. C.

J. W. Humphreys, Jr.
J. Bollerud
S. P. Vinograd
F. B. Benjamin (Project Monitor)
H. S. Brownstein
E. J. McLaughlin

Manned Spacecraft Center, Houston, Texas

D. A. Catterson
L. F. Dietlein
R. F. Johnston

Human factors standards, as required for the specification of a particular mission or program, can be defined as the qualitative and quantitative measurements of the desirable ranges and permissible limits of the environmental and man-machine system parameters which should be assumed to determine man's physiological and psychological functions. The parameters which, through their interaction, affect man's performance in any given space mission were categorized as follows:

Physiological/Psychological Functions
Environmental Parameters
Mission Phases and Tasks

In order to systematically analyze those interactions which should be considered in establishing human factors standards for future programs, a matrix was prepared to examine the effect of the Environmental Parameters on Physiological/Psychological Functions. The effect of mission type and duration on the significance of the matrix intersections was evaluated using the following coding system:

- | | |
|--------|---|
| Code 0 | Empirical and theoretical factors regarding the relationships are unknown. |
| Code 1 | The environmental parameter is critical to human function in the Apollo Project. |
| Code 2 | The environmental parameter is not critical to human function in the Apollo Project, but may be in future manned space flight projects. |
| Code 3 | The environmental parameter does not appear to be critical or applicable to human function in Apollo or in future missions. |

A copy of the matrix and detailed report examining the coding is available on request.

It soon became clear that the environmentally induced degradation of human function and performance to be assumed by mission planners and system designers is very sensitive to mission-specific variables. These include duration and nature of the overall mission; the type and sequencing of tasks and subtasks; and synergism between environments. In order to derive an appropriate set of standards for a given mission, it is necessary to understand these subtle interactions. This is especially important in contingency planning where exposure to prior stressful situations significantly alters the human response to a new environment. It was therefore felt that the first step in establishing a basis for future standards would be a comprehensive analysis of human responses to different environments with emphasis on the subtle pitfalls to be encountered in extrapolating to the space environment many of the data obtained from previous studies of the Earth and atmospheric environments.

In compliance with this specific purpose, the present document includes only the environmental-physiological interface under normal and abnormal environmental conditions. Because of extrapolation problems and the need for data on post-landing emergencies, extreme environments on Earth are included. The reaction of specific body organs and systems are covered only as they define the physiological and psychological responses to the degree required by life scientists working with mission planners. Much of the compendium is directed toward individuals writing specifications and standards for specific manned systems. For this group, effects of the environment on psychomotor performance are stressed. Physiological and psychological mechanisms are covered only as they shed some light on current unknowns and permit extrapolation from inadequate human or animal data. The compendium, therefore, represents a compromise between the specific needs of the engineering community and those of consultants in the life sciences. It is not meant to be a design handbook in the usual engineering sense.

To prevent further delay, the document is being published at this time, although, in some areas, the information is still incomplete or lacking. The absence of specific information and reference to current studies is indicated at the appropriate points. If in any area, adequate information is unavailable and if this lack of information is crucial for astronaut function and performance, there is an indicated need for future research work. The compendium has already been used for establishing gaps in aeromedical research. In many cases, the combination of voluminous Earth-based data and limitation of space in this compendium tend to make the account in the text more representative than comprehensive. It is hoped that as the data are checked and continuously updated by experts in the various fields, any serious errors of omission or commission will be corrected.

These volumes are the result of a considerable effort by a number of scientists and engineers. The basic organizational approach may have wide applications for many phases of manned space flight as well as for other human endeavors. The actual information is limited to space operations, but even within this limited frame, the material presented has to be further refined and the coverage increased as new data are made available. It was

suggested by many individuals that the compendium be presented as a loose-leaf book so that the updating could be limited to specific additions or deletions in pamphlet form. However, it has been the experience of the NASA Technical Publications Branch that, in the long run, periodic revision of the entire document is a more efficient way of handling the updating process from the point of view of both the user and the publisher.

The many suggestions offered by members of the NASA working group and by interested individuals in NASA and other organizations have been most valuable in defining the needs and scope of this project. Special thanks are due the board of scientific review for their critiques and valuable suggestions. Any errors which persist are specifically the fault of the editor in misinterpreting these suggestions. The members of the board of review were:

Microwave	Dr. D. G. Cogan Dr. S. M. Michaelson
Light	Dr. J. H. Taylor Dr. R. F. Brissenden Dr. J. A. Buesseler Dr. W. F. Grether
Ultraviolet	Dr. H. F. Blum Dr. D. G. Cogan
Radiation	Col. J. E. Pickering Dr. W. H. Langham Dr. D. Grahn Dr. C. A. Tobias Dr. C. C. Lushbaugh
Magnetic Fields	Dr. D. Beischer
Electric Current	Dr. A. R. Moritz Dr. W. B. Kouwenhoven
Thermal Environment	Dr. A. P. Gagge Dr. W. V. Blockley
Linear Acceleration	Dr. R. M. Chambers Dr. W. J. White Dr. M. McCally
Rotary Acceleration	Dr. A. Graybiel Dr. R. W. Stone, Jr. Dr. W. J. White
Zero and Sub-Gravity	Dr. E. C. Wortz Mr. D. E. Hewes Dr. J. M. Christiansen Dr. H. J. Von Beckh

Zero and Sub-Gravity (continued)	Dr. S. J. Gerathewohl
Impact	Dr. G. C. Mohr Dr. J. J. Swearingen Dr. E. B. Weis
Vibration	Dr. H. E. von Gierke Dr. F. Pradko
Sound and Noise	Dr. A. Glorig Dr. K. D. Kryter
O ₂ -CO ₂ -Energy	Dr. B. Balke Dr. U. C. Luft Dr. K. E. Schaefer
Contaminants	Dr. A. A. Thomas Dr. H. E. Stokinger
Nutrition	Dr. D. H. Calloway Dr. C. F. Consolazio Dr. A. Keys
Water	Dr. P. Webb Dr. A. R. Slonim
Anthropometric and Temporo-spatial Environment	Mr. G. A. Rathert, Jr. Dr. R. Trumbull Dr. J. F. Kubis Dr. A. Damon

The Editor wishes to express his thanks to Drs. T. Morris Fraser and Douglas E. Busby for permitting summary materials from published and unpublished review studies performed at the Lovelace Foundation to be used directly at several points in the compendium.

Many thanks are due Miss Dorothy Tyson, Mrs. Irene Brian, and the other members of the secretarial and document library staffs of the Department of Aerospace Medicine and Bioastronautics, Lovelace Foundation, for the typing and proofreading of this compendium. The art work of Mr. Fred Rupprecht editor and technical writer, and of Mr. Martin J. Schortje, Jr., and co-workers in the Department of Medical Illustration of the Lovelace Foundation are gratefully acknowledged. Appreciation is also extended to Mr. Don L. Hoxie of the NASA Technical Publications Branch for his help in establishing the format and printing requirements of this document.

Special thanks are due Dr. Fred B. Benjamin of the Office of Space Medicine, NASA Headquarters for his enthusiastic aid in coordinating and monitoring the varied aspects of this project.

The Editor

Notes for the User

The compendium is divided into 16 environmental categories as indicated in the general table of contents at the end of these notes. Each of the 16 environments has its own table of contents subdividing the text into sub-sections required for a logical presentation of the subject. (See volumes I-III.)

Conversion tables covering physical, biological, and engineering terms used in this compendium follow the last section of text. (See volume IV.)

At the end of the compendium is an alphabetic subject index covering all of the sections. Following each subject notation in the alphabetic index is the environmental section, page number in that section, and also the figure or table number where that subject is covered or even mentioned. In some cases the figure or table may be self explanatory; in others, perusal of the text is required for appreciation of the full meaning and utility limits of the figure or table. A table of environments precedes the index for handy reference. (See volume IV.)

Acknowledgements for figures and tables have been noted in the following way:

"After"-graphic material photocopied directly from stated reference.

"Modified from"-minor changes made in graphic material from stated reference.

"Adapted from"-major changes made in graphic material or data presentation of the stated reference.

At several points throughout the text whole sections were taken almost directly from recent summaries of the subject. Subtitles covering these sections will be referenced to the author of the summary and/or a statement made in the text to the same effect. It is felt that scattered quotation marks in summary material only confuse the reader. Quotation marks will be reserved for those quoted statements with which the author specifically wishes to agree or disagree.

Since it is planned to update this compendium periodically, notification of any errors of omission or commission and suggestions for improvement of content or format by the user will be much appreciated. Kindly address comments to:

Director of Space Medicine
Code MM
National Aeronautics and Space Administration
Washington, D. C. 20546

GENERAL TABLE OF CONTENTS

1. Microwave Radiation	E. M. Roth
2. Light	E. M. Roth, S. Finkelstein
3. Ionizing Radiation	E. M. Roth
4. Magnetic Fields	E. M. Roth
5. Electric Current	S. Finkelstein, E. M. Roth
6. Thermal Environment	T. A. Bottomley, E. M. Roth
7. Acceleration	E. M. Roth, W. G. Teichner R. L. Craig
8. Vibration	E. M. Roth, A. N. Chambers
9. Sound and Noise	A. N. Chambers, E. M. Roth
10. Oxygen-CO ₂ -Energy	E. M. Roth
11. Inert Gas	E. M. Roth
12. Pressure	E. M. Roth
13. Contaminants	E. M. Roth, W. G. Teichner A. O. Mirarchi
14. Nutrition	E. M. Roth
15. Water	E. M. Roth
16. Anthropometry and Temporo-spatial Environment	E. M. Roth

Conversion Tables

Alphabetic Index

1. MICROWAVE RADIATION

Prepared by

E. M. Roth, M. D., Lovelace Foundation

TABLE OF CONTENTS

1.	MICROWAVE RADIATION	1-1
	Absorption and Penetration	1-1
	Thermal Factors in Microwave Absorption	1-4
	Microthermal Effects	1-6
	Nonthermal Effects.	1-7
	Microwave Effects on Animals	1-7
	Total Body Effects	1-8
	Nervous System.	1-8
	Eye	1-8
	Testis.	1-9
	Microwave Effects in Humans	1-9
	Human Tolerance Limits for Microwaves	1-11
	Microwave Cross-Section of Man	1-15
	Microwaves and Ionizing Radiation.	1-15
	References	1-18

MICROWAVE RADIATION

The radiofrequency portion of the electromagnetic spectrum is subdivided into wave bands according to the schematic noted in Table 1-1. The term

Table 1-1

**Wave Band Division and Designation
in the Radiofrequency Spectrum**

<u>Radiofrequency Bands</u>		
Wave Band	Frequency	Wavelength
VLF	<30 kHz	> 10 km
LF	30-300 kHz	10-1 km
MF	300-3,000 kHz	1-0.1 km
HF	3-30 MHz	100-10 m
VHF	30-300 MHz	10-1 m
UHF	300-3,000 MHz	1-0.1 m
SHF	3-30 GHz	10-1 cm
EHF	30-300 GHz	10-1 mm

<u>Radar Frequency Bands</u>		
Radar Band	Frequency	Wavelength
P	225-390 MHz	133.3 - 76.9 cm
L	390-1550 MHz	76.9 - 19.3 cm
S	1.55 - 5.2 GHz	19.3 - 5.77 cm
X	5.2 - 10.9 GHz	5.77 - 2.75 cm
K	10.9 - 36 GHz	2.75 - 0.834 cm
Q	36 - 46 GHz	8.34 - 6.52 mm
V	46 - 56 GHz	6.52 - 5.36 mm

microwaves will be taken to include electromagnetic energy with wavelengths in the range of 1-300 cm or wave frequencies between 30,000 and 100 megahertz (MHz). Millimeter and submillimeter waves are currently being explored for use in space communications (14 , 33). Basic data on the engineering aspects of microwave hazards with methods for calculating power and energy factors are available (20 , 79 , 80).

Absorption and Penetration

The absorption coefficient (μ) of microwaves in tissue is defined by the exponential relationship

$$I = I_0 e^{-\mu d}$$

giving the attenuation of intensity from I_0 to I which a plane wave suffers as it propagates through a layer of thickness d . The inverse of μ or depth of penetration, D , is the distance covered by the radiant form of energy until its intensity is reduced to $1/e = 0.37$, its original value. In the microwave

case, both μ and D are determined by the electrical and magnetic characteristics of the propagating matter. Biologic materials have no magnetic losses and their magnetic permeability is for all practical purposes identical with that of free space.

The heat (H) developed per unit volume is obtained from the derivative of this equation:

$$H = \mu I \quad (1)$$

Hence, from a knowledge of μ , it is possible to determine the distribution of heat sources. The absorption coefficient and, therefore, depth of penetration in tissue appears to be an inverse function of the wavelength and follows the equation:

$$\mu^2 = \left(\frac{2\pi}{\lambda}\right)^2 2\epsilon \left[\sqrt{1 + \left(\frac{60\lambda}{\epsilon\rho}\right)^2} - 1 \right] \quad (2)$$

where (λ = wavelength in air in cm, ϵ = dielectric constant, ρ = $1/K$ = specific resistance in Ohm-cm (60, 61). Hence ϵ and K are found to be the essential material constants which determine the development of heat in tissue. In the case of several different layers of material the simple equations are subject to corrections which take into account that waves are in part reflected at each interface separating different tissues. The principles which determine the electrical properties of tissues and cell suspensions have been outlined and empirical data have been analyzed and well summarized (12, 59, 61, 65).

The dielectric constants and specific resistances of different tissues are known and can be used to calculate penetration depths (10, 21, 27, 62, 66). The data are summarized in Table 1-2. Both dielectric constant and conductivity are temperature dependent. However, the temperature dependence of the conductance is much more pronounced than that of the dielectric constant. In the band of 50-100 MHz, the value of $100 \frac{\Delta\epsilon}{\epsilon} / {}^\circ C$ for most tissues ranges only from -0.4 to 1.3 and the $100 \frac{\Delta\rho}{\rho} / {}^\circ C$, from -4.9 to -1.3.

The depth of penetration of microwaves in tissue has been determined. Figure 1-3 represents the frequency dependence of penetration. Tissue with a low water content is penetrated by the radiation to a considerably larger extent than tissue with high water content such as muscle. In each case, the depth of penetration decreases rapidly with increasing frequency. For example, the wavelength of 2500 MHz provides a depth of penetration of about 9 mm in muscle. For a frequency of about 900 MHz, the depth of penetration is double that attained with 2500 MHz. The comparatively high depth of penetration in fatty tissue seems to indicate an ability of the waves to penetrate the subcutaneous fat without major energy loss and thereby to become available for heat transfer in the deep tissues. This would only be true if all the energy which reaches the muscular and other deep tissues would be absorbed by them. Partial reflection of electromagnetic waves will occur at the inter-

Table 1-2
Dielectric Constant and Specific Resistance of Body Tissues at 37°C
(After Schwan⁽⁶¹⁾)

	FREQUENCY IN MHz								
	25	50	100	200	400	700	1000	3000	8500
<i>Dielectric constant ϵ</i>									
Muscle	103-115	85-97	71-76	56	52-54	52-53	49-52	45-48	40-42
Heart muscle				59-63	52-56	50-55			
Liver	136-138	88-93	76-79	50-56	44-51	42-51	46-47	42-43	34-38
Spleen	200	135-140	100-101						
Kidney	200	119-132	87-92	62	53-55	50-53			
Lung				35	35	34			
Skin			65		40-48		43-46	40-45	36
Brain	160	110-114	81-83						
Fat		11-13		4.5-7.5	4-7		5.3-7.5	3.9-7.2	3.5-4.5
Bone marrow		6.8-7.7					4.3-7.3	4.2-5.8	4.4-5.4
<i>Specific resistance ρ</i>									
Muscle		113-147		95-105	85-90	73-79	75-79	43-46	12
Heart muscle				95-115	85-100	78-95			
Liver	185-210	173-195	154-179	110-150	105-130	85-115	98-106	49-50	15-17
Spleen		128-151							
Kidney		90-145		90	85	76-77			
Lung		260-450		160	140	130			
Skin		120-140		110-130			90-110	37-50	14
Brain	220	190-210	180-195	1050-3500	900-2800		870-1200	440-900	240-370
Fat		1700-2500					1000-2300	445-860	210-600
Bone marrow		2800-5000							

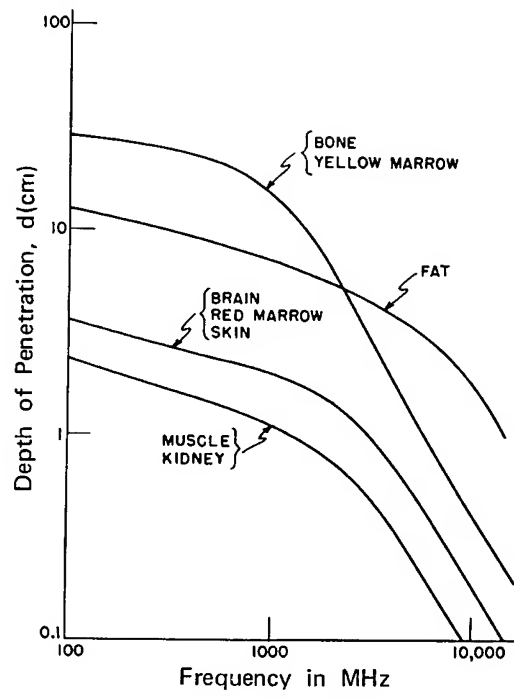


Figure 1-3

Depth of Penetration d of Typical Tissues as Function of Frequency.
Average Fat Data Have Been Chosen, Not Reflecting Variability of d with Water Content.

(Adapted From Schwan (60, 67))

face separating different media. The relative amount of the total energy, which will be reflected, is determined by the dielectric constants and specific resistance values of the different media (61).

A large part of the total energy which penetrates through subcutaneous fat and reaches the muscular tissue is reflected. The reflected waves superimpose with the incident waves to form a standing wave pattern. Typical patterns of the resultant distribution of heat sources are given in Figure 1-4, for various frequencies. They illustrate the pronounced effect due to the processes of partial reflection at fat muscle boundaries.

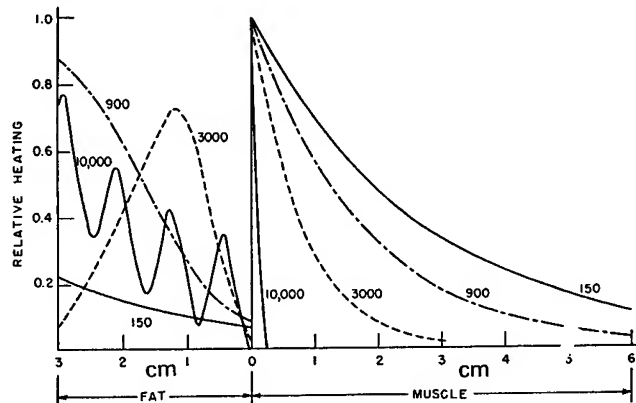


Figure 1-4

Distribution of Heat Sources in Subcutaneous Fat and Muscle. The Data Demonstrate How the Distribution of Heat Sources Changes with Frequency. All Frequencies Are Given in MHz.

(After Schwan (61))

Because of the complex reflections which would result, it appears impossible to construct a dosimeter which measures reproducibly the local absorbed energy. Biological effects must therefore be correlated with "distant field" power density measured in watts/cm².

The relative distribution of heat sources, as pictured in the fat-muscle complex, is not affected by the presence of the skin layer. However, at the boundary separating skin and subcutaneous fat an additional pronounced reflection results, reducing the total amount of energy delivered into the fat-muscle complex.

Thermal Factors in Microwave Absorption

The total distribution of heat sources in the skin-subcutaneous-fat-muscle complex and by summation, total heat outputs in skin, fat and muscle have been determined (62, 66). Under the simplifying assumption that the radiation strikes at a right angle to the surface of the body, Figures 1-5 and 1-6 represent absorption data for various skin thicknesses and amounts of subcutaneous fat at various frequencies. The figures illustrate that at frequencies lower than 1000 MHz, most of the energy reaches the deeply

Figure 1-5

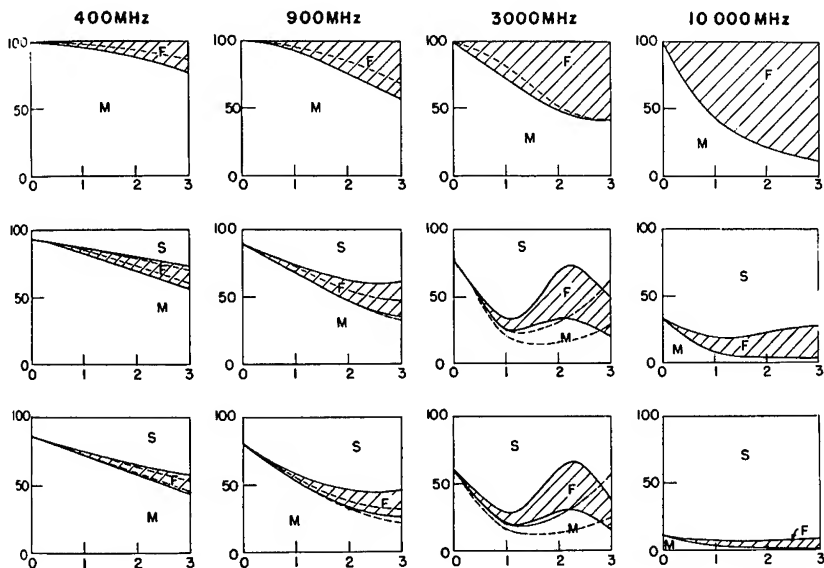
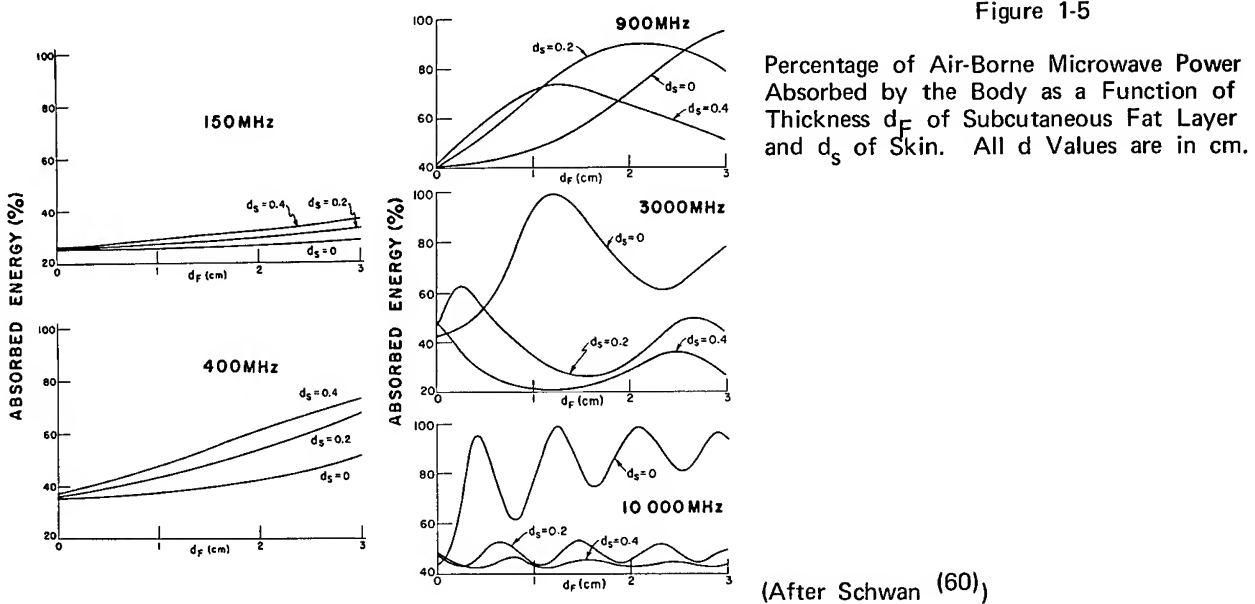


Figure 1-6

Heat Development in Skin (S), Subcutaneous Fat (F) and Deeper Situated Tissues (M) Are Given in Per Cent of Total Energy Absorbed by the Body as Function of Thickness of Subcutaneous Fat in cm. The Upper Row of Graphs Holds for a Skin Thickness $K = 0$, the Middle Row for $K = 0.2$ cm and the Lower One for $K = 0.4$ cm. The Solid Curves Pertain to Fat with High Water Content and the Dashed Curves to Dryer Fat. The Shaded Areas Emphasize the Heat Developed in Fat in the Wet Case. For Any Particular Combination of Values of Frequency, Thickness of Skin and Fat, the Sum of All Heat Contributions Developed in the Three Layers is 100 Per Cent in This Presentation.

(After Schwan and Li⁽⁶²⁾)

situated tissues and that for frequencies above 3000 MHz most of the radiant energy is absorbed in the skin. Between 1000 and 3000 MHz, transition from deep heating to surface heating takes place. At frequencies well below 1000 MHz and at high frequencies above 3000 MHz, the percentage of absorbed energy is nearly independent of skin and subcutaneous thickness and is about 40% of the airborne energy. In the range from 1000 to 3000 MHz, 20 to 100% of the airborne energy may be absorbed by the body depending on the thickness of skin and subcutaneous fat. The complexity of the situation prevailing in the 1000-3000 MHz band reflects the fact that in the mentioned frequency range, both skin and fatty tissue layers of the exposed body can act as a tuning element to "match" or grossly "mismatch" impedances of various tissue combinations and air.

The specific temperature attained at any depth is a function of the percent of energy absorbed, the specific weight and heat of the tissue and the heat exchange with blood and other tissue. The complexity of these interactions precludes a rigid analysis from first principles of local deep body temperatures attained under specific conditions of wavelengths, power density, and time. It is estimated from theoretical models that strong differences, which characterize the temperature elevations for various frequencies in the beginning of the application of the microwave energy, disappear in time (11). The spatial temperature distribution changes but little with time for all frequencies in excess of 3000 MHz. This reflects the fact that depth of penetration becomes so small above 3000 MHz that heat conduction rather than true penetration of radiant energy determines deep tissue temperature to a great extent. Radiation of such high frequency that heat tends to be developed at the body surface, is much less apt to cause intolerable elevation of total body temperature than radiation of lower frequencies. Presence of thermal receptors in the skin, however, increase the sensitivity of this part of the body to heat loads. Presently available knowledge makes it difficult to state how much more heat generated at the body surface is tolerable than heat generated in the deep tissues. A more differentiated dosage statement must wait, therefore, until more research has been done concerning this aspect of heat physiology.

Data are available on thermal effects of electro-magnetic fields below 100 MHz (61). These fields have been used in ultra-short wave diathermy.

Microthermal Effects

Since membranes which surround body cells have little effect on electrical properties of tissues at frequencies above 300 MHz, electromagnetic waves and fields proceed without being affected by the cell membranes (61). Hence, the cell interior and exterior are exposed to the same electric field and since their electrical characteristics are found to be fairly similar, are warmed up to nearly the same extent. As a consequence, electromagnetic waves cause rather uniform "volume" heating, not only on a macroscopic, but also on a microscopic level. This volume heating is probably due entirely to the movement of ions of the tissue electrolytes with the electrical field.

The similarity of the electrical properties of the cell interior and exterior, which is observed at ultra-high frequencies, leaves little room for specific actions of electrical fields on the individual cells, unless it is considered possible that certain molecular components respond selectively to the electrical field and that these are responsible for detectable reactions. Even more definitely can one exclude the possibility of a specific thermal effect on a microscopic level (56, 57). Such specific thermal heating is impossible even if vastly different dielectric properties of cells and surrounding medium are assumed. For the nearly identical values which hold in the frequency range of interest here, it is even more impossible. This follows from a numerical discussion incorporating dielectric data for cytoplasm and membranes of cells utilizing formulas already published (30, 64). It is still considered by some that low intensity effects of microwaves may be based on microthermal reactions (46). However, selective heating on a macroscopic level, due to differences in the electrical properties of various tissues may be anticipated as seen in Figures 1-2 and 1-3. Specific irradiation of the skull with heating of the brain may be more critical than other body sites (29, 40).

Nonthermal Effects

The possibility of nonthermal effects has been the subject of much interest. However, a review of the literature, which claims the existence of such effects, fails to be quantitatively convincing (61). This by no means excludes the possibility of nonthermal effects. More research, especially conducted from a more quantitative point of view, is needed to clarify this point. The only example of nonthermal effects which has been the subject of much detailed analysis is the tendency of microscopic particles to become rearranged under the influence of electrical fields and form chains of particles in the field direction. This pearl-chain effect was first reported in emulsions of fat particles exposed to high frequency fields (41). A more complete treatment of this and related phenomena has recently been given, but no specific biological effects can be deduced (55, 63, 70). Other nonthermal effects on proteins, enzymes, water, nervous tissue, etc., quoted in the Soviet and American literature are biologically interesting but have never been clearly shown to be related to specific symptoms and signs in man (2, 3, 5, 6, 17, 18, 23, 24, 36, 43, 50, 52, 69, 70, 74, 78).

Microwave Effects on Animals

Because of the early recognition of microwave hazards and control of exposure situations, few data are available on the accidental exposure of humans to excessive levels of microwaves.

Many animal studies with microwaves have been limited to small fur bearing creatures with high coefficients of heat absorption, small body surface, and relatively poor heat regulating systems compared to humans. The whole body of the animal is usually immersed in the beam. However, studies have been made of dogs, monkeys, and sheep. Unfortunately, the many factors which influence the response of animals, such as frequency or wavelength,

time (period of exposure), irradiation cycle rate, air current, environmental temperature, position of the animal in influencing resonant conditions and standing waves, effect of reflections, difference in the sensitivity of organs and tissues, use of anesthesia or tranquilizer drugs, and, last but not least, the type of animal, make comparisons very difficult. The effects can be summarized as total body, ocular, and testicular.

Total Body Effects

The magnitude of the rise in body temperature depends upon the degree of imbalance between heat production and heat loss. If the rise of temperature is excessive, the damage produced is indistinguishable from that due to fever of any origin. (See Thermal Environment, No. 6). During the rise in temperature, reactions indicative of a nonspecific pituitary-adrenal response to stress occur, including a sharp decrease in eosinophils and lymphocytes, and a rise in leukocytes (19, 29, 37, 42, 43, 45, 69). Severe hyperpyrexia carried to the point of death results in diffuse degenerative lesions throughout the body, including renal tubular degeneration, myocardial degeneration and necrosis, hemorrhagic lesions in the gut, respiratory tract, liver, and brain. Fatally exposed animals develop acidosis, hyperpnea, and tetany, and finally die of respiratory arrest (31). (See Figure 1-7).

Nervous System

Exposure of animals to microwaves of low intensity, which do not produce any appreciable thermal effect ($<10\text{mW/cm}^2$) lead to functional changes according to some Russian workers (15, 23, 25, 35, 36, 46). Such changes take place mainly in the nervous and cardiovascular systems (change in excitation and inhibition relationships in cerebral cortex, change in rhythm of cardiac activity, etc.). Possible neuro-endocrine response such as increased thyroid activity has also been found in dogs (43). These changes were observed both with chronic and with single exposures and have been termed as nonthermal, specific effects of microwaves (23). The varied effects of microwaves on animal behavior have been recently reviewed (75).

Eye

Localized microwave radiation at certain frequencies, either continuous or pulsed, causes a rise in intraocular temperature and the formation of opacities in the lens (5, 9, 19, 34, 53, 61, 68, 82, 83). Over the several wavelengths studied, from 400-3000 MHz, the threshold for damage after exposure of more than about 20 minutes was in the range of $100-200\text{ mW/cm}^2$. For less than about 20 minutes, the damage threshold increases. (See Figure 1-7). In the frequency range of 5400 to 5500 MHz, a power density of about 800 mW/cm^2 for 20 minutes causes lenticular changes in the eyes of 50 percent of exposed rabbits (83). At subthreshold power levels, there is still some question regarding the cumulative effects on the lens (5, 68). Differences in patterns of peak pulse levels and off time between pulses may be critical factors.

Testis

The characteristic lesion found in the testis is a degeneration of the epithelium lining the seminiferous tubules, and a sharp reduction in the number of maturing spermatocytes in the lumen. There is patchy irregular distribution of damage within the testis, adjacent tubules often showing markedly different degrees of degeneration. The damage is almost certainly reversible except in severe cases (19, 31). A very conservative threshold for testicular damage in the dog exposed to 3000 MHz microwaves under tranquilizer sedation for several hours is around 5mW/cm^2 (19).

Figure 1-7 summarizes threshold curves in the dog for 3000 MHz microwaves of relatively high absorptivity. These curves separate dose rate levels which do no damage from those which are dangerous. For prolonged exposure, these threshold levels are independent of exposure time, while for short exposure, the response is a function of dose and time making it dose-rate dependent. Different curves pertain to the three specific effects because different levels of critical temperature elevation must be considered. For example, for continuous exposure, cataracts result if the eye temperature reaches at least 45°C , but much lower temperature elevations in excess of 1°C are considered intolerable from the point of view of testicular damage, even though not necessarily fatal. These represent animal data most pertinent to man.

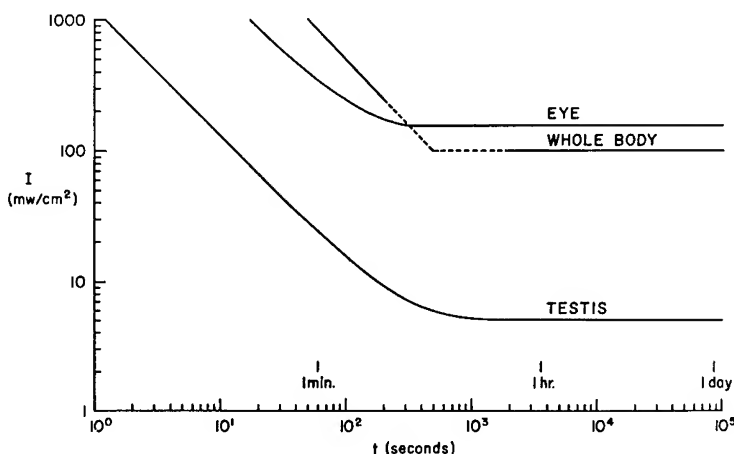


Figure 1-7

Threshold Field Intensities as a Function of Time of Exposure to 3000 MHz Microwaves (10 cm) for Three Sensitive Structures in the Dog.

(After Ely and Goldman (19))

Microwave Effects in Humans

Knowledge regarding human exposures to radar has been on a retrospective basis. In the U.S.A., a large group of radar-exposed employees, along with a control group, were put under a four-year surveillance program (4). During this period, they underwent repeated physical and eye examinations.

Detailed hematological and other laboratory investigations were carried out. The examinations failed to detect any significant changes in the physical inventories of the subjects. The incidence of death and chronic disease, sick leave and subject complaints was comparable in both groups. A high percentage of eye pathology was identified, but none with causal relation to the hyperthermia produced by microwave absorption. Fertility studies revealed essentially the same findings for both groups. Laboratory studies and chest x-rays were noncontributory with respect to radar exposures.

Only a small percentage of the exposed subjects had been aware of the heat or other subjective warning phenomena (4). Neither these tests nor subjective complaints are considered reliable indices of exposure. The sensation of heat or vibration may accompany overexposure to radar in some cases (4). Only 17% of subjects experienced a heat sensation when in close proximity to "X" band radar; 6% were aware of buzzing or pulsating sensation when in an "S" band field. Less than 1% experienced other sensations, such as sparking between dental fillings and metallic tastes. The buzzing sensations which tend to peak at the 600-1500 MHz region have received recent study (7, 22). Occasionally, epigastric distress and/or nausea may occur at power densities as low as $5-10 \text{ mW/cm}^2$, and are most commonly associated within the frequency range from 8×10^3 to 12×10^3 MHz (80). A feeling of warmth may be experienced when the heating effect occurs mainly on the skin. This phenomenon is most commonly associated within the frequency range from 8×10^3 to 26×10^3 MHz (80).

An eye survey of a large group of microwave workers - both civil and military - has been concluded (85). Barring an occasional case of cataract in workers accidentally exposed to high microwave flux, the overall eye findings in workers and an equally large control group were clinically insignificant. The extent of minor lenticular imperfection does not serve as a clinically useful indicator of cumulative exposure to microwave radiation. No relationship between lens imperfection and microwave cataract was found. In other surveys and reports of isolated cases, quantitation of power densities was inadequate to set a definite microwave threshold for cataract formation in humans (8, 28). Recently, 26 cases of lenticular changes were found in microwave workers having a high probability of exposure to more than 10 mW/cm^2 . One of these cases has progressed to cataract and loss of vision (84). These new cases suggest to the investigator that "the threshold for human cataractogenesis may approximate 100 Mev/cm^2 instead of the previously accepted state-of-the-art value lying between 350 and 500 mW/cm^2 ," but no statistical evidence is presented. In the Soviet Union, several cataract surveys have been reported (17, 38, 71). Some cataracts having a tendency to progress have been observed among microwave workers but no threshold data are available (17).

Many poorly defined symptoms have been attributed to microwaves. The Soviet observers have conducted a series of examinations on their radar workers and control groups (15, 16, 17, 18, 32, 35, 46). Unfortunately, quantification of exposure levels has been poorly defined. Chronic irradiation under industrial conditions produces extremely polymorphic changes in the state of the human organism, causing functional changes in various organs

and systems. The degree of their manifestation and the presence of characteristic symptoms are determined by the intensity and duration of the microwave influence as well as by peculiarities of the exposed individual. The clinical syndrome is basically characterized by the presence of asthenia and vegetative reactions. The asthenic reactions such as headache, increased fatigability, increased irritability and sleepiness are not usually sharply pronounced, and have no distinguishing features. Similar observations have been made in a number of laboratories in the U. S. A. and United Kingdom (69). Cardiovascular changes such as arterial hypotension and hypertension (39), bradycardia, sinus arrhythmia, lengthening of the conduction time in the heart, reduction of the amplitude of the spikes of ECG are noted. The asthenic and vegetative reactions mentioned above are entirely reversible. Intensification of the activity of thyroid tissue was detected in almost all the workers investigated by one Soviet author (17). In some surveys, a small increase in volume of the thyroid gland was noted; however, in all surveys, clinical symptoms of hyperfunction were detected only in isolated cases (17, 35, 72). Exposure of Soviet medical personnel to 170-1000 mW/cm² of 1.6 to 2450 MHz diathermy devices has led to symptoms such as headache, irritability, insomnia, chest pain, hand tremor, etc. (73). The significance of these Soviet findings above and below 10 mW/cm² is not clear and their use in establishment of threshold or allowable microwave exposure levels is open to serious question. There is a lack of information on the measurement of actual exposure levels.

Data are available pertaining to irradiation of restricted parts of the human body as performed, for example, in clinical practice (11, 26). At a frequency of 2500 MHz and power input of 100 watts over an area of 100 cm², the initial rapid temperature rise of about 1°C per minute lasts only for a few minutes in the deep tissues under this area. In vascular tissues such as muscle, the temperature peak occurs at about 20 minutes and then decreases again to a value between initial body temperature and peak temperature, reflecting the effect of more efficient cooling of the irradiated segment due to vasodilatation.

Human Tolerance Limits for Microwaves

Determination from first principles of power density limits for continuous exposure has been difficult. Current approaches in the U. S. A. take into consideration only the thermal factors. For continued or interrupted exposure of the body beyond several minutes duration, one can estimate an approximate limit of power density when only the gross volume heating effect is considered (62, 66). The steady-state temperature elevation depends on the ratio of irradiated part of the body surface to total body surface and will increase with the area of irradiation. This means that a power density of about 0.3 watts/cm² must result in a temperature rise of more than 1°C if the area irradiated beyond several minutes is larger than 100 cm². If linearity is assumed between tolerance flux figure and ratio of nonirradiated to irradiated body surface, a figure of 0.03 watts/cm² may be found dangerous if at least half of the body (i. e., about 1 m²) is exposed. Average heat dissipation under normal circumstances is about 0.005 watts/cm². This figure

is based on an energy uptake in form of food of 3000 Kcal per day, an efficiency of somewhat below 30 percent and a body surface of about 2 m^2 . Only under unusually fortunate circumstances is the body surface able to handle tenfold higher heat flux figures. However, double the above rate seems well within the capacity of the human body. This means that it is permissible to develop inside the human body an additional amount of energy which corresponds to 0.005 watt/cm^2 , averaged over the total body surface. In view of the fact that the shadowing factor limits exposure to half of the body surface, a figure of 0.01 watt/cm^2 absorbed energy appears as tolerable and is, therefore, suggested as a tolerance dosage (62, 66). This value should not be exceeded except under unusual circumstances, where cooling efficiency of body surface is excellent.

One must also consider short time exposure to very high intensities where heat flow is not very effective, i. e., whenever time of exposure is small compared with the time constants which characterize heat exchange in the human body. If temperature elevation of more than 1°C is considered intolerable in the case of total body irradiation, $0.3 \text{ watt minutes/cm}^2$ can be calculated as the limiting value. Since depth of penetration of radiation decreases with increasing frequency, this figure should be replaced by higher values at frequencies below 1000 MHz and by lower values above 3000 MHz, the adjustment for heating of the skin makes the exact nature of this adjustment quite uncertain.

If 0.01 watt/cm^2 for long time exposure and $0.1 \text{ watt hour/cm}^2$ for short exposures are not to be exceeded in case of total body exposure, the following tolerance levels for specific frequency ranges can be deduced:

For microwave frequencies below 500 MHz with a coefficient of absorption of about 30 to 40 percent, true deep heating is possible. An incident energy flux of less than 0.03 watt/cm^2 can probably be tolerated.

For frequencies from 1000 to 3000 MHz with possibly complete absorption by skin, subcutaneous fat, and deep tissues, 0.01 watt/cm^2 may be considered tolerable.

For frequencies in excess of 3000 MHz which are absorbed in the surface of the body with a coefficient of absorption of airborne energy of 40 to 50 percent and excellent heat dissipation from surface structures, a power density level of 0.2 watt/cm^2 should be tolerable but this is the least certain of these predictions.

The above analysis assumes that heat development occurs more or less uniformly through the total medium (volume heating). However, local heating at a subcellular level may present specific heating effects in the degradation of cellular function. There is as yet no specific evidence for

such a local thermal effect (61). The above analysis also reflects tolerance limited by heating of the skin and peak power factors from pulsed microwaves.

In view of the above analysis, and the data of Figure 1-7, the most common power density standard for maximum continuous total body exposure of humans to any wavelength has been 10 mW/cm^2 (66). More recent evaluation by the U.S.A. Standards Institute has resulted in a proposed standard for exposure of any time duration as (81): "For normal environmental conditions and for electromagnetic radiation of frequencies from 10 to 100,000 MHz the radiation protection guide is 1 mW hr/cm^2 in any 0.1 hour period. This means: (a) 10 mW/cm^2 for periods of 0.1 hour or more or (b) 1 mW hr/cm^2 for periods up to 0.1 hour. In the case of pulsed fields, the radiation should be averaged over complete trains of pulses, including intervals between pulse trains."

The recent USAF extrapolation of these standards reads (80):

Exposure of personnel within limited occupancy area is permitted only for the length of time given by the following equation:

$$T_p = \frac{6000}{W^2}$$

Where: T_p = permissible time of exposure in minutes during any 1-hour period.

W = power density in area to be occupied in mW/cm^2 .

The above equation is applicable only to power densities between 10 mW/cm^2 and 100 mW/cm^2 . (See Figure 1-8 for graphic presentation). It is not feasible to control limited exposures of less than 2 minutes and consequently this formula should not be applied to intensities over 55 mW/cm^2 .

The U. S. Navy Standards adds to the 10 mW/cm^2 level the fact that incident energy level should not exceed 300 millijoules per sq. cm. per 30 second interval (7).

Calculation of power density levels at any point in a radar beam should follow USAF recommendations (79, 80). An adequate estimate of safe exposure below 10 mW/cm^2 with stated limitations can be obtained from Table 1-9 (49).

The differences between these various recommendations are relatively minor and have as yet not been unified by any single government standard. In emergency situations where the above limits must be exceeded for emergency operations, it is suggested that an anti-microwave suit be used (54). Reduction of body temperature by exposure to a cold environment will also decrease thermal hazards of exposure.

The Soviet limits of safe exposure are more than one order of magnitude less than the U.S. levels.

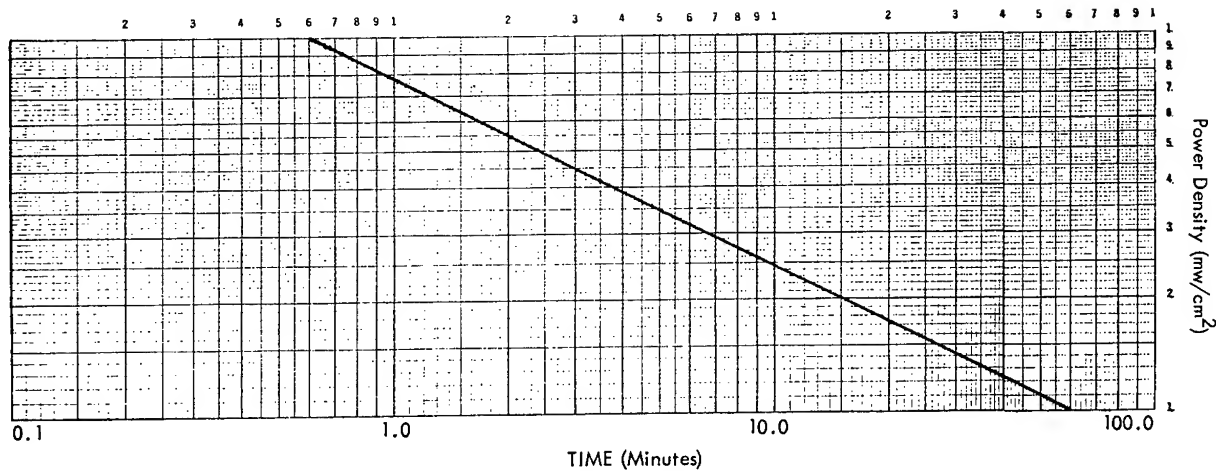


Figure 1-8

Permissible Exposure Time

$$T_p = \frac{6000}{W^2}$$

EXAMPLE:

KNOWN: Power density = $W = 25 \text{ mw/cm}^2$

$$T_p = \frac{6000}{(25)^2} = \frac{6000}{625} = 9.6 \text{ min}$$

(After AFM 161-7 (80))

Permissible exposure time may be obtained by use of figure.

Known power density = 25 mw/cm^2 .

Enter figure on vertical axis at 25 mw/cm^2 .

Follow horizontal entry line to intersection of curve.

Project vertical line from intersection to horizontal axis.

Read approximately 9.6 minutes.

Table 1-9

Safe Distance Formulas

If Average Power in Watts (W) Is:	Safe Distance in Feet Is:
Less than $3D^2$	SAFE
Between $3D^2$ and $5.8D^2$	$\frac{2.85 W}{\text{Wave length in cm.}}$
Over $5.8D^2$	$\frac{6.85 D\sqrt{W}}{\text{Wave length in cm.}}$
Chart applies to pencil-beam radar with parabolic or microwave lens antenna of diameter D feet.	
Safe distances based on power density of .010 watt/ cm^2 .	

(After Overman (49))

- In the case of irradiation during the entire working day - no more than 0.01 mW/cm^2 .
- In the case of irradiation for no more than two hours per working day - no more than 0.1 mW/cm^2 .
- In the case of irradiation for no more than 15 to 20 minutes per working day - no more than 1.0 mW/cm^2 .
(In this case, the use of protective goggles is mandatory).

No adequate data supporting such low levels are available (47). The vague "asthenia" syndromes reported above may have been a factor (16, 17, 18, 35, 46) as were the nonthermal neural effects seen in animal studies (15).

No formal limits have been set for electromagnetic fields below 10 MHz (61). No limits have been suggested for unusual situations where strong magnetic fields are present with weak electric fields and vice versa.

Microwave Cross-Section of Man

The microwave cross-section of man is a microwave parameter which may be of value in such operations as search and rescue. Unfortunately, there are no data available on man in a pressure suit, especially an aluminized suit. Data are available on the monostatic and bistatic radar cross sections of a 200 lb man at 410, 1120, 2890, 4800, and 9375 MHz (58). The measurements were made with a cw Doppler technique using both horizontal and vertical polarizations and for various facing aspects. Figures 1-10 to 1-14 present the data from several points of view.

The cross sections vary from 0.33 to 2.33 square meters, with the extremes at 410 mc; the smaller for horizontal polarization at side view and the larger for vertical polarization at rear view. The cross section is least for side view, and somewhat greater for rear than front view. As expected, there is a general decrease in polarization dependence as the frequency is increased. The microwave cross section is approximately proportional to the weight of man. The theory of microwave cross sections in biological systems is available (1).

Microwaves and Ionizing Radiation

The generation of microwaves at high power levels causes production of pulsed X-rays (13). Magnetrons, klystrons, and traveling wave tubes are the primary source of the radiation. It is recommended that shielding of these sources and operational procedures be instituted to keep human exposure to levels below those recommended in the Ionizing Radiation, (No. 3).

Subtle changes resulting from microwave exposure have been shown to alter the response of animals to ionizing radiation. Prior exposure to 2800 MHz microwaves increased the LD₅₀ for X-rays in several species of animals (44, 51, 76, 77) and decreased specific symptoms and lethality in dogs after

x-irradiation of the head (44). Simultaneous exposure decreased resistance to the x-irradiation. The specific effects of frequency, microwave, and X-ray doses and dose rates, and temporal separation of the two radiation modes have not yet been adequately determined, nor has the significance of this synergism been established for human exposure.

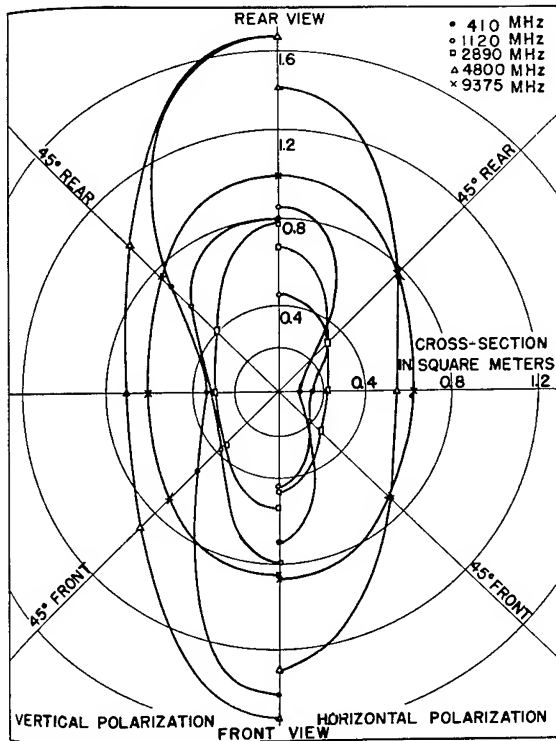


Figure 1-10

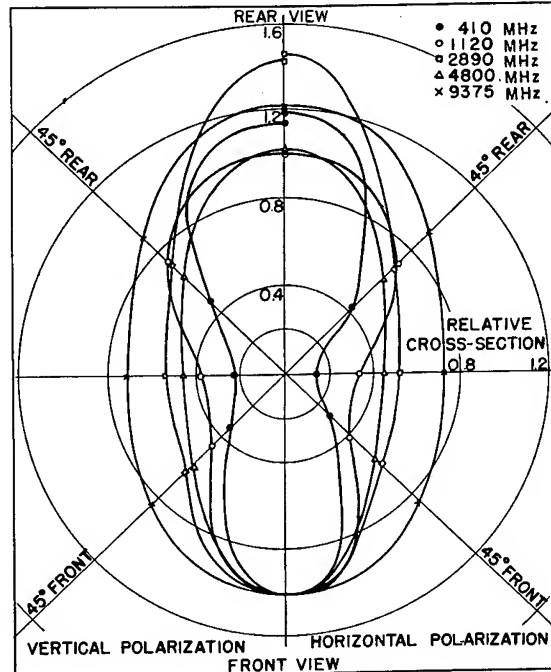
Average Bistatic Radar Cross Section of a Man as a Function of Target Aspect Angle, with Frequency and Polarization as Parameters.

(After Schultz et al (58))

Figure 1-11

Average Relative Bistatic Radar Cross Section of a Man as a Function of Target Aspect Angle, with Frequency and Polarization as Parameters.
(The Curves Are Normalized with Respect to the Radar Cross Section of the Front Aspect.)

(After Schultz et al (58))



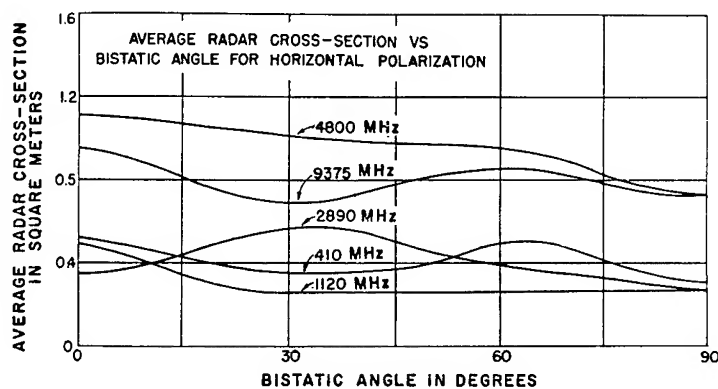


Figure 1-12

Average Bistatic Radar Cross Section of a Man as a Function of Bistatic Angle, for Horizontal Polarization with Frequency as a Parameter.

(After Schultz et al (58))

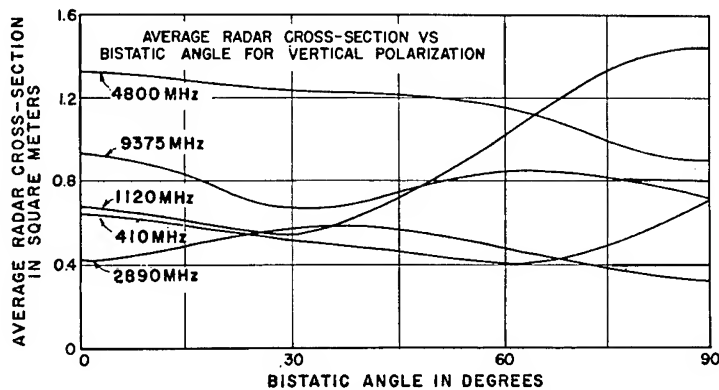


Figure 1-13

Average Bistatic Radar Cross Section of a Man as a Function of Bistatic Angle for Vertical Polarization with Frequency as a Parameter.

(After Schultz et al (58))

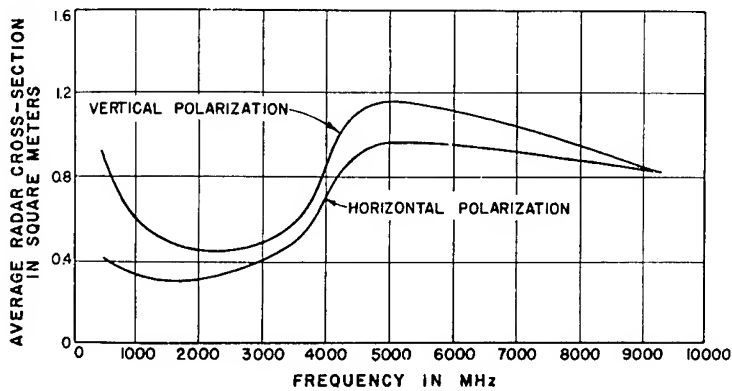


Figure 1-14

Average Radar Cross Section of a Man as a Function of Frequency with Polarization as a Parameter.

(After Schultz et al (58))

REFERENCES

- 1-1. Anne, A., Saito, M., Salati, O. M., et al., Relative Microwave Absorption Cross Sections of Biological Significance, in Peyton, M. F., Biological Effects of Microwave Radiation, Proceedings of the Fourth Annual Tri-Service Conference, Vol. 1, Plenum Press, New York: 1961, pp. 153-176.
- 1-2. Bach, S. A., Biological Sensitivity to Radio-Frequency and Microwave Energy, Fed. Proc., 24: S22-S26, 1965.
- 1-3. Bach, S. A., Luzzio, A. J., Brownell, A. S., Effects of Radio-Frequency Energy on Human Gamma Globulin, Peyton, M. F. (ed.), Biological Effects of Microwave Radiation, Proceedings of the Fourth Annual Tri-Service Conference, Vol. 1, Plenum Press, New York: 1961, pp. 117-133.
- 1-4. Barron, C. I., Baraff, A. A., Medical Considerations of Exposure to Microwaves (Radar), JAMA, 168 (9): 1194-1199, 1958.
- 1-5. Carpenter, R. L., An Experimental Study of the Biological Effects of Microwave Radiation in Relation to the Eye, RADC-TDR-62-131, Rome Air Development Center, Griffiss AFB, N. Y., Feb. 1962 (AD-275840).
- 1-6. Carr, P. H., Harmonic Generation of Microwave Phonons by Radiation Pressure and by the Phonon Phonon Interaction, AFCRL-66-802, Air Force Cambridge Research Laboratories, L. G. Hanscom Field, Bedford, Mass., Dec. 1966.
- 1-7. Christianson, C., Rutkowski, A., Electromagnetic Radiation Hazards in the Navy, NASL-TM-5, U. S. Naval Applied Science Laboratory, Brooklyn, N. Y., 1967.
- 1-8. Cleary, S. F., Pasternack, B. S., Lenticular Changes in Microwave Workers, Arch. Environ. Health, 12: 23-29, 1966.
- 1-9. Cogan, D. G., Fricker, S. J., Lubin, M., et al., Cataracts and Ultra-High-Frequency Radiation, A.M.A. Arch. Indust. Health, 18: 299-302, 1958.
- 1-10. Cook, H. F., The Dielectric Behavior of Some Types of Human Tissues at Microwave Frequencies, Brit. J. Appl. Phys., 2: 295-300, 1951.

- 1-11. Cook, H. F., A Physical Investigation of Heat Production in Human Tissues When Exposed to Microwaves, Brit. J. Appl. Phys., 3: 1, 1952.
- 1-12. Debye, P. F. W., Polar Molecules, Chemical Catalog Co., Inc., New York, 1929.
- 1-13. DeMinco, A. P., Generation and Detection of Pulsed X-Rays from Microwave Sources, in Peyton, M. F., Biological Effects of Microwave Radiation, Proceedings of the Fourth Annual Tri-Service Conference, Vol. 1, Plenum Press, New York: 1961, pp. 33-46.
- 1-14. Derr, V. E., Propagation of Millimeter and Submillimeter Waves, NASA-CR-863, Aug. 1967.
- 1-15. Dodge, C., Soviet Research on the Neural Effects of Microwaves, LC-ATD-66-133, Library of Congress, Aerospace Technology Division, Washington, D. C., Nov. 1966. (AD-645979)
- 1-16. Drogichina, E. A., Konchalovskaya, N. M., Glotova, K. V., et al, Autonomic and Cardio-vascular Disorders During Chronic Exposure to Super-High Frequency Electromagnetic Fields, LC-ATD-66-124, Library of Congress, Aerospace Technology Division, Washington, D. C. (Translation of Gigiya Truda i Professional'nyye Zabolevaniya, 10(7): 13-17, 1966).
- 1-17. Drogichina, E. A., The Clinic of Chronic UHF Influence on the Human Organism, in Letavet, A. A., Gordon, Z. V., The Biological Action of Ultrahigh Frequencies, JPRS-12471, Joint Publications Research Service, Washington, D. C., Feb. 15, 1962. (Translation of O Biologicheskom Vozdeistvii Sverkhvysokikh Chastot, Moscow, Acad. of Med. Sci., USSR, 1960, pp. 22-24.)
- 1-18. Drogichina, E. A., Sadchikova, M. N., Clinical Syndromes Arising Under the Effect of Various Radio Frequency Bands, JPRS-29694, Joint Publications Research Service, Washington, D. C., April 1965. (Translation of Gigiya Truda i Professional'nyye Zabolevaniya, 9(1): 17-21, Jan. 1965).
- 1-19. Ely, T. S., Goldman, D. E., Heating Characteristics of Laboratory Animals Exposed to Ten-Centimeter Microwaves, NMRI-NM-001-056.13-02, Naval Medical Research Institute, Bethesda, Md., Mar. 1957.
- 1-20. Engelbrecht, R. S., Mumford, W. W., Some Engineering Aspects of Microwave Radiation Hazards, in Peyton, M. F., (ed.), Biological Effects of Microwave Radiation, Proceedings of the Fourth Annual Tri-Service Conference, Vol. I, Plenum Press, N. Y., 1961, pp. 55-70.

- 1-21. England, T. S., Dielectric Properties of the Human Body for Wave-Lengths in the 1-10 cm. Range, Nature, 166: 480-481, 1950.
- 1-22. Frey, A. H., Some Effects on Human Subjects of Ultra-High Frequency Radiation, Amer. J. Med. Electronics, 2(1):28-31, 1963.
- 1-23. Gordon, Z. V., The Problem of the Biological Action of UHF, in Letavet, A. A., Gordon, Z. V. (eds.), The Biological Action of Ultrahigh Frequencies, JPRS-12471, Joint Publications Research Service, Washington, D. C., Feb. 15, 1962. (Translation of O Biologicheskom Vosdeystvii Sverkhysokikh Chastot, Moscow, Acad. of Med. Sci., USSR, 1960, pp. 5-7.)
- 1-24. Gordon, Z. V., Problems of Industrial Hygiene and of the Biological Effect Produced by Radio-Waves of Different Bands, JPRS-27032, Joint Publications Research Service, Washington, D. C., October 1964, pp. 61-71. (Translation of Vestnik Academic Meditsinski Nauk SSSR, 19(7): 42-49, 1964).
- 1-25. Gvozdikova, G. M., Anan'yev, V. M., Zenina, I. N., et al., Sensitivity of the Rabbit Central Nervous System to a Continuous Ultra-High Frequency Electromagnetic Field, in Recent Works on "Skin Vision", The Central Nervous System and Radiation Sickness, JPRS-26725, Joint Publications Research Center, Washington, D. C., Oct. 1964, pp. 31-37. (Translation of article in Bull. Exp. Biol. Med., Moscow, 29(8):63-68, 1964).
- 1-26. Herrick, J. F., Krusen, F. H., Certain Physiologic and Pathologic Effects of Microwaves, Elec. Engrg., 72: 239, 1953.
- 1-27. Herrick, J. F., Jelatis, D. G., Lee, G. H., Dielectric Properties of Tissues Important in Microwave Diathermy, Fed. Proc., 9: 60, 1950.
- 1-28. Hirsch, F. G., Parker, J. T., Bilateral Lenticular Opacities Occurring in a Technician Operating a Microwave Generator, A. M. A. Arch. Ind. Hyg. and Occup. Med., 6: 512-517, 1952.
- 1-29. Howland, J. W., Thomson, R. A. E., Michaelson, S. M., Biomedical Aspects of Microwave Irradiation of Mammals, Peyton, M. F. (ed.), Biological Effects of Microwave Radiation, Proceedings of the Fourth Annual Tri-Service Conference, Vol. I, Plenum Press, New York: 1961, pp. 261-284.
- 1-30. Hug, O., Pape, R., Nachweis der Ultraschallkavitation im Gewebe, Strahlentherapie, 94: 79-99, 1954.

- 1-31. Kalant, H., Physiologic Hazards of Microwave Radiation: A Survey of Published Literature, Canad Med. Assn. J., 81: 575-582, 1959.
- 1-32. Klimkova-Deutscheova, E., Effect of Radiation on Human EEG, FTD-TT-64-267/2, Foreign Technology Division, Wright-Patterson AFB, Ohio, 1964. (Translation of Ceskoslovenska Neurologie, 26(3): 1963, pp. 22-23). (AD-450604).
- 1-33. Kulke, B., Millimeter-Wave Generation with Electron-Beam Devices, NASA-TN-D-3727, Feb. 1967.
- 1-34. Lerman, S., Radiation Cataractogenesis, N. Y. State J. Med., 62(19): 3075-3084, Oct. 1962.
- 1-35. Library of Congress, Biological Effects of Microwaves, Compilation of Abstracts, LC-ATD-P-65-68, Aerospace Technology Division, Washington, D. C., Sept. 1965.
- 1-36. Livshits, N. N., The Role of the Nervous System in Reactions to UHF Electromagnetic Fields, Biophysics, 2(3): 372-384, 1957.
- 1-37. McLaughlin, J. T., Health Hazards from Microwave Radiation, Western Med., 3: 126-132, Apr. 1962.
- 1-38. Minecki, L., Bilski, R., The Health of Persons Exposed to the Effect of High Frequency Electromagnetic Fields, in Minecki, L., Bilski, R., Medical Reports (Selected Articles), FTD-TT-61-380, Foreign Technology Division, Wright-Patterson AFB, Ohio, Dec. 1961. (Translation of Medycyna Pracy, 12(4): 329-335).
- 1-39. Monayenkova, A. M., Sadchikova, M. N., Hemodynamic Indices During the Action of Super-High Frequency Electromagnetic Fields, LC-ATD-66-123, Library of Congress, Aerospace Technology Division, Washington, D. C., 1966. (Translation of Gigiyena Truda i Professional'nyye Zabolevaniya, 10(7): 13-21, 1966.
- 1-40. Murray, J. L., Some Biological Aspects of Microwave Radiation, (Master's Thesis), Department of Radiation Biology, The University of Rochester School of Medicine and Dentistry, Rochester, N. Y., 1963. (AD-415814).
- 1-41. Muth, E., Ueber die Erscheinung der Perlschnurketten-bildung von Emulsionspartikelchem unter Einwirkung eines Wechselfeldes, Kolloid-Zeitschrift, 41: 7-102, 1927.

- 1-42. Michaelson, S. M., Thomson, R. A. E., Howland, J. W., Comparative Studies on 1285 and 2800 Mc/sec Pulsed Microwaves, Aerospace Med., 36(11): 1059-1064, 1965.
- 1-43. Michaelson, S. M., Thomson, R. A. E., Quinlan, W. J., Jr., Effects of Electromagnetic Radiations on Physiologic Responses, Aerospace Med., 38(3):293-298, 1967.
- 1-44. Michaelson, S. M., Thomson, R. A. E., Odland, L. T., et al., The Influence of Microwaves on Ionizing Radiation Exposure, Aerospace Med., 34: 111-115, 1963.
- 1-45. Michaelson, S. M., Thomson, R. A. E., Howland, J. W., Physiologic Aspects of Microwave Irradiation of Mammals, Amer. J. Physiol., 201(2): 351-356, 1961.
- 1-46. Osipov, Yu. A., The Health of Workers Exposed to Radio-Frequency Radiation, in Gigiyena Truda i Vliyaniye na Rabotayuschikh Electromagnithykj Poley Radiochastot (Occupational Hygiene and the Effect of Radio-Frequency Electromagnetic Fields on Workers.) Med. Publ. House, Leningrad, 1965, pp. 104-144.
- 1-47. Osipov, Yu. A., Measures of Protection, Therapy, and Prophylaxis to be Taken During Work With Radio-Frequency Oscillators, JPRS-32735, Joint Publications Research Service, Washington, D. C., Nov. 1965. (Translation of Gigiyena Truda i Vliyaniye na Rabotaycheshchikh Electromagnitnykh Bleg Radiochastot, 1965, Chapt. 8, pp. 156-202).
- 1-48. Osipov, Yu. A., Kalyada, T. V., Temperature Reaction of the Skin During Irradiation with Microwaves of Low Intensity, JPRS-23287, Joint Publications Research Service, Washington, D. C., Feb. 1964. (Translation of Gigiyena i Sanitariya, no. 10, 1963, pp. 73-78).
- 1-49. Overman, H. S., Quick Formulas for Radar Safe Distances, in Peyton, M. F., (ed.), Biological Effects on Microwave Radiation, Proceedings of the Fourth Annual Tri-Service Conference, Vol. I, Plenum Press, New York: 1961, pp. 47-54.
- 1-50. Pennock, B. E., The Measurement of the Complex Dielectric Constant of Protein Solutions at Ultra High Frequencies: Dielectric Properties of Hemoglobin Bound Water, (Doctoral Thesis) ONR-TR-41, Office of Naval Research, Washington, D. C., 1967.(University of Pennsylvania, Phila. Pa.)

- 1-51. Presman, A. S., Levitina, N. A., Influence of Non-Thermal Microwave Radiation on the Survivability of Gamma-Irradiated Animals, AEC-TR-5428, U. S. Atomic Energy Commission, Division of Technical Information, Washington, D. C. (Translation of Radiobiologiya, 2(1): 258-260, 1962).
- 1-52. Presman, A. S., Problems of the Mechanism of the Biological Effect of Microwaves, JPRS-22580, Joint Publications Research Service, Washington, D. C., Jan. 1964.
- 1-53. Richardson, A. W., Lomax, D. H., Nichols, J., et al., The Role of Energy, Pupillary Diameter, and Alloxan Diabetes in the Production of Ocular Damage by Microwave Irradiations, Amer. J. Ophthal., 35: 993-1000, 1952.
- 1-54. Rutkowski, A., Christianson, C., Development of RAD HAZ Suit and RF Measuring Techniques, NASL-9400-20-1, U. S. Naval Applied Science Laboratory, Naval Base, Brooklyn, N. Y., May 1965. (AD-463422).
- 1-55. Saito, M., Schwan, H. P., Schwarz, G., Response of Non-spherical Biological Particles to Alternating Electric Fields, Biophysical J., 6(3): 313-327, 1966.
- 1-56. Schaefer, H., Schwan, H., Zur Frage der Selektiven Erhitzung Kleiner Teilchen im Ultrakurzwellen-Kondensatorfeld, Annalen Physik, 43: 99-135, 1943.
- 1-57. Schaefer, H., Schwan, H., Zur Frage der Selektiven Überhitzung von Einzelzellen im Biologischen, Strahlentherapie, 77: 123-30, 1947.
- 1-58. Schultz, F. V., Burgener, R. C., King, S., Measurement of the Radar Cross Section of a Man, Proc. IRE, 46: 476-481, Jan. - Apr. 1958.
- 1-59. Schwan, H. P., Piersol, G. M., Absorption of Electromagnetic Energy in Body Tissues: I. Biophysical Aspects, Am. J. Phys. Med., 33: 371-404, 1954.
- 1-60. Schwan, H. P., Absorption and Energy Transfer of Microwaves and Ultrasound in Tissues: Characteristics, in Glasser, O. (ed.), Medical Physics, Vol. 3, Year Book Publishers, Chicago: 1960, pp. 1-7.
- 1-61. Schwan, H. P., Biophysics of Diathermy, in Licht, S. H. (ed.), Therapeutic Heat, E. Licht, New Haven: 1958, pp. 55-115.
- 1-62. Schwan, H. P., Li, K., Capacity and Conductivity of Body Tissues at Ultrahigh Frequencies, Proc. IRE, 41: 1735-1740, Sept. - Dec. 1953.

- 1-63. Schwan, H. P., Carstensen, E. L., Li, K., Comparative Evaluation of Electromagnetic and Ultrasonic Diathermy, Arch. Phys. Med., 35: 13-19, 1954.
- 1-64. Schwan, H., Die Temperaturabhängigkeit der Dielektrizitätskonstante von Blut bei Niederfrequenz, Naturforschung, 3b: 361-367, 1948.
- 1-65. Schwan, H. P., Electrical Properties of Tissue and Cell Suspensions, in Lawrence, J. H., Tobias, C. (eds.), Advances in Biological and Medical Physics, Vol. 5. Academic Press, New York, 1957.
- 1-66. Schwan, H. P., Li, K., Hazards Due to Total Body Irradiation by Radar, Proc. IRE, 44: 1572-1581, Sept. - Dec. 1956.
- 1-67. Schwan, H. P., Survey of Microwave Absorption Characteristics of Body Tissues, in Pattishall, E. G., Banghart, F. W. (eds.), Biological Effects of Microwave Energy, Proceedings of the Second Tri-Service Conference, ARDC-TR-58-54, Rome Air Development Center, Griffiss AFB, N. Y., July 8-10, 1958, pp. 126-145. (AD-131477).
- 1-68. Seth, H. S., Michaelson, S. M., Microwave Cataractogenesis, J. Occup. Med., 7: 439-442, 1965.
- 1-69. Seth, H. S., Michaelson, S., Microwave Hazards Evaluation, Aerospace Med., 35(8): 734-739, 1964.
- 1-70. Sher, L. D., Schwan, H. P., Mechanical Effects of A. C. Fields on Particles Dispersed in a Liquid (Doctoral Thesis), Office of Naval Research, Washington, D. C., 1963. University of Pennsylvania, Philadelphia, Pa.
- 1-71. Shimkovich, I. S., Shilyaev, V. G., Cataract of Both Eyes Which Developed as a Result of Repeated Short Exposures to an Electromagnetic Field of High Density Vestn. Oftal., 72(4): 12-16, Jul. - Aug. 1959. (Abstracted in Lazarus, H. B., Levedahl, B. H., Effects of Radiation on the Mammalian Eye, A Literature Survey, TID-3912, DTIE-U. S. Atomic Energy Commission, Oak Ridge, Tenn., Nov. 1962, p. 447).
- 1-72. Smirnova, M. I., Sadchikova, M. N., Determination of the Functional Activity of the Thyroid Gland by Means of Radioactive Iodine in Workers Exposed with UHF Generators, in Letavet, A. A., Gordon, Z. V., (eds.), The Biological Action of Ultra-High-Frequencies, JPRS-12471, Joint Publications Research Service, Washington, D. C., Feb. 1962, pp. 47-49. (Translation of O Biologicheskom Vosdeystvii Sverkhysokikh Chastot, Moscow, Acad. of Med. Sci., USSR, 1960. pp. 50-51).

- 1-73. Smurova, Ye. I., Rogovaya, T. Z., Yakub, I. L., Troitskiy, S. A., General Health of Persons Working with HF, UHF, and VHF Generators in Physiotherapy Machines. (Translation of Kazanskiy Meditsinskiy Zhurnal, no. 2: 82-84, 1966).
- 1-74. Susskind, C., and Staff, Nonthermal Effects of Microwave Radiation, RADC-TDR-62-624, Rome Air Development Center, Griffiss AFB, N. Y., Oct. 1962.
- 1-75. Thompson, W. D., Bourgeois, A. E., Effects of Microwave Exposure on Behavior and Related Phenomena, ARL-TR-65-20, 6571 Aeromedical Research Lab., Wright-Patterson AFB, Ohio. 1965.
- 1-76. Thomson, R. A. E., Michaelson, S. M., Howland, J. W., Microwave Modification of X-Ray Lethality in Mice, RADC-TDR-63-352, Rome Air Development Center, Griffiss AFB, N. Y., Aug. 1963.
- 1-77. Thomson, R. A. E., Michaelson, S. M., Howland, J. W., Microwave Radiation and Its Effect on Response to Ionizing Radiation (Abstract), Preprints of Scientific Program, Aerospace Medical Association, 37th Annual Meeting, Apr. 18-21, 1966, Las Vegas, Nevada.
- 1-78. Turner, J. J., The Effects of Radar on the Human Body (Results of Russian Studies on the Subject), Bell Telephone Labs., Inc., Whippny, N. J., July 1962. (Summary based on Letavet, A. A., Gordon, Z. V., (eds.), The Biological Action of Ultra-High Frequencies, JPRS-12471, Joint Publications Research Service, Washington, D. C., Feb. 1962.)
- 1-79. U. S. Air Force, Electromagnetic Radiation Hazards, T. O. 31Z-10-4, Washington, D. C., Oct. 1961.
- 1-80. U. S. Army, U. S. Air Force, Control of Hazards to Health from Microwave Radiation, AFM-161-7, (TB-MED-270/AFM-161-7), Washington, D. C., Dec. 1965.
- 1-81. U. S. Navy, Washington, D. C., Safety Level of Electromagnetic Radiation with Respect to Personnel, USAS-95. 1-1966, USA Standard, 1966.
- 1-82. Williams, D. B., Monahan, J. P., Nicholson, W. J., et al., Biologic Effects Studies on Microwave Radiation: Time and Power Thresholds for the Production of Lens Opacities by 12.3 Cm Microwaves, SAM-55-94, School of Aviation Medicine, Randolph AFB, Texas, Aug. 1955.

- 1-83. Zaret, M. M., Ocular Effects of Microwave Radiation, Annual Progress Report, The Zaret Foundation, Inc., Scarsdale, New York, 1967. Grant No. DA-MD-49-193-67-G9224. (AD-654447).
- 1-84. Zaret, M. M., Ophthalmic Hazards of Microwave and Laser Environments, Annual Progress Report, The Zaret Foundation, Inc., Scarsdale, New York, May 1967, Contract no. DA-49-193-MD-2592. (AD-654523).
- 1-85. Zaret, M. M., Cleary, S. F., Pasternack, B., et al., A Study of Lenticular Imperfections in the Eyes of a Sample of Microwave Workers and a Control Population, RADC-TDR-63-125, Rome Air Dev. Center, Griffiss AFB, N. Y., Mar. 15, 1963. (Discussions, pp. 61-71).

2. LIGHT ENVIRONMENT
A. VISIBLE LIGHT
B. ULTRAVIOLET LIGHT

Prepared by

E. M. Roth, M. D., Lovelace Foundation
S. Finkelstein, M. D., Lovelace Foundation

TABLE OF CONTENTS

2. LIGHT	2-1
A. VISIBLE LIGHT	2-1
Characteristics of the Human Sensor	2-1
Nomenclature	2-1
The Light Environment	2-8
Visual Performance and Visibility	2-13
Visual Acuity.	2-14
Optical Aberrations of the Eye	2-24
Search and Visibility	2-25
Color	2-28
Visual Acuity as A Function of the Color of Illuminant	2-28
Color Recognition Thresholds	2-32
Color Specification	2-32
Duration of Visual Exposure and	
Intermittent Illumination	2-36
Visual Fields	2-38
Movement Discrimination and Ocular Pursuit . . .	2-42
Dark Adaptation.	2-42
Glare and Flash Blindness Phenomena.	2-51
Glare	2-51
Irradiation Phenomena	2-56
Flashblindness.	2-58
Retinal Burns	2-65
Laser Burns (Coherent Light)	2-66
Skin Effects.	2-68
Environmental Factors in Vision	2-68
Toxic and Drug Effects on Vision	2-68
Visual Performance in Actual Space Flight	2-69

Visual Considerations in the Design of the Spacecraft Cabins and Space Suits	2-73
General Recommendations for Spacecraft Illumination.	2-73
Role of Color in Habitability	2-76
Viewing Ports and Visors	2-78
Instrumentation and Displays	2-81
Telescopic Devices	2-82
Dials and Scales.	2-82
CRT (Cathode Ray Tubes) Displays	2-87
Complex Visual Displays	2-91
Visual Problems in Space Operations	2-92
Observation of Other Space Vehicles	2-92
Identification of the Shape and Other Details of a Satellite	2-94
Visibility of Objects on Earth from Spacecraft . .	2-96
Vision in Rendezvous and Docking	2-96
Acquisition	2-97
Establishment of Intercept.	2-99
Range, Braking and Docking Phases	2-101
Visual Requirements for Lunar Landing	2-105
Visual Performance on the Moon	2-108
B. ULTRAVIOLET RADIATION.	2-110
Effects of Ultraviolet Light on the Skin	2-111
Sunburn	2-113
Thickening of Skin.	2-114
Tanning	2-114
Phototoxicity and Photallergy	2-115
Effects of Ultraviolet on the Eye	2-115
Eye Protection Against Ultraviolet	2-117
Eye Trauma in Space Operations.	2-120
References	2-121

LIGHT ENVIRONMENT

A. VISIBLE LIGHT

Visible light is that band of the electromagnetic spectrum from 380 to 750 millimicrons or nanometers (nm), capable of stimulating the photoreceptors of the eye thereby producing a sensation called vision. The physical phenomenon of light may be viewed in two different ways: as energy quanta (photons) or as waves passing through a medium. The interaction of visible light with biological systems can be interpreted as a manifestation of both viewpoints.

Characteristics of the Human Sensor

Light is sensed by the retinal photon receptors of the eye after passing along the optical path as seen in Figure 2-1. Light rays reflected from an object in the external world pass through the cornea at the front of the eye, through the liquid (aqueous humor) in the anterior chamber directly behind the cornea, then through the lens and vitreous humor onto the retina. Data on the spectral transmission of the ocular media are available (63).

The rods and cones of the retina transduce the light into neuro-electrical phenomena. The neural elements of the retina are gathered into the optic nerve at the blind spot and pass by discrete pathways to the highest visual center in the brain in the occipital cortex.

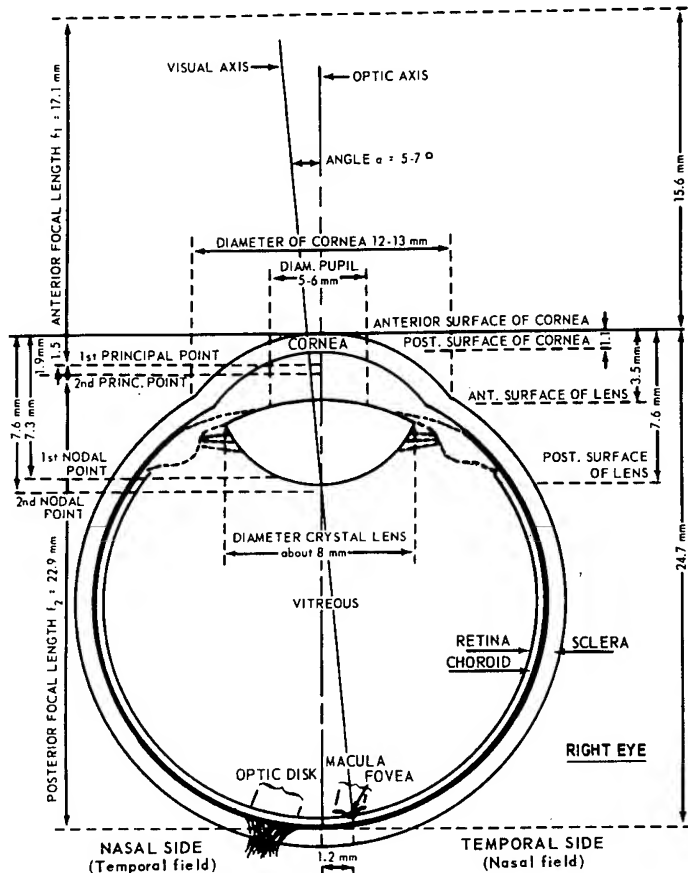
The human visual system is a very versatile one, with ample capabilities of adaptation to a variety of environmental changes. This versatility dictates that many variables in the physical and biological environment must be assessed in evaluating human standards for visual performance (117).

Nomenclature

A summary of terms and symbols commonly used in physiological optics is presented in Table 2-2.

Figure 2-3 lists and graphically demonstrates the relationship between intensity and illuminance units frequently used in the literature. Table 2-4 is a nomograph allowing conversion of the many equivalent units of luminance in common use. Table 2-5 allows conversion of other parameters.

The new unit of luminous intensity is the candela or new candle. A candela is equal to 1/60th of the luminous intensity of 1 cm² of a blackbody surface at the solidification point of platinum and represents about .981 candles.

a.**b.**

Constant	Eye Area or Measurement	
Refractive index	Cornea	1.37
	Aqueous humor	1.33
	Lens capsule	1.38*
	Outer cortex, lens	
	Anterior cortex, lens	
	Posterior cortex, lens	
Radius of curvature, mm	Center, lens	1.41
	Calculated total index	1.41
	Vitreous body	1.33
	Cornea	7.7
	Anterior surface, lens	9.2-12.2
Distance from cornea, mm	Posterior surface, lens	5.4-7.1
	Post. surface, cornea	1.2
	Ant. surface, lens	3.5
	Post. surface, lens	7.6
Focal distance, mm	Retina	24.8
	Anterior focal length	17.1
	[14.2]**	
	Posterior focal length	22.8
Position of cardinal points measured from corneal surface, mm	1. Focus	-15.7
	2. Focus	24.4
	1. Principal point	[21.0]
	2. Principal point	1.5
	1. Nodal point	[1.8]
	2. Nodal point	1.9
Diameter, mm	1. Optic disk	[2.1]
	Macula	7.3
	Fovea	[6.5]
Depth, mm	Anterior chamber	7.6
		[6.8]

*Cortex of lens and its capsule

**Values in brackets refer to state of maximum accommodation

The diagram and table give dimensions and optical constants of the human eye. Values in brackets shown in the table refer to state of maximum accommodation. The drawing is a cross section of the right eye from above.

The horizontal and vertical diameters of the eyeball are 24.0 and 23.5 mm, respectively. The optic disk, or blind spot, is about 15 degrees to the nasal side of the center of the retina and about 1.5 degrees below the horizontal meridian.

Figure 2-1

Schematic and Optical Constants of the Eyeball

(After White (446) Adapted from Spector, ed.(394))

Table 2-2
Summary of Terms and Symbols Commonly Used in Optics

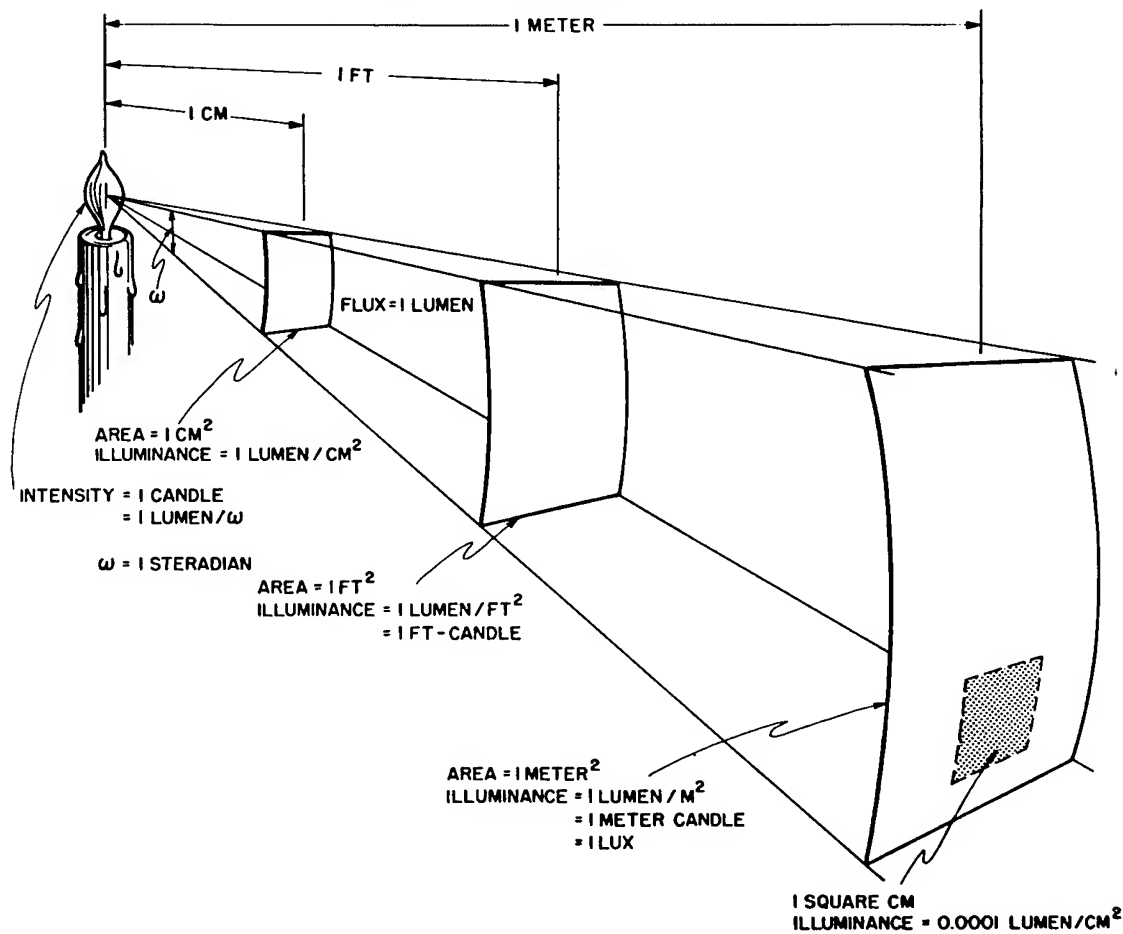
Term	Symbol	Units
LIGHT		
Velocity in vacuo	c	2.99776×10^{10} cm/sec
Frequency	ν	cycles/sec or Hertz
Wavelength	λ	millimicrons or nanometers
Velocity in any medium m	V_m	cm/sec
Index of refraction	n	ratio $n = c/V_m$
Temperature	T	degrees absolute, K
Work	W	joule = 10^7 ergs = 10^7 dyne-cm
Energy (see end note)	E or U	joule = 10^7 ergs = 10^7 dyne-cm
Power	P	watt = joule/sec
Planck's constant	h	6.624×10^{-27} erg-sec
RADIOMETRY		
Radiant energy (see end note)	E or U	joule
Radiant flux	P	watt = joule/sec
Unit solid angle	ω	steradian = $1/4\pi$ sphere
Radiant intensity	J	watt/ ω
Irradiance	H	watt/m ²
Radiance	N	watt/ ω /m ²
PHOTOMETRY		
Luminous flux	F	$\frac{1}{685}$ watt at $\lambda = 555$ m μ
Luminous intensity (candlepower)	I	lumen/ω = candle
Illuminance	E	lumen/m^2 = lux = meter-candle = 0.0929 ft-candle
Luminance	B	$\text{lumen}/\omega/m^2$ = candle/m ² = 0.3142 millilambert = 0.2919 foot-lambert
Retinal illuminance	$L \cdot S$	troland (uncorrected for Stiles-Crawford effect) = luminance of 1 candle/m ² on a surface viewed through an artificial pupil of area $S = 1 \text{ mm}^2$ or $= \frac{1}{\text{Brightness in millilamberts}} \times \frac{10}{\pi} \times \text{Area in mm}^2$

Table 2-2 Continued

COLORIMETRY

Transmittance	T_λ	Ratio $T_\lambda = P_{\lambda T}/P_{\lambda_0}$, where P_{λ_0} is incident flux and $P_{\lambda T}$ is transmitted flux at wavelength λ .
Reflectance	R_λ	Ratio $R_\lambda = P_{\lambda R}/P_{\lambda_0}$, where $P_{\lambda R}$ is reflected flux at wavelength λ .
Relative scotopic luminosity (also called relative scotopic luminous efficiency; formerly called scotopic visibility; also infrequently and informally, spectral sensitivity.)	V_λ'	Ratio of luminous efficiency of light at wavelength λ for standard observer at low levels of luminance to luminous efficiency maximum at 505 m μ .
Relative photopic luminosity (also called relative photopic luminous efficiency; formerly called photopic visibility; also infrequently and informally, spectral sensitivity.)	V_λ	Ratio of luminous efficiency of light at wavelength λ for standard observer at high levels of luminance to luminous efficiency maximum at 555 m μ .
Luminous flux	F	$\text{lumens} = 685 \int_0^\infty P_\lambda T_\lambda V_\lambda d\lambda$ <p style="text-align: center;">(for transmitted light)</p> $\text{lumens} = 685 \int_0^\infty P_\lambda R_\lambda V_\lambda d\lambda$ <p style="text-align: center;">(for reflected light)</p>
Dominant wavelength (spectral centroid)	λ_c	$\lambda_c = \frac{\int_{\lambda=0}^\infty P_\lambda T_\lambda V_\lambda \lambda d\lambda}{\int_{\lambda=0}^\infty P_\lambda T_\lambda V_\lambda d\lambda}$ <p style="text-align: center;">(for transmitted light)</p> $= \frac{\int_{\lambda=0}^\infty P_\lambda R_\lambda V_\lambda \lambda d\lambda}{\int_{\lambda=0}^\infty P_\lambda R_\lambda V_\lambda d\lambda}$ <p style="text-align: center;">(for reflected light)</p>
Tristimulus functions for the standard observer. Also called distribution coefficients.	$\bar{x}, \bar{y}, \bar{z}$	Amounts of the three CIE primaries required to match a unit amount of energy at each wavelength.
Tristimulus values	X, Y, Z	Sums of weighted values from spectral energy data at all wavelengths.
Chromaticity coefficients	x, y, z	$x = \frac{X}{X + Y + Z}$ $y = \frac{Y}{X + Y + Z}$ $z = \frac{Z}{X + Y + Z}$
(Adapted from Graham ⁽¹⁷⁷⁾)		

Intensity (I)	1 lumen /steradian = 1 candle = 1 candle power = 1.02 candelas
Illuminance (E)	lumens/cm ² 1 lumen/m ² = 1 meter candle = 1 lux 1 lumen/ft ² = 1 ft-candle (ft-c)
Luminous Emittance (L)	lumens/cm ² lumens/m ² lumens/ft ²
Luminance (B)	lumens/steradian/m ² (or cm ²) lamberts (L) = millilamberts (mL) × 10 ³ = microlamberts (μ L) × 10 ⁶ for a perfectly diffusing surface, 1 lambert = 1/ π candles/cm ² , foot-lambert (ft-L) = 1.076 mL



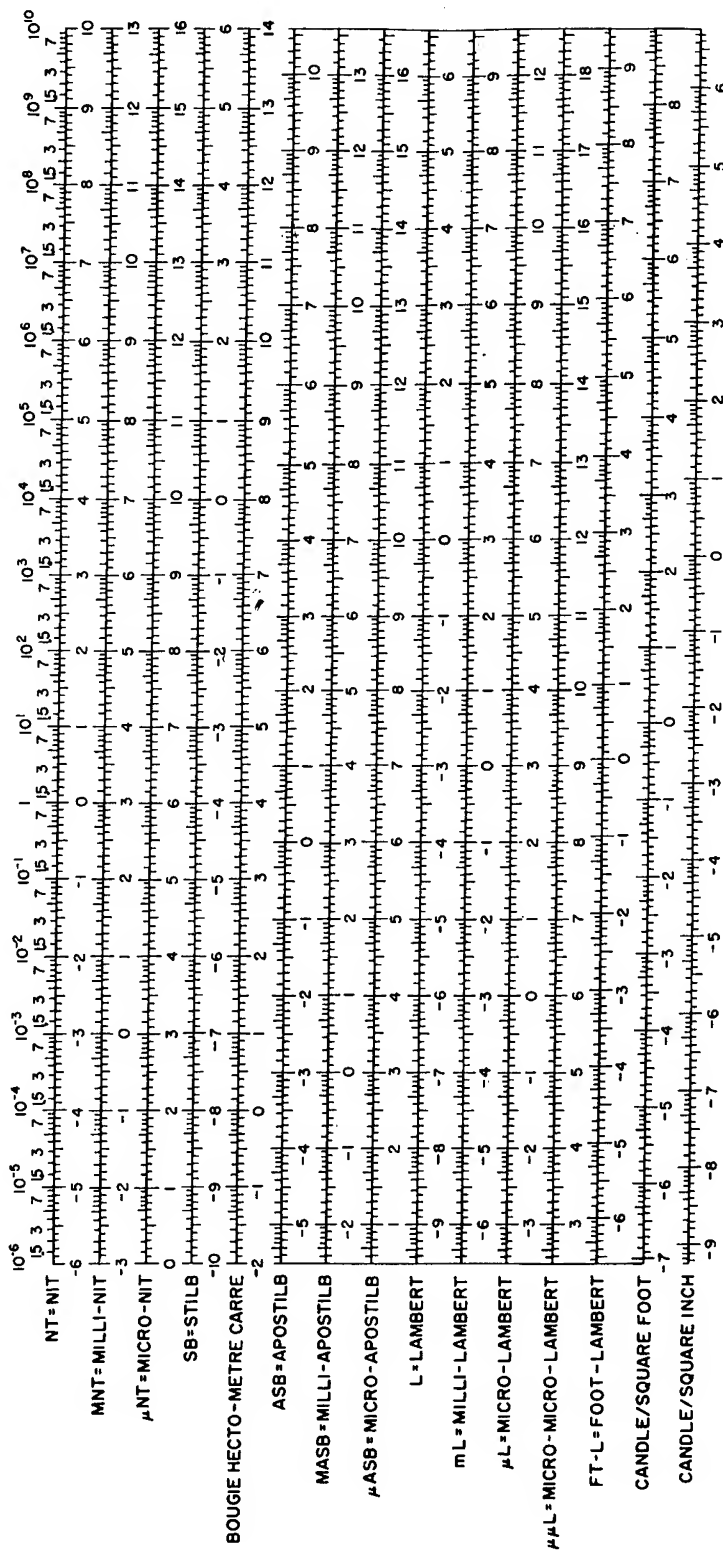
Relationships Between Intensity Units of Source and Illuminance Units on Surfaces at Various Distances

Figure 2-3

(After Sears (375))

Table 2-4

Nomograph of Equivalent Values of Commonly Used Units of Luminance, Below Each Bar Logarithmic Units and their Subdivisions Are Given. Above the Nit Bar Natural Figures and Subdivisions Are Given. Above Each Bar Subdivisions for Natural Figures Are Given.



(After Rose (363))

Table 2-5
CONVERSION FACTORS

To convert any quantity listed in the left-most column to any quantity listed to the right, multiply by the factor shown.

Luminous Flux (Intensity of a Source)					Illuminance (Illumination incident upon a surface)				
	Candle-power	Lumens	Watts	Ergs/second		Foot-candles	Meter-candles	Lumens/ft ²	Lumens/meter ²
Candlepower	1	4π	0.005882π (at 555m μ *)	$5.882\pi \times 10^4$ (at 555m μ **)		1	10.764	1	10.764
Lumens	$\frac{1}{4\pi}$	1	0.001471 (at 555m μ *)	1.471×10^4 (at 555m μ **)		0.0929	1	0.0929	1
Watts	$\frac{170}{\pi}$ (at 555m μ *)	680 (at 555m μ *)	1	10^7		Lumens/ft ²	10.764	1	10.764
Ergs/second	$\frac{170}{\pi} \times 10^{-7}$ (at 555m μ *)	680×10^{-7} (at 555m μ *)	10^{-7}	1		Lumens/meter ²	0.0929	1	0.0929

Luminance (Surface brightness or reflected light)					
	Candles/foot ²	Candles/meter ²	Footlamberts	Apostilbs***	Lamberts (Lumens/cm ²)
Candles/foot ²	1	10.764	π	10.764π	$\frac{\pi}{929}$
Candles/meter ²	0.0929	1	0.0929π	π	$\pi \times 10^{-4}$
Footlamberts	$\frac{1}{\pi}$	$\frac{10.764}{\pi}$	1	10.764	10.764×10^{-4}
Apostilbs***	$\frac{0.0929}{\pi}$	$\frac{1}{\pi}$	0.0929	1	10^{-4}
Lamberts (Lumens/cm ²)	$\frac{929}{\pi}$	$\frac{10^4}{\pi}$	929	10^4	1

Quantity of Energy Received By a Surface				
	Meter-candle-Seconds	Footcandle-Seconds	Ergs/cm ²	Watt-seconds/cm ² or Joules/cm ²
Meter-candle-Seconds	1	0.0929	1.471 (at 555m μ **)	1.471×10^{-7} (at 555m μ *)
Footcandle-Seconds	10.764	1	15.83 (at 555m μ **)	15.83×10^{-7} (at 555m μ *)
Ergs/cm ²	0.680 (at 555m μ *)	0.0632 (at 555m μ *)	1	10^{-7}
Watt-seconds/cm ² or Joules/cm ²	6.80×10^4 (at 555m μ *)	6.32×10^4 (at 555m μ *)	10^7	1

	Lumen-Seconds	Candle-power-Seconds	Watt-seconds or Joules	Ergs
Lumen-Seconds	1	$\frac{1}{4\pi}$	0.001471×10^{-7} (at 555m μ *)	0.001471×10^{-7} (at 555m μ **)
Candlepower-Seconds	4π	1	0.005882 (at 555m μ *)	0.005882×10^{-7} (at 555m μ **)
Watt-seconds or Joules	680 (at 555m μ *)	$\frac{170}{\pi}$ (at 555m μ *)	1	10^7
Ergs	680×10^7 (at 555m μ *)	170×10^7 (at 555m μ *)	10^7	1

*True only for monochromatic light at 555m μ . For other wavelengths in the visible region, multiply by the relative visibility factor for that wavelength.

**True only for monochromatic light at 555m μ . For other wavelengths in the visible region, divide by the visibility factor for that wavelength.

***Defined as 1 lumen per meter²; occasionally incorrectly called meter-lambert.

(Adapted by Taylor and Silverman⁽⁴⁰⁴⁾ from Eastman Kodak⁽¹³⁶⁾)

The Light Environment

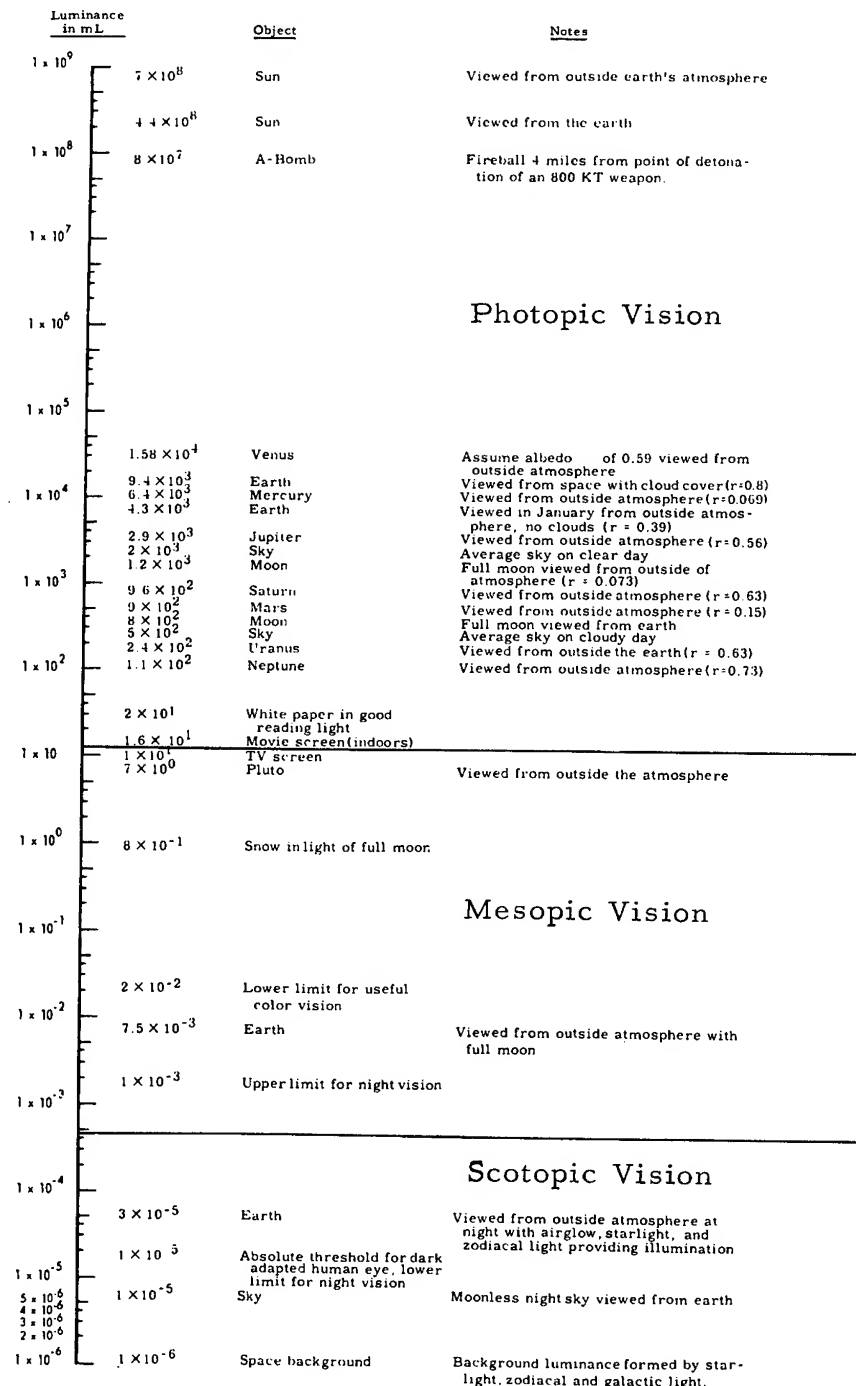
In order to define the visual factors in space operations, a knowledge of the physical light environment is required (16, 244, 354).

Table 2-6 covers the characteristic luminance on Earth and space. Photopic vision refers to that vision in which the cones of the eye are the prime receptors. In scotopic vision, the rods are the prime receptors, and in mesopic vision, both retinal elements are used.

Figure 2-7 represents the daily variation of natural illumination on Earth. More detailed coverage of these data, including haze effects, is available (73, 132). The illuminance of the Sun just outside the Earth's atmosphere is approximately 12,700 foot-candles.

Table 2-8 covers the luminance of some pertinent astronomical phenomena. A more detailed evaluation of the night sky is available (352).

Figure 2-9 presents the illuminance of stars for each stellar visual magnitude and threshold stellar magnitude as a function of background luminance. Table 2-9a is based on 3.90×10^{-8} foot candles as the illuminance of a second magnitude star (459). The stars are isometrically point sources and the light from the Sun, Moon, and other extended sources is collimated to within 32 minutes of arc of the subtended angle of the source. There appears to be some confusion in the literature as to the size of the source which can be considered a point source to the eye. The psychophysical definition of a point source is given by Ricco's law which states that the product of the threshold contrast and the solid angle subtended by the target are constant for any given adaptation level. Figure 2-18 shows the maximum visual angle for a point source at different background luminances. Note that the angle increases with decreasing background luminance. In the debriefings of all astronauts of the Gemini and Mercury space flights, there has been a continual insistence by the astronauts that "stars cannot be seen in the daytime," the only qualification of this statement being that planets and the Moon or perhaps the brightest stars (for example, Sirius) could be seen. This may have been due to the ambient light in the space cabin contributed by the spacecraft corona (see Figure 2-12), the density of the window or scattered window light (319). However, the intensity of ocular scattering may also be sufficient by itself to make impossible the observation of first-magnitude stars if the level of illumination on the face of the observer exceeds about 1000 lux (100 ft-c) (15). "Unless the viewing window of the space capsule is protected by a conical sunshade it will be difficult to reduce the interior illumination below this critical figure, even if the other window is obscured by a blind, as 1000 lux is only about 1 percent of the outdoor daylight level. This fogging effect of ocular scattering is often experienced by city-dwelling astronomers who find that it is impossible to see the Milky Way within about 90 degrees of the direction of a single street lamp that produces an ambient light level only about 0.01 percent that of daylight. That ocular scattering, rather than atmospheric scattering, produces the observed loss of contrast in the visual image of the sky can be shown by stepping into the shadow of the lamppost."



This enormous range of luminances is based on a solar illuminance of 12,700 Ft-c. A uniformly diffusing sphere at the earth's distance from the Sun would have a luminance of 13,655 mL and the apparent luminances of the Sun, Earth, Moon, Venus, and Jupiter have been recalculated on that basis. Albedo (r) as used in this figure is the ratio of the incident collimated light in a planetary body or spherical object to the light reflected and collected over 4π steradians and is considered to be invariant with wavelength. Only Jupiter and Venus are large enough to be characterized by their surface brightness.

Figure 2-6
Characteristic Luminance on Earth and in Space

(Modified from White⁽⁴⁴⁶⁾)

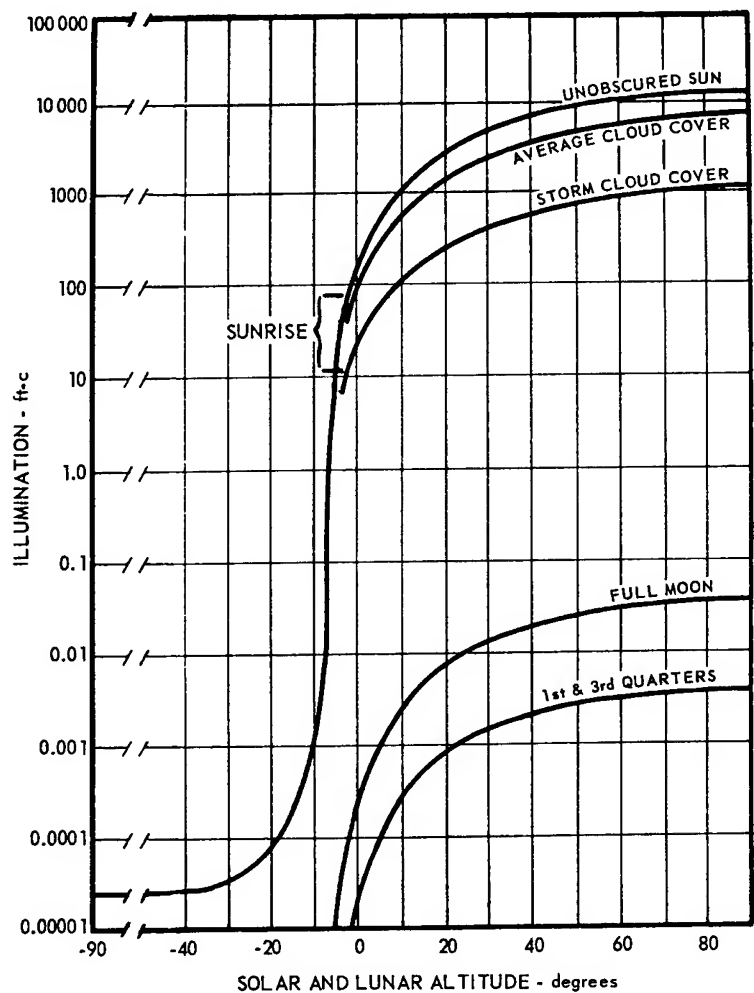


Figure 2-7

Range of Natural Illumination Levels on Earth.

This Graph Shows the Range of Natural Illumination on Earth from the Sun and the Moon, as the Values Increase from Minimum Before Sun- or Moonrise to Maximum at the Zenith.

(After White⁽⁴⁴⁶⁾) Adapted from Brown⁽⁷³⁾

Table 2-8
Luminance of Astronomical Phenomena
as Viewed from Earth

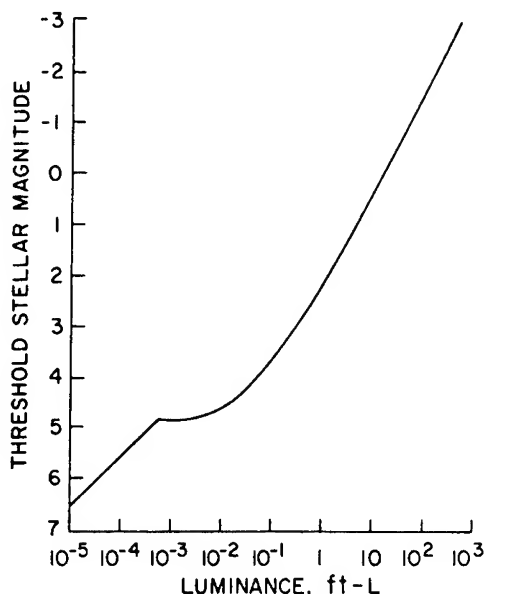
Phenomenon	Luminance, foot-lamberts
Milky Way, dimmest region, near Perseus	2.9×10^{-5}
Gegenschein	4.6×10^{-5}
Visible night glow (zenith)	5.8×10^{-1}
Aurora IBC-I	$\sim 6 \times 10^{-5}$
Milky Way brightest region, near Carina	1.1×10^{-4}
Zodiacal light (30° elongation)	3.5×10^{-4}
Visible night glow (edge-on)	1.7×10^{-3}
Great Orion nebula M42	1.6×10^{-2}
Full moon	1.2×10^3
Fluorescent lamp 4500 white	1.2×10^3

(Adapted from Dunkelman⁽¹²⁸⁾ by Allen⁽¹²⁾)

Figure 2-9
Visibility of the Stars
(After Allen⁽¹²⁾)

M_V	Illuminance (ft-cd)
-2	1.55×10^{-6}
-1	6.18×10^{-7}
0	2.46×10^{-7}
1	9.79×10^{-8}
2	3.90×10^{-8}
3	1.55×10^{-8}
4	6.18×10^{-9}
5	2.46×10^{-9}
6	9.79×10^{-10}
7	3.89×10^{-10}
8	1.55×10^{-10}

a. Stellar Visual Magnitude and Illuminance



b. Star Visibility Versus Background Luminance

Figure 2-10 summarizes pertinent parameters of the visual environment of space. Extensive reviews of the photometry of the Moon and planets are available (27, 244, 393). The reflectance of the Earth as viewed from outside the atmosphere has a greater range than the range of observed reflectance from all other planets and satellites. The reflectance of the Earth varies from 0.03 for large bodies of water to 0.85 for cloud cover. More detailed reflectance data for local areas on Earth are available (132). Other solar system reflectance values range from 0.07 for Mercury to 0.7 for Neptune. Optical data needed for predicting the view of Earth, Moon and planets from space have been presented (351).

Optical properties of the Moon pertinent to human visual function have received recent review (12, 244, 316, 364, 410). The natural illumination of the lunar surface comes from direct sunlight; reflected sunlight primarily from Earth, but in some small degree from other planets in the solar system; and from starlight. The intensity of the sunlight falling on the lunar surface is about 1.4 times that which reaches the surface of the Earth or 12,700 foot-candles. The solar disc has a luminance of 6.4×10^8 ft L subtending a visual angle of 0.5 degrees. Data are available on the mean illumination of the Moon by different phases of crescent Earth (316).

From telescopic data, the rough and broken lunar surfaces (craterwalls) reflect from 20 to 30% of the incident light while the smooth and darker layers of the maria between 6 and 7% (253, 328, 402). The Moon has a highly directional reflectance. The variation of reflectance with phase angles is shown

Table 2-10
Primary Parameters of the Visual Environment of Space
(After Jones et al⁽²⁴¹⁾)

	90° Solar Illumination	Surface Reflectance*	Mean Atmos. Transmission
Earth (Night illumination with full moon = 0.04 ft-c)	10,800 ft-c	Ocean .03 Ground .15 Snow .80	.70-.80**
EVA (Earth Orbit)	12,700 ft-c	Aluminum .55 Dark Paint .10 White Paint .80	1.00
Moon (Full earth = 1.25 ft-c 30° phase = 0.80 ft-c 90° phase = 0.26 ft-c)	12,700 ft-c	Maria .07 Crater Wall .20	1.00
Mars	7,600 ft-c	Maria .17 Continents .18	.80

*Lunar reflectances from references (105)

Mars reflectances from reference (193)

**Function of diameter and distribution of scattering particles.

in Figure 2-11. The average normal albedo of the lunar surface in the vicinity of the Surveyor spacecraft was about 6%. The range of reflectance of local lunar areas is even greater than 0.06 to 0.30 (12, 112, 316). The highest luminances (not in shadow) may vary from 0.08 to 0.42 of a white target in full sunlight on the surface of the Earth. "Limb darkening" on the lunar surface decreases the lower value to approximately 0.003. Thus, the apparent luminance varies from 0.003 to 0.40 of the luminance of the hypothetical white target, or a range approximately 100 to 1. In comparison, the range of luminance on Earth outdoors on a partially cloudy day, with part of the landscape in full sunlight and part in cloud shadow, can be more than 1000 to 1.

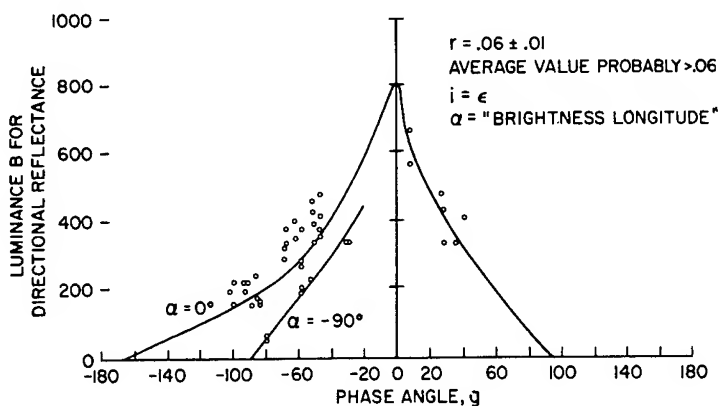


Figure 2-11

Lunar Reflectance Values

The Open Circles Are the Data Obtained from Preliminary Analysis of Surveyor I Data. The Solid Lunar Curve is the Federeetz Curve Obtained from Telescopic Observations from the Earth

(From Preliminary USGS/JPL Data^(12,227,410))

It thus appears that brighter areas may have an apparent luminance in excess of 1000 ft-L (410). Owing to the lack of atmospheric scattering, it may be expected that the deepest shadows will approach effectively zero luminance (10^{-6} ft-L or less). Without sun, illumination levels are likely

to be in the neighborhood of 10 ft-C for full Earth conditions, with a resulting maximum luminance of something over 1 ft-L, but decreasing markedly with Earth phase angle. Starshine alone is estimated to produce about 3×10^{-5} ft-C, and, unlike Earth and Sun, of a diffuse rather than unidirectional nature, so that a general average luminance might approach 10^{-5} ft-L without the severe shadow-casting effects just noted. Absence of atmospheric haze on the lunar surface may be considered in visual range determinations, although dust may be a factor (132, 144, 353).

In the vicinity of the spacecraft in orbit or on the lunar or planetary surface, the "spacecraft corona effect" must be included in the light path (319). This results from a cloud of particles traveling with the spacecraft. The surface brightness of the corona, in sunlight, has been computed as a function of the mass ejection rate of particulate matter from the spacecraft (Figure 2-12). This may have contributed to the inability of the astronauts to see stars previously predicted as visible (see Figure 2-9 and discussion).

Recommendations for dim light photography, photographic tracking, and visual observations of space phenomena from manned spacecraft are available (120, 127).

Visual Performance and Visibility

The interactions of the visible light environment with the eye should be considered as a dynamic and continuously changing process. The dynamism of this operation applies to every situation - to a change in the environment, in the sense organ, or in both. It is very important to consider all psychophysiological cues that will optimize visual function (462).

An excellent detailed review of physiological optics has recently been published and is recommended for definitive data on the more esoteric aspects of this subject (177).

The determination of visibility in any environment requires basic information of human visual performance. Much of the basic data to be presented were determined as special test cases with circular targets of known position in a uniformly luminous background using binocular vision. To such data must be added case-specific variables of luminous environment, unknown location, movement, variable duration of viewing, environmental stress, and psychological factors to permit accurate estimation of visibility in field or space conditions. Many of these variables have been covered in a recent review of visibility (132).

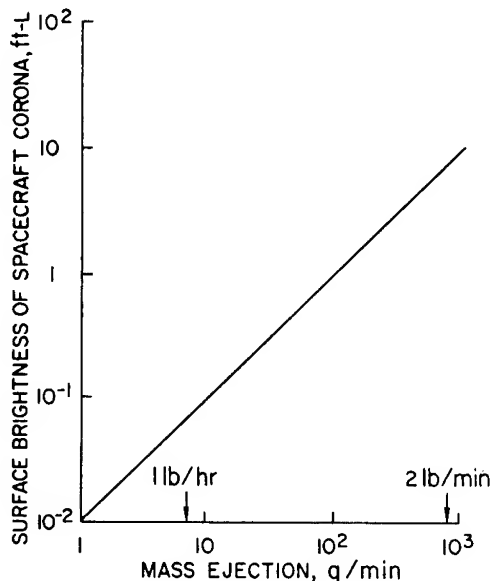


Figure 2-12

Surface Brightness of Spacecraft Corona Versus Mass Ejection Rate in Space.

(After Ney and Huch (319))

Table 2-13 summarizes some of the major physiological and physical factors which determine visual performance. In the present discussion, these variables will be covered in their more general aspects. In section 3, those conditions sensitive to specific aspects of space operations will be selected for discussion.

Table 2-13
**Variables That Must Be Kept Constant or Carefully Controlled
 When Measuring Some of the Principal Kinds of Visual Performance**

Type of Visual Performance	Variables to Be Controlled												
	Level of Illumination	Region of Retina Stimulated	Stimulus Size	Stimulus Color	Contrast Between Test Object and Background	Adaptive State of the Eye	Duration of Exposure	Distance at Which Measured	Number of Cues Available	Movement	Other Objects in Field	Monocular vs. Binocular	Stimulus Shape
Visual Acuity	X	X	(MV)*	X	X	X	X	X	X	X	X	X	X
Depth Discrimination	X		X	X	X	X	X	X	X	X	X	X	
Movement Discrimination	X	X	X	X	X	X	X	X	(MV)*	X			X
Flicker Discrimination	X	X	X	X	X	X	X						X
Brightness Discrimination	X	X	X	X	(MV)*	X	X			X		X	X
Brightness Sensitivity		X	X	X	(MV)*	X	X			X			X
Color Discrimination	X	X	X	(MV)*	X	X	X	X	X	X			

* Variable being measured

(After Wulfeck et al⁽⁴⁶²⁾)

Visual Acuity

Visual acuity is an important limiting factor in all human detection, target recognition, or other visual tasks. Acuity, like many other visual capacities, is measured and defined in terms of thresholds. One type of visual threshold is a value determined statistically at which there is a 50% probability of the target being seen. In most practical situations a higher probability of seeing, such as 95 or 100% is required. The general relation between threshold size and probability of detection is an ogive function of the general simplified form shown in Figure 2-14. This curve covers a specific test case and should be used only as a very rough guide for estimating the relationship between visual angle and probability of detection under different conditions. It can be seen that doubling the visual angle for 50% probability of detection should give almost 100% detection if the location of the object is known. Threshold data are usually based on the 50% probability of detection. As a rough rule of thumb, these visual angle values should be doubled to give near 100% threshold values. More specific conversion factors for near 100% probabilities are available (52).

There are several ways in which visual acuity has been defined and measured, each of which has significance for detection and recognition of detail. These are defined in Figure 2-15.

The luminance contrast between target and background determines the minimum visual angle which can be detected. Luminance contrast is a measure of how much target luminance (B_t) differs from background luminance (B_b). The equation for obtaining contrast is:

$$C_B = \frac{B_b - B_t}{B_b} \text{ and } C_B = \frac{B_t - B_b}{B_b} \text{ or } C_B \times 100 = \% C_B \quad (1)$$

Contrast can vary from zero to minus one for targets darker than their backgrounds, and from zero to infinity for targets brighter than their backgrounds. Most studies of this aspect of vision consider targets brighter than their backgrounds.

Relation between target size and background luminance for targets of various contrasts is shown in Figures 2-16 and 2-17.

Thresholds in Figure 2-16 are at the 50% probability of detection. By multiplying the values by 2 (log 0.3), the values may be converted to about the 95% probability of detection. The graph shows that a reduction in any one factor — background luminance, size, or contrast — may be compensated for by an increase in one or more of the others. The relation between minimum separable acuity and background luminance of Figure 2-15 is nearly reproduced for the 100% contrast curve in this graph. The chief effect of reducing contrast is a shift of the curve upward in the direction of increased target size for 50% probability of resolving parts of a target. The family of curves also shows the discontinuity at about 0.0003 mL that marks the transition from rod to cone vision.

Figure 2-17 presents similar data for luminance contrast thresholds. Variations in luminance contrast threshold ($\Delta B/B$, where B is luminance) are shown as functions of background luminance and target size. (Pupil diameter is shown as it varies with background luminance.) Two relationships are shown very clearly by this graph: When it gets darker, objects must be a lot blacker or lighter than their background to be seen; and, at any level of luminance, small objects must have more contrast in order to be seen than large objects. In Figures 2-16 and 2-17, the subjects knew where the target would appear on the background and exposure duration varied from case to case. The times were empirically determined so that, when doubled, they did not yield a lower value of threshold contrast.

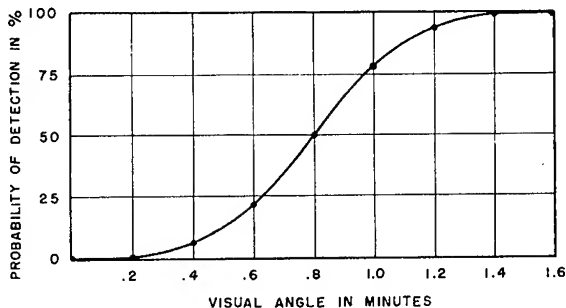
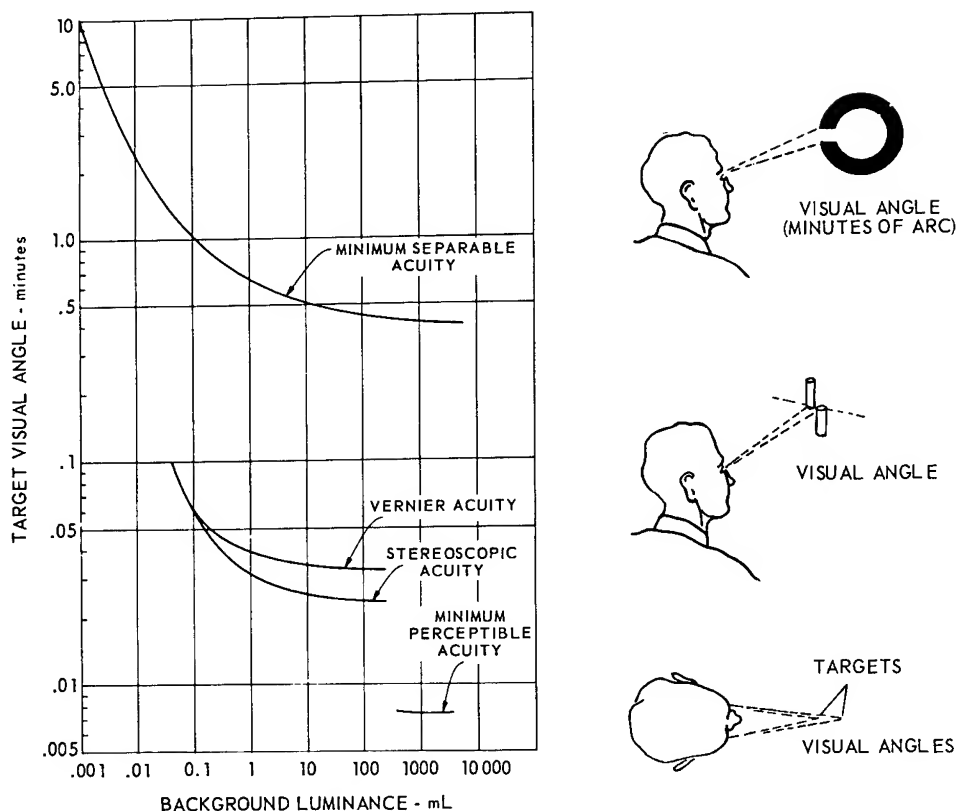


Figure 2-14

An Example of Probability of Detection at Different Visual Angles for a Specific Test Case.
(After Baker and Grether^(2b) Adapted from Blackwell⁽⁴⁹⁾)



Variations in spatial acuity with background luminance for high contrast targets, considering the natural pupil and binocular vision. Minimum separable acuity defines the smallest space the eye can see between parts of a target. The relationship shown is for a black Landolt-ring on a white background. For white targets on black backgrounds, the relationship between acuity and luminance holds up to about 10 mL, above which acuity decreases because the white parts of the display blur. Vernier acuity is the minimum lateral displacement necessary for two portions of a line to be perceived as discontinuous. The thickness of the lines is of little importance. Stereoscopic acuity defines the just perceptible difference in binocular parallax of two objects or points. Parallactic angle is one of the cues used in judging depth. Beyond 2500 feet, one eye does as well as two for perceiving depth. Minimum perceptible acuity refers to the eye's ability to see small objects against a plain background. It is commonly tested with fine black wires or small spots (either darker or lighter) against illuminated backgrounds. For all practical purposes, these numbers represent the limits of visual acuity. Another type of acuity, not shown in the graph, is minimum visible acuity. This term refers to the detection by the eye of targets that affect the eye only in proportion to target intensity. There is no lower size limit for targets of this kind. For instance, the giant red star Aldebaran (magnitude 1) can be seen even though it subtends an angle of 0.0003 minutes (0.056 sec) of arc at the eye. (The conditions under which these data were obtained were nearly optimal for a given level of illumination. Changes in contrast, retinal location, rapid changes in illumination, and vibration would decrease the resolution capabilities of the eye.)

Figure 2-15

Variation in Visual Acuity with Background Luminance

(Vernier and Stereoscopic Acuity Data from Berry⁽³⁶⁾; Minimum Perceptible Acuity Data from Hecht et al.⁽²¹²⁾; Minimum Separable Acuity Curve after Moon and Spencer⁽³⁰²⁾ Adapted by White⁽⁴⁴⁶⁾)

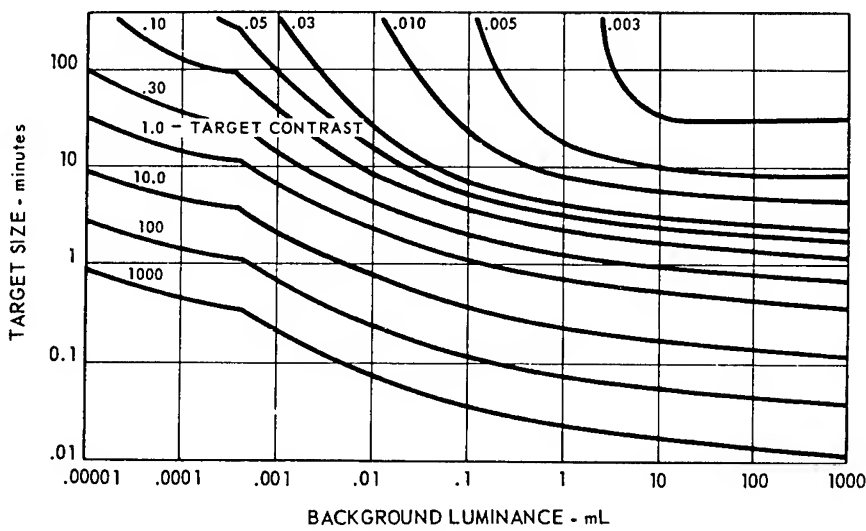


Figure 2-16

Relation Between Target Size, Threshold Background Luminance, and Contrast
(After Blackwell⁽⁴⁷⁾)

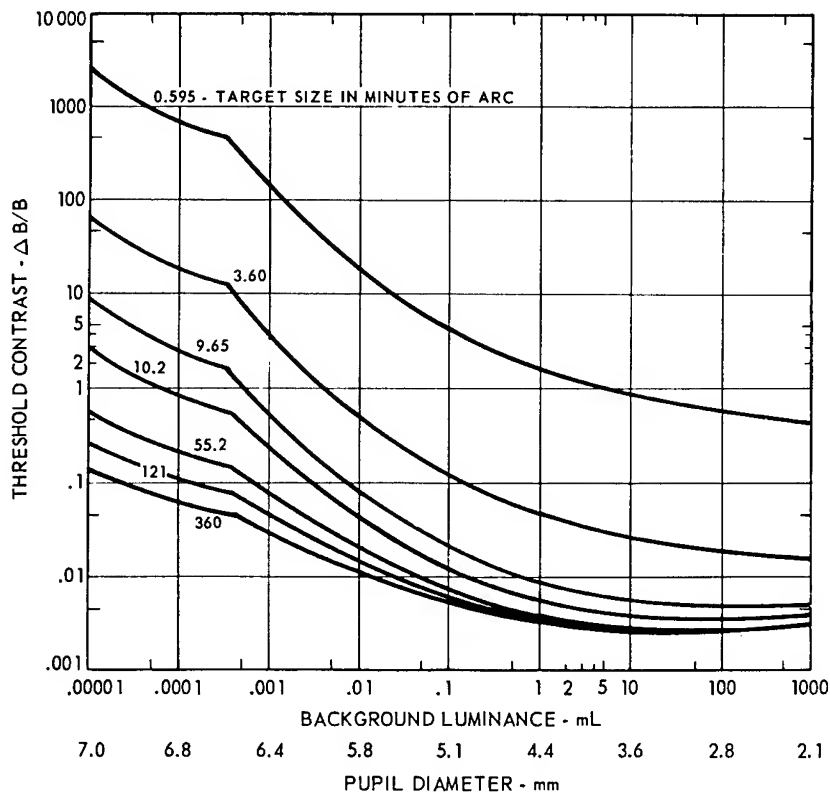


Figure 2-17

Contrast Thresholds for Different Target Sizes, Background Luminance, and Pupil Diameter at Each Level
(After Blackwell⁽⁴⁷⁾)

Point sources of light are defined by Ricco's law as those in which the product of threshold contrast and solid angle subtended by target are constant. Figure 2-18 represents the maximum visual angle satisfying the point source criterion at different luminance levels. Figure 2-9 presents the threshold illuminance and stellar magnitude at different background luminance levels. Figure 2-55 gives retinal image sizes for point sources at different pupillary diameters.

Increasing the size of light sources will increase their effective brightness and visibility. Figure 2-19 shows the minimum visual angle a light source can subtend at the eye and still be seen at different luminance levels of the source.

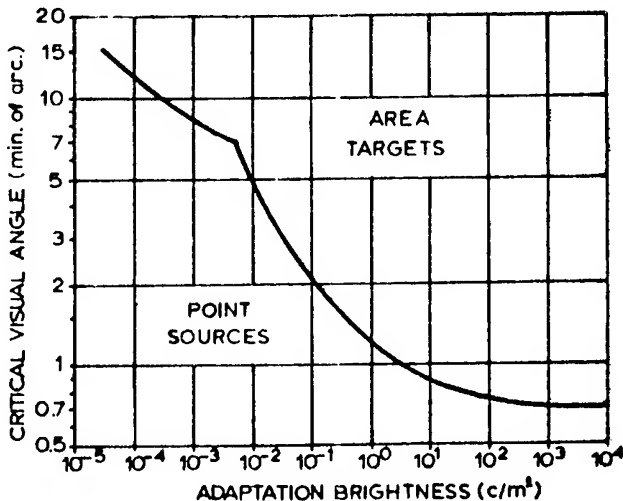


Figure 2-18

Critical Visual Angle for Point Sources Versus Area Targets.

(Adapted from Blackwell⁽⁴⁷⁾ by Seyb⁽³⁸⁰⁾)

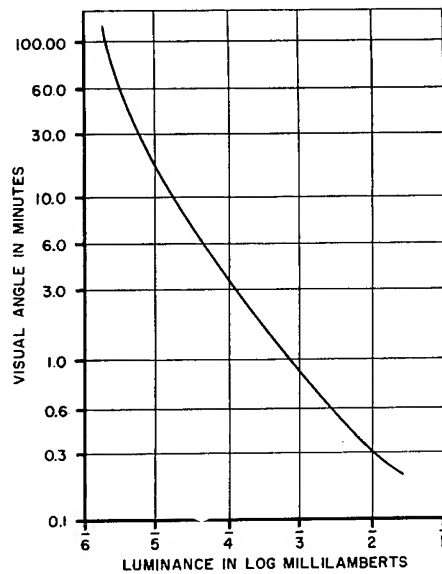


Figure 2-19

Minimum Visual Angle of a Light Source Versus Source Luminance.

(After Wulfeck⁽⁴⁶²⁾ Adapted from Data of Lash and Prideaux⁽²⁵⁹⁾)

For spacecraft and their markings, the target may not be circular but rectangular. When dark bars are seen on a brighter background, minimum separation between bars can be determined for specific background illumination and contrast conditions. This is shown in Figure 2-20.

There is a distinct difference between resolution of bright bar figures on a dark background and dark bars on a bright background. Figure 2-21 shows these differences as a function of retinal illuminance while observing the bars. The measure of visual acuity is the smallest distance two bars can be separated and still be seen as separate. As the illumination of the retina increases beyond about 3.2 photons (0.5 log units), the ability of the eye to discriminate between the bars begins to get worse instead of better. In other words, reflecting bars by day and luminous bars by night must be bright enough but not too bright. (For pupils of 2mm diameter, 10 photons = 1 mL.)

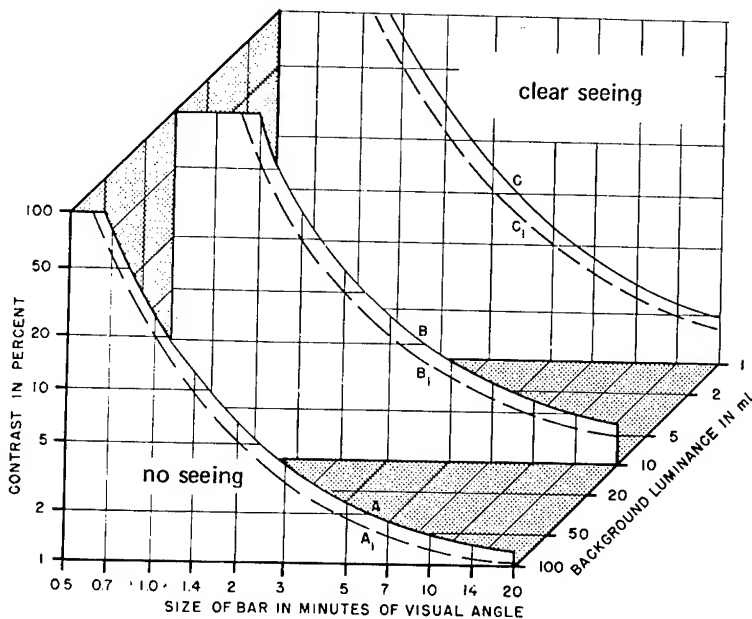


Figure 2-20

Background Luminance and Contrast Required for Bars Subtending Various Angles to be Seen Under Daylight Conditions.

(After Cobb and Moss⁽¹⁰⁰⁾)

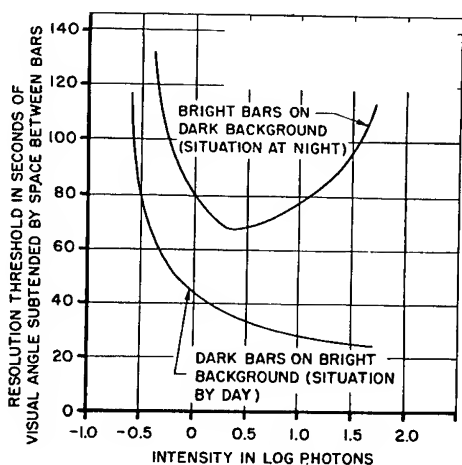


Figure 2-21

Ability to Discriminate Bright Bars Against Dark Background

(After Wilcox⁽⁴⁵¹⁾)

Figure 2-22 shows the effect of area of rectangular stimulus on threshold contrast $\Delta B/B$ for 5 ratios of length to width of rectangles. For large areas, threshold contrast for fixed area decreases as shape approaches a square. When area exceeds 100 min^2 , shape again becomes unimportant. The visibility of objects in fields of high brightness is also strongly dependent on the shape factor (212). A thin wire one degree long may be seen silhouetted against a sky of high brightness of about 4000 ft Lamberts if its diameter were only $1/2$ second of visual angle. Silhouetted squares must be 18 seconds long. Square objects, however, are more efficiently seen. To be seen with the same certainty, squares may be less than three times the area of line stimuli. Filters will have different relative effects on visibility of objects of different shape under the same background illuminance (212).

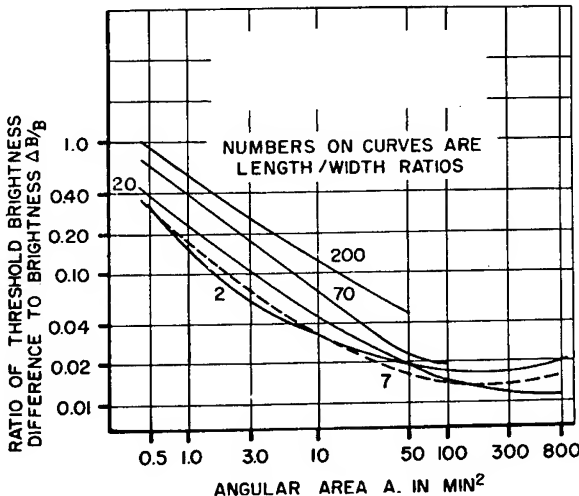


Figure 2-22

Contrast Threshold as a Function of Shape of the Stimulus

(Adapted by Wulfeck et al⁽⁴⁶²⁾ from Lamar et al⁽²⁵⁶⁾)

In the inspection of satellites at relatively close distances, the detection of critical detail may be important. Typical detection problems are seen in Figures 2-23a and 2-23b giving visual acuity limits for targets either brighter or darker than the background for different background luminance conditions. These curves permit prediction of visual acuity for discrimination of the shape of targets of known luminance on a background of known luminance, to luminance which the human eye is adapted (17, 371). The visual acuities correspond to the visual angles subtended by the critical detail which was needed for distinction of a square from a circle of equal area, when varying sizes.

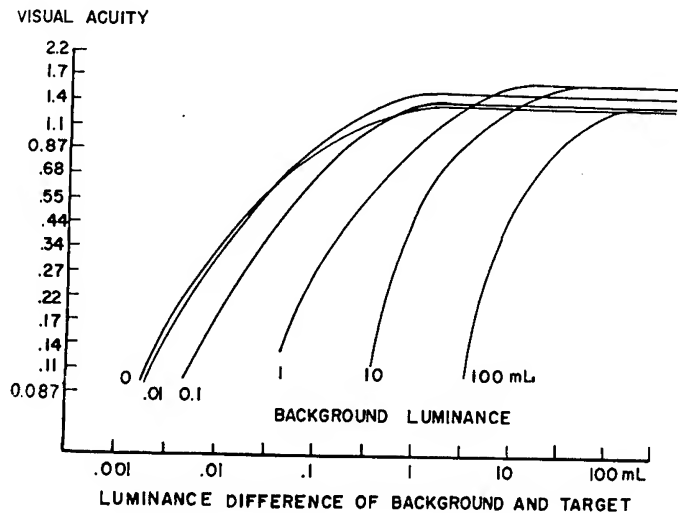
Secondary factors often play a key role in visual tasks. Subjective sharpness of the contour border between two areas of sharply different contrast may be important in determining detail of objects under space conditions (362). Similar problems of contour sharpness are present in near vision requiring accommodation (109) and at the retinal periphery (45).

In low levels of illuminance, scotopic sensitivity shows many interesting irregularities (107, 361). Color perception is especially affected as will be discussed below.

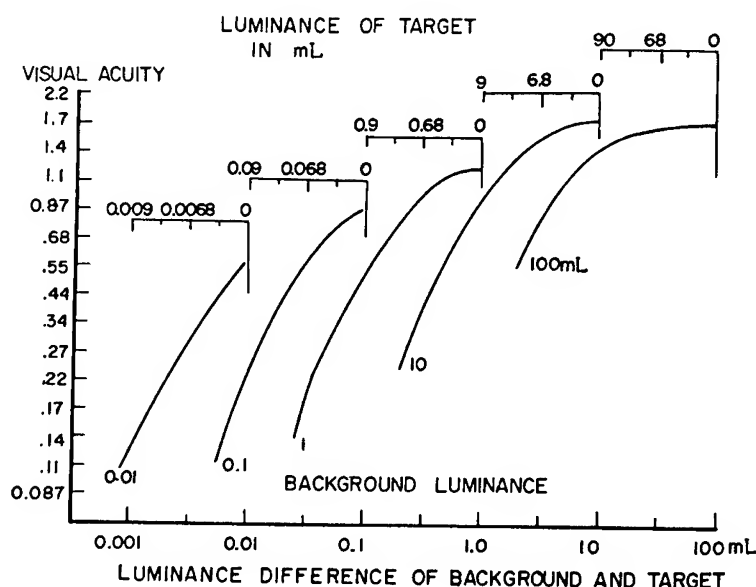
The judgment of relative brightness of several objects is a complex task which has received much study (359).

The position of target on retina as a factor in determination of visibility is seen in Figure 2-24. Figure 2-24a shows a visual acuity curve for discriminating objects at 0° , 4° , and 30° away from visual axis on retina. The advantage of foveal vision decreases with the background luminance levels. At about .001 ft L all parts of the visual field are equisensitive. Data are avail-

Figure 2-23
 Visual Acuity for Detecting Shape of Targets
 (After Schmidt⁽³⁷¹⁾ Adapted from Aulhorn⁽¹⁷⁾)



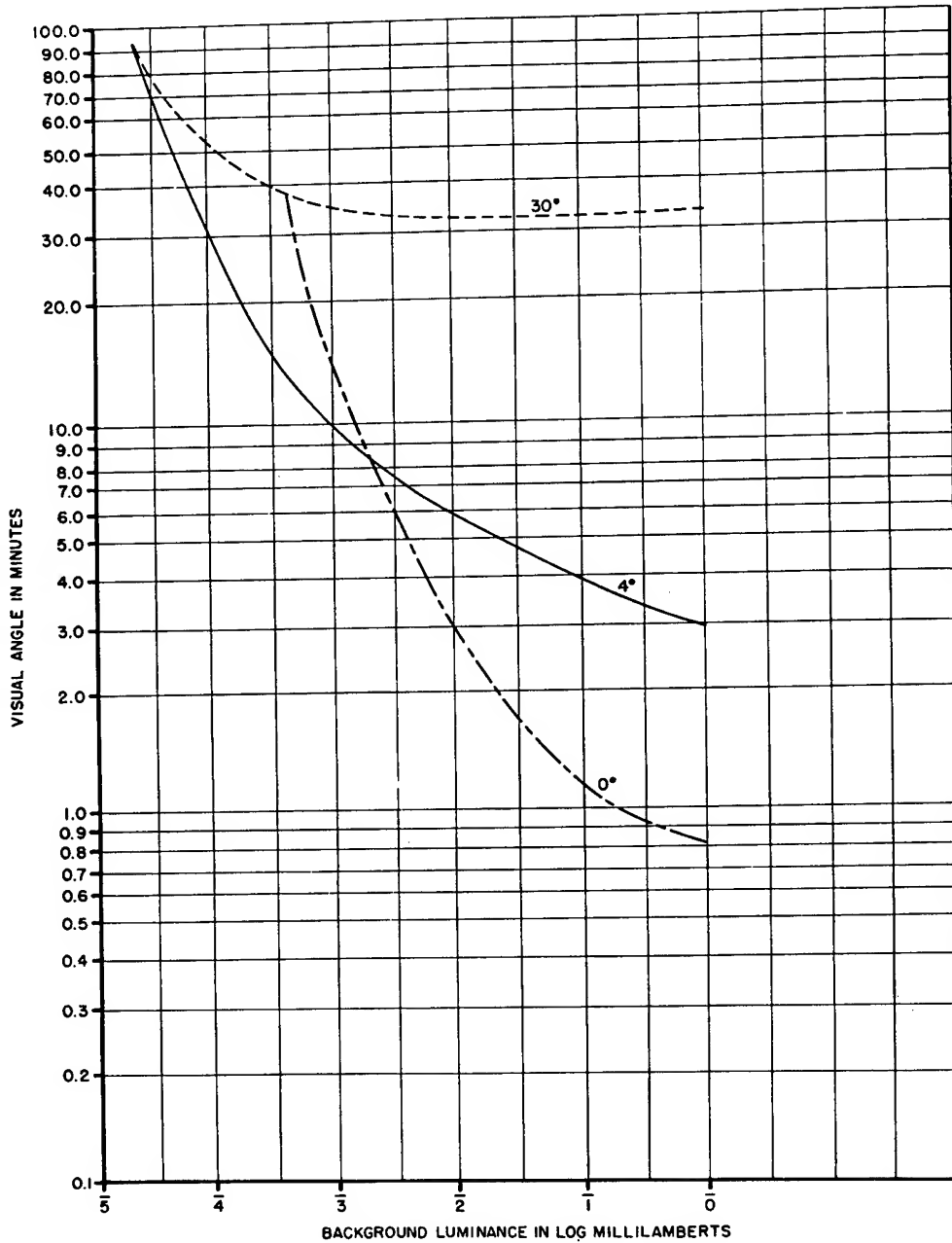
a. Brighter than Background



b. Darker than Background

(See text for definition of Acuity)

Figure 2-24
Position of Target on Retina as a Factor in Visibility



- a. Visual Acuity Curves at Different Angles Away from the Visual Axis on the Retina as a Function of Background Illuminance.

(After Wulfeck et al⁽⁴⁶²⁾ Adapted from Mandelbaum and Rowland⁽²⁸⁵⁾)

able on contrast thresholds as a function of retinal position and target size during brief target exposure (407).

Figure 2-24b shows the relative photopic acuity at a fixed level of background illuminance for different angular positions from the visual axis. The blind spot is the site of the optic disc and nerve. Such values must be considered when determining objects not directly along the visual axis.

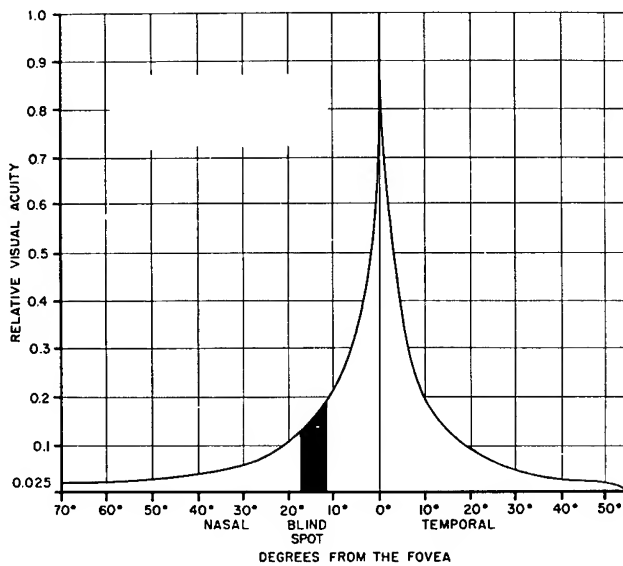


Figure 2-24b
Relative Visual Acuity at Different Angles from the Fovea
for Photopic Vision.

(After Wulfeck et al⁽⁴⁶²⁾ Adapted from Wertheim⁽⁴³⁹⁾)

The Stiles-Crawford effect is a factor which relates to the design of optical aids (397). A given increase in pupillary area is accompanied by a smaller proportional increase in the effectiveness of the light for vision. A marginal ray is generally less effective as a stimulus for vision than a ray that reaches the same point on the retina by passing through the center of the pupil. The relative luminous efficiencies of rays entering the pupil at various points away from center are shown in Figure 2-25. Marginal rays are sometimes less than one-third as effective as are central rays. Control experiments have shown that all the rays reach the retinal surface with nearly equal intensity; hence the disproportionately low efficiency of the marginal rays is a consequence of their direction of incidence on the receptors (178).

The rods do not manifest the Stiles-Crawford effect as do the cones. Hence, it is possible to appraise the effectiveness of dim lights for the dark-adapted eye in proportion to the pupillary area prevailing at the time the observations are made. The practical consequence of the Stiles-Crawford

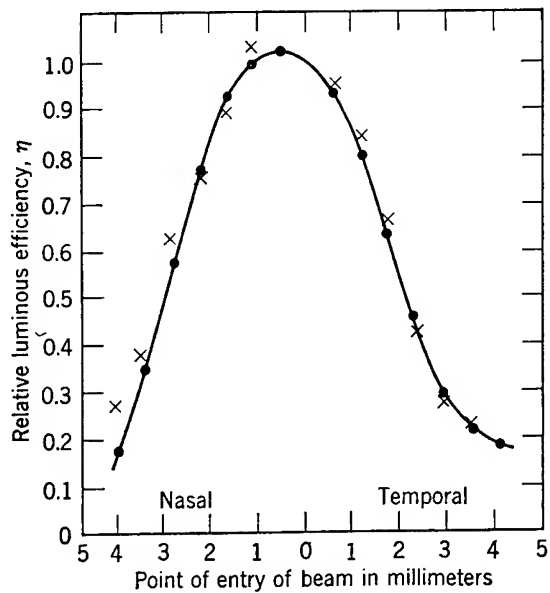


Figure 2-25

The Relative Luminous Efficiency of Light Entering the Pupil at Various Points in a Horizontal Plane Through the Center of the Eye.

Subject BHC: x left eye, ● right eye.

In this figure, η is expressed as the ratio between the intensity of a central ray and that of a marginal ray, the two having been adjusted to produce equal brightness as shown by the fact that no flicker occurs with temporal alternation of stimuli.

(After Stiles and Crawford⁽³⁹⁷⁾)

effect is that retinal illuminance per se cannot be taken as an appropriate indication of the effectiveness of visual stimulation. Thus, the troland is a unit of equivocal significance for vision at ordinary photopic levels of luminance. Nevertheless, it is a useful measure for many circumstances. Both pupil size and luminance should be clearly specified for a given situation, and under these conditions one may speak of the product in terms of trolands uncorrected for Stiles-Crawford effect. (See Table 2-2.)

Optical Aberrations of the Eye

A detailed analysis of the optical aberrations of the human eye is beyond the scope of this presentation. Data on the clinical aspects of the problem are available (1, 126, 178). The following discussion summarizes the problems from the point of view of the designer of optical equipment (178).

The surfaces of the cornea and lens are not perfectly spherical, and the optical density of the lens varies from one point to another. Furthermore, changes in accommodation produce changes in the surfaces of the lens, with corresponding changes in the aberrations of the system. (147, 226). Aberrations are greatest in the periphery of the cornea and the lens. Pupillary constriction thus improves the quality of the image formed on the retina by excluding light that passes through the peripheral portions of the cornea and the lens. Thus, problems of spherical aberration are greatest when the pupil is larger or the fired luminance is low.

The effects of "night myopia" have been attributed by some mainly to spherical aberration,(251) although others have attributed this phenomenon mainly to accommodative effects (330).

For all small pupil diameters (i.e., less than 2.5 mm, or perhaps 4 mm in individual cases) the effects of spherical aberration may be negligible by comparison with those of diffraction (80, 178).

One may conclude that spherical aberration probably does not have an important influence on measurements of visual acuity at moderate to high intensity levels for the normal eye. It may, however, be a significant factor in night vision, where pupillary apertures are large enough to bring in significant blurring by aberration effects on the marginal rays.

Chromatic aberration is another problem, especially in the viewing of angularly small objects (117, 147, 178, 203, 204, 225, 433). Here the seriousness of the effect on acuity is largely a function of the wavelength distribution of the light used for viewing the test object.

For all low to moderate levels of intensity, acuity is better when sodium or mercury vapor lamps were employed rather than tungsten incandescent lamps (373). At the levels of intensity above 4000 meter-candles, however, the various illuminants were all found to yield similar acuity scores. Monochromatic blue light yields poor acuity values, and light from the red end of the spectrum, while not so bad as blue, is definitely inferior to green or yellow for best acuity. These matters are further complicated by the influence of accommodation, which appears to be most strongly activated by yellow light and less so by lights of other hues (434). The macular pigment absorbs a relatively large proportion of the blue light that would otherwise affect the retina. This has been interpreted to mean that the macular pigment serves as a filter that, among other things, acts to reduce the chromatic aberration of the eye for any white light that contains considerable amounts of blue light.

Errors of diffraction are usually more significant than errors of chromatic or spherical aberration (117, 126, 178). The fairly constant level of visual activity in the range of pupil diameters from 2.5 to 5 mm probably represents a balance between the reduction in diffraction and the increase in optical aberrations. The testing and correction of refractive error of the eye is well covered by many textbooks of ophthalmology (117, 126). Enhancement of night vision depends heavily on correction of aberrations resulting from dilated pupils (343).

Search and Visibility

Much study has gone into visual search techniques and strategy with variable target and ambient conditions (43, 46, 50, 53, 77, 92, 167, 168, 169, 170, 171, 172, 173, 174, 201). Recent reviews are available on visual detection of targets in search (132, 141, 151, 305, 407).

Optimization of search strategy involves the concept of the visual detection lobe (132, 209). Recent work has covered eye movements in search (108, 143, 377, 453, 454, 456, 463), critical visual variables in the early period of search (428, 429), and search time as a function of visual acuity of the observer (140, 235). The dwell time in typical detection task is the time the eyes remain stationary between fixations and approaches a value of

1/3 of a second (441). For discrimination tasks, the value may increase up to one second or more (159). The stimulus duration is therefore a key variable in search strategy and visibility predictions (see Figures 2-33 and 2-34).

If one does not eliminate the assumed integrating effects of the 30 to 50 per second components of the normal oscillatory movements, it has been shown that contrast threshold values depend primarily on the target size and position. The probability of detecting a target of particular size and location is ultimately determined by the number and kind of retinal elements and their momentary threshold; receptor interconnections; the frequency and angular extent of eye movements; and the duration of target (407). Visual response in the field condition must therefore be converted from basic laboratory data often representing optimum conditions. Probability functions can be determined from contrast thresholds at $P = 0.5$ for other probabilities (52). Many of the field variables can be roughly quantitated.

Figure 2-26 gives multiplication factors to be used in roughly correcting for visual accuracy and speed during non-standard visual tasks. Figure 2-26a suggests the amount that illumination must be increased to obtain increased accuracy of vision. These data on visual task performance as a function of other factors (speed, acceleration, etc.) have been based on 50% reading accuracy. The multiplying factor was determined by evaluating data on reading instruments and on identifying the area occupied by a target (382). Since the shape of the curve is influenced by contrast, adaptation of the eye, acuity, speed of vision, and task difficulty, this curve must be used only as a rough estimate of error reduction.

Figure 2-26b suggests the amount that illumination must be increased to obtain increased speed of vision. The speed of vision is expressed in discriminations per second with discrimination task being the identification of the opening in a Landolt ring (capital letter C). The determination of the number of discriminations per second involved in a given task would be based on a correlation between the time to do this task and the time to identify C openings with all conditions being identical.

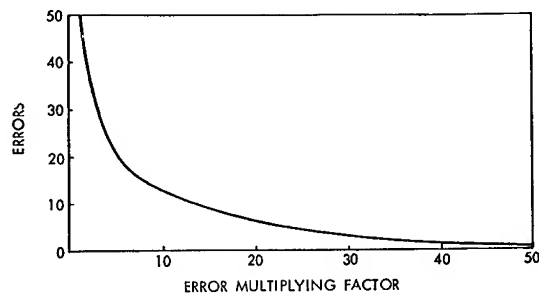
Figure 2-26c suggests multiplication factors for contrast thresholds (Figures 2-16, 2-17, 2-20, 2-23) when inadequate knowledge is available regarding various target properties (48, 49, 52, 132). They have been obtained from relatively few experiments and should be used with caution.

Vigilance is a key factor in search for targets which occur infrequently. Data on the visual aspects of vigilance are available (137, 233). Several models of vigilance have been proposed recently (72, 81, 233, 282, 374, 403) and current studies are being directed to fitting visual search problems to these models (232, 270, 299). Visual alertness may be estimated from electroencephalographic data (34). The effect of simultaneous auditory noise and other extraneous stimuli on vigilance is also under study (71, 188, 202, 437, 467).

For general use, a contrast correction factor of 1.19 for vigilance alone has been recommended (30). This factor is probably satisfactory when the

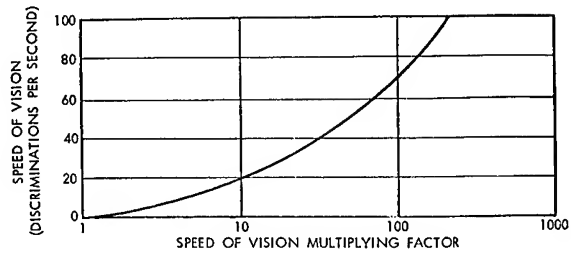
Figure 2-26

Correction Factors for Visual Accuracy and Speed in Search Operations



- a. Illumination Increase Required to Reduce Error in Vision

(After Shearer and Downey⁽³⁸²⁾)



- b. Illumination Increase Required to Heighten Speed of Vision

(After Shearer and Downey⁽³⁸²⁾)

Target Properties					Correction Factor (↓)
Location ±4° or more	Time of occurrence	Size (3 used)	Duration (3 used)		
+	+	+	+	1.00	
+	-	+	+	1.40	
+	-	+	-	1.60	
+	-	-	+	1.50	
+	-	-	-	1.45	
-	+	+	+	1.31	

+, knowledge; -, lack of knowledge

- c. Contrast Correction Factors to be Applied When Observer Is Deprived of Knowledge of Various Target Properties.

(Adapted from Blackwell^(48, 49) by Duntley⁽¹³²⁾)

stimuli occur randomly and with an average frequency of 1 or 2 in 20 min, higher occurrence rates requiring less correction.

Trained observers perform better than inexperienced ones, and the magnitude and time course of practice effects are greater for more complex visibility tasks. A recent study indicates the character of the practice effects found in a simple laboratory detection experiment, and shows that a correction factor of 1.90 in contrast will compensate for the difference between trained and naive observers (311). This value is in excellent agreement with the factor reported of 2.00 for a different data collection method (32). All of these contrast multiplication factors are sequentially applied in determining the contrast needed for a given probability of detection.

Final target acquisition times are very sensitive to specific visual functions in question (356). In a complex task each factor must be considered individually and in interaction before adequate predictions can be made. Many of the more clear-cut personal and environmental influences will be discussed below.

Determination of visual range for a high probability of detection within the Earth's atmosphere is a complex calculation (132, 252, 293). Figures

2-27a and 2-27b represent graphs permitting range estimates in daylight and starlight within the Earth's atmosphere. Similar graphs are available for other lighting conditions (133). Sighting ranges have also been calculated for night and twilight light operations under field conditions (380). For stationary targets, the sighting range is practically the same as maximum detection range; for moving and approaching targets, the sighting range can be considered the upper limit of the maximum detection range. Visual detection lobe theory has been recently applied to air to ground observations and range calculations (209).

The strategy and optimization of search for objects at sea has received extensive review (252). Data are also available for visibility under the sea (134, 245, 246), under white-out conditions (243), and in jungle terrain (123).

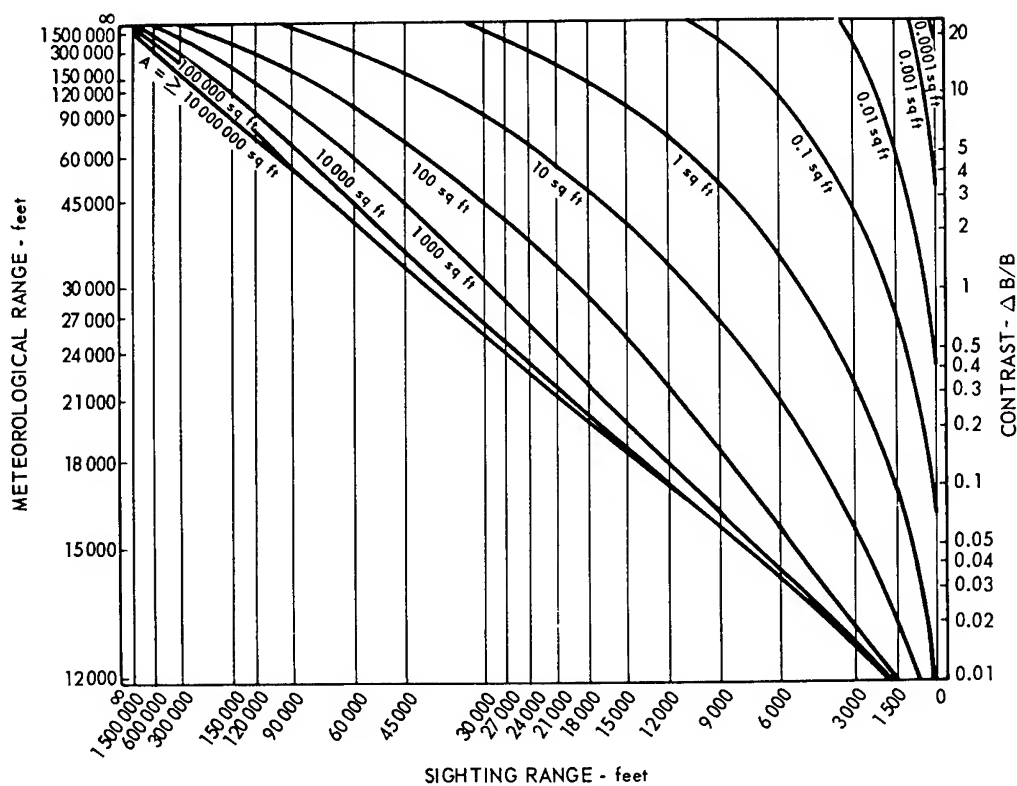
Color

Color is an important factor in the design of cockpit displays and in optimization of visual detection and identification (25). Figure 2-28 shows the eye is twice as sensitive to a yellow-green of $550 \text{ m}\mu$, as it is to a blue of $450 \text{ m}\mu$, and many times more sensitive to a yellow-green than to violet and red, at the ends of the visible spectrum. The situation is further complicated by differences in the responses of individuals (177). Spectral sensitivity curves are a function of the level of illumination, in that the relative function of rods and cones are dependent on this factor.

Visual Acuity as a Function of the Color of Illuminant

The color of the illuminant can be controlled either at the light source or by filters between the source and the observer's eyes. Both methods give the same effect. Colored illuminants cause the loss or reduction of color contrast and the distortion of the normal luminance relations. Objects of the same color as the illuminant will be relatively increased in luminance and may become invisible against a light background. Objects of complementary color will be darkened and may be invisible against a dark background. This effect can be used to advantage in some highly specific applications. In most cases this distortion of normal brightness and color relationships is a serious handicap, and greatly reduces the total information which can be resolved by the eye.

Experimental findings concerning visual acuity and color of the illuminant have been somewhat contradictory (26, 146). When there is a large luminance contrast between test object and background, visual acuity varies only slightly with wavelength and is generally best near the middle of the visible spectrum, if all test objects are of equal luminance. Reducing the luminance contrast between test object and background degrades acuity similarly at all wavelengths so there is little, if any, interaction between wavelength and contrast (89). Visual acuity with red and blue backgrounds of different luminance is shown in Figure 2-29. (See also chromatic aberration.)



This graph shows the sighting range (distance in feet) of targets viewed against the sky, background luminance 1000 mL (full daylight) at probability of detection of 95%. Meteorological range is the distance at which apparent brightness contrast is reduced by atmospheric scatter to 2% of inherent contrast between the object and sky. Contrast is the ratio of the luminance difference between target and background and the luminance of the background ($\Delta B/B$).

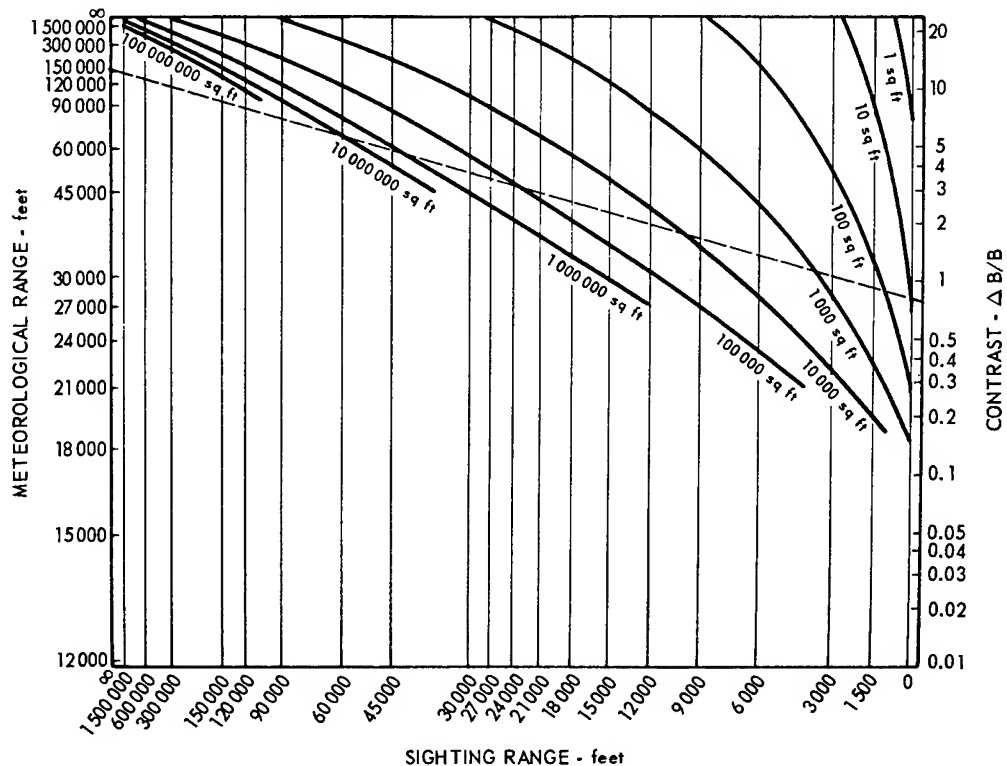
A straight line connecting meteorological range and contrast will intersect a family of curves for various target sizes, which are shown as areas (A) in square feet. The visual range is obtained by projecting up or down to the range scale. By selecting meteorological range at its infinity point, the graph may be used to find threefold contrast for any object of a given size at any assigned distance.

The graph does not apply to long narrow targets, but does apply to targets that are not very out-of-round.

Figure 2-27a

Visual Range in Natural Light - Daylight

(After Middleton⁽²⁹³⁾ Adapted from Duntley⁽¹³³⁾)



This graph shows the sighting range of circular targets against the sky with a background luminance 0.0001 mL (starlight). The following is an example of the use of the nomogram: Find the range that an object 100 sq ft in area could be seen in starlight when the meteorological range is 150,000 feet and the contrast of the object and sky is 0.8. A straight line across meets the given range and contrast. The range is read off where the line intersects the 100 sq ft curve. Under these conditions a 100 sq ft target will be sighted with a probability of 95% at 1200 feet.

Figure 2-27b

Visual Range in Natural Light - Starlight

(After Middleton⁽²⁹³⁾ Adapted from Duntley⁽¹³³⁾)

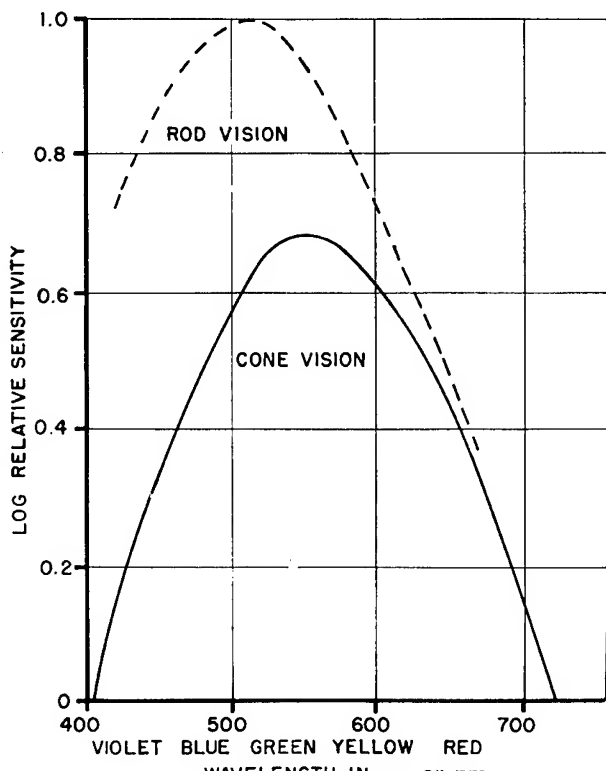


Figure 2-28

Standard Luminosity Curves: Relative Sensitivity to Radiant Flux as a Function of Wavelength

(After Hecht and Williams⁽²¹³⁾)

The extent to which acuity can be improved depends upon the particular colors used. The highest color contrast possible produces visual acuity which is equivalent to the acuity produced by a brightness contrast of 35% (135). However, acuity is increased much more by increasing brightness contrast than by increasing color contrast.

There is a frequent need to see and to identify objects on the basis of the color of the objects' surfaces. One major consideration is the ability with which the object may be seen against its background. Since detectability is increased when color and brightness contrast between the object and the background are increased, such objects as life rafts, parachutes, survival tents, path markers, and other such objects should have carefully chosen colors and brightness. Generally speaking, orange (International Orange) is seen best at great distances. Detectability can be further increased by addition of fluorescence which increases brightness and contrast. The unnaturalness of these colors also results in heightened conspicuity (406). Fluorescent orange, neon red, and red are recommended for survival equipment that must be seen at great distances. However, if the background is predominantly orange, red, or brown, objects should be green for maximum detectability. Against blue-green foliage or water, orange, red, or neon red of high brightness are best.

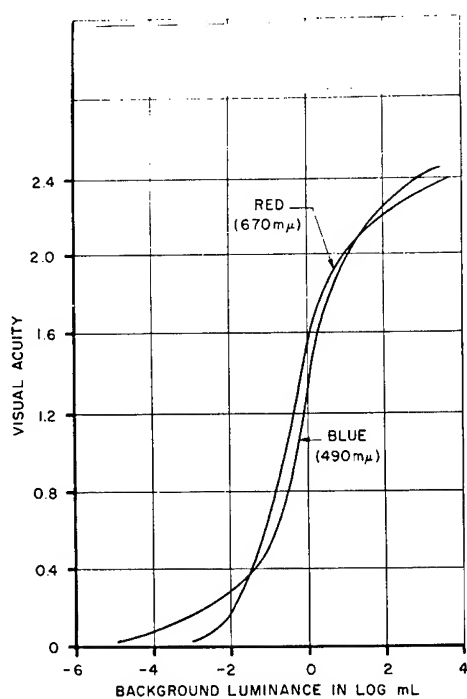


Figure 2-29

Visual Acuity as a Function of Color of Illumination

(After Chapanis⁽⁹³⁾ Adapted from Schlaer et al⁽³⁸⁴⁾)

Color Recognition Thresholds

Signal lights used in air and marine navigation are viewed at great distances. The visual angles subtended by such sources are small and can be considered as points sources of light. The recognition of a signal light color depends upon (1) the intensity of the light source, (2) the brightness of the background, and (3) the particular colors observed. Figure 2-30 shows the illumination at the eye of a point source signal light that will be correctly identified 90% of the time for various colors viewed against various neutral background brightnesses. It indicates that yellow signal lights require the greatest intensity. This study also revealed that red and green signal lights were rarely interchanged, that is, red was rarely called green and green was rarely called red. On the other hand the yellow light was frequently confused with red. The confusion of color determination at threshold has been recently reviewed (149, 357, 435).

These data apply to situations where the observer knows the location of the signal. In actual situations the observer usually knows only the general direction of a signal light. For such situations the threshold recognition values should be doubled (48, 164, 177). The signals can be seen at lower intensities than shown on the graph, but the colors may not be identified correctly. Intermittency of color flashes is also a factor to be considered (435).

Color Specification

Color may be considered as having three psychological components: hue, saturation, and brightness. Most systems of color specification make use of these three concepts in one form or another.

Hue is the aspect of color commonly denoted by such names as red, yellow, green, blue, orange, and many others. The most closely related physical property of light is wavelength -- though the hue purple does not correspond to any wavelength in the spectrum.

Saturation is defined as the degree to which a sensation of hue differs from a gray of the same brightness. Colors that are 100 percent saturated are called spectrum colors. When white light is added to a spectrum color, the spectrum color decreases in saturation. For example, a spectrum red becomes more or less pink when it is mixed with white light; it is still red in hue, but its saturation has decreased.

The sensation of brightness is related to the amount of luminous flux reaching the eye from an object or light source. Other things being equal,

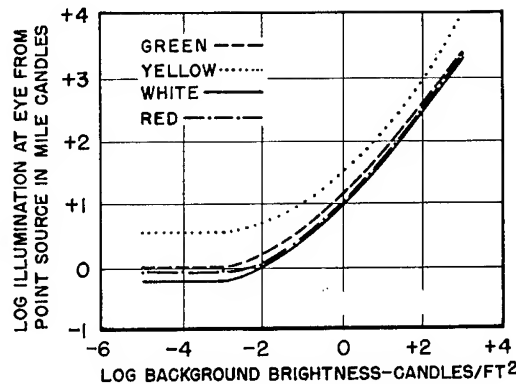


Figure 2-30

Color Recognition of Point Sources of Light

(After Baker and Grether (25) Adapted from Hill (217))

a source of high intensity or luminance will seem bright-colored -- bright red, bright blue, etc., -- while a source of low intensity or luminance will seem dark - or dull-colored. A sample of red that seems dark on a cloudy day will seem bright on a sunny day; the hue and saturation remain the same, but more luminous flux is reaching the eye.

Systems of color specification must relate colors to a standard light source (39, 65). The most objective method in color specification is the tristimulus colorimetric method (177). The International Commission on Illumination (ICI) chromaticity diagram is an example of this approach. Color may also be specified by visually matching samples with printed, dyed, or painted standards. The Munsell Atlas contains painted samples of all the colors in the system, presented in a three-dimensional array with hue, saturation, and brightness recorded on the axes (309, 310). Color may be used in coding, that is, specifying the correct identification of an object by its color. For example, wires, resistors, pipe lines, gas cylinders, and many other objects are color coded. Since errors in reading the color code may be disastrous, it is important to understand the sensitivity of color discrimination.

Hue discrimination is usually measured in terms of the smallest difference in wavelength that two test fields can have and still be interpreted as of different hues. Figure 2-31 shows variations in hue discrimination through the visible spectrum. Changes in hue discrimination are not equal for equal increments of wavelength (λ). At high luminance (10 mL or better) and saturated colors, 128 hues can be distinguished. The difference threshold in the blue-green and yellow portions of the spectrum is of the order of one millimicron ($m\mu$). At the red level of the spectrum, the difference must be as great as 20 $m\mu$ before it is detected. Data are also available on brightness saturation discrimination but these are not primary factors in coding (462).

A large proportion (6%) of the healthy male population possesses a significantly reduced ability to distinguish color differences. Only .003% of the population are completely color blind, that is, they see only various shades of gray. Since color coding is frequently used with unselected populations, at least with respect to color vision, the selection of the particular colors for coding becomes an important consideration. The four colors listed in Table 2-32a are considered ideal for coding because color deficient individuals can also easily recognize them (25). The numbers refer to the Federal Specification TT-C-595, 'Colors for Ready Mixed Paints,' with the exception of blue (10B 7/6) which is a Munsell notation (309, 310). However, more than four colors will frequently be required

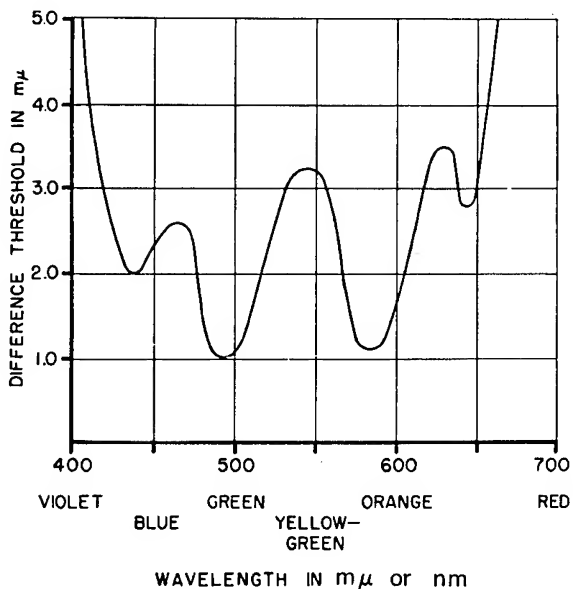


Figure 2-31
Hue Discrimination
(After Wulfeck et al (462))

Table 2-32
Color Code Recommendations for Pigments and Indicator Lights
(After Baker and Grether⁽²⁵⁾ and NASA CSD-A-096⁽⁴²³⁾)

a. Ideal For Color-Blind Persons					
	Black	1770			
	White	1755			
	Yellow	1310			
	Blue	10B 7/6			
b. For Use When More Colors Are Needed					
Red	1110	Blue	10B 7/6	White	1755
Orange	1210	Purple	2715	Black	1770
Yellow	1310	Gray	1625	Buff	1745
c. Coding of Simple Indicator Lights					
LIGHT	RED	AMBER	GREEN	WHITE	
1/2 inch diameter steady	Malfunction, action stopped, failure, stop action	Delay, check, recheck	Go ahead, in tolerance, acceptable, ready	Functional or physical position, action in progress	
1 inch diameter steady	Master summation, (system or subsystem)	Extreme caution (Impending danger)	Master summation, (system or subsystem)	N/A	
1 inch diameter flashing (3-5/sec.)	Killer warning (personnel or equipment)	N/A	N/A	N/A	

to code objects. The nine colors listed in Table 2-32b were selected to be the least confusing for individuals with normal and color-defective vision (14).

Color-coded signal lights are used on display panels, maintenance equipment, and in navigational aids to air, marine, and surface vehicles (65). Only three colors are recommended for signals if color defective observers are expected to respond correctly to these signals. These three colors are aviation red, aviation green, and aviation blue as defined by the Army-Navy Aeronautical Specification AN-C-56, 'Colors, Aeronautical Lights and Lighting Equipment.' Aviation blue is distinguished from red and green only at moderate distances. It must be noted that the specific requirements for these colors must be adhered to if the code is to be used by color deficient personnel because there are many reds, greens, and blues that will be confused. Also, no attempt should be made to include white or yellow in conjunction with the three recommended colors because the color-deficient individuals may confuse red with yellow and green with white.

A color-coding scheme for indicator lights on instrument panels conforming to the identification colors listed in MIL-C-25050 as suggested for the Apollo system are noted in Figure 2-32c (3).

Red - Red is used to alert an operator that the system or any portion of the system is inoperative and that a successful mission is not possible until appropriate corrective or override action is taken. Examples of lights which are coded red are those which display such information as: no-go, error, failure, malfunction, etc.

Amber - Amber is used to advise an operator that a condition exists which is marginal insofar as system effectiveness is concerned, that an unsatisfactory or hazardous condition is being approached or exists but that the system can still operate (battery approaching replacement time, etc.).

Green - Green is used to indicate that a unit or component is in tolerance or a condition is satisfactory and that it is all right to proceed (go ahead, in tolerance, ready, acceptance, normal, etc.).

White - White is used to indicate those system conditions that are not intended to provide a right or wrong implication, such as indications of alternative functions or are indicative of transitory conditions, where such indication does not imply success of operations.

Blue - Blue is used as an advisory type light, but preferential use of blue is discouraged.

The flash rate for flashing warning lights should vary from 3 to 5 flashes per second with on time being approximately equal to off time. The indicator should be designed so that if energized and the flasher device fails, the light will come on and burn steadily. If simple-type indicator lights (rather than legend type lights) are used for emergency conditions (personnel or equipment disaster), such functions are indicated by a 1-inch diameter red flashing light and cautionary conditions (impending danger) by a 1-inch diameter steady amber light. Master summation indications; system or subsystem, is

indicated by 1-inch diameter steady red or green lights. Indication of all other conditions is by 1/2 inch diameter steady lights. One-inch diameter lights are discriminately brighter than 1/2-inch diameter lights. With the exception of small flashing white call lights commonly used on communication panels, no other flashing lights are used. Auditory signals may be used to complement the visual display (31).

Several general reviews of factors in color coding are available (106, 240). Color mixture functions at low luminance levels have also received recent study as have distortions of color during underwater observation (246, 447). Data are also available on the visibility of colored smoke signals from the air (438). The effect of color on the internal illumination and habitability of spacecraft is discussed in another section.

Duration of Visual Exposure and Intermittent Illumination

When a target appears as a short flash up to about 0.1 sec. duration (this limit depending on the conditions), the effectiveness of the light increases linearly with exposure time as expressed in Bloch's law. On longer exposures, up to a few tenths of a second or longer, the time factor is less effective as expressed in Blondel and Rey's law (54). Finally, above a critical time the effect of a light becomes independent of the duration. These laws, which express the temporal summing ability of the visual system, may also be valid for a moving object as long as its image stimulates the same receptive fields of the retinal elements. Figures 2-33 and 2-34 are demonstrations of the effect of target size and target exposure on the contrast thresholds for stationary targets. At any luminance level, less time is required to see bigger objects. When size is held constant, less time is required to see at higher luminance levels.

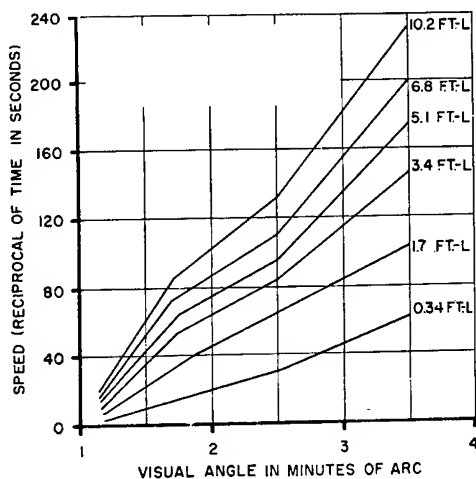


Figure 2-33

Visual Acuity as a Function of Time of Exposure to Viewed Object
(After Chapanis⁽⁹³⁾ Data of Ferree and Rand⁽¹⁴⁵⁾)

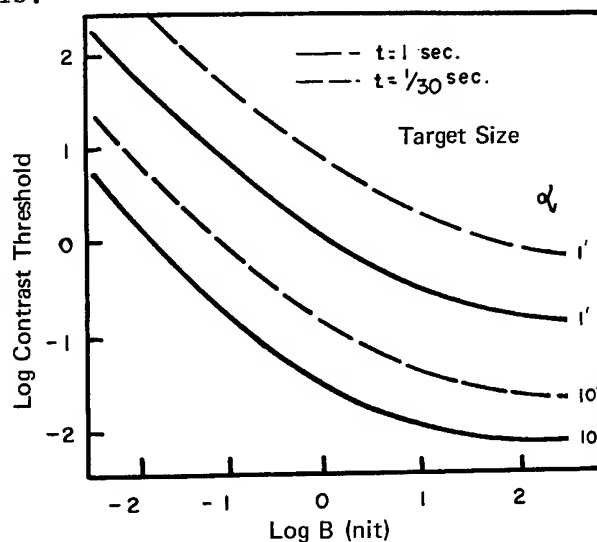


Figure 2-34

Contrast Thresholds in Dependence of Target Size and Time of Exposure
(After Schmidt⁽³⁷¹⁾ from Data of Blackwell et al⁽⁵⁰⁾)

Intermittent signal and warning lights are often more detectable than steady lights. This factor may be of value in space operations. Although a target may be bright enough to be visible, the pilot may not detect it against the star background -- particularly if its motion is very slow. Because the apparent motions at the initiation of rendezvous are, in general, very slow, this is an extremely important problem in acquisition. If the light is interrupted so as to flash off and on, it would be much more readily detected than a steady light (54, 312). The problem then concerns the optimum flash rate and flash duration. The effect of flash duration on the apparent intensity of a light seen by the human eye is shown in Figure 2-35. In this figure, a steady light which is just barely discernible is used as a datum reference with a relative intensity level of unity. The figure shows that little increase in relative intensity is required down to flash durations approaching 0.2 second. For flash durations less than one-tenth second, however, the required relative intensity increases as an inverse function of time. For example, if the flash duration is about 0.003 seconds, the intensity relative to the steady light must be increased by a factor of about 100. The curve of Figure 2-35 can be approximated by the equation:

$$E = E_O \left(\frac{t + a}{t} \right) \quad (2)$$

where

- E = intensity of flashing source required to appear as bright as E_O
- E_O = intensity of steady source
- t = duration of flash, sec.
- a = curve fitting constant equal to 0.21 second

This expression is known as Talbot's law.

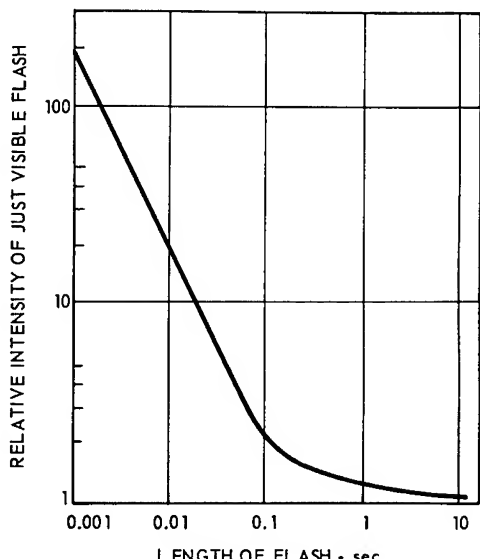


Figure 2-35
Visibility of Flashing Sources of Light

This Figure shows how intense a flash of light must be in order to be seen at the 50% probability level. Note that very short flashes must be much more intense than long flashes if they are to be seen. The detection of colored lights requires about the same illumination at the eye as detection of white light.

(Adapted from Blondel and Rey⁽⁵⁴⁾)

There are many variables altering the perception of intermittent light signals (157, 158, 247, 275, 435). Repeated flashes of light frequently lead to contradictory responses at the same wavelength. The variability in color recognition near the threshold is well known (149, 435). An observer who is expecting a brief and small, circular, colored light signal in the darkness and required to identify the color of the signal may be especially confused (435). When the signal is perceived as a circle, there is a good probability of correctly identifying its color. When it is perceived as a mere light sensation, quite shapeless, the signal may appear as achromatic regardless of actual color. When the signal appears distorted in shape between the two extreme situations described above, little confidence may be given that the assumed color response is correct. The perception of circular shape requires a less intense stimulus for red stimuli than for other colors.

The perceived brightness of intermittent light is greater below fusion than at higher frequencies (brightness enhancement) (28, 421). The maximum enhancement above the Talbot plateau level appears to be at about 4-5 cps (103).

Visual noise interferes with perception of intermittent stimuli and may cause false alarms in operational situations (358, 360). In search situations, the effect of flash distribution and illumination level of low intensity stimuli may be important (450).

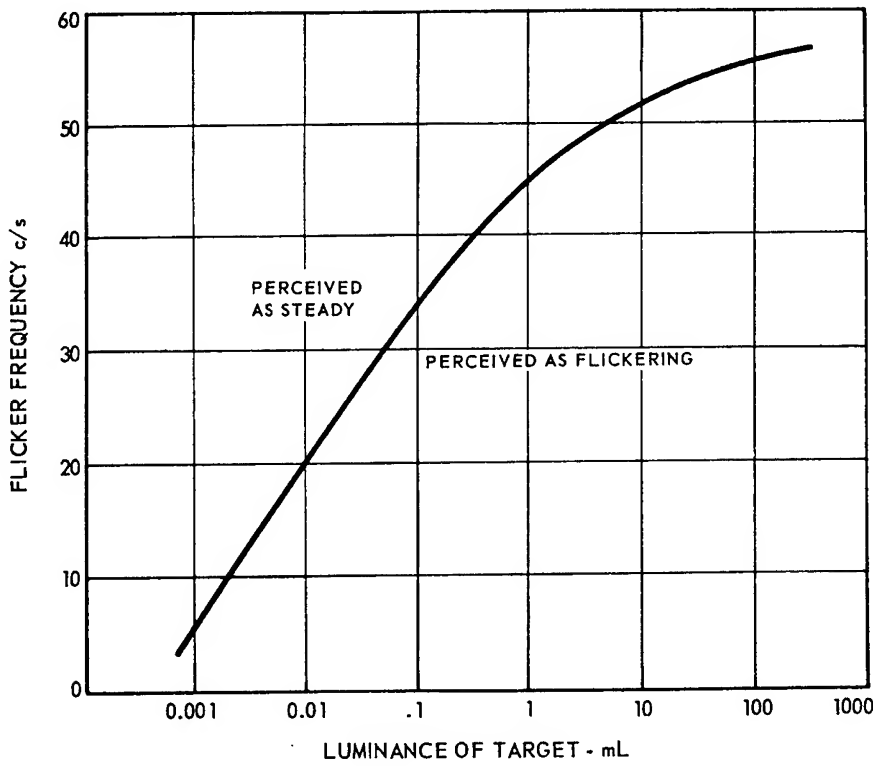
It has been noted that the threshold for visibility at night is about 0.13 km-c (.05 mi-c) but in operational conditions for semi-trained subjects who have large and ill-defined solid angles to search, 0.94 km-c (.36 mi-c) would be a more reasonable threshold for detectability. In scotopic and mesopic vision, the rod perception of contrast may be improved by intermittent illumination of peak luminance level equal to an equivalent steady illumination. There are ideal wave forms and frequencies for each color (44).

In the case where the subject knows the position in space where a flash is to occur, the simple reaction time is a decreasing, negatively accelerated function of flash luminance (261). Flash duration has no clear effect on reaction time.

The flickering effect of intermittent light at around 8 pulses per second may be disturbing to some people (6). A small percent of the population may even develop epileptic seizures from the flicker (35, 290, 418). At high frequency of flicker, fusion of the image occurs and the light is perceived as steady. Figure 2-36 represents this phenomenon as a function of luminance. The data are valid only for white light on the fovea. The flicker fusion frequency is dependent on the functional state of the central nervous system.

Visual Fields

The limit of field of vision possible with eyes and head fixed or free to move about is seen in Table 2-37. The monocular and binocular fields for achromatic targets with eyes fixed are seen in Figure 2-38a and c. Chromatic targets alter the field of vision as seen in Figure 2-38b. Helmets and



The graph shows the relation between critical fusion frequency (CFF) and luminance. The curve defines the boundary between those combinations of target luminance and flicker frequency that are perceived as flickering and those perceived as steady. CFF is the lowest frequency (c/s) of flashing that can be perceived as steady. Luminance is the variable with the greatest influence on CFF. Other variables are target size, color, lengths of the light-dark cycle, brightness of the surround, region of the retina stimulated, and individual differences. The data shown in the graph are based on a two-degree, achromatic stimulus at zero degrees of angular eccentricity.

Figure 2-36

Temporal Discrimination of White Light at the Fovea

(Adapted from Hecht and Verrijp⁽²¹¹⁾ by White⁽⁴⁴⁶⁾)

Table 2-37
 Binocular Visual Fields with Head and Eye Movement
 (After Wulfeck et al⁽⁴⁶²⁾ from data of Hall and Greenbaum⁽¹⁹⁵⁾)

MOVEMENT PERMITTED	TYPE OF FIELD AND FACTORS LIMITING FIELD	HORIZONTAL LIMITS		VERTICAL LIMITS	
		Temporal Ambinocular Field (each side)	Nasal Binocular Field (each side)	Field Angle Up	Field Angle Down
Moderate movements of head and eyes, assumed as: Eyes: 15° right or left 15° up or down Head: 45° right or left 30° up or down	Range of fixation	<u>60°</u>		<u>45°</u>	
	Eye deviation (assumed)	15°	15°	15°	15°
	Peripheral field from point of fixation	95°	(45°)	46°	67°
	Net peripheral field from central fixation	110°	60°***	61°	82°
	Head rotation (assumed)	45°	45°	30°*	30°*
Head fixed Eyes fixed (central position with respect to head)	Total peripheral field (from central body line)	155°	105°	91°	112°**
	Field of peripheral vision (central fixation)	95°	60°	46°	67°
	Limits of eye deviation (= range of fixation)	74°	55°	48°	66°
	Peripheral field (from point of fixation)	91°	Approx (5°)	18°	16°
	Total peripheral field (from central headline)	165°	60°***	66°	82°
Head maximum movement Eyes fixed (central with respect to head)	Limits of head motion (= range of fixation)	72°	72°	80°*	90°*
	Peripheral field (from point of fixation)	95°	60°	46°	67°
	Total peripheral field (from central body line)	167°	132°	126°	157°**
	Maximum movement of head and eyes	72°	72°	80°*	90°*
	Maximum eye deviation	74°	55°	48°	66°
	Range of fixation (from central body line)	146°	127°	128°	156°**
	Peripheral field (from point of fixation)	91°	Approx (5°)	18°	16°
	Total peripheral field (from central body line)	237°	132°	146°	172°**

*Estimated by the authors on the basis of a single subject.

**Ignoring obstruction of body (and knees if seated). This obstruction would probably impose a maximum field of 90° (or less, seated) directly downward; however, this would not apply downward to either side.

***This is the maximum possible peripheral field; rotating the eye in the nasal direction will not extend it, because it is limited by the nose and other facial structures rather than by the optical limits of the eye. The figures in parentheses on the line above are calculated values, chosen to give the maximum limit thus indicated.

Notes: The ambinocular field is defined here as the total area that can be seen by either eye; it is not limited to the binocular field, which can be seen by both eyes at once. That is, at the sides, it includes monocular regions visible to the right eye but not to the left, and vice versa.

The term binocular is here restricted to the central region that can be seen by both eyes simultaneously (stereoscopic vision). It is bounded by the nasal field-limits of the eyes.

Figure 2-38
Monocular and Binocular Visual Fields

Figure a is a perimetric chart that shows the average monocular visual field for the right eye. Numbers are degrees; the eccentricity angle in degrees is the distance by which a target is displaced from the fovea. The head and eyes are motionless. The nasal field is to the left, and the temporal field to the right of the chart. Visual fields are mapped with a two-degree, achromatic circular target with a luminance of about 10 mJ. Age (after 40 years) tends to narrow field limits. Errors of refraction (except presbyopia) have no significant effect on the size of the form field, but affect the size of color fields.

(After Ruch and Fulton, eds. (366))

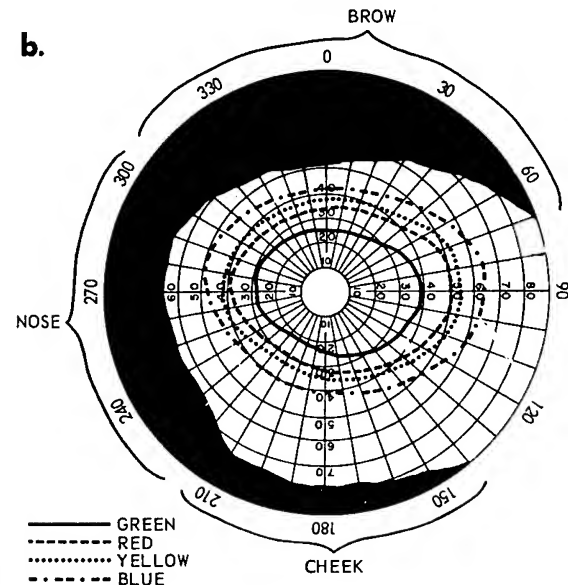


Figure c shows the normal field of view of a pair of human eyes. The central white portion represents the region seen by both eyes. The gray portions, right and left, represent the regions seen by the right and left eyes, respectively. The cut-off by the brows, cheeks, and nose is shown by the black area. Head and eyes are motionless in this case.

(After Ruch and Fulton, eds. (366))

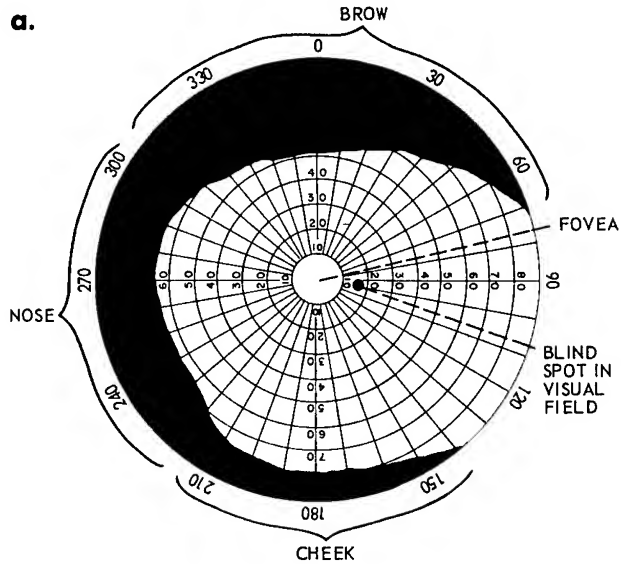
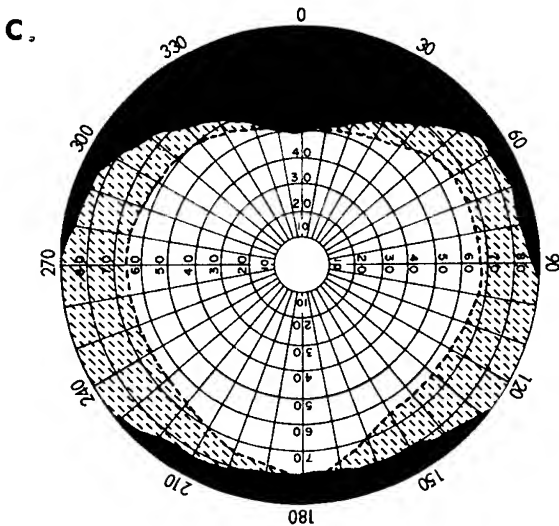


Figure b is a perimetric chart that shows average monocular visual field for both achromatic and chromatic targets for the right eye. The chart shows that the visual field for form is normally the largest; those for blue, yellow, red and green are successively smaller in the order given. A three-degree red target that is beyond 60° eccentricity will appear colorless; at 20° the target will appear as red. Increasing the brightness of the target or its size will tend to move color zones outward on the chart. Color fields are less stable than is the field for form.

(After Boring et al (64))



visors will alter the field of vision and fields must be determined specifically for each design in question. (See recommendations below and Figure 16-24).

Movement Discrimination and Ocular Pursuit

Movement of a target relative to the background is a factor to be considered in detection of satellites in a starfield and in other ocular pursuit tasks. Figure 2-39 covers the ability to discriminate movement in the frontal (a) plane and in depth (b and c). Discrimination of movement in depth is a complex function of importance in docking and extravehicular activity. Figure 2-39b & c represents the basic data which may be converted to angular data for extrapolation to space conditions.

Figure 2-73 covers angular rate perceptions for small luminous targets in a starfield, specifically obtained for evaluation of visual satellite acquisition tasks in rendezvous.

Visual acuity is affected by motion (83, 296). Dynamic visual acuity is the recognition of details when the observer or the target or both are moving in comparison to the static visual acuity where all are fixed. As seen in Figure 2-40 dynamic visual acuity shows a predictable impairment with increasing angular velocity, starting noticeably to deteriorate with a speed rate of 20° per sec. The eye is unable to match the exact rate of movement of the object at greater speed, resulting in a motion of the image on the retina which reduces the contrast and thus the visual acuity. Peripherally, the impairment is more noticeable than centrally. In the case of a single target with increasing speed the deterioration first increases slowly then more rapidly. Decrement in visual acuity with motion is about the same when the subject or the object is moving and the other remains static (296). A higher dynamic visual acuity is obtainable when normal head movements are possible than when the head is fixed (111). Legibility criteria for moving alphanumeric symbols are available (266).

The masking effects of moving light stimuli on the luminance threshold of a stationary stimulus have been studied (276). False movements in the visual fields often result from vestibular and other illusionary phenomena (449). These will be covered in detail in Acceleration (No. 7).

Dark Adaptation

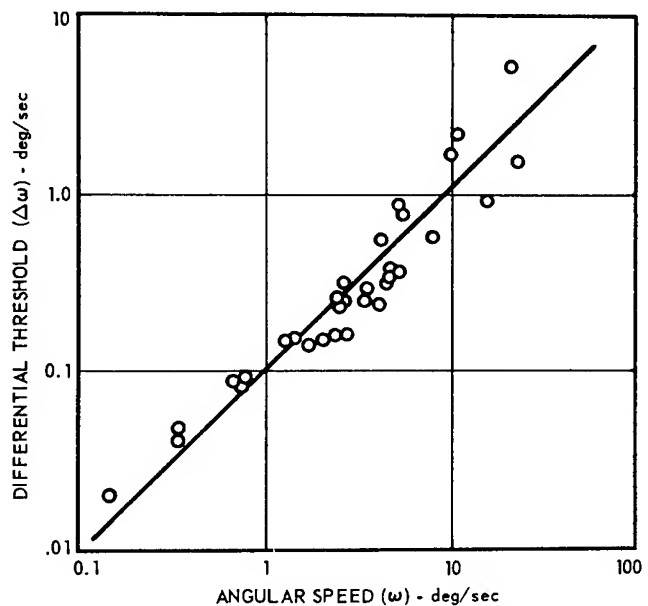
The eye becomes much more sensitive to light in darkness (231). Very little of this can be attributed to the dilation of the pupil shown in Figure 2-41 which is hardly enough to account for the many orders of magnitude of difference in sensitivity which occur when one adapts to darkness after exposure to a high illumination (76).

Another basis for the tremendous improvement of vision under dark adapted conditions is the fact that the concentration of photosensitive materials is increased. When the eye is placed in darkness, a concentration which was roughly in balance with conditions of illumination at a high level is

Figure 2-39

Discrimination of Movement

a. In the Frontal Plane



The differential threshold ($\Delta\omega$) is the amount that the angular speed of an object moving at right angles to the line of sight must change to be detected as a new speed. Data points shown on the graph are thresholds gathered from eight different experiments, for abrupt changes in speed from ω_1 to ω_2 .

When an object stationary in the visual field ($\omega_1 = 0$) is suddenly set in motion, the minimum speed which is perceived as motion ("rate threshold") varies from 1 to 2 minutes of arc per second (0.017 to 0.033 deg/sec).

Threshold for movement in peripheral vision is higher than the threshold in central vision. Effects of illumination and contrast on differential threshold are imperfectly known at this time. The rate threshold is higher at low illumination levels and when no fixed visual reference is available.

(After White⁽⁴⁴⁶⁾ Adapted from Brown⁽⁷⁹⁾ and Graham⁽¹⁷⁸⁾)

Figure 2-39 (continued)

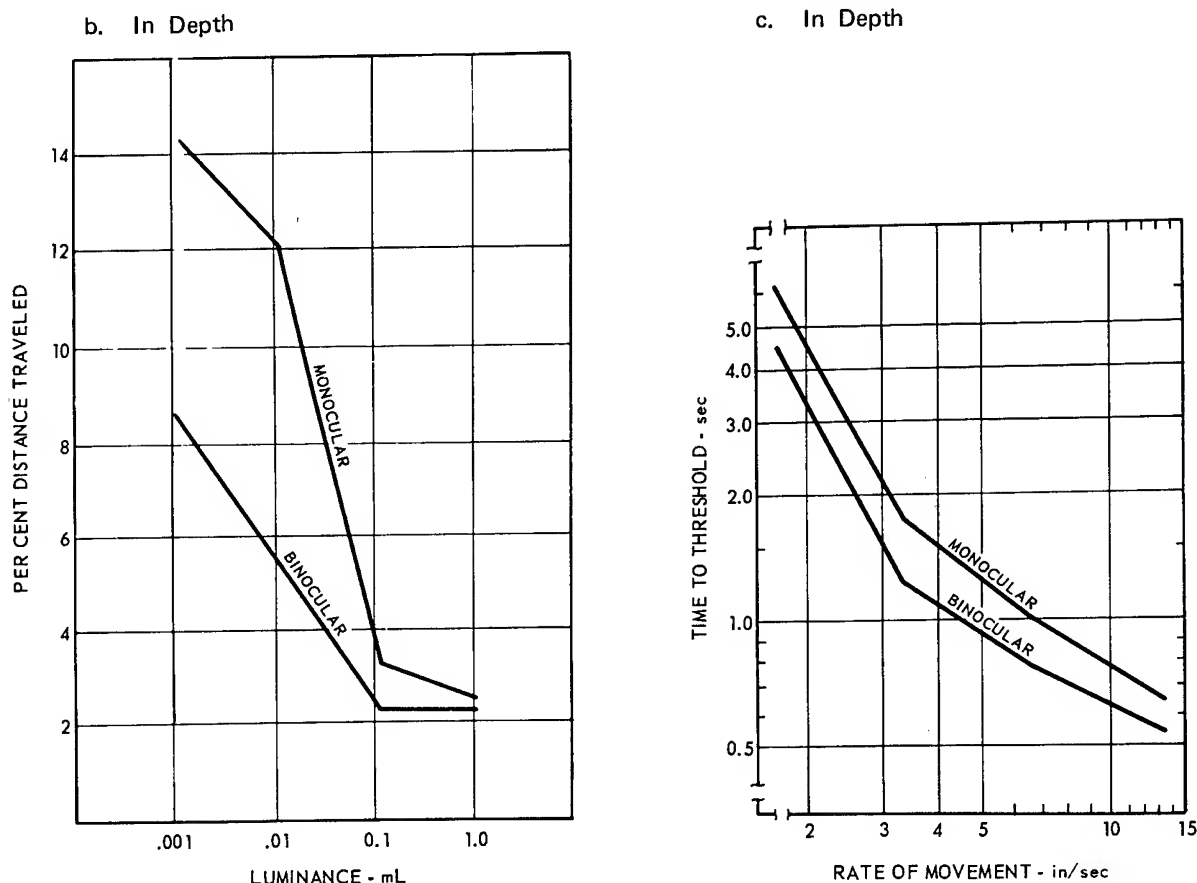


Figure **b** shows successful perception of movement in depth of a luminous target on a black field as a function of change in visual angle (per cent distance traveled) and of luminance. Figure **c** shows the time required to perceive movement in depth as a function of rate of change of visual angle (target speed). Both curves are for 75% correct responses, where 50% correct would be chance performance, since the target moved both toward and away from the observer, who had to choose the correct direction.

The target was a lamp measuring 3.5 inches in diameter which was moved back and forth on a track from an initial distance of 25 feet. At the initial distance, the lamp subtended a visual angle of 40 minutes of arc. A 2% change in distance, which was detected as movement at the higher luminance levels, represented a 2% change in visual angle, or a change of about 0.8 minutes of arc. The range of target speeds from 1.65 to 13.2 inches per second produced initial changes in visual angle from about .25 minutes of arc to 2 minutes of arc.

(After White⁽⁴⁴⁶⁾ Adapted from Baker and Steedman⁽²³⁾)

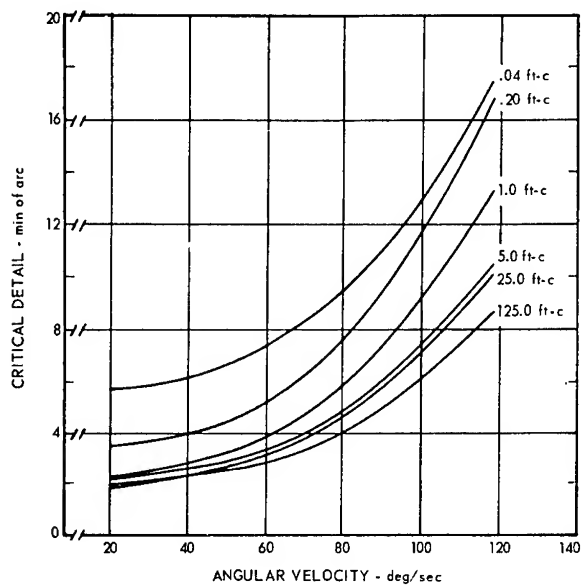
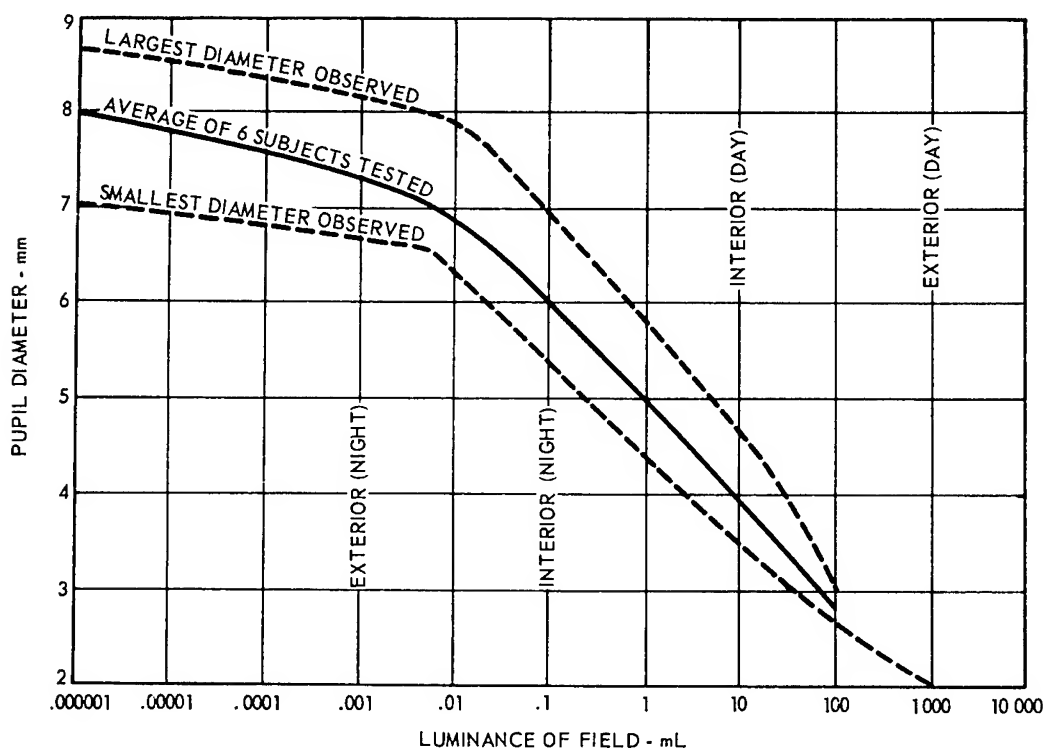


Figure 2-40.
Dynamic Visual Acuity
During Ocular Pursuit

The effects of increased angular velocity of rotation on visual acuity at each of six levels of illumination are shown in the graph. The relationship shown is for a black Landolt-ring on a white background. The data show that visual acuity declines progressively as angular velocity increases, and that acuity is benefited by increasing the illumination on the target.

(After White (446) Adapted from Miller (296))



There are a number of factors which affect the size of the pupil. The relationship shown here is diameter and variations in the luminance of a large uniform field. It is not possible at this time to predict the size of the pupil for non-uniform distributions of luminances in the visual field.

Figure 2-41

Pupillary Diameter and Luminance

(After IES Lighting Handbook (222))

supplanted by the much higher concentration which is found in the dark adapted eye. There is, however, a large change in sensitivity, many orders of magnitude, which takes place after more than 90% of the photo-sensitive materials have been regenerated (368). There is therefore, no direct relation between sensitivity and concentration. Other changes must also be occurring. One of the things which is probably occurring is a transition in the nature of the eye's capability of utilizing energy distributed over area. This is reasonable because the eye is not as capable of resolving visual detail in the dark adapted state and at low luminances. It would appear that spatial resolution capacity has been exchanged for sensitivity to flux level in the retina. The "critical duration" of the eye, the utilization time beyond which energy cannot be summated over time for the achievement of a given energy threshold level, becomes longer at lower levels of illumination. Increased sensitivity to flux is thus achieved not only at a cost of reduced spatial resolution apparently, but also of temporal resolution. The eye is not as sensitive to a pulsating light at lower luminance as it is at a high luminance. The higher the luminance, the faster the pulsation the eye can detect (Figure 2-36).

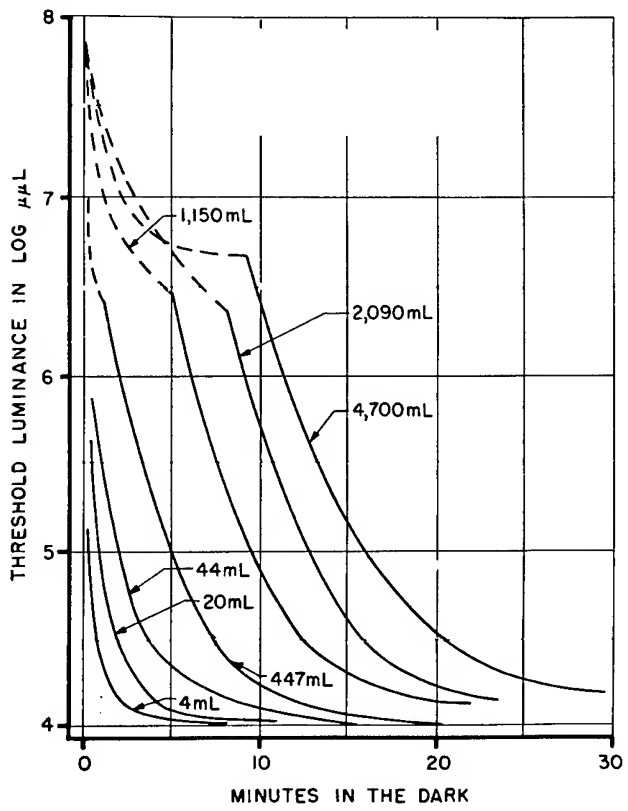
Light sensitivity at a given moment depends on the length of time the eye has been exposed to a certain level of illumination. Factors that influence absolute sensitivity to light are: (1) the duration of, and (2) average pre-exposure luminance, (3) the size, shape, contrast conditions and viewing time of the test object, (4) the color of the pre-exposure light and the test light in measuring sensitivity, (5) the region of the retina stimulated, and (6) physiological status of the individual (231). The data of any investigator must therefore be used with great caution in predicting dark adaptation under different conditions (389).

Figure 2-42 shows examples of several variables of prior exposure on dark adaptation. Rods and cones differ in the time factors associated with their activities. As shown by slope change in Figure 2-42a, the rods are much slower in action than the cones. The time required to adapt to a given threshold level is shorter when the pre-exposure brightness is lower, and when the pre-exposure light is composed of wavelengths in the red portion of the spectrum (Figure 2-42b and 2-42c). Note that the thresholds may differ by an order of magnitude depending on specific subjects and test conditions.

Figure 2-43 shows effect of test conditions on dark adaptation such as area of test object (210), wavelength of test stimulus (93), region of retina used (210) and population difference (388) - all under the specific conditions used in gathering the data. Hypoxia and nutritional state of subjects are major factors in dark adaptation (93, 231, 388, 424). The problem of optimizing cockpit color lighting for preservation of dark adaptation has received recent review (291, 389).

When the eye has been adapted to a given luminance, the luminance that is just visible immediately after is the instantaneous threshold. Figure 2-44 shows a plot of pre-adapting luminance in mL against the instantaneous threshold. The curve is a straight line except at the higher luminances where factors other than adaptation are present. This graph is for a square target that subtends 10 minutes of arc, and assumes that the observer is pre-adapted to a given wide field luminance. An observer adapted to a luminance of 1.0 mL

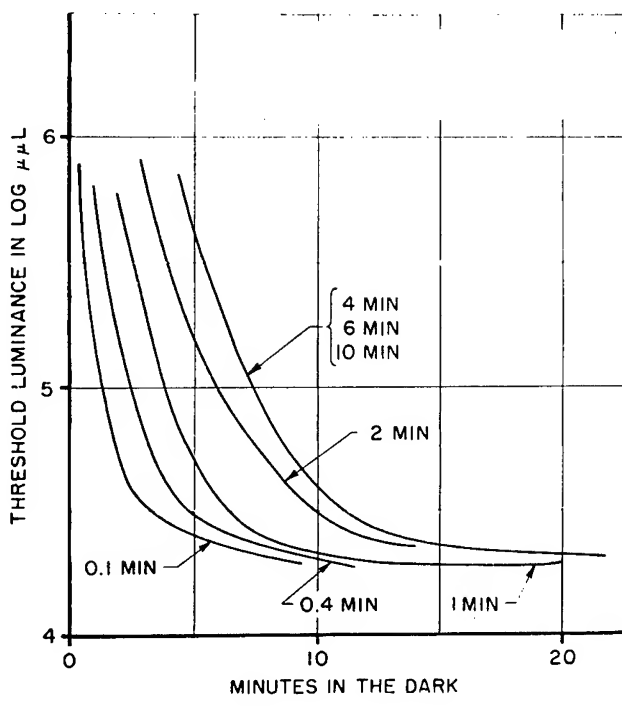
Figure 2-42
Dark Adaptation as a Function of Previous Light Exposure



a. Intensity of Previous Light

Dark-adaptation curves for one subject following exposures to lights of various luminances for four minutes. The broken lines indicate the color of the test light (violet) could be identified at threshold. The thresholds in this example are one order of magnitude higher than usually shown.

(After Chapanis (93) from Data of Haig (192))



b. Duration of Previous Light

Dark-adaptation curves for one subject following exposure to light of 447 mL for various durations. Only the rod portions of the curves are shown here. Thresholds are one order of magnitude higher than usually found.

(After Chapanis (93) from Data of Haig (192))

c. Dark Adaptation Curve as a Function of Color of Previous Light

(After Peskin and Bjornstad (339))

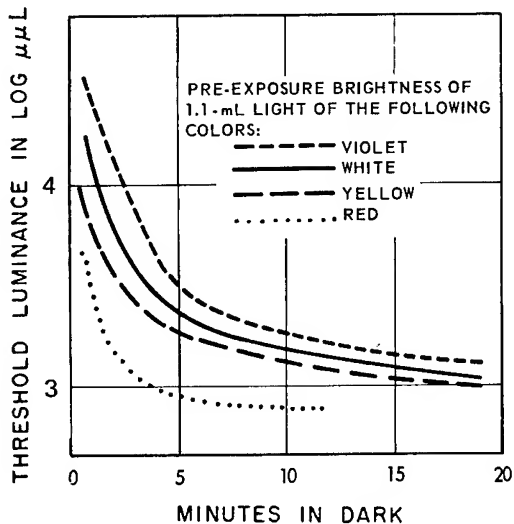
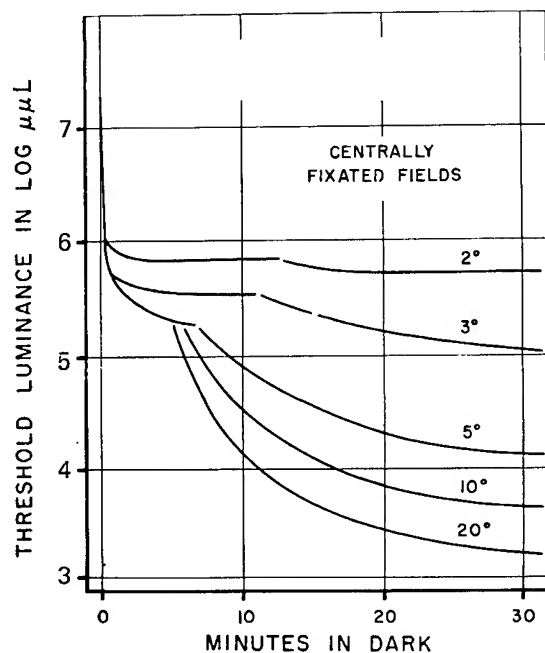


Figure 2-43
Dark Adaptation as a Function of Test Light Exposure



a. Area of the Test Object.

Dark-adaptation curves for centrally fixated areas of different size.

(After Bartley⁽²⁹⁾ from Data of Hecht et al⁽²¹⁰⁾)

b. Wavelength of the Test Stimulus

Dark-adaptation curves measured with lights of different wavelengths. Although lights were equated in brightness initially, they are no longer equally bright even at cone threshold. The differences are further exaggerated during rod dark adaptation.

(After Tufts Handbook⁽⁴¹⁶⁾ Data from Chapanis⁽⁹³⁾)

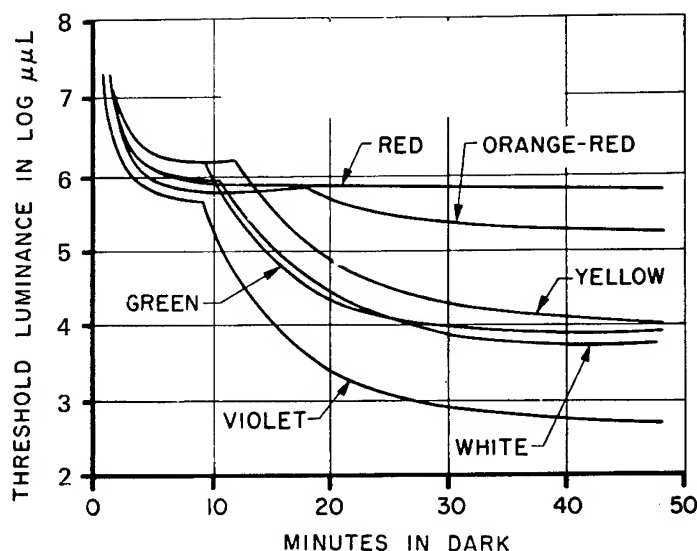
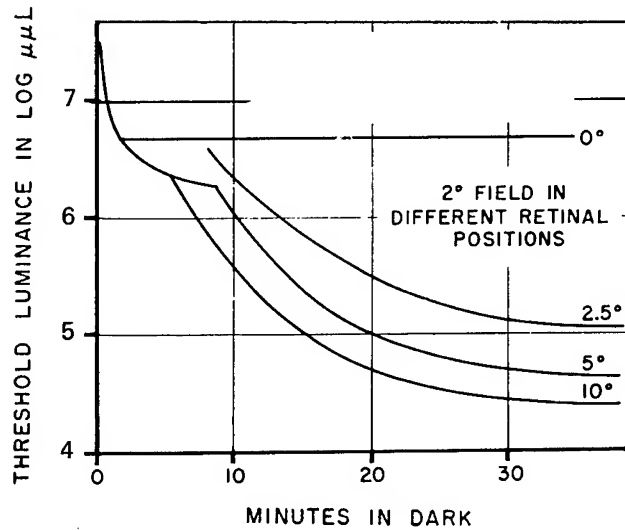


Figure 2-43 (continued)



c. Region of the Retina Stimulated.

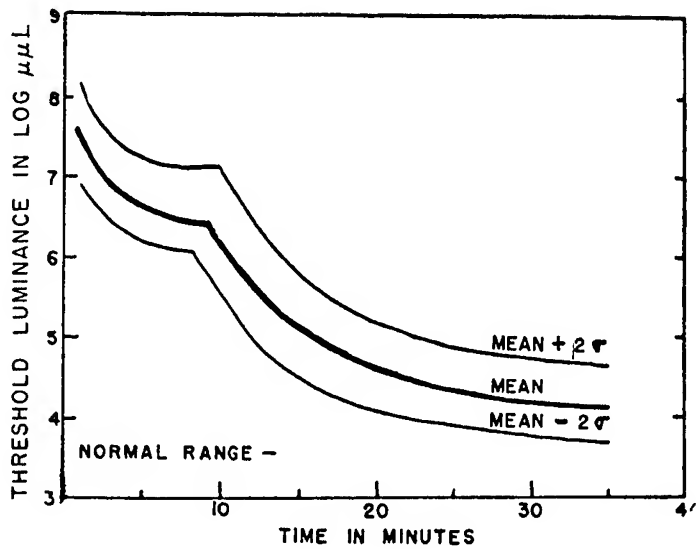
Dark-adaptation curves measured with a 2-degree test object placed at various angular distances from the fixation point.

(After Bartley⁽²⁹⁾ from data of Hecht et al⁽²¹⁰⁾)

d. Population Factor

Rate of dark adaptation after preadaptation to 1100 millilamberts. A 1-degree white test field located 15 degrees from fixation in nasal field. The area between the upper and lower curves includes 95 percent of those tested.

(After Sloan⁽³⁸⁸⁾)



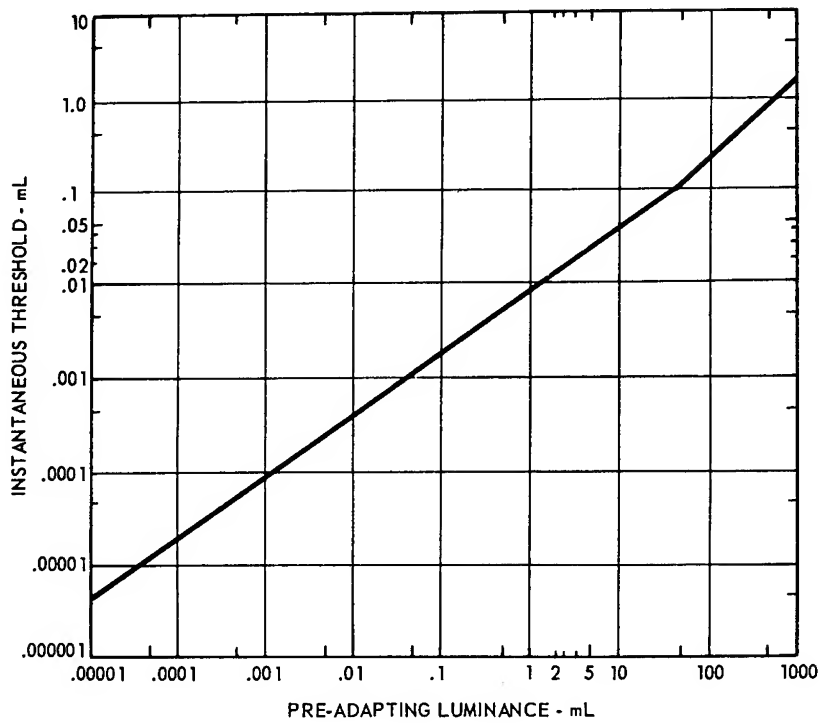


Figure 2-44

Instantaneous Threshold for Light

(Adapted from Nutting⁽³²²⁾)

can see a 10 minute square target about one hundredth as bright immediately after the pre-adapting field is turned off. If the observer in question were exposed to a field luminance of 1000 mL but the target luminance was 0.0001 mL, the predicted luminance threshold in Figure 2-42a indicates he must wait about 10 minutes after entering a dark room before he can see the target light. Figure 2-44 is for simple light detection and does not permit a prediction of instantaneous visual acuity threshold, which requires discrimination of form. Dark adaptation data pertinent to cathode ray tube (CRT) displays are seen in Figures 2-67 to 2-69.

Training techniques may aid in optimizing night vision, especially during lunar surface operations (286, 417).

Glare and Flash Blindness Phenomena

Glare is defined as any degree of light falling upon the retina in excess of that which enables one to see clearly; that is, any excess of light which hinders instead of helps vision. Glare can be further differentiated into:

- (1) Veiling glare: created by light uniformly superimposed on the retinal image which reduces contrast and, therefore, visibility
- (2) Dazzling glare: adventitious light scattered in the ocular media so as not to form part of the retinal image
- (3) Scotomatic or blinding glare (flash blindness): produced by light of sufficient intensity to reduce the sensitivity of the retina.

Although all three types of glare are present in the case of high-intensity light, the effects of the first two are primarily evident only when the source is present. The third type, scotomatic or blinding glare, is especially significant in flash blindness where it produces symptoms (afterimages) which persist long after the light itself has vanished. The afterimage is a prolongation of the physiological processes which produced the original sensation response after cessation of stimulation.

Glare

Regardless of whether the glare source is direct or indirect (reflected or specular), it can cause discomfort, or it can affect the visual performance, or it can do both. The visual discomfort or annoyance from glare is a common well-understood experience and has been confirmed by many experiments. In connection with certain experimental studies, it has been found that people sometimes become more physically tense and restless under glare conditions than under nonglare conditions.

In general, visual acuity is at a maximum when the eyes are adapted to the brightness level of the target and background. But acuity is reduced when the target and background are at a lower brightness than the greater surround. The curve in Figure 2-45 shows the effect of surround brightness both darker and lighter than the target and the immediate background (278). Acuity is best when the surround is a little darker than the target. Thus, it is suggested that for best acuity, targets should not be in a shadow or near a large area of much higher brightness. Recent reviews of surround brightness and size on visual performance are available (223, 224).

Visual acuity is best when the eyes have not been exposed to high levels of brightness. As a general rule if visual displays have to be read by people who have just been exposed to high levels of brightness (the open sea, clouds, desert, or snow), the level of brightness of the displays should be higher than would normally be necessary - they should be at least 0.01 as bright as the pre-exposure field (see Figure 2-44).

From a practical standpoint, data are available which provide a basis for specifying increased display contrast requirements when the area surrounding the display is substantially brighter than the background within the display.

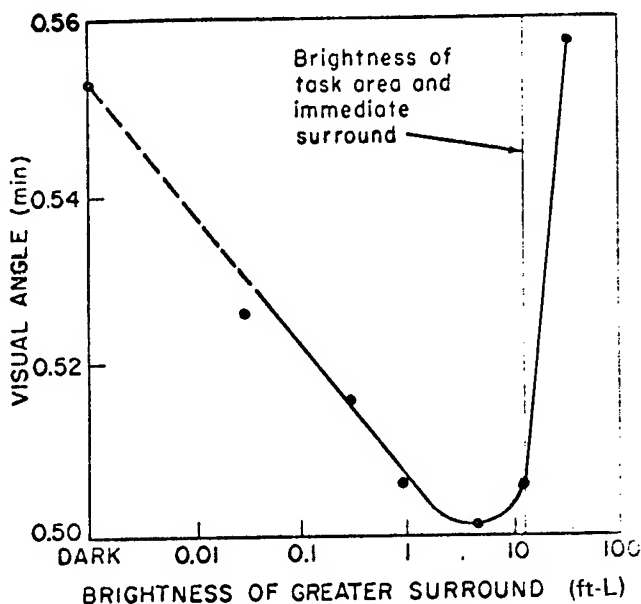


Figure 2-45

Threshold Visual Angle as Determined by Brightness of the Greater Surround.

(After Lythgoe (278))

Under these conditions, the contrast threshold is fairly sensitive to the surround-to-background ratio. The increase in a subject's contrast threshold appears to be proportional to the increase in surround brightness. This conforms to findings with point glare sources whose effects also appeared to be proportional to their brightness (219). For threshold contrast with a given background brightness, surround-to-background brightness ratios greater than "one", and background angles in the $5^\circ - 45^\circ$ range, the following empirical formula fits the experimental data fairly well ($\pm 10\%$): (224)

$$C' = C_{ref} \left(0.9815 + \frac{0.0185 \text{ BS}}{\text{BB}} \right) \quad (3)$$

where C' = threshold contrast for a given ratio, $\frac{\text{BS}}{\text{BB}} > 1$

C_{ref} = threshold contrast when $\text{BS}/\text{BB} = 1$

BS = surround brightness

BB = background brightness

The experimental results show some evidence suggesting that surrounds considerably darker than the background also adversely affect visual performance, i.e., raise the contrast limen. (See Figure 2-45.)

Changing background angle, which determines the proximity of the inner edge of the extended surround to the stimulus object, over a range of from 5° to 45° , even with the highest surround-to-background brightness ratios, appears to have a surprisingly small effect upon the contrast limen (224). The change in threshold is much smaller than that predicted on the basis of experimental results obtained by others using point sources of glare (219, 302). However, findings concerning background angle effects must be interpreted with caution since background angle was only varied from session to session rather than during a given session as was the surround-to-background

brightness ratio. There is reason to believe that factors other than the experimental variables contributed substantially to day-to-day variability. Also some tasks may be more strongly affected by background angle than others.

A log-log plot of contrast threshold versus background brightness ($BS/BB = 1$) showed a very nearly linear relationship over the background brightness range of from 0.17 mL to 18.43 mL (to 129 mL for one subject) tested. The following formula expresses this relationship for the mean data:

$$\log C_{ref} = -0.368 - 0.253 (\log BB) \quad (4)$$

where C_{ref} = Contrast limen (for $BS/BB = 1$)
 BB = Background brightness
 (BS) = Surround brightness

While the effect of glare on visual performance can be of serious consequence by itself, the visual discomfort brought about by glare can also be a matter of some concern. Though the cause is physical, the discomfort brought about by it is often of a subjective nature. The evaluation of discomfort, then, must make use of subjective responses as criteria (13,189, 190,272).

Involved in such procedures is the concept of the "borderline between comfort and discomfort" (BCD) (272). The variables which govern whether a visual environment is comfortable or not include two groups. First are those that are basic to the situation, such as brightness of the (glare) source or luminous area, its visual size, and the brightness of the surrounding field or area and adaptation brightness. Second are certain factors that have a modifying effect, including the position of the source in the visual field, the number of sources in the visual field, and their configuration and arrangement. Indices of discomfort related to these variables are available (155, 191).

The effect of angle of the glare source relative to the visual axis on visual performance has received study (273,278). Sudden glare in the line of sight under conditions of low brightness background has received much study for highway illumination (346). Many of the findings are pertinent to the space environment. They are summarized in Figure 2-46a to d where comparison is made of several studies of glare sources presented on line of sight (219,272, 323). Figure 2-46a and c show the variation expected under different experimental conditions. Figure 2-46b indicates that the equation relating the BCD to adaptation brightness (F) varies as the angular size of glare source in steradians. The equations are of the general form:

$$B = aF^b \quad (5)$$

where B = BCD in footlamberts
 F = adaptation brightness in footlamberts
 Q = source size in steradians and determines values of a and b

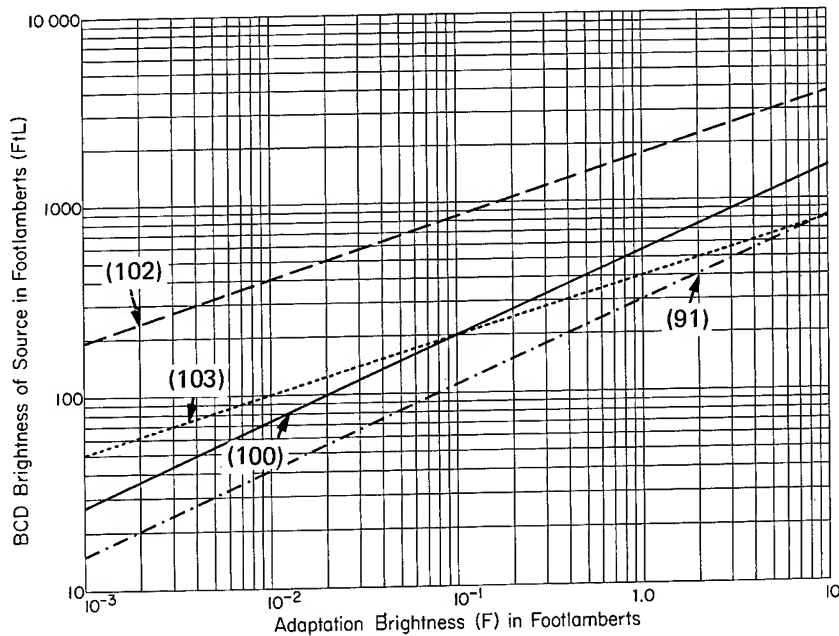


Figure 2-46a

Comparison of the Results of Various Researchers for a Source Size (Q) of 0.0011 Steradian. The Sources Are Located on Line of Sight.

(After Putnam and Faucett⁽³⁴⁶⁾)

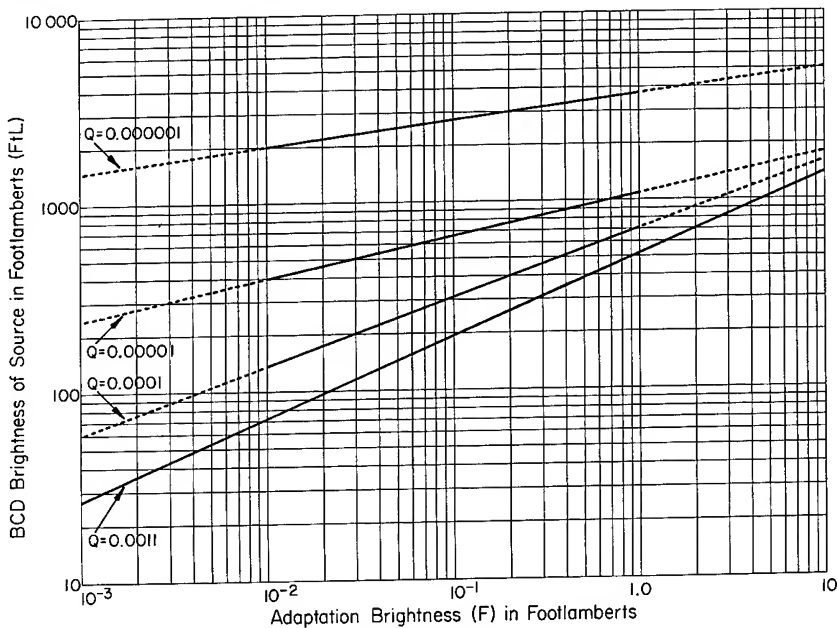


Figure 2-46b

The Relationship Between BCD Brightness of a Source and Adaptation Brightness (F). The Source Is on the Line of Sight and Subtends a Solid Angle of Q Steradians

(After Putnam and Faucett⁽³⁴⁶⁾)

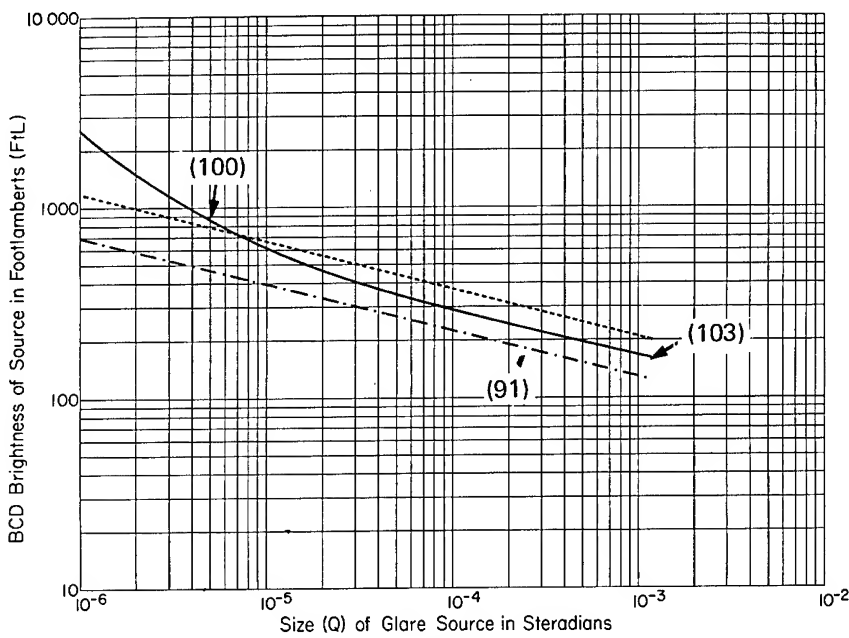


Figure 2-46c

Comparison of the Results of Various Researches for an Adaptation Brightness of 0.10 Footlambert. The Sources Are Located on Line of Sight.

(After Putnam and Faucett⁽³⁴⁶⁾)

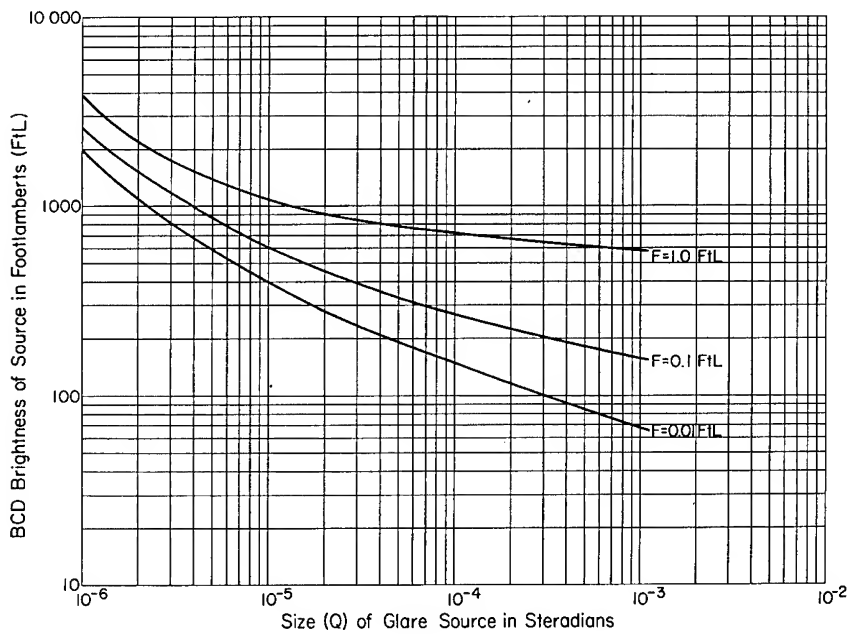


Figure 2-46d

The Relationship Between BCD Brightness and Size of Source for Three Different Adaptation Brightnesses. The Sources Are Located on the Line of Sight.

(After Putnam and Faucett⁽³⁴⁶⁾)

$$\begin{aligned}
 B &= 529F^{0.44} & (Q = 0.0011) \\
 B &= 734F^{0.36} & (Q = 0.0001) \\
 B &= 1115F^{0.23} & (Q = 0.00001) \\
 B &= 3759F^{0.14} & (Q = 0.000001)
 \end{aligned}$$

When these data are plotted for a constant adaptation brightness (F) the curves in Figure 2-46c and 2-46d result. These curves can be represented by the following equations. These equations are all in the general form:

$$\begin{aligned}
 B &= aQ^{-b} + c & (6) \\
 B &= 0.68Q^{-0.60} + 531 & (F = 1.0) \\
 B &= 0.43Q^{-0.62} + 124 & (F = 0.1) \\
 B &= 0.16Q^{-0.68} + 53 & (F = 0.01)
 \end{aligned}$$

The brightness (B) at the borderline between comfort and discomfort is therefore a complex function of the adaptation brightness (F) and the size (Q) of a source when F varies from 1.0 to 0.01 footlamberts and Q from 0.0011 to 0.000001 steradian. The experimental results show that the BCD brightness in these ranges of adaptation brightness and source size does not vary linearly as would be indicated by extrapolations of several investigations (Figure 2-46c). As the glare source becomes smaller than 10^{-5} steradian, the BCD brightness of the glare source becomes greater at an increasing rate, indicating that very high brightnesses may not be uncomfortable if the source is extremely small. Such data are of importance in evaluating glare effects on the Earth, in orbit, and on the lunar surface. In the presence of a non-scattering vacuum the relative effects of glare in distorting the usual cues for depth and size, perception and rate of closure may be altered (367, 410). This will require further study.

Irradiation Phenomena

An observer attempting to measure the boundary between a bright area and a darker area will perceive the boundary to lie toward the darker area. Astronomers refer to this effect as "irradiation" and define it in operational terms as the spreading of a bright image on the retina of the eye making the diameter of any bright object to appear to be larger than it really is (30, 415).

The magnitude of the effect of irradiation on astronomical angular measurements with optical instruments varies with the luminance of the bright limb, the contrast of the bright limb against the background, the optical system used, the dark adaptation of the observer, and the individual observer. In astronomy, corrections for irradiation are empirical and are derived from performance records of experienced observers. For example, the Nautical Almanac uses an irradiation correction of 1.2 minutes of arc for measurements of the altitude of the upper limb of the Sun with the marine sextant.

Several investigations have been performed which are related to the problem of visually sighting a space vehicle near the sun (104, 105). Measures of the minimal angle of resolution (MAR) for two small self-luminous objects against an unilluminated background have also been studied and have indicated that MAR tends to increase as a function of object luminance. For two point sources against different background illuminations, the MAR was found to depend entirely upon contrast and not upon the absolute value of background luminance (325). The MAR increases linearly as a function of the logarithm of the luminance ratio from an I_s/I_b of 100 to at least 5×10^4 . The MAR associated with the highest contrast ratio in this study was found to be 4.0 minutes of arc for glare-source luminance of 4000 ml at a background of 0.07 millilamberts. At luminance ratios of less than 100, the MAR is constant at about 1.8 minutes of arc.

Other of the visual variables involved in celestial navigation will be greatly affected if the observer looks at or near the sun or other intense source. Perception of a moving point source in close proximity to a source of high luminance and the correspondence between physical form and perceived shape are factors to be considered in such a task. The variables include (1) glare-source shape, (2) glare-source intensity, (3) point-source direction of movement in eight frontal-plane meridians, and (4) point-source direction within each meridian. In a recent study of this important problem, five highly trained observers viewed a stimulus configuration through an artificial pupil which provided a $10-1/2^\circ$ field of view (194). The moving "star" was used as a test spot to determine the characteristics of the luminous field gradient produced by the glare source of only 4250 ft L. It was found that the distance, in visual angle, from the perceived edge of a glare source at which a star disappears (or reappears) is directly related to the luminance of the glare source. This appears to be a curvilinear function which accelerates rapidly at about 1000 ft L and again begins to decelerate at about 4000 ft L as shown in Figure 2-47.

This finding is somewhat greater than those obtained for two point sources (325). The star disappears and reappears at different apparent distances from the edge of the glare source, depending upon what kind of edge geometry exists. An example of a straight edge can be found on the sides of the square and triangular mirrors. The edge of the circular mirror provides an example of a curved edge. The star disappears and reappears farther from the curved edges than it does for straight line edges under equivalent luminance conditions. Figure 2-48 presents these data.

The irradiation phenomenon results in distortion of shapes of the object (194, 367). The apparent size of the glare source increases as a function of its luminance. This effect can also be seen in Figure 2-49. The response variance tends to be larger under the higher luminance conditions than under lower luminance conditions; however, variance does not appear to be significantly affected by either the shape of the glare source or the meridian of travel of a test star (194).

It can be concluded that as a result of the irradiation phenomenon, (1) navigational sightings should be confined to a vision envelope which does not include any extremely bright sources aimed in the direction of the eye.

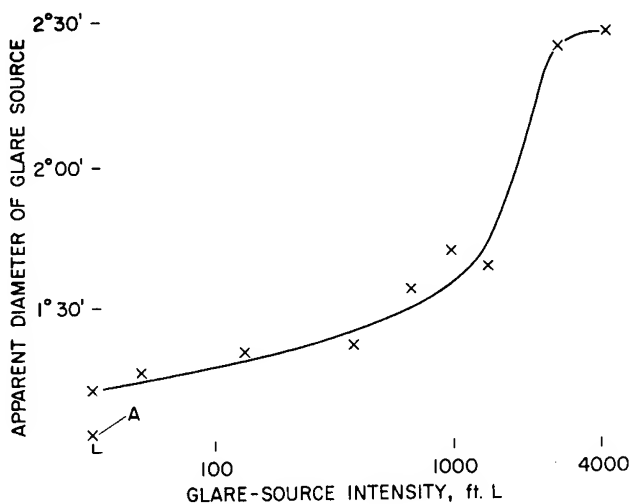


Figure 2-47

Effect of Glare Source Intensity upon Its Apparent Size.

Note: A zero intensity or control condition

After Haines⁽¹⁹⁴⁾

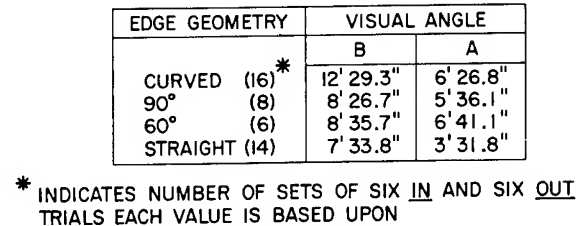
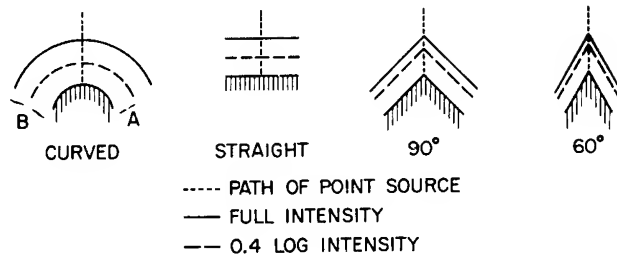


Figure 2-48

Effect of Glare-Source Edge Geometry Upon Point Source Disappearance and Reappearance Position.

(After Haines⁽¹⁹⁴⁾)

(2) Visual identification of highly luminous objects in space, on the basis of their shape, may lead to incorrect identification. (3) If navigational sightings are performed using high luminance sources as reference objects of approximately 2000 ft L apparent luminous intensity or greater, one must expect rather large errors in estimating star eclipse angles (from the edge of the luminous source). (4) Under high luminance conditions one is likely to perceive size and shape characteristics of the glare source which may misrepresent the actual glare producing object. (5) If a star is going to be chosen as a navigational referent with respect to either the perceived edge of the sun's photosphere, which is unlikely, or some man-made object having a high luminance (direct or reflected), optical filters will have to be used to reduce the photic flux to such a level that the physical edge of the referent can be accurately perceived (86, 242, 332).

The recovery time after relatively prolonged exposure to low levels of glare in highway situations has received quantitative study (234). Similar studies are required to confirm the reciprocity law under conditions of lunar and extravehicular operations. The data for exposures of short duration presented below should not be directly used under such conditions.

Flashblindness

In flashblindness the afterimage is essentially a temporary blind area or scotoma in the field of vision. In spacecraft, this could be produced by the flash following meteoroid penetration (365). The time duration of this blind area is proportional to the intensity and duration of the light exposure. The greater the intensity and/or the longer the duration of exposure, the more intense and, to a certain extent, the more persistent the afterimage. Ordinarily, the sequence of events following stimulation of the retina by a flash of

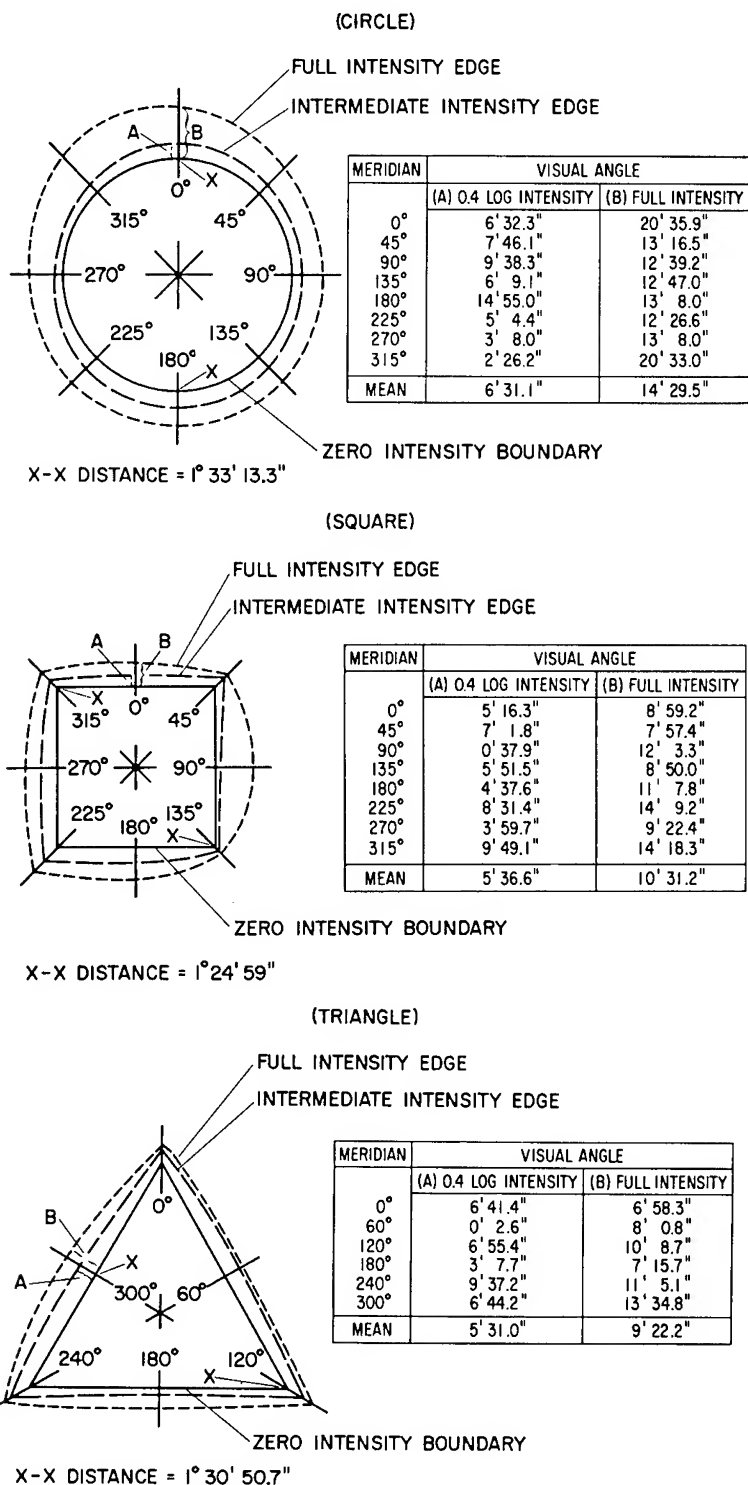


Figure 2-49

Effect of Glare-Source Luminance Upon Perceived Size and Shape of Circles, Squares, and Triangles.

(After Haines⁽¹⁹⁴⁾)

light is the primary sensation of light followed by a series of positive and negative afterimages. With moderate light intensities, afterimages are not noticed because of the complex action of successive stimulation and continuous movement of the eye. However, if the original stimulation is of sufficient duration and intensity, the sensation will persist with an intensity adequate to reduce or entirely obliterate foveal perception until the effect is dissipated. This is the primary factor in flashblindness. Papers from a recent symposium on the loss of vision from high intensity light are now available (2).

The amount of visually effective light entering the eye, because it is an indication of the amount of photopigment bleached, seems to be the essential factor in the formation of the afterimage (63, 95, 297). A useful unit for specifying the amount of visually effective light is the troland-second, because it includes the area of the eye pupil and has the dimensions of retinal illuminance assuming perfect ocular transmission (see Table 2-2). The data may also be presented as cal/cm² at the retina. A glossary of radiometric and photometric concepts used in flash blindness and retinal burn research is available (19).

Attempts have been made to relate the intensity of light flashes to the alterations in sensitivity of the dark-adapted eye. At relatively low illuminances of less than 50 lumens/ft², there is found no alteration in the course of dark adaptation and a general correlation with the reciprocity law for momentary losses of sensitivity (10, 400). The reciprocity law indicates that within certain limits $L \times T = K$ when L is in units of luminance of the dazzle and T is the duration of the dazzle. At a light source of moderate intensity, validity of the law has been confirmed (110, 154, 248). The law appears to hold up to 30,000 m-L-sec. Above this level the effect of intensity factor becomes relatively greater than duration (306). Also, for energy in the range of 3×10^7 troland-sec., reciprocity appears to fall; flash durations of 1 millisecond being less effective than longer flashes (298). Theories on reciprocity failure have been presented (458).

In establishing criteria for visual recovery time after exposure to flash, there is some difficulty in comparing the results of different investigations, because the recovery times depend on the total effective integrated energy in the flash, the duration of the flash, the size of the critical detail in the target used to determine the recovery, and the luminance of the target. The pulse shapes may also be an important factor for the very long durations. The recovery time of visual performance following high-intensity flashes is related to the decay of the afterimage brightness which is a function of the amount of photopigment bleached by the flash. The afterimage reduces the perceived contrast of a visual display in the same manner as the addition of a uniform luminance over the display (297).

Figure 2-50 summarizes data from several studies on effect of flash energy in lambert-seconds and recovery time for perception of targets at two different levels of target illumination. These are higher than the usual instrument illumination levels in night vision (Table 2-60 and Refs. 231).

Figure 2-51 represents the effect of target luminance on recovery time after different flash energies.

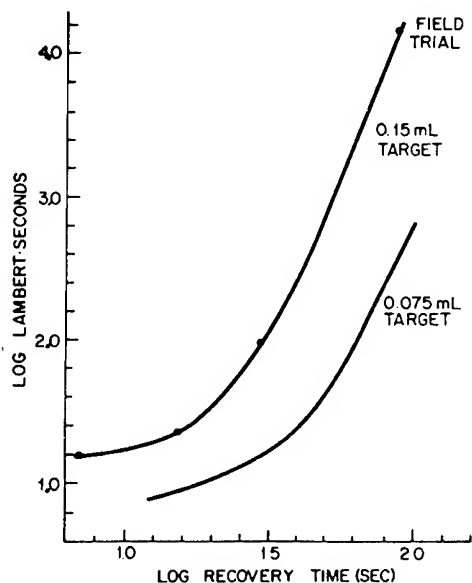


Figure 2-50

The Relationship Between the Logarithm of the Recovery and the Logarithm of the Flash Energy in Lambert-Seconds. Upper Curve from Whiteside⁽⁴⁴⁷⁾ and Lower Curve from Metcalfe and Horne⁽²⁹²⁾ for a Carbon Arc Source.

(After Miller⁽²⁹⁷⁾)

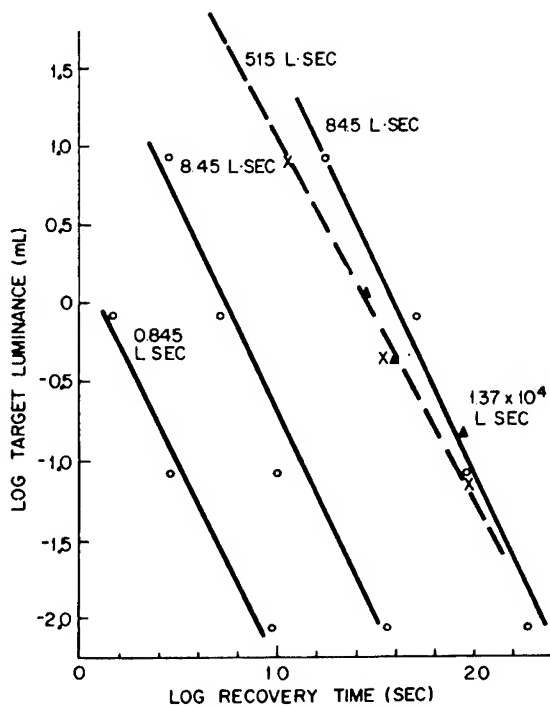


Figure 2-51

The Relationship Between the Logarithm of the Recovery Time and the Logarithm of Target Luminance. O - O from Russell⁽³⁶⁹⁾, x - x from Metcalfe and Horn⁽²⁹²⁾, and Δ from Whiteside⁽⁴⁴⁷⁾.

(After Miller⁽²⁹⁷⁾)

The recovery times following a flash appear to depend on the type of target used for measuring visual performance. There is an approximately linear relationship between the logarithm of the recovery time and the logarithm of the target luminance from 130 mL to 1 mL for the Snellen letters following high-intensity flashes. For luminances below 1 mL, the recovery times became increasingly longer than the simple relationship would predict. This is seen in Figure 2-52 where recovery times at different equivalent illuminance levels for targets of different sizes after varied levels of effective light energy impinging on the retina. Recovery time is measured as the time interval from flash to the first correct letter response in two successive correct responses. The recovery times for the detection of various targets and target luminances can be generalized by specifying the equivalent field illuminance for threshold of the targets. The equivalent field illuminance is the retinal illuminance required for threshold detection of the targets when they are viewed against a uniform field.

There is a linear relationship between the logarithm of the recovery time and the visual acuity for different size Snellen letters expressed as the reciprocal of the critical detail in minutes of arc. The effect of target size is seen in Figure 2-53.

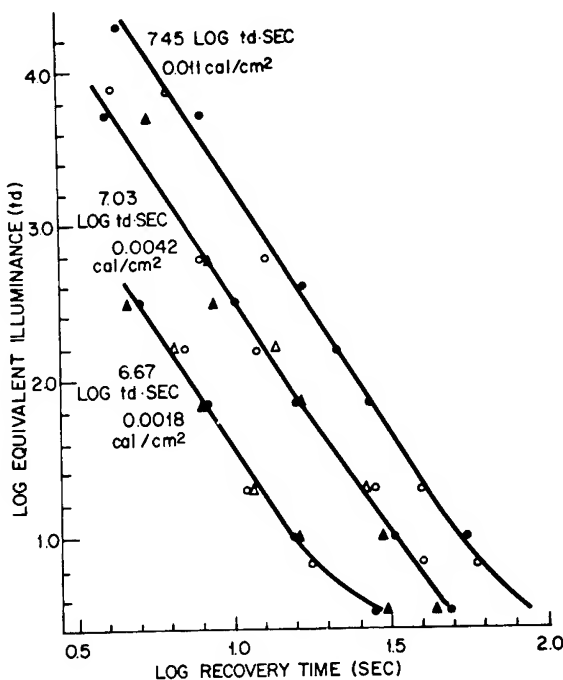


Figure 2-52

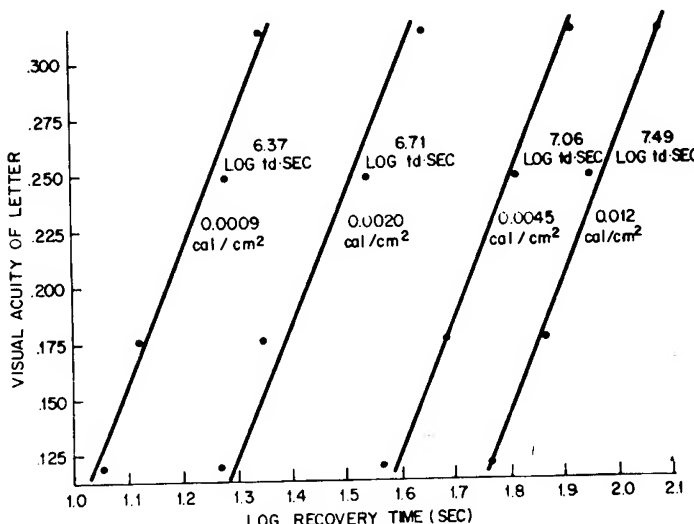
The Relationship Between the Log of the Recovery Time and the Log of the Equivalent Field Illuminance for Different Flash Energies Hitting the Retina (td sec or cal/cm^2). Open Symbols Are Times for a 28.4 Minute Letter; Closed Are for 16.2 Minute Letter. Circles Are for 1.4 msec. Flash with Luminance Varied; Triangles Are for Constant Luminance, Duration Varied.

(After Miller⁽²⁹⁷⁾)

Figure 2-53

Log Mean Recovery Times for 4 Subjects for Various Letter Sizes at 0.07 mL.

(After Miller⁽²⁹⁷⁾)



There is variability from subject to subject in the slope of the recovery function (378, 379). The pupillary factor is demonstrated as seen in Figure 2-54. Figure 2-41 gives expected pupillary diameters for different luminance levels.

The data derived from many sources for the size of the retinal image of a point source are plotted in Figure 2-55a as a function of the pupil diameter. It is evident from Figure 2-55a that the data obtained lack reliability. To be safe, one best assume the course indicated by the dotted line, which means a blur disc of almost constant size, namely 1 min of arc up to pupil diameters of 6 mm. Pupil diameters below 2 mm rarely occur; above 6 mm the increase in incident light hardly produces an increase in retinal light concentration as the light from the pupil border is so badly focused.

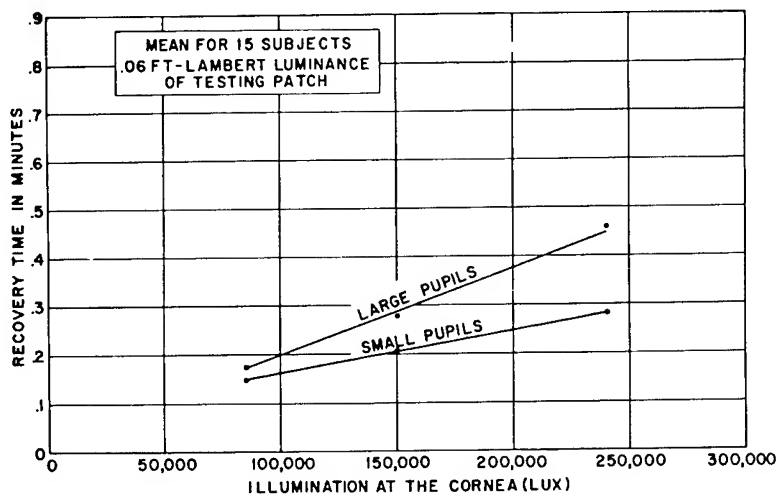


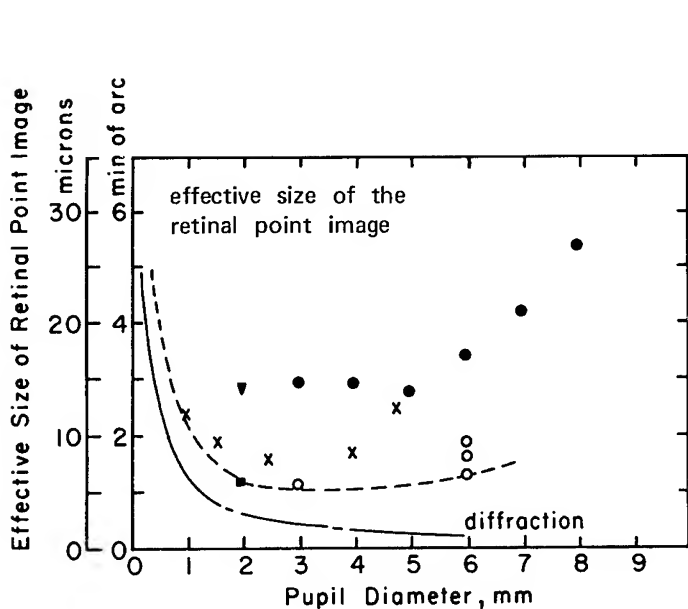
Figure 2-54

Effect of Pupil Diameter on Recovery Times (Mean of 15 subjects).
Luminance of Testing Patch was 0.06 ft-lambert.

(After Severin et al⁽³⁷⁹⁾)

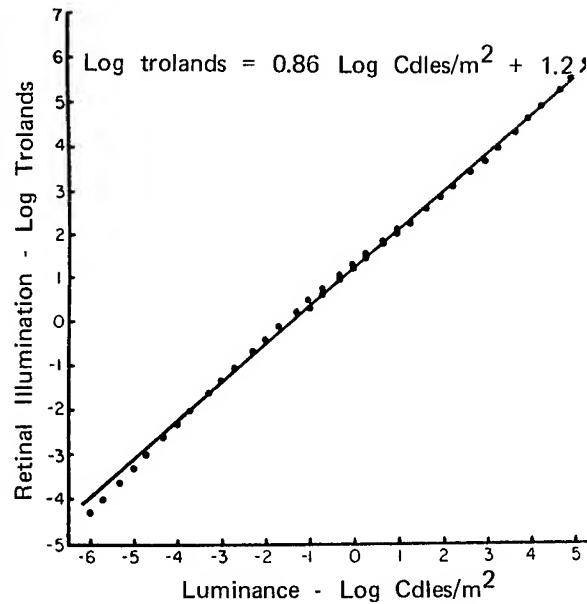
Figure 2-55

Retinal Illumination and Image Size Under Different Pupillary and Ambient Light Conditions.



- a. The Minimum Size of the Retinal Image of a Point Source as Derived from Several Investigations (See text)

(After Vos⁽⁴³⁰⁾)



- b. Retinal Illumination as a Function of Luminance.

(After Hill and Chisum⁽²¹⁶⁾ and from data of LeGrand⁽²⁶⁰⁾)

Retinal illumination as a function of the luminance of the visual field with pupil size taken into account is shown in Figure 2-55b. The retinal illumination changes only 0.86 log unit for each log unit change in luminance of the visual field.

Other recent findings are available and can be summarized (297): The only wavelengths of radiation in the flash that influenced the recovery times for foveal performance were those in the visible region. Infrared beyond 850 nm had no effect on recovery following the flashes, even when it accounted for more than 50% of the total flash energy. There is no significant cumulative effect on recovery times with successive flashes after the second flash when they were presented at intervals of 3 or 4 minutes. There is a small but statistically significant effect on foveal recovery times for different flash-field diameters from 2.5° to 10° . The smaller fields produced longer recovery times of the order of 10%. Preadaptation to relatively high-luminance levels lengthens the recovery time in proportion to the amount of photopigment bleached by the preadaptation. The amount of pigment bleached by the flash will be in addition to that caused by the adapting luminance.

Attempts have been made to write equations for visual recovery times after flash exposure. One equation appears to afford the best fit for all observers. This was an equation of the following form (75):

$$t - t_0 = a + b / (\log B - \log B_0) \quad (7)$$

where t = perception time in seconds

t_0 = 0.20 sec for all conditions of adaptation

B = display luminance in ft L

B_0 = minimum luminance at which the display can be perceived under optimum conditions.

(-1.4 log ft L for visual acuity of 0.26;

- 2.3 log ft L for visual acuity of 0.08.)

Perception time t must approach a minimum t_0 as display luminance B is increased, and it may safely be assumed that a value B will be reached beyond which there will be no further reduction of t . If this is the case, then the constant, a , must be of the following form:

$$a = -b / (\log B_{\max} - \log B_0) \quad (8)$$

where B_{\max} is the luminance at which t_0 is reached.

Assuming a value of 2.7 for $\log B_{\max}$, equations (7) and (8) can be combined and rewritten as follows:

$$t = 0.2 + b \frac{(2.7 - \log B)}{(\log B/B_0)(2.7 - \log B_0)} \quad (9)$$

It was found that the logarithm of b is proportional to the logarithm of A for data representing both of the two acuity levels, where A represents adapting flash energy in ft L sec. A simple power function therefore serves to relate b to A :

$$b_{0.08} = 0.108A^{0.58} \quad (10a)$$

$$b_{0.26} = 0.022A^{0.68} \quad (10b)$$

The difficulties presented by failure of the reciprocity law at short flash durations of less than 1-3 msec. have been pointed out (75). Equations are also available for the retinal burn problem (196, 307, 308, 431) and planning charts, for flashblindness and retinal burns following nuclear blasts (10).

Retinal Burns

Illumination at the eye of 240,000 lumens/ft² represents the probable level required for retinal burns. This is also given as 0.5 to 1.5 cal/cm² (118). This energy must be delivered at a rate of at least 0.7 cal/cm²-sec, however, or the rate of heat dissipation in the tissue will be sufficient to prevent elevation of the temperature to a degree where a burn will result. The threshold appears to depend upon the time of irradiation and upon the size of the irradiated area. See compilation of results available which leads to threshold data as shown in Figure 2-56. The data of Figure 2-55 may be used to arrive at values of J/cm² at the retina for external illumination.

Two solutions to the meteoroid or other flash problems are either to prevent the light from reaching the eye or, if this is impossible, to increase the luminance of the instruments after exposure of the eye by flooding them with white lighting (365). Auxiliary storm lights have been used in aircraft for years to combat the relatively mild flash blindness (afterimage formation and loss of dark adaptation) resulting from exposure to lightning flashes. Such lights could probably be used after meteoroid flash as well as after sudden exposure to other sources giving scotomatic glare effects.

Visor materials can attenuate light flashes. When a given filter is placed before the eyes, the change in retinal illumination depends not only on the visual transmittance of the filter but also on the size of the pupil. The size of the pupil, however, varies inversely with retinal illumination. Thus, if the retinal illumination is decreased, the pupil will increase in size and vice versa. Because of this interaction between pupil size and retinal illumination any change in luminance of the visual field will result in a final level of retinal illumination which depends on the change in pupil size as well as the change in luminance. The effective density of a filter is the ratio of the retinal illumination with the filter in front of the eyes to the retinal illumination without the filter. Figure 2-55b indicates that retinal illumination changes only 0.86 log unit for each log unit change in the luminance of visual field behind the filter. It must be remembered, however, that flashes shorter than the pupillary reaction time are attenuated only by the filter factor.

Data on the transmission of light through standard visor materials are available (4, 82, 87, 216). The Class 3, gold-coated visors were designed for eye protection against weapon flashes and are MIL-L38169(USAF)

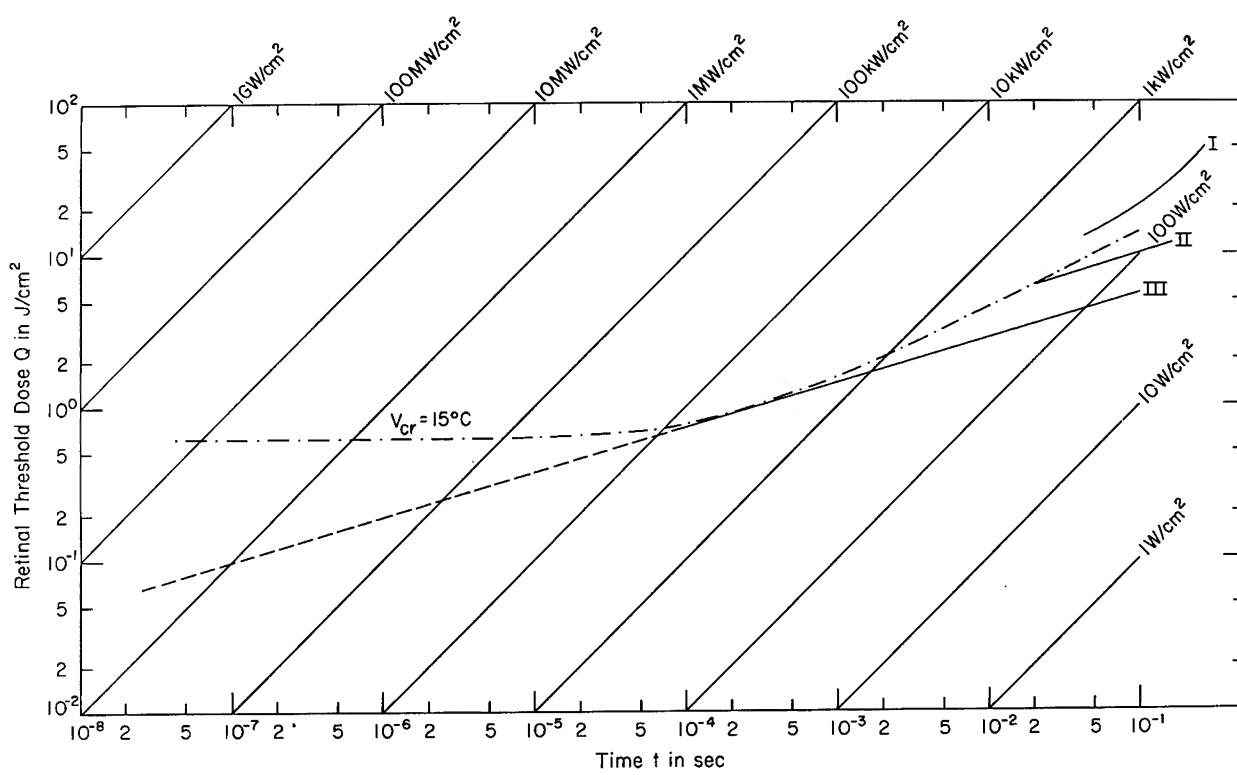


Figure 2-56

The Maximum Dose Q (in J/cm^2) to Produce Retinal Burn, as a Function of Time of Irradiation, with the Irradiated Retinal Area as Parameter. Note that the Threshold Level Is Lower in the Later Experiment Due to Better Diagnostic Techniques. I. Ref.196 Image Size 240μ . II. Ref.196 Image Size 700μ . III. Ref.197 Image Size 1000μ .

(Adapted by Vos⁽⁴³⁰⁾ from Data of Ham et al^(196, 197))

and MIL-V-22272B (WP). The specified luminous transmittances for these visors are 2 percent \pm 0.5 percent and 2.75 percent \pm 0.25 percent respectively. The corresponding optical densities are 1.70 plus 0.12, minus 0.10 and 1.56 plus 0.04, minus 0.02 respectively. The relative difference in retinal illumination that the eye would receive from a light flash is 0.86 log units for each unit of density of a fixed filter visor as compared to when no visor is worn. Therefore, the effective densities of the Class 3 visors with nominal densities of 1.70 and 1.56 are 1.46 and 1.34 respectively. (See Section B.Ultraviolet for ultraviolet transmission of these fixed visor systems.)

The use of reversible, variable-density, filter devices to reduce glare and flashblindness in high risk environments has been studied (70, 116, 124, 242, 332). A survey of photochromic materials for potential use in variable filter devices is available (37). The effects of blue-cutoff filters used in photochromic goggles on color discrimination are under study (94).

Laser Burns (Coherent Light)

Design of lasers for navigation and other purposes in space operation brings a new hazard to the skin and eye. Several excellent reviews are available on this subject (196, 197, 221, 249, 267, 268, 279, 315, 338, 430, 464, 465, 466).

All structures of the eye can be damaged, but the retina is the most sensitive structure. Thresholds of retinal damage for different wavelengths are under study and speculation (208, 430, 431, 425). Theories of damage span the gap from pure thermal burn (see Figure 2-56) through explosive steam damage, shock waves, Raman and Brillouin scattering, to ionization from intense electric field gradients (208, 342). Failure of the pure thermal model is especially prominent in the giant pulse, Q-switched laser with the actual threshold ten times lower than expected. Here even for minimum image size, the retinal image acts infinitely large (430).

A conservative practice appears to be limitation of total integrated energy into the eye of less than 10^{-8} Joules for pulsed beams (237, 238, 239). For pulses greater than 30 nanoseconds, an energy factor of 5 times lower should probably be used but no specific recommendations have been made (237, 238). Neither have specific recommendations been made for lasers of shorter wavelength than 633 nm. For purposes of calculations, in the green spectral region, the allowable energy level of 10^{-8} J might be reduced slightly due to the shorter wavelength and increased absorption in the pigment epithelium.

For continuous lasers, the power level in the eye should be kept below 10^{-6} watts.

The BG-18 and A0570 glasses have been recommended for laser protection (237, 238, 239, 398, 430). Standard BG-18 glass is approximately 4.5 mm thick and has an optical density of 10 at 694 nm to $1.3\ \mu$ which includes the two most common pulsed lasers. Using the University of California criteria for pulsed lasers, this would appear to be satisfactory for a 100 Joule laser pulse (237, 238). It should be remembered that glass may not retain its integrity with such an exposure. Spalling occurs above 2 cal/cm^2 irradiation densities with a neodymium Q-switched laser; yet even at 8 cal/cm^2 , the filter, though cracking, remains to give adequate protection. It has been advised to construct the filter of two cemented halves, so that only the front half cracks under extreme exposure without impairment of its optical safety (398). For this reason, a limit of 20 Joules for the 4.5 mm glass is recommended over the spectral region given above. No direct viewing of pulsed lasers should be allowed regardless of the eye protection used.

At 694 nm the BG-18 glass is increasing its transmission rapidly with decreasing wavelength. It therefore is not applicable for the common HeNe gas laser operating at 633 nm. For continuous lasers the AO-570 glass is used. This glass has an appreciable attenuation at 633 nm with an optical density of about 4.2. Using the University of California criteria this glass would then attenuate sufficiently for lasers of about 30 mW at this wavelength. In actual practice AO 570 glass is recommended for use at power levels up to 100 mW over the spectral region from 633 nm to $1.0\ \mu$. This continuous power is allowed because the critical value of 10^{-6} watt entering the eye contains somewhat more safety factor than is necessary for this portion of the spectrum.

Other approaches have been used for calculating the thickness of BG-18 glass required for protection against different laser types (430). These

equations cover both the near-distance situation where the complete beam enters the pupil and the far-distance situation where magnification of collimating optics and telescopic systems as well as the specular reflection of windows and metal surface must be accounted for. No official U. S. Government Standards have been published, but the issue is currently before the NAS-NRC Committee on Vision.

Skin Effects

The threshold of pulsed laser effects for human skin damage varies with color. White skin of Caucasians has tolerated energy as high as 5-10 Joules without change. At these levels, Negro skin will scale superficially, char, crust, - even ulcerate (175). Above 20-25 Joules in white skin, acanthosis and bizarre nuclei are seen. At about 100 Joules, anesthetic areas and vascular changes are found. Skin burns are covered in greater detail in the Thermal Section, (No. 6).

Environmental Factors in Vision

The acceleration, vibration, oxygen, and nutritional conditions can significantly alter visual performance. The interactions will be covered in the appropriate Sections. (See Sections, No. 7, 8, 10, and 14).

Toxic and Drug Effects on Vision

The most probable toxic material in a spacecraft atmosphere effecting vision is carbon monoxide. Figure 2-57 shows the effect of this gas upon visual light sensitivity. See also Contaminants (No. 13).

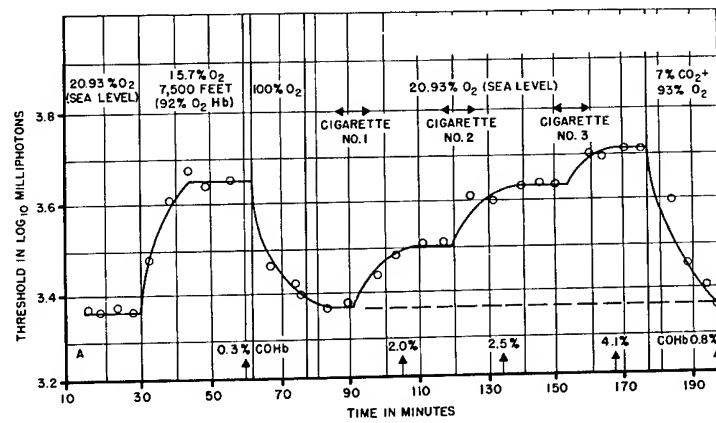


Figure 2-57

The Effect of Smoking on Visual Light Sensitivity as Compared with the Effect of Altitude.

The Effect of Inhaling the Smoke of Three Cigarettes Is Equal to an Altitude of About 8000 Feet.

(After Wulfeck et al (462) Adapted from McFarland (281))

The effects of drugs on the visual system are complex, especially the psychotropic drugs which alter the sensorium at the higher centers. A recent review of this area covers most of the key factors to be involved (14 , 66 , 331, 345, 414, 440). Such factors must be considered in the choice of drugs for use in space operations (84).

Visual Performance in Actual Space Flight

There appears to be no severe effect of orbital flight on visual performance. Preflight, inflight and postflight tests of the visual acuity of the members of the Gemini V and Gemini VII crews showed no statistically significant change in their visual capability in zero gravity (131).

Observations of a prepared and monitored pattern of rectangles made at a ground site near Laredo, Texas, confirmed that the visual performance of the astronauts in space was within the statistical range of their respective preflight thresholds. Observations of the Texas ground-pattern site were made under very favorable weather conditions. Heavy clouds blanketed the site throughout the remainder of the mission, however, and no further observations of the site were possible. Successful observations of the ground pattern were made by the command pilot through a clear portion of his window. No direct sunlight fell on the window during those observations. These observations occurred at 27:04:49 and 49:26:48 ground elapsed time (g.e.t.) on the second and third days of the flight, respectively. The circled points represent the apparent contrast and angular size of the largest rectangles in the ground pattern. Apparent contrast was calculated on the basis of measured directional luminances of the white panels and their backgrounds of plowed soil, of atmospheric optical properties measured in the direction of the path, of sight to the point of closest approach, and of a small allowance for contrast loss in the spacecraft window based upon window scan data and readings of the inflight photometer at the time of the two observations. Angular sizes and apparent contrast were both somewhat larger for revolution 31 than for revolution 17 because the slant range was shorter and because the spacecraft passed north of the site, thereby causing the background soil to appear darker. The orientations of those rectangles indicated by double circles were reported correctly, but those represented by single circles were either reported incorrectly or not reported at all. The solid line in Figure 2-58 represents the preflight visual performance of Borman as measured in the vision research van. The dashed lines represent the $-\sigma$, $+\sigma$, and $+2\sigma$ contrast limits of his visual performance. The positions of the plotted points indicate that his visual performance was precisely in accordance with his preflight visual thresholds.

The result of Soviet visual studies in orbit are not much different from those in the U.S.A. (344). Visual acuity of Leonov and Belyayev in Voshkod-2 were measured by hatched mires placed at 300 mm from the eye. Both cosmonauts had visual acuities of 1.7 in the laboratory. In orbit, these decreased to 1.64 for Leonov and to 1.34 for Belyayev. Visual efficiency as measured by reliability was reduced by 20 to 25%; and working time, by more than a factor of 2. The degradation of efficiency was attributed to uncompen-

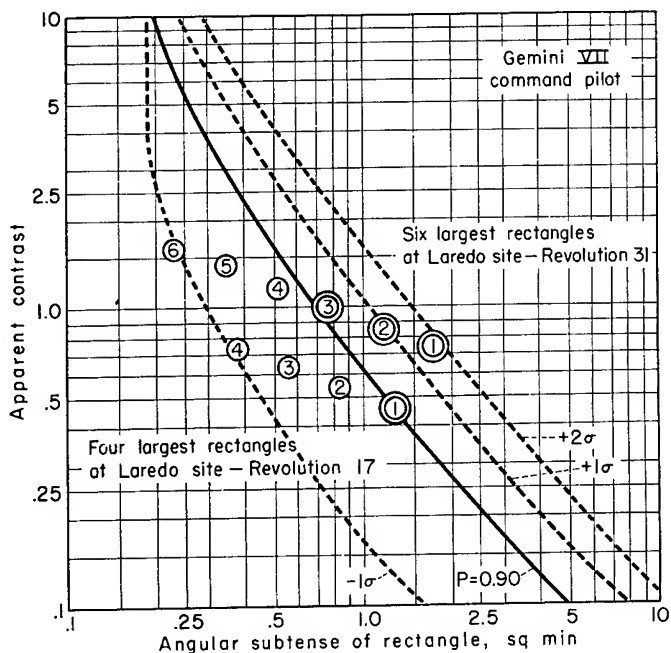


Figure 2-58

Apparent Contrast Compared with Angular Size of Rectangles in Gemini VII. (See text for details.)

(After Duntley et al⁽¹³¹⁾)

sated changes in coordination of oculomotor movement brought about by weightlessness. However, no data are present to support this contention.

Color vision was tested in flight by having the cosmonauts compare the intensity of the colors red, green, blue, light blue, purple, and yellow with the intensity of staggered black and white wedges. The wedges made it possible to measure the intensity of objective colors within an error of 5 to 6 percent for the averaged measurements. By establishing responses for different conditions of color adaptation, simultaneous and consecutive contrast, etc., a mean quadratic error of the monomial equation for the intensity of the colored and black and white fields was obtained. The measurements made at different times with the use of different charts showed that the value of the error for the colors used amounted to $\pm 7.8\%$. In Vostok-2, the mean decrease in intensity for all colors tested was 26.1% for Belyayev and 25% for Leonov. The maximum deviations were for purple, light blue and green; and the minimum, for red. The reasons for this change in color perception are not known.

One of the surprises in the manned space flight program has been the ability of astronauts to perceive unexpectedly fine detail on the surface of the earth. L. G. Cooper's visual acuity on the Mercury-Atlas 9 flight was measured as 20/12 on the Snellen scale, versus the conventional 20/20 as "perfect" (121). E. H. White on Gemini 4, also from an altitude somewhat over 100 miles, reported that he too could see roads, boat wakes, strings of street lights, airfield runways and smoke from trains and buildings. Whereas previous estimates for the resolving ability of the human eye, with white-black contrast, were about 1 minute of arc, these observations demonstrated an ability to resolve a half a minute or less (121, 344). These results come in the face of the above suggestions that if any change in visual acuity were to be found in men in space it would be a minor degradation in ability.

The simplest explanation is the fact that many of these targets were of linear shape. The width of lines and bars can be resolved more easily than circles of the same diameter (see discussion of Figures 2-19 to 2-22). One must also include previous experience of the astronauts in detecting landmarks from secondary cues. However, it must be remembered that photographs taken by the astronauts have tended to be more distinct than pictures taken from high-altitude aircraft. Edward White reported that indeed he could see much greater detail on the surface from 100 miles than he could when flying at 40,000 feet. Photographs taken during the Gemini 4 flight, for example, revealed a dark, finger-like streak through the terrain of central Texas that was unknown to geologists despite the fact that the terrain had been surveyed by aerial photographs (85).

A possible explanation of the superior photographs, bearing also on the superior visual acuity, stems from local turbulence in the atmosphere, small nonhomogeneous bubbles in the atmosphere and dust particles in the atmosphere (121). The first two phenomena tend to distort and blur fine image details when they intervene between viewer and target, but the effect will diminish as a function of the distance from the effects since the angle they project relative to the target will diminish. The dust particles can cause back-scattering of light, increasing background luminance and reducing contrast, but again with an effect diminishing with range. These phenomena cannot fully explain an increased human acuity in space, however, because the limit of 1 minute of arc has been derived over the years under laboratory conditions in which, of course, atmospheric effects do not bear on the results. Given an excellent lens, sensitive film and the proper exposure, a camera can see whatever light reaches it, but the eye has an intrinsic threshold both for light energy and contrast beyond which it does not respond. What space flight suggests is that this threshold is lower than had been supposed; remove gravity and possibly the eye can operate more effectively as a sensor, approaching or perhaps reaching its threshold.

Further evidence is provided by a series of zero-g aircraft experiments which found an increase in man's ability to discriminate brightness while weightless, the difference being greatest at the lowest illumination levels (443). By measuring the difference in illumination between the brightness of the target and background required for the subjects to perceive that a difference exists, USAF's Aerospace Medical Research Laboratory found the following improvements in zero g as compared to baseline 1-g measurements:

Illumination (ft-lamberts)	Maximum Difference in Illumination for Detection (%)	
	1 g	0 g
0.03	15.1	12.6
0.28	7.1	6.5
30	4.5	4.0

Since the brief period of weightlessness aboard the aircraft immediately followed a positive g pull-up, it is possible that the eyes of the subjects were sufficiently affected by the increased gravity to bias the results during zero-g before the lens had time to recover.

The effect of zero gravity to improve vision can be two-fold. On the one hand the removal of friction and damping forces on the eye produced by gravity can permit the eye motions to proceed more efficiently in correcting drift. On the other hand, it is possible that part of the explanation for the observed increase in visual acuity lies in part in the effect of weightlessness on the vestibule mechanisms of the inner ear. The effect on the vestibular mechanisms may be such to encourage physiological nystagmus in such a manner as to aid vision by the normal technique of eye motion (143). Electro-oculograms of Soviet cosmonauts have in fact provided evidence that asymmetric oculo-motor reactions and nystagmus are different in orbit from those observed on the ground (7 , 254). (See also Acceleration, No. 7.) More work is required on the oculo-vestibular interaction in zero gravity before this hypothesis can be incorporated into the explanation of enhanced visual acuity in space-to-Earth observation.

These findings suggest that laboratory visual acuity data can be combined with environmental optical data to predict correctly man's limiting visual capability to discriminate small objects on the surface of the Earth in daytime under routine orbital conditions. Data are also available on the visual observation of other planets from space (351). A new vision tester for use in future space missions is currently under study (218). Attempts are being made to generate computer programs for prediction of space-to-planet visual capabilities under the many different operational conditions (130).

Data on the observation of stars from Mercury and Gemini spacecraft are covered in the discussion of Figures 2-9 and 2-12 (15 , 445). Little from the reports of the astronauts indicates that the accelerative forces encountered in space flight have had a detrimental effect on vision. The only case of affected vision was reported by Shepard (383). At one point some head vibration was observed. The degradation of vision associated with this vibration was not serious. There was a slight fuzzy appearance of the instrument needles. At T + 1 min 21 sec, he was able to observe and report the cabin pressure without difficulty. The indications of the various needles on their respective meters could be determined accurately at all times. Grissom (184) reported no interference with communication or vision which would seem to confirm Shepard's conclusion that the degradation was due to vibration rather than to acceleration. With respect to the g force experienced during reentry, Shepard reported (383) that reentry and its attendant acceleration pulse of 11 g was not unduly difficult. The functions of observation, motion, and reporting were maintained, and no respiration difficulties were encountered. Glenn noted large oscillations at the end of powered flight but made no note of visual degradation (317).

In the Gemini program, the launch has been free from any objectionable vibration with one exception. On the Gemini V flight, longitudinal oscillations, or POGO, were encountered. The crew indicated that the vibration level was severe enough to interfere with their ability to read the instrument panel. However, POGO lasted only a few seconds and occurred at a non-critical time during this one flight. Unpublished data are available at NASA Ames Laboratory on human response to POGO-like longitudinal vibrations (eyeball in and out) obtained in simulator studies (88). The Saturn boosters appear to have POGO problems.

VISUAL CONSIDERATIONS IN THE DESIGN OF THE SPACECRAFT CABINS AND SPACE SUITS

The preceding data have been presented so as to allow prediction of visual capabilities on the ground and in space. They can be used for specific problems in operational analysis as well as design. The following section covers the general design recommendation for spacecraft illumination, instrumentation and displays considering overall habitability as well as specific operational problems.

General Recommendations for Spacecraft Illumination

Experience in submarines and naval vessels has provided guidelines for optimizing the visual background and decor within the spacecraft. The following suggestions are offered as a result of this and other experiences (5, 48, 152, 271, 301, 389, 412, 419).

In the design of the lighting subsystem, it is necessary to consider those factors which are basic to the provision of artificial illumination most adequate for maintaining comfortable, healthful and effective functioning of normal eyes. These factors are: quality or color of light, intensity of light, and distribution of illumination and brightnesses within the environment. Arrangement of these factors should give compartments a more pleasing appearance and proportions; all three should be combined to induce in the occupants a sense of tranquility, comfort, and "hominess".

The use of color, as a characteristic of a reflecting medium, will be considered in more detail later. Illuminants, however, which vary in spectral characteristics, have an inherent color, which in laboratory situations, at least, affects to some extent the visual acuity. For threshold seeing, spectral yellow, or the yellow light from sodium vapor lamps, is somewhat more effective than other artificial illuminants, although the difference is not of operational significance and does not improve the acuity over that from a similar level of diffused daylight. In ordinary situations (e.g., print reading) the qualities of daylight, mercury arc light, tungsten filament light, and fluorescent lamps are all about equally effective as illuminants, although fluorescent light has been criticized because of its harsh, cold appearance.

The intensity of light has to be considered in relation to: 1) visual acuity; 2) size of object to be discriminated; 3) speed of vision; 4) brightness contrast; and 5) efficiency of performance (48). These have been covered in the previous section. These data suggest that visual acuity increases rapidly up to about 5 foot-candles, and more slowly thereafter, when the object to be discriminated is of about 3-6 minutes of arc. For smaller objects, vision improves perceptibly up to 40 to 50 foot-candles. The greater the brightness contrast, the better is the visual efficiency, and both acuity and speed of vision continue to improve slightly up to and beyond 100 foot-candles. However, little is gained in acuity by increasing the illumination beyond 25 foot-candles, and there is no practical gain at all when the intensity is higher than 50 foot-candles. For large objects,

subtending four minutes of arc and above, there is no practical improvement in visual discrimination with illumination above 20 foot-candles. For smaller objects, there is improved visual discrimination at higher levels up to a limit of about 40-50 foot-candles.

The data on speed of vision may be summarized as follows: a) for objects subtending three minutes of arc or larger, and with good contrast between object and background, speed of vision is near maximum at about 15-20 foot-candles; b) for small objects on a background of low reflectance significant decreases in time for seeing occur with illumination intensities up to about 50 foot-candles.

With respect to brightness contrast, when the contrast between object and background is high, discrimination of arc sizes of three to six minutes is not significantly improved by illumination above 20 foot-candles. With an object of 1-minute size, performance improves significantly up to a practical limit of about 50-60 foot-candles. The greater the brightness contrast, the better is the visual discrimination, although, as will be noted in the examination of light distribution, the effort of seeing is more fatiguing with high contrast. Excessive illumination will not compensate for small object size or poor contrast.

Brightness contrast is also of significance in consideration of distribution of illumination, and in this connection it must be distinguished from glare. The effects of glare can be minimized by increasing the brightness contrast between the object and its immediate background, and by increasing the illumination on the visual object. Elimination of the glare source, however, by removal, or by use of diffuse or indirect lighting, is superior. For best overall vision, with minimum fatigue, the brightness ratio between the central field and surround should not exceed three or five to one; ratios of ten to one should be avoided (Figure 2-45). The extent to which excessive brightness contrast is diminished is largely determined by the degree to which the lighting is indirect, that is, reflected from all directions. When light is properly diffused there are no shadows, no dark corners, and no areas of relatively high brightness. Light fixtures in the field of vision should have a surface brightness of not over 2 candles per square inch and preferably less (412). Thus, vision is generally best when the surround is at the same brightness as the central field unless the visual object approaches the thresholds of acuity or discrimination, in which case, supplementary lighting can be utilized to increase the brightness ratio, provided the latter does not exceed three or perhaps five to one (271). Intensity and distribution, however, must be coordinated. To increase intensity without distribution will only make a bad situation worse. In fact, when distribution is poor, relatively low intensities must be employed to avoid visual discomfort.

In relation to illumination, color serves two purposes in the perceived environment. It determines the reflectance of colored objects in that environment, and it has a psychosocial influence on the emotional set of individuals in that environment. From the point of view of visual perception, the reflection factor of walls, ceilings, and furnishings of any living or working space is more important than the color used, since the reflecting

surfaces become, in effect, secondary sources of illumination. The reflectance of a surface is the ratio of the light flux reflected from the surface to that striking the surface. Dependent upon the surface, it may be diffuse, specular, or compound. Diffuse reflectance arises from a matte surface; specular reflection comes from a highly polished (mirror) surface and gives rise to glare. A compound surface has qualities of both. The color of an object arises out of selective reflectance and absorption of particular wavelengths of the incident light. For any specified level of illumination a region with highly reflecting surfaces requires a less intense light source than one with low reflecting surfaces. Table 2-59 indicates the reflectance factors for various surface finishes.

Table 2-59
General Reflectance Factors for Various Surface Finishes

Color	Percent of Reflected Light	Color	Percent of Reflected Light
White	85		
Light cream	75	Dark gray	30
gray	75	red	13
yellow	75	brown	10
buff	70	blue	8
green	65	green	7
blue	55		
Medium yellow	65	Wood finish	
buff	63	maple	42
gray	55	satinwood	34
green	52	English Oak	17
blue	35	walnut	16
		mahogany	12

(After AFSCM 80-3⁽⁵⁾)

Recommended workplace reflectances for different areas include the following: console panel 20-40%; instruments 80-100%; floors 15-30%; walls 40-60%; ceilings (i.e., above eye level) 60-95% (5).

For decorative purposes, contrast is desirable. Lack of contrast variation tends to be monotonous and undesirable. Good decorative schemes cannot readily be achieved with a one to one ratio. The blending of highlights and shadows adds attractiveness to the living space, and can be better achieved with higher ratios, while still remaining within acceptable limits. It should be recommended, however, that the unique characteristics of space system stations, such as restricted internal volume, irregular compartment configurations, multipurpose regional usage, compact working consoles, and special power supplies, may make application of conventional illumination standards inappropriate.

General recommendations for instrument, cockpit and console lighting for aircraft are consolidated in Table 2-60 and should be applicable to work areas of spacecraft. An extensive review of illumination recommendations for specific visual tasks is available (183). Charts, tables and calculation sheets have been prepared to aid the designer in rapidly calculating lighting distribution and average illumination conditions in symmetrical rooms (324).

Table 2-60
Instrument, Cockpit, and Console Lighting

CONDITION OF USE	RECOMMENDED SYSTEM	BRIGHTNESS OF MARKINGS	BRIGHTNESS ADJUSTMENT
Instrument lighting, dark adaptation critical	Red flood, indirect, or both with operator choice	.02 to 0.1 ft.L	Continuous thru range
Instrument lighting, dark adaptation not critical	Red flood or low color temperature white, indirect or both with operator choice	.02 to 1.0 ft.L	Continuous thru range
Instrument lighting, no dark adaptation required	White flood	1 to 20 ft.L	May be fixed
Control console lighting, dark adaptation required	Red edge lighting, additional red flood lighting desirable.	.02 to 1.0 ft.L	Continuous thru range
Control console lighting, dark adaptation not required	White flood	1 to 20 ft.L	May be fixed
Possible exposure to bright flashes	White flood	10 to 20 ft.L	Fixed
Simulated instrument flying (blue amber)	White flood	10 to 20 ft.L	Fixed
Very high altitude, daylight restricted by cockpit design	White flood	10 to 20 ft.L	Fixed
Chart reading, dark adaptation required	Flood, operator's choice of red or white	0.1 to 1.0 ft.L on white portions of chart	Continuous thru range
Chart reading, dark adaptation not required	White flood	5 ft.L or above	May be fixed

(After Baker and Grether⁽²⁵⁾)

Role of Color in Habitability (152)

The psychosocial aspects of color have received much study (40, 41, 42, 327). Color is perceived within the context of texture and setting. Sometimes it is identified with a surface, sometime with a volume, a film, an illumination, or illuminant. The perception of color is determined by the factors outlined in Figures 2-28 to 2-31 but is influenced by the mental set. It is more than the mere consciousness of color, or even consciousness of modes of appearance of color, but is influenced by the connotations of the color and its associations in the light of past experience. Distinctive color preferences exist. Studies of numerous investigators show the following order of preference of six common colors among over 20,000 observers: blue, red, green, violet, orange, yellow (142).

Although dominant wavelength, or hue, is significant in the determination of color preference, luminance (or reflectance), and purity, are also important. The appeal of a color increases with increasing luminance until

the comfort limit is exceeded, following which there is an increasingly violent loss of appeal. Somewhat similarly, appeal increases with increase in purity up to the spectrum limit in many individuals, although a substantial minority favor weak unsaturated colors (327). The increase in affective value noted in these circumstances is in relation to tests with very small areas of color; it is probable that when areas are large, as in compartment walls, these factors do not apply. The size of the colored area, saturation or tint, hue or shade, and harmony of color patterns tend to combine to give specific emotional responses (152, 327, 412).

Thus, color should provide both reflecting surfaces and pleasing combinations. Saturated colors and color of low reflectance should be avoided on large areas; tints of appropriate color should be used instead. A proper proportion of reflectance should be maintained on consoles, panels, instruments, floors, ceilings, and walls. Variety in color of decoration is desirable. To maintain a pleasing environment, with appealing contrasts, different colors should be used in the same compartment, and still different combinations in other compartments. Tints and light grays possess several advantages; they make a compartment appear more spacious and ceilings appear higher. Some of the favored colored tints are buff with umber, ivory, cream, blue, coral, and peach. Flat or matte-surface paints should be used to avoid specular reflection. A light that enhances warmth and softness of colored objects is desirable, and furthermore illumination should be such that it does not markedly alter the color of natural objects, e.g., skin complexion and food.

Within these limitations, a variety of colors can be selected for the interior of spacecraft and space dwellings. Cool, work-stimulating colors are recommended for the work area, with bright contrasting accents on trim; warm, relaxing colors are recommended for public rest and recreation areas, again with contrasting accents and trim; while subdued, "homey" colors will be appropriate for personal areas. General lightening of color values will assist in providing brighter interiors with a lower level of illumination. The latter, as much as feasible, should be indirect, diffuse and non-glaring.

The following recommendations have been suggested for the illumination system of spacecraft (152, 418):

- (1) White light illumination be provided for most mission phases.
- (2) The intensity be variable from 0.1 m-L to about 40 m-L with the highest intensity for launch and flashblindness emergencies.
- (3) An intensity of 10 m-L be provided as the maximum value for non-launch conditions with local illuminance levels recommended above.
- (4) Provisions be made for turning off all internal lights with critical instruments being self-illuminated (according to Table 2-60) and for maintaining interior/exterior light balance.

- (5) Flexible floodlights should be provided to reduce extreme contrast to less than 5:1 between target area and general surround.
- (6) The reflectivity of suits, equipment, and interior paints be used to increase the evenness and diffuseness of lighting.
- (7) Color of interior should be pleasing, of low saturation and appropriate reflectance, and of warm and restful quality in public and personal areas.
- (8) Red filters (6400 \AA) be provided for dark adaptation for all light sources, and the color of critical markings and legends be designed so that they can be seen when red lighting is used.
- (9) Trans-illuminated displays should be used and shielded to prevent their being masked by high-intensity light sources. (389) For night operation, the average cockpit display luminance should be minimized.
- (10) Lights, indicators, and self-illuminated instruments be located to prevent reflections from windows and other instruments.
- (11) Filters, or shutters be provided for the windows to reduce undesirable illumination.
- (12) Filters or shutters be readily operable to aid the astronaut in programming light to achieve optimal light levels.
- (13) The color and intensity of caution and warning lights be considered, as they influence ambient illumination levels and dark adaptation, particularly for the dark side of the Earth (389).
- (14) Inadvertent light leaks, particularly from high-intensity sources, be identified and corrected before the mission for each spacecraft, to ensure that low levels of interior illumination and dark adaptation can be maintained.

Viewing Ports and Visors

The viewing ports of spacecraft often require extreme accuracy for sighting and resolution, especially where optical experiments are being performed. The efficiency of the visual system is a function of the clarity of the optical window, lighting, and the angles between line of sight and window. The data of Figure 2-61 were obtained from subjects who looked through aircraft glass, clean plexiglas, and dirty plexiglas. Deterioration of optical properties of glass in Mercury and Gemini capsules by exhaust from the escape tower and by deposition of sublimated gasket material has been reported (409).

A review of windows for aerial photography is available (150) as are data on optical characteristics of a Gemini window (436).

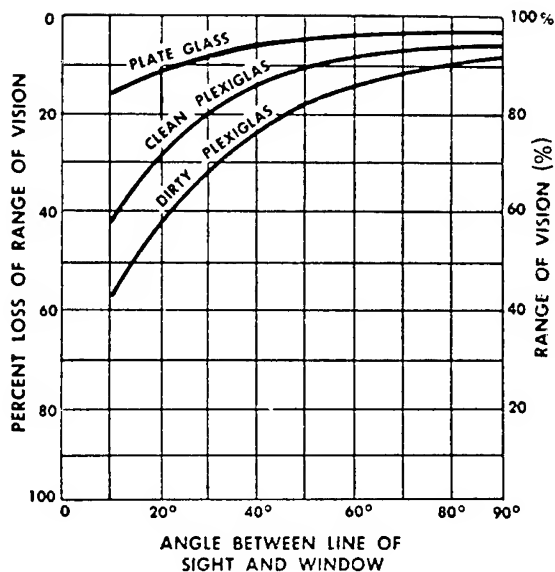


Figure 2-61

Clearness of View

(After Olenski and Gooden⁽³²⁶⁾)

There are several visual problems caused by helmets and visors:

1. Field restrictions.

Helmets should permit the widest possible visual field. Visors with the largest possible area should be used and visual fields determined with and without head movement.

In the Apollo helmet and visor system (423) it has been suggested that the crewman be able to see downward to a point on the front torso centerline 6 inches below the neck ring. With the crewman standing and nodding in an erect PGA, he should be able to see the toes of the boots. When the crewman is subjected to a sustained acceleration of 10 g's eyeballs in, enclosed by a pressurized suit, and secured to the command module couch, vertical field of vision should not be reduced by fault of the helmet upward or downward.

The recommended unrestricted range of vision is as follows:

- a) Horizontal Plane: 120° left, 120° right.
- b) Vertical Plane: 105° down, 90° up.

Minimum vision requirements in a compound direction (example: upper left-hand corner) are defined by an ellipse through the specified vertical and horizontal points. With the head moved forward, eye relief for the primary pressure retention visor is 2.06 inches. This eye relief applies over a vertical range from 45° up to 10° down.

2. Optical distortions.

Optical distortions can be produced by curvature of visors, point-to-point differences in thickness, prism errors, changes in head position, non-neutrality, etc. No visible distortion or optical defects detectable by the "unaided eye" at the typical "as worn" position should be visible. The definition of "unaided eye" is a person who has a visual acuity of 20/20 or better.

For the Apollo visor system it has been recommended (423) that the refractive power in any meridian not exceed by more than plus or minus 0.06 diopters the power inherent in a spherical lens with concentric surfaces having the proper radii of curvature and thickness. The inherent power of the visor is calculated by use of the following formulae:

$$F = F_1 + F_2 - \frac{t}{n}; F_1 = \frac{n' - n}{r_1}; F_2 = \frac{n - n'}{r_2} \quad (11)$$

where F = Power of the lens in diopters

F_1 = Power of the convex surface in diopters

F_2 = Power of the concave surface in diopters

n = Index of refraction of air

n' = Index of refraction of the material

r_1 = Radius of first or convex surface

r_2 = Radius of second or concave surface

t = Thickness in meters

Prismatic deviation includes the inherent prismatic power resulting from non-parallel surfaces of the material. The vertical prismatic deviation between the right eye and the left eye should not be more than 0.18 diopters at any point in the area of vision. The vertical prism at any point in the area should not exceed 0.18 diopters at either eye.

The horizontal prismatic deviation is stated for specific regions of the typical visor given in Figure 3.1-7 of Ref. 423. The algebraic sum of the horizontal prismatic deviation at point "C" for the left eye and at point "C" for the right eye should not exceed 0.75 diopters. The algebraic difference between the horizontal deviation at point "C" for the left eye and at point "C" for the right eye should not exceed 0.18 diopters.

3. Optical transmission.

The transmission of light through the visor should be controlled to minimize the effects of glare and flashblindness, ultraviolet damage to the cornea, infrared heating, and haze. The light transmission and optical characteristics of plastic visors used in military helmets for aircrew are available (4, 82, 87, 216).

For the Apollo system it has been recommended that the luminous transmittance of the pressure-retention, primary visor should not be less than 80 percent throughout the critical areas of vision noted in Figure 3.1-7 of Ref. 423. Other visor areas should not vary in transmittance by more than $\pm 5\%$ of the critical area transmittance. The total luminous transmittance through all visors including the antiglare supplemental visors, is a maximum of 10%. The transmittance for the left and right eyes do not differ by more than 5%. The haze value of the visor should not exceed 5%.

The spectral transmittance of the pressure visor may vary with wave lengths between 380 and 770 nm, the average percentage deviation within nine spectral bands should be less than 12. (See Figure 3.1-7 of Ref. 423 for sample calculations.)

For control of electromagnetic transmittance in the visor system, the following has been recommended: (423)

- a) Ultraviolet - The transmission of ultraviolet radiation in the range 220-320 nm be such that the total energy incident on the cornea and facial skin shall not exceed 1.0×10^5 ergs cm^{-2} in any 24 hours period. (See Ultraviolet light, Section 2, part B.)
- b) Infrared Transmittance - The transmittance of infrared radiation beyond 770 nm not exceed a total value of 10 percent with all visors in place.
- c) Visible - The primary visor have a transmittance in the visible range of at least 85%. The maximum transmittance through the primary visor and the least dense sector of one secondary visor should be 60%. The maximum transmittance utilizing all visors should be 2%.

The temperature of the facial skin can also be used as a limit in the design of the visor system. It is recommended that in sunlight, the facial skin temperature should not exceed 100°F.

It has also been recommended that the chromaticity coordinates of the anti-glare visor be within the limits indicated in Fig. 3.1-8 of Reference 423 when computed by the techniques of Reference 2-1.

4. Visual impairment due to fogging.

Fogging of visors due to a combination of high humidity in the helmet and low temperature of the visor surface must be prevented. Serious degradation of performance can result from this design problem. Anti-fog coatings or heating can be used to allow fog-free conditions under zero air flow and 100% humidity. About 33 watts/in² of thermal input may be required for thermal control of fogging (355).

Instrumentation and Displays

The visual factors in the design of instruments and displays have been summarized by several good reviews (25, 148, 280, 304, 457). The following discussion represents only the more generalized visual aspects of the problem. The original reviews should be consulted for specific design details when required.

Telescopic Devices

Manned star tracking in navigation has received much study (11, 149, 320, 321). It has been shown that man can track to a 1 sigma accuracy of 0.05 milliradians in elevation and 0.12 milliradians in azimuth using a manually slewed, eight-power telescope. A 1 sigma tracking error of 0.01 mill is possible using a 28 power rate control telescope. The minimum field of view required for tracking has also been studied (11). Results indicate that star recognition time varies significantly as an inverse function of field of view size; star recognition times for viewing fields of 10, 15, and 20 degrees are significantly greater than for viewing fields of 30, 35, 40, and 45 degrees; star recognition performance does not appreciably change for viewing fields greater than 25 degrees; the majority of star identification errors (81 percent) occurs for viewing fields of 25 degrees or less; the time required to recognize stars, up to some maximum proficiency level is significantly related to the amount of training the knowledge of the star constellation. Data on effects of magnification and observation time on telescopic target identification in simulated orbital reconnaissance are available (386).

Dials and Scales

In the design of dials and scales, the scale base-length reading distance, number of scale divisions, and scale interval are key variables (311). Figure 2-62a is a nomograph showing this relationship.

Alteration of scale units for low cockpit luminance conditions has been studied (445). At the viewing distance of 28 inches and minimum night lighting of 0.01 to 0.002 ft lamberts, the graduation interval should not fall below 0.11 inches and the width of minor graduation marks should be approximately 0.032 inches for optimum speed and accuracy of reading. The following scale numbering and graduation interval values have been recommended in the Apollo system (423): (1) Scale graduations progress by 1, 2, or 5 units or a decimal multiplier of those numbers; (2) The number of minor graduations between major markings does not exceed nine; (3) An increase in numerical progression reads from left to right or bottom to top; (4) Major graduation marks are whole numbers; and (5) Maximum contrast between scale face and markings is maintained, i.e., black scale markings against white background.

For rapid and accurate readings under illumination conditions as low as 0.003 foot lamberts, the dimensions in Figure 2-62b are recommended. This figure is based on a 28-inch viewing distance. For other distances, multiply these dimensions by the factor:

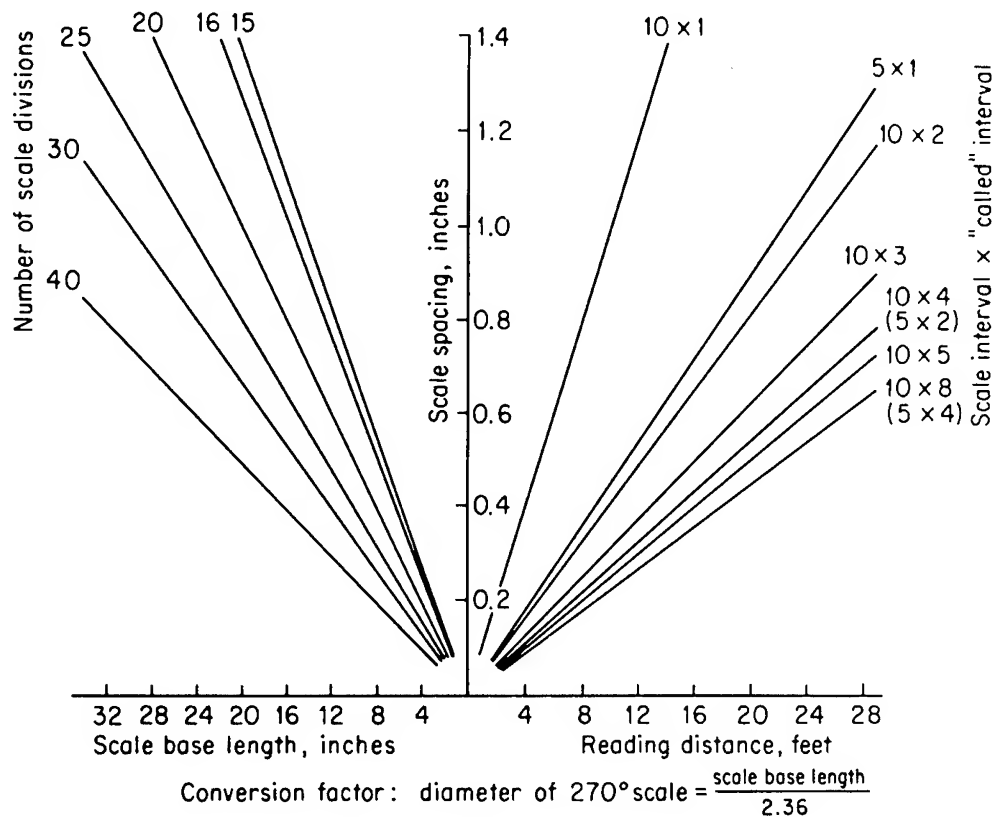
$$\frac{\text{Viewing Distance in Inches}}{28} = \frac{\text{Graduation Mark Dimension and Spacing}}{(12)}$$

When illumination levels exceed 1 to 2 foot lamberts and where reading time is not critical, smaller graduation marks of the same general proportions may be used and the separation between marks can be reduced to a minimum of 0.35 inches.

Figure 2-62

Dial and Scale Design

a. Dial and Scale Design Nomograph.



Nomograph showing relationship between reading distance, scale interval, "called" interval, and scale base length. The method of using the nomograph to find the dial size when the maximum reading distance is known can be illustrated by a 200-lb pressure gauge subdivided into 20 scale divisions at 10-lb intervals, to be read at a distance of 20 ft, to a "called" interval of 2 (the smallest value to be read). Enter the right side of the nomograph at 20 ft and more vertically until the 10×2 line is cut (10×2 is the scale interval, 10 multiplied by the "called" interval, 2 lb). From this 10×2 line horizontally to the 20 line (there being 20 marked scale divisions) and down to the base line to give a scale base length of $17\frac{1}{2}$ in.; to obtain the diameter, divide by 2.36 to give 7.4 in. In practice this means using a standard gauge with an 8-in. dial blank. The nearness of scale base length of $17\frac{1}{2}$ in. at 20-ft reading distance to a 1:1 ratio has led the British Standard Institution to suggest the use of a scale base length of 1 in. for each 1-ft reading distance as a useful working relationship. To obtain the maximum reading distance when the dial size is known, the procedure described above is reversed. It may be noted that should the 200-lb gauge be subdivided into 40 scale divisions, giving a 5×2 interpolation, the scale diameter will be 9.1 instead of 7.4 in. In fact, any method of a subdivision other than 10×2 gives a less favorable result, which suggests that for industrial scales, subdivision into 20 parts and interpolation into 5ths is optimum.

(After McCormick⁽²⁸⁰⁾ Adapted from Murrell, Laurie, and McCarthy⁽³¹¹⁾)

Figure 2-62 (continued)

- b. Minimum Recommended Circular Scale Diameters Under Illuminating Conditions as Low as 0.003 ft Lamberts in Apollo.

After NASA CSD-A-096 (423)

Number of Graduation Marks	Viewing Distance		
	20	28	36
Diameter of Circular Scales			
35			1.00
45		1.00	1.23
50		1.11	1.43
63	1.00	1.40	1.80
100	1.59	2.23	2.87
150	2.39	3.35	4.30
200	3.18	4.45	5.73
250	3.98	5.57	7.77
300	4.77	6.68	8.60
350	5.57	7.80	10.00

The number of graduation marks required on a circular scale imposes a limit on the minimum diameter of the scale. The minimum distance between graduation marks viewed from a distance of 28 inches is 0.07 inches. For other viewing distances, Figure 2-62b shows recommended minimal diameters for three viewing distances and various numbers of graduation marks.

Letter location on scales and dials has been recommended as follows (423): On circular stationary scales, orient all numbers to be read horizontally instead of medially. On moving scales, orient all numbers to be upright at the reading position.

The general design requirements for moving-pointer, fixed-scale type indicators (circular) are presented for the Apollo system (423). Clockwise movement of the pointer should result from (1) clockwise movement of an associated rotary control, or (2) movement forward, upward, or to the right of an associated lever or switch, vehicle or component. In cases where positive and negative values around a zero value are being displayed, the zero should be located preferably at the 12 o'clock position although the 9 o'clock position is also acceptable. The positive values should increase with clockwise movement of the pointer and the negative values increase with counter-clockwise movement. Except on multi-revolution instruments such as the clock, there should be an obvious scale break between the two ends of the scale of not less than 1-1/2 divisions. The numerals are usually placed inside of the graduation marks to avoid constriction of the scale. If space is not limited, the numbers may be placed outside of the marks to avoid having the numbers covered by the pointer.

In the design of moving-pointer, fixed-scale type indicators (linear and curved, or arc scales), pointer movements are recommended as above (423). In cases where positive and negative values around a zero value are being displayed, the positive values should increase with movement of the pointer

up to the right and the negative values increase with movement of the pointer down or to the left. Movement of the pointer up or to the right should result from (1) clockwise movement of an associated rotary control, or (2) movement upward, forward, or to the right of an associated lever or switch. Numerals should be placed on the side of the graduation marks away from the pointer to avoid having the numbers covered by the pointer. For curved or arc scales, the numerals will be placed inside of the graduation marks to avoid constriction of the scale. If space is not limited, the numbers may be placed outside of the marks to avoid having the numbers covered by the pointer. The pointer is located to the right of vertical scales and at the bottom of horizontal scales.

Fixed-pointer, moving-scale indicators are not recommended for general use (423). If, however, the situation dictates their use, the progression of numbers and response to control should follow those recommended for moving-pointer systems. The numbers on the indicator should progress in magnitude in a clockwise direction around the dial face. In case of vertical or horizontal moving straight scales, numbers should increase from bottom to top or from left to right. If the associated control has a direct effect on the behavior of the vehicle, the scale should rotate counter-clockwise with (1) clockwise movement of the associated knob, wheel, or crank; (2) movement forward, upward, or to the right of a lever; or (3) movement forward, upward, or to the right of the vehicle or component. However, if the associated control has no direct effect on the behavior of the vehicle, the scale should rotate counter-clockwise with counter-clockwise movement of the associated knob or crank. The pointer of lubber line position should be at 12 o'clock for right-left directional information and at 9 o'clock for up-down information. For purely quantitative information, either position may be used. If the display is used for setting, such as tuning in a desired wavelength, it is usually advisable to cover the unused portion of the dial face. The open window should be large enough to permit at least one numbered graduation to appear at each side of any setting.

The desirable size of numerals and letters is affected by the distance at which they are to be read. For the usual reading distance of about 28 in., it has been reported that two different sizes of block capital letters seem to satisfy the concurrent desirability for uniform size with occasional larger letters for emphasis (74). These two sizes are 9/64 in. for the bulk of the letters and 11/64 in size for emphasis. Illumination, reading conditions, distance, and the importance of accuracy should of course be taken into account in selecting the size of letters or numerals for use as labels or markings (280, 304).

A formula has been developed that takes into account illumination, reading conditions, viewing distance, and the importance of reading accuracy (280, 340):

$$H \text{ (height of letter in inches)} = 0.0022 D + K_1 + K_2 \quad (13)$$

where D = viewing distance

K_1 = correction factor for illumination and viewing condition

K_2 = correction for importance (for important items such as emergency labels, $K_2 = 0.075$; for all other conditions, $K_2 = 0.0$).

This formula has been applied to various viewing distances, in combination with the other variables, and the heights of letters and numerals derived therefrom. These values are given in Table 2-63. It should be kept in mind that these are approximations of desirable heights; values within reason of those given would generally produce relatively comparable legibility. Needless to say, one should not apply such a formula arbitrarily, without taking into account special facets of the particular situation. A set of recommended heights for the Apollo System at 28" viewing distance, low brightness (down to 0.03 ft L) range from 0.05 to 0.20 in. for noncritical, normal situations, up to a range of 0.20 to 0.30 in. for critical, adverse situations (304, 423).

Table 2-63

Table of Heights of Letters and Numerals (H) Recommended for Labels and Markings on Panels, for Varying Distances and Conditions
Derived from Formula H (in.) = $0.0022 D + K_1 + K_2$

(After McCormick⁽²⁸⁰⁾ Adapted from Peters and Adams⁽³³⁹⁾)

Viewing distance, inches	0.0022 D value	Nonimportant markings			Important markings		
		$K_1 = 0.06$	$K_1 = 0.16$	$K_1 = 0.26$	$K_1 = 0.06$	$K_1 = 0.16$	$K_1 = 0.26$
14	0.0308	0.09	0.19	0.29	0.17	0.27	0.37
28	0.0616	0.12	0.22	0.32	0.20	0.30	0.40
42	0.0926	0.15	0.25	0.35	0.23	0.33	0.43
56	0.1232	0.18	0.28	0.38	0.25	0.35	0.45

Illumination level, fc	Reading situation	K_1 value
Above 1.0	Favorable	0.06
Above 1.0	Unfavorable	0.16
Below 1.0	Favorable	0.16
Below 1.0	Unfavorable	0.26

In a study relating to legibility of numerals at distances of several feet, a relationship between height of numerals and legibility was established as shown in Figure 2-64. Each of the three areas indicates, generally, the relative legibility of numerals seen under reasonably normal viewing conditions for persons with normal vision.

The use of color contrast to improve alpha numeric legibility has received recent review (283). The recommended use of color in the design of indicator warning lights is shown in Table 2-32c.

Both for maintaining dark adaptation and avoiding objectionable reflections, it is necessary to use the minimum instrument illumination which will

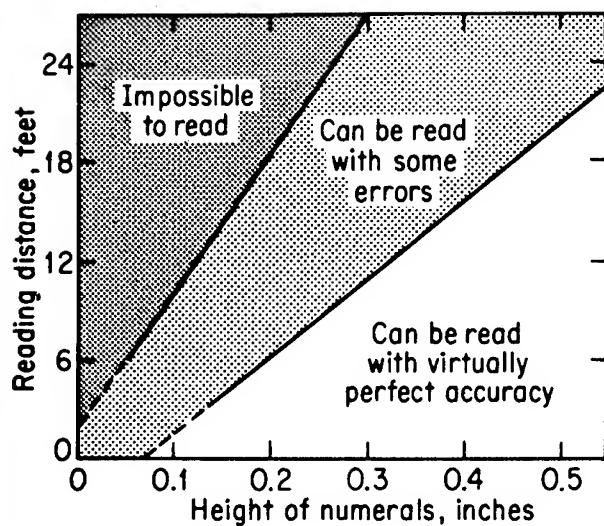


Figure 2-64

Figure Showing Relationship Between Height of Numerals and Legibility of Numerals at Various Distances. The Indications of Degrees of Legibility of Those Height-Distance Relationships in the Three Areas are Generally Valid for Persons with Reasonably Normal Vision.

(After McCormick (280) Adapted from Murrell, Laurie, and McCarthy (311))

permit adequate instrument reading. Figure 2-65 shows the relationship between the brightness of instrument markings and relative efficiency of instrument reading.

In the design of counter systems it is recommended that numbers change by snap action in preference to continuous movement (423). Space between numerals should be no more than 1/2 the numeral width. The height to width ratio of numerals for counter displays should be 1:1 rather than 5:3 as recommended for dials and scales. Numbers should not follow each other faster than about 2 per second if the observer is expected to read the numbers consecutively. Counters used to indicate sequencing of equipment should be designed to reset automatically upon completion of the sequence. Manual provision for resetting is usually provided. The rotation of the counter reset knob is conventionally clockwise to increase the counter indication or to reset the counter. Counters are mounted as close to the panel surface as possible to maximize viewing angle and minimize parallax and shadows.

CRT (Cathode Ray Tubes) Displays

In the design of radar and other displays of the CRT type, the minimum size, shape, and brightness contrast of target on scope is a key factor as is duration of presentation (160, 457, 462). Figure 2-66 shows the relation of a target size to accuracy and relative speed of identification of display targets of this latter type. From the curve, it is evident that, when the visual angle subtended by the largest dimension of the target is smaller than 12 min, there is an increase in relative search-to-identification time and an

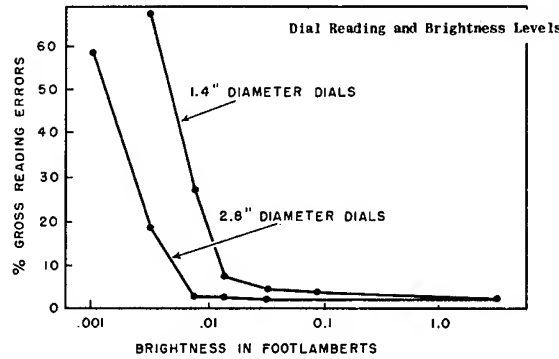


Figure 2-65

Dial Reading and Brightness Levels

(After Baker and Grether (25) from Data of Chalmers et al (90))

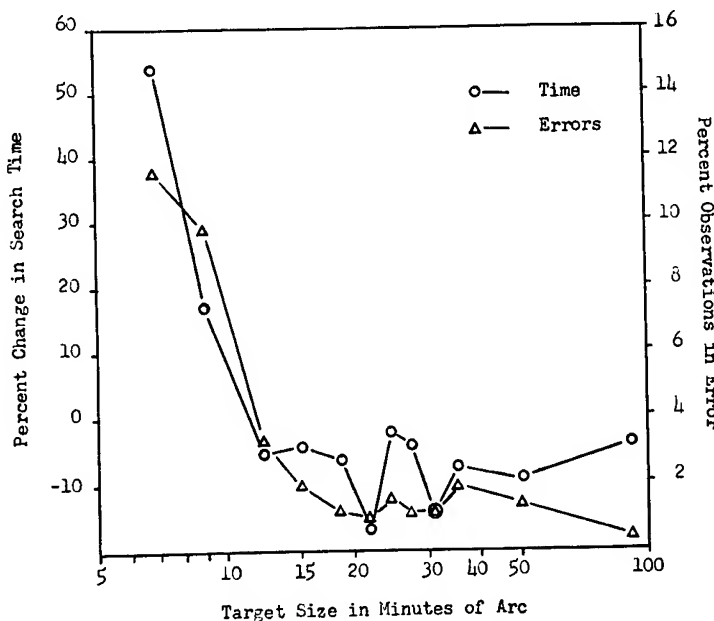


Figure 2-66

Effect of Target Size on Identification Time in Search on CRT Scopes.

(After Steedman and Baker⁽³⁹⁶⁾)

increase in the number of errors in identification. These and other research data indicate that it probably is safe to assume that targets should subtend, as a minimum, 12 min of arc to insure reasonably accurate identification (457).

Dark adaptation can affect detection on CRT (cathode ray tube) displays. The visibility of threshold targets is best when the operator is visually adapted to the level of the scope brightness. The time lost in the detection of a target on a CRT scope as a function of the pre-exposure brightness for various scope brightnesses is shown in Figure 2-67 (199). The signal, which subtended a visual angle of 20 min of arc at the eye has a 99% probability of detection for an operator whose eyes were adapted to the brightness level of the task. In this experiment, a detection time of 5 sec is equivalent to immediate detection because it took that long for the subjects to move from the adaptation screen to the CRT scope.

It can be concluded that (304):

- For very dim scopes (0.0001-mL background brightness) the operator can be pre-exposed to brightnesses as high as 0.01 mL without impairing target visibility.
- For dim scopes (0.022-mL background brightness) the operator can be pre-exposed to brightnesses as high as 2 mL without impairing target visibility.
- For moderately bright scopes (0.22-mL background brightnesses) the operator can be pre-exposed to brightnesses as high as 20 mL without impairing target visibility.
- A completely dark-adapted operator will suffer a slight loss in detecting threshold targets on scopes with background brightnesses of about 0.02 mL and above.

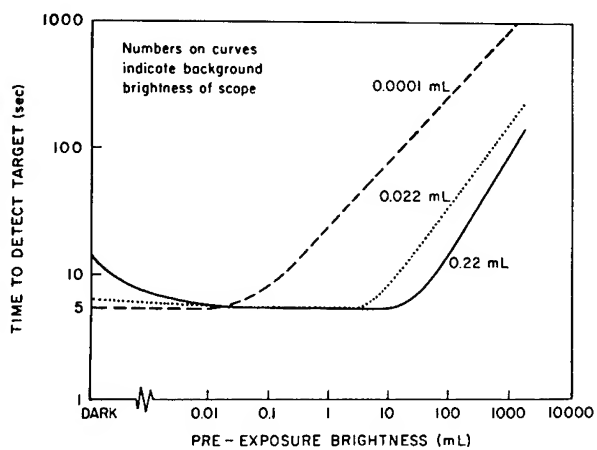


Figure 2-67

Effect of Pre-exposure Brightness on Time to Detect Target on CRT Scopes of Different Brightness Values.

(After Hanes and Williams⁽¹⁹⁹⁾)

If the operator must do other visual tasks at higher brightness levels than those required for the above, visibility will not be seriously affected if the higher brightnesses are not more than 100 times as bright as the average brightness of the radar scope. In other words, if the operator must scan daylight skies (about 2,000 mL), the average scope brightness should be set up to 20 mL or more to maximize visibility under these circumstances (280, 462).

The intensity contrast of the target on a scope is also a factor for CRT displays (199, 217, 457, 462). The curves in Figure 2-68 show the time required for a target to be detected as a function of the pre-exposure brightness for targets of various intensities. In every case, the scope background brightness is 0.022 mL, and the target subtends a visual angle of 20 min of arc. As before, the detection time of 5 sec represents immediate detection. The lowest contrast (13%) is for a target having about 99% probability of detection for operators adapted to the brightness level of the task. The other targets are above this threshold level.

It is evident that, with stronger signals (higher contrasts) the range of tolerable adapting brightnesses is much greater. Indeed, for this background brightness (0.022 mL), a target that is 2 1/2 times as bright as the background can be seen immediately after the operator has adapted to 2,000 mL. Thus, if a given radar operation does not require the detection of weak signals, greater tolerances in the operator's brightness adaptation are permissible.

After the eye has been exposed to relatively high brightnesses for about 2.5 min, it reaches, for all practical purposes, a "steady state" of adaptation. This means that longer periods of pre-exposure have little further effect on

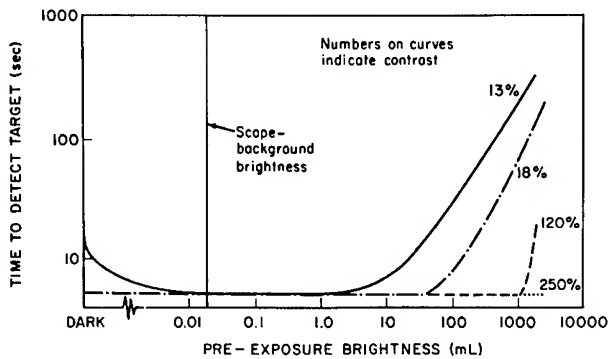


Figure 2-68

Effect of Intensity Contrast and Pre-exposure Brightness on Target Detection of CRT Scopes.

(After Hanes and Williams⁽¹⁹⁹⁾)

the immediate sensitivity of the eye. If shorter periods of pre-exposure are used, however, the sensitivity is affected proportionately less. This relationship is shown in Figure 2-69, in which, for any given exposure duration, the value on the ordinate is used as a multiplier of the exposure brightness to give the steady-state-adaptation level of the eye. This relationship shows that, if the eye is exposed to 2,000 mL (daylight brightness) for 15 sec, the eye has a sensitivity loss equivalent to that of being exposed to 200 mL ($15/150 \times 2,000$ mL) for 150 sec or more. These adjusted values then can be used with the data of Figure 2-68.

The brightness and color of the scope phosphor will determine the specific loss of night vision caused by a CRT scope (413, 462). This may interfere with night vision of a crewman by the effect on dark adaptation or by direct glare of the scope during a visual exercise. The effect of color is similar to that seen on Figure 2-42c. Recovery takes the least time when a red CRT screen is used, only 10 percent longer with a yellow screen, but nearly twice as long with a green screen. The visual characteristics of various phosphors are available (462). The selection of cockpit and instrument color lighting for dark adaptation has been recently reviewed (291, 389).

In CRT displays, detectability of targets of varied contrast and geometric coding may be adversely affected by visual "noise" or "snow" on the scope background. The effects of this noise on the perception of forms in electrovisual display systems have been studied extensively (113, 114). Visual noise with a combined contrast and contour degradation impairs form discrimination to a much greater extent than reducing contrast alone. A typical finding is seen in Figure 2-70. The generation of noise on a prototype electrovisual display as "granularity" of the display was varied, as well as the brightness contrast. Landolt ring targets were used against the variations in background noise to measure the effects of the visual noise on visual discriminations. The variations in granularity of the background affected primarily the clarity of the contours of the visual targets. By variations in the display, it was possible to vary the contour degradation and the brightness contrast. The sharper slope of the solid curves (in comparison with the dotted ones) indicates the greater influence on visual discrimination of the combination of contour degradation and contrast, as compared with contrast alone.

Effects of delay of image motion on target detection using side-looking radars are under study (32). Visual phenomena such as anomalous movement on CRT scopes under certain phosphor conditions are also under study (129).

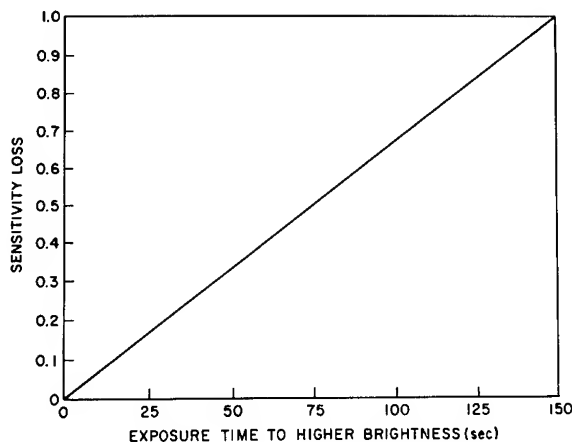


Figure 2-69

Rate of Loss of Dark Adaptation After Exposure to Light. (See text)

(After Mote and Riopelle⁽³⁰⁶⁾)

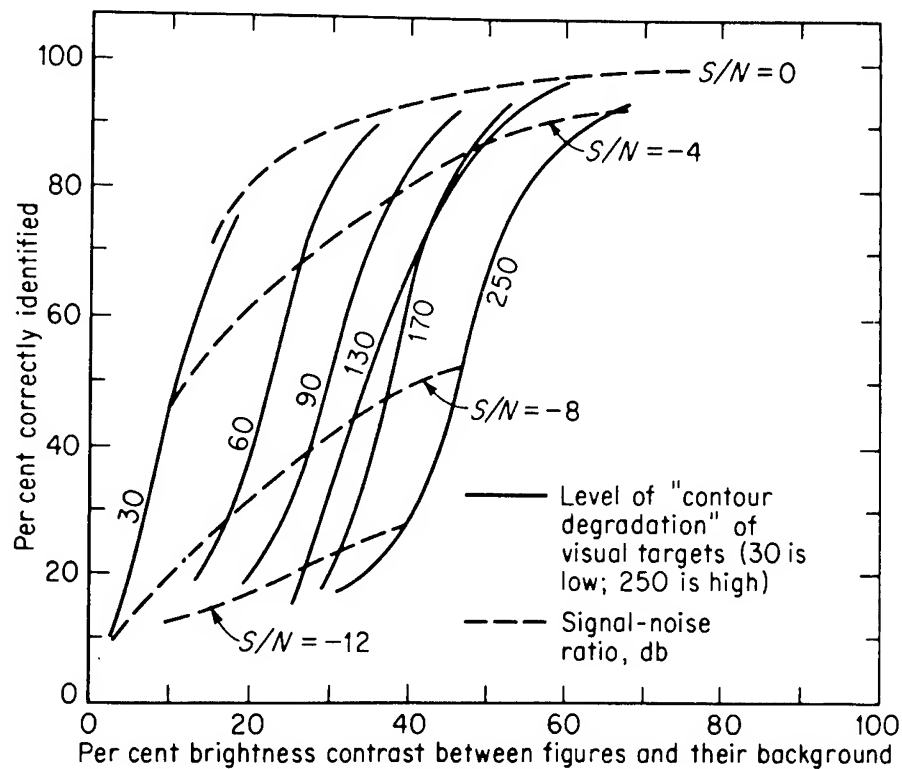


Figure 2-70

Relationship Between Aspects of Visual Noise and Identification of Landolt-Ring Targets on Electrovisual Displays. The Sharper Slopes of the Solid Curves Show the Combined Effects on Visual Discrimination of "Contour Degradation" of the Target Forms Accompanied by Changes in Brightness Contrast, as opposed to the Flatter Slopes of the Dotted Curves Which Represent Essentially Changes in Contrast with "Contour Degradation" Held Constant.

(After McCormick⁽²⁸⁰⁾ Adapted from Crook and Coules⁽¹¹⁴⁾)

Complex Visual Displays

Target recognition and acquisition of information may be difficult on complex displays (24, 138, 236, 258, 385, 387, 452). Optical enhancement techniques for visual displays have been studied (422). Displays covering multiple inputs may be color coded (51, 115, 122, 258, 389) and make use of electroluminescent techniques (341). Color mixture functions at low levels of luminance are under study (347).

Visual factors in the design of large scale displays have been evaluated (257). Recent reviews of instrumentation and displays for night visibility (404, 389) and of visual factors in the design of contact analog devices (86) are available. It has been shown that peripheral displays can be used with effectiveness to decrease deterioration of tracking performance which results from visual switching in complex displays of advanced vehicles (420).

Display requirements for prelaunch checkout or launch control of advanced space vehicles (129, 163, 338) and planetary surface vehicles (185) have been outlined.

VISUAL PROBLEMS IN SPACE OPERATIONS

Space operations present several visual problems not usually present on Earth. There are several requirements of a predictive nature needed to optimize contact with exterior visual environment. These data can be used to simulate such visual problems (12, 284). Many of the figures and tables in the previous sections are applicable when supplemented with the appropriate data and concepts.

The following section will review the visual problems of satellite observation, rendezvous and docking, lunar landing, and operations on the lunar surface.

Observation of Other Space Vehicles

It is often of importance to detect orbiting space vehicles from a great distance in order that sufficient time be available to carry out the necessary navigational maneuvers. For a stationary target, the visual range for detection as something different than the surround without identification of its shape, can be predicted, knowing its size, its luminance, the luminance of the background, to which the observer's eye should be well adapted and the contrast threshold for this situation. The details of these calculations have been described (371, 372) and have been covered in Figure 2-23.

A satellite frequently appears as a sunlit object against the background of the space sky which has a luminance of about 10^{-5} nt or 10^{-6} mL. Sometimes a satellite may be seen as a brighter or darker object against the sunlit Earth, the luminance of which depends on how much of the ground is covered by clouds. In rare instances, the nonilluminated satellite may appear against the surface of the sun or against the airglow line. At night it may appear as a moonlit object against the dark night sky or the surface of the dark Earth.

The adaptation of the astronaut is determined by the average luminance of the surface which he is viewing. He probably never observes the same area for more than a few minutes because of his different duties. Since light adaptation requires only a few minutes, the sensitivity of his eyes may rapidly reach a plateau when he is looking at the sunlit surface of Earth or when inspecting the instrument panel. The cabin illumination increases when the window faces the sun or the sunlit Earth. On the other hand, dark adaptation is a slow process requiring at least 15-30 minutes (depending on previous conditions) to achieve a fairly stationary high sensitivity (Figure 2-42 and 2-43). In orbit, a terminal dark adaptation may be difficult to obtain in view of the short range day-night cycle. In a low orbit, there is a shift from day to night and vice versa about every 45 minutes.

Some of the visual ranges may be higher than those computed for vision on Earth for the following reason. When observing the instrument panel first and then looking toward the dark sky, the eyes are adapted first to a higher luminance, for which the threshold was established. (Figures 2-16 and 2-17). When looking out into space, a sudden rise of sensitivity occurs within fractions of a second, known as alpha-adaptation, followed by the

slower beta-adaptation process. During the scanning of the sky the sensitivity of the eyes slowly rises. There are a few data available about sudden changes in adaptation and pertinent studies are still in progress.

The contrast sensitivity may be affected further by the retinal region stimulated, motion, time of exposure of the target and empty visual field myopia (448). In the presence of an empty visual field subjects cannot relax accommodation completely. Accommodation remains in a state of constant activity, fluctuating about a level of from 0.5 to 2.0 diopters. One is unable to focus at infinity if infinity contains no detail subject to sharp focus. Under these conditions, unable to focus farther than a point about 1 to 2 m. away, one becomes effectively myopic by this amount. Empty visual field myopia can increase the light threshold by a factor of log 0.3 or double the minimum visual angle (329, 448). It is difficult to say how serious a factor empty visual field myopia would be in space flights since an astronaut is not constantly scanning a homogeneous field. When looking at the sky, he perceives celestial bodies which are objects for focusing at infinity. Many of these factors are covered in the previous section and are applicable to space operations.

In the present context, these factors are interrelated in a complex way. Uniform sensitivity exists over the retina at the limit of scotopic and mesopic vision ($\log -3mL$) up to at least a 25° peripheral angle. In the scotopic stage there is a steep increase in sensitivity from the fovea toward the parafovea and then a more or less leveling off. The fovea is blind for targets of low luminances. Values determined for parafoveal vision are also nearly correct for a more peripheral region. When the adapting luminance is above the scotopic level, the trend of sensitivity becomes reversed. Sensitivity is now highest in the fovea and decreases steadily toward the periphery, the decrease steepening with increasing adapting luminance. Thus, foveal threshold values are not valid in the retinal periphery (see Figures 2-24 and 2-25).

The findings on stationary targets may only be applicable in space when both satellites move with the same speed and in the same orbit. Other situations are possible: the target may move slower than the observer and thus may apparently move backwards, their pathways may cross each other or the target may move toward the observer. For these different situations there are not yet sufficient data available in the literature. The threshold luminances for a point light source simulating a satellite and moving horizontally at an angular speed of 1 to 4 degrees per sec have been calculated (187). On a star-studded night sky as background, the threshold for detection is about 1 stellar magnitude brighter than for detection of a stationary target on a starless background. The difference increased rapidly as vision began to change over to cone or photopic vision. A moving target stimulates not just one point on the retina but successive retinal regions. In scotopic vision, successively stimulated retinal receptors may be of equal or similar sensitivity, whereas, in photopic vision the image of the target will stimulate less sensitive areas as soon as it moves from the fovea. Thus, under these circumstances higher threshold intensities are required. Data on detection times for moving targets in rendezvous are discussed below.

Another variable is the time of exposure. A satellite may be visible for only a limited time, especially in a restricted field of view. This factor is covered in Figure 2-33. Data on sensorimotor latency factors in flight operations are available (52).

Computations of sighting probability for visual search in space have been made (183, 255, 313, 455). Factors which favor probability of success in visual search are: high contrast ratio between target and background, large target size, slow closure or movement rates of the target relative to the observer, and restricted area of search. Factors which reduce probability are: irregular illumination of target, interference with scanning efficiency by other tasks, thickness and clarity of the window glass, low angle of incidence for viewing through window, glare from the sun for some target directions, empty field myopia, and the visual blind spot in each eye. The variables are so numerous that practical use of such calculations must be reserved until more empirical data are available.

Identification of the Shape and Other Details of a Satellite

When an object in space has been detected as a lighter or darker silhouette, some nearer observation distance is required before its shape can be recognized. The recognition of a shape and other details is a complex function of visual acuity. Table 2-71 shows the visual range or the

Table 2-71

Visibility of a Satellite in Space

(After Schmidt⁽³⁷¹⁾)

Illumination of satellite	Astronaut adapted to	Visual acuity	Visual angle of critical detail	Visual range of identification, km*
Sunlit, full-phase +F	space sky +F	1.7	35"	5.9
Moonlit, full-phase	night sky	.25	4'	.86
Nonilluminated +F	sunlit earth +F	1.5	40"	5.2
Nonilluminated	airglow line	.25	4'	.86

*For a spherical satellite 5 meters in diameter with visual transmittance of window = .5 and 10% probability of detection. +F refers to a neutral density filter of 0.1 transmittance.

farthest distance at which one can identify the shape of a satellite. The visual range for specific objects can be computed by using curves of Figure 2-23 and by assuming that the visual angle of the critical detail represents 1/5 of the diameter of the satellite (371). At the identification distance, the sunlit satellite is at least 10 times too bright to be observed comfortably (346). Therefore, the transmittance, 0.1, of a neutral density filter was used for the computation. Table 2-71 demonstrates that the shape of the satellite is recognized at about the same distance whether it is illuminated by the sun seen against the night sky or is perceived as a silhouette against the background of the sunlit Earth. The chances for identification

of a moonlit satellite are as low as those of a nonilluminated satellite seen against the airglow line and they are definitely worse for a nonilluminated satellite appearing against the night sky or the night time Earth.

Differences in colors would aid in recognition of details but they are far less decisive than brightness contrast. Visual acuity shows a dependence on the exposure time: a 0.5 to 1.0 seconds exposure is optimal (Figures 2-33 and 2-34). The recognition of a shape also depends on psychological factors such as previous experience and training of the observer. A familiar form is resolved more easily than an unfamiliar form; an expected form, more easily than the unexpected (48, 49, 52).

Motion of a satellite relative to the star background is the factor most helpful in its detection. The threshold for perception of motion in laboratory studies under optimal conditions is equal to 1 to 2 minutes of arc per second. The displacement threshold (the minimal angular displacement required to perceive a motion) in presence of stationary objects is 20 seconds of arc. In the absence of fixed comparative objects the values are higher. The star-studded sky is then an appropriate background for the detection of a moving satellite (See Figure 2-39). The motion threshold is affected by the same variables as the other visual functions mentioned, e.g., background and adaptation state of the observer, intensity of the target, retinal region stimulated, size of the target, and exposure time up to a certain critical value.

In the absence of other lights, it has been observed that a stationary light after at least 9 seconds of fixation in an empty surround starts to move in an erratic manner. This optical illusion, known as "autokinetic movement", may also play a role when a satellite is observed against the dark sky (181). The vestibular apparatus appears to play no part in its genesis but eye muscle imbalance may play a role (149, 164). The operational significance of this subjective phenomenon is not as yet clear.

In space operations, the estimation of the distance of another spaceship is of crucial importance. The recognition of the distance is a complex function which involves the integration of immediate visual impressions and previous experience (4, 179, 180, 182). For a moving light point far out in space, many cues of depth perception are invalid, especially the primary factor of stereopsis. An important factor for recognition of an absolute distance, that is a distance with reference to the observer, is the presence of a terrain. In case a terrain is lacking, distance judgment becomes unreliable and, without size cues, only relative distances are recognized, namely that one object is nearer than the other. An important empirical distance factor is the apparent size. In order for this factor to give information about the distance of an object in a homogeneous surround, the real size of the object must be known. When the actual size of the target is unknown, its distance will be indeterminate, since the same angular size can correspond to a small object nearby or a large object at great distance (See Figure 2-74).

One secondary distance factor is motion perspective or motion parallax or the gradual change in the rate of apparent displacement of objects in the

field when the observer is moving. When fixating the horizon toward which the locomotion is aimed, the ground below shows a flow opposite to the motion of the traveler (161). The visual field appears to expand anteriorly from a stationary focus to which attention is aimed. The visual field behind contracts inward to a focus. The farther objects have a slower rate of speed than the nearer objects. The astronauts repeatedly mention the flow of the surface of Earth opposite to the direction of their orbit. The drift is quite apparent over clear areas or broken clouds whereas a solid cloud cover with no pronounced texture mediates a very slow floating feeling. When gaze is fixated on the target satellite, it should show no such parallactic motion because the pursuit movements of the eyes keep its image on the fovea, unless its actual motion is so fast that it makes fixation impossible. The celestial bodies, as more distant objects, should show a parallactic with-motion. When the gaze is fixated on a star, the satellite as a nearer object should show a parallactic against motion which may conflict with its actual motion.

Another empirical factor in distance recognition is the aerial perspective; that is, the progressively increasing haziness of objects as their distance from the observer increases (gradient of haziness). The clearer the outline of an object, the nearer it is perceived. In space there is no gradient of haziness. The light and dark areas on the surface of a satellite produce sharp boundaries (367). Clearer contours and clearer details may cause an underestimation of its distance, in comparison to what is known from observation on Earth. This, in turn, should make it appear smaller because the retinal image actually corresponds to farther distance. As long as the satellite subtends visual angles large enough to affect the eye as a luminous surface, its brightness is determined by its luminance and is independent of its distance, but, as soon as the visual angle becomes so small that it affects the eye as a point light source, its brightness decreases with increasing distance and thus might serve as a distance cue (Figure 2-18).

Visibility of Objects on Earth from Spacecraft

Theoretical aspects regarding the detection of Earth targets from space with and without periscopic aid have been covered (313). Quantitative data obtained during actual space flight are now being processed (131). An example of the findings on revolutions 17 and 31 of Gemini VII are presented in Figure 2-58. Computer programs are being prepared to allow prediction of Space to Earth visibility (130).

Vision in Rendezvous and Docking

The visual tasks associated with rendezvous and docking are summarized in Table 2-72.

Table 2-72
Visual Rendezvous Operations
(After Pennington and Brissenden⁽³³⁶⁾)

PHASES OF RENDEZVOUS	VISUAL TASKS	TARGET PARAMETERS
1. ACQUISITION	DETECTION	INTENSITY, COLOR SIGNAL SEQUENCE
2. ESTABLISHMENT OF INTERCEPT	ANGULAR RATE DISCRIMINATION	MOTION CUES
3. RANGE AND RANGE RATE ESTIMATION	"	"
4. BRAKING OPERATIONS	DISTANCE AND CLOSURE RATE JUDGEMENT	SIZE, SHAPE, MOTION CUES
5. DOCKING	ATTITUDE	ASPECT

Visual information for rendezvous, docking, and navigation has been outlined (19, 33, 67, 68, 69, 205, 207, 228, 229, 230, 263, 264, 269, 334, 335, 337, 349, 350, 370, 381, 461). Visual data can be used to predict accuracy of navigation techniques proposed for different phases of space flight (198, 200, 288, 289). These show that visual control is efficient in many areas and can be used in secondary or backup control techniques. Space flight data suggest the critical nature of visual problems in rendezvous and docking maneuvers (313).

Acquisition

Visual observation from another spacecraft of a satellite moving against a starfield background has obvious operational importance in any rendezvous mission where the target satellite must be detected and located to effect terminal guidance. The operator may be required to act as a backup system in the event of radar or other failure. It has been shown that a pilot can accomplish rendezvous using only visual sighting of the target position (264). Also an accurate knowledge of visual detection ranges can aid in planning launch time to obtain favorable illumination during acquisition phases.

The ability of the observer to detect a target satellite as a point source target moving slowly in a starfield has been covered above and quantified by recent studies (381). In contrast to detection problems on Earth, the target is identical in appearance to the other objects from which it is to be distinguished. If the satellite is illuminated by solar or Earth light and the target intensity is within the range of visible stellar intensities, only its motion relative to the fixed stars and actual presence of a new object in the

starfield can serve as cues to the observer. (An asymmetrical rotating satellite may produce a variation of intensity with time.) The surface characteristics of a given target, the viewing angle and the direction of incident light are needed to determine its photometric intensity. The problem is compounded by the fact that the field of view, background luminance, adaptation level of the observer and allowable search time will influence an observer's detection performance. During a typical transfer orbit, a change in illumination geometry and line-of-sight angular motion occurs (314). Even if the terminal phase occurs in solar illumination, the target may be less visible than it was before the terminal phase, if for example, the target moves between the chaser and the sun.

For the acquisition phase of rendezvous, several studies have been published on detection of a moving point source against a starfield. Given sufficient time, it is possible to see an isolated star of magnitude 8.5 (See Figure 2-9). However, in a field of stars the threshold of perception is closer to a 5th or 6th magnitude star, the former being equivalent to $10^4 \mu\mu$ lamberts (336). (See Table 2-71 and the discussion of Figures 2-9 and 2-12.) Dark adaptation (Figures 2-42 and 2-43), target surface features (287), color (Figures 2-28, 2-29, and 2-30), and intermittency (Figures 2-33, 2-34, and 2-35) of the acquisition lights must also be taken into account.

While the flash duration influences the apparent intensity of the light, the flash rate influences the ease of acquisition, and these two factors influence the power consumption required for the beacon. The rate must be slow enough to permit a flash duration not requiring excessive power, but still fast enough so that at least several flashes will occur during the pilot's search time of the target area. For example, in evaluating a flashing light for use in a proposed orbital acquisition and tracking experiment, it was found desirable to flash at about one cycle per second, and this appears to be a good, representative flash rate (336). The ability of Gemini and Mercury pilots to acquire and track flashing beacons is still under study (314).

The effect of angular velocity and number of background stars on detection performance has been studied (461). Angular velocities from 0 to 3.2 mrad/sec (0.18°) were used and the number of stars varied from one to six in a visual field of 10° . The subjects were required to indicate the direction of movement out of five possibilities (i.e., toward each corner and zero). Response times varied from about 2.5 sec to 40 sec over the range of velocities. Significant first order interactions were found among all combinations of subjects, number of stars, and velocities. For fields composed of one, two and three stars, the subjects reported an inability to establish a reference for determining the direction of motion. Errors in reporting direction increased with a decreasing target rate.

The effects of target intensity and velocity on the subject's ability to detect a point source target when a different starfield was used on each trial has also received study (401). The range of conditions included photopic and mesopic targets (+2 to +5 magnitude). As part of the same study a second experiment was conducted to investigate the effects of target intensity, velocity and practice on detection performance when the same starfield was used on repeated trials. Both experiments showed that target angular rate

strongly affected detection time, but this dependence decreased with practice. Memory for the starfield played an important role in target detection. By the last session of the experiment, differences in detection time between different conditions of target velocity and intensity had decreased. Variations in target intensity produced a variation in search time for the initial sessions in both experiments, but the magnitude of variation decreased with practice. In terms of detection time, there was apparently little difference in time for a mesopic target as compared to that for a photopic target. Recent studies indicate that detection time also depends upon target velocity, starfield density and field of view (381). Differences in target velocity produced the greatest variability in performance with an average detection time of 220 sec for 0.1 mrad/sec rate and 45 sec for 2.4 mrad/sec rate. There is an appreciable difference in mean detection time between the two modes of starfield presentation -- 15 sec for the same starfield background contrasted with 150 sec for the unique or novel background. Detection time for the unique starfield group depended on target velocity and target intensity but for the group exposed to the same starfield, detection time became independent of these variables after a number of trials. There was no positive or negative transfer of training from one type of starfield presentation to the other.

On the basis of these results two models were proposed to explain the observer's search strategy for each type of presentation. In novel or unique starfields, the observer initially uses brief fixations and rapidly scans the starfield to detect the moving target. If this strategy fails he then fixates on specific clusters of stars and memorizes their pattern, later returning to each cluster to determine if a change in the pattern has occurred. When the observer detects a change he identifies the target by ascertaining the change in a relative position of one of three or four stars forming a pattern. For searches in the same starfield, the observer uses only two or three fixations, detects the new object by comparing the memorized pattern with the presented pattern.

Unaided visual search has been compared with search aided by a finely ruled reticle in a telescope (19). The reticle caused the target to blink as it moved across the field. A $22^\circ 38'$ starfield was used with the target always appearing in the central 12° . An average density starfield (not stated) was used with a range of stellar magnitudes from +0.5 to +6.0. The target intensity was +3.0 magnitude. The subjects were given two trials with and two trials without the reticle. For a target velocity of 0.1 mrad/sec, the mean detection time was 169 sec without the reticle and about 40 sec with the reticle. The number of misses and incorrect identifications, if any, were not reported.

Optimization of search strategies under variable starfield backgrounds of a moving spacecraft remains to be performed.

Establishment of Intercept

One technique for the intercept phase of rendezvous is to bring the angular rate of the line of sight of the target vehicle in an inertial reference system to zero and then to control closure rate to effect a safe rendezvous. In simulations utilizing this technique with visual references for background

and target, it was found that pilots could detect the target and establish the intercept course (228). The terminal rendezvous maneuver can be controlled even without instruments for range, space angles, and time derivatives of these parameters, if the pilot has sufficient background reference to make angular measurements on the order of 1 millirad (69). A simple table or slide-rule type of computer is sufficient for converting the angular measurements to range and range rate. An accurate instrument, however, is required for obtaining the 0.1-millirad/sec line-of-sight rate needed to perform visual rendezvous. This instrument must have angular resolution equal to 1 millirad over an observation time of 10 sec or more, and a timer that can be read to within 0.1 sec.

Laboratory studies have shed some light on the critical aspects of this tracking problem. The effects of target angular velocity and of initial separation from a reference point on the time to identify direction of motion of a point source have been determined (68). The starfield background consisted of 106 stars in a 22° field with random separation angles. Stellar intensities were not given but the moving spot was slightly brighter than background. Tests were conducted with dim light spots on a black surface, and were estimated to have intensity equivalent to fifth-magnitude stars. The light spots subtended 1.7 milliradian but definition was such that the outer annulus of about 0.2 milliradian was fuzzy. The moving spot was slightly brighter than the background stars. The target was centered in a 3-star triangle or a 4-star square and different directions of motion were used. Initial separations from a reference star ranged from 12.5 to 60 mrad (0.71 to 3.4 degrees). The subjects knew the location of the target so that search and detection were not required. The subject's task was only to report the direction of motion. Target velocities were varied from 0.1 mrad/sec (0.057°)/sec to 2.0 mrad/sec (1.14° sec). The time to detect the target varied from 2 sec to 35 sec for rates from 0.1 to 2.0 mrad/sec.

Figure 2-73 shows results of one series where the rate of motion is plotted against the overall average detection time for six subjects.

If the initial spacing is 12.5 milliradians, a pilot can detect an angular rate of 0.1 milliradian per second in about 10 seconds for a 1-milliradian traversed angle. Figure 2-73 also shows a tendency to recognize motion to the right more readily than motion to the left for the closest initial positioning of the objects. One can calculate from these data the angles through which the object moves during the time required to detect the motion.

If the target moved across the reference background in random directions, the task of identifying both the

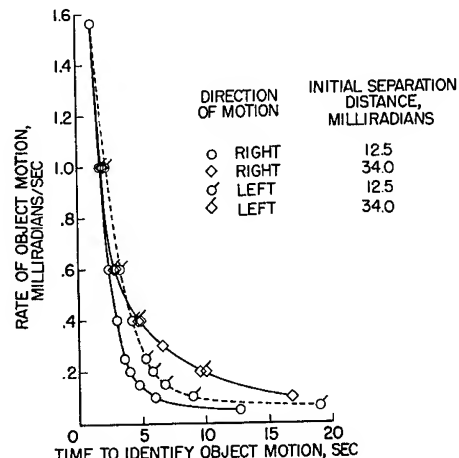


Figure 2-73

Typical Angular-Rate Perception

(After Brissenden⁽⁶⁸⁾)

existence and direction of motion became more difficult than just detecting motion in a predetermined plane. The time required for this task when only the correct estimates of the direction of object motion are used is available. Fatigue is a distinct factor in these studies.

Figure 2-74 is typical of results of how well subjects can detect separation from a superimposed condition at various speeds. The object and the reference both subtend 1.7 milliradians. The "detection" curve is parallel to the actual separation curve at speeds of separation above 0.1 milliradian per second. At 0.1 milliradian per second, detection of separation required 17 seconds. At rates less than this, detection times converged on actual times required for the objects to separate, and reaction time was such a small percentage of the test time that its effect was secondary.

Errors in reporting the direction of motion increased almost linearly from 2% for the target initially superimposed on a star to about 25% for 30 mrad of initial separation but decreased little beyond this separation. It was not stated whether or not the detection times included incorrect responses.

Range, Braking and Docking Phases

After acquisition, correction to an intercept course, and initial braking have been accomplished, (leading up to something less than two miles separation distance between the chaser and the target) the final braking and docking phases are initiated. The pilot observes aspect and closure rate as information to complete the maneuver. The visual conditions here are entirely different from those of the early phases where the target was seen as a point source.

When target objects are nearby, change in visual angle, size cues, shapes, lighting patterns, and color becomes more significant variables. This information is sufficient to enable the pilot to control the range and range rate by direct visual contact, while orienting his vehicle for the docking and final latching maneuver. The appropriate data in section 2 can be used for design prediction as can more specific data from other sources (20, 21, 38, 43, 46, 50, 53, 77, 92, 139, 162, 166, 167, 168, 169, 170, 171, 172, 173, 174, 201, 405).

The apparent size of the target vehicle is used by the pilot to estimate the separation distance between the vehicles. The ability of the pilot to judge object separation distance with no visual cues except the apparent size of the target is known (336). After a period of dark adaptation, subjects were asked at night to estimate the range of several models of known size placed at random distances. Figure 2-75 shows the average distance judgments of several observers for various configurations. The solid line represents perfect estimates. Beyond 500 feet, estimations were better than expected, but with a tendency towards overestimating the range of the large objects and underestimating the range of the smaller target objects. All estimates (except for the balloon) were fairly accurate from 500 feet in to zero. The effects of illumination, color, and aspect are currently being studied.

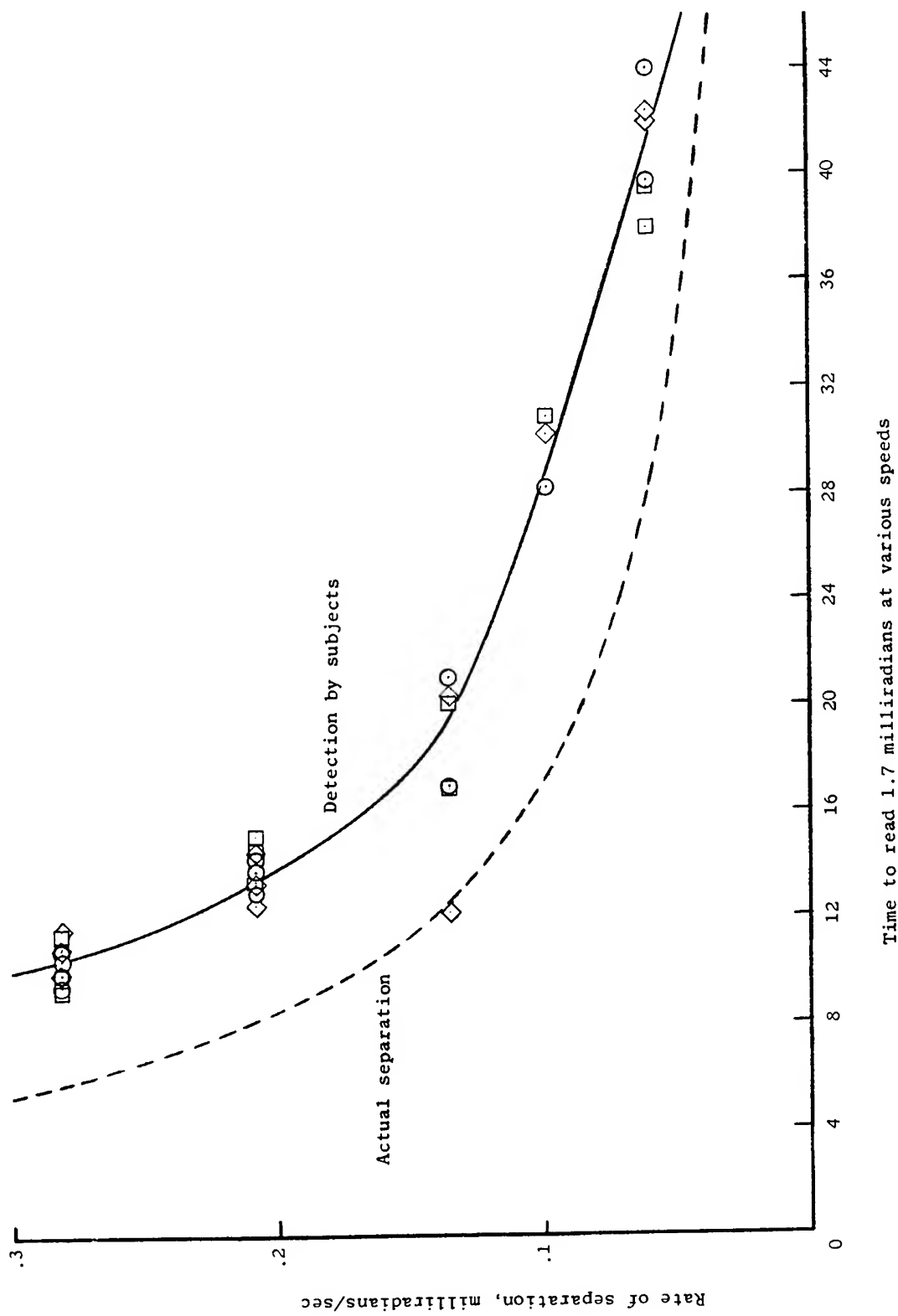


Figure 2-74

Typical Plot of Maximum Separable Acuity. 1.7-Milliradian-Diameter Object Initially Superimposed on Background Reference of Same Size.

(After Brissenden (68))

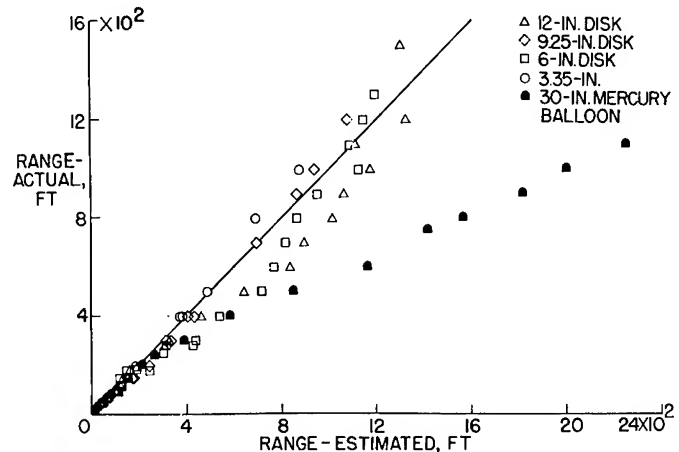


Figure 2-75

Distance Judgement with No Visual Cues Except
Size of Target

(After Pennington and Brissenden⁽³³⁶⁾)

Estimation of velocity is a key factor in visual docking (78). In the visual-docking maneuver the rate of change of size can be used to determine the rate of closure between two vehicles (263). Attention has been given to the question of visual sensitivity when the target is in motion along the line of sight as an important factor in judgment of closure rate. Under these conditions the problem may be conceived in terms of the discrimination of a change in angular size over time. In a dark field, the threshold as a function of the velocity and luminance of the target has been determined (23). The conditions approached those of a homing and docking maneuver, since the object, a 3.5 in. luminescent lamp, subtending an angle of about 40' of arc, corresponding to the angle subtended by a 5 ft object viewed from about 430 ft. Detection improved as the luminance increased from 0.001 to 0.1 ft L, with little added improvement when the luminance was raised to 1.0 ft L. The rate of movement also affected the threshold, the amount depending upon the threshold criterion used. Movements were detected when the visual angle increased or decreased, by amounts ranging from about 1.5 percent to about 8 percent. Using the 95 percent correct threshold criterion, the detection threshold was between 8 percent visual angle change (at slow speeds) and 5 percent (at higher speeds). The threshold generally decreased as the criterion was relaxed, the 65 percent correct criterion yielding thresholds of about 1.5 percent.

It has been predicted that at closure rates of about 3 ft/sec, detection of movement would occur with 95 percent reliability when the distance traveled was about 8 percent of the initial distance, while at rates of about 20 ft/sec detection would occur when the distance was about 5 percent of the initial distance. Assuming that thrust is applied on the basis of such detections at the outset of a homing and docking maneuver, one may anticipate between 5 and 8 percent error in the distance at which initial thrusts were applied to establish the approach rates. These would be expected to undergo adjustment as approach continued.

A more recent study has been primarily concerned with vertical descent to the lunar surface, and in the simulation a projection of the lunar surface was servo-driven in a closed-loop system for closure cues. The pilot applied a braking thrust to stop the apparent closure velocity; the thrust voltage was fed to an analog computer and then to the landscape-

projector drive system. The results seen in Figure 2-76 obtained for one observer over the range of visual angles considered may be applied to docking. The ratio of closure rate \dot{S} to distance S , define (for this particular test subject) the boundary of this \dot{S}/S ratio. This threshold was based on a reply time of 2 seconds dictated by time lags inherent in the test procedure. The figure is of interest because it shows that the maximum perception of closure occurs at visual angles, as subtended by the target outline, from 70° to 90° . This boundary agrees with an analytical derivation of the relation between \dot{S} and S . For this subject, it was found that a representative value for the closure threshold

$$\frac{\dot{S}_{\min}}{S} \text{ fell between } 0.013 \text{ and } 0.016.$$

In docking, the pilot should be able to judge the closure rate to about 0.15 feet per second from a distance of 10 feet. It is clear that estimation of closure rates is subject to strong training effects (22).

Simulation studies have added much to the use of many of these concepts in operational design (33, 98, 205, 206, 228, 265, 269, 334, 337, 348, 349, 350). Operator performance in the control of remote maneuvering units during satellite inspection is currently under study (96, 97). Most translation errors existing at termination of pilot-controlled docking appear to be caused by visual cues (337). Pilots are capable of visually aligning the Gemini and Agena within about 1° of roll and 2° of pitch and yaw using direct (acceleration-command) control mode. Inaccuracies tend to arise from parallax problems in observation of indexing bars and by inability to separate attitude and translation errors.

Oscillation of visual target vehicle can effect efficiency of docking in the visual mode (349). A brief study has been made with a fixed-base simulator employing closed-circuit television to determine the effects of target sinusoidal oscillations in three angular degrees of freedom on pilot-controlled Gemini-Agena docking. Flights were initiated at a range of about 300 feet and were performed by using both the rate-command and direct (acceleration command) attitude-control modes with only visual observation of the target for guidance. Vehicle mass and moments of inertia simulated the parachute configuration of the Gemini spacecraft with a one-half fuel load. The results of the study apply to a fully illuminated target with rear-mounted visual-aid bars for additional boresight information and are as follows:

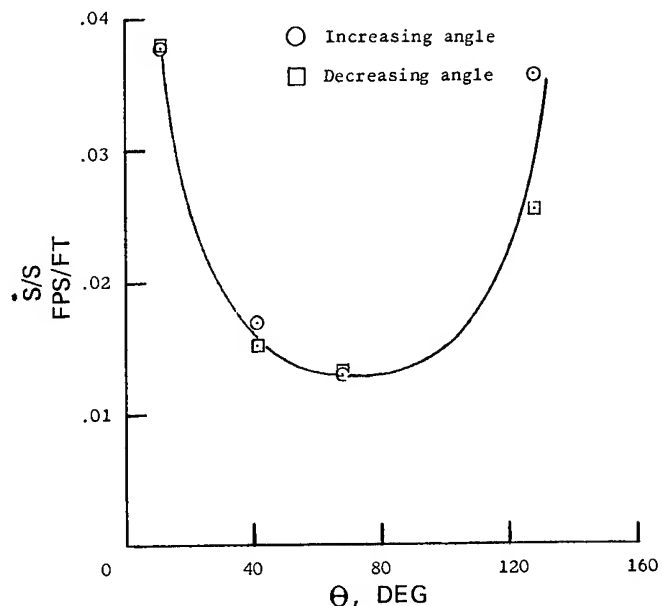


Figure 2-76

Threshold of Velocity Perception

(After Lina and Assadourian⁽²⁶³⁾)

- For docking flights using either the rate-command or direct attitude-control modes, task performance and pilot ratings comparable with those for a rigidly stabilized target were obtained with the target oscillating at $\pm 5^\circ$ amplitude in each of three angular degrees of freedom at oscillation periods of 160 seconds or greater. Fuel consumption and flight time increased, pilot ratings were less favorable, and the percentage of successful dockings decreased as the period of the oscillations was reduced below 160 seconds.
- For the rate-command, attitude-control mode, limited results on the effect of oscillation amplitude indicate that for an amplitude of 2.5° , target oscillations have little influence on the docking task except at small values of period (30 to 40 seconds or less) where docking-ring velocity tolerances can more easily be exceeded. For the amplitude range between $\pm 2.5^\circ$ and $\pm 10^\circ$, increasing the motion amplitude for a given value of period (below about 120 seconds) results in increases in fuel used, increases in flight time required, and less favorable pilot ratings.
- Suggestions are available for optimizing docking cues during day and night operations (269, 284, 337). No concrete data are as yet available on the effect of sunlight and glare on docking control. More data are required on star navigation capabilities in rotating vehicles and the effect of glare on this function (see Figure 2-46).
- Visual aspects of lunar orbit establishment and translation and hover maneuvers over the lunar surface have been studied and preliminary simulator data are available (294, 295).

Visual Requirements for Lunar Landing

The visual parameters for establishing a circumlunar orbit and accomplishing survey of the lunar surface in preparation for landing have been determined (105, 295). In preparation for landing, the rate at which the objects traverse the visual field also has to be taken into account (see Figures 2-39 and 2-40). Study of the effect of stimulus velocity on acuity thresholds revealed that the threshold value increased by a factor of four as stimulus velocity was increased to 140° of visual angle/sec (274). Subjects were required to identify the orientation of Landolt C stimuli exposed for 0.4 sec. Acuity thresholds increased from 3 to 11 min of arc as stimulus velocity increased. Beyond $140^\circ/\text{sec}$ the perceptual task was impossible for most subjects; stimuli were reported blurred beyond recognition.

For the clear perception of a contour, however, the perceptual response breaks down at lower rates of target movement. A contour subtending 30 min of visual angle and moving horizontally across a 5° visual field could not be perceived for rates greater than $15^\circ/\text{sec}$ (390, 391, 392). Presenting the contour in a stationary position a few hundred milliseconds prior to the movement, permitted the contour to be perceived at higher rates. It was observed, however, that for velocities beyond $40^\circ/\text{sec}$ contour perception was impossible for any amount of stationary exposure time. In addition,

increasing the contrast and illumination level improved contour perception for higher velocities.

The velocity of lunar landmarks across the visual field is determined by the (a) orbital and de-orbital speed, and (b) altitude of the spacecraft. At speeds of 5000 ft/sec and altitudes ranging from 50,000 ft to 100 miles the maximum apparent velocity of lunar objects is slightly less than $6^{\circ}/sec$, which is within the range of human capability for contour perception (350). The rotation of the moon is not considered in these calculations since the speed of rotation is only 15.18 ft/sec at the equator and contributes a minor effect on the apparent velocity of landmarks perceived from the spacecraft. It appears that angular motion of the target should present little difficulty to the astronaut in locating and identifying lunar landmarks for initiating a deorbit and landing sequence on the moon with unaided eyes.

In planning for manned lunar landings, one must consider the capabilities of a pilot to make final corrections required to land a vehicle on the lunar surface. For the lunar landing, judgment of vertical velocity has fundamental similarity to the necessary ability displayed by a helicopter pilot in making a vertical landing. However, in the case of the helicopter landing, small distances and velocities are involved, whereas the lunar landing deceleration might, under emergency conditions, encompass much larger distances.

Human judgment of speed (or vertical velocity) relative to a two-dimensional object is based on rate of change of the subtended visual angle. Analysis of the problem is presented as follows (263):

Assuming,

h distance perpendicular to reference plane, ft

\dot{h} velocity normal to plane, ft/sec

\dot{h}_{min} threshold perception of velocity, ft/sec

s distance on the reference plane between features which are equally spaced from the perpendicular line of sight, ft

Δt_{max} maximum image-retention time of the eye, sec

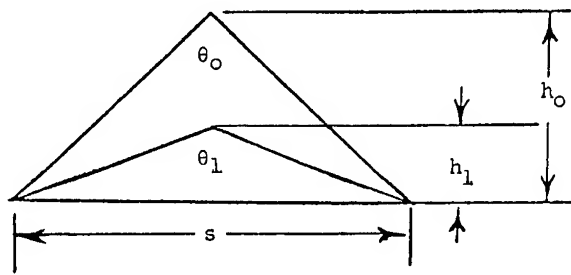
θ total visual angle which is subtended by the reference base-line distance s , radians unless otherwise indicated

$\Delta\theta_{min}$ angular resolution of the eye, radians

$\dot{\theta}$ rate of change of visual angle, radians/sec

$\dot{\theta}_{min}$ threshold perception of visual angular rate, radians/sec

a descent from height h_0 to height h_1 will result in an increase of the visual angle from θ_0 to θ_1 when an object of size s on the ground is seen. The visual reference distance s may be the size of a single object such as a boulder or it may be the distance between two objects. In the case of a



descent above a reference circle or crater, the increase in visual angle would be seen as an apparent growth in diameter.

The relation between height size of object, and subtended visual angle is

$$\tan \frac{\theta}{2} = \frac{s}{2h} \quad (14)$$

The threshold of perception of relative velocity is related to the threshold of detecting visual-angle rate. The relationship, obtained by differentiating equation (14) with respect to time, is

$$\frac{\dot{h}_{\min}}{h} = -\dot{\theta}_{\min} \left(\frac{1 + \tan^2 \frac{\theta}{2}}{2 \tan \frac{\theta}{2}} \right) \quad (15)$$

and can also be expressed

$$\dot{h}_{\min} = -\dot{\theta}_{\min} \left(\frac{h^2}{s} + \frac{s}{4} \right) \quad (16)$$

by substituting equation (10) in equation (15). If $\dot{\theta}_{\min}$ is a constant and has no dependence on visual angle, then for the case of a single reference object, the most sensitive velocity cue will be at impact with the surface. When the view is unobstructed, however, distinctive terrain features may be seen over a wide range of visual angles. In this case, it is necessary to find the object size at a given height that will minimize the vertical velocity at the threshold; this is done by differentiating equation (16) with respect to s , holding $\dot{\theta}_{\min}$ and h constant, to give

$$\frac{dh_{\min}}{ds} = -\dot{\theta}_{\min} \left(\frac{-h^2}{s^2} + \frac{1}{4} \right) = 0 \quad (17)$$

$$h = \frac{s}{2} \quad (18)$$

The maximum sensitivity to velocity would therefore be provided by terrain features on a 90° visual cone. However, for human control, it is the product on the right side of equation (11) that must be minimized ($\dot{\theta}_{\min}$ cannot be assumed a constant with no dependence on θ). Measurements necessary to determine variations in the threshold of the angular-velocity perception of the eye over a range of visual angles have been made (263). The threshold is defined as the minimum angular rate that can be detected visually with a high degree of probability in 2 seconds. Figure 2-76 and discussion cover the results of these studies. These values seem reasonable in view of human visual resolution and maximum major retention times. Additional helicopter descent studies indicate the $(\frac{h}{\dot{h}})$ values are conservative enough for design assumptions (263). These data can also be used for calculation of the point on approach path in lunar landing where emergency visual mode with velocity detection may be brought into play.

Visual determination of altitude on the lunar surface has been simulated (262). Surface feature techniques, when the surface feature is viewed from directly above, seems considerably more accurate for altitude determination than do horizon-matching techniques.

Visual Performance on the Moon

The lunar optical environment has been covered in section 1. Figure 2-17 shows the manner in which contrast and size of objects are related at a wide range of adapting luminances. The near coincidence of the curves at 1000, 100, and 10 mL for objects subtending 10 minutes or more is important to note, for it indicates that eye-protective filters which transmit 10% total or one percent of visible light will not significantly impair contrast discrimination at the higher ambient levels of field luminance. It is clear that the expected luminance levels on the lunar surface (Fig. 2-10 & Table 2-11) are, in the main, well within the operational tolerances of ordinary seeing. There are, however, certain special properties of the lunar visual environment which are unlike any naturally-occurring terrestrial ones (410).

The lack of a lunar atmosphere has several important consequences for the lunar explorer. The first consequence of a missing atmosphere is the absence of diffused light. Shadowed parts of the moon's surface will be very black; the contrasts in the scene will be extremely high and it seems likely that details of the shadowed areas can only be seen by use of some reflective device or auxiliary light source. Another property of the atmosphere on Earth, generally known as atmospheric haze, is habitually used in the estimation of distance and size of features. Since this cue will not be available, and because objects of familiar size may not be available for direct visual comparison, it is believed that the judgment of size and distance will have to be aided by special devices (theodolites, rangefinders) and by special observing techniques (motion parallax), at least at distances where man's accommodation and convergence cues are inoperative and stereopsis no longer helps. Correction for "irradiation" factors must be considered (194) (see Figure 2-49). Simulated studies in dust-free environments suggest some of the illusions which may arise (367).

Distance estimates of surface and flying objects on or near the lunar surface may offer some difficulty because of the unusual lighting conditions. Size, distance, motion and numerosity cues must be considered in analysis of the problem (153). (See also references on the discussion of range estimates during braking and docking maneuvers.) The use of these cues in night operations is another problem which needs further study (417).

Since the sky above the horizon will appear essentially black (unless the Sun or Earth is in the field of view) the adaptive capabilities of the man on the lunar surface may be taxed and his visual performance under such conditions cannot confidently be predicted from existing data (410). For the sunlit and earthlit conditions, the highly directional nature of the illumination will, especially at low angles, combine with the low average surface reflectance to produce wide extremes in the appearance of the terrain (112) (Figure 2-11). Small change in the sun's azimuth and elevation markedly alters the contrast conditions. With an apparent luminance of around 6.4×10^8 ft-L, and subtending a half degree, the sun constitutes a glare source of tremendous magnitude. If the man on the lunar surface must operate with the solar disc in his visual field, it is imperative that suitable protective devices be provided which will prevent discomfort or temporary or permanent visual disability. It has been argued that the man will always operate so as to avoid looking into or near the sun, but we must recognize the probability that accidental exposure will occur. Figure 2-46b suggests that an attenuation factor of about 10^5 will be required for direct viewing of the solar disc without discomfort. Furthermore, the eye-protective devices which have been proposed are far from ideal from the visual standpoint, tending to introduce contrast and acuity losses by reason of scattering or distortion (410).

Other potentially serious glare sources may be introduced by man himself. The need for thermal regulation of lunar excursion vehicles and, eventually, fixed habitats, has dictated that their surfaces be so treated as to be highly reflective. These surfaces are likely, therefore, to be very much brighter than the surrounding scene, especially if seen partly or wholly against the dark sky and may produce serious glare problems and temporary flash blindness. The reciprocity law and visual acuity during recovery should be confirmed under specific luminance x time conditions expected for lunar surface operations.

Preliminary data are available on performance of vision-based tasks in a lunar light simulator (376). The most unfavorable situation occurs when the astronaut's body or other obstacle blocks off light to the task equipment, creating deep shadows. Performance time decrement associated with control tasks varies between 18 and 50% under these conditions. Backlighted panels and display markings and reflecting bezels are recommended. Storage areas or containers require more lighting than in equivalent Earth design. Visual simulation for evaluation of lunar surface roving vehicles is currently under study (427).

Visualization of a vehicle in orbit as it appears near the lunar horizon is required in order to compute a launch time for optimum rendezvous, i.e., rendezvous in a direction away from the sun and prior to entering the

moon's shadow. In this case the astronaut is looking toward the sun. The minimum angle of separation between the command module and the sun for detectability, therefore, appears to be a function of two variables, viz., the brightness of the command module and the degree of impairment of visual resolution due to the glare effects of the sun. The surface of the moon, also a glare source, does not offer a serious problem since the average reflectivity coefficient is relatively low and methods for shielding these reflections are readily available, e.g., binoculars. The data on minimal angle of resolution (MAR) for two small luminous objects may be used in evaluating this problem and the "irradiation" factors of Figures 2-47 to 2-49 (194, 325, 326).

B. ULTRAVIOLET RADIATION

The major source of ultraviolet radiation expected during a space mission is the sun. Transmission of light by the atmosphere obeys the following equation very closely for any given wavelength, λ :

$$I_\lambda = I_{0\lambda} e^{-m_\lambda \sec z} \quad (19)$$

wherein I_λ is the intensity of radiation of wavelength λ arriving at the surface of the Earth, $I_{0\lambda}$ is the intensity of this radiation arriving at the outer margin of the Earth's atmosphere, m_λ is dependent only on λ and z is the angle which the sun subtends with the zenith, called the zenith angle. The length of atmosphere through which the sun's rays must pass (air mass) is directly proportional to the secant of z . The magnitude of m determines the extent of variation of the intensity I of any wavelength with zenith angle, and hence with latitude, season and time of day. For wavelengths for which m is large, the effect of increasing zenith angle is greater than for wavelengths for which m is small. An idea of the effect of zenith angle on the spectrum of sunlight at sea level may be gained from Figure 2-77 where curve 0 represents the spectrum of sunlight outside the Earth's atmosphere, curve 1 with the sun at zenith, and curve 2 with the sun at 60° from zenith (300). The strong effect of ozone absorption is seen at the short wavelength (ultraviolet) end of the spectrum; the effect of the absorption bands of water vapor, in the long wavelength (infrared) region. Detailed data on solar light absorption are available (250, 354).

The transmission of light of a given wavelength by an absorbing system in which scattering of light is negligible, may be described by Lambert's Law:

$$I = I_0 (1 - R)^2 e^{-\alpha t} \quad (20)$$

where I_0 is the intensity of the light entering the system. I is the intensity at depth t , α is a constant generally called the absorption coefficient, and R is the reflective coefficient.

In a system where there is a good deal of scattering, such as human skin, an equation of similar form may be applied:

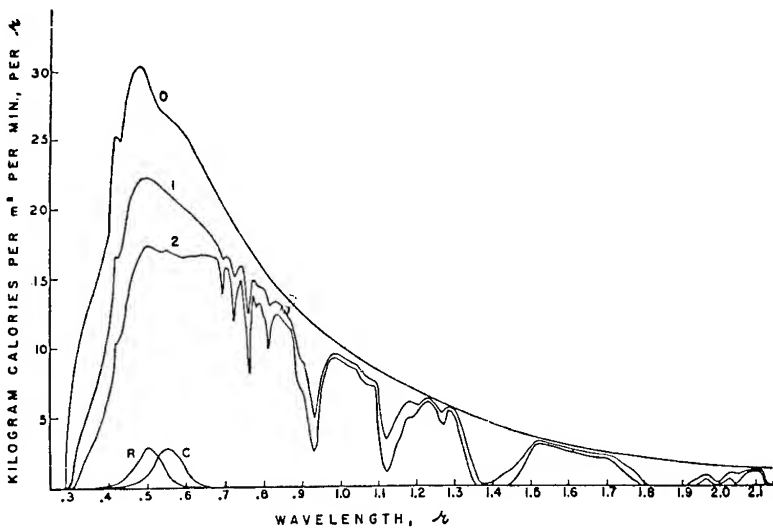


Figure 2-77

Spectral Distribution of Sunlight

0 - outside earth's atmospheres

1 - at sea level with sun at zenith

2 - at sea level with sun at 60°

R - relative sensitivity of the human eye, scotopic vision

C - relative sensitivity of the human eye, photopic vision

(After Blum⁽⁶⁰⁾)

$$I = I_0 e^{-m(\alpha, s)} \quad (21)$$

where $m(\alpha, s)$ is a function called the attenuation coefficient, which contains an absorption function, α , and a scattering function, s . The functions α and s are mutually dependent, but vary to different extents with the optical character of the medium and with the wavelength.

Effects of Ultraviolet Light on the Skin

The absorption of light by the skin is of interest to the designer of optical skin sensors as well as to those interested in ultraviolet effects.

Figure 2-78 represents the spectral absorption of light by white (W) and negro (N) skin.

Representation of the skin structures is diagrammatic, giving a schematized conception in which the dimensions should not be taken as generally representative, since the skin may vary widely in its thickness: c - corneum (horny layer of epidermis), m - Malpighian layer of epidermis, sw. - sweat gland, seb. - sebaceous gland, p - the most superficial blood vessels, arterioles, capillaries, and venules, h - hair follicle, s - hair shaft. The curves w and n give only rough estimates of depths at which

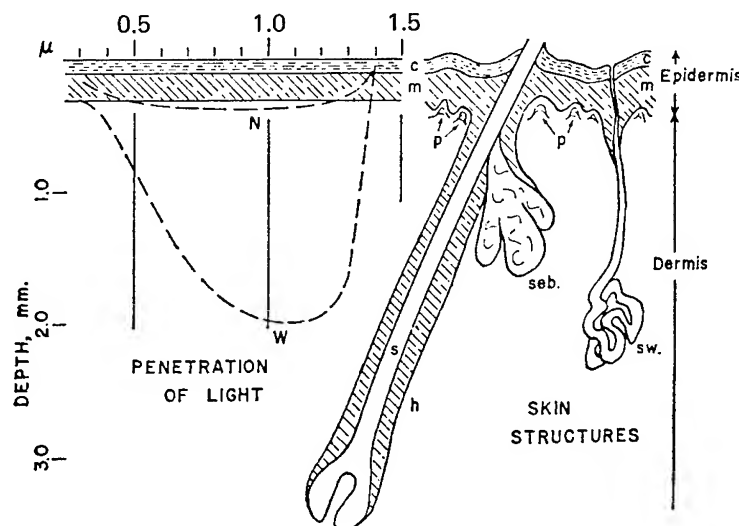


Figure 2-78

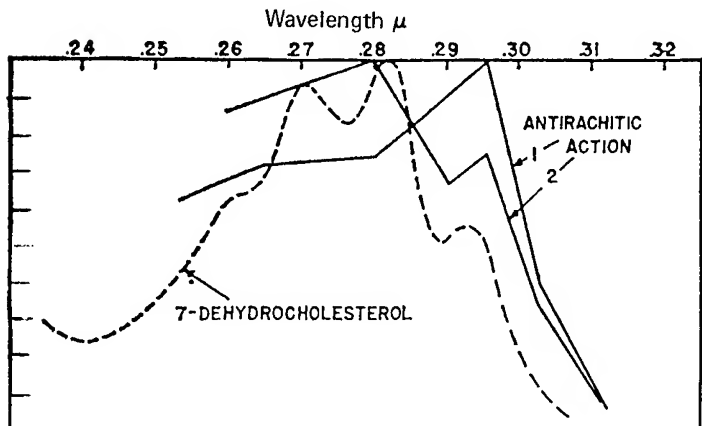
Penetration of Skin by Light
(After Blum⁽⁵⁵⁾)

radiation of the corresponding wavelengths is reduced to 5 percent of its incident value. There are insufficient data to make more than rough estimates, and these curves should be regarded as suggestive only.

The penetration of ultraviolet rays of wavelengths shorter than $0.32\text{ }\mu$ into the skin is of particular interest since these wavelengths produce specific physiologic and pathologic effects, the most obvious of which is sunburn. The thickness of the corneum varies widely from part to part of the body, and the depth of penetration of rays of these wavelengths varies accordingly. On the palms of the hands and soles of the feet, where this layer is very thick, virtually all of this radiation is absorbed before reaching the Malpighian layer. On the other parts of the body, the thickness may depend largely upon previous exposure to ultraviolet rays. Figure 2-79a shows the antirachitic (Rickets-preventing) action spectrum in two independent rat studies and the absorption spectrum of pro-vitamin D for conversion to active vitamin D in the skin. Figure 2-79b shows the erythema (redness) spectrum for the skin and absorption by the corneum which has a maximum near $0.28\text{ }\mu$ corresponding to an absorption maximum for protein, a large component of this layer.

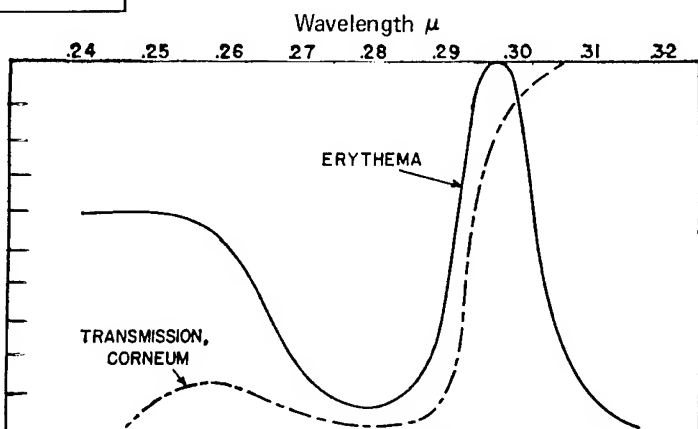
The fraction of radiation which has passed through the corneum is largely absorbed by the cells of the Malpighian layer by such strongly absorbing substances as proteins and nucleic acids. Here, scattering is probably considerably less, the optical boundaries being much less sharp than in the corneum. In general, very little radiation of wave lengths shorter than $0.32\text{ }\mu$ penetrates deeper than the epidermis, but a small fraction may reach the papillary layer of the dermis and have its effect there. Another absorbing component of the epidermis needs particular mention, the melanin pigment, which gives the brown and black color to skin. This is a finely granular substance found in skin, hair, and some other organs of mammals. There is a good deal of variety in chemical composition. From its chemical composition, melanin may be expected to show a maximum of absorption at about the same position as that of protein, at $0.28\text{ }\mu$; but, since the former is present in a much smaller amount in the corneum than the latter, its contribution to total absorption might be expected to be small. Melanin is a good scattering agent, however, and

Figure 2-79
Biological Action Spectrum of Ultraviolet Light
(After Blum⁽⁵⁸⁾)



a. Antirachitic Spectra (Rat Studies 1 and 2) and Absorption Spectrum of Provitamin D (7-dehydrocholesterol). The Ordinates are in Arbitrary Action and Absorption Units on a Linear Scale from 0 to 1.0.

b. Erythema Spectrum for Human Skin; Spectral Transmission of a Sample of Human Corneum. The Ordinates are in Arbitrary Action and Absorption Units on a Linear Scales from 0 to 1.0. Transmission of the Corneum is in Percent Extending Linearly from 0 to 25%.



may increase the absorption path. The quantitative role of melanin in protecting the skin against ultraviolet light is difficult to assess.

Transmission by the epidermis increases sharply for wavelengths longer than $0.32\text{ }\mu$; the light penetration into the skin as a whole increases to a maximum in the near infrared around $1.0\text{ }\mu$, then falls to virtual extinction at about $1.4\text{ }\mu$ due to strong absorption by water. Absorption by carotenoids and by hemoglobin in the long ultraviolet and shorter wavelengths of the visible can be neglected. Both these substances are important factors in determining the color or complexion of white skins, but have a minor effect on the total penetration of sunlight.

Sunburn

Exposure of skin to ultraviolet light results in the sunburn complex (56). Exposure of the skin to bright summer sunlight for half an hour or longer is followed, after a latent period of 3 to 6 hours, by dilatation of the minute vessels of the exposed area, manifested grossly as erythema (57, 216, 333). The erythema is accompanied by swelling, often so slight as to be almost imperceptible. If the exposure is prolonged, marked edema (swelling), desquamation (peeling), or blistering may follow, and there may be pain or

itching. The erythema fades in the course of a few days, being gradually replaced by "suntan" due to a rearrangement and increase of melanin in the epidermis. The suntan may persist for months or even years. In addition the suntan may darken by a process beginning almost immediately upon exposure, and ceasing with the exposure. The long latent period between exposure and the physiological responses may be accounted for by assuming that the physiologically active substances are elaborated by the injured cells at relatively slow rates.

Figure 2-79 shows an action spectrum for the erythema of sunburn of human skin obtained by determining, for a range of wavelengths, the dose of radiation required to elicit a just perceptible reddening. Numerous factors contribute to the complexity of the erythema response, and each may have somewhat different action spectra. This would help to explain the apparent paradox that reciprocity (dose-rate \times time = constant) holds very well when erythema production is studied with monochromatic radiation, whereas with polychromatic radiation this is not the case (62). The erythema spectrum has sometimes been used as a standard for comparison of the action of sunlight with the action of artificial sources; but it is clear that with these complicating factors there may be considerable inaccuracy involved.

Thickening of Skin

A result of the action of ultraviolet radiation on the epidermis is a rapid proliferation of the cells of the Malpighian layer. This leads to thickening of that layer and also of the corneum, as many of the Malpighian cells die and are incorporated into the horny layer (60). Thickening of the corneum results in a marked decrease in the amount of sunburn-producing radiation that reaches the Malpighian layer; that is, the effectiveness of the corneum as a filter is increased, with a resultant reduction in sensitivity to sunburn. In white-skinned people, the thickening of the corneum is clearly a principal cause of the apparent immunity to sunburn that is experienced after exposure to sunlight or other source of ultraviolet radiation. This point is not generally understood, and it is commonly thought that the tanning of the skin, that is, the production of melanin pigment in the epidermis, is the only thing that gives protection from sunburn.

Tanning

The tanning process is itself quite complicated. In white races the melanin pigment, which confers the tan color, is found principally in the deepest part of the Malpighian layer (60, 62, 214, 215). About twenty hours after the exposure to ultraviolet light, some of this melanin begins to migrate toward the surface, and following this there is production of new pigment in the basal layer. Later, with the death of cells from the Malpighian layer and their incorporation into the corneum, the melanin gets into that layer too. In Negro skin the melanin is present in greater quantity and is also distributed more uniformly through the epidermis, including the corneum. Negro skin not only contains more melanin but also is thicker (411), both factors apparently contributing to the greater opacity that is associated with low susceptibility to sunburn (60). Ultimately, if the skin is not exposed, the melanin not only bleaches but also may disappear completely; but the

disappearance may take months or even years, whereas susceptibility to sunburn will have returned in several weeks.

Phototoxicity and Photallergy

Certain drugs and disease states increase the sensitivity of the skin to long wave ultraviolet and even visible light. Several excellent reviews are available (18, 59).

Effects of Ultraviolet on the Eye

Light reaches a much greater depth in the eye (2.3 cm) than in any other part of the body. The media of the various parts of the eye, including the retina, are highly transparent to the wavelengths of visible light (approximately 0.39μ to 0.65μ), with little absorption and scattering (63). At the short end of the visible spectrum, however, about 50% of the light is scattered (101). Absorption of all wavelengths is virtually complete in the retinal pigment layer. There is no horny layer, as in the skin. The outer layer of the eye, the cornea, is a membrane consisting of extracellular collagen and polysaccharide. A thin layer of viable cells is kept moist by secretion from the lacrimal glands. Some attenuation of ultraviolet of greater than 0.32μ wavelength takes place in the lens. Wavelengths shorter than 0.32μ , on the other hand, penetrate very little, apparently not reaching the lens to any great extent. As in the case of skin, water absorption sets the long wavelength limit at about 1.4μ . A diagram of the estimated spectral intensity of sunlight reaching the level of the retina is shown in Figure 2-80. Fluorescence

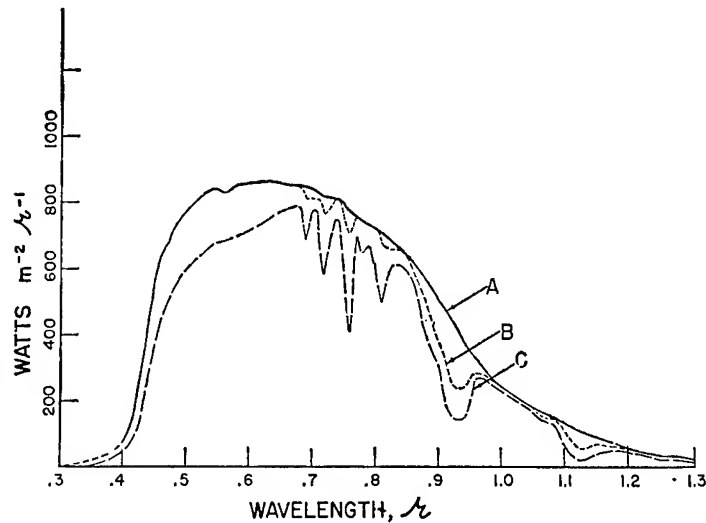


Figure 2-80

Estimates of Sunlight Reaching the Human Retina. A - Sun at Zenith, Dry Air; B and C - Air Containing 20 mm. Precipitable Water; B, Sun at Zenith, and C, Sun 60° from Zenith.

(After Blum⁽⁵⁶⁾)

of the optical media by ultraviolet light of about 0.36μ can degrade vision by decreasing contrast conditions through a glare effect.

Wavelengths shorter than 0.32μ that cause sunburn are absorbed very superficially in the eye, where they may cause damage to the cells of the cornea, called keratitis. The manifest symptoms are pain, disturbances of vision, and photophobia (light intolerance), with congestion of the conjunctiva, excessive secretion, and swelling, according to the extent of the injury. When

such symptoms occur after exposure in the neighborhood of snow fields, where there is a good deal of diffuse reflection, the condition is often referred to as "snow blindness". These wavelengths are absorbed so superficially that they do not cause damage to structures at any depth. Arc welders also get keratitis from UV emission in the arc (395).

The spectral dependence of energy required for threshold keratitic damage has not been determined for humans but is known for rabbits (102). The data are probably valid for humans.

The most characteristic sign of keratitis with threshold reactions is a stippled appearance within the corneal surface epithelium as seen by trans-illumination with the slit lamp and after staining with fluorescein. This stippling may be seen to be due to multiple punctate erosions (101). With more severe reactions there is a corresponding increase in the number of granules, ultimately forming a mosaic. With relatively severe exposures the cornea becomes uniformly hazy. It is of interest that the cloudiness of the stroma occurs only with amounts of radiation which would be expected on the basis of transmission measurements to penetrate the cornea in sufficient quantities to produce a threshold reaction in the endothelium or inner lining layer.

Figure 2-81 represents the action spectrum of keratitis and the absorption spectrum of several glasses 2 mm in thickness.

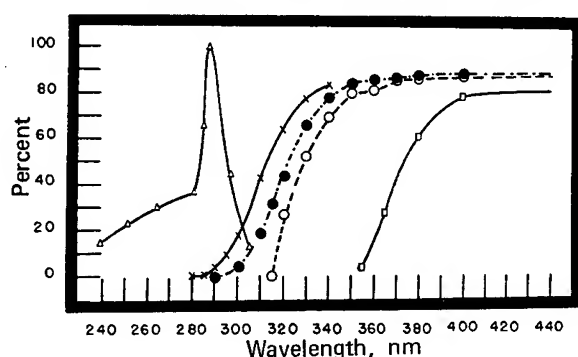


Figure 2-81

Curves Illustrating the Action Spectrum (Rabbits) of Keratitis (Line and Triangles) and the Absorption by Glass of 2 mm. Thickness of the Following Types: Crown or Spectacle Glass (Line and Crosses), Window Glass (Line and Dark Circles), Plate Glass (Line and Hollow Circles), and Flint Glass (Line and Rectangles).

(After Cogan and Kinsey (102))

The action spectrum rises abruptly with a peak of 288 nm, and shows by extrapolation that the long wavelength limit lies somewhere between 306 and 326 nm. The absorption curve of corneal epithelium peaks at 265 nm. There is no evidence of selective absorption at the wavelength corresponding to the peak of the action spectrum causing keratitis. This suggests that the amount of photosensitive substance present is small, e.g., an enzyme, or alternatively, that the abiotic effects are due to absorption by some small fraction of the protein complex having absorption maximums similar to the keratitis maximum. The energy necessary to elicit a threshold reaction in the cornea at the wavelength of peak sensitivity is of the order of 0.15×10^6 ergs. This is to be compared with the value of 2.0×10^6 ergs when the whole ultraviolet portion of the spectrum is utilized (102, 125, 426).

The lens does absorb some of the longer wavelengths of the ultraviolet. When the lens is removed these reach the retina where they stimulate the rods; the eye thus perceiving shorter wavelengths more than normally (431).

Retinal blindness caused by looking directly at the sun is not produced by ultraviolet but by focusing of light in the visible spectrum on the retinal structures (See Section A - Visible Light). Claims that ultraviolet rays may damage the retina seem unfounded. It is doubtful that either the ultraviolet or the total energy from sunlight can cause cataract in human eyes, that is, opacification of the lens. This may be brought about, however, by radiation from lower temperature sources, such as glass blowers' furnaces (glass blowers' cataract), which may have much more emission in the infrared than does sunlight (60).

Eye Protection Against Ultraviolet

The absorption of ultraviolet by optical media follows Lambert's Law of Equation 2-20. Part of the incident radiation is reflected at the front surface; part of it is absorbed in passing through the substance; and part is reflected at the back surface. In the case of glass about 4 percent of the radiation is reflected at each glass air surface when the radiation is incident normal to the surface. Another 4 percent is reflected at the surface where the light emerges, so that even if the glass had no absorption (and consequently 100 percent internal transmittance), its external transmittance would only be 92 percent.

A convenient way of presenting information about the internal transmittance of substances, I/I_0 , is to give the values of the absorption coefficient at various wavelengths. Knowing this, the transmittance for any particular thickness may be calculated from Equation 2-20. For convenience in calculating, this relation is given graphically in Figure 2-82a where values of transmittance are plotted as a function of a with the thickness of the absorbing medium as a parameter. Figure 2-82b shows the values of transmittance as a function of the thickness of the medium with absorption coefficient as a parameter.

Data are available on the absorption coefficient of many different glasses and plastics (250). The transmission of glass in the ultraviolet is determined largely by the iron oxide content (ferric state) which absorbs strongly in this region. Impurities of less than 0.01 percent may have profound effects. Figure 2-81 indicates the absorption characteristics of the common glasses. A 2mm. thickness of crown glass reduces the exposure hazard approximately fifteenfold at 305 millimicrons, forty-five fold at 297 millimicrons and a hundred fold at 268 millimicrons (320). A 2 mm. thickness of flint glass affords essentially complete protection at all wavelengths. Pyrex and Corex, heat resistant glasses, have higher transmissions than plate or flint glasses. Vycor glasses, approaching silica in their properties, show very high transmission in the ultraviolet. These have been used for windows in the Mercury series (165). Fused quartz can be used where optimum ultraviolet transmission is required. Various glasses, crystalline minerals, and solutions can be used as filters for specific ultraviolet bands (250). Exposure to sunlight will gradually oxidize the absorbing minerals and increase the absorption of UV in glasses and plastics. This solarization must be accounted for when precise control of the ultraviolet transmission is required. Noviol glasses can be used in eye-protective devices where

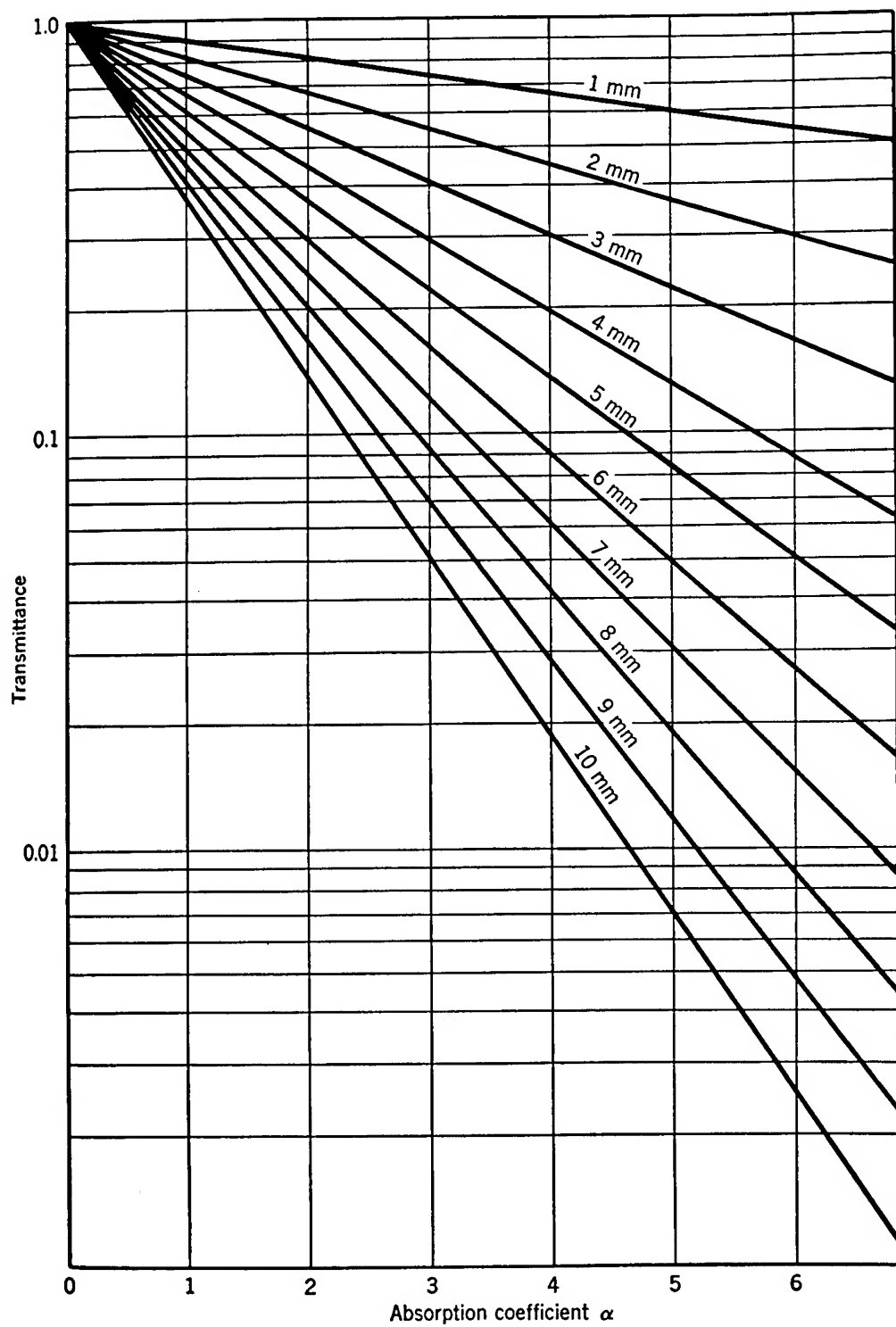


Figure 2-82a

Transmittance as a Function of Absorption Coefficient for Various Thicknesses
of Absorbing Medium

(After Koller⁽²⁵⁰⁾)

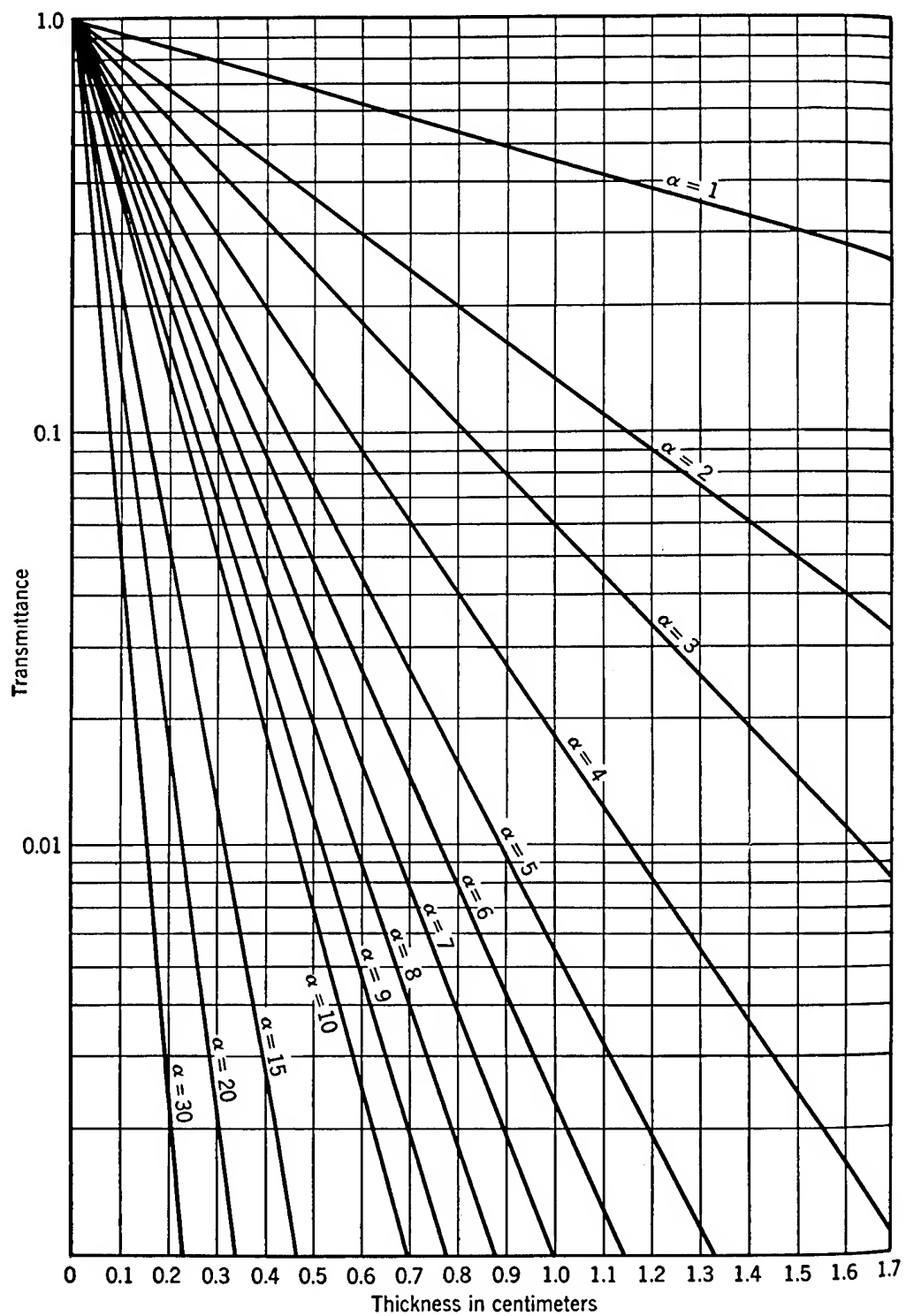


Figure 2-82b

Transmittance as a Function of Thickness for Various Values of Absorption Coefficient

(After Koller⁽²⁵⁰⁾)

high intensity ultraviolet exposure is anticipated such as in welding (250, 395). Polaroid ultraviolet filters are also available (395).

Plastic materials vary in their absorption of ultraviolet (250, 395). Care must be taken in choosing the appropriate plastic window and visor materials maximizing UV absorption. Helmet polycarbonates do require UV inhibitors. Figure 2-83 presents the UV absorbance of four compounds used in plastics to increase the natural UV absorbance. In addition to absorbing ultraviolet light from the visual pathway, these compounds also stabilize the plastics by decreasing photo-oxidation and degradation of structural integrity. These compounds do tend to discolor the plastics to a variable degree. This factor must be controlled in helmet and visor applications (176).

In orbit or on the lunar or planetary surface, the full intensity of ultraviolet radiation is experienced (see solid line in Figure 2-77). Data are available on the ultraviolet transmission of military helmet visor systems (82, 87). For the gold-coated visor (Class 3) there is less than 0.5% for any wavelength in the 290 to 320 nm erythema band. Such visor systems can absorb the visible light band to a 2% transmission level and cause no operational problems except in dusk light conditions (87).

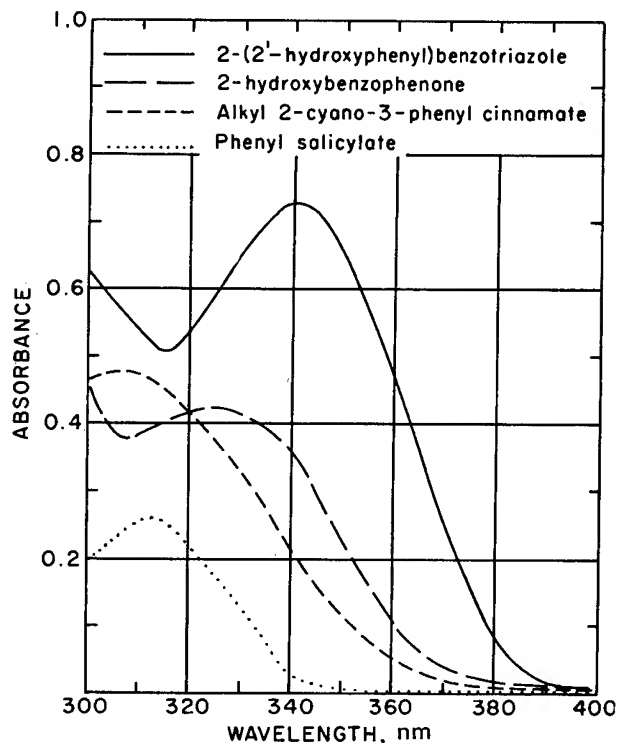
Eye Trauma in Space Operations

Weightlessness in orbit increases the chances of trauma to the eye by floating debris and chemicals. Treatment of the various eye trauma syndromes in space operations has been covered in great detail in a recent review (84).

Figure 2-83
Variations in UV Absorbance of the Four Compounds Most Commonly used as UV Absorbers in Plastics

Wavelength range shown is that most important in protection of plastics against photodegradation. Absorbers were at a concentration of 1.0 mg/100 ml in CHCl_3

(After Gordon and Rothstein⁽¹⁷⁶⁾)



REFERENCES

- 2-1. Adler, F. H., Physiology of the Eye: Clinical Application, C. V. Mosby Co., St. Louis, 3rd Edition, 1959.
- 2-2. Advisory Group for Aerospace Research and Development, Loss of Vision from High Intensity Light, AGARD-CP-11, 1966, A Symposium sponsored by the Aerospace Medical Panel of AGARD-NATO, Paris, France, Mar. 16-17, 1966. (AD-653917).
- 2-3. Aeronautical Systems Division, Colors, Aeronautical Lights and Lighting Equipment, General Requirements for #ASG#, MIL-C-25050A, Research and Technology Div., Systems Engineering Group, Wright-Patterson AFB Ohio, Dec. 2, 1963.
- 2-4. Air Force, Washington, D. C., Lenses, Goggle and Visor, Helmet, Optical Characteristics, General Specification. MIL-L-38169, Mar. 26, 1963 and Amend. 2, Sept. 21, 1964.
- 2-5. Air Force Systems Command Headquarters, Handbook of Instructions for Aerospace Personnel Subsystem Designers (HIAPSD), AFSCM-80-3, Washington, D. C., 1966.
- 2-6. Aitken, R. C., Ferres, H. M., Gedye, J. L., Distraction from Flashing Lights, Aerospace Med., 34: 302-306, Apr. 1963.
- 2-7. Akulinichev, I. T., Yemel'yanov, M. D., Maksimov, D. B., Oculomotor Activity in Cosmonauts during Orbital Flight, Izvestia Akademii Nauk SSSR, Seria Biologicheskaiia, No. 2: 274-278, Mar. Apr., 1965.
- 2-8. Alexander, W. C., Sever, R. J., Fedderson, W. E., et al., Acceleration (+G_x) Induced Hypoxemia and Crew Performance, NASA Manned Spacecraft Center, Houston, Texas. Paper presented at the Scientific Program, Aerospace Med. Assn., 35th Annual Mtg., May 11-14, 1964, Miami Beach, Fla.
- 2-9. Allen, L. K., Dallenbach, K. M., The Effect of Light Flashes during the Course of Dark Adaptation, Amer. J. Psychol., 51: 540-548, 1938.
- 2-10. Allen, R. G., Jungbauer, D. E., Isgitt, D. J., et al., Nuclear Flash Eye Effects Technical Report for Military Planners, School of Aerospace Medicine, Aerospace Medical Div., Brooks AFB, Texas, Feb. 1967. (AD-659145).

- 2-11. Allen, R. W., Hershberger, M. L., Telescope Field-of-View Requirements for Star Recognition, Human Factors, 8: 41-47, 1966.
- 2-12. Allen, W. H., Need for Validity in Simulation of the Extra-terrestrial Visual Environment, AIAA-67-251, presented at AIAA Flight Test, Simulation and Support Conference, Cocoa Beach, Fla., Feb. 6-8, 1967.
- 2-13. Allphin, W., BCD Appraisals of Luminaire Brightness in a Simulated Office, Illum. Engin. 56: 31, 1961.
- 2-14. Arden, G. B., The Sensory Effects of Drugs, Electrophysiological Investigations of the Mechanism of the Action of Drugs on the Eye, in Recent Developments in Vision Research, Whitcomb, M. A., (ed.), NAS-NRC-1272, National Academy of Sciences - National Research Council, Washington, D. C., 1966, pp. 194-209.
- 2-15. Argyle, E., Optical Environment in Gemini Space Flights, Science, 155(3760): 354, Jan. 1967.
- 2-16. Arnold Engineering Development Center, Annual Symposium on Space Environment Simulation, Fifth, May 21-22, 1964, AEDC, Headquarters, Arnold Air Force Station, Tenn., 1965. (AD-441312).
- 2-17. Aulhorn, E., Uber Die Sehscharfe Bei Herabgesetzter Beleuchtung, Ber. Deutsch. Ophth. Ges., 64: 555-559, 1961.
- 2-18. Baer, R. L., Harber, L. C., Light Sensitivity in Biologic Systems, Phototoxicity and Photoallergy Related to Visible Light, Fed. Proc., 24: S-15-S-21, 1965.
- 2-19. Baird, F. E., Schindler, R. A., Smith, R. N., An Optical Aid for Manual Acquisition and Tracking of a Target Satellite during a Rendezvous Mission, Adv. Astronautical Sci., 16: 585-598, 1963.
- 2-20. Baird, J. C., Effects of Stimulus-Numerosity upon Distance Estimates, Psychon. Sci., 6(4): 133-134, 1966.
- 2-21. Baird, J. C., Biersdorf, W. R., Quantitative Functions for Size and Distance Judgments, Percept. Psychophysics, 2: 161-166, 1967.
- 2-22. Baker, C. A., Steedman, W. C., Estimation of Visually Perceived Closure Rates, Human Factors, 4: 343-347, Dec. 1962.

- 2-23. Baker, C. A., Steedman, W. C., Perceived Movement in Depth as a Function of Luminance and Velocity, Human Factors, 3(3): 166-173, Sept. 1961.
- 2-24. Baker, C. A., Morris, D. F., Steedman, W. C., Target Recognition on Complex Displays, WADC-TR-59-418, 1959.
- 2-25. Baker, C. A., Grether, W. F., Visual Presentation of Information, WADC-TR-54-160, Wright Air Dev. Center, Wright-Patterson AFB, Ohio, 1954.
- 2-26. Baker, K. E., Some Variables Influencing Vernier Acuity. I. Illumination and Exposure Time. II. Wavelength of Illumination, J. Opt. Soc. Amer., 39: 567-576, 1949.
- 2-27. Barber, E., Radiometry and Photometry of the Moon and Planets, JPLAI-LS-345, Jet Propulsion Lab., California Inst. of Technology, Pasadena, Calif., Sep. 1961.
- 2-28. Bartley, S. H., Light Adaptation and Brightness Enhancement, Percept. Motor Skills, 7: 85-92, 1957.
- 2-29. Bartley, S. H., The Psychophysiology of Vision, in Handbook of Experimental Psychology, Stevens, S. S. (ed.), John Wiley & Sons, Inc., N. Y., 1951, Chapt. 24.
- 2-30. Bartley, S. H., Vision: A Study of Its Basis, Hafner Publishing Co., N. Y., 1963, p. 239.
- 2-31. Bate, A. J., Bates, C., Jr., A Comparison of Cockpit Warning Systems, AMRL-TR-66-180, Aerospace Medical Research Labs., Wright-Patterson AFB, Ohio, Apr. 1967.
- 2-32. Bate, A. J., Self, H. C., Target Detection on Side-Looking Radar When Image Motion Can be Temporarily Delayed, AMRL-TR-67-23, Aerospace Medical Research Labs., Wright-Patterson AFB, Ohio, Nov. 1967.
- 2-33. Beasley, G. P., Pilot-Controlled Simulation of Rendezvous between a Spacecraft and a Command Module Having Low Thrust, NASA-TN-D-1613, 1963.
- 2-34. Bergey, G. E., Sipple, W. C., Hamilton, W. A., et al., A Technique for Determining an Index of Visual Alertness from the Electroencephalogram, NADC-MR-6618, Naval Air Development Center, Aerospace Medical Research Department, Johnsville, Pa., May 1967.
- 2-35. Berry, C. A., Eastwood, H. K., Helicopter Problems: Noise, Cockpit Contamination and Disorientation, Aerospace Med., 31: 179-190, Mar. 1960.

- 2-36. Berry, R. N., Riggers, L. A., Duncan, C. P., The Relation of Vernier and Depth Discriminations to Field Brightness, J. Exp. Psychol., 40: 349-354, 1950.
- 2-37. Bertelson, R. C., Glanz, K. D., McQuain, D. B., et al. Effort to Evolve a Method of Eye Protection from Flash Blindness, National Cash Register Co., Dayton, Ohio, Dec. 1966. (AD-645730).
- 2-38. Biersdorf, W. R., Convergence and Apparent Distance as Correlates of Size Judgements at Near Distances, J. Gen. Psychol., 75: 249-264, 1966.
- 2-39. Billmeyer, F. W., Jr., Optical Aspects of Color,
Pt. I., Optical Spectra, 1(2): 59-63, Apr.-May-June 1967.
Pt. II., Putting Numbers on Color with the CIE System, Optical Spectra, 1(3): 44-48, Third Qtr., 1967.
Pt. III., Light Sources and Their Effects on Color, Optical Spectra, 1(4): 71-74, Fourth Qtr., 1967.
Pt. IV., The Perception and Description of Color, Optical Spectra, 2(1): 43-47, Jan-Feb. 1968.
- 2-40. Birren, F., Color for Interiors: Historical and Modern, Hill & Wang, Inc., N. Y., 1963.
- 2-41. Birren, F., Color, Form and Space, Reinhold Publishing Corp., N. Y., 1961.
- 2-42. Birren, F., Creative Color, Reinhold Publishing Corp., N. Y., 1961.
- 2-43. Bittini, M., Nicoletti, I., Ronchi, L., Basic Research in the Field of Vision, AFOSR TN 57-682, Air Force Office of Scientific Res., Washington, D. C., 1957.
- 2-44. Bittini, M., Ercole, A. M., Fiorentini, A., et al., Enhanced Contrast of an Indefinitely Contoured Object by Movement or Intermittent Illumination, Serie II, No. 898, Pubblicazioni Dell' Istituto Nazionale di Ottica, Arcetri-Firenze, 1960. (Also reprinted in: Atti. Fond. G. Ronchi, 15: 62-84, Jan.-Feb. 1960).
- 2-45. Bittini, M., Gloria, E., The Relationship of Subjective Sharpness Threshold to Retinal Position, Atti. Fond. G. Ronchi, 20(6): 677-685, Dec. 1965.
- 2-46. Bixel, G. A., Blackwell, H. R., The Visibility of Non-Uniform Target-Background Complexes. II. Further Experiments, OSU-RF-TR-890-2, Ohio State University Research Foundation, Columbus, Ohio, July 1961. (AD-297069).

- 2-47. Blackwell, H. R., Contrast Thresholds of the Human Eye, J. Opt. Soc. Amer., 36: 624-643, Nov. 1946.
- 2-48. Blackwell, H. R., Development and Use of a Quantitative Method for Specification of the Interior Illumination Levels on the Basis of Performance Data, Illum. Engin., 54: 317-353, 1959.
- 2-49. Blackwell, H. R., The Effects of Certain Psychological Variables Upon Target Detectability, Rep., 2455-12-F, Eng. Res. Inst., University of Michigan, 1958.
- 2-50. Blackwell, H. R., Smith, S. W., Cutchshaw, C. M., et al., The Effects of Target Size and Shape on Visual Detection. Project Michigan, Willow Run Labs., Ann Arbor, University of Michigan. I. Continuous Foveal Targets at Moderate Background Luminance, Report 2144-279-T. (AD-203073) II. Continuous Foveal Targets at Zero Background Luminance, Rep. 2144-334-T, Jan. 1959. (AD-211452) III. Effects of Background Luminance Duration, Wavelength, and Retinal Location, Rep. 2144-346-T, Dec. 1958. (AD-210277). IV. Some Relations with Previous Investigations, Rep. 2144-335-T, Feb. 1959.
- 2-51. Blackwell, H. R., Ohmart, J. G., Brainard, R. W., Experimental Evaluation of Optical Enhancement of Literal Visual Displays, ASD-TR-61-568, Aeronautical Systems Div., Wright-Patterson AFB, Ohio, 1961.
- 2-52. Blackwell, H. R., McCready, D. W., Jr., Foveal Contrast Thresholds for Various Durations of Single Pulses, Eng. Res. Inst., Rept. No. 2455-13-F, University of Michigan, 1958.
- 2-53. Blackwell, H. R., Bixel, G. A., The Visibility of Non-Uniform Target Background Complexes, I. Preliminary Experiments, OSU-RF-TR-890-1, Ohio State University, Research Foundation, Columbus, Ohio, 1960, p. 36.
- 2-54. Blondel, A., Rey, J., Sur La Perception Des Lumieres Breves A La Limite De Leur Portee, J. Phys., Paris, 1: 530-550, 1911.
- 2-55. Blum, H. F., Does the Melanin Pigment of Human Skin Have Adaptive Value? An essay in human ecology and the evolution of race, Quart. Rev. Biol., 36: 50-63, 1961.
- 2-56. Blum, H. F., Effects of Sunlight on the Human Body, in Medical Climatology, Vol. 8, Licht, S., (ed.), E. Licht, New Haven, Conn., 1964, pp. 229-256.

- 2-57. Blum, H. F., Terus, W. S., Inhibition of the Erythema of Sunburn by Large Doses of Ultraviolet Radiation, Amer. J. Physiol., 146: 97-106, 1946.
- 2-58. Blum, H. F., Photobiological Research with Particular Reference to Skin, J. A. M. A., 173: 1353, 1357, 1960.
- 2-59. Blum, H. F., Photodynamic Action and Diseases Caused by Light, Hafner Publishing Co., N. Y., Revised Edition, 1964.
- 2-60. Blum, H. F., Physiological Effects of Sunlight on Man, Physiol. Rev., 25: 483-530, 1945.
- 2-61. Blum, H. F., Solar Energy Reaching the Retina: Proposed Spectral Curve for Testing Sunscanning Glasses, Research Proj. X 435, Nav. Med. Res. Inst., Bethesda, Md., 1944.
- 2-62. Blum, H. F., Sunburn, in Radiation Biology, Vol. II, Ultraviolet and Related Radiations, Hollaender, A., McGraw-Hill, N. Y., 1955, pp. 487-528.
- 2-63. Boettner, E. A., Spectral Transmission of the Eye, Univ. of Michigan, Contract AF41(609)-2966, School of Aerospace Medicine, Brooks AFB, Texas, Jul. 1967.
- 2-64. Boring, E. G., Langfeld, H. S., Weld, H. P., Foundations of Psychology, John Wiley & Sons, N. Y., 1948.
- 2-65. Breckenridge, F. C., Colors of Signal Lights, Their Selection, Definition, Measurement, Production, and Use, NBS-Monograph-75, National Bureau of Standards, Washington, D. C., Apr. 1967.
- 2-66. Breinin, G. M., Perryman, J. H., Studies in the Pharmacology of Extraocular Muscles, in Recent Developments in Vision Research, Whitcomb, M. A., (ed.), NAS-NRC-1272, National Academy of Sciences - National Research Council, Washington, D. C., 1966, pp. 210-212.
- 2-67. Brissenden, R. F., Burton, B. B., Foudriat, E. C., et al., Analog Simulation of a Pilot-Controlled Rendezvous, NASA-TN-D-747, 1961.
- 2-68. Brissenden, R. F., A Study of Human Pilot's Ability to Detect Angular Motion with Application to Control of Space Rendezvous. NASA-TN-D-1498, Dec. 1962.
- 2-69. Brissenden, R. F., Lineberry, E. C., Jr., Visual Control of Rendezvous. Aerospace Engr., 21: 64-65, 74-78, June 1962.

- 2-70. Britten, A. J., Eye-Protective Devices, Ordnance, 45: 312-315, Nov.-Dec. 1964.
- 2-71. Broadbent, D. E., On the Dangers of Over-Arousal, MRC Applied Psychology Unit, Cambridge, England. Paper presented at the Basic Environmental Problems of Man in Space, 2nd International Symposium, Paris, June 14-18, 1965.
- 2-72. Broadbent, D. E., Vigilance, Brit. Med. Bull., 20(1): 17-20, 1964.
- 2-73. Brown, D. R. E., Natural Illumination Charts, U. S. Navy R & D Project NS 714-100, Report No. 374-1, Sept. 1952.
- 2-74. Brown, F. R., A Study of the Requirements for Letters, Numbers, and Markings to be Used on Trans-Illuminated Aircraft Control Panels. Part 4, Legibility of Uniform Stroke Capital Letters as Determined by Size and Height to Width Ratio and as Compared to Garamond Bold, Proj. TED NAM EL-609, Naval Air Material Center, Aeronautical Med. Equip. Lab., Philadelphia, Pa., March 10, 1953.
- 2-75. Brown, J. L., Experimental Investigations of Flash Blindness, Human Factors, 6: 503-516, 1964.
- 2-76. Brown, J. L., Study of Visual Perception in Humans and Animals, Sensitivity and Spectral Response Properties of Human Vision at Low Luminances, Tech. Rep. 2, Kansas State University, Manhattan, Kan., 1966. (AD-640555).
- 2-77. Brown, J. L., Phares, L., Fletcher, D. E., Spectral Sensitivity of the Eye Based on Visual Acuity, NADC-MA-6006, Naval Air Dev. Center, Johnsville, Pa., Apr. 1960.
- 2-78. Brown, R. H., Visual Sensitivity to Differences in Velocity, Psychol. Bull., 58: 89-103, Mar. 1961.
- 2-79. Brown, R. H., Weber Ratio for Visual Discrimination of Velocity, Science, 131: 1809-1810, Mar. 7, 1960.
- 2-80. Bryam, G. M., The Physical and Photochemical Basis of Visual Resolving Power. I. The Distribution of Illumination in Retinal Images, J. Opt. Soc. Amer., 34: 571-591, 1944.
- 2-81. Buckner, D. N., McGrath, J. J., Vigilance: A Symposium, McGraw-Hill, N. Y., 1963.
- 2-82. Bureau of Naval Weapons, Visors, Protective, Helmet, MIL-V-22272B (WP), Military Specifications, Washington, D. C., Jan. 28, 1965.

- 2-83. Burg, J., Visual Acuity as Measured by Dynamic and Static Tests: A Comparative Evaluation, J. Appl. Psychol., 50(6): 460-466, 1966.
- 2-84. Busby, D. E., Clinical Space Medicine: A Prospective Look at Medical Problems from Hazards of Space Operations, NASA-CR-856, 1967.
- 2-85. Cameron, W. S., Man in Space, in Introduction to Space Science, Ness, W. N., (ed.), Gordon and Breach, N. Y., 1965, p. 545.
- 2-86. Carel, W. L., Visual Factors in the Contact Analog, GE-R61ELC60, General Electric, Ithaca, N. Y., 1961.
- 2-87. Carpenter, J. A., Richey, E. O., Evaluation of Two Percent Gold Visor, SAM-TR-66-71, School of Aerospace Medicine, Brooks AFB, Texas, 1966.
- 2-88. Catterson, A. D., NASA, Manned Spacecraft Center, Houston, Texas, personal communication, 1967.
- 2-89. Cavonius, C. R., The Effect of Wavelength on Visual Acuity, ERF-RR-1/67-Cr, The Eye Research Foundation, Bethesda, Md., 1967. (AD-646575).
- 2-90. Chalmers, E. L., Goldstein, M., Kappauf, W. E., The Effect of Illumination on Dial Reading, AF-TR-6021, Wright-Patterson AFB, Ohio, 1950.
- 2-91. Chapanis, A., Garner, W. R., Morgan, C. T., Applied Experimental Psychology, John Wiley & Sons, N. Y., 1949.
- 2-92. Chapanis, A., Color Names for Color Space, Amer. Sci., 53: 327-346, Sept. 1965. (AD-626313).
- 2-93. Chapanis, A., How We See: A Summary of Basic Principles, in Human Factors in Undersea Warfare, National Research Council, Washington, D. C., 1949, pp. 3-60.
- 2-94. Chisum, G. T., Trent, K. B., Morway, P. E., Effects of Blue Cutoff Filters on Color Discrimination, NADC-MR-6704, Naval Air Development Center, Aerospace Medical Res. Dept., Johnsville, Warminster, Pa., Apr. 1967.
- 2-95. Chisum, G. T., Intraocular Effects on Flashblindness, NADC-MR-6719, Naval Air Development Center, Aerospace Medical Res. Dept., Johnsville, Warminster, Pa., Dec., 1967.
- 2-96. Clark, H. J., Control of a Remote Maneuvering Unit Satellite Inspection, AMRL-TR-66-134, Aerospace Medical Research Labs., Wright-Patterson AFB, Ohio, 1966.

- 2-97. Clark, H. J., Optimum Angular Accelerations for Control of a Remote Maneuvering Unit, AMRL-TR-66-20, Aerospace Medical Research Labs., Wright-Patterson AFB, Ohio, Mar. 1966.
- 2-98. Clark, H. J., Space Rendezvous Using Visual Cues Only, Human Factors, 7: 63-70, 1965. (Also published as: AMRL-TR-65-10, Aerospace Medical Res. Labs., Wright-Patterson AFB, Ohio).
- 2-99. Clark, W. B., Culver, J. F., Space Ophthalmological Problems, in Bioastronautics and the Exploration of Space, Proceedings of the Third International Symposium, San Antonio, Texas, Nov. 16-18, 1964, Bedwell, T. C., Jr., and Strughold, H., (eds.), pp. 149-155. (AD-627686).
- 2-100. Cobb, P. W., Moss, F. K., Four Fundamental Factors in Vision, Trans. Illum. Engng. Soc., 23: 496-506, 1928.
- 2-101. Cogan, D. G., Howe Laboratory of Ophthalmology, Harvard University Medical School, Massachusetts Eye and Ear Infirmary, Boston, Mass., personal communication, 1968.
- 2-102. Cogan, D. G., Kinsey, V. E., Action Spectrum of Keratitis Produced by Ultraviolet Radiation, Arch. Ophthal., 35: 670-677, 1946.
- 2-103. Colgan, C. M., The Effect of Observational Technique on Brightness-Enhancement, Amer. J. Psychol., 78: 471-475, 1965.
- 2-104. Conklin, J. E., Literature Review and Experimental Design for Research on Velocity Perception Related to Space Rendezvous Requirements, Interdepartmental Correspondence Ref. 2732.30/87, Hughes Aircraft Co., Culver City, Calif., May 8, 1962.
- 2-105. Conklin, J. E., Visual Requirements for Landing on the Moon, Human Factors, 4: 335-342, 1962.
- 2-106. Conover, D. W., Kraft, C. L., The Use of Color in Coding Displays, WADC-TR-55-471, Wright Air Dev. Center, Wright-Patterson AFB, Ohio, 1958. (AD-204214).
- 2-107. Conticelli, M., Training and Retinal Location Affecting the Periodic Fluctuation of Apparent Brightness during Prolonged Fixation, AFOSR-4195, Air Force Office of Scientific Research, Washington, D. C., 1962. (Reprinted from: Atti. Fond. G. Ronchi, 17: 396-404, July-Aug. 1962). (AD-637648).

- 2-108. Cook, G., Stark, L., The Human Eye-Movement Mechanism: Experiments, Modeling and Model Testing, SRL-67-0005, Frank J. Seiler Research Laboratory, U. S. Air Force Academy, Colo., June 1967. (AD-654626).
- 2-109. Crane, H. D., A Theoretical Analysis of the Visual Accommodation System in Humans, NASA-CR-606, 1966.
- 2-110. Crawford, B. H., Photochemical Laws and Visual Phenomena, Proc. Roy. Soc. London, 133B: 63-75, Jan. 1946.
- 2-111. Crawford, W. A., Visual Acuity and Moving Objects. III. The Coordination of Eye and Head Movements, FPRC Memo 150c, Institute of Aviation Medicine, Royal Air Force, Farnborough, England, July 1960.
- 2-112. Cronin, J. F., Adams, J. B., Colwell, R. N., A Proposed Multispectral Photography Experiment for AES Lunar Orbital Mission, AFCRL-66-796, Air Force Cambridge Research Labs., Hanscom Field, Bedford, Mass., 1966.
- 2-113. Crook, M. N., Coules, J., The Effect of Noise on the Perception of Forms in Electro-Visual Display Systems, Final Report, Contract DA-49-007-MD-536, Institute for Applied Experimental Psychology, Tufts University, Medford, Mass., Jan. 1959.
- 2-114. Crook, M. N., Coules, J., Reduced Contrast and Contour Degradation as Factors in Impairment of Form Discrimination, Interim Rep. 7, Contract DA-49-007-MD-536, Institute for Applied Experimental Psychology, Tufts University, Medford, Mass., Jan. 1959.
- 2-115. Crumley, L., Divany, R., Gates, S., Hostetter, R., et al., Display Problems in Aerospace Surveillance Systems, Part 1. A Survey of Display Hardware and Analysis of Relevant Psychological Variables, ESD-TR-61-33, Air Force Electronic Systems Div., L. G. Hanscom Field, Bedford, Mass., 1961.
- 2-116. Culver, J. F., Adler, A. V., Protective Glasses Against Atomic Flash, in Visual Problems in Aviation Medicine, Mercier, A., (ed.), Pergamon Press, N. Y., 1962, pp. 34-38.
- 2-117. Davson, H., (ed.), The Eye: Vol. I. Vegetative Physiology and Biochemistry, Vol. 2. The Visual Process, Vol. 3. Muscular Mechanisms, Vol. 4. Visual Optics and the Optical Space Sense, Academic Press, London, 1962.

- 2-118. De Mott, D. W., Davis, T. P., An Experimental Study of Retinal Burns: Part I. The Irradiance Thresholds for Chorio-Retinal Lesions. Part II. Entoptic Scatter as a Function of Wave Length, UR-548, University of Rochester, N. Y., May 1959. (Also in Arch. Ophthal., 62: 653-656, 1959).
- 2-119. Derksen, W., Griff, N., Glossary of Radiometric and Photometric Concepts Used in Retinal Burn and Flashblindness Research (Definitions, Symbols and Units), Progress Rep. 18, Naval Applied Science Lab., Brooklyn, N. Y., under DASA Sub-task 03.001, Dec. 1967.
- 2-120. DeRocher, W. L., Jr., Wudell, A. E., Manual Tracking for a Space-to-Space Photographic Mission, Control Systems Research, Martin Co., Denver, Colo., Jan. 1966.
- 2-121. Deutsch, S., Human Factors Challenges in Manned Space Flight, SAE-Paper 650809, Society of Automotive Engineers, National Aeronautic and Space Engineering and Manufacturing Meeting, Los Angeles, Oct. 4-8, 1965.
- 2-122. Devoe, D. B., Duva, J. S., Display Sharing Through Color Filtering, ESD-TN-60-60, Air Force Electronic Systems Div., L. G. Hanscom Field, Bedford, Mass., 1960.
- 2-123. Dobbins, D. A., Ah Chu, R., Kindick, C. M., Jungle Vision VII: Seasonal Variations in Personnel Detectability in a Semi-deciduous Tropical Forest, Res. Rep. 8, Army Tropic Test Center, Fort Clayton, Canal Zone, Jan. 1967.
- 2-124. Doyle, C. D., Aftergut, S., Development of a Reversibly Frostible Transparency for a Nuclear Flash Eye Protection Shutter, General Electric, Schenectady, N. Y., 1966. (AD-642732).
- 2-125. Duke-Elder, W. S., Pathologic Action of Light upon the Eye; Photophthalmia, Lancet, 1: 1137-1140, June 1926.
- 2-126. Duke-Elder, W. S., System of Ophthalmology, C. V. Mosby Co., St. Louis, Vol. I, 1958, Vol. II, 1961.
- 2-127. Dunkelman, L., Mercer, R. D., Dim Light Photography and Visual Observations of Space Phenomena from Manned Spacecraft, NASA-TM-X-55752, Goddard Space Flight Center, Greenbelt, Maryland, Feb. 1966.
- 2-128. Dunkelman, L., Gill, J. R., McDivitt, J. A., et al., Geo-Astronomical Observations, in Manned Space Flight Experiments Symposium, Gemini Missions III and IV, NASA-TM-X-56861, 1965.

- 2-129. Dunlap and Associates, Inc., Darien, Conn., Man-Machine Relationships in Prelaunch Checkout of Advanced Space Vehicles, Final Summary Report, NASA-CR-69172, 1965.
- 2-130. Duntley, S. Q., Visibility Laboratory, Scripps Institute of Oceanography, University of California, San Diego, Calif., personal communication, 1966.
- 2-131. Duntley, S. Q., Austin, R. W., Taylor, J. H., et al., Experiment S-8/D-13, Visual Acuity and Astronaut Visibility, in Gemini Midprogram Conference Including Experiment Results, Part II, A, NASA-SP-121, 1966, pp. 329-346. (Also: S10-Ref-66-17, Scripps Institution of Oceanography, University of California, San Deigo, Calif., July 1966)
- 2-132. Duntley, S. Q., Gordon, J. I., Taylor, J. H., et al., Visibility, Appl. Opt., 3: 549-598, May 1964.
- 2-133. Duntley, S. Q., The Visibility of Distant Objects, J. Opt. Soc. Amer., 38(3): 237-249, Mar. 1948.
- 2-134. Duntley, S. Q., Visibility in the Oceans, Optical Spectra, 1(4): 64-69, Fourth Quarter 1967.
- 2-135. Eastman Kodak Co., Influence of Color Contrast on Visual Acuity, OSRD-4541, National Defense Research Committee; U. S. Office of Scientific Research and Development, 1944.
- 2-136. Eastman Kodak Co., Tech Bits, 1: 5, 1965.
- 2-137. Egan, J. P., Signal Detection Theory and Psychophysics: A Topical Bibliography, Indiana University Hearing and Communication Laboratory, for National Academy of Sciences - National Research Council Committee on Hearing, Bioacoustics, and Biomechanics, under Grant AF-AFOSR-548-67, Dec. 1967. (AD-663906).
- 2-138. Enoch, J. M., Fry, G. A., Visual Search of a Complex Display: A Summary Report, RADC-TN-59-65, Rome Air Development Center, Griffiss AFB, N. Y., 1958.
- 2-139. Epstein, W., Franklin, S., Some Conditions of the Effect of Relative Size on Perceived Relative Distance, Amer. J. Psychol., 78: 466-470, 1965.
- 2-140. Erickson, R. A., Relation between Visual Search Time and Peripheral Visual Acuity, Human Factors, 6: 165-177, Apr. 1964.

- 2-141. Erickson, R. A., Visual Detection of Targets: Analysis and Review, NOTS-TP-3645, Naval Ordnance Test Station, China Lake, Calif., 1965. (AD-612721).
- 2-142. Eysenck, H. J., A Critical and Experimental Study of Color Preferences, Amer. J. Psychol., 54: 385-394, 1941.
- 2-143. Fender, D. H., Beeler, G. W., Jr., Human Eye Movements during Fixation, in A Report for the Year 1964-1965 of the Research and Other Activities, California Institute of Technology, Division of Engineering and Applied Science, Pasadena, Calif., 1965, p. 92.
- 2-144. Fenn, R. W., Correlation Between Atmospheric Backscattering and Meteorological Visual Range, AFCRL-66-549, Air Force Cambridge Research Labs., L. G. Hanscom Field, Bedford, Mass., 1966.
- 2-145. Ferree, C. E., Rand, G., Intensity of Light and Speed of Vision Studied with Special Reference to Industrial Situations, Part I., Trans. Illum. Engin. Soc., 22: 79-110, 1927.
- 2-146. Ferree, C. E., Rand, G., Visibility of Objects as Affected by Color and Composition of Light. Part II. With Lights Equalized in Both Brightness and Saturation, Person. J., 10: 108-124, 1931.
- 2-147. Fincham, E. F., The Accommodation Reflex and Its Stimulus, Brit. J. Ophthal., 35: 381-393, 1951.
- 2-148. Fitts, P. M., Engineering Psychology and Equipment Design, in Handbook of Experimental Psychology, Stevens, S. S., (ed.), John Wiley & Sons, Inc., N. Y., 1951.
- 2-149. Fiorentini, A., Ronchi, L., Problems Related to Visual Performance of Pilots, Istituto Nazionale di Ottica, Arcetri-Firenze, Italy, 1965. (AD-630475).
- 2-150. Forman, P. F., The Photographic Window, The Perkin-Elmer Corp., Electro-Optical Div., Norwalk, Conn., in New Developments for Aerial Photography, A Program of Talks Presented to Members of OSA, ASP, SPIE, and SPSE at a Joint Technical Meeting, Sept. 16, 1964.
- 2-151. Franklin, M. E., Whittenburg, J. A., Research on Visual Target Detection. Part I. Development of an Air-to-Ground Detection/Identification Model, HSR-RR-65/4-Dt, Human Sciences Research, Inc., McLean, Va., 1965. (AD-619275).

- 2-152. Fraser, T. M., The Intangibles of Habitability during Long Duration Space Missions, The Lovelace Foundation for Medical Education and Research, Albuquerque, N. M., Contract NASr-115, 1967. (In Press).
- 2-153. Frederickson, E. W., Follettie, J. F., Baldwin, R. D., Aircraft Detection, Range Estimation, and Auditory Tracking Tests in a Desert Environment, HUMRRO-TR-67-3, Human Resources Research Office, The George Washington Univ., Washington, D. C., Mar. 1967.
- 2-154. Fry, G. A., Alpern, M., Effects of Flashes of Light on Night Visual Acuity, WADC-TR-52-10, Pt. I., Wright Air Development Center, Wright-Patterson AFB, Ohio, Nov. 1951.
- 2-155. Fry, G. A., The Evaluation of Discomfort Glare, Illum. Engin., 51: 722-728, 1956.
- 2-156. Gauer, O. H., Zuidema, G. D., (eds.), Gravitational Stress in Aerospace Medicine, Little Brown, Boston, 1961.
- 2-157. Gerathewohl, S. J., Conspicuity of Flashing Light Signals: Effects of Variation Among Frequency, Duration and Contrast of the Signals, Project 21-1205-0012, Rep. No. 1, School of Aviation Med., Randolph Field, Texas, 1954.
- 2-158. Gerathewohl, S. J., Conspicuity of Flashing and Steady Light Signals, II. High Contrasts, Project 21-24-014, Rep. No. 2, School of Aviation Med., Randolph Field, Texas, 1952.
- 2-159. Gerathewohl, S. J., Eye Movements during Radar Operations, J. Aviat. Med., 23: 597-607, 1952.
- 2-160. Gerathewohl, S. J., Rubinstein, D. A., Investigation of Perceptual Factors Involved in the Interpretation of PPI-Scope Presentations, II. A Pilot Study on Form Discrimination, Project 21-24-009, Rep. No. 2, School of Aviation Med., Randolph Field, Texas, 1952.
- 2-161. Gibson, J. J., The Perception of the Visual World, Riverside Press, Cambridge, Mass., 1958.
- 2-162. Gibson, J. J., Report to the Office of Naval Research on Published Research Studies and Other Contributions between 1957 and 1967 Supported in Whole or Part under Contract No. NONR-401(14), Cornell Univ., Ithaca, N. Y., Apr. 1967. (AD-652392).

- 2-163. Gilchrist, J. D., Anderson, P. A., Research on Computational and Display Requirements for Human Control of Space Vehicle Boosters, Part I: Theory and Results, NASA-CR-89606, Aug. 1967.
- 2-164. Gillies, J. A., (ed.), A Textbook of Aviation Physiology, Pergamon Press, N. Y., 1965.
- 2-165. Goetzl, C. G., Rittenhouse, J. B., Singletary, J. B., (eds.), Space Materials Handbook, 2nd Edition, ML-TDR-64-40A, Air Force Materials Lab., Wright-Patterson AFB, Ohio, Jan. 1965.
- 2-166. Gogel, W. C., Mertens, H. W., Perceived Depth between Familiar Objects, FAA-AM-67-20, Federal Aviation Administration, Office of Aviation Medicine, Oklahoma City, Okla., Aug. 1967.
- 2-167. Gogel, W. C., The Perception of Depth from Binocular Disparity, FAA-CARI-63-10, Federal Aviation Agency, Oklahoma City, Okla., 1963.
- 2-168. Gogel, W. C., The Perception of Space with Binocular Disparity Cues, AMRL-379, Army Medical Res. Lab., Fort Knox, Ky., Apr. 1959.
- 2-169. Gogel, W. C., Mertens, H. W., Problems in Depth Perception: Perceived Size and Distance of Familiar Objects, FAA-AM-66-22, Federal Aviation Agency, Oklahoma City, Okla., 1966.
- 2-170. Gogel, W. C., The Size Cue to Visually Perceived Distance, FAA-AM-64-13, Federal Aviation Agency, Oklahoma City, Okla., 1964.
- 2-171. Gogel, W. C., Size Cues and the Adjacent Principle, FAA-CARI-63-28, Federal Aviation Agency, Oklahoma City, Okla., 1963.
- 2-172. Gogel, W. C., A Test of the Invariance of the Ratio of Perceived Size to Perceived Distance, Amer. J. Psychol., 76: 537-553, 1963.
- 2-173. Gogel, W. C., The Visual Perception of Size and Distance, FAA-CARI-62-15, Federal Aviation Agency, Oklahoma City, Okla., 1962.
- 2-174. Gogel, W. C., The Visual Perception of Spatial Extent, FAA-CARI- 63-20, Federal Aviation Agency, Oklahoma City, Okla., 1963.

- 2-175. Goldman, L., Dermatologic Manifestations of Laser Radiation, Fed. Proc., Suppl. 14: S92-S93, 1965.
- 2-176. Gordon, D. A., Rothstein, E. C., Ultra-violet Absorbers, Chemicals and Additives, in Modern Plastics Encyclopedia, for 1966, Vol. 43 1A, McGraw-Hill, N. Y., Sept. 1965, pp. 434-456.
- 2-177. Graham, C. H., (ed.), Vision and Visual Perception, John Wiley & Sons, Inc., N. Y., 1965.
- 2-178. Graham, C. H., Visual Perception, in Handbook of Experimental Psychology, Stevens, S. S., (ed.), John Wiley & Sons, N. Y., 1951, pp. 868-920.
- 2-179. Gregory, R. L., Distortion of Visual Space as Inappropriate Constancy Scaling, Nature, 199(4895): 678-680, 1963.
- 2-180. Gregory, R. L., Eye and Brain. The Psychology of Seeing, World University Library, McGraw-Hill, N. Y., 1966.
- 2-181. Gregory, R. L., Zangwill, O. L., The Origin of the Autokinetic Effect, Quart. J. Exp. Psychol., 15: 252-261, 1963.
- 2-182. Gregory, R. L., Visual Perception of Movement, AFOSR-66-1532, Air Force Office of Scientific Research, Washington, D. C., 1966. (AD-637510).
- 2-183. Grether, W. F., Visual Search in the Space Environment, in Visual Capabilities in the Space Environment, Baker, C. A., (ed.), Pergamon Press, N. Y., 1965, pp. 29-35.
- 2-184. Grissom, V. I., Pilot's Flight Report, in Results of the Second U. S. Manned Suborbital Space Flight, July 21, 1961, NASA, Manned Spacecraft Center, Washington, D. C., 1961, pp. 47-58.
- 2-185. Grumman Aircraft Engineering Corp., Man-System Locomotion and Display Criteria for Extra-Terrestrial Vehicles, NASA-CR-71757, 1965.
- 2-186. Guignard, J. C., Irving, A., Effects of Low Frequency Vibration on Man, Engineering, 190: 364-367, 1960.
- 2-187. Gulatedge, I. S., Koomen, M. J., Packer, D. M., et al., Visual Thresholds for Detecting an Earth Satellite, Science, 127: 1242-1243, 1958.
- 2-188. Gunn, W. J., Loeb, M., Correlation of Performance in Detecting Visual and Auditory Signals, AMRL-713, Army Medical Research Lab., Fort Knox, Ky., Jan. 1967.

- 2-189. Guth, S. K., McNelis, J. F., A Discomfort Glare Evaluator, Illum. Engin., 54: 398-406, 1959
- 2-190. Guth, S. K., Eastman, A. A., Lighting for the Forgotten Man, Amer. J. Opt., 32: 413-421, 1955.
- 2-191. Guth, S. K., A Method for the Evaluation of Discomfort Glare, paper presented at National Technical Conference of the Illuminating Engineering Society, Dallas, Texas, Sept. 9-14, 1962. (Preprint No. 45).
- 2-192. Haig, C., The Course of Rod Dark Adaptation as Influenced by Intensity and Duration of Preadapting to Light, J. Gen. Physiol., 24: 735-751, 1941.
- 2-193. Haines, R. F., Changes in Size and Shape of a Highly Luminous Target, NASA, Ames Research Center, Moffett Field, Calif., 1966. (unpublished study).
- 2-194. Haines, R. F., The Effects of High Luminance Sources upon the Visibility of Point Sources, NASA-TM-X-56561, 1965.
- 2-195. Hall, M. V., Greenbaum, L. J., The Areas of Vision and Cockpit Visibility, Trans. Amer. Acad. Ophthal., 55: 74-88, Sept-Oct. 1950.
- 2-196. Ham, W. T., Jr., Wiesinger, H., Schmidt, F. H., et al., Flash Burns in the Rabbit Retina as a Means of Evaluating the Retinal Hazard from Nuclear Weapons, Amer. J. Ophth., 46: 700-723, 1958.
- 2-197. Ham, W. T., Jr., Williams, R. C., Mueller, H. A., et al., Ocular Effects of Laser Radiation, Part I, Acta Ophth., 43: 390-409, 1965.
- 2-198. Hamer, H. A., Mayo, A. P., Error Analysis of Several Methods of Determining Vehicle Position in Earth-Moon Space from Simultaneous Onboard Optical Measurements, NASA-TN-D-1805, June 1963.
- 2-199. Hanes, R. M., Williams, S. B., Visibility on Cathoderay Tubes: The Effects of Light Adaptation, J. Opt. Soc. Amer., 38: 363-377, 1948.
- 2-200. Hannah, M. E., Mayo, A. P., A Study of Factors Affecting the Accuracy of Position Fix for Lunar Trajectories, NASA-TN-D-2178, Jan. 1964.

- 2-201. Harcum, E. R., Rabe, A., Blackwell, H. R., Visual Recognition Along Various Meridians of the Visual Field, Project Michigan, Vision Res. Labs., Willow Run Labs., Univ. of Michigan, Ann Arbor, Mich. I. Preliminary Experiments, Rep. 2144-50-T, June 1957. II. Nine-Element Typewritten Targets, Rep. 2144-293-T, Dec. 1958. III. Patterns of Blackened Circles in an Eight-Circle Template, Rep. 2144-294-T, Nov. 1958. (AD-210340). IV. Linear Binary Patterns at Thirty-Six Orientations, Rep. 2144-296-T, Nov. 1958. (AD-208220). V. Binary Patterns Along 12 Meridians, Rep. 2144-302-T, Nov. 1958. (AD-206346). VI. 8-Element and 10-Element Binary Patterns, Rep. 2144-303-T, Nov. 1958. (AD-209357). VII. Effect of Target Length Measured in Angular Units, Rep. 2144-304-T, Nov. 1958. (AD-209358). VIII. Patterns of Solid Circles and Squares, Rep. 2144-306-T, Dec. 1958. (AD-210598). IX. Monocular and Binocular Recognition of Patterns of Squares and Circles, Rep. 2144-307-T, Nov. 1958. (AD-208332). X. Binary Patterns of the Letters "H" and "O", Rep. 2144-308-T, Nov. 1958. (AD-206295). XI. Identification of the Number of Blackened Circles, Rep. 2144-314-T, Dec. 1958. (AD-210599).
- 2-202. Harris, W., The Object Identification Test: A Stress-Sensitive Perceptual Test, Technical Report 209-1, Human Factors Research, Inc., Goleta, Calif., Feb. 1967.
- 2-203. Hartridge, H., The Chromatic Aberration of the Human Eye and Its Physiological Correction, Experientia, 6: 1-10, 1950.
- 2-204. Hartridge, H., The Visual Perception of Fine Detail, Phil. Trans., 232: 516, 1925.
- 2-205. Hatch, H. G., Jr., Rendezvous Docking Simulator, in A Compilation of Recent Research Related to the Apollo Mission, NASA-TM-X-890, 1963, pp. 187-192.
- 2-206. Hatch, H. G., Jr., Pennington, J. E., Cobb, J. B., Dynamic Simulation of Lunar Module Docking with Apollo Command Module in Lunar Orbit, NASA-TN-D-3972, 1967.
- 2-207. Hatch, H. G., Jr., Riley, D. R., Cobb, J. B., Simulating Gemini-Agena Docking, Astronaut. Aeron., 2: 74-81, 1964.
- 2-208. Hayes, J. R., Wolbarsht, M., A Thermal Theory of Laser Induced Retinal Damage, in Preprints of Scientific Program, 1967 Annual Scientific Meeting, Aerospace Medical Association, April 10-13, 1967, Washington, D. C., pp. 296-297.

- 2-209. Heap, E., Air to Ground Applications of Visual Detection Lobe Theory, RAE-TN-ARM-715, Royal Aircraft Establishment, Ministry of Aviation, London, Jan. 1962.
- 2-210. Hecht, S., Haig, C., Wald, G., The Dark Adaptation of Retinal Fields of Different Size and Location, J. Gen. Physiol., 19: 321-339, 1935.
- 2-211. Hecht, S., Shlaer, S., Verrijp, C. D., Intermittent Stimulation by Light, J. Gen. Physiol., 17: 237-282, Nov. 1933.
- 2-212. Hecht, S., Ross, S., Mueller, C. G., The Visibility of Lines and Squares at High Brightnesses, J. Opt. Soc. Amer., 37: 500-507, 1947.
- 2-213. Hecht, S., Williams, R. F., The Visibility of Monochromatic Radiation and the Absorption Spectrum of Visual Purple, J. Gen. Physiol., 5: 1-33, Sept. 1922.
- 2-214. Henschke, U., Schultze, R. Untersuchungen zum Problem der Ultraviolett-Dosimetrie. III. Über Pigmentierung durch langwelliges Ultraviolett, Strahlentherapie, 64: 14-42, 1939.
- 2-215. Henschke, U., Schultze, R., Untersuchungen zum Problem der Ultraviolett-Dosimetrie, IV. Wirkung der Sonnenstrahlung auf die Haut, Strahlentherapie, 64: 43-58, 1939.
- 2-216. Hill, J. H., Chisum, G. T., Effective Density of the Class 3 Visors, NADC-ML-L6501, Naval Air Development Center, Johnsville, Pa., May 1965.
- 2-217. Hill, N. E. G., The Recognition of Colored Light Signals which are Near the Limit of Visibility, Proc. Phys. Soc., (London), 59: 560-564, 1947.
- 2-218. Hoisman, A. J., Moots, A., The Use of a Visual Testing Apparatus for Space Application, Final Report, NASA-CR-73099, Apr. 1967.
- 2-219. Holladay, L. L., The Fundamentals of Glare and Visibility, J. Opt. Soc. Amer., 12(4): 271-319, Apr. 1926.
- 2-220. Hornick, R. J., Costin, R. W., Space Vehicle Vibration Effects on Human Occupants, paper presented at the Annual Meeting of the Aerospace Medical Association, April 9, 1962, Atlantic City, N. J.

- 2-221. Huston, T. O., Human Biological Interactions with Laser Light, NEL-1502, Naval Electronics Lab. Center, San Diego, Calif., Aug. 1967.
- 2-222. I. E. S., Lighting Handbook, Illuminating Engineering Society, N. Y., 3rd Edition, 1959.
- 2-223. Ireland, F. H., Effects of Surround Illumination on Visual Performance, An Annotated Bibliography, AMRL-TR-67-103, Aerospace Medical Research Labs., Wright-Patterson AFB, Ohio, 1967.
- 2-224. Ireland, F. H., Kinslow, W., Levin, E., et al., Experimental Study of the Effects of Surround Brightness and Size on Visual Performance, AMRL-TR-67-102, Aerospace Med. Res. Labs., Wright-Patterson AFB, Ohio, Sept. 1967.
- 2-225. Ivanoff, A., Chromatic Aberration of the Eye, Documenta Ophthalmologica, 3: 322-323, 1949.
- 2-226. Ivanoff, A., Les Aberrations de Chromatisme et de Sphericite de l'oeil, Rev. Opt., 26: 145-171, 1947.
- 2-227. Jaffe, L. D., Shoemaker, E. M., Dwornik, S. E., et al., Surveyor I Mission Report, Part II. Scientific Data and Results, JPL-TR-32-1023(Pt. 2), Jet Propulsion Laboratory, California Institute of Technology, Pasadena, Calif., 1966.
- 2-228. Jaquet, B. M., Riley, D. R., An Evaluation of Gemini Hand Controllers and Instruments for Docking, NASA-TM-X-1066, Mar. 1965.
- 2-229. Jaquet, B. M., Riley, D. R., Fixed-Base Gemini-Agena Docking Simulation, in A Compilation of Recent Research Related to the Apollo Mission, NASA-TM-X-890, 1963, Chapt. 9, pp. 67-78.
- 2-230. Jaquet, B. M., Simulator Studies of Space and Lunar Landing Techniques, in Lectures in Aerospace Medicine, School of Aerospace Med., Feb. 3-7, 1964, Brooks AFB, Texas, 1964, pp. 145-166.
- 2-231. Jayle, G. E., Ourgaud, A. G., Baisinger, L. F., et al., Night Vision, Charles C. Thomas, Springfield, Ill., 1959.
- 2-232. Jerison, J. H., Pickett, R. M., Stenson, H. H., The Elicited Observing Rate and Decision Processes in Vigilance, Human Factors, 7: 107-128, 1965.

- 2-233. Jerison, H. J., Pickett, R. M., Vigilance: A Review and Re-evaluation, in Visual Capabilities in the Space Environment, Baker, C. A., (ed.), Pergamon Press, N. Y., 1965, pp. 37-64.
- 2-234. Johansson, G., Ottander, C., Recovery Time after Glare. An Experimental Investigation of Glare After-Effect under Night Driving Conditions, Scand. J. Psychol., 5: 17-25, 1964.
- 2-235. Johnston, D. M., Search Performance as a Function of Peripheral Acuity, Human Factors, 7: 527-535, 1965.
- 2-236. Johnston, W. A., Howell, W. C., Influence of Prolonged Viewing of Large-Scale Displays on Extraction of Information, RADC-TR-67-411, Rome Air Development Center, Griffiss AFB, N. Y., Sept. 1967.
- 2-237. Jones, D. E., Comment on "Eye Protection Criteria for Laser Radiation", (Revised comment on UCRL-7811, pp. 14-19), in Hazards Control Quarterly Report No. 17, UCRL-12004, Lawrence Radiation Lab., Univ. of California, Livermore, Calif., 1964, pp. 37-38.
- 2-238. Jones, D. E., Montan, D. N., Eye Protection Criteria for Laser Radiation, in Hazards Control Quarterly Report No. 16, UCRL-7811, Lawrence Radiation Lab., Univ. of California, Livermore, Calif., 1964, pp. 14-19.
- 2-239. Jones, D. E., Sykos, M., The Laser Eye Protection Program at LRL, in Hazards Control Quarterly Report No. 18, UCRL-12167, Lawrence Radiation Lab., Univ. of California, Livermore, Calif., 1964, pp. 34-38.
- 2-240. Jones, M. R., Color Coding, Human Factors, 4: 355-365, 1962.
- 2-241. Jones, W. L., Allen, W. H., Parker, J. F., Advanced Vision Research for Extended Spaceflight, Aerospace Med., 38(5): 475-478, 1967.
- 2-242. Jones, W. L., Parker, J. F., Flash Blindness Protection, ACLANT Medical Officers Symposium on Biomedical Effects of Nuclear Weapons, National Naval Medical Center, Bethesda, Md., Oct. 29, 1963.
- 2-243. Kasten, F., Horizontal Visual Range in Polar Whiteout, USACRREL-SR-54, Army Cold Regions Research and Engineering Lab., Hanover, N. H., May 1962. (AD-653149).

- 2-244. Katzoff, S., The Electromagnetic-Radiation Environment of a Satellite. Part I. Range of Thermal to X-Radiation, NASA-TN-D-1360, Sept. 1962.
- 2-245. Kent, P. R., Vision Underwater, NMRL-498, Naval Submarine Medical Center, Submarine Base, Groton, Conn., July 1967.
- 2-246. Kinney, J. A. S., Cooper, J. C., Adaptation to a Homochromatic Visual World, NMRL-499, Naval Submarine Medical Center, Submarine Base, Groton, Conn., July 1967.
- 2-247. Kinney, J. A. S., Color Induction Using Asynchronous Flashes, NMRL-496, Naval Submarine Medical Center, Submarine Base, Groton, Conn., 1967. (Reprinted from Vision Res., 7: 299-318, 1967).
- 2-248. Kinney, J. A. S., Connors, M. M., Recovery of Foveal Acuity Following Exposure to Various Intensities and Durations of Light, NMRL-464, Naval Medical Research Lab., Groton, Conn., Dec. 1965. (Reprinted from Amer. J. Psychol., 78: 432-440, Sept. 1965)
- 2-249. Kinney, M., Occupational Laser Hazards - A Survey of the Literature, Rep. T5-1245/3111, Autonetics, Div. of North American Aviation, Inc., Downey, Calif., 1965. (AD-617913).
- 2-250. Koller, L. R., Ultraviolet Radiation, John Wiley & Sons, N. Y., 2nd Ed., 1965.
- 2-251. Koomen, M., Tousey, R., Scolnik, R., Spherical Aberration of the Eye, J. Opt. Soc. Amer., 39: 370-376, 1949.
- 2-252. Koopman, B. O., Search and Screening, OEG Rep. 56, Operations Evaluation Group, Office of the Chief of Naval Operations, Navy Department, Washington, D. C., 1946.
- 2-253. Kopal, Z., The Moon Our Nearest Celestial Neighbor, Academic Press, N. Y., 1960.
- 2-254. Kosenkov, M. M., Kuz'minov, A. P., Some Results and Problems of Observation under Spaceflight Conditions, FTD-TT-65-1/1, Foreign Technology Division, Wright-Patterson AFB, Ohio, Jan. 10, 1965. (Source: III International Symposium on Bioastronautics at San Antonio, Texas, Nov. 16-18, 1964, pp. 3-7).

- 2-255. Lamar, E. S., Operational Background and Physical Considerations Relative to Visual Search Problems, in Visual Search Techniques, Proceedings of a Symposium, Apr. 7-8, 1959, Washington, D. C., Morris, A., Horne, E. P., (eds.), NAS-NRC-712, 1960, pp. 1-9.
- 2-256. Lamar, E. S., Hecht, S., Shlaer, S., et al., Size, Shape, and Contrast in Detection of Targets by Daylight Vision, I. Data and Analytical Description, J. Opt. Soc. Amer., 37: 531-545, 1947.
- 2-257. Landis, D., Slivka, R. M., Jones, J. M., et al., Evaluation of Large Scale Visual Displays, RADC-TR-67-57, Rome Air Development Center, Griffiss AFB, N. Y., 1967. (AD-651372).
- 2-258. Landis, D., Slivka, R. M., Jones, J. M., et al., Experiments in Display Evaluation, Technical Rep. 1-194, The Franklin Institute Research Labs., Philadelphia, Pa., July 1967.
- 2-259. Lash, J. D., Prideaux, G. F., Visibility of Signal Lights, Illum. Engin., 38: 481-492, 1943.
- 2-260. LeGrand, Y., Light, Color and Vision, John Wiley & Sons, N. Y., 1957, p. 104.
- 2-261. Lewis, M. F., Mertens, H. W., Reaction Time as a Function of Flash Luminance and Duration, FAA-AM-67-24, Federal Aviation Administration, Office of Aviation Medicine, Oklahoma City, Okla., Nov. 1967.
- 2-262. Lichtenstein, J. H., Suit, W. T., An Experimental Investigation of Two Visual Methods of Altitude Determination, NASA-TM-X-1392, May 1967.
- 2-263. Lina, L. J., Assadourian, A., Investigation of the Visual Boundary for Immediate Perception of Vertical Rate of Descent, NASA-TN-D-1591, 1963.
- 2-264. Lineberry, E. C., Jr., Brissenden, R. F., Kurbjun, M. C., Analytical and Preliminary Simulation of a Pilot's Ability to Control the Terminal Phase of a Rendezvous with Simple Optical Devices and a Timer, NASA-TN-D-965, Oct. 1961.
- 2-265. Ling-Temco-Vought, Inc., NASA Lunar Module Visual Simulation Study, Vol. I - Lunar Mission Descent, Ascent, and Rendezvous, LTV-00.884 (Vol. I), 1966. Vol. II - Lunar Module Rendezvous in Earth Orbit, LTV-00.884(Vol. 2), 1967.

- 2-266. Lippert, S., Lee, D. M., Dynamic Vision: The Legibility of Moderately Spaced Alphanumeric Symbols, Human Factors, 7: 555-560, 1965.
- 2-267. Litwin, M. S., Glew, D. H., The Biological Effects of Laser Radiation, JAMA, 187, 842-847, 1964.
- 2-268. Litwin, M. S., Earl, K. M., (eds.), Proceedings of the First Annual Conference on Biologic Effects of Laser Radiation, Armed Forces Institute of Pathology, Washington, D. C., 30 April-1 May 1964, Fed. Proc., 24: 1, Part 3, Suppl. No. 14, pp. S1-S177, Jan-Feb. 1965.
- 2-269. Long, E. R., Jr., Pennington, J. E., Deal, P. L., Remote Pilot-Controlled Docking with Television, NASA-TN-D-3044, Oct. 1965.
- 2-270. Luce, T. S., Vigilance as a Function of Stimulus Variety and Response Complexity, Human Factors, 6: 101-110, 1964.
- 2-271. Luckiesh, M., Brightness Engineering, Illum. Engin., 39: 75-92, 1944.
- 2-272. Luckiesh, M., Guth, S. K., Brightness in Visual Field at Borderline between Comfort and Discomfort, Illum. Engin., 44: 650-670, 1949.
- 2-273. Luckiesh, M., Moss, F. K., The New Science of Seeing, in Interpreting the Science of Seeing into Lighting Practice, Vol. 1, General Electric Co., Cleveland, Ohio, 1927-1932.
- 2-274. Ludvigh, E., Miller, J. W., Study of Visual Acuity during the Ocular Pursuit of Moving Test Objects, J. Opt. Soc. Amer., 48(11): 799-802, Nov. 1958.
- 2-275. Luria, S. M., Color-Name as a Function of Stimulus Intensity and Duration, NMRL-494, U. S. Naval Submarine Medical Center, Submarine Base, Groton, Conn., 1967.
- 2-276. Luria, S. M., Effects of Continuously and Discontinuously Moving Stimuli on the Luminance Threshold of a Stationary Stimulus, NMRL-454, Naval Submarine Medical Center, Submarine Base, Groton, Conn., 1965.
- 2-277. Luria, S. M., Kinney, J. A. S., The Interruption of Dark Adaptation, NMRL-347, Naval Medical Research Lab., Submarine Base, Groton, Conn., Feb. 1961.
- 2-278. Lythgoe, R. J., The Measurement of Visual Acuity, Rep. No. 173, Medical Research Council, London, England, 1932.

- 2-279. McCartney, A. J., A Consideration of the Biological Effects of Laser, AMRL-654, Army Medical Research Laboratory, Fort Knox, Ky., 1966. (Also in: Mil. Med., 130: 1069-1077, Nov. 1965).
- 2-280. McCormick, E. J., Human Factors Engineering, McGraw-Hill, N. Y., 1957.
- 2-281. McFarland, R. A., Human Factors in Air Transportation: Occupational Health and Safety, McGraw-Hill, N. Y., 1953.
- 2-282. Mackworth, N. H., Researches on the Measurement of Human Performance, Medical Research Council Special Report Series 268, H. M. Stationery Office, London, England, 1950. Reprinted in Selected Papers on Human Factors in the Design and Use of Control Systems, Sinaiko, H. W., (ed.), Dover, N. Y., 1961, pp. 174-331.
- 2-283. McLean, M. V., Brightness Contrast, Color Contrast and Legibility, Human Factors, 7: 521-526, 1965.
- 2-284. McPhail, C. D., Apollo External Visual Simulation Display Systems, AIAA-67-253, paper presented at AIAA Flight Test Simulation and Support Conference, Cocoa Beach, Fla., Feb. 6-8, 1967.
- 2-285. Mandelbaum, J., Rowland, L. S., Central and Paracentral Visual Acuity at Different Levels of Illumination, Project No. 220, Rep. No. 1, Air Force School of Aviation Medicine, Randolph Field, Texas, 1944.
- 2-286. Marriott, F. H. C., Visual Search by Night, APRC-66/NC3, Army Personnel Res. Comm. Medical Research Council, London, Sept. 1966. (AD-809474).
- 2-287. Martin, D. J., The Visibility of an Object in a Space Environment NASA-L-1872, presented at the 30th Annual Meeting, Institute of the Aeronautical Sciences, N. Y., Jan. 21-24, 1962.
- 2-288. Mayo, A. P., Jones, R. L., Adams, W. M., Accuracy of Navigation in Various Regions of Earth-Moon Space with Various Combinations of Onboard Optical Measurements, NASA-TN-D-2448, Sept. 1964.
- 2-289. Mayo, A. P., Hamer, H. A., Hannah, M. E., Equations for Determining Vehicle Position in Earth-Moon Space from Simultaneous Onboard Optical Measurements, NASA-TN-D-1604, Feb. 1963.

- 2-290. Melton, C. E., Higgins, E. A., Saldivar, J. T., et al., Exposure of Men to Intermittent Photic Stimulation under Simulated IFR Conditions, FAA-AM-66-39, Federal Aviation Agency, Oklahoma City, Okla., 1966.
- 2-291. Mercier, A., Whiteside, T. C. D., The Effect of Red Versus White Instrument Lighting on the Dark Adaptation Index, FPRC-1255, Flying Personnel Research Comm., Ministry of Defense, London, May 1966.
- 2-292. Metcalf, R. D., Horn, R. E., Visual Recovery Times from High Intensity Flashes of Light, WADC-TR-58-232, Wright Air Dev. Center, Wright-Patterson AFB, Ohio, 1958.
- 2-293. Middleton, W. E. K., Vision Through the Atmosphere, Univ. of Toronto Press, Toronto, 1958.
- 2-294. Miller, G. K., Jr., Fixed-Base Visual-Simulation Study of Manually Controlled Translation and Hover Maneuvers Over the Lunar Surface, NASA-TN-D-3653, Oct. 1966.
- 2-295. Miller, G. K., Jr., Sparrow, G. W., Visual Simulation of Lunar Orbit Establishment Using a Simplified Guidance Technique, NASA-TN-D-3524, 1966.
- 2-296. Miller, J. W., Study of Visual Acuity during the Ocular Pursuit of Moving Test Objects, II. Effects of Direction of Movement, Relative Movement, and Illumination, J. Opt. Soc. Amer., 48(11): 803-808, Nov. 1958.
- 2-297. Miller, N. D., Visual Recovery, SAM-TR-65-12, School of Aerospace Medicine, Brooks AFB, Texas, 1965.
- 2-298. Miller, N. D., Visual Recovery from High Intensity Flashes II, Final Rep., Contract AF41(609)-2426, Ohio State Univ., Columbus, Ohio, 1966. (AD-642731).
- 2-299. Montague, W. E., Webber, C. E., Adams, J. A., The Effects of Signal and Response Complexity on Eighteen Hours of Visual Monitoring, Human Factors, 7: 163-172, 1965.
- 2-300. Moon, P., Proposed Standard Solar-Radiation Curves for Engineering Use, J. Franklin Inst., 230: 583-618, 1941.
- 2-301. Moon, P., Scientific Basis of Illuminating Engineering, Dover Publications, Inc., N. Y., 1936. (Paperback Edition).
- 2-302. Moon, P., Spencer, D. E., Visual Data Applied to Lighting Design, J. Opt. Soc. Amer., 34: 605-617, Oct. 1944.

- 2-303. Moran, J. A., Tiller, P. R., Investigation of Aerospace Vehicle Crew Station Criteria, AFFDL-TDR-64-86, Flight Dynamics Lab., Wright-Patterson AFB, Ohio, July 1964.
- 2-304. Morgan, C. T., Cook, J. S., III., Chapanis, A., et al., Human Engineering Guide to Equipment Design, McGraw-Hill, N. Y., 1963.
- 2-305. Morris, A., Horne, E. P., (eds.), Visual Search Techniques, Proceedings of Symposium sponsored by the Armed Forces NRC Committee on Vision, NAS-NRC Publ. 712, National Academy of Sciences - National Res. Council, Washington, D. C., 1960.
- 2-306. Mote, F. A., Riopelle, A. J., The Effect of Varying the Intensity and the Duration of Pre-exposure upon Subsequent Dark Adaptation in the Human Eye, J. Comp. Physiol. Psychol., 46: 49-55, 1953.
- 2-307. Muller, A. F., Wilson, P. W., Jr., Eye Effects Mathematical Models, Project Task No. 630103, School of Aerospace Medicine, Brooks AFB, Texas, June 1967. (AD-653984).
- 2-308. Muller, A. F., Wilson, P. W., Jr., Research Toward the Development of Eye Effects Safe Separation Charts, Final Rep., Contract AF41(609)-2437, Technology, Inc., San Antonio, Texas, July 1966. (AD-641191).
- 2-309. Munsell, A. H., Munsell Book of Color, Munsell Color Book Co., Inc., Baltimore, 1942.
- 2-310. Munsell, A. H., Munsell Book of Color. Defining, Explaining and Illustrating the Fundamental Characteristics of Color; A Revision and Extension of the Atlas of the Munsell Color System, Munsell Color Book Co., Baltimore, Md., 1929.
- 2-311. Murrell, K. F. H., Laurie, W. D., McCarthy, C., The Relationship between Dial Size, Reading Distance and Reading Accuracy, Ergonomics, 1: 182-190, 1958.
- 2-312. Nachmias, J., Brightness and Visual Acuity with Intermittent Illumination, J. Opt. Soc. Amer., 48(10): 726-730, 1958.
- 2-313. Narva, M. A., Muckler, F. A., Visual Surveillance and Reconnaissance from Space Vehicles, in Visual Capabilities in the Space Environment, Baker, C. A., (ed.), Pergamon Press, N. Y., 1965, pp. 121-141.

- 2-314. National Aeronautics and Space Administration, Manned Spacecraft Center, Houston, Texas, Gemini Midprogram Conference Including Experiment Results, NASA-SP-121, 1966.
- 2-315. National Aeronautics and Space Administration, Lasers and Masers, A Continuing Bibliography with Indexes, NASA-SP-7009 (01), July 1966.
- 2-316. National Aeronautics and Space Administration, Natural Environment and Physical Standards for the Apollo Program, NASA-M-DE-8020-008B, Office of Manned Spaceflight, Washington, D. C., Apr. 1965.
- 2-317. National Aeronautics and Space Administration, Results of the First United States Manned Orbital Space Flight, Manned Spacecraft Center, Houston, Texas, Feb. 20, 1962.
- 2-318. National Aeronautics and Space Administration, Surveyor I, A Preliminary Report, NASA-SP-126, June 1966.
- 2-319. Ney, E. P., Huch, W. F., Optical Environment in Gemini Space Flights, Science, 153: 297-299, 1966.
- 2-320. Norris, R. E., Gouyd, C. A., The Effect of Simulated TOW Launch Transients on Operator Tracking, HAC-TM-HM-88, Hughes Aircraft Co., Culver City, Calif., 1964.
- 2-321. Norris, R. E., Gouyd, C. A., HLMR Acquisition and Tracking Field Trials, Phase II, Sight Evaluation, HAC-IDC-2732-50/92, Hughes Aircraft Co., Culver City, Calif., 1964.
- 2-322. Nutting, P. G., Effects of Brightness and Contrast in Vision, Trans. Illum. Engin. Soc., 11: 939-946, 1916.
- 2-323. Nutting, P. G., Report of Standards of Committee on Visual Sensitometry, J. Opt. Soc. Amer., 4: 55-79, 1920.
- 2-324. O'Brien, P. F., Numerical Analysis for Lighting Design, Illum. Engin., 60: 169-178, Apr. 1965.
- 2-325. Ogle, K. N., On the Resolving Power of the Human Eye, J. Opt. Soc. Amer., 41: 517-520, 1951.
- 2-326. Olenski, Z., Goodden, N. W., Clearness of View from Day-Fighter Aircraft, (Part of "Ability to See"), RAE-Aero-1862, Royal Aircraft Establishment, Farnborough, England, Oct. 1943. (AD-115868).

- 2-327. Optical Society of America, Committee on Colorimetry, The Science of Color, Thomas Y. Crowell Co., N. Y., 1953.
- 2-328. Orlova, N. S., Selected Articles on Light Scattering and Photometric Relief of the Lunar Surface, NASA-TT-F-75, Sept. 1962. (Translation of article in Astronomicheskiy Zhurnal Akademii Nauk SSSR, 33(1): 93-100, 1956).
- 2-329. Otero, J. M., Plaza, L., Salavarri, F., Absolute Threshold and Night Myopia, J. Opt. Soc. Amer., 39: 167, 1949.
- 2-330. Otero, J. M., Influence of the State of Accommodation on the Visual Performance of the Human Eye, J. Opt. Soc. Amer., 41: 942-948, 1951.
- 2-331. Otis, L. S., The Effects of Drugs on Vision, in Recent Developments in Vision Research, Whitcomb, M. A., (ed.), NAS-NRC 1272, National Academy of Sciences - National Res. Council, Washington, D. C., 1966, pp. 216-222.
- 2-332. Parker, J. F., Target Visibility as a Function of Light Transmission Through Fixed Filter Visors, Rep. 64-2, Bio-Technology, Inc., Arlington, Va., 1964.
- 2-333. Partington, M. W., The Vascular Response of the Skin to Ultra-violet Light, Clin. Sci., 13: 425-439, 1954.
- 2-334. Pennington, J. E., Effects of Display Noise on Pilot Control of the Terminal Phase of Space Rendezvous, NASA-TN-D-1619, 1963.
- 2-335. Pennington, J. E., Some Aspects of Man's Visual Capabilities in Space, in A Compilation of Recent Research Related to the Apollo Mission, NASA-TM-X-890, 1963, pp. 59-65.
- 2-336. Pennington, J. E., Brissenden, R. F., Visual Capability of Pilots as Applied to Rendezvous Operations, IAS-Paper 63-15, presented at the IAS 31st Annual Meeting, N. Y., Jan. 21-23, 1963.
- 2-337. Pennington, J. E., Hatch, H. G., Jr., Long, E. R., et al., Visual Aspects of a Full-Size Pilot-Controlled Simulation of the Gemini-Agena Docking, NASA-TN-D-2632, 1965.
- 2-338. Pepler, R. D., Wohl, J. G., Display Requirements for Pre-launch Checkout of Advanced Space Vehicles, RAND-RM-4200-NASA, RAND Corp., Santa Monica, Calif., May 1964.

- 2-339. Peskin, J. C., Bjornstad, J., The Effect of Different Wavelengths of Light on Visual Sensitivity, AML-MR-694-93A, Air Materiel Command, Wright-Patterson AFB, Ohio, 1948.
- 2-340. Peters, G. A., Adams, B. B., These Three Criteria for Readable Panel Markings, Product Engineering, 30(21): 55-57, 1959.
- 2-341. Petertyl, S. V., Fuller, P. R., Wysocki, C. A., et al., Development of High Contrast Electroluminescent Displays, AFFDL-TR-66-183, Flight Dynamics Lab., Wright-Patterson AFB, Ohio, Mar. 1967.
- 2-342. Pitha, C. A., Laser Damage: A Selected Literature Survey, AFCRL-67-137, Air Force Cambridge Research Labs., L. G. Hanscom Field, Bedford, Mass., 1967.
- 2-343. Pomerantzeff, O., Enhancement of Night Vision by Correction of Optical Aberrations of the Eye, Rep. 1, Retina Foundation, Department of Retina Research, Boston, Mass., under contract DADA-17-67-C-0029, Army Medical Research and Development Command, Washington, D. C., Apr. 1967. (AD-815995).
- 2-344. Popov, V., Boyko, N., Vision in Space Travel, RSIC-698, Redstone Scientific Information Center, Redstone Arsenal, Ala., Aug. 1967. (Translation of Aviatsiya i Kosmonautika, No. 3: 73-76, 1967).
- 2-345. Potts, A. M., Ocular Pharmacodynamics, in Recent Developments in Vision Research, Whitcomb, M. A., (ed.), NAS-NRC, Publ. 1272, 1966, pp. 192-193.
- 2-346. Putnam, R. C., Faucett, R. E., The Threshold of Discomfort Glare at Low Adaptation Levels, Illum. Engin., 46: 505-510, Oct. 1951.
- 2-347. Richards, W., Luria, S. M., Color Mixture Functions at Low Luminance Levels, NMRL-439, Naval Submarine Medical Center, Submarine Base, Groton, Conn., 1964. (Reprinted from: Vision Res., 4: 281-313, 1964).
- 2-348. Riley, D. R., Jaquet, B. M., Pennington, J. E., et al., Comparison of Results of Two Simulations Employing Full-Size Visual Cues for Pilot-Controlled Gemini-Agena Docking, NASA-TN-D-3687, 1966.
- 2-349. Riley, D. R., Jaquet, B. M., Cobb, J. B., Effect of Target Angular Oscillations on Pilot-Controlled Gemini-Agena Docking, NASA-TN-D-3403, 1966.

- 2-350. Riley, D. R., Jaquet, B. M., Bardusch, R. E., et al, A Study of Gemini-Agena Docking Using a Fixed-Base Simulator Employing a Closed-Circuit Television System, NASA-TN-D-3112, 1965.
- 2-351. Ritter, O. L., Strughold, H., Seeing Planets from Space, Astronautics and Aerospace Engineering, 1(6): 82-87, July 1963.
- 2-352. Roach, F. E., The Light of the Night Sky: Astronomical Interplanetary and Geophysical, Space Science Reviews, 3(4): 512-540, 1964.
- 2-353. Roberts, L., The Action of a Hypersonic Jet on a Dust Layer, LAS-63-50, Inst. Aerospace Science, Annual Meeting, 31st, N. Y., Jan. 21-23, 1963.
- 2-354. Robinson, N., (ed.), Solar Radiation, Elsevier Publishing Co., Amsterdam, 1966.
- 2-355. Rocco, R. M., Research and Development of Helmet Face-pieces for Space Protective Assemblies, AMRL-TR-66-193, Aerospace Medical Res. Labs., Wright-Patterson AFB, Ohio, 1967.
- 2-356. Ronchi, L., Freedman, S. J., Comparative Study of Acquisition Times for Various Visual Functions, Serie II, No. 1103, Pubblicazioni Dell' Istituto Nazionale di Ottica, Arcetri-Firenze, 1965. (Reprinted from: Atti Fond. G. Ronchi, 20(1): 88-101, Jan-Feb. 1965).
- 2-357. Ronchi, L., Tittarelli, R., Detection of Circular Light Signals in Relation to Shape and Color Identification, Preliminary Report, SAM-TR-66-14, School of Aerospace Med., Brooks AFB, Texas, 1966.
- 2-358. Ronchi, L., Sulli, R., Low Luminance Background: A Handicap for Signal Perception, Atti. Fond. G. Ronchi, 21(6): 729-737, Nov-Dec. 1966.
- 2-359. Ronchi, L., On the Factors Influencing the Judgment of Brightness, Serie II, No. 1076, Pubblicazioni Dell' Istituto Nazionale di Ottica, Arcetri-Firenze, 1964. (Reprinted from: Atti. Fond. G. Ronchi, 19(4): 408-412, Jul-Aug. 1964).

- 2-360. Ronchi, L., Fujiwara, S., Tittarelli, R., Response to Low-Frequency Intermittent Stimulation and Visual Noise, Serie II, N. 1077, Pubblicazioni Dell' Istituto Nazionale di Ottica, Arcetri-Firenze, 1964. (Reprinted from: Atti Fond. G. Ronchi, 19(4): 413-427, Jul-Aug. 1964).
- 2-361. Ronchi, L., Fujiwara, S., A Statistical Treatment of Irregularities of Scotopic Sensitivity, Serie II, No. 1070, Pubblicazioni Dell' Istituto Nazionale di Ottica, Arcetri-Firenze, 1964. (Reprinted from: Atti Fond. G. Ronchi, 19(3): 305-314, May-June 1964)
- 2-362. Ronchi, L., Bittini, M., Adachi, I., Subjective Sharpness of a Contour as a Function of Luminance and Contrast, Optik, 20: 132-140, 1963.
- 2-363. Rose, H. W., Nomograph of Equivalent Values of Commonly Used Units of Luminance, Table 2.2, in Vision in Military Aviation, Chapter 2. The Nature and Measurement of Light, Wulfeck, J. W., Weisz, A., Raben, M. W., et al, (eds.), WADC-TR-58-399, Nov. 1958, p. 16.
- 2-364. Roth, E. M., Bioenergetic Considerations in the Design of Space Suits for Lunar Exploration, NASA-SP-84, 1966.
- 2-365. Roth, E. M., Space-Cabin Atmospheres, Part II - Fire and Blast Hazards, NASA-SP-48, 1964.
- 2-366. Ruch, T. C., Fulton, J. F., (eds.), Medical Physiology and Biophysics, W. B. Saunders Co., Philadelphia, Pa., 1960.
- 2-367. Runyan, T. L., Dick, J. M., Illumination for Extravehicular Tasks, DAC-P-3876, Douglas Aircraft Co., Inc., Santa Monica, Calif., Mar. 1966.
- 2-368. Rushton, W. A. H., Cohen, R. D., Visual Purple Level and the Course of Dark Adaptation, Nature (London), 173: 301-302, 1954.
- 2-369. Russell, J. L., The Temporary Blinding Effect of Flashes of Light, Report No. E and I-1085, Royal Aircraft Establishment, South Farnborough, Hants, England, 1937.
- 2-370. Ryken, J. M., Emerson, J. E., Onega, G. T., et al., Study of Requirements for the Simulation of Rendezvous and Docking of Space Vehicles, AMRL-TDR-63-100, Aerospace Medical Res. Labs., Wright-Patterson AFB, Ohio, 1963.

- 2-371. Schmidt, I., Satellite-to-Satellite Visibility, in Lectures in Aerospace Medicine, School of Aerospace Med., Brooks AFB, Texas, Feb. 3-7, 1964, pp. 100-118.
- 2-372. Schmidt, I., Space of Potential Visibility of Artificial Satellites for the Unaided Eye, in Proceedings of the International Astronautical Congress, 8th, Barcelona, 1958, p. 373.
- 2-373. Schober, H., Wittmann, K., Untersuchungen über die Sehschärfe bei verschiedenfarbigen Licht. Das Licht, Z. praktische Leucht- u. Beleuchtungs-Aufgaben, 8: 199-201, 1938.
- 2-374. Scott, T. H., Literature Review of the Intellectual Effects of Perceptual Isolation, Rep. HR-66, Dept. of National Defence, Defence Research Board, Canada, 1957.
- 2-375. Sears, F. W., Principles of Physics, in Optics, Vol. III, Sears, F. W., (ed.), Addison-Wesley Press, Cambridge, Mass., 1946, pp. 1-323.
- 2-376. Seminara, J. L., Kincaid, W. K., Jr., Control Task Performance in the Lunar Visual Environment, LMSC-685055, Biotechnology Organization, Lockheed Missiles & Space Co., Sunnyvale, Calif., Feb. 1968.
- 2-377. Senders, J. W., Elkind, J. I., Grignetti, M. C., et al., An Investigation of the Visual Sampling Behaviour of Human Observers, NASA-CR-434, 1966.
- 2-378. Severin, S. L., Recovery of Visual Discrimination After High Intensity Flashes of Light, SAM-62-16, School of Aerospace Med., Brooks AFB, Texas, Dec. 1961.
- 2-379. Severin, S. L., Newton, N. L., Culver, J. F., A Study of Photostress and Flash Blindness, SAM-TDR-62-144, School of Aerospace Med., Brooks AFB, Texas, 1962.
- 2-380. Seyb, E. K., Sighting Range at Night and Twilight Brightness, SHAPE-TM-151, SHAPE Technical Centre, The Hague, (Netherlands), Mar. 1967. (AD-811315).
- 2-381. Shea, R. A., Summers, L. G., Visual Detection of Point Source Targets, NASA-CR-563, 1966.
- 2-382. Shearer, J. E., Downey, P., Design Study for Cabin Lighting of Orbital Flight Vehicle, WADD-TR-60-122, Wright Air Development Division, Wright-Patterson AFB, Ohio, 1960.

- 2-383. Shepard, A. B., Pilot's Flight Report Including Inflight Films, in Proceedings of a Conference on Results of the First U. S. Manned Suborbital Space Flight, NASA, Manned Spacecraft Center, Houston, Texas, 1961, pp. 69-75.
- 2-384. Shlaer, S., Smith, E. L., Chase, A. M., Visual Acuity and Illumination in Different Spectral Regions, J. Gen. Physiol., 25: 553-569, Mar. 1942.
- 2-385. Siegel, A. I., Fischl, M. A., Dimensions of Visual Information Displays, Applied Psychological Services, Wayne, Pa., under Contract N00014-66-C0183, Office of Naval Research, Sept. 1967.
- 2-386. Simon, C. W., Craig, D. W., Effects of Magnification and Observation Time on Target Identification in Simulated Orbital Reconnaissance, Human Factors, 7: 569-583, 1965.
- 2-387. Simon, C. W., Rapid Acquisition of Radar Targets from Moving and Static Displays, Human Factors, 7: 185-205, 1965.
- 2-388. Sloan, L. L., Rate of Dark Adaptation and Regional Threshold Gradient of the Dark-Adapted Eye: Physiologic and Clinical Studies, Amer. J. Ophthalm., 30: 705-720, 1947.
- 2-389. Smith, H. A., Goddard, C., Effects of Cockpit Lighting Color on Dark Adaptation, AFFDL-TR-67-56, Flight Dynamics Lab., Wright-Patterson AFB, Ohio, May 1967.
- 2-390. Smith, W. J., Gulick, W. L., Dynamic Contour Perception, J. Exp. Psychol., 53: 145-151, 1957.
- 2-391. Smith, W. M., Gulick, W. L., A Statistical Theory of Dynamic Contour Perception, Psychol. Rev., 69: 91-108, 1962.
- 2-392. Smith, W. M., Gulick, W. L., Visual Contours and Movement Perception, Science, 124: 316-317, 1956.
- 2-393. Snyder, E. F., Development of a Lunar Photometric Function from Experimental Data, Chrysler Corporation, in Proceedings of the Interdisciplinary Symposium on Apollo Application Programs (12-13 Jan. 1966), Society of Engineering Science, Huntsville, Ala., NASA-TM-X-53558, George C. Marshall Space Flight Center, Huntsville, Ala., Dec. 1966, pp. 61-116.
- 2-394. Spector, W. S., (ed.), Handbook of Biological Data, WADC-TR-56-273, Wright Air Dev. Center, Wright-Patterson AFB, Ohio, Oct. 1956. (AD-110501).

- 2-395. Stair, R., Spectral-Transmissive Properties and Use of Eye-Protective Glasses, NBS-Circular-471, National Bureau of Standards, Washington, D. C., Oct. 8, 1948. (Also includes the Supplementary Notes on the Spectral Transmittance of Glasses for Driving at Night, (this accompanies NBS Circ-471), Nov. 10, 1955).
- 2-396. Steedman, W. C., Baker, C. A., Target Size and Visual Recognition, Human Factors, 2: 120-127, 1960.
- 2-397. Stiles, W. S., Crawford, B. H., The Luminous Efficiency of Rays Entering the Eye Pupil at Different Points, Proc. Roy. Soc. (London), 112B: 428-450, Mar. 1933.
- 2-398. Straub, W. H., Protection of the Human Eye from Laser Radiation, HDL-TR-1133, Harry Diamond Labs., Washington, D. C., July 1963.
- 2-399. Strughold, H., The Human Time Factor in Flight, II. Chains of Latencies in Vision, J. Aviat. Med., 22: 100-108, 1951.
- 2-400. Suchman, E. A., Weld, H. P., The Effect of Light Flashes during the Course of Dark Adaptation, Amer. J. Psychol., 51: 717-722, 1938.
- 2-401. Summers, L. G., Shea, R. A., Ziedman, K., Unaided Visual Detection of Target Satellites, J. Spacecraft, 3: 76-79, 1966.
- 2-402. Sytinskaya, N. N., Summary Catalog of the Absolute Values of the Visual Reflecting Power at Full Moon of 104 Lunar Objects, STL-TR-61-5110-24, Space Tech. Lab., Los Angeles, Calif., 1961.
- 2-403. Tanner, W. P., Jr., Swets, J. A., A Decision-Making Theory of Visual Detection, Psychol. Rev., 61: 401-409, 1954.
- 2-404. Taylor, J. B., Silverman, S. M., Some Aspects of Night Visibility Useful for Air Force Operations, AFCRL-66-862, Air Force Cambridge Research Labs., L. G. Hanscom Field, Bedford, Mass., 1966.
- 2-405. Taylor, J. G., The Behavioural Basis of Perceived Size and Distance, Canad. J. Psychol., 19: 1-14, Mar. 1965.
- 2-406. Taylor, J. H., Scripps Institution of Oceanography, Visibility Lab., Univ. of California, La Jolla, Calif., personal communication, 1968.

- 2-407. Taylor, J. H., Contrast Thresholds as a Function of Retinal Position and Target Size for the Light-Adapted Eye, SIO-Ref-61-10, Scripps Institution of Oceanography, Univ. of California, La Jolla, Calif., Mar. 1961.
- 2-408. Taylor, J. H., Practice Effects in a Simple Visual Detection Task, Nature, 201: 691-692, 1964.
- 2-409. Taylor, J. H., Survey of Research Relating to Man's Visual Capabilities in Space Flight, Final Report, under Contract NOBS-86012, Scripps Institution of Oceanography, Univ. of California, La Jolla, Calif., June 1964. (AD-606802).
- 2-410. Taylor, J. H., Visual Performance on the Moon, Scripps Institution of Oceanography, Univ. of California, San Diego, Calif., paper presented at the XVIIth Congress of the International Astronautical Federation, Madrid, Spain, Oct. 1966.
- 2-411. Thomson, M. L., Relative Efficiency of Pigment and Horny Layer in Protecting the Skin of Europeans and Africans against Solar Ultraviolet Radiation, J. Physiol., 127: 236-246, 1955.
- 2-412. Tinker, M. A., Lighting and Color, in Human Factors in Under-sea Warfare, National Academy of Sciences - National Res. Council, Committee on Undersea Warfare, Washington, D. C., 1949, pp. 357-374.
- 2-413. Tousey, R., Report on Effect of CRT Screens on Night Vision, U. S. Naval Res. Lab., Washington, D. C.
- 2-414. Trumbull, R., Some Potential of Research on Drugs and Vision, in Recent Developments in Vision Research, Whitcomb, M. A., (ed.), NAS-NRC-1272, National Academy of Sciences - National Res. Council, Washington, D. C., 1966, pp. 223-225.
- 2-415. Tschermak-Seysenegg, A. von, Introduction to Physiological Optics, Charles C. Thomas, Springfield, Ill., 1952, p. 19.
- 2-416. Tufts Inst. for Appl. Exp. Psychol., Handbook of Human Engineering Data for Design Engineers, Tech. Rep. No. SDC-199-1-1, Tufts Univ., Medford, Mass., Revised 1951.
- 2-417. Uhlauer, J. E., Zeidner, J., The Army Night Seeing Tester, Development and Use, HFRB-TRR-1120, Human Factors Research Branch, TAG Research and Development Command, U. S. Army, May 1961. (AD-258349).

- 2-418. Ulett, G. A., Flicker Sickness, Arch. Ophthal., 50: 685-687, 1953.
- 2-419. Urmer, A. H., Jones, E. R., The Visual Subsystem Concept and Spacecraft Illumination, in Visual Capabilities in the Space Environment, Baker, C. W., (ed.), Pergamon Press, N. Y., 1965, pp. 101-109.
- 2-420. Vallerie, L. L., Peripheral Vision Displays, NASA-CR-808, 1967.
- 2-421. Valsi, E., Bartley, S. H., Bourassa, C., Further Manipulation of Brightness Enhancement, J. Psychol., 48: 47-55, 1959.
- 2-422. Vanderplas, J. M., Visual Capabilities of Performing Rendezvous in Space, in Visual Capabilities in the Space Environment, Baker, C. A., (ed.), Pergamon Press, N. Y., 1965, pp. 149-154.
- 2-423. Van Dyke, J. W., Performance/Design and Product Configuration Requirements, Extravehicular Mobility Unit for Apollo Block II Missions, CSD-A-096, NASA, Manned Spacecraft Center, Crew Systems Division, Houston, Texas, Jan. 1966.
- 2-424. Van Liere, E. J., Hypoxia, University of Chicago Press, Chicago, 1963.
- 2-425. Vassiliadis, A., Peppers, N. A., Peabody, R. R., et al., Investigations of Laser Damage to Ocular Tissues, AFAL-TR-67-170, Air Force Avionics Lab., Wright-Patterson AFB, Ohio, Mar. 1967.
- 2-426. Verhoeff, F. H., Bell, L., The Pathological Effects of Radiant Energy on the Eye, Proc. Amer. Acad. Arts & Sciences, 5: 629-818, 1916.
- 2-427. Vinz, F. L., Knighton, M. H., Lahser, H. F., et al., Visual Simulation Facility for Evaluation of Lunar Surface Roving Vehicles, NASA-TN-D-4276, Feb. 1968.
- 2-428. Volkmann, J., Corbin, H. H., Further Experiments on the Range of Visual Search, ESD-TDR-65-169, Electronic Systems Div., L. G. Hanscom Field, Bedford, Mass., 1965. (AD-622414).
- 2-429. Volkmann, J., Corbin, H. H., Eddy, N. B., et al, The Range of Visual Search, ESD-TDR-64-535, Electronic Systems Div., L. G. Hanscom Field, Bedford, Mass., 1964.

- 2-430. Vos, J. J., Some Considerations on Eye Hazards with Lasers, TDCK-46027, National Defence Research Council, T. N. O., Medical Biological Lab., Rijswijk, Netherlands, 1966.
- 2-431. Vos, J. J., Theory of Retinal Burns, Bull. Math. Biophysics, 24: 115-128, 1962.
- 2-432. Wald, G., Alleged Effects of the Near Ultraviolet On Human Vision, J. Opt. Soc. Amer., 42: 171, 1952.
- 2-433. Wald, G., Human Vision and the Spectrum, Science, 101(2635): 653-658, June 1945.
- 2-434. Walls, G. L., Factors in Human Visual Resolution, J. Opt. Soc. Amer., 33: 487-505, Sept. 1943.
- 2-435. Walraven, P. L., On the Mechanism of Color Vision, Report Institute for Perception RVO-TNO, Soesterberg, The Netherlands, 1962.
- 2-436. Walsh, T. M., Warner, D. N., Jr., Davis, M. B., The Effects of a Gemini Left-Hand Window on Experiments Requiring Accuracy in Sighting or Resolution, NASA-TN-D-3669, 1966.
- 2-437. Watkins, W. H., Feehrer, C. E., Investigations of Acoustic Effects upon Visual Signal Detection, ESD-TR-64-557, Electronic Systems Div., L. G. Hanscom Field, Bedford, Mass., 1964.
- 2-438. Weasner, M. H., Carlock, J., Detection and Identification of Colored Smoke, Human Factors, 8(5): 457-462, Oct. 1966.
- 2-439. Wertheim, T., Uber die Indirekte Sehscharfe, Z. Psychol., 7: 172-187, 1894.
- 2-440. Westheimer, G., Drugs and Eye Movement Responses in Man, Recent Developments in Vision Research, Whitcomb, M. A., (ed.), NAS-NRC-1272, National Academy of Sciences - National Res. Council, Washington, D. C., 1966, pp. 215.
- 2-441. White, C. T., Ford, A., Eye Movements during Simulated Radar Search, J. Opt. Soc. Amer., 50: 909-913, 1960.
- 2-442. White, W. J., Acceleration and Vision, WADC-TR-58-333, Wright Air Development Center, Wright-Patterson AFB, Ohio, 1958.

- 2-443. White, W. J., The Effects of Transient Weightlessness on Brightness Discrimination, AMRL-TDR-64-12, Aerospace Medical Research Labs., Wright-Patterson AFB, Ohio, Mar. 1964.
- 2-444. White, W. J., Riley, M. B., Effects of Positive Acceleration on the Relation Between Illumination and Instrument Reading, WADC-TR-58-322, Wright Air Development Center, Wright-Patterson AFB, Ohio, 1958. (AD-206663).
- 2-445. White, W. J., Sauer, S. C., Scale Design for Reading at Low Brightness, WADC-TR-53-464, Wright Air Development Center, Wright-Patterson AFB, Ohio, 1954.
- 2-446. White, W. J., Vision, in Bioastronautics Data Book, Webb, P., (ed.), NASA-SP-3006, 1964, pp. 307-341.
- 2-447. Whiteside, T. C. D., Dazzle from Nuclear Weapons. Vision Research Reports, NAS-NRC-835, National Academy of Sciences - National Res. Council, Washington, D. C., 1960, pp. 79-96.
- 2-448. Whiteside, T. C. D., The Problems of Vision in Flight at High Altitudes, Butterworth, London, 1957, pp. 30-33, 42-55, 89-92, 105-113.
- 2-449. Whiteside, T. C. D., Visual Perception of Movement, Ann. Roy. Coll. Surg. Eng., 33: 267-281, 1963.
- 2-450. Wienke, R. E., The Effect of Flash Distribution and Illumination Level upon the Detection of Low Intensity Light Stimuli, Human Factors, 6: 305-311, June 1964.
- 2-451. Wilcox, W. W., The Basis of the Dependence of Visual Acuity on Illumination, Proc. Nat. Acad. Sci., 18: 47-57, 1932.
- 2-452. Williams, A. C., Jr., Simon, C. W., Haugen, R., et al., Operator Performance in Strike Reconnaissance, WADD-TR-60-521, Wright Air Development Center, Wright-Patterson AFB, Ohio, 1960.
- 2-453. Williams, L. G., A Study of Visual Search Using Eye Movement Recordings, Rep. 12009-IR-1, Honeywell, Inc., St. Paul, Minn., 1966. (AD-629624).
- 2-454. Williams, L. G., A Study of Visual Search Using Eye Movement Recordings, Rep 12009-IR-3, Systems and Research Center, Honeywell, Inc., St. Paul, Minn., Mar. 1967.
- 2-455. Williams, L. G., Target Conspicuity and Visual Search, Human Factors, 8(1): 80-92, 1966.

- 2-456. Williams, L. G., Visual Search: Eye Fixations as Determined by Instructed Target Characteristics, Rep-T-125, Honeywell, Inc., St. Paul, Minn., 1965. (AD-620336).
- 2-457. Williams, S. B., Visibility on Radar Scopes, in A Survey Report on Human Factors in Undersea Warfare, Committee on Undersea Warfare, National Research Council, Washington, D. C., 1949.
- 2-458. Williams, T. P., Photoreversal of Rhodopsin Bleaching, J. Gen. Physiol., 47: 679-689, 1964.
- 2-459. Willstrop, R. V., Absolute Measures of Stellar Radiation, Part II, Mem. Roy. Astron. Soc., 69: 83-143, 1965.
- 2-460. Wilson, R. C., Canfield, A. A., The Effects of Increased Positive Radial Acceleration upon Pupillary Response, in Psychological Research on the Human Centrifuge: Final Report, Warren, N. D., Bryan, D. L., Wilmorth, N. E., et al., N6-ori-77, Task Order 3, Dept. of Psychology, Univ. of Southern California, Los Angeles, Calif., 1951.
- 2-461. Woodhull, J. G., Bauerschmidt, D. K., Human Perception of Line-of-Sight Rates, HAC-2732.20/135, Hughes Aircraft Co., Culver City, Calif., 1962.
- 2-462. Wulfeck, J. W., Weisz, A., Raben, M. W., et al., Vision in Military Aviation, WADC-TR-58-399, Wright Air Development Center, Wright-Patterson AFB, Ohio, 1958. (AD-207780).
- 2-463. Young, L. R., Zuber, B. L., Stark, L., Visual and Control Aspects of Saccadic Eye Movements, NASA-CR-564, 1966.
- 2-464. Zaret, M. M., Ripps, H., Siegel, I. M., et al., Laser Photocoagulation of the Eye, Arch. Ophth., 69: 97-104, 1963.
- 2-465. Zaret, M. M., Grosof, G., Ocular Hazards of Laser Radiation, AMRL-TDR-63-132, Aerospace Medical Res. Labs., Wright-Patterson AFB, Ohio, 1963.
- 2-466. Zaret, M. M., Ophthalmological Effects of Intense Light Beams, AL-TDR-64-217, Air Force Avionics Lab., Wright-Patterson AFB, Ohio, 1965. (AD-468093).
- 2-467. Zuercher, J. D., The Effects of Extraneous Stimulation on Vigilance, Human Factors, 7: 101-105, 1965.

3. IONIZING RADIATION

Prepared by

E. M. Roth, M. D., Lovelace Foundation



TABLE OF CONTENTS

3.	IONIZING RADIATION	3-1
	Space Radiations	3-1
	Nomenclature and Dosage Factors	3-4
	Reference Equivalent Space Exposure (RES)	3-6
	Dose Distribution Factors	3-7
	Dose Protraction.	3-8
	Interaction of Radiation With Biological Materials.	3-10
	Energy LET and Quality Factors	3-10
	Flux (Current)-To-Tissue Dose Conversion	
	Factors for Nucleons	3-31
	Shielding and Tissue Range	3-33
	Tissue Range and Tissue Self-Shielding	3-38
	Typical Depth-Dose Patterns in Space	
	Under Shielding	3-42
	Early Effects of Acute Radiation at High Dose Rates	3-46
	Lethality	3-49
	Prodromal Symptoms	3-51
	Hematological Syndrome	3-53
	Skin Reactions	3-57
	Quality	3-59
	Dose Fractionation	3-59
	Dose Rate.	3-60
	Depth Distribution and Area Factors	3-60
	Germinal Epithelium	3-62
	Progressive Performance Decrement	3-63
	Late or Delayed Effects of Radiation	3-67
	Ocular Lens	3-68
	Permanent or Late Skin Effects.	3-70
	General Life-Shortening and Carcinogenesis	3-73

Life-Shortening	3-73
Genetic Manifestations	3-78
Secondary Factors in Radiation Injury	3-80
Environmental Factors	3-80
Anti-radiation Therapy	3-82
Performance After Radiation.	3-82
Radiation Dose Limits in Space Operations	3-83
Risk Analysis	3-84
Planning Operational Dose (POD)	3-85
Maximum Operational Dose (MOD)	3-85
Dosimetry for Characterization of Space	
Radiation Exposure	3-86
Dose Limits for Ground Personnel	3-89
References	3-90

IONIZING RADIATION

Operational evaluation of the radiation hazard to man is dependent on the nature and timing of the radiation flux incident on the vehicle, the composition and three-dimensional thickness of the shielding, the geometrical position of the human behind the shielding, the self-shielding of the body, the current-to-dose conversion factors in the body, and the pathophysiology of radiation damage. The following are data which may be used for calculation of specific organ doses, radiation shielding, and mission risk-hazard analysis for man. Emphasis will be placed on the interaction between radiation and man. The physical nature of space radiation and the molecular aspects of radiobiology will be covered only as they contribute directly to the evaluation of radiobiological risks and operational problems.

SPACE RADIATIONS

The physical nature of the radiation environment has received much study and review. Space radiation can be defined as falling into three categories: primary cosmic or galactic radiation; the geomagnetically trapped radiations of the Van Allen belts; and solar wind and flare events. Cosmic radiation is now preferably called galactic radiation to distinguish it from trapped radiation and solar-particle fluxes. The current hypotheses assume that these nuclei have traveled for eons in galactic space, gradually being accelerated in turbulent magnetic fields or arise from supernovas or other events near the center of our own galaxy. The galactic radiation spectrum has been described in great detail but is continually changing as new data are obtained from geophysical satellites and other sources (87, 90, 162, 243). Table 3-16 presents the composition of the primary cosmic-ray flux outside the atmosphere at northern latitudes. The truly primary galactic radiation (i. e., the flux containing no secondaries produced locally in a compact absorber), consists of 85 percent hydrogen nuclei (protons, 14 percent helium nuclei (alpha particles), and 1 percent of the heavier nuclei up to iron ($Z = 26$) as regular constituents and so-called superheavy nuclei beyond iron occasionally recorded. These particles transfer energy to matter by ionization along their pathway, by terminal absorption ("thindowns"), and by inelastic collision ("star formation"), which result in highly localized areas of very dense ionization. The intensity of galactic radiation in the vicinity of the Earth varies with the 11-year solar cycle, with magnetic storms, and possibly with the appearance of supernovae near the solar system.

Trapped particle radiation is a problem in the Van Allen belts, where protons and electrons are injected and trapped in the Earth's magnetic field. Though the topological conditions and direction of injection are still obscure, it is currently thought that the trapped particles arise from protons and electrons from the primary cosmic-ray beam backscattered from the Earth's atmosphere - the source of the bulk of this component is neutrons decaying into protons and electrons; protons from the solar wind; and primary cosmic-ray protons, which are assumed to be of minor importance.

Estimation of exposures during space flight in these toroidal belts is most difficult because of the complicated geomagnetic and particle interactions determining the geometric distribution of the radiation. Magnetic storms can influence the nature of the belts (163, 235, 296). The inner belts contain not only protons, but sizable fluxes of soft electrons of natural origin and from fission electrons injected into the trapping region by high altitude nuclear weapons testing.

A summary of the particles' energies has been recently presented from which the following data are taken directly (145). In going vertically up from sea level at the geomagnetic equator, the flux of trapped protons in the inner belt is found to start rising sharply at 1.16 Earth radii (about 1,000 km altitude above sea level) and reaches a first maximum at 1.5 Earth radii (3,185 km), with an integral flux of slightly more than 10,000 protons/cm² sec of 40 MeV minimum energy. In the heart of the inner belt, a flux of 2,000 protons/cm² sec per unit solid angle in the energy interval from 40 to 110 MeV, corresponds to a range interval in aluminum from 2 to 12 g/cm². Since the radiation sensors on Relay I discriminated fluxes only in the energy intervals from 1.1 to 14 MeV, from 18.2 to 35 MeV, and from 40 to 110 MeV, the slope in the last interval can only be inferred indirectly by extrapolation plotting of the three flux fractions. The flux then drops slightly and reaches a second flat maximum smaller than the first one at 2.2 Earth radii and finally drops below 100 protons/cm² sec at 2.8 Earth radii. The corresponding altitude profiles toward higher magnetic latitudes show gradually smaller fluxes up to geomagnetic latitude 37.5°, which marks the boundary at which the fluxes of high-energy protons and electrons drop to insignificant levels.

A phenomenon of special importance for satellite missions in near-Earth orbits is the so-called South Atlantic anomaly. It is a region where the mirror points of the trajectories of trapped protons in the inner belt dip down more closely to the Earth than at any other longitude, due to an asymmetry of the geomagnetic field. Dose rates below 1.5 g/cm² shielding come close to 100 mrads/hr at altitudes as low as 120 miles, as direct dose-rate measurements on the Gemini IV mission indicate. Since the point of intersection of a satellite orbit with the geographic equator continuously drifts westward due to the rotation of the Earth, any mission comprising a large enough number of revolutions passes through the anomaly on some orbits. Although the time of a single passage is less than 15 min and the accumulated passage time on a mission of many orbits remains well below 10 percent of the total time in orbit, the proton exposure in the anomaly accounts for more than 90 percent of the total exposure. The accumulated exposure in the anomaly will be a limiting factor for long-duration, low-orbital missions.

A large fraction of the artificially injected electron fluxes shows lifetimes of at least several years, and it might still take 30 years for the natural radiation levels to be restored. It now seems reliably established that electrons injected into regions of $L < 1.2$ Earth radii, corresponding to an altitude of 1,275 km above sea level at the geomagnetic equator, are rapidly removed by the Earth's atmosphere. Electrons injected into L regions beyond 1.7 (4,460-km altitudes) are also removed comparatively rapidly by magnetic fluctuations due to solar activity. These are the same fluctuations that cause

the large variations of natural flux levels noted above. In the intermediate altitude region between 1.2 and 1.7 L, however, artificially injected electrons become semipermanently trapped with $1/e$ decay times of the order of 5 to 10 years. In January 1963, the flux at 1.5 L in the plane of the geomagnetic equator was 5×10^8 electrons/cm² sec for the energy band from about 0.5 to 5 MeV and 1.5×10^7 electrons/cm² sec for the band higher than 5 MeV. The combined exposure hazard from protons and electrons in the heart of the artificial electron belt, which happens to coincide with the heart of the natural inner proton belt, was predominantly due to electrons 6 months after creation of the artificial belt. Whereas the decay times for the fluxes in the outer regions and the inner fringes of the artificial belt are on the order, respectively, of months and weeks, they grow to the order of at least several years in the center of the belt. In the natural outer belt of electrons, fluxes show large irregular fluctuations. At 4.0 L (sea-level altitude of 3 Earth radii at the magnetic equator), peak electron intensities closely approach the maximum values found in the heart of the artificial belt at 1.5 L.

Models of the trapped radiation environment are available as are computer codes for their use in establishing dose rates (91, 184, 284, 285).

Solar plasma comes from the Earth in three ways: the solar wind, solar corpuscular streams, and solar flare emissions or plasma shells. Solar wind is a perpetual outflow from the solar corona all over the sun. The solar wind is distinguished from the other two flows which are called ejected flows. The magnetic fields and low energy particles of the solar wind have been recently reviewed (163, 195, 235). The solar wind does not appear to represent a significant human hazard.

The solar corpuscular stream is an intermittent emission continuing for weeks and months, apparently from the same region of the sun. These spiral streams interact with the solar wind and the cosmic galactic radiation (163). The solar flare emissions are of much shorter duration, usually lasting about an hour or less. The solar ejected flows vary from one event to the next in the differential energy spectrum and intensity of the proton and alpha particles. Analyses of these spectral data are available (14, 30, 93, 142, 162, 242, 295). The proton:alpha flux ratio for equal rigidity intervals in four events were 1:1 and in 3 events were >5:1. Calculations of the exponential rigidity-flux relationship and rigidity-kinetic energy relationship for the time-integrated spectra are available (184). Values of P_0 or characteristic rigidity are uniformly distributed between 45 and 150 mV for all events of solar cycle 19 when the largest solar particle events were recorded. (See discussion of Table 3-33). The typical characteristic rigidity is 100 mV and may be used for first-order dose computations. Data are now available on large events during the quiet sun period (237).

Reviews of Soviet studies on the geophysical aspects of space radiations are available (35, 255).

NOMENCLATURE AND DOSAGE FACTORS

The basic terms for expressing the exposure field and absorbed dose of radiation are seen in Figure 3-1. RBE (relative biological effectiveness)

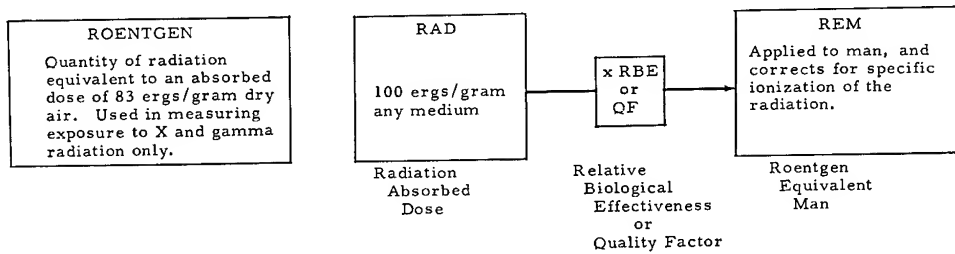


Figure 3-1

Radiation Terms

expresses the effectiveness of a particular type of radiation in producing the same specific biological response as 250 kVp X-radiation or gamma radiation having a linear energy transfer (LET) equivalent to 3.5 kilovolts per micron of water and delivered at the rate of about 10 rads per minute. When an RBE is used not for a specific biological endpoint but for general considerations of health protection, it is referred to as QF or quality factor (41). The exact degree of relative effectiveness is dependent also on the criterion of effect, the tissue or organ of interest, the dose rate, and whether the response is early or delayed (41, 76). High-LET radiations (arbitrarily taken as those radiations having a mean LET greater than $3.5 \text{ keV}/\mu$) are more effective per rad than the conventional x and gamma rays normally used as standard radiations. For late or delayed effect of low dose rate, the QF-LET relationship shown in Table 3-2 has been proposed (122). To a first approximation,

Table 3-2
Values of QF_L for Late or Delayed Effects as a Function of Average LET
(After ICRP(122))

LET _a (keV/ μ IN WATER)	QF
X rays and electrons of any LET	1
3.5 or less	1
3.5-7	1-2
7-23	2-5
23-53	5-10
53-175	10-20

this relationship may be represented as:

$$QF_L = 0.8 + 0.16 \bar{L} \quad (1)$$

where \bar{L} is the mean LET in keV/ μ . No official committee or organization has made specific recommendations with respect to the QF-LET relationship for early effects. Accurate calculation of the biological effect should refer to detailed LET spectra where available.

In general, early responses to large doses delivered at high dose rates are less dependent on LET than are late responses to low doses at low dose rates. The relationship generally follows the equation:

$$QF_E = 0.9 + 0.05 \bar{L} \quad (2)$$

For gross evaluation it is suggested that the general QF_E-LET relationships shown in Table 3-3 be applied to early responses from high-intensity space-radiation exposure (145). For computer programming of more exact dosage

Table 3-3

Suggested QF_E Values for Early Effects of High-Intensity Space-Radiation Exposure
(After Langham (ed.)-NAS-NRC⁽¹⁴⁵⁾)

	COMPONENT	QF
Skin responses	Low LET (≤ 3.5 keV/ μ)	1
	High LET (> 3.5 keV/ μ)	3
Prodromal syndrome	Total flux	1
Hematological responses	Total flux	1
Lethality, hematological syndrome	Total flux	1
Lethality, intestinal syndrome	Low LET (≤ 3.5 keV/ μ)	1
	High LET (> 3.5 keV/ μ)	3
Atrophy of germinal epithelium	Low LET (≤ 3.5 keV/ μ)	1
	High LET (> 3.5 keV/ μ)	3

schedules under operational conditions, more specific energy-LET-QF relationships can be used when available. It must be kept in mind that RBE or QF is dose-rate dependent (41, 76). In general, radiation of low LET tends to be more sensitive to dose rate factors than does radiation of high LET. Particles of high LET may have higher RBE or QF at low dose rates than at higher dose rates. Specific examples will be noted below. In all cases, the biological dose equivalent for late and early responses should be calculated separately.

Examples of RBE or QF values for late effects at low dose rates used in ground laboratories are seen in Table 3-4. In some animal studies, RBE's of over 35 have been reported for genetic changes after neutron irradiation (251). At high dose rates, the QF_E of Table 3-3 may be used for neutrons and the other radiations of Table 3-4 (134).

Table 3-4

Typical QF_L for Late Effects at Low Dose Rate in Ground-Based Exposure

Type of radiation	RBE or QF
X-rays	1
Gamma rays	1
Beta particles, 1.0 mev	1
" " 0.1 mev	1
Neutrons, thermal energy	2.8
" 0.0001 mev	2.2
" 0.005 mev	2.4
" 0.02 mev	5
" 0.5 mev	10.2
" 1.0 mev	10.5
" 10.0 mev	6.4
Protons, greater than 100 mev	1 - 2
" 1.0 mev	8.5
" 0.1 mev	10
Alpha particles, 5 mev	15
" " 1 mev	20

For more specific calculations of organ doses in experimental ground-based studies, the energy-LET-QF relationship will be covered in more detail below.

Reference Equivalent Space Exposure (RES)

Quantitative evaluation of the factors that modify radiation responses is singularly the greatest uncertainty in establishing human response criteria for space radiation exposure. The most obvious modifying factors are radiation quality, dose rate (as influenced both by protraction and fractionation), and dose distribution (both topical and depth). For space applications it has been suggested that "dose equivalent" in "rems" used in conventional occupational radiation protection, be replaced by "reference equivalent space exposure" (RES) in "reference equivalent units" designated "reu" (145). Conceptually, the method of evaluation is the same as that employed in conventional radiation protection. The space radiation dose (D) is multiplied by a radiation quality factor (QF) and subsequently by other appropriate modifying factors to give the reference equivalent space exposure:

$$\text{RES (reu)} = D \text{ (rads)} \times \text{QF} \times (f_1 \cdot f_2 \dots f_n), \quad (3)$$

where $f_1 \dots f_n$ are the appropriate modifying factors for early vs. late effects, dose protraction, and dose distribution of the particular response being evaluated. In principle, this procedure is applicable to evaluation of both early and late radiation responses. However, inadequate knowledge of the quantitative influence of the relevant modifying factors such as dose dis-

tribution and dose protraction and their interdependence necessitates the choice of a set of values for each specific situation on the basis of rather arbitrary simplifications and generalizations.

Dose Distribution Factors

Dose distribution in space radiation exposure will be highly non-uniform with respect to depth, area, volume, and region or organ systems exposed. More detailed evaluation will be made for each organ system. At present, only very arbitrary simplifying generalizations will be made.

With respect to depth-dose distribution the acquired dose is calculated or measured at the average depth or anatomical site (volume) of interest for the particular response. The point of interest for skin responses is at a depth of 0.1 mm; for hematological depression, a depth of 5 cm; for hematopoietic and gastrointestinal lethality, a depth of 11 cm; and for prodromal response and general physiological injury a 15-cm diameter sphere in the mid-epigastric region. At these depths the penetration factor (f_p) will be considered to be one.

With regard to region or volume exposed, it has been suggested for prodromal, hematological and early lethal responses a dose involving a major portion of the trunk be considered as capable of eliciting full response and be assigned a "volume factor" (f_v) of one (145). Exposure of the extremities exclusive of the trunk would be much less effective. Based on fraction of total body mass and active bone marrow, an arbitrary choice of a f_v of 1/5 might be suggested for the extremities when only the hematological response is considered.

Skin and germinal epithelium responses must be considered specifically. A severe response of even a small skin area, regardless of location, could be highly uncomfortable particularly under a space suit. Furthermore, dose values are usually established for skin areas of ~ 35 to 100 cm^2 ; and early erythema and desquamation are somewhat area-dependent up to ~ 300 to 400 cm^2 . The area-effect over this range amounts to an increase in effective dose of ~ 25 percent. It is suggested, therefore, that an area-effectiveness factor (f_a) of ~ 1.25 be applied to the doses given when exposure involves skin areas greater than $\sim 150 \text{ cm}^2$.

In the case of the germinal epithelium response is considered a local effect. Because of the limited size and localization of the testicles, it is reasonable to assume that they either will or will not be in the exposure field in which case f_v will either be unity or zero. In mentioning the germinal epithelium it is emphasized that the response in this case is considered of no significance in evaluating risk of early performance decrement but may have social or emotional significance to the astronaut.

Dose Protraction

The effect of dose protraction has been studied to some degree for most of the early signs and symptoms (32 , 41 , 73 , 148 , 172 , 191 , 201 , 205 , 228 , 231 , 238). Some suggestions are possible regarding general "dose-effectiveness" factors (f_r) that are useful for exposure periods up to three or four weeks. To derive the factors, it has been assumed that the decrease per rad in biological effect associated with a dose-rate decrease can be compensated for by an increase in total dose required to produce the given effect (145). Thus the ratio of total doses required for low dose-rate versus high dose-rate exposure will determine the "dose-rate-effectiveness" factors. This is not the same as taking a ratio of dose rates, however, since for some tissues the latter may change by a factor of 10 or more while being accompanied by a change in effect of only about 2. There is also considerable difference in protraction period over which the change from maximum to minimum effect occurs in the various tissues and systems.

Table 3-5 attempts to encompass all of these variables for exposure periods varying from a few hours to a few weeks with respect to total doses

Table 3-5

Suggested Dose-Rate or "Rate-Effectiveness" Factors (f_r) for Early Responses
Following Exposure to Low-LET Radiations at High Intensity. (See text for specific definitions)
(After Langham (ed.)-NAS-NRC⁽¹⁴⁵⁾)

	Duration of Exposure to Produce Same Response Level		
	Skin Erythema and Desquamation	Prodromal Signs	Hematological Depression and Lethality
<u>A. High Dose-Rate</u>			
Duration of Exposure for Maximum Effectiveness	1 - 2 hours or less	2 - 4 hours or less	1 - 2 days or less
<u>B. Low Dose-Rate</u>			
Duration of Exposure for Minimum Effectiveness	4 - 6 days or longer	2 - 4 days or longer	3 - 4 weeks
Ratio of Total Doses to Produce Same Response Level (B/A)	3	2.5	2
Rate-Effectiveness Factor (f_r)	1/3	1/2.5	1/2

high enough to elicit the more significant early responses. The rate-effectiveness factors (f_r) are given as the reciprocals of the ratios of total doses.

In general, "maximum dose" implies no repair is possible. For the prodromal syndrome, fractionated doses longer than 7 days apart can be considered as single doses with no residual effects from the prior doses. For the hematological syndrome, the range of population sensitivity will spread with prolongation beyond 3-4 weeks and an increasingly larger fraction will show no effects as the doses are separated by longer intervals. The terms

"high" dose rate and "low" dose rate are difficult to define for all situations. What is considered a high and a low dose rate for early responses might be quite different from high and low dose rates for progressive and late responses. Furthermore, a high and a low dose rate for early skin responses might be different from those for early hematological and prodromal responses. In general, Table 3-5 attempts to take these variations into consideration for the important early responses. As an example of the use of this table, a given prodromal sign (e.g., nausea) may have a 10 percent probability of occurrence following an exposure of 50 rads delivered over 2 to 4 hours (dose rate 12 to 25 rads/hr), while an exposure of 125 rads (2.5×50) would produce the same probability of response if the dose was protracted over 2 to 4 days (dose rate 30 to 60 rads/day). It is suggested, therefore, that the space radiation dose (D) be multiplied by the appropriate rate-effectiveness factor (f_r) from Table 3-5 to evaluate RES when exposures are protracted over periods comparable to those specified.

Radiation recovery rates are influenced by LET and for this reason, the f_r values given in Table 3-5 are specified for low-LET radiations. Technically, the rate-effectiveness factors should be applied only to the low-LET components of space radiation. Correction of f_r for LET appears unnecessary under shielding conditions that result in only a small fraction of the absorbed dose at the site of interest being delivered at high LET. Information on early skin responses suggests, however, that the slopes of the time-dose response curves decrease with increasing LET. For early skin responses under exposure conditions of very light to nominal shielding, where from ~ 10 to ~ 75 percent of the absorbed dose at 0.1-mm depth from solar flare events may be due to densely ionizing components, adjustments should be made by assuming f_r is unity for that fraction of the dose delivered at or above some arbitrary cut-off for high LET e.g., ~ 15 keV/ μ .

Application of the information given in this section to an evaluation of a risk of early performance decrement may be illustrated (using skin erythema as the early response) by a hypothetical mission during the triplet solar flare event of July 10-16, 1959. No attempt is made to make the assumptions conform necessarily to the actual conditions. If it is assumed that the average effective shielding of the spacecraft was 2 g/cm^2 , the accumulated skin dose (D) during the 6-day period of the triplet flare would have been 674 rads. Let it be assumed also that the QF_E was 1.45, the skin area involved was a major portion of the front surface of the body, the dose received was measured at a depth of 0.1 mm, and 25 percent was delivered at a LET of >15 keV/ μ . Under these conditions, $QF_E = 1.45$, $f_a = 1.25$, $f_p = 1$, and $f_r = (1/3 \times 0.75 + 1 \times 0.25) = 0.5$. The reference equivalent space exposure, evaluated from Equation 1 would be:

$$\text{RES} = 674 \times 1.45 \times 1.25 \times 1 \times 0.5 = 610 \text{ reu.}$$

Since 1 reu is equivalent in effectiveness to 1 rad of reference radiation, comparison of RES with the reference radiation dose-response relationship given in Table 3-47 suggests that the probability of an erythema response under the specified conditions would have been of the order of 50 percent.

Since most exposures to radiation in space flight are expected to be at low dose rates, the dose factors noted for early effects following high dosage of radiation must be modified. Under space flight conditions a gradually accumulating injury to the bone marrow may be expected. Since injury and recovery may be concurrent for long periods of time, the dose distribution and protraction factors applied to acute injury cannot be directly applied to this situation. Suggestions for dosage factors covering these "progressive performance decrements" will be presented in a separate section below. Dosage factors for late or delayed injury following acute exposures will also be covered as a separate entity.

INTERACTION OF RADIATION WITH BIOLOGICAL MATERIALS

In order to calculate the rate of energy transfer, QF or RBE, tissue range, and stopping power of space radiations, data are needed on the interaction with tissue. Since the bulk of absorption takes place in bone or muscle, much of the data have been generated for these model tissues. Table 3-6 represents the model composition of muscle and bone which can be used in the many calculations noted above.

To apply the general purpose nucleon transport codes to the calculation of usable current-to-dose conversion factors of sufficient generality of application, the nuclear density must be known. A tissue of composition $C_{21}H_{140}O_{57}N_3$ with a density of 1 gm/cm³, results in the nuclear densities seen in Table 3-7. The average ionization potentials can be used in the stopping-power formulas for the computation of particle ranges in tissue.

Energy -LET and Quality Factors

The stopping power and rate of energy loss given as MeV/cm or keV/micron (LET) for protons in standard muscle and bone is given in Table 3-8. The calculations of DE/DZ, DE/DX, and LET (127) were made from the ICRU data of Table 3-6 (190), and the energy loss equations of references 11, 17, and 218. The resulting information can be applied to the dosimetric measurement of the protons found in the space environment and can be used in the design of tissue-equivalent radiation detectors. Similar data on proton path length, straggling factors, percent scattering, and probability of inelastic nuclear interaction are available for muscle and other materials (125).

When particles of high energy pass through solid materials, star formation occurs with the release of many nucleons and mesons of different type. These stars are not as frequently generated in biological materials because of the low Z values. The secondary particles from wall materials can pass through biological tissue. Tables 3-9 and 3-10 represent the stopping power and range of muons, pions, kaons, and protons in muscle and bone for a wide range of energies. Powers of 10 are indicated by the symbol E; e.g., 1.234E02 means 1.234×10^2 . The mean excitation energy, I_{adj} , (in eV) is indicated by the symbol I. These data for protons replace previous data

Table 3-6
Composition of ICRU Muscle and Bone

Data compiled by Janni⁽¹²⁷⁾ from the Report of the International Commission on Radiological Units and Measurements (ICRU)⁽¹⁹⁰⁾

a. Muscle*

<u>Element</u>	<u>Atomic number</u>	<u>Atoms/molecule</u>	<u>Percent by weight</u>	<u>Atomic weight</u>
H	1	10.11905	10.20	1.01
C	6	1.02415	12.30	12.01
N	7	0.24986	3.50	14.01
O	8	4.55625	72.90	16.00
Na	11	0.00348	0.08	23.00
Mg	12	0.00082	0.02	24.33
P	15	0.00646	1.20	30.98
S	16	0.01559	0.50	32.07
K	19	0.00767	0.30	39.11
Ca	20	0.00017	0.01	40.09

b. Bone**

<u>Element</u>	<u>Atomic number</u>	<u>Atoms/molecule</u>	<u>Percent by weight</u>	<u>Atomic weight</u>
H	1	6.3491	6.40	1.01
C	6	2.31474	27.80	12.01
N	7	0.19275	2.70	14.01
O	8	2.5625	41.00	16.00
Mg	12	0.00822	0.20	24.32
P	15	0.22599	7.00	30.97
S	16	0.00628	0.20	32.07
Ca	20	0.36677	14.70	40.08

* Density of muscle is 1 gram per cm^3 ; electron density 3.313×10^{23} electrons/gm

** Density of bone is 1.85 gram per cm^3 ; electron density 3.193×10^{23} electrons/gm

Table 3-7
Composition and Mean Excitation Potentials
for Model Tissue
(After NBS⁽¹⁸⁹⁾, Kinney and Zerby⁽¹³⁹⁾)

<u>Element</u>	<u>Nucleon density (nuclei/cm^3) $\times 10^{-24}$</u>	<u>Mean excitation potential, eV</u>
H	6.265×10^{-2}	17.5
O	2.55075×10^{-2}	99.0
C	9.3975×10^{-3}	74.44
N	1.3425×10^{-3}	86.0

Table 3-8
 Stopping Power and Rate of Energy Loss of Protons
 in Standard Muscle and Bone
 (After Janni⁽¹²⁷⁾)

a. ICRU Muscle

PROTON ENERGY MEV	DE/DZ MEV CM ² /GM	DE/DX MEV/CM	L E T KEV/MICRON
0.50	408.62	408.62	40.86
0.60	365.03	365.03	36.50
0.70	331.02	331.02	33.10
0.80	302.30	302.30	30.23
0.90	279.13	279.13	27.91
1.00	259.74	259.74	25.97
2.00	158.70	158.70	15.87
3.00	117.37	117.37	11.74
4.00	94.26	94.26	9.43
5.00	79.28	79.28	7.93
6.00	68.72	68.72	6.87
7.00	60.83	60.83	6.08
8.00	54.67	54.67	5.47
10.00	45.73	45.73	4.57
20.00	26.08	26.08	2.61
30.00	18.76	18.76	1.88
40.00	14.87	14.87	1.49
50.00	12.44	12.44	1.24
60.00	10.77	10.77	1.08
80.00	8.62	8.62	0.86
100.00	7.28	7.28	0.73
200.00	4.49	4.49	0.45
300.00	3.51	3.51	0.35
400.00	3.03	3.03	0.30
500.00	2.74	2.74	0.27
800.00	2.33	2.33	0.23
1000.00	2.21	2.21	0.22

Table 3-8 (continued)

b. ICRU Bone

PROTON ENERGY MEV	DE/DZ MEV CM ² /GM	DF/DX MEV/CM	L E T KEV/MICRON
0.50	369.42	683.43	68.34
0.60	329.59	609.75	60.97
0.70	298.75	552.69	55.27
0.80	273.26	505.53	50.55
0.90	252.56	467.25	46.72
1.00	235.24	435.19	43.52
2.00	144.91	268.08	26.81
3.00	107.65	199.15	19.91
4.00	86.68	160.36	16.04
5.00	73.02	135.10	13.51
6.00	63.41	117.31	11.73
7.00	56.21	103.99	10.40
8.00	50.58	93.58	9.36
10.00	42.38	78.41	7.84
20.00	24.29	44.94	4.49
30.00	17.51	32.40	3.24
40.00	13.90	25.72	2.57
50.00	11.64	21.54	2.15
60.00	10.09	18.67	1.87
80.00	8.08	14.95	1.49
100.00	6.83	12.64	1.26
200.00	4.22	7.80	0.78
300.00	3.31	6.12	0.61
400.00	2.85	5.27	0.53
500.00	2.58	4.77	0.48
800.00	2.20	4.06	0.41
1000.00	2.08	3.85	0.39

Table 3-9
 Stopping Power, MEV/CM²/G
 (See text for explanation of symbols)
 (Adapted from Berger and Seltzer⁽²⁴⁾)

ENERGY MEV	MUON		PION		KAON		PROTON	
	MUSCLE I= 66.2	BONE I= 85.1						
2.0	2.901E 01	2.680E 01	3.638E 01	3.353E 01	1.029E 02	9.356E 01	1.679E 02	1.513E 02
4.0	1.651E 01	1.533E 01	2.070E 01	1.918E 01	5.740E 01	5.232E 01	9.876E 01	8.980E 01
6.0	1.193E 01	1.110E 01	1.491E 01	1.385E 01	4.158E 01	3.827E 01	7.049E 01	6.424E 01
8.0	9.520E 00	8.870E 00	1.185E 01	1.102E 01	3.293E 01	3.038E 01	5.509E 01	5.037E 01
10.0	8.023E 00	7.483E 00	9.939E 00	9.258E 00	2.746E 01	2.538E 01	4.622E 01	4.249E 01
14.0	6.256E 00	5.842E 00	7.680E 00	7.164E 00	2.088E 01	1.935E 01	3.520E 01	3.245E 01
18.0	5.243E 00	4.901E 00	6.380E 00	5.957E 00	1.703E 01	1.581E 01	2.869E 01	2.651E 01
22.0	4.587E 00	4.290E 00	5.533E 00	5.170E 00	1.448E 01	1.346E 01	2.437E 01	2.255E 01
26.0	4.127E 00	3.862E 00	4.936E 00	4.615E 00	1.267E 01	1.179E 01	2.127E 01	1.970E 01
30.0	3.787E 00	3.545E 00	4.494E 00	4.204E 00	1.131E 01	1.053E 01	1.893E 01	1.756E 01
34.0	3.526E 00	3.302E 00	4.153E 00	3.886E 00	1.025E 01	9.549E 00	1.711E 01	1.588E 01
38.0	3.319E 00	3.108E 00	3.882E 00	3.634E 00	9.403E 00	8.762E 00	1.564E 01	1.452E 01
42.0	3.152E 00	2.952E 00	3.662E 00	3.429E 00	8.705E 00	8.115E 00	1.443E 01	1.341E 01
46.0	3.015E 00	2.825E 00	3.480E 00	3.259E 00	8.122E 00	7.574E 00	1.341E 01	1.247E 01
50.0	2.901E 00	2.718E 00	3.326E 00	3.114E 00	7.627E 00	7.115E 00	1.255E 01	1.167E 01
60.0	2.682E 00	2.513E 00	3.034E 00	2.842E 00	6.663E 00	6.220E 00	1.086E 01	1.011E 01
70.0	2.531E 00	2.368E 00	2.827E 00	2.649E 00	5.962E 00	5.569E 00	9.630E 00	8.972E 00
80.0	2.421E 00	2.266E 00	2.672E 00	2.504E 00	5.429E 00	5.073E 00	8.687E 00	8.098E 00
90.0	2.337E 00	2.188E 00	2.556E 00	2.390E 00	5.010E 00	4.683E 00	7.942E 00	7.408E 00
100.0	2.272E 00	2.128E 00	2.465E 00	2.306E 00	4.671E 00	4.369E 00	7.338E 00	6.847E 00
110.0	2.222E 00	2.081E 00	2.391E 00	2.238E 00	4.393E 00	4.109E 00	6.838E 00	6.383E 00
120.0	2.182E 00	2.044E 00	2.331E 00	2.183E 00	4.159E 00	3.892E 00	6.418E 00	5.992E 00
130.0	2.150E 00	2.014E 00	2.282E 00	2.137E 00	3.961E 00	3.707E 00	6.059E 00	5.659E 00
140.0	2.123E 00	1.989E 00	2.241E 00	2.099E 00	3.790E 00	3.549E 00	5.749E 00	5.371E 00
150.0	2.102E 00	1.968E 00	2.207E 00	2.067E 00	3.642E 00	3.411E 00	5.478E 00	5.119E 00
160.0	2.084E 00	1.951E 00	2.178E 00	2.040E 00	3.513E 00	3.290E 00	5.240E 00	4.898E 00
170.0	2.069E 00	1.937E 00	2.154E 00	2.017E 00	3.397E 00	3.181E 00	5.029E 00	4.701E 00
180.0	2.057E 00	1.926E 00	2.133E 00	1.998E 00	3.296E 00	3.086E 00	4.840E 00	4.526E 00
190.0	2.047E 00	1.916E 00	2.115E 00	1.981E 00	3.205E 00	3.002E 00	4.671E 00	4.368E 00
200.0	2.039E 00	1.908E 00	2.099E 00	1.966E 00	3.123E 00	2.925E 00	4.518E 00	4.226E 00
220.0	2.026E 00	1.896E 00	2.074E 00	1.942E 00	2.983E 00	2.794E 00	4.252E 00	3.979E 00
240.0	2.018E 00	1.889E 00	2.055E 00	1.924E 00	2.866E 00	2.686E 00	4.030E 00	3.772E 00
260.0	2.012E 00	1.885E 00	2.041E 00	1.910E 00	2.768E 00	2.593E 00	3.841E 00	3.596E 00
280.0	2.009E 00	1.882E 00	2.031E 00	1.900E 00	2.683E 00	2.515E 00	3.679E 00	3.445E 00
300.0	2.008E 00	1.881E 00	2.023E 00	1.893E 00	2.613E 00	2.449E 00	3.538E 00	3.314E 00
320.0	2.008E 00	1.882E 00	2.017E 00	1.888E 00	2.551E 00	2.386E 00	3.414E 00	3.197E 00
340.0	2.009E 00	1.883E 00	2.013E 00	1.885E 00	2.498E 00	2.337E 00	3.306E 00	3.095E 00
360.0	2.010E 00	1.885E 00	2.010E 00	1.883E 00	2.451E 00	2.293E 00	3.209E 00	3.005E 00
380.0	2.013E 00	1.888E 00	2.009E 00	1.882E 00	2.409E 00	2.254E 00	3.123E 00	2.925E 00
400.0	2.015E 00	1.891E 00	2.008E 00	1.881E 00	2.372E 00	2.220E 00	3.046E 00	2.853E 00

Table 3-9 (continued)

ENERGY MEV	MUON		PION		KAON		PROTON	
	MUSCLE I= 66.2	BONE I= 85.1						
420.0	2.018E 00	1.894E 00	2.008E 00	1.882E 00	2.338E 00	2.189E 00	2.976E 00	2.788E 00
440.0	2.022E 00	1.898E 00	2.008E 00	1.883E 00	2.308E 00	2.162E 00	2.913E 00	2.729E 00
460.0	2.025E 00	1.902E 00	2.009E 00	1.884E 00	2.282E 00	2.137E 00	2.855E 00	2.675E 00
480.0	2.029E 00	1.906E 00	2.011E 00	1.886E 00	2.257E 00	2.114E 00	2.802E 00	2.625E 00
500.0	2.032E 00	1.910E 00	2.012E 00	1.888E 00	2.236E 00	2.094E 00	2.754E 00	2.580E 00
520.0	2.036E 00	1.914E 00	2.014E 00	1.890E 00	2.216E 00	2.076E 00	2.710E 00	2.539E 00
540.0	2.040E 00	1.918E 00	2.016E 00	1.892E 00	2.199E 00	2.060E 00	2.667E 00	2.500E 00
560.0	2.044E 00	1.922E 00	2.019E 00	1.895E 00	2.183E 00	2.045E 00	2.630E 00	2.465E 00
580.0	2.048E 00	1.926E 00	2.021E 00	1.898E 00	2.168E 00	2.031E 00	2.596E 00	2.427E 00
600.0	2.052E 00	1.930E 00	2.024E 00	1.901E 00	2.155E 00	2.018E 00	2.563E 00	2.397E 00
620.0	2.056E 00	1.934E 00	2.027E 00	1.904E 00	2.142E 00	2.007E 00	2.534E 00	2.370E 00
640.0	2.060E 00	1.939E 00	2.029E 00	1.907E 00	2.131E 00	1.996E 00	2.506E 00	2.344E 00
660.0	2.063E 00	1.943E 00	2.032E 00	1.910E 00	2.121E 00	1.986E 00	2.480E 00	2.320E 00
680.0	2.067E 00	1.947E 00	2.035E 00	1.913E 00	2.111E 00	1.977E 00	2.455E 00	2.297E 00
700.0	2.071E 00	1.951E 00	2.038E 00	1.916E 00	2.102E 00	1.969E 00	2.432E 00	2.276E 00
720.0	2.075E 00	1.955E 00	2.041E 00	1.919E 00	2.094E 00	1.961E 00	2.411E 00	2.256E 00
740.0	2.079E 00	1.958E 00	2.044E 00	1.922E 00	2.087E 00	1.954E 00	2.390E 00	2.238E 00
760.0	2.082E 00	1.962E 00	2.047E 00	1.925E 00	2.080E 00	1.948E 00	2.371E 00	2.220E 00
780.0	2.086E 00	1.966E 00	2.050E 00	1.928E 00	2.074E 00	1.941E 00	2.353E 00	2.203E 00
800.0	2.089E 00	1.970E 00	2.053E 00	1.932E 00	2.068E 00	1.936E 00	2.337E 00	2.188E 00
820.0	2.093E 00	1.974E 00	2.056E 00	1.935E 00	2.063E 00	1.931E 00	2.321E 00	2.173E 00
840.0	2.096E 00	1.977E 00	2.059E 00	1.938E 00	2.058E 00	1.926E 00	2.305E 00	2.159E 00
860.0	2.100E 00	1.981E 00	2.062E 00	1.941E 00	2.053E 00	1.921E 00	2.291E 00	2.146E 00
880.0	2.103E 00	1.984E 00	2.065E 00	1.944E 00	2.049E 00	1.917E 00	2.277E 00	2.133E 00
900.0	2.107E 00	1.988E 00	2.068E 00	1.947E 00	2.045E 00	1.914E 00	2.265E 00	2.121E 00
920.0	2.110E 00	1.991E 00	2.070E 00	1.950E 00	2.041E 00	1.910E 00	2.253E 00	2.110E 00
940.0	2.113E 00	1.995E 00	2.073E 00	1.953E 00	2.038E 00	1.907E 00	2.241E 00	2.099E 00
960.0	2.116E 00	1.998E 00	2.076E 00	1.956E 00	2.035E 00	1.904E 00	2.231E 00	2.089E 00
980.0	2.119E 00	2.001E 00	2.079E 00	1.959E 00	2.032E 00	1.902E 00	2.220E 00	2.080E 00
1000.0	2.123E 00	2.004E 00	2.082E 00	1.962E 00	2.030E 00	1.899E 00	2.211E 00	2.071E 00
1200.0	2.151E 00	2.034E 00	2.108E 00	1.989E 00	2.013E 00	1.885E 00	2.136E 00	2.000E 00
1400.0	2.176E 00	2.060E 00	2.132E 00	2.014E 00	2.008E 00	1.881E 00	2.088E 00	1.955E 00
1600.0	2.198E 00	2.083E 00	2.153E 00	2.036E 00	2.009E 00	1.883E 00	2.057E 00	1.925E 00
2000.0	2.235E 00	2.122E 00	2.189E 00	2.074E 00	2.019E 00	1.896E 00	2.024E 00	1.894E 00
2400.0	2.266E 00	2.154E 00	2.219E 00	2.105E 00	2.035E 00	1.912E 00	2.011E 00	1.883E 00
2800.0	2.292E 00	2.180E 00	2.245E 00	2.132E 00	2.052E 00	1.930E 00	2.008E 00	1.882E 00
3200.0	2.314E 00	2.203E 00	2.267E 00	2.155E 00	2.068E 00	1.948E 00	2.010E 00	1.885E 00
3600.0	2.334E 00	2.224E 00	2.287E 00	2.176E 00	2.084E 00	1.964E 00	2.016E 00	1.892E 00
4000.0	2.351E 00	2.242E 00	2.305E 00	2.194E 00	2.099E 00	1.980E 00	2.023E 00	1.900E 00
5000.0	2.388E 00	2.280E 00	2.342E 00	2.232E 00	2.133E 00	2.015E 00	2.045E 00	1.923E 00

Table 3-10
 Range, G/CM²
 (See text for explanation of symbols)
 (Adapted from Berger and Seltzer⁽²⁴⁾)

ENERGY MEV	MUON		PION		KAON		PROTON	
	MUSCLE I= 66.2	BONE I= 85.1						
2.0	3.813E-02	4.154E-02	3.042E-02	3.324E-02	1.124E-02	1.250E-02	7.233E-03	8.162E-03
4.0	1.338E-01	1.447E-01	1.067E-01	1.157E-01	3.839E-02	4.230E-02	2.335E-02	2.594E-02
6.0	2.785E-01	3.005E-01	2.223E-01	2.403E-01	7.989E-02	8.749E-02	4.767E-02	5.265E-02
8.0	4.677E-01	5.036E-01	3.741E-01	4.035E-01	1.344E-01	1.466E-01	8.008E-02	8.820E-02
10.0	6.976E-01	7.502E-01	5.593E-01	6.024E-01	2.012E-01	2.189E-01	1.198E-01	1.315E-01
14.0	1.268E 00	1.362E 00	1.022E 00	1.099E 00	3.700E-01	4.014E-01	2.200E-01	2.403E-01
18.0	1.971E 00	2.113E 00	1.597E 00	1.715E 00	5.835E-01	6.315E-01	3.467E-01	3.775E-01
22.0	2.789E 00	2.989E 00	2.273E 00	2.438E 00	8.392E-01	9.068E-01	4.985E-01	5.417E-01
26.0	3.711E 00	3.974E 00	3.040E 00	3.259E 00	1.135E 00	1.225E 00	6.747E-01	7.320E-01
30.0	4.724E 00	5.057E 00	3.891E 00	4.169E 00	1.470E 00	1.585E 00	8.745E-01	9.474E-01
34.0	5.820E 00	6.227E 00	4.818E 00	5.160E 00	1.842E 00	1.984E 00	1.097E 00	1.187E 00
38.0	6.991E 00	7.477E 00	5.815E 00	6.225E 00	2.250E 00	2.422E 00	1.342E 00	1.451E 00
42.0	8.229E 00	8.799E 00	6.877E 00	7.359E 00	2.692E 00	2.897E 00	1.608E 00	1.738E 00
46.0	9.527E 00	1.018E 01	7.998E 00	8.557E 00	3.168E 00	3.408E 00	1.896E 00	2.048E 00
50.0	1.088E 01	1.163E 01	9.175E 00	9.813E 00	3.677E 00	3.953E 00	2.205E 00	2.379E 00
60.0	1.447E 01	1.546E 01	1.233E 01	1.318E 01	5.084E 00	5.461E 00	3.064E 00	3.303E 00
70.0	1.832E 01	1.957E 01	1.575E 01	1.683E 01	6.674E 00	7.164E 00	4.044E 00	4.355E 00
80.0	2.236E 01	2.389E 01	1.939E 01	2.072E 01	8.435E 00	9.048E 00	5.139E 00	5.530E 00
90.0	2.657E 01	2.839E 01	2.322E 01	2.481E 01	1.035E 01	1.110E 01	6.345E 00	6.823E 00
100.0	3.091E 01	3.302E 01	2.721E 01	2.907E 01	1.242E 01	1.331E 01	7.656E 00	8.228E 00
110.0	3.536E 01	3.778E 01	3.133E 01	3.348E 01	1.463E 01	1.568E 01	9.069E 00	9.742E 00
120.0	3.991E 01	4.263E 01	3.557E 01	3.800E 01	1.697E 01	1.818E 01	1.058E 01	1.136E 01
130.0	4.452E 01	4.756E 01	3.991E 01	4.264E 01	1.944E 01	2.081E 01	1.218E 01	1.308E 01
140.0	4.921E 01	5.255E 01	4.433E 01	4.736E 01	2.202E 01	2.4357E 01	1.388E 01	1.489E 01
150.0	5.394E 01	5.761E 01	4.883E 01	5.216E 01	2.471E 01	2.645E 01	1.566E 01	1.680E 01
160.0	5.872E 01	6.271E 01	5.339E 01	5.703E 01	2.751E 01	2.943E 01	1.753E 01	1.880E 01
170.0	6.353E 01	6.786E 01	5.801E 01	6.196E 01	3.041E 01	3.253E 01	1.948E 01	2.088E 01
180.0	6.838E 01	7.303E 01	6.268E 01	6.694E 01	3.340E 01	3.572E 01	2.151E 01	2.305E 01
190.0	7.325E 01	7.824E 01	6.738E 01	7.197E 01	3.647E 01	3.900E 01	2.361E 01	2.530E 01
200.0	7.815E 01	8.347E 01	7.213E 01	7.704E 01	3.963E 01	4.238E 01	2.579E 01	2.763E 01
220.0	8.799E 01	9.399E 01	8.172E 01	8.728E 01	4.619E 01	4.938E 01	3.035E 01	3.251E 01
240.0	9.788E 01	1.046E 02	9.141E 01	9.763E 01	5.303E 01	5.668E 01	3.519E 01	3.768E 01
260.0	1.078E 02	1.152E 02	1.012E 02	1.081E 02	6.014E 01	6.426E 01	4.027E 01	4.311E 01
280.0	1.178E 02	1.258E 02	1.110E 02	1.186E 02	6.748E 01	7.210E 01	4.560E 01	4.880E 01
300.0	1.277E 02	1.364E 02	1.209E 02	1.291E 02	7.503E 01	8.016E 01	5.114E 01	5.472E 01
320.0	1.377E 02	1.470E 02	1.308E 02	1.397E 02	8.278E 01	8.844E 01	5.690E 01	6.087E 01
340.0	1.476E 02	1.577E 02	1.407E 02	1.503E 02	9.071E 01	9.691E 01	6.285E 01	6.723E 01
360.0	1.576E 02	1.683E 02	1.506E 02	1.609E 02	9.879E 01	1.056E 02	6.900E 01	7.379E 01
380.0	1.675E 02	1.789E 02	1.606E 02	1.715E 02	1.070E 02	1.143E 02	7.531E 01	8.053E 01
400.0	1.775E 02	1.895E 02	1.705E 02	1.822E 02	1.154E 02	1.233E 02	8.180E 01	8.746E 01

Table 3-10 (continued)

ENERGY MEV	MUON		PION		KAON		PROTON	
	MUSCLE I= 66.2	BONE I= 85.1						
420.0	1.874E 02	2.000E 02	1.805E 02	1.928E 02	1.239E 02	1.324E 02	8.845E 01	9.455E 01
440.0	1.973E 02	2.106E 02	1.905E 02	2.034E 02	1.325E 02	1.416E 02	9.524E 01	1.018E 02
460.0	2.072E 02	2.211E 02	2.004E 02	2.140E 02	1.412E 02	1.509E 02	1.022E 02	1.092E 02
480.0	2.170E 02	2.316E 02	2.104E 02	2.246E 02	1.500E 02	1.603E 02	1.092E 02	1.168E 02
500.0	2.269E 02	2.421E 02	2.203E 02	2.352E 02	1.589E 02	1.698E 02	1.164E 02	1.244E 02
520.0	2.367E 02	2.526E 02	2.303E 02	2.458E 02	1.679E 02	1.794E 02	1.238E 02	1.323E 02
540.0	2.465E 02	2.630E 02	2.402E 02	2.564E 02	1.770E 02	1.890E 02	1.312E 02	1.402E 02
560.0	2.563E 02	2.734E 02	2.501E 02	2.670E 02	1.861E 02	1.988E 02	1.388E 02	1.482E 02
580.0	2.661E 02	2.838E 02	2.600E 02	2.775E 02	1.953E 02	2.086E 02	1.464E 02	1.564E 02
600.0	2.759E 02	2.942E 02	2.699E 02	2.880E 02	2.046E 02	2.185E 02	1.542E 02	1.647E 02
620.0	2.856E 02	3.045E 02	2.798E 02	2.986E 02	2.139E 02	2.284E 02	1.620E 02	1.731E 02
640.0	2.953E 02	3.149E 02	2.896E 02	3.091E 02	2.232E 02	2.384E 02	1.700E 02	1.816E 02
660.0	3.050E 02	3.252E 02	2.995E 02	3.195E 02	2.326E 02	2.485E 02	1.780E 02	1.902E 02
680.0	3.147E 02	3.354E 02	3.093E 02	3.300E 02	2.421E 02	2.586E 02	1.861E 02	1.988E 02
700.0	3.244E 02	3.457E 02	3.191E 02	3.404E 02	2.516E 02	2.687E 02	1.943E 02	2.076E 02
720.0	3.340E 02	3.559E 02	3.289E 02	3.509E 02	2.611E 02	2.789E 02	2.025E 02	2.164E 02
740.0	3.436E 02	3.662E 02	3.387E 02	3.613E 02	2.707E 02	2.891E 02	2.109E 02	2.253E 02
760.0	3.533E 02	3.764E 02	3.485E 02	3.717E 02	2.803E 02	2.993E 02	2.193E 02	2.343E 02
780.0	3.629E 02	3.866E 02	3.583E 02	3.821E 02	2.899E 02	3.096E 02	2.277E 02	2.433E 02
800.0	3.724E 02	3.967E 02	3.680E 02	3.924E 02	2.996E 02	3.199E 02	2.363E 02	2.524E 02
820.0	3.820E 02	4.069E 02	3.777E 02	4.028E 02	3.092E 02	3.303E 02	2.448E 02	2.616E 02
840.0	3.915E 02	4.170E 02	3.875E 02	4.131E 02	3.190E 02	3.407E 02	2.535E 02	2.708E 02
860.0	4.011E 02	4.271E 02	3.972E 02	4.234E 02	3.287E 02	3.511E 02	2.622E 02	2.801E 02
880.0	4.106E 02	4.372E 02	4.069E 02	4.337E 02	3.384E 02	3.615E 02	2.710E 02	2.895E 02
900.0	4.201E 02	4.472E 02	4.165E 02	4.440E 02	3.482E 02	3.719E 02	2.798E 02	2.989E 02
920.0	4.296E 02	4.573E 02	4.262E 02	4.543E 02	3.580E 02	3.824E 02	2.886E 02	3.083E 02
940.0	4.391E 02	4.673E 02	4.359E 02	4.645E 02	3.678E 02	3.929E 02	2.975E 02	3.178E 02
960.0	4.485E 02	4.774E 02	4.455E 02	4.747E 02	3.776E 02	4.034E 02	3.065E 02	3.274E 02
980.0	4.580E 02	4.874E 02	4.551E 02	4.850E 02	3.875E 02	4.139E 02	3.155E 02	3.370E 02
1000.0	4.674E 02	4.973E 02	4.647E 02	4.952E 02	3.973E 02	4.244E 02	3.245E 02	3.466E 02
1200.0	5.610E 02	5.964E 02	5.602E 02	5.964E 02	4.963E 02	5.301E 02	4.166E 02	4.450E 02
1400.0	6.534E 02	6.940E 02	6.545E 02	6.963E 02	5.958E 02	6.364E 02	5.114E 02	5.462E 02
1600.0	7.448E 02	7.906E 02	7.479E 02	7.951E 02	6.954E 02	7.426E 02	6.080E 02	6.494E 02
2000.0	9.252E 02	9.807E 02	9.321E 02	9.897E 02	8.941E 02	9.544E 02	8.043E 02	8.591E 02
2400.0	1.103E 03	1.168E 03	1.114E 03	1.181E 03	1.091E 03	1.164E 03	1.003E 03	1.071E 03
2800.0	1.278E 03	1.352E 03	1.293E 03	1.370E 03	1.287E 03	1.373E 03	1.202E 03	1.284E 03
3200.0	1.452E 03	1.535E 03	1.470E 03	1.556E 03	1.481E 03	1.579E 03	1.401E 03	1.496E 03
3600.0	1.624E 03	1.716E 03	1.646E 03	1.741E 03	1.674E 03	1.783E 03	1.600E 03	1.708E 03
4000.0	1.795E 03	1.895E 03	1.820E 03	1.924E 03	1.865E 03	1.986E 03	1.798E 03	1.919E 03
5000.0	2.217E 03	2.337E 03	2.250E 03	2.376E 03	2.338E 03	2.487E 03	2.289E 03	2.442E 03

which were erroneously calculated (17). The data for protons are slightly different from those of Table 3-8 because of different assumptions regarding the molecular properties of the tissues in question. Similar data are available for other materials (24).

Similar stopping powers, ranges, and radiation yield(bremsstrahlung efficiency) for electrons are seen in Tables 3-11 and 3-12. These can be used for secondary electrons or primary electrons in the Van Allen belts. These tables replace previous data which were erroneously calculated (25). Similar data are available on other non-biological materials (24). The angular distribution of thick-target bremsstrahlung including multiple electron scattering is now under study (248). Figure 3-13 compares the rate of energy loss for electrons and protons in tissue. Neutron mean free paths in ICRU muscle vs. energy are seen in Figure 3-14.

In the past, stopping power and range for ions $>Z = 18$ have been poorly investigated either theoretically or experimentally. The Omnitron accelerator may make available ions up to 500 MeV/atomic mass unit (amu) and Z numbers through 92. A program has been recently written which computes range, energy, and stopping power data. These are available for hydrogen, helium 4, carbon 12, neon 20, argon 40, krypton 84, xenon 131, and uranium-238 incident upon water, aluminum, copper, silver, lead, and uranium (262). Programs are available in Chippewa, Fortran, and Fortran IV. The calculations have been corroborated by comparison with experimental data available on ions of $Z < 10$ (197). Figures 3-15 a, b, and c represent only water, aluminum, and lead targets most pertinent to the space radiation problem. The stopping power has been plotted as a function of ion residual range. The symbols on each curve match points corresponding to various energies. The Ne-C and Xe-U crossovers are low energy, and although possibly a physical reality, occur in regions of low confidence of the calculations. Discontinuities and irregularities in several of the curves are caused by different equations and assumptions used for calculation of $Z < 10$ and for 4 separate energy regions of $Z > 10$ (262).

As noted in the discussion of Figure 3-15 a, b, and c, calculation of LET's for the primary galactic cosmic-ray flux is difficult. Table 3-16 shows theoretical considerations of dose and energy distribution in tissue from the constituents of the primary cosmic-ray flux. The sections, energies, and angles of emissions, as well as relative frequencies of alternate decay schemes for the various types of secondaries, are not well enough known to allow more than a tentative designation for this table. Data are available for some of the nuclei above iron in the primary cosmic ray spectrum (90). A large percentage of the absorbed dose appears to be derived from particles giving very heavy ionization.

Figure 3-17 presents examples of primary cosmic-ray data graphically. Contrary to conditions for electrons, where the LET reaches its maximum at the very end of the particle track, the maximum LET occurs for nuclear particles a very short distance before the end (2 micra T for protons, 46 micra T for Ca nuclei) and then drops steeply to zero. As the exact shape of this final descent of the LET to zero is not known, the exact height of the

Table 3-11

Electrons in Muscle

(After Berger and Seltzer⁽²⁴⁾)

ENERGY MEV	STOPPING POWER			RANGE G/CM ²	RADIATION YIELD
	COLLISION MEV CM ² /G	RADIATION MEV CM ² /G	TOTAL MEV CM ² /G		
0.010	2.292E 01	4.971E-03	2.292E 01	2.467E-04	1.236E-04
0.015	1.670E 01	4.874E-03	1.670E 01	5.061E-04	1.674E-04
0.020	1.334E 01	4.810E-03	1.335E 01	8.435E-04	2.072E-04
0.025	1.123E 01	4.766E-03	1.123E 01	1.254E-03	2.443E-04
0.030	9.763E 00	4.735E-03	9.768E 00	1.733E-03	2.794E-04
0.035	8.686E 00	4.705E-03	8.691E 00	2.276E-03	3.128E-04
0.040	7.859E 00	4.702E-03	7.863E 00	2.882E-03	3.449E-04
0.045	7.202E 00	4.710E-03	7.207E 00	3.547E-03	3.761E-04
0.050	6.669E 00	4.726E-03	6.673E 00	4.269E-03	4.066E-04
0.055	6.225E 00	4.749E-03	6.230E 00	5.045E-03	4.365E-04
0.060	5.851E 00	4.777E-03	5.856E 00	5.873E-03	4.659E-04
0.065	5.531E 00	4.808E-03	5.536E 00	6.752E-03	4.948E-04
0.070	5.254E 00	4.843E-03	5.259E 00	7.679E-03	5.234E-04
0.075	5.012E 00	4.881E-03	5.017E 00	8.653E-03	5.516E-04
0.080	4.799E 00	4.921E-03	4.804E 00	9.672E-03	5.795E-04
0.085	4.609E 00	4.952E-03	4.614E 00	1.073E-02	6.071E-04
0.090	4.440E 00	4.995E-03	4.445E 00	1.184E-02	6.344E-04
0.095	4.287E 00	5.041E-03	4.292E 00	1.298E-02	6.615E-04
0.100	4.149E 00	5.087E-03	4.154E 00	1.417E-02	6.884E-04
0.150	3.261E 00	5.609E-03	3.267E 00	2.792E-02	9.497E-04
0.200	2.811E 00	6.169E-03	2.817E 00	4.451E-02	1.201E-03
0.250	2.543E 00	6.781E-03	2.550E 00	6.323E-02	1.446E-03
0.300	2.366E 00	7.420E-03	2.373E 00	8.359E-02	1.687E-03
0.350	2.244E 00	8.088E-03	2.252E 00	1.052E-01	1.926E-03
0.400	2.155E 00	8.754E-03	2.164E 00	1.279E-01	2.162E-03
0.450	2.088E 00	9.432E-03	2.097E 00	1.514E-01	2.397E-03
0.500	2.036E 00	1.011E-02	2.046E 00	1.755E-01	2.629E-03
0.550	1.996E 00	1.078E-02	2.007E 00	2.002E-01	2.859E-03
0.600	1.964E 00	1.146E-02	1.976E 00	2.253E-01	3.086E-03
0.650	1.939E 00	1.214E-02	1.951E 00	2.508E-01	3.311E-03
0.700	1.918E 00	1.282E-02	1.931E 00	2.766E-01	3.534E-03
0.750	1.901E 00	1.350E-02	1.915E 00	3.026E-01	3.754E-03
0.800	1.887E 00	1.418E-02	1.902E 00	3.288E-01	3.973E-03
0.850	1.876E 00	1.487E-02	1.891E 00	3.552E-01	4.190E-03
0.900	1.867E 00	1.556E-02	1.882E 00	3.817E-01	4.405E-03
0.950	1.859E 00	1.625E-02	1.875E 00	4.083E-01	4.619E-03
1.000	1.852E 00	1.694E-02	1.869E 00	4.350E-01	4.831E-03
1.100	1.843E 00	1.834E-02	1.861E 00	4.886E-01	5.252E-03
1.200	1.836E 00	1.975E-02	1.856E 00	5.424E-01	5.668E-03
1.300	1.832E 00	2.116E-02	1.854E 00	5.963E-01	6.081E-03

Table 3-11 (continued)

ENERGY MEV	STOPPING POWER			RANGE G/CM2	RADIATION YIELD
	COLLISION MEV CM2/G	RADIATION MEV CM2/G	TOTAL MEV CM2/G		
1.400	1.830E 00	2.259E-02	1.853E 00	6.503E-01	6.490E-03
1.500	1.829E 00	2.402E-02	1.853E 00	7.043E-01	6.895E-03
1.600	1.829E 00	2.546E-02	1.854E 00	7.582E-01	7.299E-03
1.700	1.830E 00	2.687E-02	1.857E 00	8.121E-01	7.698E-03
1.800	1.831E 00	2.833E-02	1.859E 00	8.660E-01	8.096E-03
1.900	1.833E 00	2.981E-02	1.862E 00	9.197E-01	8.492E-03
2.000	1.835E 00	3.130E-02	1.866E 00	9.733E-01	8.887E-03
2.200	1.839E 00	3.432E-02	1.874E 00	1.080E 00	9.674E-03
2.400	1.844E 00	3.739E-02	1.882E 00	1.187E 00	1.046E-02
2.600	1.850E 00	4.050E-02	1.890E 00	1.293E 00	1.124E-02
2.800	1.855E 00	4.354E-02	1.899E 00	1.398E 00	1.203E-02
3.000	1.861E 00	4.673E-02	1.907E 00	1.504E 00	1.280E-02
3.500	1.874E 00	5.495E-02	1.929E 00	1.764E 00	1.476E-02
4.000	1.886E 00	6.346E-02	1.950E 00	2.022E 00	1.673E-02
4.500	1.898E 00	7.230E-02	1.970E 00	2.277E 00	1.871E-02
5.000	1.908E 00	8.129E-02	1.990E 00	2.530E 00	2.072E-02
5.500	1.918E 00	9.045E-02	2.008E 00	2.780E 00	2.274E-02
6.000	1.927E 00	9.977E-02	2.026E 00	3.028E 00	2.477E-02
6.500	1.935E 00	1.092E-01	2.044E 00	3.273E 00	2.682E-02
7.000	1.942E 00	1.188E-01	2.061E 00	3.517E 00	2.887E-02
7.500	1.949E 00	1.285E-01	2.078E 00	3.758E 00	3.093E-02
8.000	1.956E 00	1.384E-01	2.094E 00	3.998E 00	3.299E-02
8.500	1.962E 00	1.483E-01	2.110E 00	4.236E 00	3.506E-02
9.000	1.967E 00	1.593E-01	2.127E 00	4.472E 00	3.715E-02
9.500	1.973E 00	1.695E-01	2.142E 00	4.706E 00	3.925E-02
10.000	1.978E 00	1.798E-01	2.158E 00	4.939E 00	4.135E-02
20.000	2.043E 00	3.986E-01	2.441E 00	9.289E 00	8.266E-02
30.000	2.079E 00	6.311E-01	2.710E 00	1.317E 01	1.214E-01
40.000	2.103E 00	8.701E-01	2.973E 00	1.670E 01	1.570E-01
50.000	2.123E 00	1.113E 00	3.236E 00	1.992E 01	1.894E-01
60.000	2.138E 00	1.360E 00	3.498E 00	2.289E 01	2.189E-01
80.000	2.163E 00	1.859E 00	4.021E 00	2.822E 01	2.710E-01
100.000	2.182E 00	2.363E 00	4.545E 00	3.289E 01	3.152E-01
200.000	2.241E 00	4.927E 00	7.167E 00	5.027E 01	4.654E-01
300.000	2.275E 00	7.521E 00	9.796E 00	6.215E 01	5.542E-01
400.000	2.299E 00	1.013E 01	1.243E 01	7.119E 01	6.139E-01
500.000	2.318E 00	1.274E 01	1.506E 01	7.849E 01	6.574E-01
600.000	2.334E 00	1.536E 01	1.769E 01	8.461E 01	6.908E-01
800.000	2.358E 00	2.061E 01	2.296E 01	9.451E 01	7.391E-01
1000.000	2.377E 00	2.585E 01	2.823E 01	1.023E 02	7.727E-01

Table 3-12

Electrons in Bone

(After Berger and Seltzer⁽²⁴⁾)

ENERGY MEV	STOPPING POWER			RANGE G/CM2	RADIATION YIELD
	COLLISION MEV CM2/G	RADIATION MEV CM2/G	TOTAL MEV CM2/G		
0.010	2.101E 01	6.373E-03	2.101E 01	2.711E-04	1.726E-04
0.015	1.536E 01	6.282E-03	1.537E 01	5.533E-04	2.341E-04
0.020	1.231E 01	6.206E-03	1.231E 01	9.195E-04	2.898E-04
0.025	1.037E 01	6.172E-03	1.038E 01	1.364E-03	3.418E-04
0.030	9.030E 00	6.159E-03	9.036E 00	1.882E-03	3.913E-04
0.035	8.041E 00	6.153E-03	8.047E 00	2.469E-03	4.387E-04
0.040	7.281E 00	6.169E-03	7.287E 00	3.123E-03	4.846E-04
0.045	6.678E 00	6.196E-03	6.684E 00	3.841E-03	5.292E-04
0.050	6.186E 00	6.231E-03	6.193E 00	4.619E-03	5.730E-04
0.055	5.778E 00	6.271E-03	5.785E 00	5.455E-03	6.159E-04
0.060	5.434E 00	6.316E-03	5.440E 00	6.347E-03	6.581E-04
0.065	5.139E 00	6.365E-03	5.145E 00	7.292E-03	6.998E-04
0.070	4.883E 00	6.417E-03	4.890E 00	8.290E-03	7.409E-04
0.075	4.660E 00	6.472E-03	4.666E 00	9.337E-03	7.814E-04
0.080	4.463E 00	6.528E-03	4.469E 00	1.043E-02	8.216E-04
0.085	4.288E 00	6.571E-03	4.294E 00	1.157E-02	8.612E-04
0.090	4.131E 00	6.631E-03	4.138E 00	1.276E-02	9.003E-04
0.095	3.990E 00	6.693E-03	3.997E 00	1.399E-02	9.392E-04
0.100	3.862E 00	6.757E-03	3.869E 00	1.526E-02	9.778E-04
0.150	3.041E 00	7.442E-03	3.049E 00	3.001E-02	1.351E-03
0.200	2.623E 00	8.154E-03	2.631E 00	4.778E-02	1.706E-03
0.250	2.374E 00	8.941E-03	2.383E 00	6.781E-02	2.050E-03
0.300	2.210E 00	9.765E-03	2.219E 00	8.960E-02	2.388E-03
0.350	2.092E 00	1.063E-02	2.103E 00	1.128E-01	2.723E-03
0.400	2.011E 00	1.148E-02	2.022E 00	1.371E-01	3.054E-03
0.450	1.949E 00	1.235E-02	1.961E 00	1.622E-01	3.380E-03
0.500	1.901E 00	1.321E-02	1.914E 00	1.880E-01	3.701E-03
0.550	1.864E 00	1.407E-02	1.878E 00	2.144E-01	4.019E-03
0.600	1.835E 00	1.493E-02	1.850E 00	2.412E-01	4.333E-03
0.650	1.811E 00	1.578E-02	1.826E 00	2.684E-01	4.642E-03
0.700	1.791E 00	1.664E-02	1.808E 00	2.959E-01	4.948E-03
0.750	1.775E 00	1.750E-02	1.793E 00	3.237E-01	5.250E-03
0.800	1.762E 00	1.836E-02	1.780E 00	3.517E-01	5.550E-03
0.850	1.751E 00	1.925E-02	1.770E 00	3.799E-01	5.847E-03
0.900	1.742E 00	2.012E-02	1.762E 00	4.082E-01	6.141E-03
0.950	1.734E 00	2.098E-02	1.755E 00	4.366E-01	6.433E-03
1.000	1.728E 00	2.185E-02	1.750E 00	4.652E-01	6.722E-03
1.100	1.720E 00	2.359E-02	1.743E 00	5.224E-01	7.294E-03
1.200	1.714E 00	2.533E-02	1.740E 00	5.798E-01	7.856E-03
1.300	1.711E 00	2.708E-02	1.738E 00	6.374E-01	8.411E-03

Table 3-12 (continued)

ENERGY	STOPPING POWER			RANGE	RADIATION YIELD
	COLLISION	RADIATION	TOTAL		
MEV	MEV CM2/G	MEV CM2/G	MEV CM2/G	G/CM2	
1.400	1.710E 00	2.883E-02	1.739E 00	6.949E-01	8.959E-03
1.500	1.709E 00	3.059E-02	1.740E 00	7.524E-01	9.501E-03
1.600	1.710E 00	3.236E-02	1.742E 00	8.098E-01	1.004E-02
1.700	1.711E 00	3.400E-02	1.745E 00	8.672E-01	1.056E-02
1.800	1.713E 00	3.580E-02	1.749E 00	9.244E-01	1.109E-02
1.900	1.715E 00	3.761E-02	1.753E 00	9.815E-01	1.161E-02
2.000	1.717E 00	3.944E-02	1.757E 00	1.039E 00	1.212E-02
2.200	1.723E 00	4.317E-02	1.766E 00	1.152E 00	1.315E-02
2.400	1.728E 00	4.697E-02	1.775E 00	1.265E 00	1.418E-02
2.600	1.734E 00	5.084E-02	1.785E 00	1.377E 00	1.520E-02
2.800	1.741E 00	5.483E-02	1.795E 00	1.489E 00	1.622E-02
3.000	1.747E 00	5.883E-02	1.805E 00	1.600E 00	1.724E-02
3.500	1.761E 00	6.907E-02	1.830E 00	1.875E 00	1.980E-02
4.000	1.775E 00	7.963E-02	1.854E 00	2.147E 00	2.237E-02
4.500	1.787E 00	9.053E-02	1.878E 00	2.415E 00	2.495E-02
5.000	1.798E 00	1.016E-01	1.900E 00	2.679E 00	2.754E-02
5.500	1.809E 00	1.129E-01	1.922E 00	2.941E 00	3.014E-02
6.000	1.818E 00	1.243E-01	1.943E 00	3.200E 00	3.274E-02
6.500	1.827E 00	1.359E-01	1.963E 00	3.456E 00	3.534E-02
7.000	1.835E 00	1.477E-01	1.983E 00	3.709E 00	3.795E-02
7.500	1.843E 00	1.596E-01	2.003E 00	3.960E 00	4.056E-02
8.000	1.850E 00	1.716E-01	2.022E 00	4.209E 00	4.317E-02
8.500	1.857E 00	1.838E-01	2.040E 00	4.455E 00	4.578E-02
9.000	1.863E 00	1.969E-01	2.060E 00	4.699E 00	4.839E-02
9.500	1.869E 00	2.093E-01	2.078E 00	4.940E 00	5.101E-02
10.000	1.874E 00	2.218E-01	2.096E 00	5.180E 00	5.362E-02
20.000	1.945E 00	4.885E-01	2.434E 00	9.599E 00	1.040E-01
30.000	1.983E 00	7.718E-01	2.755E 00	1.346E 01	1.499E-01
40.000	2.010E 00	1.063E 00	3.073E 00	1.689E 01	1.909E-01
50.000	2.029E 00	1.360E 00	3.389E 00	1.999E 01	2.276E-01
60.000	2.045E 00	1.660E 00	3.705E 00	2.281E 01	2.606E-01
80.000	2.070E 00	2.267E 00	4.337E 00	2.780E 01	3.172E-01
100.000	2.089E 00	2.880E 00	4.969E 00	3.210E 01	3.642E-01
200.000	2.147E 00	5.994E 00	8.141E 00	4.766E 01	5.172E-01
300.000	2.180E 00	9.144E 00	1.132E 01	5.803E 01	6.033E-01
400.000	2.204E 00	1.231E 01	1.451E 01	6.581E 01	6.599E-01
500.000	2.222E 00	1.548E 01	1.770E 01	7.204E 01	7.003E-01
600.000	2.237E 00	1.865E 01	2.089E 01	7.724E 01	7.310E-01
800.000	2.260E 00	2.501E 01	2.727E 01	8.559E 01	7.747E-01
1000.000	2.278E 00	3.137E 01	3.365E 01	9.218E 01	8.048E-01

Figure 3-13

Energy Loss Per Unit Path Length for Protons and Electrons in Model Biological Materials
(After Janni et al⁽¹²⁸⁾)

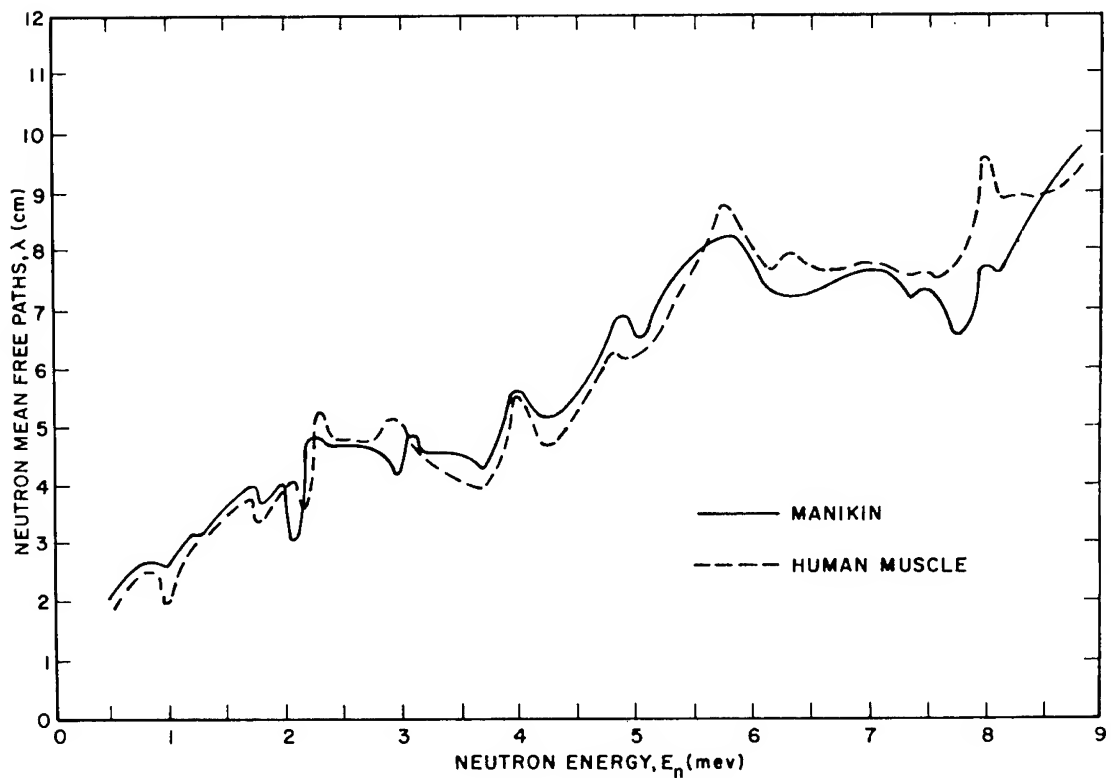
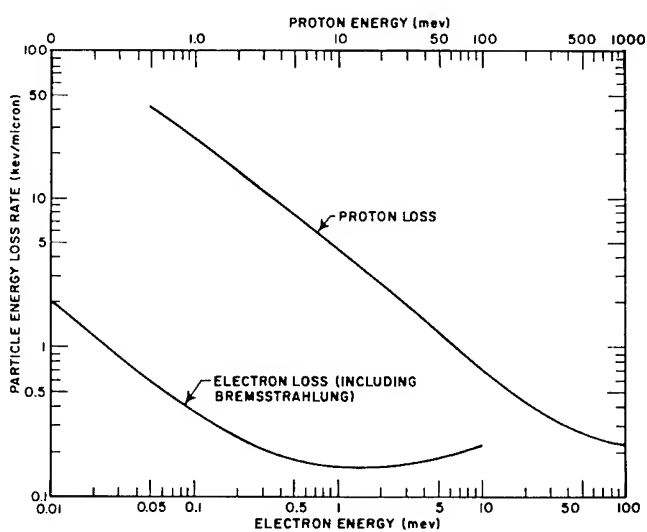


Figure 3-14

Neutron Mean Free Paths for ICRU Muscle Tissue and a Tissue Equivalent Manikin

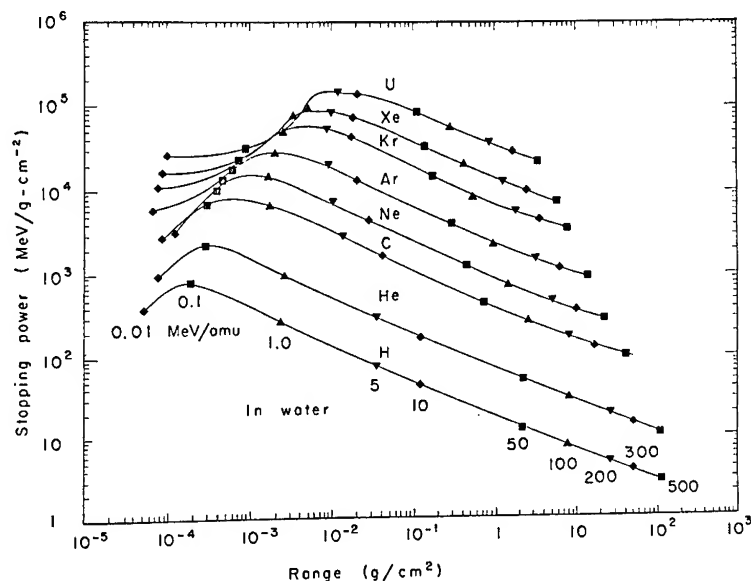
(After Janni et al⁽¹²⁸⁾)

Figure 3-15

Stopping-Power Curves as a Function of Range for Various Ions as Calculated by a UCRL Computer Program. Various Ion Energies in Units of MeV/amu Are Designated on Each Curve by the same Symbols as Noted for H. (See text for details).

(After Steward and Wallace⁽²⁶²⁾)

a. In Water



b. In Aluminum

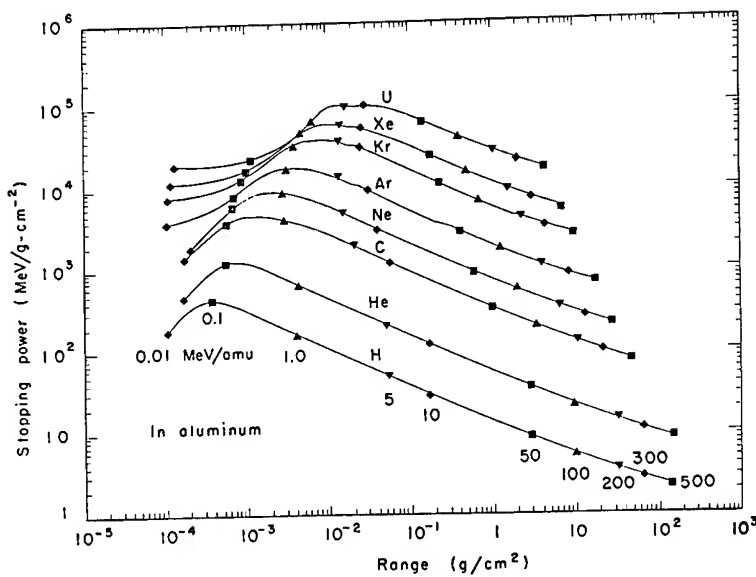


Figure 3-15 (continued)

c. In Lead

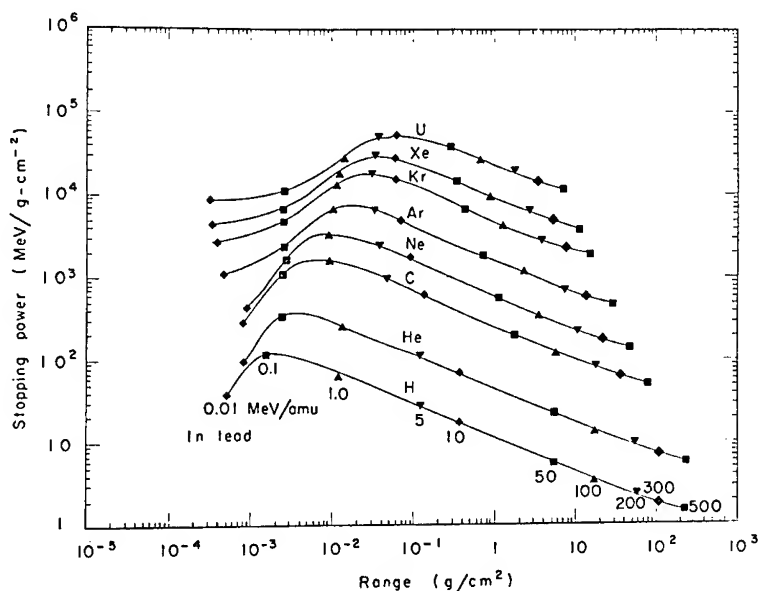


Table 3-16
Composition of the Primary Cosmic-Ray Flux
Outside the Atmosphere in Northern Latitudes
(After Langham-NAS-NRC⁽¹⁴⁵⁾)

TYPE NUCLEUS						
	He		CNO	Mg	Ca	Fe
	H	PROTONS				
Z ^a :	1	2	7	12	20	26
Particle flux ^b	4,460	633	32	8.4	2.9	1.4
Absorbed dose contribution (mrads/24 hr)	4	2.3	1.4	0.99	0.13	0.28
LET (keV/ μ tissue)						
Minimum	0.21	0.84	10.5	30.3	84	142
Maximum	57.8	252	1,230	1,780	2,570	3,500
Absorbed dose to centrally traversed cell (rads) ^c						
Minimum	0.07	0.24	0.36	1	2.85	4.8
Maximum	20	85	420	610	870	1,200

^aZ numbers from 7 to 26 are group representatives.

^bParticle intensity: particles traversing sphere of 1 cm² cross section per hour from all directions.

^cDose per particle calculated for a 10- μ cell at center of track.

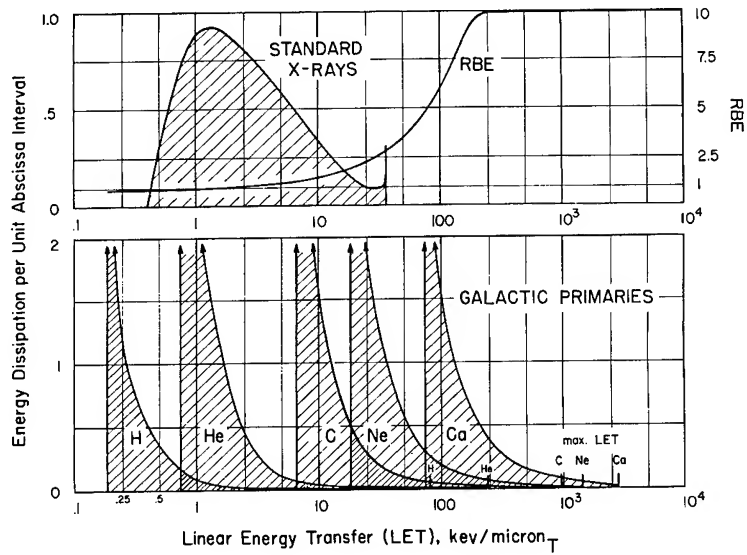


Figure 3-17

LET Distributions of Standard X-Rays
and of Heavy Galactic Primaries
in Tissue and RBE/LET Function.

(After Schaefer⁽²³⁹⁾ and Cormack and
Johns⁽⁵⁷⁾)

spike at the upper end of the LET distribution remains uncertain. For this reason the spikes in the lower graph of Figure 3-17 are drawn with the same arbitrary height for all five components. Accordingly, the spikes should be interpreted merely as denoting the position of the steep terminal rise of the curve on the LET scale. A quantitative assessment of the extremely small fraction of the energy dissipation at the maximum LET would require a separate and entirely different approach. The fractional dose at the maximum LET represents, radiobiologically, an essentially unknown quantity best described dosimetrically with the term "microbeam" (145, 247).

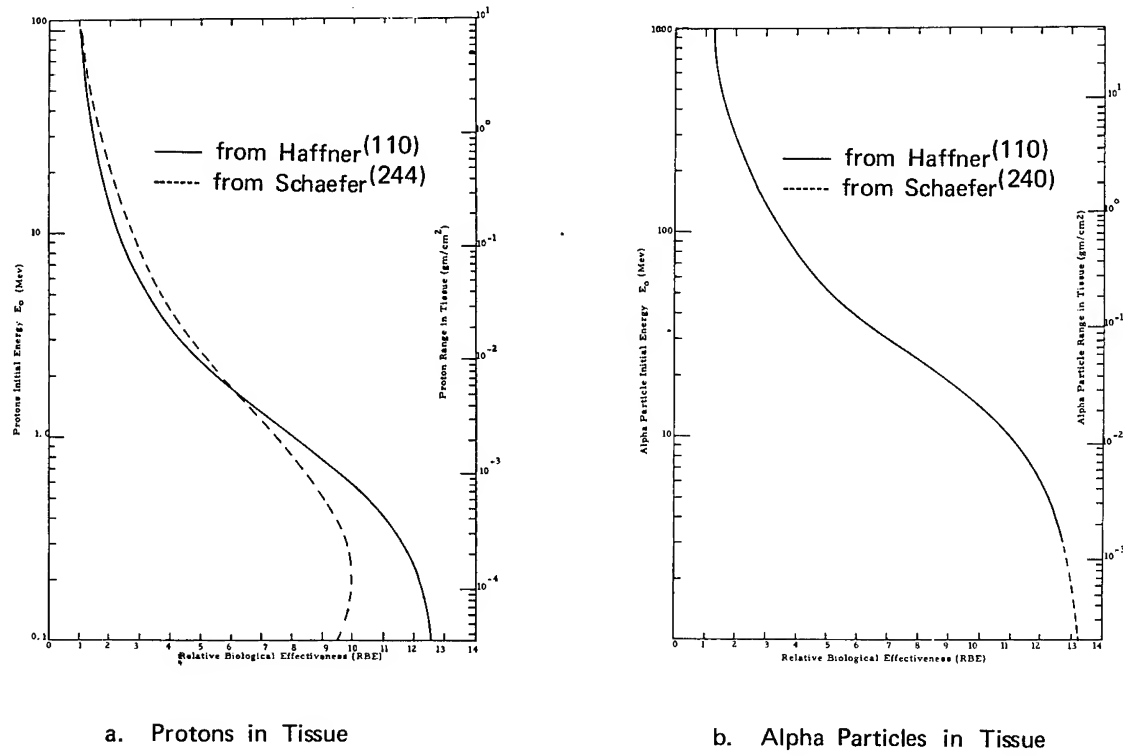
This track of a very heavy charged particle in tissue is characterized by a very small central core of ionization caused by the particle itself, surrounded by a much wider area of ionization caused by the secondary particles ejected from the central core. Thus most of the volume of the track is attributable to secondary radiation, and a living cell in the path of the track would probably be affected predominantly by proton and electron radiation. It has been suggested that only about 5 to 10 millirads/day of the 40 millirads/day galactic ray dose at solar minimum have a LET above 30 keV/ μ (238, 239).

A large part of galactic radiation exposure falls into the region of low and very low LET values. For the proton component in particular, the bulk of the energy dissipation takes place at LET values even below the lowest LET of standard x-rays. In fact, the LET distribution of galactic protons closely resembles the one for Co-60 gamma rays. This is to be expected since for both radiations a large part of the energy dissipation is produced by secondary relativistic particles of single charge. Since LET depends only on charge and speed, but not on mass, there is no difference in the energy loss between electrons and protons of the same speed.

For calculation of local, effective tissue doses especially under conditions of low shielding, a reasonably satisfactory dependence of the RBE or QF on the

local Linear Energy Transfer (LET), has been obtained and experimentally verified (to some extent) by Rossi (215, 243). The relationship between RBE or QF and local LET for protons, alphas, and electrons of specific energy can be determined (110, 128, 240, 244). Figure 3-18a and b shows that for alphas and protons, RBE values vary from unity at high particle energies

Figure 3-18
RBE Versus Energy or Particle Range



increasing to 12 at low energies where electron acquisition becomes important. The upper critical energies, at which the $\text{LET} = 4 \text{ keV}/\mu\text{m}$ and, therefore, the RBE equals 1, are 10.8 MeV for protons and 249 MeV for alpha particles. The composite RBE values in infinite tissue (50 percent bone and 50 percent muscle) for protons and alpha particles between their initial and final energies are 2.1 and 2.2, respectively. Above 0.5 MeV, the two independent calculations are in good agreement (110, 240). Below 0.5 MeV (6 microns residual range), the Haffner calculations predict somewhat higher RBE values. Probably saturation effects (there are only so many atoms per unit path length for the particles to ionize), which the Haffner calculation did not take into account, are responsible for the differences. From the overall shielding viewpoint the differences are unimportant.

The RBE may be determined instantaneously or as the mean RBE of a particle during dissipation of its entire energy. The differences are seen in Figure 3-19.

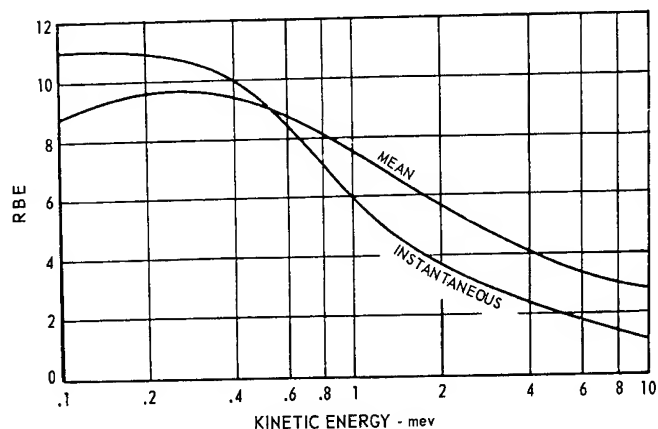


Figure 3-19

Mean Versus Instantaneous RBE Values for Protons.

Instantaneous and mean RBEs are shown for protons of different energies, corresponding to the instantaneous linear energy transfer at energy E, and the mean RBE for dissipation of the entire energy from E down to zero.

(After Grahn⁽¹⁰³⁾ from the data of Schaefer⁽²⁴⁴⁾)

At higher LET's, the RBE saturates and begins to decrease. The curve varies for different biological systems. After acute doses, mammalian cells tend to respond as seen in Figure 3-20.

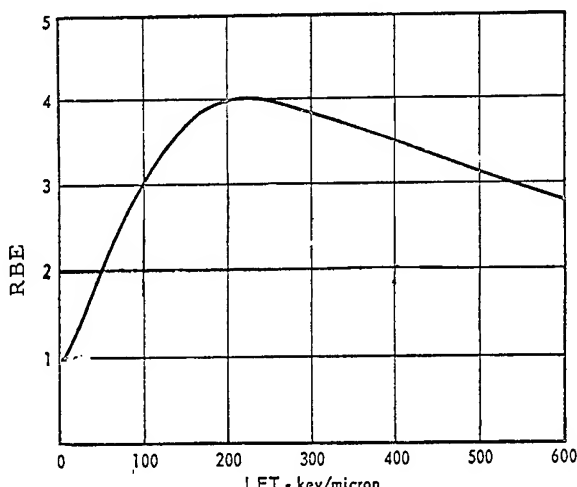


Figure 3-20

The Relative Biological Effectiveness (RBE) is Plotted as a Function of Linear Energy Transfer (LET) for Survival of Mammalian Cells Following Exposure to Charged Particles at About 8.3 mev/nucleon

(After Grahn⁽¹⁰³⁾ Based on data from Sondhaus⁽²⁵⁸⁾)

The proton RBE for many biological endpoints has been studied for different energies in many biological systems (135, 145, 154). As predicted by LET considerations and the calculations of Figure 3-18, the empirical RBE (lethality) for protons and alpha particles >500 MeV is equal to or less than 1 (72, 259, 267). Depending on the particular type of radiation injury used as criterion, RBE values of 0.6 to 0.9 have been determined (135, 145). RBE values compared to Co⁶⁰ gamma rays of 1 have been reported for iridocyclitis and erythema, and of 2, for epilation and desquamation in monkeys irradiated focally with 14, 39, 185, and 730 MeV protons (209, 298). However, in similarly irradiated animals, 730 MeV protons induced cataracts in 12 to 18 months at doses as low as 750 rads, whereas lower energy protons (14, 40, and 187 MeV) were ineffective even at doses as high as 2000 rads. This

observation of cataractogenesis with high energy but not with low energy protons is of interest, since damage to the lens is generally considered to be less pronounced with increasing energies of fast neutrons (158). More recent data, however, indicate that several hundred rads of protons in all of the energies under consideration can probably produce cataracts (18, 19).

As a given particle degrades in tissue, the RBE will rise as its energy transfer per micron rises. At the same time, a heterogeneous beam of protons will have an average RBE that tends to drop with increasing depth in tissue as the lower energy component becomes fully absorbed and the higher energy component continues its traverse. For gamma radiation, average body dose (ABD) is higher than midline tissue dose (MTD); and for protons, it is lower in large animals (267). Figure 3-21 represents calculations for depth-dependence of RBE for C-nuclei, alphas, and protons of 3 different rigidities: $P_0 = 50, 125, \text{ and } 300 \text{ mv}$. The conservative RBE-LET relationship recommended by the ICRP was employed with a constant RBE of 10 being used for all values of LET above $150 \text{ keV}/\mu$. The alpha and C-nuclei show a pronounced decrease of local RBE extending down to tissue depths well beyond 1 gm/cm^2 .

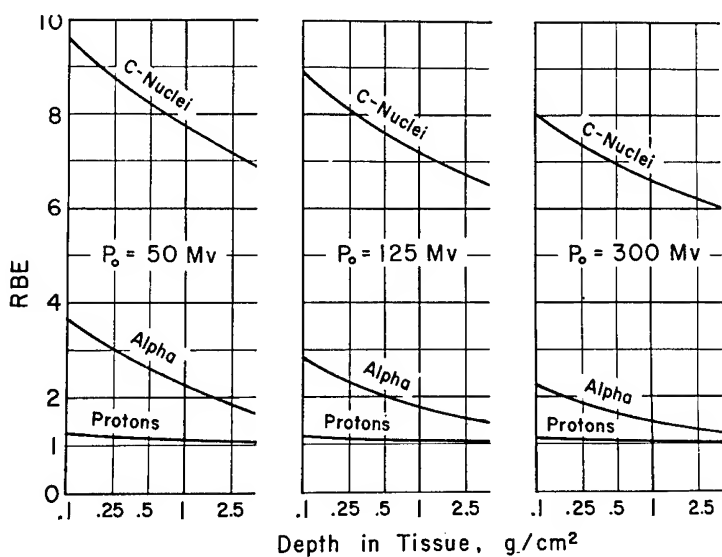


Figure 3-21

Local RBE or QF in Tissue
at Increasing Depth

(After Schaefer⁽²⁴²⁾)

The concept of RBE cannot be applied in those cases where special types of effects are produced by passage of very high LET particles and star formation in cosmic ray events (215). It is seen in Figure 3-17 that the proton contribution to the total dose from galactic primaries should be assigned an RBE well below 1.0. For the alpha component, the bulk of the energy dissipation falls well within the LET limits of standard x-rays, assuring that for this dose contribution an RBE of 1.0 is appropriate. The picture changes as one proceeds to heavier components. For C nuclei, a sizable portion of

the energy dissipation extends into the LET region for which the RBE factor exceeds 2.0. If the mean RBE for the absorbed dose from the C component is computed by numerical methods from the LET and RBE curves, a value of 1.56 is obtained. The corresponding mean RBE values for Ne and Ca nuclei are 2.86 and 6.64, respectively. Weighting these mean RBE values for the individual components according to their respective shares in the total dose and using a mean RBE of 0.75 for the proton contribution, one arrives at an overall mean RBE of 1.82 for the total dose from galactic primaries. This value might appear unexpectedly low in the light of other estimates in the literature (239). The discrepancy is due mainly to the fact that a ceiling value of 10 for the RBE was used whereas in other estimates values up to 20 have been assumed. Justification or preference for either value is largely subjective, though the higher values may be reasonable for protracted exposure and delayed effects.

It is possible to calculate the dose delivered to cells in a microbeam track core and the approximate range of LET of the particles. This has been attempted in Table 3-16. One cannot, however, assign LET or QF values to these microbeams (145). Attempts have been made to circumvent this problem but not enough data are available to substantiate the hypotheses (66).

The RBE or QF for electrons of all energies above .03 MeV is assumed to be unity (215).

The quality, nature, flux, and distribution of secondary radiations are dependent on the characteristics (flux, energy, mass, and charge) of the primary beam and on the materials and geometry of the spacecraft shielding as well as on the tissues of the crew. Present assessments of RBE or QF for secondary radiation doses for long-duration missions are estimates only, derived by complex analysis and evaluation of each organ system individually (290). Insofar as the QF's of various secondary radiations are concerned, it seems reasonable to assume a value of unity for secondary electrons and electromagnetic radiations, since their LET characteristics do not differ greatly from those of conventional x and beta rays. The QF of secondary protons may be assumed to be the same as for primary protons of comparable LET. As with protons, QF values for secondary neutrons are complicated by the dependence of effectiveness on energy, biological response (whether early or delayed), the organ or tissue under consideration (ocular lens vs. bone marrow, for example), and, to some degree, on depth within the body. Presently the most accepted values are those proposed by the NCRP (188). These values are shown graphically in Figure 3-22 and represent late effects of protracted exposure at a depth of 3 mm in tissue. The broken-line portion of the curve is an extension based on the observations of the secondary-proton spectrum (289). QF values applicable to early effects have not been specified by the NCRP or similar committees, but experimental observations on animals suggest values appreciably lower than those for production of late effects (41). Reported RBE values of fission neutrons (mean energy 0.5 to 1 MeV) for production of 30-day lethality and other early responses in experimental animals range from ~1 to ~3 (145).

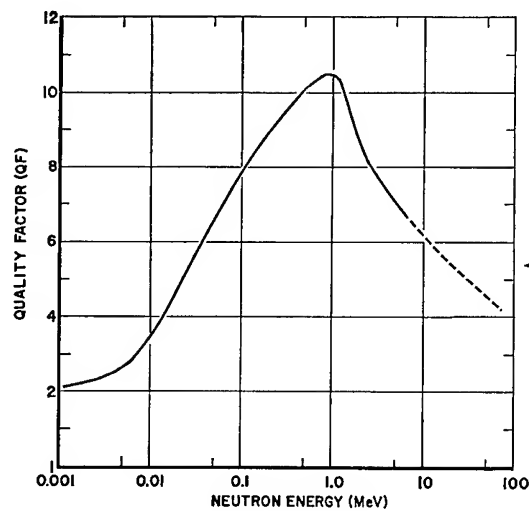


Figure 3-22

QF of Neutrons for Late Effects as a Function of Energy. Calculated for a Depth of 3 mm in Tissue Under Conditions of Protracted Exposure.

(After Langham-NAS-NRC⁽¹⁴⁵⁾ from the data of NCRP⁽¹⁸⁸⁾)

For the major space radiations, the LET decreases with increasing shield thickness and with increasing depth in the body, approaching (behind nominal shielding) that of conventional electromagnetic radiation at the depth of the bone marrow and the gastrointestinal tract. The greatest contribution of QF to the estimation of the biological dose equivalent therefore would be for early skin responses behind light shielding, as in the case of extravehicular operations.

Flux (Current)- To-Tissue Dose Conversion Factors for Nucleons

Conversion of particle flux data to tissue rads and rems is most difficult. The interaction of high-energy nucleons with matter initiates a complex avalanche of secondary particles with lower energy which proceeds through the medium, increasing in population and decreasing in total energy as energy is deposited in the medium. In general, a non-elastic interaction with a nucleus produces, first of all, several secondary nucleons which are due to direct interactions of the incident particle with the nuclear constituents and which have energies ranging from a few MeV up to a large fraction of the incident particle energy. There is left a highly excited, recoiling nucleus which rids itself of most of its excess energy by evaporating nucleons and heavy particles of relatively low energy of the order of a few MeV. Any energy left after evaporation presumably goes into the production of electromagnetic radiation. As a consequence of the significant contribution of the heavy particles and secondary protons to the rem dose, it is not reasonable to expect that the rem dose at any depth from incident protons can be calculated very accurately unless the secondary radiation created in the body is taken into consideration. For the case of incident neutrons this is obviously true, because only through secondary radiations is it possible for neutrons to deposit energy.

The data of Figure 3-23 and Table 3-24 were calculated by the Monte Carlo technique for the study of the transport of nucleons of energies up to 400 MeV through quite arbitrary geometrical configurations (138, 139, 169,

170, 295). The intranuclear cascade is treated by a subroutine version of Bertini's code (27) which is itself a Monte Carlo nucleon transport calculation on an intranuclear scale and gives the velocities and types of particles resulting from direct interaction processes. The evaporation portion of the cascade is handled by Dresner's subroutine (77). Protons below 50 MeV are allowed to proceed to the end of their range with no nuclear interaction, while neutrons below this energy are transported by neutron transport code (77). The data on Tables 3-6 and 3-7 were used for tissue factors in the calculations. In order to provide current-to-dose conversion factors which could be used to estimate upper and lower bounds on the doses for most practical cases of interest, the nucleons were made to impinge on a 30 cm tissue slab both normally in a broad beam and isotropically, with the expectation that these two extremes of incident angular distribution would represent the bounding cases.

The dose as a function of depth was calculated in units of rads and rems. Because of the uncertainties connected with the QF (quality factor) versus LET curves, the dose data were recorded in energy intervals in a manner that any preferred set of QF's could be employed to calculate the rem dose with relative ease. The energy deposition resulting from protons as they passed through the energy ranges 0-1, 1-5, 5-10, 10-50, and >50 MeV was recorded separately. Average QF values, for each interval, of 8, 3, 1.25 and 1, respectively, were calculated from QF versus LET curves (190, 215). The values of the energy of the protons were correlated with the LET values by means of the stopping-power formulas. A constant value of 20 for the QF above a . LET value of 1750 MeV/cm was used. This constituted a quite arbitrary assumption that a saturation effect takes place and can be represented by a constant QF at high LET values. It should be noted, that under all circumstances, the QF value of 20 is applied to the dose from the heavy evaporation particles and recoil nuclei in calculating the rem dose, since their LET value is generally above 1750 MeV/cm.

Figures 3-23a and b present the average total whole-body rad and rem doses for both normally incident neutrons and protons. Also shown is the average whole-body rad dose that would be received if the proton beam were totally absorbed. In comparison with the latter curve, it is easy to see that below 215 MeV, little error would be introduced if the whole-body rad dose were calculated on the basis that all the energy is totally absorbed. The reason for the primary proton dose having a discontinuity at 215 MeV is that above this energy the proton beam penetrates 30 cm of tissue and some of the energy is not deposited. The decrease in dose with increasing energy above 215 MeV is accounted for by the decrease in stopping-power with increasing energy in this energy range. Thus, less energy is deposited in the 30 cm of tissue as the energy increases.

The flux-to-dose conversion factors for average dose, 5 cm dose, and surface dose as well as maximum dose along the particle path can be calculated by an expression of the form:

$$\log_{10} D = A + BE + CE^2 \quad (4)$$

where D is the dose in rem per nucleon per cm^2 and E is the energy in MeV. Table 3-24 contains the values of the coefficients.

Computer codes have been used to generate depth-dose curves for protons in spherical targets for cases where the usual slab techniques are inadequate (290). Depth dose due to an incident isotropic flux of monoenergetic protons, including the effect of primary and first-generation secondary protons can be determined in spheres of arbitrary size containing tissue-equivalent material. The sphere is chosen because it is, for present purposes, the simplest reference solid useful in showing the effects of the variables. Dose rate due to primary protons and three classes of proton secondaries are treated by the code. The secondary protons cover cascade, evaporation, and elastically scattered (hydrogen nuclei) particles.

In Figure 3-25, the dose rate contributed by each of the proton classes described above is recorded as a function of depth in the sphere. At each depth, the dose rate deposited by protons in each of eight energy intervals (0-1, 1-2, 2-5, 5-10, 10-20, 20-40, 40-80, and $80-\infty$ MeV) was tabulated separately for each energy interval and each class of protons. Only the total and primary dose contributions are indicated though others are available (290). Similar deposition data are available for 32 and 35 MeV protons (268).

Tissue current-to-dose conversion factors for neutrons with energies from 0.5 to 60 MeV have been recently programmed (123).

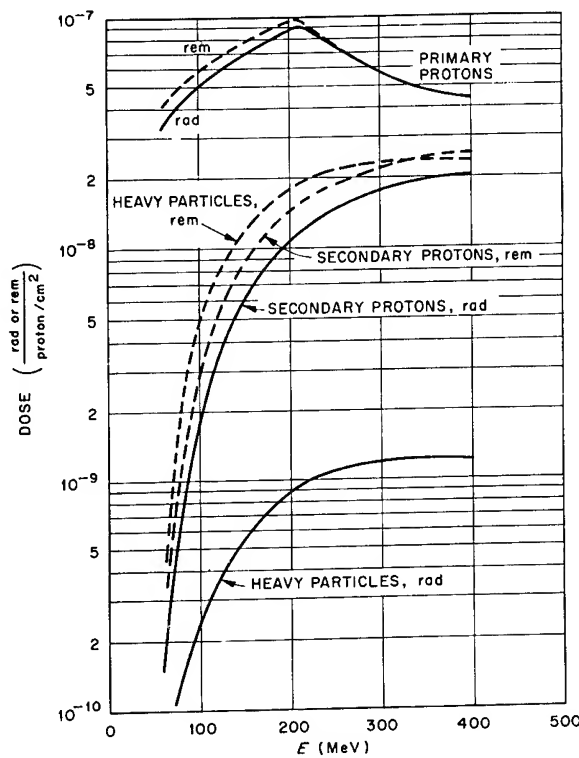
Flux to rad conversion functions may be combined with RBE-energy functions for protons (Figure 3-18a) to give rem dose/unit flux for each particle energy after acute doses (100, 110). Figure 3-26 represents such conversions.

Shielding and Tissue Range

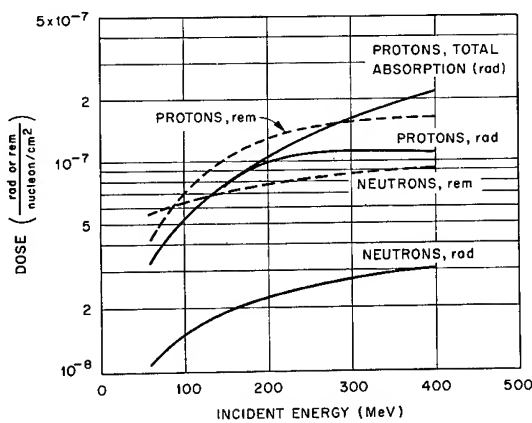
The design of shielding requires an understanding of the residual exposure of the human target behind the shield. The stopping power and ranges of various spacecraft materials for protons, mesons, electrons (24), and heavy ions (262), have been calculated and can be used with Tables 3-9 to 3-12 to determine radiation input to internal organs. Proton penetration codes are being continually refined (249, 250). Bremsstrahlung from electrons hitting thick targets are receiving current re-evaluation (248).

Table 3-27 gives the minimum kinetic energy and rigidity of protons and alpha particles which can penetrate typical shielding projected for future missions. In the actual situation, of course, the thickness of shielding will be heterogeneous in 4π geometry and will allow an influx of variable particles, kinetic energies and rigidities to hit the human target (280). For the Apollo vehicle, for instance, the range of shielding extends from 1.75 g/cm^2 to 212 g/cm^2 , with lower thicknesses predominantly on the anterior side of the astronauts and larger ones on the posterior side afforded by the heat shield and fuel tanks, rocket engine, and other heavy equipment in the service module. In such systems, the dose distribution throughout the body becomes

Figure 3-23
 Flux-to-Dose Conversion for High Energy Protons and Neutrons
 (After Kinney and Zerby⁽¹³⁹⁾)



- a. Average Total Rad and Rem Doses Versus Incident Energy for Normally Incident Protons in Tissue (30 cm slab)



- b. Average Total Rad and Rem Doses Versus Incident Energy for a Unit Flux of Isotropically Incident Protons and Neutrons in Tissue (30 cm slab)

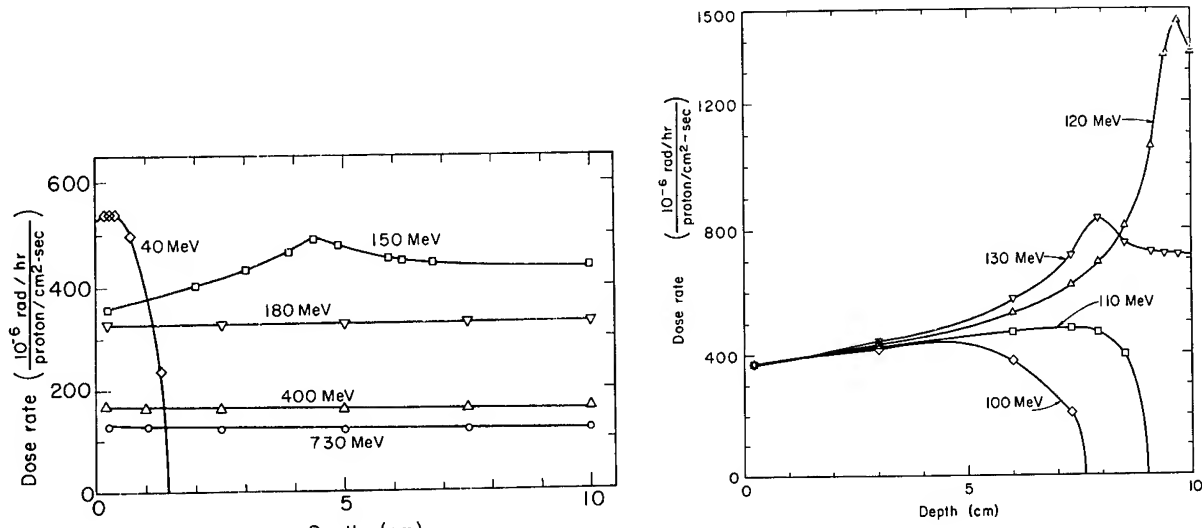
Table 3-24

Coefficients of the Expansion for the Rem Dose Log D for Various Cases

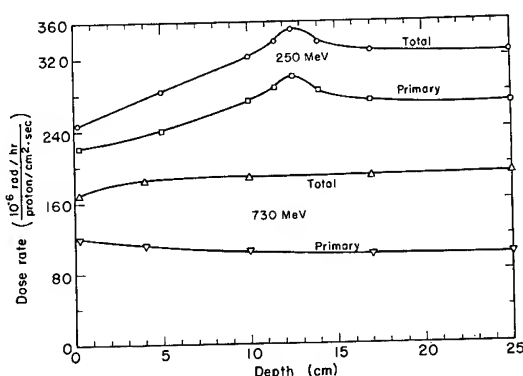
(After Kinney and Zerby⁽¹³⁹⁾)

<i>Normally incident protons</i>	
Average dose-----	$-7.72 + 6.4 \times 10^{-3}E - 1.1 \times 10^{-5}E^2$; $60 < E < 215$
5-cm-deep dose-----	$-6.20 - 4.3 \times 10^{-3}E + 5.5 \times 10^{-6}E^2$; $215 < E < 400$
Surface dose-----	$-6.27 - 4.6 \times 10^{-3}E + 6.4 \times 10^{-6}E^2$; $80 < E < 400$
Maximum dose-----	$-6.64 - 2.2 \times 10^{-3}E + 2.9 \times 10^{-6}E^2$; $60 < E < 400$
	$-6.02 - 1.2 \times 10^{-3}E$; $60 < E < 215$
	$-6.62 - 1.1 \times 10^{-3}E$; $215 < E < 400$
<i>Normally incident neutrons</i>	
Average dose-----	$-7.43 + 2.7 \times 10^{-4}E$; $60 < E < 400$
5-cm-deep dose-----	-7.38 ; $60 < E < 400$
Surface dose-----	$-7.59 + 3.7 \times 10^{-4}E$; $60 < E < 400$
Maximum dose-----	$-7.35 + 3.8 \times 10^{-4}E$; $60 < E < 400$
<i>Isotropically incident protons</i>	
Average dose-----	$-7.79 + 7.9 \times 10^{-3}E - 1.7 \times 10^{-5}E^2$; $60 < E < 215$
	$-7.07 + 1.2 \times 10^{-3}E - 1.3 \times 10^{-6}E^2$; $215 < E < 400$
5-cm-deep dose-----	$-6.57 - 5.4 \times 10^{-4}E$; $80 < E < 400$
Surface dose-----	$-6.30 - 2.7 \times 10^{-3}E + 3.7 \times 10^{-6}E^2$; $60 < E < 400$
Maximum dose-----	$-6.26 - 2.9 \times 10^{-3}E + 4.1 \times 10^{-6}E^2$; $60 < E < 400$
<i>Isotropically incident neutrons</i>	
Average dose-----	$-7.26 + 5.6 \times 10^{-4}E$; $60 < E < 400$
5-cm-deep dose-----	$-7.18 + 3.9 \times 10^{-4}E$; $60 < E < 400$
Surface dose-----	$-7.26 + 4.5 \times 10^{-4}E$; $60 < E < 400$
Maximum dose-----	$-7.18 + 4.0 \times 10^{-4}E$; $60 < E < 400$

Figure 3-25
Proton-Depth Dose Patterns in Spheres of 10 and 25 cm Radius
 (Total primary plus secondary proton depth-dose patterns
 due to monoenergetic isotropic fluxes of protons.)
 (After Wallace et al (290))



a and b. 10-cm-radius Sphere of Tissue Equivalent Material
 (Two graphs used for clarity)



c. 25-cm-radius Sphere of Tissue-Equivalent Material

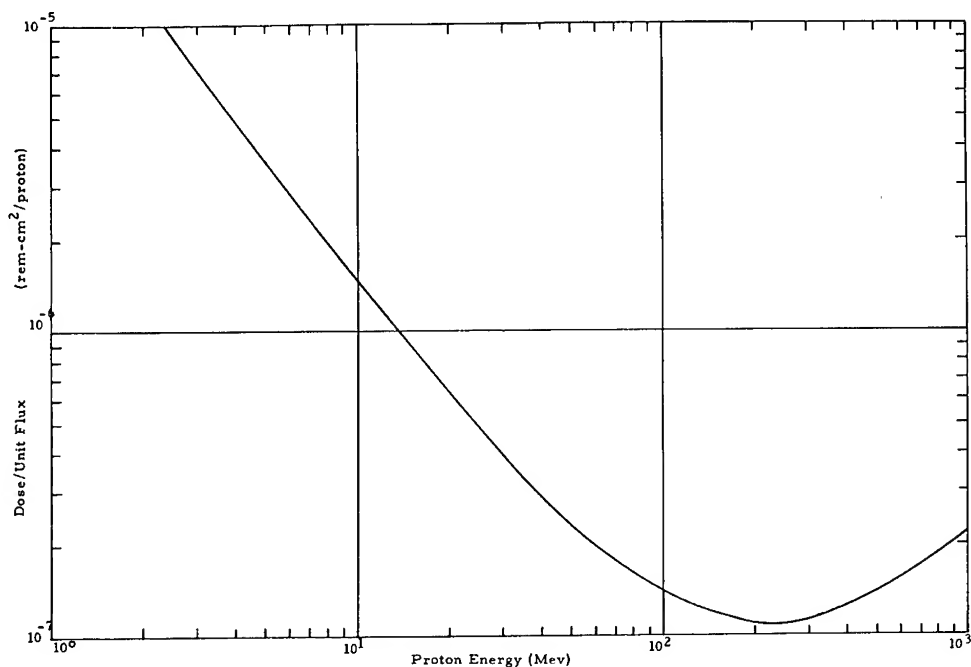


Figure 3-26

Flux to Rem Dose Conversion Function for Protons in Tissue
(After Haffner⁽¹¹⁰⁾)

Table 3-27

Minimum Kinetic Energies and Rigidities for Protons and Alpha Particles Required for Penetration of Typical Shield Thicknesses

(After Schaefer⁽²⁴³⁾)

Space System	Min. Shield Equivalent, g/cm ²	Kinetic Energy, Mev		Magnetic Rigidity, Mv	
		Protons	Alpha Particles	Protons	Alpha Particles
Space suit	0.1	8.4	33.6	125	252
Gemini vehicle	0.2	12.3	49.2	152	303
-	0.5	20.5	82.0	197	392
-	1.0	30.1	120	240	492
Apollo vehicle	1.5	37.8	151	269	545
Permanent lunar base	2.0	44.2	177	290	588

extremely complex. Figure 3-28 compares the typical flux of primaries which pass through typical shielding during exposure to solar flare and galactic protons. The relative levels vary with time because the magnetic field caused by the solar wind can screen off the galactic particles of low rigidity. The actual flux hitting the human target is not the primary flux noted above,

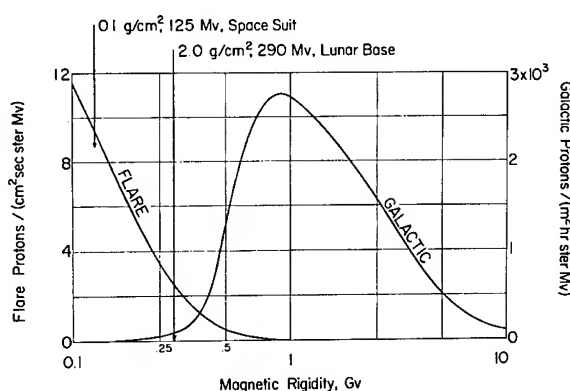


Figure 3-28

Comparison of the Differential Rigidity Spectra of Galactic Protons and of Protons of a Typical Solar Particle Beam
 (Note the great disparity of ordinate units differing by a factor of 36 million). Galactic spectrum is based on the data of Freier and Waddington⁽⁹²⁾; flare spectrum pertains to event of 17 July 1959.
 (After Schaefer⁽²⁴³⁾)

but the secondary and higher order products after absorption process in the barrier.

Tissue Range and Tissue Self-Shielding

For rough calculation of self-shielding or shielding by other humans, the simple range-energy relations of charged particles in matter can be used (293):

$$R = \delta E^n \quad (5)$$

where R = range, gm/cm^2
 E = energy, MeV
 δ = constant - specific for each particle
 n = constant - same for all charged particles

For bone and muscle, these constants are:

$$\begin{aligned} \text{Bone } n &= 1.779, \quad \delta_{\text{proton}} = 2.30 \times 10^{-3} \\ \text{Muscle } n &= 1.786, \quad \delta_{\text{proton}} = 2.03 \times 10^{-3} \end{aligned}$$

Taking the human body to be 50% bone and 50% muscle (the bone is usually weighted more heavily in this way because of the importance of the marrow), the δ constant for protons becomes 2.17×10^{-3} and that for alpha particles 1.87×10^{-4} .

The range in tissue and stopping power vs. particle energy conversion can be seen in Tables 3-9 to 3-11. However, geophysical data are often expressed not as particle energy but in magnetic rigidity. Rigidity and depth of penetration or range are disparate magnitudes. Since rigidity is the momentum per unit charge, and alpha particles have twice the charge of

protons, equal integral fluxes of the same rigidity represent different fluxes in terms of momentum, energy, or range spectrum. Figure 3-29 may be used to convert rigidity spectra to tissue ranges. It shows that for a given rigidity the corresponding ranges of protons and alpha particles differ greatly.

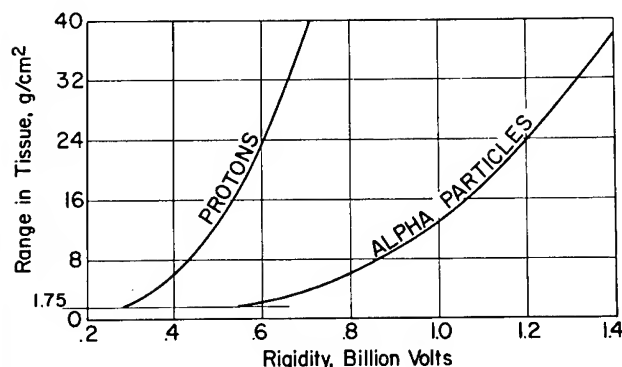


Figure 3-29

Range/Rigidity Function of Protons and Alpha Particles in Human Tissues

(After Schaefer⁽²⁴⁰⁾)

Since the presence of shielding by tissue will alter the RBE of the emergent particles, the spectrum of the particles impinging the tissue must be considered in any operational configuration. If a particle integral energy spectrum is present of the form,

$$\Phi(E > E_0) = AE_0^{-a} \quad (6)$$

where E and E_0 represent the range of external spectral energies to be considered, RBE due to particles in a given energy interval is the integral of the product of the relationship of this power equation and the RBE factors of Figure 3-18. The time-integrated energy spectra of solar proton events appear to follow such a law down to ~ 10 MeV. Solar alpha particle spectra may follow a similar law. However, spectra behind tissue shields will be modified thus:

$$E_i = \left[E_0^{n_s} - (E')^{n_s} \right]^{1/n_s} \quad (7)$$

where E_0 = particle energy outside shield

E_i = particle energy inside shield

E' = particle cutoff energy of shield

n_s = constant for charged particles in the metallic shield material or in shielding tissue

Using the values of the constants n and δ in Equation (5), the particle cutoff energy E' for tissue shielding for any finite tissue thickness X may be calculated. Figures 3-30a and b give the emergent cutoff energy E' as a function of the initial energy E_0 for protons at any tissue thickness. Figures 3-31a and b give similar values for alpha particles.

The feasibility of partial body shielding against ionizing radiation has been recently reviewed (198, 253).

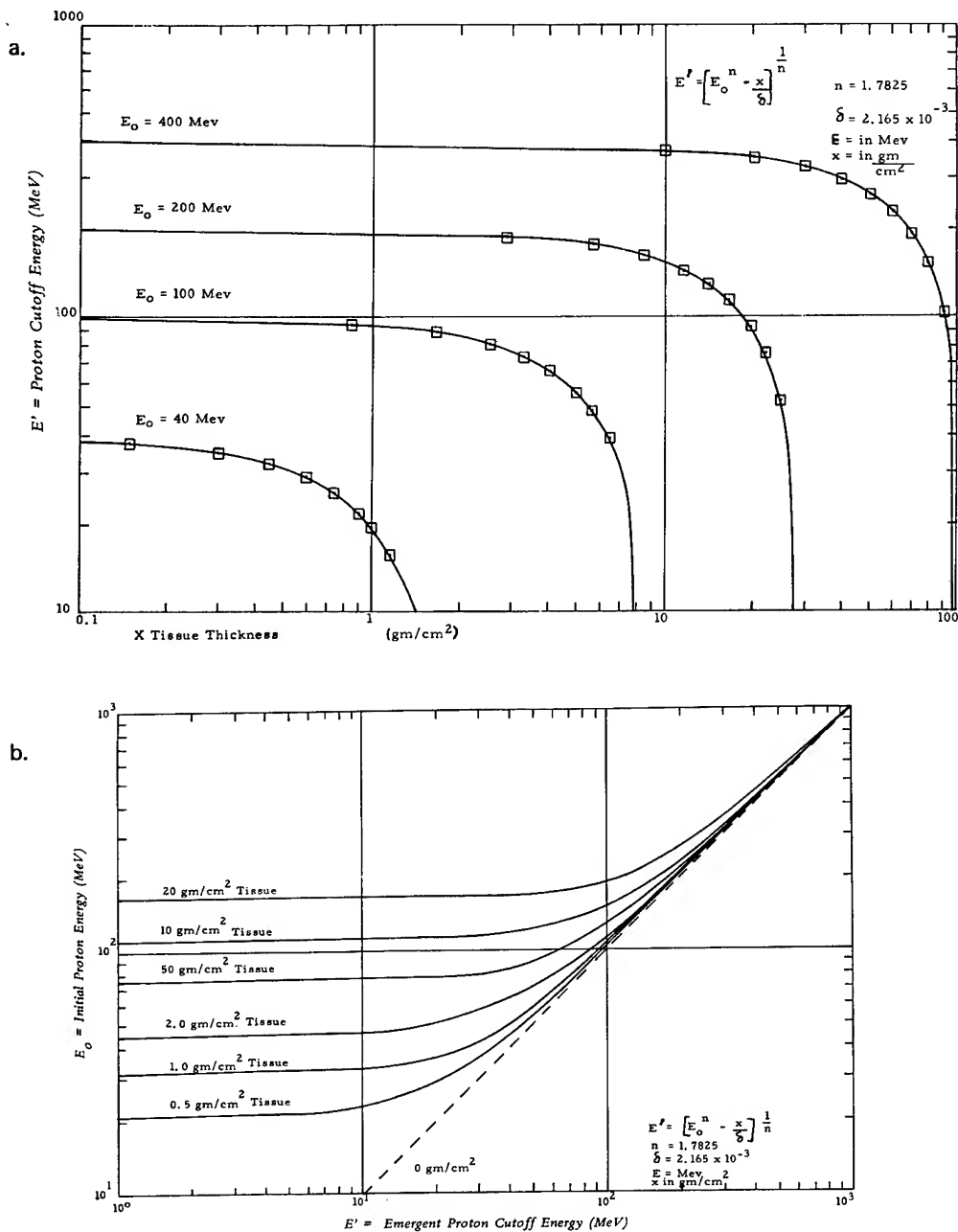


Figure 3-30

Emergent Proton Cutoff Energy at Any Depth of Tissue for Different Initial Energies
(After Haffner⁽¹¹⁰⁾)

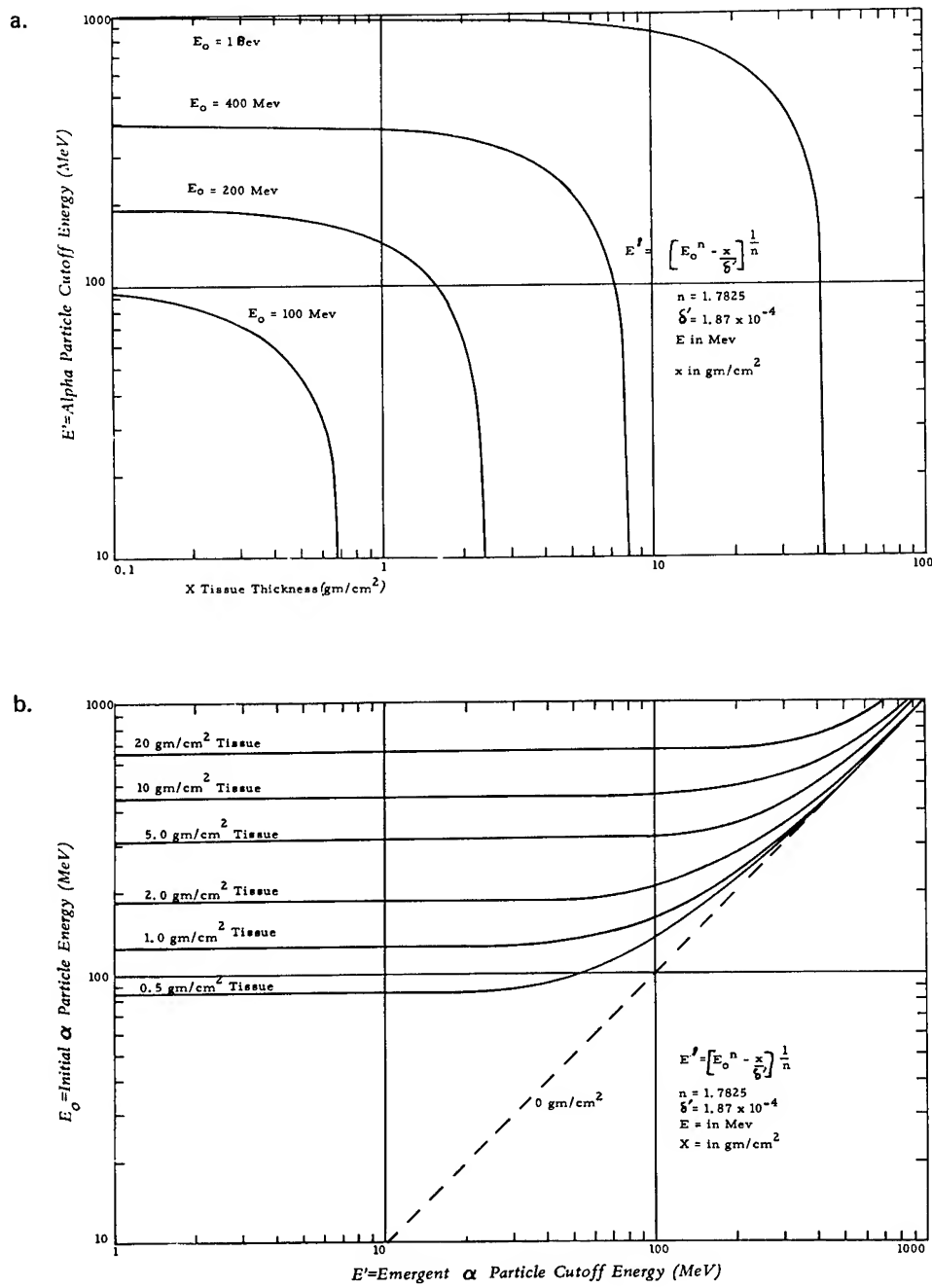


Figure 3-31

Emergent Alpha Particle Cutoff Energy at Any Depth of Tissue for Different Initial Energies
(After Haffner⁽¹¹⁰⁾)

Typical Depth-Dose Patterns in Space Under Shielding

Several examples will be given of the typical depth-dose under shielding of space radiation. Unfortunately, data are deficient on the charge and momentum spectra of solar flare particles measured directly in satellites. Current estimates are based on uncertain and incomplete data (162, 295).

Figure 3-32 shows the calculated dose from only protons at various depths in tissue for inner Van Allen belt and the Solar Proton Event of May 12, 1959, assuming cabin provides only 2 gm/cm^2 of shielding. The greater drop of tissue depth-dose from flare protons as compared to Inner Belt protons is a function of the differences in the integral energy spectra (see inset). The greater frequency of higher energy protons in the Inner Belt increases the dose rate in deep tissues. Note the importance of knowing the integrated energy spectrum of the proton radiation when considering the critical targets -- i. e., bone marrow, spleen, and intestinal locations beneath the surface. It is to be emphasized that no critical organ is located at a discrete depth below the surface. Since the body self-shielding is non-uniform, a more detailed analysis is necessary to determine the effect of a given radiation exposure on specific organs or organ systems.

Table 3-33 shows typical depth doses beneath the 14 largest events of solar cycle 19 under homogeneous shielding of different values. Since flare events occur essentially at random during the active part of the solar cycle, and since the magnitude of the individual flare dose does not show any correlation with the phase in the active half-cycle, the preferred way of formulating the flare hazard for the entire active period is to establish the probability of encountering, on a mission of given duration and for a randomly chosen launch date, an arbitrarily selected dose (145). It can be derived from Table 3-33 that 92 percent of the total dose is delivered in eight critical time intervals, none of them exceeding 10 days' duration, spaced at random over the 6 years. Sixty-four percent of the total is condensed still more to a few large increments on the ominous dates of February 23, 1956; July 10, 14, and 16, 1959; and November 12 and 15, 1960. As a consequence, the dose-probability plot is not a smooth curve but exhibits an irregular pattern. It should also be emphasized that the dosage received in the operational situation would be asymmetric and so the doses of Table 3-33 cannot be used directly to estimate probability of symptoms (253). Calculations have been made on the probability per week of different organs receiving varied doses under different shielding conditions when exposed to spectra typical of solar cycle 19 (80). Radiation shielding considerations and depth dose predictions have also been prepared for interplanetary flights (142).

Figure 3-34 compares degradation of depth dose for specific solar flares rigidities and inner Van Allen belt protons.

Figure 3-35 shows a rigidity spectrum of a typical solar flare of solar cycle 19 converted into a differential range spectrum in tissue for protons and alphas assuming a 1:1 flux ratio. The range spectra allow direct comparisons of fluxes that would reach the same depth in tissue or shielding material. For low and very low shielding the alpha flux drops much more

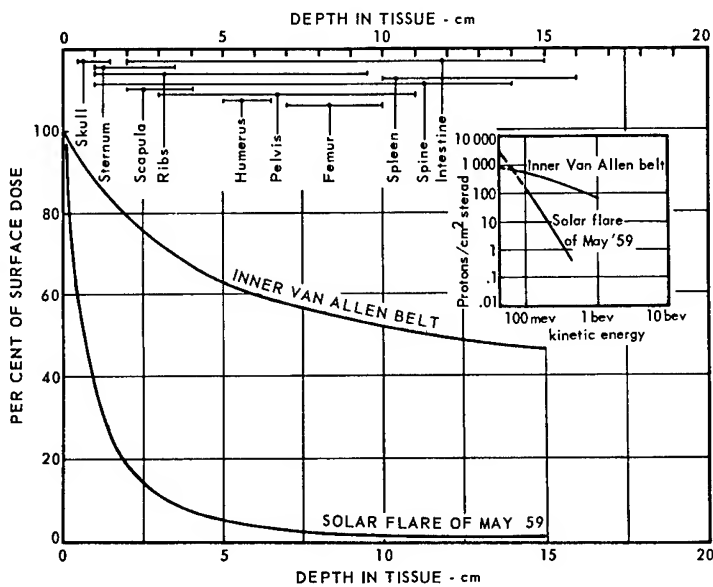


Figure 3-32

Depth Dose Under Solar Flare and Inner Van Allen Belt Exposure Under 2 gm/cm^2

(After Grahn⁽¹⁰³⁾ Adapted from Schaefer⁽²⁴⁶⁾)

Table 3-33

Radiation Doses for the 14 Largest Solar-Particle Events of Solar Cycle 19

(After Langham (ed.)-NAS-NRC⁽¹⁴⁵⁾)

DATE OF EVENT	SHIELDING (g/cm ²):	DOSE AT TISSUE SURFACE (rads)				DOSE AT 4-cm TISSUE DEPTH (rads)				
		1	2	5	10	1	2	4	6	10
Feb. 23, 1956	280	180	89	48	73	64	51	42	30	
Mar. 23, 1958	148	54	10	2.1	6.4	4.5	2.55	1.53	0.66	
July 7, 1958	150	54	9.5	1.93	6	4.3	2.35	1.4	0.59	
Aug. 16, 1958	23.7	8.6	1.6	0.34	1.02	0.72	0.41	0.24	0.11	
Aug. 22, 1958	45	14.7	2.24	0.38	1.33	0.91	0.49	0.27	0.11	
Aug. 26, 1958	75	22.3	3	0.43	1.76	1.17	0.57	0.3	0.11	
May 10, 1959	470	206	55	15.6	38	29.3	18.2	12.5	6.4	
July 10, 1959	420	210	69	24.5	50	40	27.5	19.5	11.5	
July 14, 1959	650	273	72	19.5	48	36	22.8	15.1	7.5	
July 16, 1959	382	191	63	22.3	46	36	25	17.7	10.5	
Nov. 12, 1960	484	263	100	43	75	62	46	34	20.8	
Nov. 15, 1960	288	151	53	20.5	39.6	31.7	23	16.6	10.1	
July 12, 1961	25.7	8.4	1.28	0.22	0.76	0.52	0.28	0.15	0.06	
July 18, 1961	128	63	20.4	7.2	15	12	8.1	5.7	3.3	
Grand total of all 50 events of Cycle 19	3,914	1,837	584	217	426	342	241	176	107	

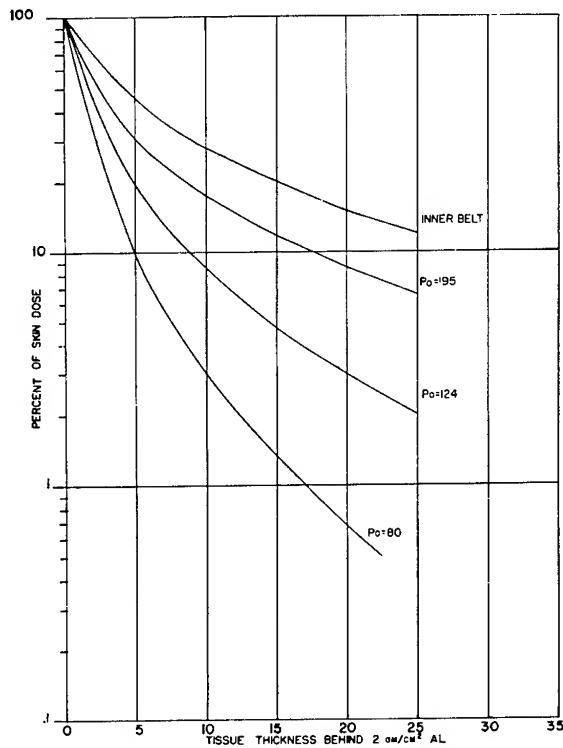


Figure 3-34

Variation of the Percent of Skin Dose as a Function of Tissue Depth for the Three Solar Flare Rigidity Spectra in the Range Expected

(After Jones et al⁽¹³⁴⁾)

steeply at greater depths than the proton flux. This indicates that possible objectionable exposures from solar flare alpha particles can occur only for low shielding as, for instance, for an astronaut outside the vehicle merely protected by his space suit with equivalent shielding of only 0.3 gm/cm^2 for suit and thermal-meteorite coverall.

Figure 3-16 gives spectral absorbed dose contribution of typical primary galactic cosmic ray particles and the dose per particle calculated for a 10μ cell at the center of the track of heavy particles. The only available empirical data on absorption of galactic radiation with buildup of secondaries is in the atmosphere. It has been estimated that the corresponding buildup in a compact scatterer containing high-Z materials would be substantially higher. A total dose of 30 to 50 mrads/24 hr would seem a conservatively high estimate (145, 243). A major uncertainty is introduced by the neutron component of the secondary radiation. Neutrons play an important role in the development of nucleonic cascades, yet data obtained by various authors on the altitude profile of the neutron flux in the atmosphere and the corresponding transition of the local neutron energy spectrum seem to differ greatly. This particular limitation of present knowledge on the transition of the galactic beam is all the more important for assessments of tissue dosages because the neutron component would require elevated QF or RBE, thus substantially

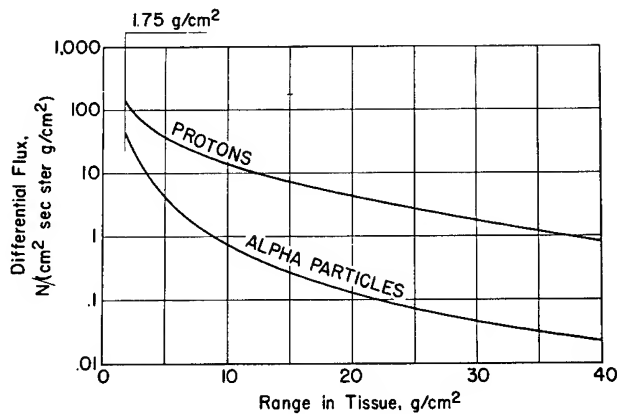


Figure 3-35

Differential Range Spectrum for Protons and Alpha Particles of Solar Flare 19 Assuming a 1:1 Flux Ratio of These Particles.

(After Schaefer⁽²⁴⁰⁾)

enhancing the dose equivalents (see Figure 3-22). Discrepancies still exist with respect to the exact configuration of the lower side of the galactic energy spectrum extending down to thermal energies. However, it now seems well established that, contrary to the spectra of trapped or flare-produced particle fluxes with their very large fluxes at low energies, the galactic spectrum maintains its maximum flux at high energies with values decreasing toward lower energies. As a consequence, dose rates from the galactic field even under worst conditions (solar minimum; location outside the magnetosphere; low shielding) should not greatly exceed the estimate of 50 mrads/24 hr (145).

The actual doses received in space flight to date fall within these predicted ranges for quiet solar years. American and Soviet space flights have been well below the trapped radiation belts (275). The apogee and perigee for the highest prolonged Gemini flight were 100 and 215 miles respectively for 128 orbits. The highest Soviet flight was the Voshkod 2 with perigee and apogee at 107 miles and 308 miles respectively for 17 orbits. Beneath 3.2 mm of Al, the mean total radiation doses of the Soviet Cosmonauts in the Vostok series were measured as ranging from 8.4 to 17 ± 2 mrads/day (286). Ninety percent of the dose was from the primary cosmic radiation and 10 percent from the inner belts at an orbital vector of 65° and apogeas of 409 km. In U. S. astronauts the highest dose rates in the South Atlantic anomaly were recorded as 107 mrad/hr in the portable ionization chamber and 363 mrads/hr in the fixed chamber of Gemini IV (14). Differential spectra of Gemini IV and VI are available(126). Over the 10 day period of Gemini VII, the dose rate per man averaged about 11 mrad/day (26, 241). Emulsions on MA8 and MA9 showed that the inherent shielding of the capsule was sufficient to absorb electrons and secondary brehmssstrahlung from the artificial belt.

Long duration missions on the moon require the use of electrical power sources other than solar cells. Such power sources are radioisotopic and rely on plutonium 238, curium 244, strontium 90, and others as the heat generator (187, 234). Thermoelectric or thermionic converters are used to convert the heat into electrical power. Since a 100 MeV alpha particle requires only 0.8 gm/cm^2 of aluminum for absorption (0.3 cm thick or 0.12 inch), the shield around the unit will, for all practical purposes, absorb or attenuate the alpha particles. This leaves a radiation environment of neutrons and gamma rays from primary decay and secondary emission in the shield.

The external radiation characteristics of lunar, SNAP, radioisotopic thermoelectric generator (RTG) modules or units at a distance of 1 meter are as follows (96):

<u>Neutrons</u>	<u>Snap 19</u>	<u>Snap 27</u>
mrem hr^{-1}	1.5	125
$\text{neutrons cm}^{-2} \text{ sec}^{-1}$	10.5	8.75×10^2
<u>Gamma</u>		
mrads hr^{-1}	2	$11 (\perp \text{to long RTG axis})$ $1.7 (\parallel \text{to long RTG axis})$
$\text{photons cm}^{-2} \text{ sec}^{-1}$	14	77

For either the neutron or the gamma radiation, the mean energy is nearly 1 MeV for these Pu 238 RTG's. For a cluster of RTG's, the total radiation dose is the sum of the individual doses, accounting for the distance from each RTG. Data are available on the shielding and radiation fields for other SNAP and reactor systems proposed for spacecraft and lunar surface operations (10 , 22 , 129 , 141 , 187).

EARLY EFFECTS OF ACUTE RADIATION AT HIGH DOSE RATES

Table 3-36 represents the expected early effects of acute whole-body irradiation. It should be emphasized that these thresholds do not hold true for partial body and protracted radiation of the same total dosage. They do not cover exposure to simultaneous environmental stress of other types. The latency periods and relative duration of symptoms are dependent upon the penetration, quality factors, total dose, dose distribution, and intensity of the exposure. In very general terms, limiting systemic and/or tissue responses are:

1. Acute gastrointestinal or prodromal symptomatology, i. e., nausea, vomiting, diarrhea. These may appear within an hour or two and subside within a day at any dose above about 50-100 r at the midline.
2. Acute hematopoietic symptomatology, i. e., thrombocytopenia, leukopenia, hemorrhage, intercurrent infection. These symptoms will appear within a few days to a week and can reach a clinically aggravating level at doses of 50-150 r or more to the marrow within several weeks to a month.
3. Widespread erythema and skin blistering. Under certain circumstances, such as extravehicular operations, high intensity surface exposure with little deep tissue dosage may occur. Depending upon the quality of the radiation, erythema will appear within a few hours to days following exposures of 400 r to 800 r. Severe damage will occur at doses above 1400-2000 r. Due to the restrictions and abrasive contacts of the space suit, even a partial body moderate erythema could become extremely uncomfortable and somewhat incapacitating.
4. Degradation of general operational skills through direct and indirect physiologic and neurologic injury, i. e., lassitude, fatigability. At lower doses, acute systemic radiation injury is accompanied by nebulous symptoms of reduced performance capacity interfering with information processing, decision-making, emotional stability, and motivation often related to the prodromal symptomatology. At higher doses, vascular shock, cerebral edema, and hypoxia of the central nervous system all contribute to the entity often referred to as the "central nervous system syndrome."

Table 3-36
Expected Early Effects from Acute Whole-Body Radiation on Earth
 (Modified from Glasstone⁽¹⁰²⁾)

<u>Dose in Rads</u>	<u>Probable Effect</u>
0 to 50	No obvious effect, except, possibly, minor blood changes and anorexia.
50 to 100	Vomiting and nausea for about 1 day in 10 to 20% of exposed personnel. Fatigue, but no serious disability. Transient reduction in lymphocytes and neutrophils.
100 to 200	Vomiting and nausea for about 1 day, followed by other symptoms of radiation sickness in up to 50% of personnel; < 5% deaths anticipated. A reduction of approximately 50% in lymphocytes and neutrophils will occur.
200 to 350	Vomiting and nausea in 50 to 90% of personnel on first day, followed by other symptoms of radiation sickness, e.g., loss of appetite, diarrhea, minor hemorrhage; 5 to 90% deaths within 2 to 6 weeks after exposure; survivors convalescent for about 3 months.
350 to 550	Vomiting and nausea in most personnel on first day, followed by other symptoms of radiation sickness, e.g., fever, hemorrhage, diarrhea, emaciation. Over 90% deaths within 1 month; survivors convalescent for about 6 months.
550 to 750	Vomiting and nausea, or at least nausea, in all personnel within four hours from exposure, followed by severe symptoms of radiation sickness, as above. Up to 100% deaths; few survivors convalescent for about six months.
1000	Vomiting and nausea in all personnel within 1 to 2 hours. Probably no survivors from radiation sickness.
5000	Incapacitation almost immediately (several hours). All personnel will be fatalities within one week.

Figure 3-37 presents the mean survival time of man vs. the acute rad dose of whole-body x-ray radiation. The major cause of death is indicated for the appropriate dose range. The possibility of GI tract death and CNS damage occurring at lower doses with protons and alpha particles will be covered below. Defects in all functions of these organ systems can be expected.

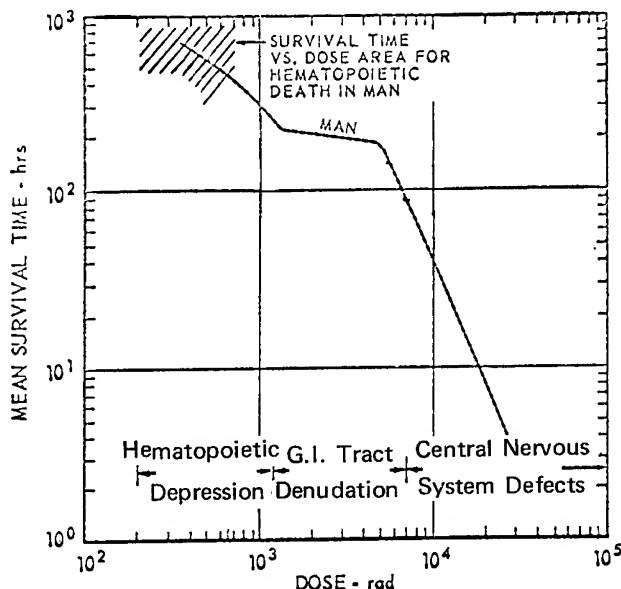


Figure 3-37

The Relationship Between Mean Survival Time and Acute Radiation Dose for Man

This curve is extrapolated from animal studies and very few human studies. It holds only for acute total body radiation. Note spread of data.

(After Grahn⁽¹⁰³⁾ Adapted from Langham⁽¹⁴⁶⁾)

Whenever possible, the above responses will be examined in a probabilistic manner. Not all individuals may show the symptoms mentioned above at the stated dose levels. In defining upper-limit emergency doses, the lowest limit will be the first determinant, modified by depth-dose protraction, distribution, and dose rate. For example, at high dose rate whole-body exposure to a penetrating radiation will undoubtedly cause the dose for prodromal responses to be determinant. A more protracted exposure will bring hematopoietic injury into the determining position, and when moderate to high doses of very low energy radiations prevail under certain unshielded exposure conditions, skin injury will be determinant.

Alteration of these response patterns by space radiation is not clear. Protons, like neutrons, are more effective in producing gastrointestinal symptoms following whole-body irradiation of several species (68, 69, 70, 72, 134, 154, 259, 267). How much protons will modulate the usual x-ray response in humans is not clear since the effect is postulated to be a complex function of relative secondary electron flux in bone, bone size, marrow geometry, ionization density, LET, dose distribution, and dose rate. Early reports that hemorrhage appears earlier and is more severe in large animals irradiated by proton than by x-ray (69, 70, 108, 178) have not always been substantiated (267). Symptoms of the nervous system are variable. Death is reported in animals exposed to 2000 rads of 187 MeV proton within 100 to 200 days after exhibiting central nervous system (CNS) symptoms (216). It has also been found that 6000 rads of 40 MeV protons to the whole-body

(given in two parts - upper and lower halves) caused convulsive seizures and death in about 48 hours following exposure, suggesting a CNS radiation effect. Possible latent or long-term effects based on this observation of a gradual onset of lethargy, anorexia, and ataxia exhibited among survivors of whole-body, proton-irradiated animals at 2 1/2 to 5 1/2 months irradiation have been suggested but not always found (267). In extrapolating from animal data, profound species differences must be kept in mind (39, 61). The above animal data should not be used as examples of dose-specific symptoms expected in man after proton irradiation but as background information about possible aberrant responses in humans to be guarded against when extrapolating to proton radiation effects from x-ray or gamma data obtained from radiation of humans.

Even less is known about high energy alpha particles. Differences in the timing and severity of response between high energy protons and alpha particles in small animals have been demonstrated (258). Extrapolation to humans is not as yet possible from these data.

Lethality

In studying human lethality after irradiation many LD₅₀ doses have been proposed ranging up to 700 rads (28, 63, 102, 114, 154, 178, 179). The spontaneous 60-day death rate for persons between 25 and 44 years is .02% (148). Data obtained from irradiation of patients (160, 292), atom bomb casualties (39, 292), large animal studies (60), and evaluation committees (145, 185, 278) have been reviewed, and the best probabilistic early-lethality curve for acute total-body irradiation has been proposed as seen in Figure 3-38. This study suggests an LD₅₀ value of 286 ± 25 for normal man. The suggested values for LD₁₀ and LD₉₀ are given in Table 3-39. These recommendations can be compared with previous LD₅₀ estimates for humans indicated by different committees and groups as seen in Table 40.

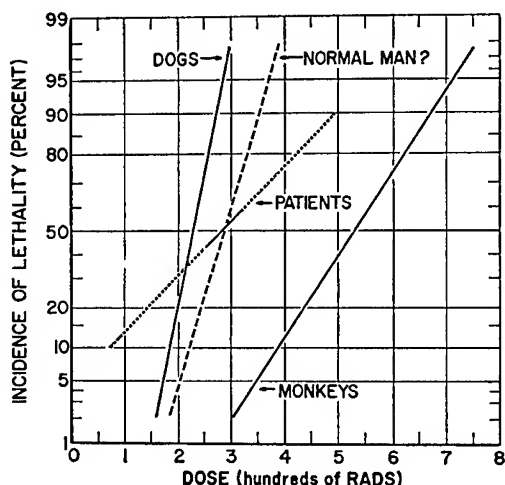


Figure 3-38

Derived Dose-Lethality Relationships for Dogs, Monkeys and Human Patients and a Postulated Relationship for Normal Man.

(After Langham (ed.)-NAS-NRC(145))

Table 3-39

Estimated High-Intensity Whole-Body Dose Levels for Production of Hematopoietic Lethality*
 (After Langham (ed.)-NAS-NRC⁽¹⁴⁵⁾)

Response Probability Level (percent)	Dose (rads)**
10	220
50	285
90	350

*Symptoms begin within a few hours with the prodromal reaction, followed by progressive hematological depression terminating in death in 2 to 8 weeks.

** Point of interest for dose estimation: 11-cm depth;
 QF assumed to be unity.

Table 3-40

Estimates of LD₅₀ of Man for High-Intensity Radiation Exposure

(After Langham (ed.)-NAS-NRC⁽¹⁴⁵⁾)

Source	Exposure (R)	Dose (rads) ^a	Reference
Patients, pathology of atomic bomb casualties	~ 450	~ 300 ^b	Warren and Bowers (292)
Committee evaluation	400-600	260-400 ^b	NAS-NRC (185)
Marshallese observations, large-animal studies	~ 350	~ 300	Bond and Robertson (39)
Committee evaluation	--	300-500 ^c	Cronkite and Bone (60)
Whole-body exposure of patients	370 ^b	243±22	United Nations (278)
Whole-body exposure of patients	380 ^b	250±28	Lushbaugh et al (160)
Whole-body exposure of patients and accident cases	430 ^b	285±25	Langham (ed.)NAS-NRC (145)
			Figure 3-38

^a Average absorbed dose near midline of the body.

^b Assuming radiation of the quality of ¹³⁷Cs gamma rays.

^c Nature of radiation and point of dose assessment not specified.

Partial-body, nonuniformly-distributed doses are less effective than a uniform whole-body dose for production of lethality in the dosage range of the early hematological syndrome. Except when exposure involves a major portion of the trunk, this decrease in effectiveness is true, even when the dose is expressed in terms of integral absorbed energy (kilogram-rads). A dose to the extremities exclusive of the trunk would be much less effective. Based on fraction of total body mass and active bone marrow, an arbitrary choice of a volume factor (f_v) of 1/5 has been suggested for the extremities (145). Dose distribution effects on lethality are covered in section on Dose Distribution Factors and Progressive Performance Decrement).

In animals, the LD₅₀ dose increased with decreasing energy (decreasing depth dose) (106). Sparing a portion of the bone marrow by nonuniform dose distribution (either by irradiating only a portion of the body or by decreasing depth-dose distribution) results in increased protection against early death (145). Under operational space conditions, the geometry of a high-intensity exposure through influence on depth-dose distribution may have a pronounced effect on lethal response if the shielding geometry of the spacecraft and position of the crewmen are such that dose delivery approximates unilateral exposure. Use of midline tissue dose to characterize exposure seems to give the most acceptable correlation with response for exposure geometries other than unilateral exposure (39). The quality factors of Table 3-3 may be applied. Protraction factors for lethal doses are given in Table 3-5, Figure 3-53, and the discussion of Progressive Performance Decrement.

Prodromal Symptoms

In spite of individual idiosyncracy, the dosage parameters for prodromal reaction follows a definite pattern (99, 102, 148, 157). After a short latent period, a feeling of fatigue is followed by depression and emotional disturbance accompanied by anorexia, nausea, retching, salivation, and vomiting. Intestinal cramps and diarrhea occur prodromally at lethal doses. Symptoms reach a peak in about 4 to 6 hours and then improve rapidly. For 200 and 300 rads the peak may occur as quickly as 2 hrs after exposure. The degree of upset and duration of recovery depend on size and location of dose, on individual sensitivity, and, most importantly, on the dose rate. Radiation to the epigastrium is particularly productive of prodromal systems. The volume factor (f_v) for irradiation of extremities should be the same as that for lethality or hematologic response, or 1/5 that for whole-body radiation (145). Anti-nauseant and tranquilizer therapy are effective in reducing symptoms.

The time of onset of the prodromal complex of nausea and vomiting, empirically derived, may be seen in Figure 3-41.

The dose response is a probabilistic function expressed often as the 50% symptom dose or SD₅₀. The probability of symptomatic response may be expressed as a normal or logarithmic function:

$$Y = a + b(D) \quad (8)$$

or

$$Y = a + b(\log D). \quad (9)$$

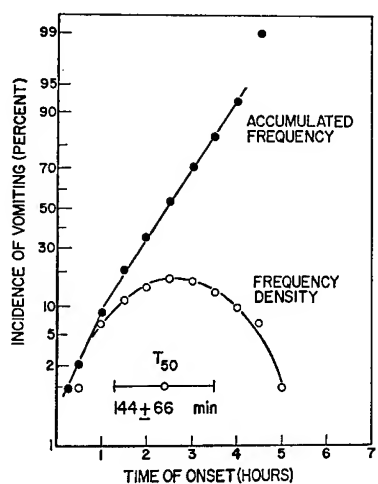


Figure 3-41

Anticipated Elapsed Time Between Irradiation and Onset of Severe Nausea and Vomiting in a Sample of 100 Persons Exposed to Radiation Doses in the Lethal Range.

(After Langham (ed.)-NAS-NRC⁽¹⁴⁵⁾ Adapted from Gerstner⁽⁹⁹⁾)

In either case, Y is the probability of the response as percent transformed into probit units, D is the radiation dose, a is the intercept, and b is the slope constant. Such dose-response relationships can be used to predict a dose that will elicit any given level of response in an infinitely large number of subjects, providing the fiducial limitations of the data are known. Data from atom bomb casualties, nuclear accident victims, and irradiation of cancer patients have recently been summarized (145).

The most well-controlled data were obtained from 165 patients treated for neoplastic disease by isotropic gamma radiation in the Cesium 137 total-body radiation facility at the Medical Division of the Oak Ridge Associated Universities (159, 160). The data were normalized to an effective rad dose of the prodromally sensitive epigastrium (100 r to the midline results in only 66 rads to a 10 cc epigastric volume). A dose rate of 1.5 r/min was used.

Table 3-42 gives the extrapolated SD₁₀, SD₅₀, and SD₉₀ with account

Table 3-42

Estimated High-Intensity Radiation Dose Levels for Production of Early Prodromal Response

(After Langham (ed.)-NAS-NRC⁽¹⁴⁵⁾ from data of Lushbaugh et al^(145,159,160))

CLINICAL SIGN	ABSORBED DOSE FOR PROBABILITY OF RESPONSE (rads)		
	10 PERCENT	50 PERCENT	90 PERCENT
Anorexia	40	100	240
Nausea	50	170	320
Vomiting	60	215	380
Diarrhea	90	240	390

Point of interest for dose estimate: a 26-cm diameter sphere in the mid-epigastric region; QF assumed to be unity.

made of the concurrent signs of disease by Abbott's method. Because of the nature of the patients and the uncertainty of the corrections for concurrent

illness, this table should be considered conservative with higher SD values and wider range of distribution than would be expected in a normal population. The data shown in Figure 3-41 and Table 3-42 are extrapolated from x-ray and gamma experiments and may not be quantitatively appropriate for space radiation, especially when depth dose variations are brought to bear. Appropriate modification of these probabilities for multi-energetic protons and alpha particles as well as for specific dose rate factors is not known from empirical data. Quality factors should follow suggestion of Table 3-3 since the radiation at midepigastic region should typically give a low enough LET to have a QF of 1.

Dose protraction is known to affect prodromal symptomatology (see Table 3-5). Increased sensitivity to large second doses has been noted as well as the prolongation of fatigability and listlessness for as long as 60 days after sublethal exposures (145). Predictions for chronic low level exposure will be covered below under Progressive Performance Decrement on p. (3-63).

Hematological Syndrome

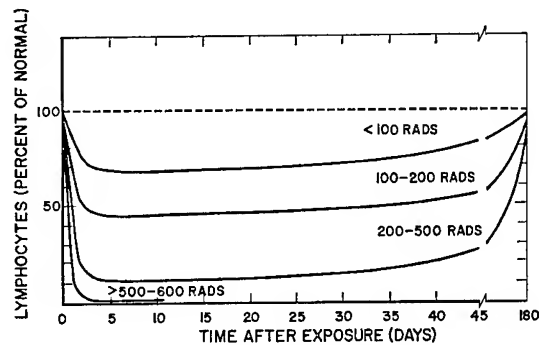
Hematological responses to radiation are largely dependent on damage to the marrow and lymphoid tissue (55 , 202). Damage to the chromosomal mechanisms of the cell inhibit normal division and reproduction of the elements, resulting in decrease in blood counts. Signs and symptoms develop in relation to depression of specific elements. Whole-body irradiation with doses in the lethal range (above about 200 to around 600 rads) causes a typical illness characterized by early transient nausea and vomiting (the prodromal syndrome) followed by a latent period of several days or a week or more, the length of which is inversely related to the dose (see Table 3-36). Signs and symptoms then develop relating to depression of blood elements; infections and fever, relating to granulocyte depression and impairment of immune mechanisms; and bleeding and possibly anemia, relating to platelet depression. Anemia from red-blood-cell depression does not usually occur. These symptoms may lead to death if the bone marrow is incapable of responding in time by adequate cellular regeneration.

The time-course of changes in most of the peripheral-blood elements is fairly well correlated with the dose of radiation to the bone marrow. The description is taken from recent reviews of the subject (55 , 145). Based on dose relationship of these changes, the following categories of prognosis in irradiated persons may be made: (1) survival almost certain (dose <100 rads); (2) survival probable (dose 100 to 200 rads); (3) survival possible (dose 200 to 500 rads); and (4) survival very improbable (dose greater than 500 to 600 rads). Figures 3-43 a to d indicate roughly the smoothed average time-course, based on the human cases from accidental exposure, for lymphocytes, neutrophils, and platelets in these four categories (37 , 44 , 62 , 109 , 115 , 117 , 124 , 145 , 159 , 254 , 288). The changes are represented as percentages of normal counts (the average levels for the population), and the curves portray generally the time-course of changes as a function of radiation dose.

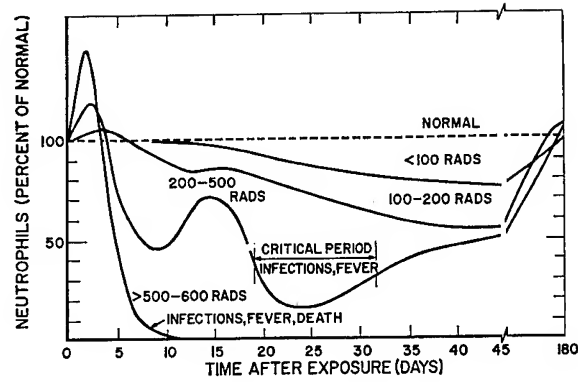
Figure 3-43

The Time Course of Blood Changes After Different Doses of Radiation of QF = 1.

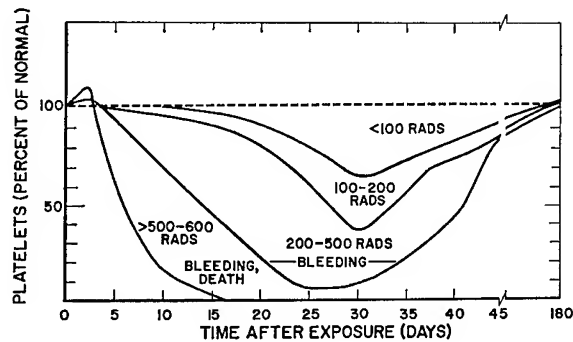
(After Langham (ed.)-NAS- NRC⁽¹⁴⁵⁾ from many sources (see text))



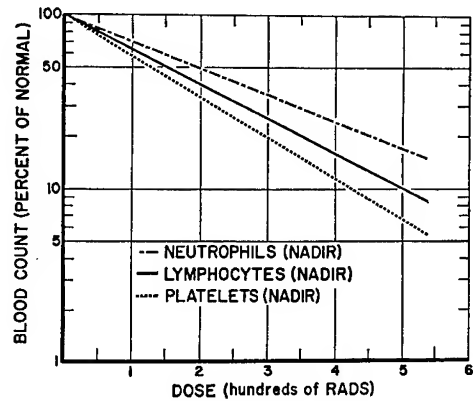
- a. Smoothed Average Time-Course of Lymphocyte Changes in Human Cases from Accidental Radiation Exposure as a Function of Dose.



- b. Smoothed Average Time-Course of Neutrophil Changes in Human Cases from Accidental Radiation Exposure as a Function of Dose.



- c. Smoothed Average Time-Course of Platelet Changes in Human Cases from Accidental Radiation Exposure as a Function of Dose.



- d. Idealized Average Dose-Response Relationship for Lymphocytes, Neutrophils, and Platelets in which the Nadir of Each Blood Element is Plotted Against Dose.

The lymphocyte count (Figure 3-43a) is significantly depressed in 1 to 2 days even with doses of less than 100 rads and approaches zero at that time with near-lethal doses. The return to normal is slow and may be incomplete months and even years later, as has been the case with the exposed Marshallese people (56). Neutrophils increase in the first few days after exposure to doses greater than 100 rads (Figure 3-43b). This initial leukocytosis is even greater with higher doses. The neutrophil count then declines steadily and either levels off or has an "abortive rise" after about 8 to 20 days unless a lethal dose has been given. Absence of this latter phenomenon following substantial radiation dose is a grave prognostic sign. Following the abortive rise, further depression ensues, the nadir being reached earlier with higher doses (8-10 days with lethal doses to 40-45 days with sublethal doses). If profound neutropenia occurs, serious or fatal febrile infections may develop. If the bone marrow is able to regenerate sufficiently before overwhelming infection and death occur, the neutrophil count will climb toward normal during the ensuing weeks, and recovery of the individual is likely. Complete return to normal counts may be delayed for months, or, with higher doses, the counts may actually rise above normal levels for a time.

Changes in platelet counts are shown in Figure 3-43c. Lowest levels are reached in about 24 to 32 days following all but lethal doses where levels may approach zero by 10 to 15 days. Bleeding is likely to develop when the platelets approach zero. With bone-marrow regeneration, platelet recovery may begin rapidly but be incomplete for months or years.

Figure 3-43d shows an idealized average dose-response relationship for lymphocytes, neutrophils, and platelets in which the nadir of each of the blood elements is plotted against dose.

Daily fluctuations in individual counts and normal variations among individuals limit the usefulness of blood counts as a direct biological dosimeter or precise detector of radiation damage. However, repeated hematological examinations afford valuable prognostic information. The lymphocyte count is valuable as an early criterion of radiation injury. If there are 1,200 or more lymphocytes/mm³ at 48 hr after exposure, it is unlikely that the individual has received a fatal dose. Lower lymphocyte counts at this time indicate more serious exposure. Neutrophil and platelet counts are of value in following subsequent progress of exposure cases and as general indicators of the seriousness of the exposure.

Although precise information is lacking on the threshold doses necessary to produce symptoms from blood-cell depression, it might be stated generally that only a few individuals would show hematological symptoms following a whole-body dose of 200 rads, but that a majority would show them following about 300 rads.

The key points of the curves in Figure 3-43 are summarized in Table 3-44.

Radiation doses to different parts of the bone marrow undoubtedly will vary widely under space flight conditions owing to variations in shielding

of the spacecraft, in energy and penetrability of the space radiations, and in distribution of active bone marrow throughout the body. The principal locations of active bone marrow are the pelvis, spine, ribs, and proximal ends of the bones of the extremities (8). The depth of the bone marrow varies from about 1 to 15 cm. For calculation and assessment of dose to the blood-forming tissues, the average effective depth of the active marrow is given as 5 cm. Although no definitive statements can be made at this time regarding the quantitative influence of nonuniform dose distribution on early hematological response, animal experiments show definitely that uniform whole-body exposure is more effective than nonuniform exposure for the production of hematological effects, even when expressed as integral absorbed dose in kilogram-rads (4, 113, 171).

Table 3-44

Estimated High-Intensity Radiation Dose Levels for Production of Hematological Depression*
(After Langham (ed.)-NAS-NRC(145))

CIRCULATING ELEMENT	ABSORBED DOSE FOR REDUCTION FROM NORMAL (rads) **		
	25 PERCENT	50 PERCENT	75 PERCENT
Platelets ***	50	120	250
Lymphocytes ***	60	150	300
Neutrophils ***	80	190	390

*Symptoms appear within 1 to 10 days after bone marrow exposure.

**Point of interest for dose estimation average depth of 5cm: QF assumed to be unity.

*** ~3,25, and 30 days, respectively, for lymphocytes, neutrophils, and platelets.

Quantitative approaches to the evaluation of effects and recovery from nonuniform exposure have been proposed (38, 202). Under nonuniform irradiation the unequal distribution of dose to the bone marrow should permit a higher rate of survival than if the same average dose were distributed uniformly. This is due to the exponential nature of dose effect on survival of bone-marrow stem cells. Furthermore, it is considered possible that stem cells from unirradiated marrow migrate to irradiated areas and hasten regeneration. However, migration of stem cells may not be as significant in humans as in small rodents. The strong dependence of early hematological effects on the region of the body irradiated suggests that emergency partial shielding of the bone marrow be considered. Local shielding of the pelvic region would probably be the most beneficial since about 40 percent of the bone marrow is located there. Such a procedure would markedly increase the chance of survival in cases of high dose exposure. The volume factor (f_v) for irradiation of extremities should be about 1/5 that for whole-body irradiation (145). (See Distribution, page 3-7.)

From several studies it is apparent that marrow exposures will be of varying fractions of weakly-penetrating space radiation at high LET and highly-penetrating radiation at low LET. (See Figures 3-25, 3-32, 3-34, and 3-35). For rough estimation, work with primates suggests that the overall LET is $\leq 3.5 \text{ keV}/\mu$ and that a QF of 1 should be used for the entire flux as seen in Table 3-3 (68, 69, 70, 71, 135, 145, 153, 154).

Suggestions for dose protraction factors are given in Table 3-5.

Skin Reactions

Early responses of the skin to radiation exposure may be particularly important to manned space-flight operations, especially those involving extravehicular activity and light to moderate shielding. A few systematic clinical investigations have been relied upon heavily in deriving the limited dose-response relationships for human skin that are established at this time (7 , 21 , 78 , 81 , 131 , 161 , 206 , 213 , 214).

The levels of early skin response in order of increasing severity are usually designated as (1) erythema, (2) dry desquamation, (3) moist desquamation (vesiculation), (4) slough of skin layers, and (5) chronic ulceration. The first four levels of reaction are often followed by restoration of the irradiated skin to near-normal or pre-exposure conditions; however, clinically evident permanent changes occur regularly after doses that yield at least a dry desquamation response.

Table 3-45 represents the air dose-response of the skin for early symptoms following acute x-radiation.

Table 3-45
Radiation Damage to the Skin*

(After Grahn⁽¹⁰³⁾ Adapted from Saenger⁽²³²⁾ and Cronkite et al⁽¹⁸³⁾)

<i>Epilation -loss of hair</i>	<i>Erythema (first degree burns)</i>	<i>Moist desquamation and blistering (second degree burns)</i>	<i>Ulceration (third degree burns)</i>
Rare at less than 200 r			
Partial epilation at 350-450 r	Response is dependent on energy, dose rate, area exposed, & com- plexion of the individual. Full effect in 1 to 3 weeks after:		
Complete epilation in 16-18 days at > 450 r	200-400 r (<150 kev) 500-600 r (200-400 kev) 800-1000 r (>400 kev)		
Permanent epilation at > 700 r	Response in first hours at 1000 r	Effect in 1-2 weeks at > 1000 r	Rapidly progressive effect at > 2000 r

*These statements are based on air doses. Dose estimates are at 0.1 mm depth where 1 r \cong 1 rad.

The ED's for skin responses have been evaluated in the light of uncertainties regarding effects of quality of radiation, local skin areas, end-points, etc. The only reactions with adequate statistical data are erythema and moist desquamation for fields of less than 100 cm^2 (145). The estimated responses are seen in Figure 3-46. It is probable that the dose response curves for more severe erythema and dry desquamation would lie between these curves. The statistical projections are summarized in Table 3-47. The factors modifying radiation effects on the skin are numerous and more closely studied than many of the other responses. They include (1) quality (LET) of the radiation, (2) dose fractionation and total time over which irradiation occurs, (3) dose rate, (4) depth-dose distribution, (5) area of skin irradiated, (6) anatomical region exposed, and (7) presence of other irritants or trauma.

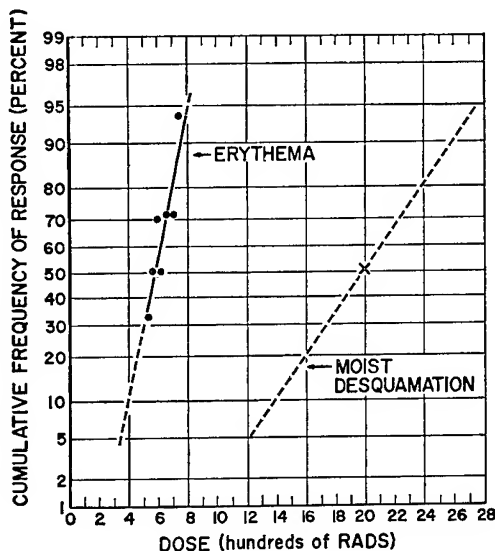


Figure 3-46

Dose-Frequency Relationship of Minimal Erythema⁽¹⁷⁷⁾ and Moist Desquamation^(7,81,131,206) (Clinical Tolerance Response) for Acute Exposure 200kVp X-rays for Areas of $<100 \text{ cm}^2$ and Dose Rates $\geq 30 \text{ rads/min}$
 (After Langham (ed.)-NAS-NRC⁽¹⁴⁵⁾)

Table 3-47
 Estimated Doses of High-Intensity Radiation ($QF=1$) at 0.1 mm Depth
 for Production of Erythema and Desquamation of the Skin
 (After Langham (ed.)-NAS-NRC⁽¹⁴⁵⁾)

CLINICAL SIGN	ABSORBED DOSE FOR PROBABILITY OF RESPONSE (rads)		
	10 PERCENT	50 PERCENT	90 PERCENT
Erythema	400	575	750
Desquamation	1,400	2,000	2,600

An overall modifying factor (QF_E) weighted for LET should be applied to the dose values given here (See Table 3-3). An area effectiveness factor of 1.25 is suggested to reduce the dose values given here when exposure involves skin areas up to or greater than 150 cm^2 .

Corneal lesions can occur after 2500 r of 100 kVp x-rays and lower energy cathode radiation (220).

Quality

The sensitivity of skin to low energy protons and alpha of high LET has already been covered. Primate studies with 1440 rads and 5200 rads of 32 MeV protons lacking sufficient range to penetrate to the marrow and gastro-intestinal tract, show that the skin and subcutaneous tissues can bear the weight of the injury (67, 154). During an initial quiescent period of 2 weeks, only epilation and erythema were noted on the skin, accompanied by anorexia and dehydration. In the next two weeks the erythema turned to ulceration of the skin and mucous membranes of the mouth with massive edema of the soft tissue. The lesions began to heal poorly at 5 weeks. Capillary and lymphatic damage appeared to be a prime factor. These signs progress in primates to severe fibrous contracture of the skin which leads to immobilization and often death from starvation (178, 195).

The threshold dose for the late alpha and proton effect in humans is not yet known. Animal studies with electrons of varying penetration suggest that the threshold dose at 0.1 mm for death of the critical basal layers of the epidermis is about 1200 to 1700 rads for transdermal injury; 1800 to 2500 rads for atrophy and chronic inflammation. Comparative data for pertinent protons and alpha may be extrapolated from the RBE or QF - LET relationship of Table 3-3. Some reservations should be held because of the uncertainty regarding dose-rate-dependent quality factors in skin radiation (131, 145).

For high-intensity single exposure, observed RBE values for radiations of $\text{LET} \geq 3.5 \text{ keV}/\mu$ (largely soft x-rays and fast neutrons) for production of early skin reactions have been in the range of 2 to 3. In converting absorbed dose of space radiations to local dose equivalents for production of early skin responses, it should be kept in mind that for high-LET radiations, QF appears to increase more slowly with increasing dose fractionation than for conventional x-ray exposure (145) (see Figure 3-49). Some compromise between the recommendations of Tables 3-2 and 3-3 will have to be arrived at for fractionated dosage patterns leading to subacute injury (see below).

Dose Fractionation

The repair of sublethal injury in the surviving cells and the proliferation of the surviving cells between fractions determines the dependence of ED₅₀ and TD₅₀ (doses required to produce 50 percent erythema and moist desquamation response, respectively) on fractionation number and total time required for dose administration (89). The repair of sublethal cellular injury after moderate doses is complete or very nearly so in less than 24 hr. Cellular repopulation of irradiated tissues is a much slower process. Accordingly, the ED₅₀ and TD₅₀ are sensitive to the number of equal fractions into which the total dose is divided (administered at ≥ 24 hr intervals) and are less sensitive to the total time of its administration (7, 53, 54, 82, 161, 206, 213, 214, 264).

Figure 3-48 shows the effect of daily fractionation of dose on the ED_{50} and TD_{50} of 200- to 250 kVp x-rays (30 to 60 rads/min, 35 to a 100 cm^2 area). In none of the clinical studies are there applicable data for more than about 40 fractions. If the expressions shown in Figure 3-48 are to be extrapolated to long times or to large fraction numbers, a slope constant of perhaps 0.25 may be more appropriate (145).

Figure 3-49 suggests that radiations of low LET show a greater RBE sensitivity to dose fractionation than do radiations of higher LET.

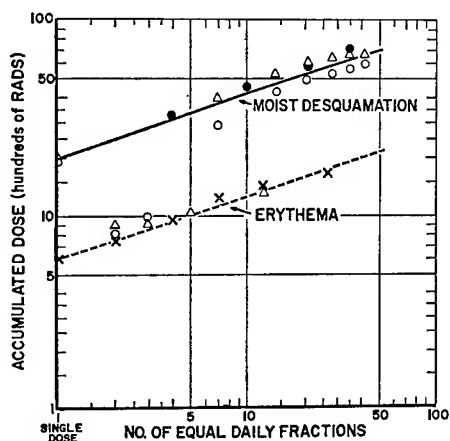


Figure 3-48

Effect of Dose Fractionation or Overall Exposure Time on Dose Producing 50 Percent Probability of Erythema (ED_{50})^(161,213,214) and Moist Desquamation (TD_{50})^(81,131,206) of Human Skin (200-250 kVp x-rays).

(After Langham (ed.)-NAS-NRC⁽¹⁴⁵⁾)

Dose Rate

A given dose of radiation administered continuously at relatively low dose rates is known to be less effective in producing early skin reactions than is the same dose given at a rate of ≥ 30 rads/min. Clinical estimates of the dependence of skin reaction on dose rate (for a single exposure only) are shown in Figure 3-50. The only empirical data are the symbols and solid lines (206). All other points are extrapolations (145).

Depth Distribution and Area Factors

It has been determined from study of effective depth-dose patterns with different isotopes that any dose to a depth of ≥ 0.9 mm should be considered as capable of producing full skin reactions (177).

The dose required to produce a given response is larger for an area of a few cm^2 than for one of a few hundred cm^2 with both x-rays (81, 131,

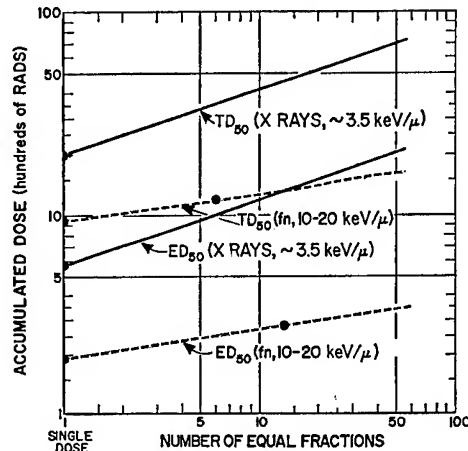


Figure 3-49

Dependence of Erythema (ED_{50}) and Moist Desquamation (TD_{50}) of Human Skin on Radiation Quality (LET). (fn = fast neutrons)

(After Langham (ed.)-NAS-NRC⁽¹⁴⁵⁾)

53 , 206) and electrons (256). Above $\sim 400 \text{ cm}^2$, the size of the area irradiated has little effect on the dose required to produce a given level of response. Figure 3-51 illustrates the effect of area irradiated on skin-tolerance dose (TD_{50}) over the range of 30 to 600 cm^2 for 25 treatments given over a period

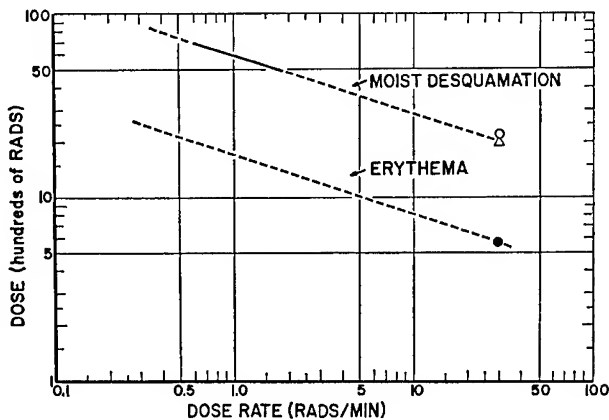


Figure 3-50

Dose-Rate Dependence (Single Exposure Only)
of Erythema (ED_{50}) and Moist Desquamation
(TD_{50}) of Human Skin (200-250 kVp x-rays).

(After Langham (ed.)-NAS-NRC⁽¹⁴⁵⁾ Adapted
from Paterson⁽²⁰⁶⁾).

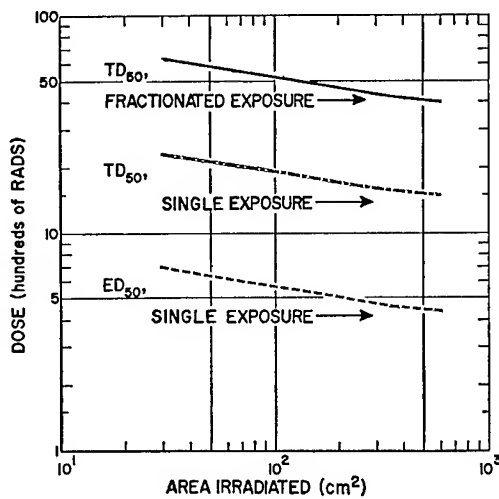


Figure 3-51

Effect of Area on Response of Human Skin to
Radiation Exposure (Upper Curve, Skin Tol-
erance Dose, TD_{50} , for 25 Treatments Given
Over 5 Weeks; Lower Curves, TD_{50} and ED_{50}
for Single Exposure).

(After Langham (ed.)-NAS-NRC⁽¹⁴⁵⁾ from data
of Paterson⁽²⁰⁶⁾).

of 5 weeks (upper curve). The lower curves demonstrate the possible effect of area irradiated on the single high-intensity exposure TD_{50} and ED_{50} . In this case, the TD_{50} and ED_{50} curves are drawn parallel to the upper curve through the established points of 2,000 and 575 rads for the high-intensity tolerance and erythema doses, respectively, for an exposed area of 100 cm^2 . In view of the limited data, it has been suggested that the erythema and tolerance-dose values perhaps should be lowered by about 20 to 25 percent if applied to situations in which the potentially exposed skin area may exceed 100 to 200 cm^2 (145). These considerations are related only to effect of area exposed on the ED_{50} and TD_{50} and do not apply to effect of area of skin involved on the degree of discomfort and the probability of producing decrement in performance. It is suggested, therefore, that in calculating RES, the space-radiation dose (D) be multiplied by an area-effectiveness factor (f_a) of 1.25 to evaluate the reference equivalent space exposure (RES) when exposure involves skin areas greater than $\sim 150 \text{ cm}^2$ (see Distribution, page 3-7).

The less sensitive regions of the body are the face, trunk, arms, and legs; more sensitive regions are the dorsa of the hands and feet, the scalp, the eyelids, and the perineum. Data are not available from which an estimate of the ED_{50} or TD_{50} for hands and feet can be made. The response threshold for skin of these regions appears to be about 15 to 25 percent less than that for skin on the trunk (145).

Irradiated skin exposed to chronic irritation or trauma, such as from tightly fitting clothing, will develop a more severe reaction than would non-traumatized skin. The increase in severity would be a function of the type of trauma and whether the area was being continually subjected to trauma during the course of the development and healing of the reaction. Exposure to elevated local temperature would also act to augment the reaction. It has been suggested that exposure of irradiated skin to trauma and irritants could effect a reduction in ED₅₀ or TD₅₀ by a factor of ~0.25 (145).

Germinal Epithelium

The sterilizing effect of radiation will not affect the success of a specific mission, but may have a second-order psychological bearing on crew effectiveness during the whole program. Due to the high radiosensitivity of the gametogenic epithelium, the gonads are probably the most sensitive organs of the human body. Table 3-52 represents the expected dose-response curve for male sterility obtained from experience with electromagnetic radiations.

Table 3-52

Radiation Damage to Gonads

(Adapted from Brown⁽⁴²⁾, Oakes and Lushbaugh⁽²⁰⁰⁾ and Heller⁽¹¹⁶⁾)

Dose	Response
15-100 rad	Progressive reduction in fertility with dose reduced sperm count (oligospermia) and increased frequency of abnormal sperm. Above 100 rads, azoospermia is usually evident at 10 weeks.
200-300 rad	Temporary, absolute sterility (azoospermia) for approximately 12-15 months after 10 weeks.
400-500 rad	Temporary sterility for 18-24 months.
500-600 rad	Probably permanent sterility, if individual survives.

The time course of decreased sperm count is related to the fact that post-spermatogonial cells are quite resistant to radiation. Cells beyond the second and third phases of spermatogenesis continue to develop. Below 300 rads, there is a normal sperm count for about 46 days with a sudden drop over the next 10 or 12 days to a nadir at about 80-120 days depending on dose (146). Above 300 rads, the sperm count falls after several weeks. Libido and potency are unaffected up to about 600 rads. The lower the dose, the more rapid the recovery. Beyond 500-600 rads, little or no recovery is seen (182). A review of gonadal response after clinical x-ray exposure is available (118).

The principal effect of radiation on the germinal epithelium is a direct one (95). Therefore, nonuniformity of dose distribution, both topically and in depth, would influence response of the germinal epithelium to space-radiation exposure. For purposes of effective dose calculation and measurement, the average depth of the testes is assumed to be 2.5 cm (145). It should be remembered that the testes are shielded in operational conditions by at least 3π steradians of body shielding. The fact that radiation effect on the

germinal epithelium is predominantly a direct one suggests the feasibility of local shielding, if necessary, to lessen the probability of response.

The QF-LET factors suggested in Table 3-3 appear appropriate for acute exposure of the germinal epithelium (20 , 145 , 199). It has been pointed out, however, that in small animals some testicular cells are very sensitive to high LET radiation; 6 rads of alpha particles causing a significant effect (270). Under conditions of fractionated or protracted exposure the QF-LET factors of Table 3-5 appear reasonable (260).

PROGRESSIVE PERFORMANCE DECREMENT

Where exposures are at low levels and where no early manifestations occur, continued or periodic exposures can lead to a progressive decay in health and in performance necessary to maintain flight operations. Quantification of this problem encompasses one of the most difficult areas for the prediction of biological effects.

Radiation injury has a comparatively slow time-course of expression and its manifestations will progressively emerge, then subside. Expression and recovery are concurrent. When the exposure is essentially continuous but at a low daily rate, injury and recovery will probably equilibrate and a steady state will be maintained for long periods. Such observations have been made in experimental animal populations and certainly would occur in man, but there are not yet sufficient data available to establish the kinetics of injury and recovery with any degree of confidence (228).

One theoretical approach to this problem has lead to the evolution of the "equivalent residual dose" (ERD) concept (32 , 73 , 148 , 172 , 191 , 231). This assumes a simple linear additive model for injury accumulation and concurrent recovery. The assumptions and constants employed in the ERD calculation have never been validated in man and are often, for specific biological end points, in conflict with much present day radiobiological data (201). The ERD concept is not based upon a correlation of physiological or cellular injury with lethality, and therefore it cannot determine in any realistic way a dose accumulation that can be related to an acute end point. Dose protraction studies in larger animals may shed more light on the problem (2 , 205 , 297).

The following discussion is taken directly from the recommendations of the Space Radiation Study Panel of the Life Sciences Committee, Space Science Board, NAS-NRC (145).

The possibility of radiation-induced progressive performance decrement will increase with increasing mission duration. The highest-intensity exposures will occur very infrequently and then only over a period of a few days, such as during solar flares. Most exposures to radiation in space flights are, therefore, expected to be at low dose rates. Since radiation effects decrease roughly proportionately with decreasing dose rate, the early effects described above for high-intensity exposures will become less marked

or even absent under sufficiently protracted exposure, even though the dose rate during an occasional episode may be relatively high. Under these conditions, as a result of a gradually accumulating injury to the blood-forming tissues, more subtle effects may occur that may be accompanied by a reduction of the spacecrew's ability to maintain normal flight operations. This injury may be characterized by vague symptoms of fatigability, headache, dyspnea, reduced resistance to general stress, increased incidence of low-grade infection, and decreased blood-oxygen transport.

In space radiation exposure, the expressions of injury and recovery are concurrent. When the exposure to reference-quality radiation is essentially continuous but at a low daily rate (perhaps 1 rad/day or less for man), the rate of injury and recovery may approach equilibrium, and a steady state may be maintained for long periods. Although the phenomenon of equilibrated injury and recovery has been quantitatively defined in experimental animal populations under specific conditions of exposure, the kinetics of injury and recovery for man cannot yet be given with any degree of confidence.

Prediction of man's response is difficult even when a regular pattern of protracted or fractionated exposure is involved. The erratic pattern of exposure that may occur in most projected space flights, and the accompanying moderate to serious depth-dose inhomogeneity, make extrapolation virtually impossible at present. Sufficient dose protraction (whether by low dose rate or by fractionation) will lessen or even preclude the occurrence of prodromal symptoms and early skin responses. Restricting one's self to injury to the blood-forming tissues, the important questions are to what extent damage to the bone marrow will be lessened and what time factors are involved.

In the absence of any well-substantiated method of estimating an individual's residual radiation damage from intermittent exposure and his capacity to tolerate additional doses, the Panel suggests that a dose-accumulation procedure as outlined below be utilized. The procedure allows for any changing effectiveness of accumulating dosage by taking dose rate into account. Although there are insufficient data to permit a high degree of precision, the Panel feels that some evaluation of dose-rate effects under the anticipated conditions of exposure is important in determining the radiation status of a spacecrew. A suggested approach is outlined below.

1. Radiation absorbed by a crew on a deep-space mission will typically result from occasional limited periods of exposure at elevated dose rates (which will vary from period to period and with time during each period) superimposed on a continuous low-dose-rate ambient cosmic-radiation background. The irregularities in dose rate can be smoothed for calculation and accumulated on a mean-daily-dose basis.
2. It is assumed that the effect per unit dose will decrease linearly with decreasing dose rate.
3. For bone-marrow responses, doses delivered at dose rates of 50 rads/day and above are assumed to produce maximum injury per rad, while exposures at rates of 1 rad/day and below are assumed to produce minimum injury per rad accumulated.

4. A dose-rate accumulation effectiveness ratio of 3 will be assumed between these limiting dose rates, and linear interpolations of the accumulation-rate factor (RFA) may be made for all intermediate dose rates (Figure 3-53). RFA should not be confused with f_r (Table 3-5), which applies only to early responses within ~ 30 days after high-intensity exposure.
5. The RFA values taken from Figure 3-53 may be applied to the space-radiation dose (D) in the general equation (3) to derive a value for RES that allows for differences in progressive bone-marrow injury as a result of differences in dose-accumulation rate. It has been suggested that, for extended missions, the acceptable mission-accumulated exposures be set on the basis of the lowest dose rate (1 rad/day or less) (see Table 3-66). This recommendation is consistent with standard practice in occupational radiation protection. In contrast to early responses where the standard exposure situation has always been the high dose rate producing maximum effect, the standard for protracted low dose-rate exposures has always been that associated with minimum effectiveness. Therefore, RES for progressive bone-marrow injury will only be subject to upward adjustments by multiplying the space dose (D) by RFA (which is always ≥ 1) to allow for increasing effect as dose rate increases above 1 rad/day. As dose rate and dose accumulation are protracted, expression of bone-marrow injury approaches that of late or delayed responses. It seems, therefore, that quality factors for late responses (QF_L) should be used for evaluating progressive bone-marrow injury. Quality factors for late responses are given in Table 3-2 and equation (1).

It was also recommended that the contribution of daily dose increments (assuming exposure of a major portion of the bone-marrow) to the accumulated RES for progressive bone-marrow injury be evaluated as

$$RES \text{ (reu)} = D \text{ (rads)} \times QF_L \times RFA \quad (10)$$

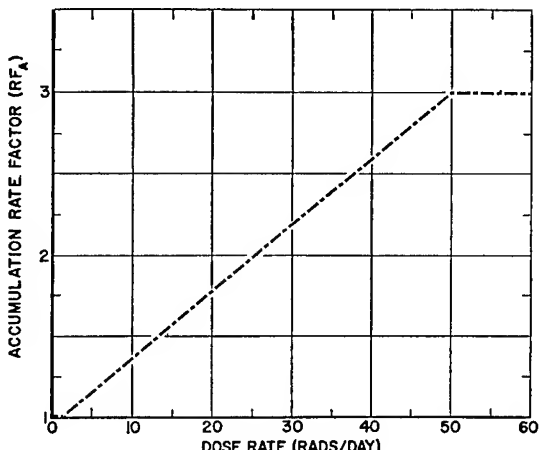


Figure 3-53

Accumulation Rate Factor (RFA) for Progressive Bone-Marlow Injury as a Function of Mean Daily Dose Rate.

(After Langham (ed.) -NAS-NRC⁽¹⁴⁵⁾)

and subtracted from a pre-established acceptable mission reference-equivalent space exposure (RES_m) expressed in reu to give a chronological record for the remaining allowable mission exposure.

An example of the manner in which a record may be kept of the accumulated marrow exposure received by a flight crew during a hypothetical 1-year mission is shown in Table 3-54. In this example, it is assumed that the

Table 3-54

Example of a Dose Accumulation Record for a Hypothetical 1-Year Mission

(After Langham (ed.)-NAS-NRC⁽¹⁴⁵⁾)

ELAPSED TIME PERIOD (days)	MEAN DOSE RATE (rads/day)	MEASURED DOSE (D) RECEIVED (rads) ^a	ESTIMATED RES RECEIVED ^b (reu)	ALLOWABLE RES_m REMAINING (reu)
		RFA		
0	—	—	—	250
0-1	10	10	1.4	236
2-150	< 1	15	1	221
151-152	20-30	45	2	131
153-364	< 1	20	1	111
365	15	15	1.5	89
TOTAL		105	162	

^aAt 5-cm depth, tissue-equivalent; total-body exposure.

^b Q_{RF_L} assumed to be unity.

acceptable RES_m , established on the basis of a risk-versus-gain philosophy, was set at 250 reu. It is assumed also that exposure involved two traversals of the geomagnetically trapped radiation fields, continuous low-level background radiation (~ 0.1 rad/day), and interception of one major solar-flare even on the 151st day. The example illustrates how such a chronological record may give some feeling as to the progressive bone-marrow exposure status of the crew during an extended mission.

The uncertainties in evaluating the risks from space-radiation exposure increase disproportionately with increasing mission duration. For missions up to 30 to 60 days, risk evaluation is based on a reasonable amount of factual information. For missions beyond 1 year, evaluation becomes more and more a matter of judgment. In an effort to provide some guidance for long-duration missions, suggestions of annual exposure-accumulation factors are given in Table 3-55. The factors are given as a set of multiples of a 1-year exposure on the assumption that the 1-year exposure is in the range of 200 to 300 reference equivalent units (reu). The factors are selected on the judgment that any derived RES values will produce no clinical signs or symptoms of hematological injury (such as infection, hemorrhage, fatigue, or fever) if exposure is generally distributed or fractionated over the indicated time periods. The factors do not increase in direct proportion with time; they drop away from simple proportionality to allow for uncertainties of damage to recovery mechanisms and for possible cumulative effects of other stresses associated with space flight.

Table 3-55
 Examples of Exposure-Accumulation Factors or Multiples
 of the 1-Year RES^a for Missions of Specified Duration
 (After Langham (ed.)-NAS-NRC⁽¹⁴⁵⁾)

MISSION DURATION (years)	MULTIPLE
1	1.0
2	1.8
3	2.4
4	2.8
5	3.0

^aAt 5-cm depth, tissue-equivalent; total-body exposure.

The NAS-NRC Panel believes that present knowledge permits a limited prediction regarding tolerance to progressive bone-marrow injury. Although it may be possible to judge from existing experience when a population is approaching the limits of its tolerance (the point where overt signs and symptoms may appear), there is no way at present to predict individual variations in sensitivity or distribution of sensitivities in the population. The variance of the population is an extremely important parameter of any quantitative prediction, and present knowledge is far from adequate. In general, the variance may be a function of age, dose rate, total accumulated dose, post-irradiation time period, radiation quality, presence of other physiologic stresses, and particular tissue or system involved. Since most or all of these factors will be variables in space flight, quantitative and accurate predictions will not be possible. With the above considerations in mind, the consensus of the Panel is that a safety factor or uncertainty factor (as the case may be) of 2 may be inherent in the exposure-accumulation multiples given in Table 3-55. As exposure and time accumulate, the safety factor becomes more of an uncertainty factor because of the gradual shift of the response pattern into the late-injury mode. The limiting consideration, therefore, is ultimately the extent to which long-term risks are acceptable.

Although it is not possible to avoid all risk of radiation injury, signs and symptoms of early and intermediate injury to the blood-forming system can be selectively avoided by controlling the exposure-accumulation rate. However, the probability of manifestation of late radiation injury and general life-shortening will increase in proportion to the total accumulated exposure.

LATE OR DELAYED EFFECTS OF RADIATION

Late or delayed manifestations of radiation damage are those that do not appear until after a latent period of months, years, or the remaining life span of the individual. These effects are nonspecific in that they cannot be correlated to any particular radiation exposure. Lack of correlation between a particular dose and ultimate manifestations of effect arises partly as a result of the relatively long latent period before appearance of injury and

partly because the effects from continuous exposures, multiple exposures, or both are additive, but not necessarily in a 1:1 ratio in their final expression.

Late responses in what would appear to be a reasonable order of relative importance to manned space flight are changes in the ocular lens, permanent impairment of skin, general life-shortening, increased incidence of leukemia and other neoplastic disease, and genetic manifestations. The genetic manifestations differ from the others in that they affect the progeny of the irradiated individual rather than his health or faculties. The others are manifestations of cumulative somatic injury.

In general, late (or delayed) effects are qualitatively the same, regardless of the nature of the radiation and whether exposure is continuous, intermittent, or from a single high-intensity dose. Although modified quantitatively by a variety of factors (including dose rate or protraction, depth-dose distribution, portion and region of the body irradiated, and nature and quality of the radiation), some delayed effects (life-shortening, increase of incidence of malignancy, and genetic manifestations) are considered nonthreshold phenomena and impose on an exposed individual a probability of response in proportion to the total accumulated dose. In this case, the associated actuarial risks provide both the necessity and the basis for limits to radiation exposure in long-duration missions and space-flight careers.

Ocular Lens

Either acute or chronic exposure of the ocular lens will result in opacities which may go on to true cataracts depending on dose (51, 52, 145, 168). The time of appearance is highly variable and may range from as early as 6 months to many years after exposure. The higher the dose, the earlier the appearance and the greater the degree of impairment. Because of the variability of clinical and accidental exposures, no definite response-probability values for production of lens opacities can be assigned to specific radiation doses. About 150 to 200 rads of reference-quality radiation is the minimum cataractogenic single-exposure dose, and some lessening of effect appears to result from dose protraction over a period of at least 2 to 12 weeks. This is summarized in Figure 3-56.

It appears also that a single dose of about 650 to 750 rads of reference radiation may have a cataractogenic probability approaching unity, 50 percent of which may be progressive, resulting ultimately in impaired vision. The slope of the time-dose response curve between single (1-day) exposure and exposure protracted over an average time of ~7 weeks suggests a ratio of protracted dose to single dose of ~2 for the doses required to produce the same level of response. The dose protraction factor for lens opacities is, thus, much less than for other tissues (79, 145, 161).

The incidence of cataract after a given dose level fractionated over 2 to 12 weeks is shown in the histogram of Figure 3-57. The available data suggest a log-normal dose-response distribution between the probability limits and predict that doses between 550 and 950 rads (average 800 rads) delivered over periods from 2 weeks to 3 months may produce an opacity in

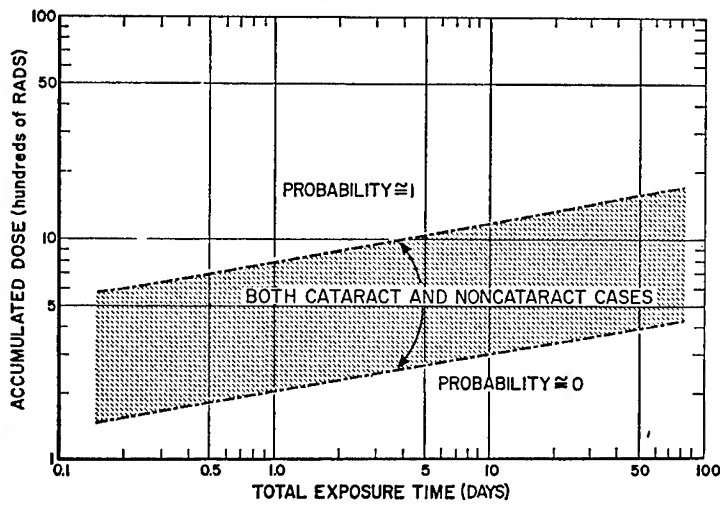


Figure 3-56

Time-Dose Relationship for Production of Late Radiation Changes in the Ocular Lens, Suggesting Probability Limits of $0 \leq p \leq 1$.

(After Langham (ed.)-NAS-NRC⁽¹⁴⁵⁾

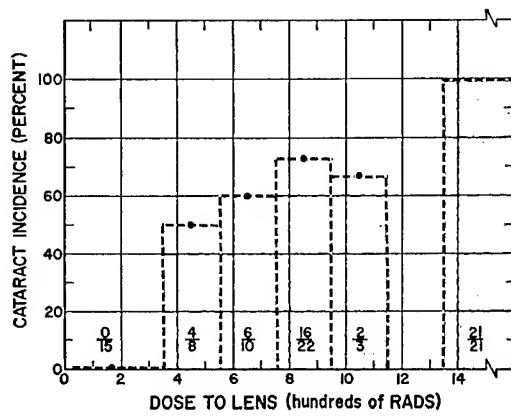


Figure 3-57

Incidence of Late Lenticular Changes in Patients Who Received Photon Exposures Fractionated over 2 to 12 Weeks.

(After Langham (ed.)-NAS-NRC⁽¹⁴⁵⁾ from data of Merriam and Focht⁽¹⁶⁷⁾)

about 70 percent of those exposed. Of these, about 30 percent may be progressive and eventually result in impaired vision. On this basis, one might estimate that about 20 percent of flight crews who receive lens exposures of ~ 800 rads of ionizing radiation (equivalent in effectiveness to 200-kVp x-rays) in an interval from a few weeks to about 3 months may develop clinically significant cataracts at some time during their lives. Table 3-58 represents a probabilistic summary of the dose response relationship after acute and protracted radiation.

Review of animal and human data suggests an RBE of at least 10 for late lenticular effects from recoil protons of neutrons under conditions of protracted

Table 3-58

Suggested Absorbed Doses^a of Reference Radiation for Production of Late Changes in the Ocular Lens

(After Langham (ed.)-NAS-NRC⁽¹⁴⁵⁾)

PROBABILITY OF RESPONSE	HIGH-INTENSITY SINGLE (1-DAY) DOSE (rads)	PROTRACTED DOSE C (rads)
Minimal ($p \geq 0$)	150	300
Median ($p \approx 0.5$) d	300	600
Maximal ($p \leq 1$)	650	1,300

- a. Point of interest for dose estimation, 3-mm depth.
- c. Dose protracted over 7 weeks or longer.
- d. Assuming log-normal distribution of response.

exposure (1, 166). Demonstrable observations of an increase in the RBE of high-LET radiations with increasing dose protraction indicate that the slope of the time-dose curve approaches zero with increasing LET. It is advisable, therefore, to use the QF-LET relationship given in Table 3-2 and the local LET spectrum at the depth of the lens when considering delayed cataractogenic effects of space-radiation exposure. Curves have been recently published on specific QF values for different proton energies in lenticular radiation (75). It has been noted that protons and neutrons may tend to produce more vacuolar degeneration of the lens in animals than do other forms of radiation (211).

Topical nonuniformity of dose distribution is highly important and suggests the feasibility of locally shielding the eyes to lessen the probability of late lenticular changes from space radiations. Because of the rapid drop-off in dose and local LET of the principal sources of space-radiation exposure, nonuniform depth-dose distribution may also be significant. The average depth to the surface of the lens is estimated as ~3mm. Dose evaluation for late cataractogenic-effects, therefore, should take into consideration dose and local QF at a depth of 3mm (145).

The RES for late changes in the ocular lens may be evaluated by the expression

$$\text{RES (reu)} = D \text{ (rads)} \times QF_L \times F_{pr} \quad (11)$$

where D is the space-radiation dose and F_{pr} is the protraction factor equal to unity for protraction times of 7 weeks and greater and linearly increasing to 2 with decreasing time to 1 day. As an example, if the pre-established acceptable exposure risk for a mission of 7 weeks or longer ($F_{pr} = 1$) corresponds to minimal probability of lens response (RES = 300 reu), and that exposure is anticipated to a space radiation having a predicted mean QFL of 3, the allowable space-radiation dose (D) would be 100 rads. If delivered in a 1-day exposure, however, the allowable dose would be only 50 rads.

It should be kept in mind that the greater the level of exposure, the greater will be the probability that any cataracts produced will be progressive and the shorter will be the latent period before development.

Chronic ulcerative lesions and opacification of the cornea can result from 100 kVpx-rays in the 2000 - 3000r range, from lower doses of soft x-rays (<75 kVp), and from β radiation of $<1-2 \times 10^6$ eV. (50, 220). Retinal vascular occlusions have also been reported following x-radiation in excess of that necessary to cause lenticular changes (50).

Permanent or Late Skin Effects

In the review of early skin effects (see Table 3-45 and discussion of Figure 3-46), it was mentioned that clinically evident permanent changes in the skin occur regularly after radiation doses that yield at least a dry desquamation response. Furthermore, induction of skin malignancy is known

to be one of the late or delayed oncogenic effects of single high-intensity and protracted radiation exposure. The characteristic late radiation changes in the skin are referred to collectively as "chronic radiodermatitis" and consist of telangiectasia, loss of hair, pigmentation, parchment-like appearance with atrophy, keratosis, malignancy, and sensitivity to mild trauma. The latter, combined with decreased capacity for healing, predisposes to chronic ulceration. As with other late effects, manifestations of chronic radiodermatitis do not occur until many months or many years after exposure, and their frequency and severity are proportional to the accumulated dose to the exposed area.

Although minimal delayed radiation changes in the skin are not serious per se, there is a general feeling by some that severe or symptomatic radiodermatitis is a dangerous lesion because it is progressive and may eventuate in carcinoma of the skin if the affected person lives long enough (43, 204). The most common type of skin tumor resulting from radiation exposure is squamous-cell carcinoma, although basal-cell carcinomas occur frequently and appear to occur more frequently in the less severe and more superficial type of radiodermatitis. The time between the first evidence of skin changes and appearance of the cancer can average 7 years, with a variance of 1 to 25 years. Tumors developing in irradiated skin appear to possess a relatively low degree of malignancy with infrequent metastases. Rates of ultimate mortality reported from radiation cancer of the skin, however, have ranged from 5 to 25 percent (145, 204).

Clinical experience has dealt largely with small exposure areas. No observations are available on delayed consequences of whole-body skin exposure. Data may become available with time as a result of total-body electron exposure in the treatment of extensive skin diseases. Whole-body exposures of primates to >900 rads of 32 mev protons, has lead, as early as 1 year, to severe fibrosis and contracture of the skin with immobilization and starvation as the cause of death (178, 195). In these primates, no tumors have been seen after 2 1/2 years.

Depending on total dose and dose protraction, late radiation changes in skin vary from minor telangiectasia of cosmetic interest only to development of the most serious sequela, metastatic carcinoma. However, quantitative dose-response relationships for the various manifestations of chronic radiodermatitis do not exist. There seems to be a correlation, however, between production of an early desquamation reaction and manifestations of minimal late effects (telangiectasias, mottled pigmentation) in that clinically-evident permanent changes are observed regularly after early desquamation. Based on this premise, the single-exposure dose-response relationship for production of minimal late changes in the skin would be parallel to and approximately the same as that for early moist desquamation shown in Figure 3-46. Indirectly at least, there are observations that support the above contention (145, 266). Back extrapolation from protracted dose schedules suggest a single-dose equivalent of ~2,800 rads (small exposure fields, ~10 cm²) for production of 50 percent probability of late necrosis (82, 145, 273).

As with early desquamation, the total dose required to produce chronic radiodermatitis should show parallel dependence on dose protraction and fractionation resembling that for early responses. This is seen in the extrapolations from tenuous observations in Figure 3-59 (82, 145, 266, 273). The late effects appear less sensitive to protraction than early effects. It should be emphasized, however, that, with sufficient protraction, enough dose can accumulate to produce severe radiodermatitis, including cancer, without ever producing any early response.

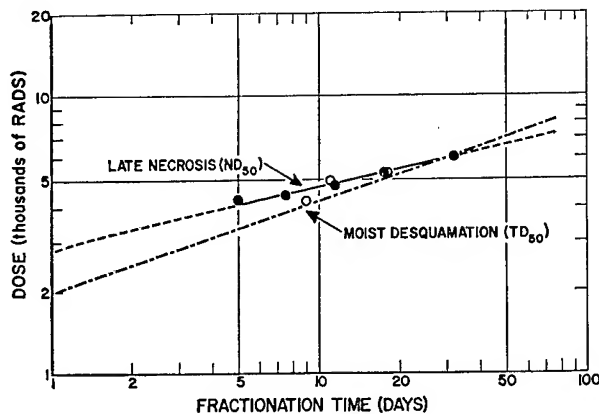


Figure 3-59

Comparison of the Time-Dose Curves for Late Radiation Necrosis and Early Moist Desquamation.

(After Langham (ed.)-NAS-NRC⁽¹⁴⁵⁾ from the data of Sulzberger et al⁽²⁶⁶⁾, Traenkle and Mulay⁽²⁷³⁾, and von Essen⁽⁸²⁾)

Table 3-60 probabilistically summarizes the suggested absorbed doses for production of late skin necrosis. As with ocular-lens changes, the time-dose response curve for skin necrosis suggests a decreasing effect with increasing dose protraction, such that the ratio of protracted dose (approximately equally distributed in daily increments over ~7 weeks or longer) to single dose (1 day) required to produce the same probability of response is ~2.3.

Table 3-60

Suggested Absorbed Doses^a of Reference Radiation for Production of Late Skin Necrosis.

(After Langham (ed.)-NAS-NRC⁽¹⁴⁵⁾)

PROBABILITY OF RESPONSE (percent)	HIGH-INTENSITY SINGLE (1-DAY) DOSE (rads)	FRACTIONATED OR PROTRACTED DOSE ^b (rads)
10	2,000	4,600
50	2,800	6,400
90	3,600	8,200

a. Point of interest for dose estimation, 0.1 mm depth; area exposed <150 cm².

b. Dose protracted over 7 weeks or longer.

The late skin effects are very sensitive to the LET factor. Fast neutrons are at least 3 to 5 times as effective as 200-kVp x-rays in producing late radiation sequelae and even more effective in producing late responses than early ones (263). It is suggested that the QF in Table 3-2 be used for late skin effects and that an area effectiveness factor (F_a) of 1.25 for areas >150 cm² be used in risk evaluations. The recommended dose protraction

factor F_{pr} is 1 for protraction times of 7 weeks and longer and the F_{pr} linearly increases to 2.3 with decreasing time to 1 day. Equation (11) may be used to calculate the RES for late effects with these QF and F_{pr} factors. As an example, if the space-radiation dose (D) to an area of $> 150 \text{ cm}^2$ accumulated (in approximately daily increments) during a mission of 7 weeks or longer ($F_{pr} = 1$) is 1,000 rads of radiation with an average QFL of 3, the RES would be 3,750 reu. Comparison of this value with the fractionated dose-response relationship indicated in Table 3-60 (on the basis of 1 reu = 1 rad of reference radiation) suggests about a 3 percent probability of necrosis or chronic radiodermatitis. If fractionated more or less equally over 25 days ($F_{pr} = 1.65$), the probability of necrosis would be of the order of 50 percent (RES = 6,200 reu). In this case, however, the appearance of early skin responses would definitely have been mission-limiting. In evaluating risk from late skin effects, it should be kept in mind that from 5 to 25 percent of cases of chronic radiodermatitis (in small areas) progress to the malignant stage, and that the area damaged may have a considerable influence on the probability of malignancy since the number of potential cells exposed to malignant conversion is proportional to area. It is not clear if there is a specific body site which shows predilection to chronic necrosis or malignant change (204, 273).

General Life-Shortening and Carcinogenesis

Life-shortening

A convincing body of data indicates that a statistical sample of an animal population exposed to radiation has a shorter median life expectancy than does an unirradiated sample of the same population. The data further show that the degree of life-shortening is a function of accumulated dose. If a group of animals receives a dose of radiation insufficient to cause early lethality, the animals appear to recover completely. Blood counts return to normal, gastrointestinal symptoms disappear, and weight returns practically to normal. Organ function tests, such as liver or kidney, are within normal limits. Nevertheless, on a statistical basis, these animals die sooner than their unirradiated controls (64, 121, 133, 137, 145, 152, 196, 261). Generally, no new or different disease syndromes have been observed as late effects in irradiated animals, and all causes of death so far studied, with only minor exceptions, are accelerated by radiation. Symptoms of delayed radiation effects appear to be so much like those of aging that the syndrome has often been termed "radiation-induced aging," and typical signs of aging confirm this impression.

There is little reason to doubt that radiation exposure would have the same qualitative effect on life expectancy and general well-being of man. With regard to space crews, selection of dose limits for early effects automatically establishes certain probabilities of general life-shortening and other late responses, and forces consideration of placing limits on the associated actuarial risks as they would apply to long-duration missions and space-flight careers. No definitive data exist on the radiation dose-response relationship for general life-shortening in man, but useful data may eventually result from the Atomic Bomb Casualty Commission's studies of the Japanese atomic-bomb survivors. At present, however, it is necessary

to rely almost entirely on animal observations, tenuous extrapolation from experimental animals to man, and limited data on the mortality rates of several age-cohorts of American radiologists.

The degree of life-shortening caused by a single radiation dose delivered to young adult rats or mice is nearly a straight-line function of dose. There is a decrease in mean survival time of about 0.04%/rad with a range of 0.01%/rad to 0.10%/rad. If it is assumed that the percentage of life-span decrement per rad is the same in all species, then a single high-intensity dose of 1 rad of x or gamma radiation would have a statistical life-shortening effect in man of ~10 days (45). Alternatively, if it is assumed that the single-exposure LD₅₀ dose for man is 300 rads and that equal fractions of the LD₅₀ for the different species produce the same percentage life-span loss, a high-intensity absorbed dose of 1 rad at the midline would have a life-shortening effect in man of ~20 days (65). It may be assumed also that flight crews (in the 30- to 40-year age interval) at the time of exposure will have only about one half their life expectancy at risk. On this basis, the life-shortening effect per rad may be modified downward from the above values. A controversy exists over the methods of extrapolation from animals to man and over whether life-shortening from single high-intensity exposure increases linearly or nonlinearly with increasing dose (152, 229). It can probably be assumed arbitrarily for space-flight applications that the actuarial risk from high-intensity exposure to radiations with an LET of 3.5 keV/ μ and below is of the order of 10 days/rad (145). About four times more gamma radiation is required at low dose rate than at high dose rate to produce comparable statistical life-shortening in mice. Application of a factor of 4 to the assumed life-shortening value of ~10 days/rad for high-intensity exposure in man gives a statistical decrement of ~2.5 days/rad for low-dose-rate exposure. This value is in general agreement with other estimates which have been made for man of 1 day/rad for continuous exposure at dose rates not in excess of ~0.5 rad/day (86). If the dose rate is increased above 0.5 to 1 rad/day, its effectiveness on life-shortening may be expected to increase, finally reaching a figure about four times the low-dose-rate value when the dose is received promptly. The dividing line between acute and chronic exposure is not known, but there is almost certainly a gradual transition from one to the other. Present knowledge of rate-dependence of life-shortening effects would hardly seem to justify attempts to refine the quantitative influence of dose protraction and fractionation beyond that given above. Table 3-61 and Figure 3-62 show the suggestion of the NAS-NRC Panel on dose protraction factors in life-shortening (145).

Comparison of fission neutron vs. gamma ray or x-ray effects suggest that the life-shortening effectiveness of low-LET radiation is more highly dose-rate dependent than high-LET radiation (145). The RBE of low-LET neutrons increases from 2 to 10 as protraction is prolonged (145). For the typical space proton dose and dose rate behind nominal shielding at the probable site of the life-shortening effect, the bone marrow, a QF = 1 can probably be assumed (3, 105, 106, 145). Table 3-63 represents a current estimate of quality factor for high-LET radiation of cosmic ray type (243). Applying upper limit estimates to total body dose for man of 40 m rad/day and 120 m rems/day for 27 incidence of the full galactic flux at solar minimum, it can be calculated that the life of a crewman will be shortened by about 1/4 a day for every day he spends in space under these conditions (238, 245).

Table 3-61
 Suggested Reference Radiation Dose-Response Relationships for General
 Life-Shortening and Increased Incidence of Leukemia
 (After Langham (ed.)-NAS-NRC⁽¹⁴⁵⁾)

RESPONSE	HIGH-INTENSITY EXPOSURE ^a	LOW-INTENSITY EXPOSURE ^b
Life Shortening ^c	~ 10 days/rad	~ 3 days/rad
Leukemia ^c	2-4 per 10^6 man-yr/rad	1-2 per 10^6 man-yr/rad

- a. Assumed to be 50 rads/day and greater.
- b. Assumed to be 1 rad/day and less.
- c. Site of interest for dose estimation, 5 cm depth; whole-body exposure.

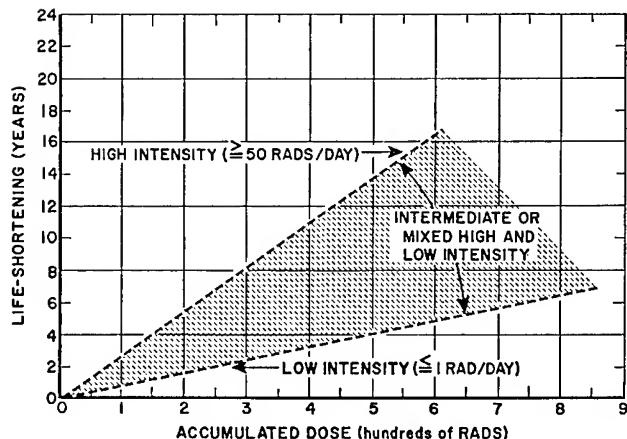


Figure 3-62

Relationship of Accumulated Dose and Intensity of Reference-Quality
 Whole-Body Radiation to Life-Shortening Probability

(After Langham (ed.)-NAS-NRC⁽¹⁴⁵⁾)

Table 3-63
 Estimates for Life-Shortening of Man from Exposure to High-LET Ionizing Radiation
 (After Schaefer⁽²⁴³⁾)

Type of Radiation	Life Shortening, days/rad	
	Acute Exposure	Chronic Exposure
Low LET (Electrons, α - or gamma rays)	12	3
High LET (Low-E protons or neutrons, medium and high-E heavy nuclei)	24	24
Extremely high LET ("Microbeams" of heavy nuclei enders)	?	?

The induction of leukemia and other neoplastic diseases contributes specifically to the statistical life-shortening effect of cumulative radiation exposure (121). Although this problem has been under study since the early 1900's there are still very few quantitative dose-response data available for man. This is not due entirely to lack of information, but rather, to the complex statistical and actuarial aspects of the problem. Since no new or unique types of cancer are produced by irradiation, one must seek differences in either the age of appearance, the frequency of occurrence, or both. Since most causes of death are increasing exponentially with age beyond young adulthood, it becomes difficult to be certain without careful statistical analysis when a change in frequency may be attributed to some factor other than sheer chance. In addition, most human data involve fairly small groups-at-risk, and, therefore, the probability of detecting a significant age-specific death rate for a given malignancy is very small. The present Atomic Bomb Casualty Commission (ABCC) studies exemplify many of these statistical difficulties.

Leukemia is one neoplastic disease that characteristically occurs significantly earlier in life in irradiated populations than in nonirradiated populations and, depending upon dose, at a significantly higher percentage (121, 277). Several studies have substantiated the higher-than-average number of deaths from leukemia in irradiated human populations. The most significant data are those obtained from the survivors of the Hiroshima and Nagasaki bombings (12, 40). Exposure in both cities involved prompt weapon-quality gamma radiation with some fission neutrons, the neutron component being higher in Hiroshima. The predicted excess death rate lies between one and two deaths per million exposed per rad per year (1 to 2 per 10^6 man-years/rad). According to present indications, this rate is likely to be maintained for at least 15 to 20 years after exposure.

All other epidemiologic studies of irradiated adult humans also give strong evidence of man's sensitivity to the leukemogenic effect of ionizing radiation (277). These studies include a group of adult British males given therapeutic irradiation of the spine for ankylosing spondylitis (58), the study of professional radiologists, and the evaluation of Danish cancer registry data (84). Virtually all induced leukemias are of either the acute granulocytic, acute lymphocytic, or chronic granulocytic forms. The incidence of chronic lymphocytic leukemia is not detectably increased by radiation. Recent suggestions that the incidence of multiple myeloma, lymphosarcoma, and Hodgkin's disease is higher among the proximally irradiated Japanese (within 1,400 m of the hypocenter) should be noted with caution, since only between one and four such cases have been observed (5). However, a survey of leukemia deaths among U.S. radiologists, does offer evidence in support of a significantly increased mortality ratio from multiple myeloma (151). The latent periods for acute forms of leukemia and for chronic leukemia have been fairly well defined as 1 to 5 years and 1 to 10 years, respectively (85). The duration of an elevated death rate from leukemia is not absolutely defined and may or may not exceed 15 years (31, 58).

There is evidence from several sources that radiation to the thyroid and pituitary gland may increase incidence of thyroid adenomas and carcinoma (7, 8, 9, 155, 212, 257, 272). The dose-response relationship is not clear.

Although risk estimates for thyroid cancer have been made for the case of children exposed to single doses, no valid estimate is available for the irradiated adult. The estimate for children is similar to the leukemia risk (about 1 per 10^6 man-years/rad), but the negative data for adults suggest that the risk may be somewhat lower for that group (145).

The evidence for skin cancer has been covered above. Osteogenic sarcoma also appears to follow radiation. The present consensus is that, if no complicating bone pathology is present, at least 3,000 to 4,000 rads are required to induce bone cancer (33, 132). No risk factor can be derived from the data since they are based on case-history reports and not on epidemiologic surveys. For the same reason, the minimum sarcoma-inducing dose cannot be considered definite. Many other unfrequent tumors have been reported in following radiation of man and animals (145). For example, the ratio of mortality from all cancers among U. S. radiologists is 40 percent higher than among a non-exposed medical-specialty group (252). Unfortunately dose-response relationships are not clear.

In the case of neutron irradiation of high LET, there appears to be much less recovery of chromosome damage and a concomitant higher RBE for tumor formation (64). High LET radiations have not unequivocally demonstrated a higher tumor induction rate than that normally associated with their acute or chronic lethal effectiveness. Soviet studies suggest that protons may have a higher carcinogenic effect in small rodents than equivalent doses of x-ray or gamma radiation (270). Until more specific knowledge is available, it is recommended that the QF-LET relationship proposed by the NCRP (Table 3-2) be used to estimate the risk of malignant disease following exposure to space radiations. The dose rate sensitivity of carcinogenesis appears to be greater than that for life-shortening (40, 121, 252). However, the exact protraction factors are far from clear. Table 3-61 and Figure 3-64 present the proposed relationship for space radiations. Since none of the human data are sufficiently accurate or extensive to favor any one of the dose response models over the other, the simplest linear relationship has been accepted as adequately descriptive of existing data, although it should be appreciated that the present evidence for man and animals does not generally support simple linearity (46, 47, 151). In view of these uncertainties in dose-response curves, any errors in risk estimate will tend to be in the conservative direction (that is, to overestimate response), particularly at doses below 100 rads (145).

The organ specificity, region, area, and volume factors for carcinogenesis are far from clear. Organs in children appear generally more sensitive than those in adults. Astronaut age of predominantly 30 to 40 will certainly reduce the probability of thyroid neoplasia, may reduce the possibility of cancer involving the skeletal, connective, and integumentary tissues, but is not likely to modify the probability of leukemia.

Since the relationships of Table 3-61 and Figures 3-62, 3-63, and 3-64 may be modified by such factors as radiation quality, dose distribution, and dose rate, any attempt to refine risk evaluations by adjusting the space-radiation dose to give reference-equivalent space exposure (RES) is probably an unjustified refinement in view of the large uncertainties in the dose-response

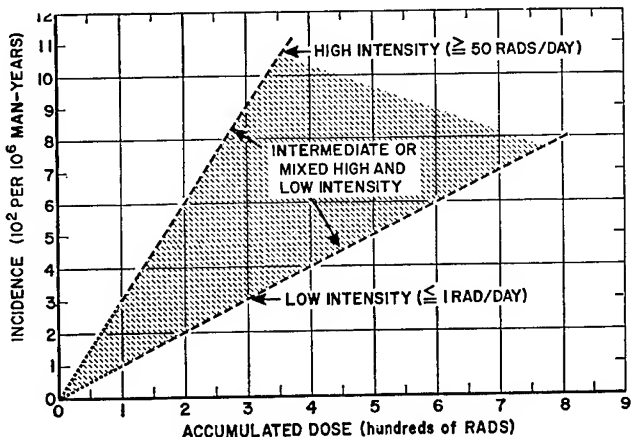


Figure 3-64

Relationship of Accumulated Dose and Intensity of Reference Quality Whole-Body Radiation to Increased Probability of Leukemia.

(After Langham (ed.)-NAS-NRC⁽¹⁴⁵⁾)

relationships. It is possible, however, to make such adjustments of RES and to record chronologically the life-shortening and leukemia-risk status of a flight crew in a manner analogous to that suggested for progressive bone marrow injury, using Equation (10) and Figure 3-53. If it is assumed that the effective tissue depth for generalized late effects is 5 cm, QFL of the major space radiations (inside current spacecraft shielding) for production of life-shortening and leukemia will be approximately unity. QFL , however, may be estimated from the calculated local LET using Equation (1). A dose-rate accumulation-effectiveness factor (RFA) for each daily-dose increment may be taken from Figure 3-53. To evaluate the probabilities of life-shortening and increased leukemia incidence, it is necessary only to multiply RES (reu) for each daily increment by the respective probability values for low-intensity reference-radiation exposure shown in Table 3-61 and sum the incremental probabilities.

Genetic Manifestations

The reports of the National Research Council Committee on Genetic Effects of Atomic Radiation present a clear review of general knowledge of the genetic effects of radiation exposure and stress the responsibility of all public and private agencies to keep the radiation dose to the population below their recommended value of 10 rads/generation, or about 0.3 rads/year (145, 180). Subsequent recommendations by the International Commission on Radiological Protection suggest a dose of 5 rads in 30 years, or about 0.17 rad/year (121). The potential radiation exposure of astronaut crews should not make a significant contribution to this average per capita figure (145). The individual astronaut will undoubtedly be subject to gonad doses well above those normally allowed persons operating under the exposure limits established for routine occupational radiation hazards. The concept of permissible dose as that which entails a negligible risk of severe somatic or genetic injury has to be set aside when considering the space-radiation problem (145, 227). Even so, knowledge of the radiation dose received by the gonads permits an estimate of the probability of mutation in the spermatogonial cells and of its expression in the offspring. Such a calculation assumes

reasonable knowledge of the following parameters (the values given in parentheses are based largely on animal data):

1. The mutation rate per rad/gene ($\mu = 5 \times 10^{-8}$)
2. The number of genes per haploid set ($n = 10^4$)
3. The probability of expression of the new mutation in the first generation heterozygote ($s = 5 \times 10^{-2}$)
4. The gonad dose (D)

For example, assuming a dose of 100 rads,

$$(5 \times 10^{-8}) (10^4) (5 \times 10^{-2}) (10^2) = 2.5 \times 10^{-3}$$

would be the probability of a new mutation in the immediate offspring. Such probability statements must be accepted with considerable reserve, but they do serve to indicate that the genetic risk to the individual astronaut is not unacceptably high (145). Since the mutation rate in the advanced germinal cell stages of the mouse is twice or three times that observed in the spermatogonia, it can be recommended that conception of offspring be avoided during the postflight period in which irradiated postgonial cell stages are still present (227).

Dose rate and fractionation effects are not yet clear (225, 227). Low dose-rate exposures are not as effective as high-intensity exposures in inducing mutations. In mice, the difference may be a factor of 4 to 10 and apparently is operative at dose rates of less than 0.1 to 1.0 rad/min. However, this dose-rate dependence is observed only in the immature germ cells, not in spermatozoa. This finding is consistent with the concept that metabolic activity is a prerequisite to repair and that low dose-rate exposure, as with somatic injury, permits concurrent repair in conjunction with less damage to repair mechanisms (172). Present data on the effects of fractionation are limited to studies on mice using high dose rates and exposure intervals where high mutagenic sensitivity is known to exist. This sensitivity itself is of some concern, however, since existing data suggest that a fractionation interval of about 1 day causes the response to a second exposure to be greater than the normal expectation for that dose (224). Widely fractionated, low dose-rate exposures (comparable to most in-flight possibilities) would probably have approximately the same mutagenic effects as continuous exposures to low dose rates, but these rate and interval parameters have not yet been tested. There is a significant increase in quality factor with increasing LET, especially in protracted exposures, but the exact relationship is not clear (226, 251).

As a general operating principle for the next few decades, the NAS-NRC Panel believes that the probability of such late responses as general life-shortening and increased likelihood of malignancy may be considered of secondary importance in evaluating the risks of manned space flight (145). This attitude contrasts sharply with the manner in which occupational risks are evaluated, where late effects are of primary importance. The relative sizes of the astronaut and occupational groups provide the major reason for attaching less importance to late effects of radiation. The astronaut population

may be about 30 to 50; occupational groups may comprise hundreds of thousands of humans. Such late radiation injury is measured in statistical terms - an increase in age-specific death rate, a reduction of after-expectation of life, an increase in incidence of malignancy. Nevertheless, an awareness must be maintained in respect to the astronaut population of the late somatic and genetic manifestations of radiation injury. As noted earlier, selection of acceptable RES values for short-term responses of the gastrointestinal and hematopoietic systems will automatically entrain certain probabilities for occurrence of leukemia, generalized life-shortening, and other late manifestations.

Establishment of a career dose appears premature. If establishment of such a dose is a necessity then some value or set of organ-specific values must be established as acceptable integrated annual dose increments. Previous attempts along this line have been made, but have been thought by others to provide unrealistically low values that have no meaning or relationship to the biological effects they are designed to protect against (104, 147, 210). There is no obvious interim approach to the problem of developing radiation guides for evaluating long-term risk without also establishing career-exposure limits. Since a lack of both radiobiological knowledge and operating experience precludes the establishment of such dose limits at the present time, an alternate suggestion is offered as an approach to the question of general life-shortening. The long-term radiation risk may be compared with the accepted risks associated with piloting high-performance aircraft. It has been estimated that the latter occupation is characterized by a life-shortening probability of approximately 10 years. If this risk is assumed to be additive with the radiation hazards, the question then becomes how much additional probability of life-shortening may be acceptable. This is covered in the section on dose limits, below.

Soviet approaches to radiation safety in space flight have been reviewed (192).

SECONDARY FACTORS IN RADIATION INJURY

Environmental Factors

A number of environment factors in space flight having potential interaction with radiation differ markedly from normal terrestrial conditions. These include weightlessness, a pure-oxygen environment, periods of vibration and thermal load, and brief periods of excessive g loads. Unfortunately, there are few data on these interactions in humans. Animal studies suggest the interactions noted in Table 3-65. In this table, additive means simple summation of effects; synergistic means an interaction that produces a greater than additive effect; antagonistic means an interaction that produces a less than additive effect; and neutral means no detectable effect of the nonradiation stress alone or in combination. Synergistic potentials predominate and suggest that the conservative end of any proposed radiation dose-effect range should probably be used for first approximations in the hazards analysis.

Though animal data supporting these conclusions are available, it should be stated that this Table represents a tentative appraisal of the problem and will require revision as new data are made available (145, 294).

A synergistic factor frequently raised in considering the design of radiation shielding is the effect of space-cabin atmosphere (222). A parallel has been drawn between the mechanism of tissue damage seen in oxidation syndromes that follow radiation (221). High pressure of oxygen has been

Table 3-65
Summary of Stress Combinations and Types of Interactions
(After Langham (ed.)-NAS-NRC(145))

COMBINED STRESSES	INTERACTION
Radiation-noise	Neutral to synergistic
Radiation-hypothermia	Neutral to synergistic
Radiation-hyperthermia	Neutral to synergistic
Radiation-hypoxia	Synergistic (antagonistic for only brief periods during exposure)
Radiation-hyperoxia	Neutral to additive
Radiation-physiological factors	Synergistic
Radiation-emotional factors	Indeterminate
Radiation-vibration	Neutral to additive to synergistic
Radiation-acceleration	Antagonistic to neutral to synergistic
Radiation-weightlessness	Additive to synergistic
Radiation-vestibular factors	Neutral to additive
Radiation-emergency situations	Neutral to synergistic
Three-stress interactions	Indeterminate

used to sensitize tissue to radiation during x-ray therapy for cancer (107). Protective effects of antiradiation drugs against oxygen toxicity have also been shown. At present there appears to be no requirement for the alteration of shielding calculations due to the presence of 5 psia - 100% oxygen in future space-cabin atmospheres. However, several studies suggest that some synergism may be present. It has been shown that mice exposed to 750 r of gamma radiation from cobalt 60 given at 90 r/min have a survival about 10% lower in 5 psia - 100% oxygen than in air (23). At 900 r given at a rate of 38 r/min, the synergism was much less. On the other hand, mice exposed to 800 r of 250 kVp x-rays at only 14 r/min have shown no synergism with 5 psia - 100% oxygen (136). The type, total dose, and the dose rate of radiation may be significant variables in these studies of synergism. In tissue culture, at least, there is a steady reduction of the oxygen effect with increase stopping power until its apparent abolition by radiation \geq than 3000 MeV/cm²/g (271). The exact stopping power at which the O₂ effect becomes undetectable in intact animals or isolated cells has not been established. Further research along this line is needed.

Alteration of the vestibular apparatus after human exposure to radiation has received recent study (176). Such alteration may play a significant role in degrading astronaut performance in zero g or during reentry and certainly requires further study.

Anti-radiation Therapy

The potential use of anti-radiation compounds in space operations has been recently reviewed (13, 16, 48, 145). The amino-thiols have received the most study and appear to be quite promising (13). However, the doses calculated as required for human protection are well within the human toxic range and can provide little protection against chronic or continuous radiation (13, 149, 193, 233, 265, 269, 276, 279). Much more data are required on toxicity mechanisms in humans. Maximum dose reduction for lethality is about 1.7 or 1.8, but this factor is much lower for other end points.

Other drugs such as PAPP and serotonin appear to be less effective than the amino-thiols, especially against radiation of high LET. Both MEA and PAPP protect mice against 440 MeV protons (203). Combination of different drug types has been tried with slightly more success than with individual drugs (165, 194, 269, 279, 283, 291). Combinations tend to alleviate the toxicity problem but certainly do not solve it.

Post-irradiation therapy consists of antinauseant and vomiting drugs (130, 143), intravenous fluids, anti-microbial agents, and supportive care. Leukocytes from leukemia patients (94) and bone marrow (6, 36, 59, 164) have been used with variable success in humans. The case for using autologous marrow in space operations has also been reviewed (48). Problems in obtaining sufficient amounts from each astronaut and the training of crews for administration of the marrow are superimposed on the basic storage difficulties. Cryogenic storage of blood and marrow in space is under consideration (173, 219).

Treatment of the irradiated skin with topical and oral cortisone has been tried with little success in relief of discomfort in early or late phases. In view of its penetrability and anti-radiation properties, the drug DMSO may offer some promise as a topical prophylactic against skin reactions (48).

In view of the lag times in arrival of solar flare particles after early electromagnetic warning signals and knowledge of the power-flux-time spectra of flares, it may be possible to predict the magnitude of integrated exposure expected during a flare from measurements made early in that same flare (93). In the future, prophylaxis with improved protective agents may well be tailored on a flare-by-flare basis. At the present state-of-the-art, however, prophylactic agents should not be entered into the basic hazard analysis even for acute flare exposures.

Performance After Radiation

The literature on the effects of radiation on the nervous system and behavior is large and complex (97, 111, 112, 145, 217, 282). The Soviet literature indicates many reflex changes in animals following radiation but the significance of parallel changes in humans is not clear (156, 287). Damage to the nervous system may even be the primary cause of death at very high dose levels (See Figure 3-37). The quantification of specific behavioral effects is confused by the prodromal syndrome which, by itself, can have profound

effects on behavior and yet may not involve irradiation of the central nervous system (see Table 3-36 and Figures 3-38 to 3-42). Whole body exposures of 100 to 130 rads of reference quality radiation can give fatigue, apathy, dizziness, headache, and depression which seriously alter behavior (150, 174, 207). Low doses of x-ray down to 10 rads can be detected by behavioral responses in some animals (98).

Observation of trained primates suggests that limiting mechanisms in each behavioral test may be key factors in interpretation of radiation effects. For example, protracted irradiation may tend to increase attentiveness to the immediate field of concern by depressing attention to peripheral information. Animals can continue to learn and can continue to express previously learned behavior (i.e., retained their learning) during and after considerable radiation to the head up to many hundreds or thousands of rads in short exposures. It should be remembered, however, that although the tests used involve fairly complex procedures they do not measure total performance under a wide range of circumstances. Some neurological deficits which affect behavior have followed exposure of the head to the higher doses just mentioned - often with concomitant morphologic changes (145).

Short of prolonged interplanetary flight, the microbeams of galactic radiation will probably not produce much of risk factor as far as brain, and eye damage are concerned (145, 299, 300). It is assumed the same holds true for the audiovestibular mechanism, though this is far from clear (176). Similar ignorance exists with respect to the retina where radiations of high LET may cause irreversible damage.

RADIATION DOSE LIMITS IN SPACE OPERATIONS

According to the NAS-NRC Panel, the rationale for an independent review of radiation protection in specific space flights should be reflected in the following points (145):

1. Radiation is only one of many recognized and accepted potential risks that may jeopardize the success of any flight mission.
2. Individual astronauts are carefully selected for their special skills and motivation. The application of existing standards of radiation safety established for large, occupationally exposed groups would unduly limit the ability of this small group of specialists to achieve their objectives.
3. The parameters of some space-radiation risks cannot be precisely predicted; therefore, optimal protective measures will not always be available or even feasible. Since any radiation shielding will add to the weight of a spacecraft, the reduction in risk to be achieved by the shielding must be balanced against the other uses to which this weight might have been put.

4. Since flight missions may vary in both duration and radiation exposure, the probability and importance of the radiation risk compared with those of other risks must be taken into account for each specific mission. A risk-versus-gain philosophy is most appropriate for this comparison, and the philosophy is particularly useful for evaluation of radiation risk. The latter is generally a cumulative one that should not require an urgent all-or-nothing type of decision as had been previously proposed (29, 101).

Risk Analysis

In view of this proposed risk versus gain philosophy and judgment, it is expected that the results of this judgment will probably vary for each mission. It has been suggested that the space radiation hazards and risks be evaluated in the following terms (145):

1. Immediate or early performance decrement (early responses) occurring within a few hours to one month following a major exposure.
2. Progressively increasing performance decrement or serious loss of performance over long periods of flight as a result of an accumulating exposure (progressive injury to the blood-forming system).
3. Probability of delayed or chronic radiation response that may require interrupting a planned series of flights and which may limit an astronaut's career.

Within each of these categories, the significant clinical symptomatology or responses must be defined on the basis of importance to crew safety and mission success. The relative significance of responses will be mission-dependent. The following suggestions may assist in identification of the important responses and in evaluation of their significance for each specific mission.

1. Any amount of radiation exposure should be considered as potentially detrimental and, therefore, the exposure should be kept at a minimum consistent with the risk versus gain philosophy.
2. Radiation guides should be set below the level that might result in an unacceptable probability of in-flight response capable of jeopardizing crew safety.
3. Elapsed time between recurrent or repeat use of an individual or crew should take into consideration the nature and extent of previous exposure, the predicted exposure risk of the contemplated mission, and the degree to which mission success may depend on individual or crew experience.

4. The dose or doses established for early effects automatically entails acceptance of certain probabilities of occurrence of generalized life shortening, leukemia, and other late manifestations.
5. The radiation responses may be subdivided into "in-flight" and "post-flight" categories. Although this subdivision is somewhat arbitrary, it is time-dependent and may be important under special circumstances, for which certain higher risks may be acceptable if it is clear that the latent period for expression of injury will automatically cause the response to occur post-flight.

In view of the above operational requirements and hazards analysis, it has been suggested that any radiation exposure that might exceed the dose limits set for the mission may be permitted if the concomitant risk incurred by action to avoid the radiation fields or to protect oneself against the potential injury is determined to be greater than the hazard associated with the excess radiation dose. There is no immediately obvious way of approaching the problem of setting limits for the long-term effects that does not also imply certain career-dose limits and the lack of operating experience precludes establishing a firm commitment here.

As a first order approach to permit test of the trajectories for the AAP program, the radiation exposure levels have been suggested according to the following provisional operational criteria (208):

Planning Operational Dose (POD): The dose which should not be exceeded without requiring a mission modification of some degree. The degree of modification will be a function of the magnitude of the excess dose and will be formulated by mission rules. This dose will be used for mission planning purposes to determine if proposed trajectories and time lines are acceptable.

Maximum Operational Dose (MOD): The dose which should not be exceeded without specific modification of the mission to prevent further radiation exposure. Such an exposure would be considered to result in a potentially harmful in-flight response in terms of crew safety and post-flight response in terms of delayed radiation injury.

In establishing the POD and MOD limits it has been suggested that each response and its effect on the mission and crew are considered independently, and no adjustments are made for known or suspected uncertainties in radio-biological data, shielding calculations, or environmental data. As an example of this approach, the preliminary radiation limits for Apollo Applications Program are presented. Current recommendations for radiation exposure guidelines for missions of 30-60 days only are listed. It should be emphasized that the radiation units shown are for use in early planning of the AAP Program and will be updated as better knowledge becomes available.

The doses are expressed in rads of a reference radiation taken to be equivalent to 250 kVp x-rays whose mean LET is ~3.5 kev/micron of track length in wet tissue. No radiation QF or RBE has been applied.

The following doses found in Table 3-66 have been established on the assumption that the crew will be exposed to small increments of dose on each orbit and no allowance is made for pulses of radiation received at higher intensities. (See Section on Progressive Performance Decrement).

Table 3-66

Provisional Radiation Dose Limits Suggested for Preliminary Evaluation of a 30-60 Day Mission

(After Grahn⁽²⁰⁸⁾)

Tissue	Depth	POD	MOD
Skin	0.1 mm	2.5 rads/day	5 rads/day
Eye	3.0 mm	1.25 rads/day	2.5 rads/day
Bone Marrow	5.0 cm	0.6 rads/day	1.0 rad/day

Dosimetry for Characterization of Space Radiation Exposure (145)

From a physical point of view, the type of radiation, flux density, and energy spectrum completely define the radiation field which produces a biological change. From a biological point of view, however, it is the energy transferred by this field to the biological entity under consideration which is most important. When the physics of interactions between tissues and incident radiations are known, then the physical specification suffices, although in many instances computer programs are required to apply such physical knowledge. The most logical choice for space radiation monitoring, in view of the above difficulty, appears to be a tissue-equivalent system (49, 83, 119, 127, 175).

The problems associated with radiation monitoring of a manned space flight must, in other words, be clearly distinguished from the acquisition of geophysical data or of information aimed primarily at computation of shielding requirements. The chief requirement is for an instrument which will yield a direct indication of absorbed dose in tissue in real time. Such a requirement rules out instruments which are only capable of measuring flux or even flux plus energy distribution because of the complexity of using such data to provide dosimetric information. The dependence on geometrical variation, angular incidence, self-shielding, lack of accurate physical data on interaction properties between the radiation and tissue, plus the degree of complexity of the computations themselves, tends to rule out this method. It seems reasonable to conclude that knowledge of the physical characteristics of the radiation environment, although it may provide data for other scientific or engineering purposes, is not immediately applicable to radiation monitoring. Such information, therefore, should be gathered and treated separately from the problem of crew safety. For the latter problem, a practical approach to a detector whose atomic composition is as close as possible to that of tissue and whose response is proportional to energy absorbed, rather than to

flux density, appears to be the best course to follow, even within the limitations and compromises necessary (15).

The NAS-NRC Panel has suggested that the development of such a system should take two lines of approach (145). First, a system to supply both rate and total absorbed dose in rads as a function of mission time should be engineered for space vehicle application. Absorbed dose should be determined in such a manner as to supply values at superficial points and at critical depths in the body. Second, a tissue-equivalent system for determining the energy absorbed per event in a representative tissue volume centered at the points where absorbed dose has been measured should be developed on a simplified basis so that energy deposited per event can be classified into several broad LET groups. Total absorbed dose and dose rate should be displayed and weighted in accordance with LET distribution if the situation warrants. Absorbed dose, dose rate in rads, and LET groups should be recorded for future reference.

Dose should obviously then be defined in terms of rads, and preferably it should be measured in a tissue-equivalent system at at least three levels, including 0, 5 and possibly 10 cm in equivalent tissue depth. If possible, doses should be measured at the 0.1 mm and 3 cm levels noted in Table 3-66. Accuracy of these determinations should be no less than ± 15 percent. If compromise is required, it would then seem that at least two measurements should be made: one at the equivalent level of the skin and a second at about 5 cm, assuming it to be the mean depth of the bone marrow. The spanning measurements suggested above are statistically better but probably would invoke a greater weight penalty and instrument sophistication. A practical approach to the solution of this problem is under development (83).

A very important question that has been debated repeatedly concerns the alternative whether the radiation field inside the vehicle should be probed with stationary sensors distributed throughout the ship or whether micro-sensors on the bodies of the crew members should be given preference. It could be argued in favor of the first alternative that stationary sensors would free the crewman from additional gear in his space suit. Furthermore, such sensors could be of greater weight and bulk, thereby allowing a more elaborate analysis of the local radiation level. In favor of the second alternative, sensors on the body would indicate the radiation level exactly at the location where it counts. It is even conceivable that the differential reading of a pair of sensors on the chest and back would provide a crude measure of depth-dose. However, the validity of the data beyond a measure of local surface doses is open to question. Multiple sensors do allow estimation of the general homogeneity of the dose and could be used to estimate the degree of partial body exposure for risk analyses (270). The main argument in favor of sensors on the body naturally rests in the advantage that it would cover all contingencies of each individual's activity. In terms of the Lunar Mission, surface dosimeters require no changes or adjustments whether the individual is in the heavily shielded Apollo vehicle or in the extremely light Lunar Module, or is engaged in extravehicular activity. To be sure, for the last named condition, it should be recognized that there are very high fluxes of low-energy electrons and protons at many locations in the space environment. These should be detected and measured on the outside of the vehicle prior to

any outboard excursion, since they can potentially produce a very high surface tissue dose.

A final question concerns the need of LET sensors as a component of dosimetric instrumentation in space. In discussing the problem, measurement of heavy nuclei is excluded. In its conventional interpretation, LET defines the inhomogeneity in the distribution of the ionization events at the microscopic level. The diameter of the ionization columns which heavy nuclei produce in tissue exceeds the dimensions of a single cell, creating a peculiar exposure pattern with a few cells exposed to very high doses and the surrounding bulk of the cell population remaining entirely unaffected. It is not generally agreed upon that the biological significance of this type of exposure cannot be dealt with adequately in terms of the conventional LET concept (236, 243). Some feel that the LET concept is still useful in this context, and with the appropriate study, could be applied to the primary galactic cosmic radiation (270). As has been indicated above, the dose of microbeam radiation will probably not play a significant role in gross brain or eye damage in most space missions of less than 1 year duration (145). However, one must keep in mind the irreversible nature of the lesions in such areas as the gonads, lens and retina from very high-LET radiation (270).

If heavy nuclei are excluded, the LET problem appears only of limited importance for the remaining types of ionizing agents represented in the galactic radiation beam (243). The two main components of the primary galactic beam (i.e., protons and alpha particles) produce LET values exceeding those of standard x-rays only at energies from a few MeV down to the Bragg peak. These energies are not represented at all in the incident beam. Low-energy protons and alpha particles originate only locally in nuclear disintegrations in absorbing material. It should be remembered that the spectacular multipronged disintegration stars which cosmic-ray primaries release in collisions with silver and bromine nuclei of nuclear emulsions are absent in materials made up of low Z components such as living tissue. The number of prongs per star in these substances is small and the star frequency low; hence, terminating protons and alpha particles contribute only insignificantly to total ionization dose. Since the remaining dose of the galactic beam is produced mainly by protons of very high energies, the question could be raised whether a QF considerably smaller than 1 would not be applicable to the total absorbed dose from the galactic beam. (See Table 3-16 and Figure 3-17).

The situation is different for the proton and alpha fluxes of solar particle beams. Protons and alpha particles reaching the end of their ionization ranges (so-called "enders") contribute noticeably to the total ionization dose in systems of medium-light shielding (1.5 g/cm^2) and become the predominant contributors to the total dose in the skin and subcutaneous tissue behind low shielding. Under the latter conditions, calculation suggests a QF of 4 to 5 for late effects from combined proton and alpha particle dose to a depth of a few mm. On the other hand, it is not possible to say unequivocally whether these very special conditions would justify the great complications which a separate determination of LET would introduce in dosimetric instrumentation. Since the conditions in question occur only under conditions of low shielding and are always accompanied by a very steep drop in absorbed dose in the first

mm, it is possible that measurement of dose in rads with application of a suitable QF factor to the skin dose would suffice. (See Figure 3-25).

Dose Limits for Ground Personnel

Maximum permissible radiation doses in adult radiation workers and ground personnel as recommended by the Federal Radiation Council (88) are:

<u>Type of exposure</u>	<u>Condition</u>	<u>Dose (rem)</u>
Radiation worker:		
(a) Whole body, head and trunk, active blood-forming organs, gonads, or lens of eye.	Accumulated dose 13 weeks	5 times number of years beyond age 18 3
(b) Skin of whole body and thyroid	Year 13 weeks	30 10
(c) Hands and forearms, feet and ankles.	Year 13 weeks	75 25
(d) Other organs	Year	15

If it is not feasible to govern exposures to internal emitters by applying air-borne radioactivity concentration standards, the following radiation protection standards can apply: (281)

<u>Type of exposure</u>	<u>Condition</u>	<u>Dose (rem)</u>
Whole body, active blood-forming organs, gonads.	Year 13 weeks	5 3
Thyroid	Year 13 weeks	30 10
Bone		Body burden of 0.1 microgram of radium-226 or its biological equivalent *
Other organs	Year 13 weeks	15 5

* Exposure must be governed so that the individual's body burden does not exceed this value 1) when averaged over any period of 12 consecutive months and 2) after 50 years of occupational exposure.

The quality factor for calculating rem values applicable to low dose exposure and risk of late effects in occupational exposure are given in Table 3-2 (41).

A Radiological Safety Handbook for the John F. Kennedy Space Center is available (186). Data are available on the hazards of radioisotope thermo-electric generators for remote stations around the world (187).

REFERENCES

- 3-1. Abelson, P. H., Kruger, P. G., Cyclotron-Induced Radiation Cataracts, Science, 110: 655-657, 1949.
- 3-2. Ainsworth, E. J., Leong, G. F., Recovery from Radiation Injury in Dogs as Evaluated by the Split-Dose Technique, USNRDL-TR-964, U. S. Naval Radiological Defense Lab., San Francisco, Calif., Dec., 1965.
- 3-3. Alpen, E. L., Jones, D. M., Hechter, H. H., et al., The Comparative Biological Response of Dogs to 250-kVp and 100-kVp X-Rays, Radiology, 70: 541-550, 1958.
- 3-4. Alpen, E. L., Jones, D. M., Effects of Concomitant Superficial X-Radiation upon Lethal Effectiveness of 250 kVp X-Rays, Radiology, 72: 81-85, Jan. 1959.
- 3-5. Anderson, R. E., Ishida, K., Malignant Lymphoma in Survivors of the Atomic Bomb in Hiroshima, Ann. Intern. Med., 61: 853-862, Nov. 1964.
- 3-6. Andrews, G. A., Discussion of Paper by E. P. Cronkite, Ann. N. Y. Acad. Sci., 114: 349-355, 1964.
- 3-7. Andrews, J. R., Coppedge, T. O., The Dose-Time Relationship for Cure of Squamous Cell Carcinoma, Amer. J. Roentgenol., 65: 934-939, 1951.
- 3-8. Anger, H. O., Van Dyke, D. C., Human Bone Marrow Distribution Shown in vivo by Iron-52 and the Positron Scintillation Camera, Science, 144: 1587-1589, 1964.
- 3-9. Angevine, D. M., Jablon, S., Late Radiation Effects of Neoplasia and Other Diseases in Japan, Ann. N. Y. Acad. Sci., 114: 823-831, 1964.
- 3-10. Arnold, E. D., Handbook of Shielding Requirements and Radiation Characteristics of Isotopic Power Sources for Terrestrial, Marine, and Space Applications, ORNL-3576, Oak Ridge National Lab., Union Carbide, Inc., Oak Ridge, Tenn., Apr. 1964.
- 3-11. Aron, W. A., The Passage of Charged Particles Through Matter, UCRL-1325, Univ. of California Radiation Lab., Berkeley, Calif., May 1951.

- 3-12. Auxier, J. A., Cheka, J. S., Haywood, F. F., et al., Free-Field Radiation-Dose Distributions from the Hiroshima and Nagasaki Bombings, Health Phys., 12: 425-429, Mar. 1966.
- 3-13. Bacq, Z. M., Chemical Protection Against Ionizing Radiation, Charles C. Thomas, Springfield, Ill., 1964.
- 3-14. Bailey, D. K., Time Variations of the Energy Spectrum of Solar Cosmic Rays in Relation to the Radiation Hazard in Space, J. Geophysical Res., 67: 391-396, Jan. 1962.
- 3-15. Baily, N. A., Sondhaus, C. A., Radiation Dosimetry Aboard Manned Space Vehicles, J. Spacecraft Rockets, 3: 1245-1251, 1966.
- 3-16. Balabukha, V. S., (ed.), Chemical Protection of the Body against Ionizing Radiation, Pergamon Press, Oxford, 1963. Distributed by Macmillan Co., N. Y., (Translation of Russian book Khimicheskaya Zashchita Organizma ot Ioniziruyushchikh i Zluchenii, Atomizdat, Moscow, 1960).
- 3-17. Barkas, W. H., Berger, M. J., Tables of Energy Losses and Ranges of Heavy Charged Particles, NASA-SP-3013, 1964.
- 3-18. Bateman, J. L., Bond, V. P., Rossi, H. H., Lens Opacification of Mice Exposed to Monoenergetic Fast Neutrons, in Biological Effects of Neutron and Proton Irradiations Proceedings, Brookhaven National Lab., Upton, N. Y., Oct. 7-11, 1963, International Atomic Energy Agency, Vienna, 1964, Vol. I, pp. 321-336.
- 3-19. Bateman, J. L., Bond, V. P., Lens Opacification in Mice Exposed to Fast Neutrons, Radiation Research Suppl. 7: 239-249, 1967.
- 3-20. Bateman, J. L., Rossi, H. H., Bond, V. P., et al., The Dependence of RBE on Energy of Fast Neutrons. 2. Biological Evaluation of Discrete Energies in the Range 0.43 to 1.80 MeV, Radiation Res., 15: 694-706, 1961.
- 3-21. Belisario, J. C., A Discussion on the Skin Erythema Dose with Roentgen Rays: Some Biological Implications, Brit. J. Radiol., 25: 326-335, 1952.
- 3-22. Beller, W. S., SNAP-27 Readied for Tests with ALSEP, Technology Week, 20(18): 23-25, May 1, 1967.
- 3-23. Benjamin, F. B., Peyser, L., Effect of Oxygen on Radiation Resistance of Mice, Aerospace Med., 35(12): 1147-1149, 1964.

- 3-24. Berger, M. J., Seltzer, S. M., Additional Stopping Power and Range Tables for Protons, Mesons, and Electrons, NASA-SP-3036, 1966.
- 3-25. Berger, M. J., Seltzer, S. M., Tables of Energy Losses and Ranges of Electrons and Positrons, NASA-SP-3012, 1964.
- 3-26. Berry, C. A., Coons, D. O., Catterson, A. D., et al., Man's Response to Long-Duration Flight in the Gemini Spacecraft, in Gemini Midprogram Conference, Feb. 23-25, 1962, NASA-SP-121, 1966, pp. 235-261.
- 3-27. Bertini, H. W., Low Energy Intranuclear Cascade Calculation, Phys. Rev., 131: 1801, 1963.
- 3-28. Billingham, J., Robbins, D. E., Ewing, D., A Method of Evaluating Radiation Risks for Manned Space Flights, NASA-Ames Research Center, Moffett Field, Calif. and NASA-Manned Spacecraft Center, Houston, Texas, presented to the Radiation Research Society, San Diego, Calif., Feb. 14, 1966.
- 3-29. Billingham, J., Status Report on the Space Radiation Effects on the Apollo Mission, in Second Symposium on Protection Against Radiation in Space, Gatlinburg, Tenn., Oct. 12-14, 1964, Reetz, A., (ed.), NASA-SP-71, 1965, pp. 139-141.
- 3-30. Biswas, S., Fichtel, C. E., Nuclear Composition and Rigidity Spectra of Solar Cosmic Rays, Astrophysical J., 139(3): 941-950, 1964.
- 3-31. Bizzozero, O. J., Jr., Johnson, K. G., Ciocco, A., Radiation-Related Leukemia in Hiroshima and Nagasaki, 1946-1964, I. Distribution, Incidence and Appearance Time, New Eng. J. Med., 274: 1095-1101, May 1966.
- 3-32. Blair, H. A., The Constancy of Repair Rate and of Irreparability during Protracted Exposure to Ionizing Radiation, Ann. N. Y. Acad. Sci., 114: 150-157, 1964.
- 3-33. Bloch, C., Postradiation Osteogenic Sarcoma. Report of a Case and Review of Literature, Amer. J. Roentgenol., 87: 1157-1162, June 1962.
- 3-34. Bloom, W., Bloom, M. A., Histological Changes after Irradiation, in Radiation Biology, Hollaender, A., (ed.), McGraw-Hill, N. Y., 1954, Ch. 17, pp. 1091-1143.
- 3-35. Bobkov, V. G., Demin, V. P., Keirim-Markus, I. B., et al., Radiation Safety during Space Flights, NASA-TT-F-356, May 1966. (Translation of Radiatsionnaya Bezopasnost' pri Kosmicheskikh Poletakh, Atomizdat, Moscow, 1964).

- 3-36. Bogoyavlenskaya, M. P., Sukyasyan, G. V., Vinograd-Finkel', V. R., et al., Transfusion of Donors' Bone Marrow in the Combined Treatment of Patients with Radiation Sickness Developing after Radiotherapy, TT-67-60799, Scripta Technica, Inc., Washington, D. C., 1966. (Translation of Meditinskaya Radiologiya, 11(1): 15-23, 1966).
- 3-37. Bond, V. P., Fliedner, T. M., Cronkite, E. P., Evaluation and Management of the Heavily Irradiated Individual, J. Nucl. Med., 1: 221-238, Oct. 1960.
- 3-38. Bond, V. P., Robinson, C. V., A Mortality Determinant in Non-Uniform Exposures of the Mammal, Rad. Res. Suppl. 7: 265-275, 1967.
- 3-39. Bond, V. P., Robertson, J. S., Vertebrate Radiobiology. Lethal Actions and Associated Effects, Ann. Rev. Nuclear Sci., 7: 135-162, 1957.
- 3-40. Brill, A. B., Tomonaga, M., Heyssel, R. M., Leukemia in Man Following Exposure to Ionizing Radiation. A Summary of the Findings in Hiroshima and Nagasaki, and a Comparison with Other Human Experience, Ann. Intern. Med., 56: 590-609, Apr. 1962.
- 3-41. Brookhaven National Laboratory, Associated Universities, Inc., Dose-Effect Modifying Factors in Radiation Protection (Report of Subcommittee M-4 Relative Biological Effectiveness of the National Commission on Radiation Protection), BNL-50073, Brookhaven National Lab., Upton, N. Y., Aug. 1967.
- 3-42. Brown, J. A. H., Human Fertility in Nuclear War, in Exposure of Man to Radiation in Nuclear Warfare, Rust, J. H., Mewissen, D. J., (eds.), Elsevier Publishing Co., Inc., N. Y., 1963.
- 3-43. Brown, J. B., McDowell, F., Fryer, M. P., Surgical Treatment of Radiation Burns, Surg. Gynec. Obstet., 88: 609-622, May 1949.
- 3-44. Brucer, M., The Acute Radiation Syndrome, A Medical Report on the Y-12 Accident, June 16, 1958, ORINS-25, Oak Ridge Institute of Nuclear Studies, Inc., Tenn., 1959.
- 3-45. Brues, A. M., Sacher, G. A., Analysis of Mammalian Radiation Injury and Lethality, in Symposium on Radiobiology, Nickson, J. J., (ed.), John Wiley & Sons, N. Y., 1952, pp. 441-465.

- 3-46. Brues, A. M., Somatic Effects, and also the Introduction to Part 2, and the Summary and Conclusions Sections, in Low Level Irradiation, Brues, A. M., (ed.), Colonial Press, Clinton, Mass., 1959, pp. 73-86, 89, 139-142.
- 3-47. Burch, P. R. J., Radiation Carcinogenesis. A New Hypothesis, Nature, 185: 135-142, 1960.
- 3-48. Busby, D. E., Clinical Space Medicine: A Prospective Look at Medical Problems from Hazards of Space Operations, NASA-CR-856, 1967.
- 3-49. Chapman, M. C., Holly, F. E., An Experiment to Measure the Tissue-Equivalent Absorbed Dose (LET) and Depth-Dose Distributions Produced by Radiations in Space, preprint of paper presented at the 1st International Congress of the International Radiation Protection Association, Rome, Italy, Sept. 7, 1966.
- 3-50. Cogan, D. G., Ocular Effects of Radiation, New Eng. J. Med., 259: 517-520, 1958.
- 3-51. Cogan, D. G., Donaldson, D. D., Reese, A. B., Clinical and Pathological Characteristics of Radiation Cataract, Arch. Ophth., 47: 55-70, Jan. 1952.
- 3-52. Cogan, D. G., Goff, J. L., Graves, E., Experimental Radiation Cataract; Cataract in the Rabbit Following Single Exposure to Fast Neutrons, Arch. Ophth., 47: 584-592, May 1952.
- 3-53. Cohen, L., Clinical Radiation Dosage. II. Inter-Relation of Time, Area and Therapeutic Ratio, Brit. J. Radiol., 22(264): 706-713, Dec. 1949.
- 3-54. Cohen, L., The Statistical Prognosis in Radiation Therapy. A Study of Optimal Dosage in Relation to Physical and Biologic Parameters for Epidermoid Cancer, Amer. J. Roentgenol., 84: 741-753, Oct. 1960.
- 3-55. Conard, R. A., Hematological Effects of Space Radiation, BNL-10221, Brookhaven National Lab., Upton, N. Y., 1966.
- 3-56. Conard, R. A., Hicking, A., Medical Findings in Marshallese People Exposed to Fallout Radiation: Results from a Ten-Year Study, JAMA, 192: 457-459, 1965.
- 3-57. Cormack, D. V., Johns, H. E., Electron Energies and Ion Densities in Water Irradiated with 200 KeV, 1 MeV and 25 MeV Radiation, Brit. J. Radiol., 25: 369-386, July 1952.

- 3-58. Court-Brown, W. M., Doll, R., Leukemia and Aplastic Anemia in Patients Irradiated for Ankylosing Spondylitis, Medical Research Council Special Series, Rep. No. 295, Her Majesty's Stationery Office, London, 1957.
- 3-59. Cronkite, E. P., The Diagnosis, Treatment, and Prognosis of Human Radiation Injury from Whole-Body Exposure, Ann. N. Y. Acad. Sci., 114: 341-349, 1964.
- 3-60. Cronkite, E. P., Bond, V. P., Diagnosis of Radiation Injury and Analysis of the Human Lethal Dose of Radiation, U. S. Armed Forces Med. J., 11: 249-260, 1960.
- 3-61. Cronkite, E. P., Bond, V. P., Effects of Radiation on Mammals, Ann. Rev. Physiol., 18: 483-526, 1956.
- 3-62. Cronkite, E. P., Bond, V. P., Conard, R. A., et al., Response of Human Beings Accidentally Exposed to Significant Fallout Radiation from a Thermonuclear Explosion, JAMA, 159: 430-434, 1955.
- 3-63. Cronkite, E. P., Bond, V. P., Dunham, C. L., (eds.), Some Effects of Ionizing Radiation on Human Beings, TID-5358, U. S. Atomic Energy Commission, Washington, D. C., July 1956.
- 3-64. Curtis, H. J., Biological Mechanisms Underlying the Aging Process, Science, 141: 686-694, 1963.
- 3-65. Curtis, H. J., Radiation Induced Aging, Med. Phys., 3: 492-497, 1960.
- 3-66. Curtis, S. B., Dye, D. L., Sheldon, W. R., Fractional Cell Lethality Approach to Space Radiation Hazards, in Second Symposium on Protection Against Radiations in Space, Gatlinburg, Tenn., Oct. 12-14, 1964, Reetz, A., (ed.), NASA-SP-71, 1965, pp. 219-223.
- 3-67. Dalrymple, G. V., Edema-A Delayed Complication of Total-Body 32 MeV Proton Irradiation, SAM-TR-65-57, School of Aerospace Medicine, Brooks AFB, Texas, Sept. 1965.
- 3-68. Dalrymple, G. V., An Investigation of the Relative Biologic Effectiveness of 138 MeV Protons as Compared to CO₆₀ Gamma Radiation, SAM-TR-65-52, School of Aerospace Medicine, Brooks AFB, Texas, Aug. 1965.
- 3-69. Dalrymple, G. V., Some Effects of 138 MeV Protons on Primates - The Radiations of Space III, SAM-TR-65-58, School of Aerospace Medicine, Brooks AFB, Texas, Sept. 1965.

- 3-70. Dalrymple, G. V., Some Effects of 400 MeV Protons on Primates, the Radiations of Space IV, SAM-TR-65-73, School of Aerospace Medicine, Brooks AFB, Texas, Oct. 1965.
- 3-71. Dalrymple, G. V., Lindsay, I. R., Ghidoni, J. J., et al., An Estimate of the Biological Effects of the Space Proton Environment, SAM-TR-65-261, School of Aerospace Medicine, Brooks AFB, Texas, 1966.
- 3-72. Darenkaya, N. G., Domshlak, M. P., Grigor'yev, G. Yu., et al., Comparative Analysis of Biological Effect of Proton Radiation with Energy of 510 MeV, in Problems of Radiation Safety in Space Flights, Nefedov, G. Yu., (ed.), NASA-TT-F-353, Dec. 1965, pp. 194-209.
- 3-73. Davidson, H. O., Biological Effects of Whole-Body Gamma Radiation on Human Beings, The Johns Hopkins Press, Baltimore, Md., 1957.
- 3-74. DeLawter, D. S., Winship, T., A Follow-Up Study of Adults Treated with Roentgen Rays for Thyroid Disease, Cancer, 16: 1028-1031, Aug. 1963.
- 3-75. Dennis, J. A., Calculated Quality Factors for Protons in Body and Eye-Lens Tissues, AERE-M-1887, Atomic Energy Research Establishment, Harwell, England, 1967.
- 3-76. Domshlak, M. P., Relative Biological Effectiveness of Various Types of Radiations, JPRS-39774, Joint Publications Research Service, Washington, D. C., Feb. 1967. (Translation of Russian book Voprosy Osschey Radiobiologiya (General Problems of Radiobiology), Domshlak, M. P., (ed.), Atomizdat, Moscow, 1966, Chapter 4).
- 3-77. Dresner, L., EVAP, A Fortran Program for Calculating the Evaporation of Various Particles from Excited Compound Nuclei, ORNL-CF-61-12-30, U. S. AEC, Oak Ridge National Lab., Oak Ridge, Tenn., Dec. 1961.
- 3-78. Duffy, J. J., Arneson, A. N., Voke, E. L., Rate of Re-cuperation of Human Skin Following Irradiation; A Preliminary Report, Radiology, 23: 486-490, Oct. 1934.
- 3-79. DuSalt, L. A., Time-Dose Relationships, Amer. J. Roentgenol., 75: 597-606, Mar. 1956.
- 3-80. Dye, D. L., Wilkinson, M., Radiation Hazards in Space, Science, 147(3653): 19-25, Jan. 1965.

- 3-81. Ellis, F., Tolerance Dosage in Radiotherapy with 200 Kv X-Rays, Brit. J. Radiol., 15: 348-350, Dec. 1942.
- 3-82. Essen, C. F. von, Roentgen Therapy of Skin and Lip Carcinoma: Factors Influencing Success and Failure, Amer. J. Roentgenol., 83: 556-570, Mar. 1960.
- 3-83. Ewing, D. E., A Space Radiation Monitoring System for Support of Manned Space Flight, Air Force Weapons Lab., Kirtland AFB, N. M., presented at 17th International Astronautical Congress at Madrid, Spain, Oct. 10-15, 1966.
- 3-84. Faber, M., [Ionizing Irradiation as a Pathogenetic Factor in Leukemia], Nord. Med., (Stockholm), 59(25): 839-842, June 1958.
- 3-85. Faber, M., Borum, K., Leukaemia and a Malignant Tumor in the Same Patient, Brit. J. Haemat., 8: 313-321, Oct. 1962.
- 3-86. Failla, G., McClement, P., The Shortening of Life by Chronic Whole-Body Irradiation, Amer. J. Roentgenol., 78: 946-954, Dec. 1957.
- 3-87. Farley, T. A., Space Technology, Vol. VI - Space Sciences, NASA-SP-114, 1966.
- 3-88. Federal Radiation Council, Background Material for the Development of Radiation Protection Standards, Staff Rep. 1, May 13, 1960.
- 3-89. Fowler, J. F., Stern, B. E., Fractionation and Dose-Rate, II. Dose-Time Relationships in Radiotherapy and the Validity of Cell Survival Curve Models, Brit. J. Radiol., 36: 163-173, Mar. 1963.
- 3-90. Fowler, P. H., Adams, R. A., Cowen, V. G., et al., The Charge Spectrum of Very Heavy Cosmic Ray Nuclei, Proc. Roy. Soc., Ser. A, 301: 39-45, Oct. 1967.
- 3-91. Freeman, J. W., Jr., The Geomagnetically Trapped Radiation in Second Symposium on Protection Against Radiations in Space, Gatlinburg, Tenn., Oct. 12-14, 1964, Reetz, Arthur, Jr., (ed.), NASA-SP-71, 1965, pp. 7-17.
- 3-92. Freier, P. S., Waddington, C. J., Electrons, Hydrogen Nuclei, and Helium Nuclei Observed in the Primary Cosmic Radiation during 1963, J. Geophys. Res., 70: 5753-5768, 1965.

- 3-93. Freier, P. S., Webber, W. R., Exponential Rigidity Spectrums for Solar Flare Cosmic Rays, J. Geophysical Res., 68: 1605-1629, 1963.
- 3-94. Freireich, E. J., Levin, R. H., Whang, J., et al., The Function and Fate of Transfused Leukocytes from Donors with Chronic Myelocytic Leukemia in Leukopenic Recipients, Ann. N. Y. Acad. Sci., 113: 1081-1089, Feb. 1964.
- 3-95. Freund, M., Borrelli, F. J., The Effects of X-Irradiation on Male Fertility in the Guinea Pig: Semen Production after X-Irradiation of the Testes, of the Body or of the Head, Radiation Res., 24: 67-80, Jan. 1965.
- 3-96. Fuchs, R. A., Experimenter's Design Handbook for the Manned Lunar Surface Program, SSD-60352R, Hughes Aircraft Co., Culver City, Calif., Jan. 1967. (Prepared under NASA contract NAS 8-20244).
- 3-97. Furchtgott, E., Behavioral Effects of Ionizing Radiations: 1955-61, Psychol. Bull., 60: 157-199, Mar. 1963.
- 3-98. Garcia, J., Koelling, R. A., A Comparison of Aversions Induced by X-Rays, Toxins, and Drugs in the Rat, Radiation Res. Suppl. 7: 439-450, 1967.
- 3-99. Gerstner, H. B., Reaction to Short-Term Radiation in Man, Ann. Rev. Med., 11: 289-302, 1960.
- 3-100. Gibson, W. A., Energy Removed from Primary Proton and Neutron Beams by Tissue, ORNL-3260, U. S. AEC, Oak Ridge National Lab., Oak Ridge, Tenn., June 1962.
- 3-101. Gill, W. L., Statement of the Approach to the Radiation Problem for Apollo, NASA Manned Spacecraft Center, Append. B to the Man in Space Committee Working paper No. 16, Jan. 12-13, 1962, Draft - March 26, 1962, submitted to National Academy of Sciences, Space Science Board, Working Group on Radiation Problems in Space Flight, 1962.
- 3-102. Glasstone, S., (ed.), The Effects of Nuclear Weapons, U. S. Atomic Energy Commission, Washington, D. C., 1962.
- 3-103. Grahn, D. G., Radiation, Argonne National Lab., Argonne, Ill., in Bioastronautics Data Book, Webb, Paul, (ed.), NASA-SP-3006, 1964, (Section 8), pp. 133-157.
- 3-104. Grahn, D. G., Langham, W. H., Methods in the Evaluation of Radiation Hazards in Manned Space Flight, in Second Symposium on Protection Against Radiations in Space, Gatlinburg, Tenn., Oct. 12-14, 1964, Reetz, A., (ed.), NASA-SP-71, 1965, pp. 59-64.

- 3-105. Grahn, D. G., Sacher, G. A., Chronic Radiation Mortality in Mice after Single Whole-Body Exposure to 250-, 135-, and 80-kVp X-Rays, Radiation Res., 8: 187-194, 1958.
- 3-106. Grahn, D. G., Sacher, G. A., Walton, H., Jr., Comparative Effectiveness of Several X-Ray Qualities for Acute Lethality in Mice and Rabbits, Radiation Res., 4: 228-242, 1956.
- 3-107. Gray, L. H., Radiobiologic Basis of Oxygen as a Modifying Factor in Radiation Therapy, Amer. J. Roentgenol., 85: 803-815, May 1961.
- 3-108. Grigor'ev, Yu. G., Darenetskaya, N. G., Domshlak, M. P., et al., [Characteristics of the Biological Action and Relative Biological Effectiveness of High-Protons], in Proc. Symposium on Biological Effects of Neutron and Proton Irradiations, Oct. 7-11, 1963, Upton, N. Y., International Atomic Energy Agency, Vienna, 1964, Vol. I, pp. 223-230. (English Trans. AEC-tr-6444, 1964).
- 3-109. Guskova, A. K., Baisogolov, G. D., Two Cases of Acute Radiation Disease in Man, in Proceedings of the International Conference on the Peaceful Uses of Atomic Energy, Aug. 8-20, 1955, Geneva, Vol. 11. Biological Effects of Radiation, United Nations, N. Y., 1956, pp. 25-34.
- 3-110. Haffner, J. W., RBE of Protons and Alpha Particles, in Second Symposium on Protection Against Radiations in Space, Gatlinburg, Tenn., Oct. 12-14, 1964, Reetz, A., (ed.), NASA-SP-71, 1965, pp. 513-525.
- 3-111. Haley, T. J., Snider, R. S., (eds.), Response of the Nervous System to Ionizing Radiation: A Symposium, Academic Press, N. Y., 1962.
- 3-112. Haley, T. J., Snider, R. S., (eds.), Second International Symposium on the Response of the Nervous System to Ionizing Radiation, Little, Brown & Co., Boston, Mass., 1964.
- 3-113. Hansen, C. L., Jr., Michaelson, S. M., Howland, J. W., The Biological Effects of Upper Body Irradiation of Beagles, UR-580, Univ. of Rochester, Rochester, N. Y., 1960.
- 3-114. Harris, P. S., Statement Before the Special Subcommittee on Radiation, Biological Environmental Effects of Nuclear War, Hearings of the Joint Comm. on Atomic Energy, Congress of the United States, Eighty-Sixth Congress, First Session on Biological and Environmental Effects of Nuclear War, U. S. GPO, Washington, D. C., June 22-26, 1959, pp. 263.

- 3-115. Hasterlick, R. J., Marinelli, L. D., Physical Dosimetry and Clinical Observations on Four Human Beings Involved in an Accidental Critical Assembly Excursion, in Proceedings of the International Conference on the Peaceful Uses of Atomic Energy, Aug. 8-10, 1955, Geneva, Vol. II. Biological Effects of Radiation, United Nations, N. Y., 1956, pp. 25-34.
- 3-116. Heller, C. G., Radiation Damage to the Germinal Epithelium of Man, Pacific Northwest Research Foundation, Seattle, Wash., 1966. (Work in progress to be reported to the Space Radiation Study Panel, Space Science Board, National Academy of Sciences, National Research Council, Washington, D. C.).
- 3-117. Hempelmann, L. H., Lisco, H., Hoffman, J. G., The Acute Radiation Syndrome: A Study of Nine Cases and a Review of the Problem, Ann. Inter. Med., 36: 279-510, Feb. 1952.
- 3-118. Hrabovszky, Z., Nikl, I., X-Ray Examinations and a Review of Indications with Regard to Hazard to Gonad Function, FTD-TT-1751, Sept. 30, 1966. (Translation of Magyar Radiologiya, No. 2: 65-88, 1964).
- 3-119. Hughes Research Labs., Malibu, Calif., Division of Hughes Aircraft Co., Research and Development Program for Radiation Measurements of Radiobiological Hazards of Man in Space, Summary Tech. Rpt., NASA-CR-73146, 1967. (Prepared under NASA contract NAS 2-2366).
- 3-120. Ingram, M., (chairman), TRIMAC Committee, Treatment of Acute Radiation Injury under Medically Austere Conditions, TRC-67-21, Univ. of Rochester, N. Y., Apr. 1967. (Prepared under office of Civil Defense Subtask 2431F).
- 3-121. International Commission on Radiological Protection, The Evaluation of Risks from Radiation, ICRP Publication 8, Pergamon Press, N. Y., 1966.
- 3-122. International Commission on Radiological Protection, Radiation Protection, Recommendations, ICRP Publication 9, Pergamon Press, N. Y., 1966.
- 3-123. Irving, D. C., Alsmiller, R. G., Jr., Moran, H. S., Tissue Current-To-Dose Conversion Factors for Neutrons with Energies from 0.5 to 60 MeV, ORNL-4032, Oak Ridge National Lab., Union Carbide Corp., Oak Ridge, Tenn., Aug. 1967.

- 3-124. Jammet, H. G., Mathe, B., Pendic, J. F., et al., Etude de Six Cas D'irradiation Totale Aigue Accidentelle, Rev. Franc. Etud. Clin. Biol., 4: 210-225, 1959.
- 3-125. Janni, J. F., Calculations of Energy Loss, Range, Pathlength, Straggling, Multiple Scattering, and the Probability of Inelastic Nuclear Collisions for 0.1 - 1000 MeV Protons, AFWL-TR-65-150, Air Force Weapons Lab., Kirtland AFB, N. M., 1966.
- 3-126. Janni, J. F., Measurements of Spacecraft Cabin Radiation Distributions for the Fourth and Sixth Gemini Flights, AFWL-TR-65-149, Air Force Weapons Lab., Kirtland AFB, N. M., 1967.
- 3-127. Janni, J. F., Proton Absorption in Dose-Equated Materials, AFWL-TR-65-3, Air Force Weapons Lab., Kirtland AFB, N. M., Apr. 1965.
- 3-128. Janni, J. F., Clark, B. C., Schneider, M. F., et al., A Dose-Equated Manikin for Space Radiation Research, AFWL-TR-65-97, Air Force Weapons Lab., Kirtland AFB, N. M., Aug. 1965.
- 3-129. Johnson, C. E., Mason, D. G., SNAP 8 Reactor and Shield Designs and Operating Experience, J. Spacecraft, 3(7): 1099-1105, 1966.
- 3-130. Johnson, E. M., The Control of Radiation Sickness with Thiethylperazine (Torecan), New Zeal. Med. J., 64: 649-650, Nov. 1965.
- 3-131. Jolles, B., Mitchell, R. G., Optimal Skin Tolerance Dose Levels, Brit. J. Radiol., 20: 405-409, Oct. 1947.
- 3-132. Jones, A., Irradiated Sarcoma, Brit. J. Radiol., 26: 273-284, June 1953.
- 3-133. Jones, D. C., Kimeldorf, D. J., Lifespan Measurements in the Male Rat, USNRDL-TR-646, U. S. Naval Radiological Defense Lab., San Francisco, Calif., May 1963.
- 3-134. Jones, R. K., Adams, D. E., Russell, I. J., The Radiobiological Consequences of Dose Distributions Produced by Solar-Flare Type Spectra, in Second Symposium on Protection Against Radiations in Space, Reetz, A., Jr., (ed.), Gatlinburg, Tenn., Oct. 12-14, 1964, NASA-SP-71, 1965, pp. 85-95.
- 3-135. Kelton, A. A., Radiation Guide Lines for Manned Space Vehicles: A Review with Recommendations, SM-47749, Douglas Aircraft Co., Inc., Missile and Space Systems Div., Santa Monica, Calif., 1965.

- 3-136. Kelton, A. A., Kirby, J. K., Total Oxygen Pressure and Radiation Mortality in Mice, DAC-P-2030, Douglas Aircraft Co., Inc., Missile and Space Systems Div., Santa Monica, Calif., 1964.
- 3-137. Kimeldorf, D. J., Phillips, R. D., Jones, D. C., Longevity in Neutron-Exposed Guinea Pigs, USNRDL-TR-941, U. S. Naval Radiological Defense Lab., San Francisco, Calif., Dec. 1965.
- 3-138. Kinney, W. E., Coveyou, R. R., Zerby, C. D., A Series of Monte Carlo Codes to Transport Nucleons Through Matter, in Proceedings of the Symposium on the Protection Against Radiation Hazards in Space, Gatlinburg, Tenn., Nov. 5-7, 1962, TID-7652, Book 2, U. S. AEC, Div. of Technical Information, Oak Ridge, Tenn., 1963, pp. 608-618.
- 3-139. Kinney, W. E., Zerby, C. D., Calculated Tissue Current-to-Dose Conversion Factors for Nucleons of Energy below 400 MeV, in Second Symposium on Protection Against Radiation in Space, Gatlinburg, Tenn., Oct. 12-14, 1964, Reetz, A., Jr., (ed.), NASA-SP-71, 1965, pp. 161-172.
- 3-140. Klass, P. J., Gemini III, IV Underscore Man's Space Role, Aviat. Week Space Tech., 83: 58, 1965.
- 3-141. Klass, P. J., Views Mixed on High-Power Generation for Spacecraft: Foggy Mission Outlook Spurs Divergence on Type of Nuclear System Required for Late 1970's to Supply Tens of Kilowatts, Aviat. Week and Space Tech., 87(11): 96-106, Sept. 11, 1967.
- 3-142. Kottler, C. F., Jr., Radiation Shielding Considerations for Interplanetary Spacecraft, Rep. RE-236, Grumman Aircraft Engineering Corp., Bethpage, N. Y., Jan. 1966.
- 3-143. Kurohara, S. S., George, F. W., III, Levitts, S., et al., Factor Concerned with "Clinical Radiation Nausea", Radiology, 86: 262-265, Feb. 1966.
- 3-144. Lacassagne, A., Gricouloff, G., Action of Radiation on Tissues, An Introduction to Radiotherapy, Grune and Stratton, N. Y., 1958.
- 3-145. Langham, W. H., (ed.), Radiobiological Factors in Manned Space Flight, NAS-NRC-1487, National Academy of Sciences, National Research Council, Washington, D. C., 1967.
- 3-146. Langham, W. H., Some Radiobiological Aspects of Early Manned Space Flight, paper presented at the 4th International Space Science Symposium (COSPAR), Warsaw, Poland, 1963.

- 3-147. Langham, W. H., Some Radiobiological Aspects of Early Manned Space Flight, Los Alamos Scientific Labs., Los Alamos, N. M., in Proc. Lunar and Planetary Exploration Colloquium, Santa Monica, Calif., May 23-24, 1962, Vol. 3, No. 2, May 1963, pp. 117-134.
- 3-148. Langham, W. H., Brooks P. M., Grahn, D., (eds.), Radiation Biology and Space Environmental Parameters in Manned Spacecraft Design and Operations, Aerospace Med., 36(2): Section II, Feb. 1965.
- 3-149. La Salle, M., Billen, D., Inhibition of DNA Synthesis in Murine Bone-Marrow Cells by AET and Cysteamine, Ann. N. Y. Acad. Sci., 114: 622-629, Mar. 1964.
- 3-150. Levin, W. C., Schneider, M., Gerstner, H. B., Initial Clinical Reaction to Therapeutic Whole-Body X-Irradiation - Some Civil Defense Considerations, SAM-TR-60-1, School of Aviation Medicine, Brooks AFB, Texas, 1959.
- 3-151. Lewis, E. B., Leukemia and Ionizing Radiation, Science, 125: 965-972, 1957.
- 3-152. Lindop, P. J., Rotblat, J., Long-Term Effects of a Single Whole Body Exposure of Mice to Ionizing Radiation, I. Life Shortening, Proc. Roy. Soc. (Biol.), 154: 332-349, July 1961.
- 3-153. Lindsay, I. R., Dalrymple, G. V., Acute Somatic Effects in Primates of Protons to 400 MeV, Radiation Res., Suppl. 7: 330-335, 1967.
- 3-154. Lindsay, I. R., Dalrymple, G. V., Ghidoni, J. J., et al., Some Effects of 55-MeV Protons on Primates, SAM-TR-65-322, School of Aerospace Med., Brooks AFB, Texas, 1966.
- 3-155. Lindsay, S., Chaikoff, I. L., The Effects of Irradiation on the Thyroid Gland with Particular Reference to the Induction of Thyroid Neoplasms: A Review, Cancer Res., 24: 1099-1107, Aug. 1964.
- 3-156. Livshits, N. N., (ed. in chief), The Effect of Space-Flight Factors on Functions of the Central Nervous System, NASA-TT-F-413, June 1967. (Translation of Vliyanie Faktorov Kosmicheskogo Poleta na Funktsii Tsentral'noy Nervnoy Sistemy. Izdatel'stvo Nauka, Moscow, 1966).

- 3-157. Lushbaugh, C. C., ORINS Human Response Studies, Oak Ridge Institute of Nuclear Studies, Oak Ridge, Tenn., in Review of Space Radiation Problems, NASA, Office of Manned Space Flight, Washington, D. C., Jan. 22, 1966.
- 3-158. Lushbaugh, C. C., Vertebrate Radiobiology (The Pathology of Radiation Exposure), Ann. Rev. Nucl. Sci., 7: 163-184, 1957.
- 3-159. Lushbaugh, C. C., Comas, F., Hofstra, R., Clinical Studies of Radiation Effects in Man: A Preliminary Report of a Retrospective Search for Dose-Response Relationships in the Prodromal Syndrome, Radiation Res. Suppl. 7: 398-412, 1967.
- 3-160. Lushbaugh, C. C., Comas, F., Saenger, E. L., et al., Radio-sensitivity of Man in Extrapolation from Studies of Total-Body Irradiation of Patients, Radiation Res., 27: 487-488, 1966. (Abstract of papers for the 14th Ann. Meeting of the Radiation Res. Soc., Coronado, Calif., Feb. 13-16, 1966).
- 3-161. MacComb, W. S., Quimby, E. H., The Rate of Recovery of Human Skin from the Effects of Hard or Soft Roentgen Rays or Gamma Rays, Radiology, 27: 196-207, Aug. 1936.
- 3-162. McDonald, F. B., Review of Galactic and Solar Cosmic Rays, in Second Symposium on Protection Against Radiations in Space, Reetz, A., Jr., (ed.), Gatlinburg, Tenn., Oct. 12-14, 1964, NASA-SP-71, 1965, pp. 19-29.
- 3-163. Mackin, R. J., Jr., Neugebauer, M., (eds.), The Solar Wind Conference Proceedings, held at The California Inst. of Technology, Pasadena, Calif., Apr. 1-4, 1964, sponsored by Jet Propulsion Lab., Pergamon Press, N. Y., 1966.
- 3-164. Mathe, G., Jammet, H., Pendic, B., et al., Transfusions et Greffes de Moelle Osseuse Homologue Chez des Humains Irradies a Haute Dose Accidentellement, [Transfusions and Grafts of Homologous Bone Marrow in Humans After Accidental High Dosage Irradiation], Rev. Franc. Etud. Clin. Biol., 4: 226-238, Feb. 1959.
- 3-165. Melville, G. S., Jr., Harrison, G. W., Jr., Leffingwell, T. P., Chemical Protection of Monkeys Against X-Irradiation, Radiation Res., 16: 579-580, 1962. (Abstracts of papers for the 10th Ann. Meeting of the Radiation Res. Soc., Colorado Springs, Colo., May 20-23, 1962).

- 3-166. Merriam, G. R., Jr., Biavati, B. J., Bateman, J. L., et al., The Dependence of RBE on the Energy of Fast Neutrons. IV. Induction of Lens Opacities in Mice, Radiation Res., 25: 123-138, 1965.
- 3-167. Merriam, G. R., Jr., Focht, E. F., A Clinical and Experimental Study of the Effect of Single and Divided Doses of Radiation on Cataract Production, Trans. Amer. Ophth. Soc., 60: 35-52, 1962.
- 3-168. Merriam, G. R., Jr., Focht, E. F., A Clinical Study of Radiation Cataracts and the Relationship to Dose, Amer. J. Roentgenol., 77: 759-785, May 1957.
- 3-169. Metropolis, N., Bivins, R., Strom, M., et al., Monte Carlo Calculations on Intranuclear Cascades. I. Low-Energy Studies, Phys. Rev., 110: 185-203, Apr. 1958.
- 3-170. Metropolis, N., Bivins, R., Strom, M., et al., Monte Carlo Calculations on Intranuclear Cascades. II. High-Energy Studies and Pion Processes, Phys. Rev., 110: 204-219, Apr. 1958.
- 3-171. Michaelson, S. M., Odland, L. T., Howland, J. W., Mechanisms of Injury and Recovery from Whole and Partial Body Exposure to Ionizing Radiation, UR-615, University of Rochester, Rochester, N. Y., 1962.
- 3-172. Michaelson, S. M., Odland, L. T., Relationship between Metabolic Rate and Recovery from Radiation Injury, Radiation Res., 16: 281-285, 1962.
- 3-173. Miller, C. E., Louderback, A. L., Opfell, J. B., Human Blood in the Space Environment - In Vitro Studies in Earth Orbit, SSD-TDR-64-1, Space Systems Div., Manned Environmental Systems Directorate, Los Angeles, Calif., Jan. 1964.
- 3-174. Miller, L. S., Fletcher, G. H., Gerstner, H. B., Systemic and Clinical Effects Induced in 263 Cancer Patients by Whole-Body X-Irradiation with Normal Air Doses of 15 to 200 r, SAM-TR-57-92, School of Aviation Medicine, Brooks AFB, Texas, 1957.
- 3-175. Mitchell, J. C., Dalrymple, G. V., Gwilym, H., et al., Proton Depth-Dose Dosimetry, SAM-TR-65-262, School of Aerospace Medicine, Brooks AFB, Texas, 1966.

- 3-176. Model', A. A., State of the Vestibular Analyzer in Persons Working with Sources of Ionizing Radiation, JPRS-32151, Joint Publications Research Service, Washington, D. C., 1965. (Translation of Meditinskaya Radiologiya, 10(5): 71-74, May 1965).
- 3-177. Moritz, A. R., Henriques, F. W., Jr., Effect of Beta Rays on the Skin as a Function of the Energy, Intensity and Duration of Radiation. II. Animal Experiments, Lab. Invest., 1: 167-185, 1952.
- 3-178. Moskaleve, I., Some Results of the Study of the Biological Effect of Neutrons and Protons, FTD-TT-63-1046, Foreign Technology Div., Wright-Patterson AFB, Ohio, Apr. 27, 1964. (Translated from: Nekotoryye Itogi Izucheniya Biologicheskogo Deystviya Neytronov I Protonov, SM-44/54, 1963, 19p.).
- 3-179. National Academy of Sciences, National Research Council, Biological Aspects of Atomic Radiation, Summary Reports, Committees on the Biological Effects of Atomic Radiation, Washington, D. C., 1960, pp. 27-38.
- 3-180. National Academy of Sciences, National Research Council, Committee on the Genetic Effects of Atomic Radiation, Summary Report, 1956, pp. 3-31.
- 3-181. National Academy of Sciences, National Research Council, Committee on the Genetic Effects of Atomic Radiation, Summary Report, 1960, pp. 3-24.
- 3-182. National Academy of Sciences, National Research Council, Committee on the Pathologic Effects of Atomic Radiation, Long-Term Effects of Ionizing Radiation from External Sources, NAS-NRC-849, Washington, D. C., 1961, pp. 41-49.
- 3-183. National Academy of Sciences, National Research Council, Man in Space Committee, Working Group on Radiation Problems, Summary Report, Space Science Board, Washington, D. C., May 1962.
- 3-184. National Aeronautics and Space Administration, Natural Environment and Physical Standards for the Apollo Program, NASA-M-DE-8020-008B, SE-015-001-1, Office of Manned Space Flight, Washington, D. C., April 1965.
- 3-185. National Academy of Sciences, National Research Council, Report of the Committee on Pathologic Effects, in The Biological Effects of Atomic Radiation, Summary Reports, Washington, D. C., 1960, pp. 27-33.

- 3-186. National Aeronautics and Space Administration, Radiological Safety Handbook, NASA-TM-X-54859 (SP-4-41-S), Safety Office, John F. Kennedy Space Center, Fla., Nov. 1, 1964.
- 3-187. National Aeronautics and Space Administration, Selection of Radioisotopes for Space Power Systems (U), NASA-TM-X-1212, Lewis Research Center, Ad Hoc Study Group, Cleveland, Ohio, Mar. 1966.
- 3-188. National Bureau of Standards, National Committee on Radiation Protection, Subcommittee on Heavy Particles (Neutrons, Protons and Heavier), Protection Against Neutrons up to 30 MeV, NBS-Handbook 63, U. S. Government Printing Office, Washington, D. C., 1957.
- 3-189. National Bureau of Standards, Permissible Dose From External Sources of Ionizing Radiation, Handbook 59, 1954, (Addendum to National Bureau of Standards Handbook 59, extends and Replaces insert of Jan. 8, 1957, Maximum Permissible Radiation Exposures to Man, Apr. 15, 1958).
- 3-190. National Bureau of Standards, Report of the International Commission on Radiological Units and Measurements (ICRU), NBS-Handbook 78, U. S. Government Printing Office, Washington, D. C., 1959.
- 3-191. National Committee on Radiation Protection and Measurements, Recommendations for Exposure to Radiation in an Emergency, NCRP-29, Section of Nuclear Medicine, Dept. of Pharmacology, Univ. of Chicago, 1962.
- 3-192. Nefedov, Yu. G., (ed. in chief), Problems of Radiation Safety in Space Flights. Physical and Biological Studies with High-Energy Protons, NASA-TT-F-353, Dec. 1965. (Translation of Problemy Radiatsionnoy Bezopasnosti Kosmicheskikh Poletov; Fizicheskiye i Biologicheskiye Issledovaniya s Protonami Bol'shikh Energiy. Atomizdat, Moscow, 1964).
- 3-193. Nelson, A., Hertzberg, O., Henricsson, I., Recovery Rate and Dose-Reduction Factor in Cysteamine-Treated Mice after Fractionated Irradiation, Ann. N. Y. Acad. Sci., 114: 630-650, Mar. 1964.
- 3-194. Newsome, J. R., Overman, R. R., The Protective Effects of B-Aminoethylisothiuronium Br·HBr and p-Aminopropiophenone Against Acute Sublethal Whole-Body X-Irradiation in Dogs, Radiation Res., 21: 530-540, Apr. 1964.
- 3-195. Nicks, O. W., A Review of the Mariner IV Results, NASA-SP-130, 1967.

- 3-196. Nims, L. F., Sutton, E., Weight Changes and Water Consumption of Rats Exposed to Whole-Body X-Irradiation, Amer. J. Physiol., 171: 17-21, Oct. 1952.
- 3-197. Northcliffe, L. C., Passage of Heavy Ions through Matter, Ann. Rev. Nucl. Sci., 13: 67, 1963.
- 3-198. Nowell, P. C., Cole, L. J., Clonal Repopulation in Reticular Tissues of X-Irradiated Mice: Effect of Dose and of Limb-Shielding, USNRDL-TR-67-79, U. S. Naval Radiological Defense Lab., San Francisco, Calif., July 1967.
- 3-199. Oakberg, E. F., Clark, E., Effect of Dose and Dose-Rate on Radiation Damage to Mouse Spermatogonia and Oocytes as Measured by Cell Survival, J. Cell. Comp. Physiol., 58(3) Pt. 2: 173-182, Dec. 1961.
- 3-200. Oakes, W. R., Lushbaugh, C. C., Course of Testicular Injury Following Accidental Exposure to Nuclear Radiations, Report of a Case, Radiology, 59: 737-743, Nov. 1952.
- 3-201. Okunewick, J. P., The Relationship between Post-Irradiation Recovery and Equivalent Residual Dose, RAND-RM-5048-TAB, The Rand Corp., Santa Monica, Calif., Oct. 1966.
- 3-202. Okunewick, J. P., Kretchmar, A. L., A Mathematical Model for Post-Irradiation Hematopoietic Recovery, RAND-RM-5272-PR, The Rand Corp., Santa Monica, Calif., July 1967.
- 3-203. Oldfield, D. G., Doull, J., Plzak, V., Chemical Protection Against 440-MeV Protons in Mice Pretreated with Mercaptoethylamine (MEA) or p-Aminopropiophenone (PAPP), Radiation Res., 26: 12-24, 1965.
- 3-204. Pack, G. T., Davis, J., Radiation Cancer of the Skin, Radiology, 84: 436-442, 1965.
- 3-205. Page, N. P., Ainsworth, E. J., Leong, G. F., The Relationship of Exposure Rate and Exposure Time to Radiation Injury in Sheep, USNRDL-TR-67-22, U. S. Naval Radiological Defense Lab., San Francisco, Calif., Jan. 1967.
- 3-206. Paterson, J. R. K., Choice of Technique, Time and Dose. Treatment of Malignant Disease by Radiotherapy, 2nd ed., The Williams & Wilkins Co., Baltimore, Md., 1963, pp. 25-47.

- 3-207. Payne, R. B., Effects of Acute Radiation Exposure on Human Performance, in Protection against Radiation Hazards in Space, Symposium, TID-7652, Book I, U. S. AEC Div. of Technical Information Extension, Oak Ridge, Tenn., 1962, pp. 343-374.
- 3-208. Pickering, J. E., National Aeronautics and Space Administration, Washington, D. C., personal communication, 1967.
- 3-209. Pickering, J. E., Biological Effects of Whole-Body Proton Irradiation, Aerospace Med., 34: 942-943, Oct. 1963.
- 3-210. Pickering, J. E., Space Radiobiology. Training and Operations: A Concept, AMD-TR-65-2, Aerospace Medical Div., Brooks AFB, Texas, June 1965.
- 3-211. Pickering, J. E., USAF Animal Program on Proton Effects, Aerospace Medical Division, Brooks AFB, Texas, in Review of Space Radiation Problems, NASA, Office of Manned Space Flight, Washington, D. C., Jan. 22, 1966, pp. 232-246.
- 3-212. Pifer, J. W., Toyooka, E. T., Murray, R. W., et al., Neoplasms in Children Treated with X-Rays for Thymic Enlargement. I. Neoplasms and Mortality, J. Nat. Cancer Inst., 31: 1333-1356, Dec. 1963.
- 3-213. Quimby, E. H., MacComb, W. S., Further Studies on the Rate of Recovery of Human Skin from the Effects of Roentgen or Gamma-Ray Irradiation, Radiology, 29: 305-312, 1937.
- 3-214. Reisner, A., Hauterythem und Rontgenbestrahlung, Ergebn. Med. Strahlenforsch., 6: 1-60, 1933.
- 3-215. Relative Biological Effectiveness Committee Report to the Intern. Commissions on Radiological Protection and on Radiological Unit and Measurements, Health Physics, 9: 357-384, 1963.
- 3-216. Rexford-Welch, S. C., Clinical Effects Consequent on the Exposure of Mammalian Ocular Tissues to High Energy Protons, in Proc. Symposium Biol. Effects of Neutron and Proton Irradiations, Oct. 7-11, 1963, Upton, N. Y., International Atomic Energy Agency, Vol. I., 1964, pp. 287-295.
- 3-217. Rice, E. A., Early Performance Decrement in Primates Following Pulsed Ionizing Radiation, SAM-TR-65-60, School of Aerospace Medicine, Brooks AFB, Texas, Aug. 1965.

- 3-218. Rich, M., Madey, R., Range-Energy Tables, UCRL-2301,
Univ. of California Radiation Lab., Berkeley, Calif.,
1954.
- 3-219. Rinfret, A. P., Medical Products Department, Linde Co.,
Div. of Union Carbide Corp., Tonawanda, N. Y., personal
communication, 1966.
- 3-220. Robbins, L. L., Aub, J. C., Cope, O., et al., Superficial
"Burns" of Skin and Eyes from Scattered Cathode Rays,
Radiology, 46: 1-23, Jan. 1946.
- 3-221. Roth, E. M., The Mechanism of Oxygen Toxicity as a Model for
Interpreting Certain Biometeorological Phenomena, Int.
J. Biometeor., 11: 79-91, 1967.
- 3-222. Roth, E. M., Space-Cabin Atmospheres, Part I. Oxygen
Toxicity, NASA-SP-47, 1964.
- 3-223. Rossi, H. H., Maximum Permissible Radiation Levels for High-
Energy Installations, in Symposium on the Conference on
Shielding of High-Energy Accelerators, New York, Apr.
11-13, 1957, TID-7545, U. S. AEC, Div. of Research,
Washington, D. C., Dec. 6, 1957, pp. 148-156.
- 3-224. Russell, W. L., Effect of Radiation Dose Fractionation on
Mutation Frequency in Mouse Spermatogonia, Genetics, 50:
282, 1964.
- 3-225. Russell, W. L., The Effect of Radiation Dose Rate and Fractiona-
tion on Mutation in Mice, in Repair from Genetic Radiation
Damage, Sobels, F. H., (ed.), Pergamon Press, Oxford,
England, 1963, pp. 205-217.
- 3-226. Russell, W. L., Studies in Mammalian Radiation Genetics,
Nucleonics, 23(1): 53-56, 62, 1965.
- 3-227. Russell, W. L., Russell, L. B., Kelly, E. M., Radiation Dose
Rate and Mutation Frequency, Science, 128: 1546-1550,
Dec. 1958.
- 3-228. Sacher, G. A., Late Effects of Continuous Irradiation: The
Relation of Hematological Injury to Lethality, LAVAL MED.,
34: 163-168, Jan. 1963.
- 3-229. Sacher, G. A., On the Statistical Nature of Mortality with
Special Reference to Chronic Mortality, Radiology, 67:
250-257, 1956.

- 3-230. Sacher, G. A., Grahn, D., Survival of Mice under Duration-of-Life-Exposure to Gamma Rays, I. The Dosage-Survival Relation and the Lethality Function, J. Nat. Cancer Inst., 32: 277-321, Feb. 1964.
- 3-231. Sacher, G. A., Trucco, E., Theory of Radiation Injury and Recovery in Self-Renewing Cell Populations, Argonne National Labs., Argonne, Ill., (unpublished data).
- 3-232. Saenger, E. L., (ed.), Medical Aspects of Radiation Accidents. A Handbook for Physicians, Health Physicists and Industrial Hygienists, U. S. AEC, Headquarters, Washington, D. C., 1963.
- 3-233. Sandberg, A., Doull, J., Influence of Exposure to Low Levels of Gamma and Fast Neutron Irradiation on the Life Span of Animals. II. Effect of the Addition of 2-Mercaptoethylamine or Para-aminopropiophenone to the Diets of Chronically Irradiated Mice and the Production of Methemoglobin by Feeding a Diet Containing Para-aminopropiophenone, Quarterly Progress Report No. 51, Univ. of Chicago, USAF Radiation Lab., 1964, pp. 116-128.
- 3-234. Sanders Associates, Inc., Nashua, N. H., Cambridge Nuclear Corp., Cambridge, Mass., Thulium 170 and Thulium 171 Isotopic Power Systems (Proposal 86HM Vol. III Appendices), prepared for NASA, Nuclear Systems and Space Power Div., Mar. 1966.
- 3-235. Scarf, F. L., Plasma in the Magnetosphere, NASA-CR-81759, Dec. 1966. (Prepared for Vol. I of Advances in Plasma Physics, Thompson, W., Simon, A., (eds.), Interscience Press, N. Y.).
- 3-236. Schaefer, H. J., Energy Dissipation Characteristics in Tissue for Ionizing Radiation in Space, Progress Report No. 15, NASA Order No. R-75, Naval Aerospace Medical Inst., Pensacola, Fla., 1966.
- 3-237. Schaefer, H. J., Flare Hazards at Solar Minimum: Dosimetric Evaluation of the Class 2 Flare of February 5, 1965, NAMI-970, Naval Aerospace Medical Inst., Pensacola, Fla., 1966.
- 3-238. Schaefer, H. J., Galactic Radiation Hazard in Long-Term Space Missions, Aerospace Med., 39(3): 271-276, 1968.
- 3-239. Schaefer, H. J., Linear Energy Transfer Spectra and Dose Equivalents of Galactic Radiation Exposure in Space, NAMI-987, U. S. Naval Aerospace Medical Center, Pensacola, Fla., Dec. 1966.

- 3-240. Schaefer, H. J., Local Dose from Proton and Alpha Particle Enders Behind Complex Shield Systems, in Second Symposium on Protection Against Radiations in Space, Gatlinburg, Tenn., Oct. 12-14, 1964, Reetz, A., Jr., (ed.), NASA-SP-71, 1965, pp. 507-512.
- 3-241. Schaefer, H. J., Measurements of the Proton Dose of the Gemini Astronauts with Nuclear Emulsions, NASA-TT-F-11237, Oct. 1967. (Translation of Messungen der Protonendosis der Gemini-Astronauten mit Kernemulsionen, Biophysik, 4: 63-67, 1967).
- 3-242. Schaefer, H. J., A Note on the Dosimetric Interpretation of Rigidity Spectra for Solar Particle Beams, NAMI-960, Naval Aerospace Medical Inst., Pensacola, Fla., Apr. 1966.
- 3-243. Schaefer, H. J., A Note on the Galactic Radiation Exposure in Geomagnetically Unprotected Regions of Space, NAMI-982, Naval Aerospace Medical Inst., Pensacola, Fla., 1966.
- 3-244. Schaefer, H. J., A Note on the RBE of Proton Radiation in Space, Project MR-005-13-1002, Subtask 1, Rep. 18, Naval School of Aviation Medicine, Pensacola, Fla., Jan. 1961.
- 3-245. Schaefer, H. J., Radiation Hazards to Man on the Moon, in Proceedings of the Second Lunar International Laboratory Symposium, Malina, F. J., (ed.), Pergamon Press, Inc., New York, Oxford, 1967, Chapt. 9, pp. 83-95.
- 3-246. Schaefer, H. J., Tissue Ionization Dosages in Proton Radiation Fields in Space, Aerospace Med., 31(10): 807-816, 1960.
- 3-247. Schaefer, H. J., Golden, A., Solar Influences on the Extra-Atmospheric Radiation Field and Their Radiobiological Implications, in Physics and Medicine of the Atmosphere and Space, Benson, O. O., Jr., Strughold, H., (eds.), John Wiley & Sons, Inc., N. Y., 1960, pp. 157-181.
- 3-248. Scott, W. W., Angular Distribution of Thick-Target Bremsstrahlung which Includes Multiple Electron Scatterings, NASA-TN-D-4063, Aug. 1967.
- 3-249. Scott, W. W., Estimates of Primary and Secondary Particle Doses behind Aluminum and Polyethylene Slabs due to Incident Solar-Flare and Van Allen Belt Protons, ORNL-RSIC-18, Oak Ridge National Lab., Union Carbide Corp., Oak Ridge, Tenn., July 1967.

- 3-250. Scott, W. W., Alsmiller, R. G., Jr., Comparisons of Results Obtained with Several Proton Penetration Codes, ORNL-RSIC-17, Oak Ridge National Lab., Union Carbide Corp., Oak Ridge, Tenn., July 1967.
- 3-251. Searle, A. G., Phillips, R. J. S., Genetic Effects of Neutron Irradiation in Mice, in Proceedings of the Symposium on the Biological Effects of Neutron and Proton Irradiations, Oct. 7-11, 1963, Upton, N. Y., International Atomic Energy Agency, Vienna, Mar. 1964, Vol. I, pp. 361-370.
- 3-252. Seltser, R., Sartwell, P. E., The Influence of Occupational Exposure to Radiation on the Mortality of American Radiologists and Other Medical Specialists, Amer. J. Epidem., 81: 2-22, Jan. 1965.
- 3-253. Shapiro, E. S., Feasibility and Potential Effectiveness of Partial-Body Shielding for Personnel Protection against Ionizing Radiation, USNRDL-TR-67-39, U. S. Naval Radiological Defense Lab., San Francisco, Calif., Apr. 1967.
- 3-254. Shipman, T. L., Lushbaugh, C. C., Petersen, D. F., et al., Acute Radiation Death Resulting from an Accidental Nuclear Critical Excursion, J. Occup. Med., Suppl. 3: 146-192, Mar. 1961.
- 3-255. Skurdin, G. A., Al'pert, Ya. L., Krasovskiy, V. I., et al., Space Research, Transactions of the All-Union Conference on Space Physics, NASA-TT-F-389, May 1966. (Translation of Issledovaniya Kosmicheskogo Prostranstva. Trudy Vsesoyuznoy Konferentsii po Fizike Kosmicheskogo Prostranstva. Izdatel'stvo Nauka, Moscow, June 10-16, 1965).
- 3-256. Smedal, M. I., Johnston, D. O., Salzman, F. A., et al., Ten Year Experience with Low Megavolt Electron Therapy, Amer. J. Roentgenol., 88(2): 215-228, Aug. 1962.
- 3-257. Socolow, E. L., Hashizume, A., Neriishi, S., et al., Thyroid Carcinoma in Man After Exposure to Ionizing Radiations: A Summary of the Findings of Hiroshima and Nagasaki, New Eng. J. Med., 268: 406-410, Feb. 1963.
- 3-258. Sondhaus, C. A., Biological Effects of High Energy Protons, in Proceedings of the Symposium on the Protection Against Radiation Hazards in Space, Gatlinburg, Tenn., Nov. 5-7, 1962, TID-7652 Book I, USAEC, Division of Technical Information Extension, Oak Ridge, Tenn., 1963, pp. 312-342.

- 3-259. Sondhaus, C. A., Effect of High-Energy Protons and A Alpha Particles on Small Mammals, in Second Symposium on Protection Against Radiations in Space, Gatlinburg, Tenn., Oct. 12-14, 1964, Reetz, A., Jr., (ed.), NASA-SP-71, 1965, pp. 97-103.
- 3-260. Spalding, J. F., Hawkins, S. B., Strang, V. G., The Relative Effectiveness of Neutrons of 1.4-MeV and 14-MeV Energies and Gamma Rays in the Reduction of Fertility in the Male Mouse, Radiation Res., 9: 369-377, 1958.
- 3-261. Stapleton, G. E., Curtis, H. J., The Effects of Fast Neutrons on the Ability of Mice to Take Forced Exercise, Manhattan Project Report No. MDDC-696, 1946.
- 3-262. Steward, P. G., Wallace, R., Calculation of Stopping Power and Range-Energy Values for Any Heavy Ion in Nongaseous Media, UCRL-17314, Lawrence Radiation Lab., Univ. of California, Berkeley, Calif., Dec. 1966.
- 3-263. Stone, R. E., Neutron Therapy and Specific Ionization, Amer. J. Roentgenol., 59: 771-785, 1948.
- 3-264. Strandqvist, M., A Study of the Cumulative Effects of Fractionated X-Ray Treatment Based on the Experience Gained at the Radiumhemmet with the Treatment of 280 Cases of Carcinoma of Skin and Lip, Acta Radiol. (Suppl.), 55: 300, 1944.
- 3-265. Sullivan, M. F., Thompson, R. C., The Influence of Fractionated X-Irradiation on the Intestine of Rats Protected by Cysteine and Partial-Body Shielding, Radiation Res., 23: 551-563, 1964.
- 3-266. Sulzberger, M. B., Baer, R. L., Borota, A., Do Roentgen-Ray Treatments as Given by Skin Specialists Produce Cancers or Other Sequelae? Follow-Up Study of Dermatologic Patients Treated with Low-Voltage Roentgen Rays, Arch. Dermat. Syph., 65: 639-655, June 1952.
- 3-267. Taketa, T. S., Biological Effects of Protons and Neutrons in Large Animals, in Second Symposium on Protection Against Radiation Hazards in Space, Gatlinburg, Tenn., Oct. 12-14, 1964, Reetz, A., Jr., (ed.), NASA-SP-71, 1965, pp. 73-84.
- 3-268. Texas Nuclear Corporation, Formal Report No. 1 under Contract AF 41(609)-2654, Nov. 3, 1965. (no title).
- 3-269. Tiunov, L. A., Vasil'yev, G. A., Val'dshteyn, E. A., Drugs for Radiation Protection, FTD-TT-65-556, Foreign Technology Div., Wright-Patterson AFB, Ohio, (Translation of Protivolumcheyye Sredstva, 1964), Feb. 17, 1966.

- 3-270. Tobias, C., Donner Laboratory, University of California, Berkeley, Calif., personal communication, 1968.
- 3-271. Todd, P., Heavy-Ion Irradiation of Cultured Human Cells, Radiation Research Suppl., 7: 196-207, 1967.
- 3-272. Toyooka, E. T., Pifer, J. W., Hempelmann, L. H., Neoplasms in Children Treated with X-Rays for Thymic Enlargement, III. Clinical Description of Cases, J. Nat. Cancer Inst., 31: 1379-1405, Dec., 1963.
- 3-273. Traenkle, H. L., Mulay, D., Further Observations on Late Radiation Necrosis Following Therapy of Skin Cancer. The Results of Fractionation of the Total Dose, Arch. Derm., 81: 908-913, June 1960.
- 3-274. Traynor, J. E., Department of Radiobiology, School of Aerospace Medicine, Brooks AFB, Texas, personal communication, 1967.
- 3-275. TRW Systems Group, Redondo Beach, Calif., TRW Space Log, Vol. 6(4), Winter 1966-67, and Vol. 7(3), Fall, 1967.
- 3-276. Tubiana, M., Discussion, Symposium on Physical Factors and Modification of Radiation Injury, Hamilton, L. D. (ed.), Ann. N. Y. Acad. Sci., 114, Art. I:, 146-147, 1964.
- 3-277. United Nations, Report of the United Nations Scientific Committee on the Effects of Atomic Radiation, General Assembly, Official Records: Nineteenth Session, Supplement No. 14 (A/5814), N. Y., 1964.
- 3-278. United Nations, Somatic Effects, in Report of the Scientific Committee on the Effects of Atomic Radiation, General Assembly, Seventeenth Session, Supplement No. 16 (A/5216), N. Y., 1962, pp. 9-13.
- 3-279. U. S. Army Medical Research and Development Command, Nuclear Energy Division, Proceedings of the Meeting on Radiation Chemoprophylaxis, July 17-18, 1964, Washington, D. C.
- 3-280. U. S. Atomic Energy Commission, Proceedings of the Symposium on the Protection against Radiation Hazards in Space, Gatlinburg, Tenn., Nov. 5-7, 1962, TID-7652, Book 2: Shielding Against Space Radiations. USAEC, Division of Technical Information, Oak Ridge, Tenn., 1963.

- 3-281. U. S. Atomic Energy Commission, Standards for Radiation Protection, Chapter 0524, AEC Manual, Washington, D. C., Aug. 12, 1963.
- 3-282. Van Cleave, C. D., Irradiation of the Nervous System, Rowman and Littlefield, New York, 1963.
- 3-283. Van Lancker, J. L., Wolf, R. C., Mowbray, J. B., Protection of Primates Against Lethal Doses of X-Radiation, Nature (Lond.), 194: 492-493, May 1962.
- 3-284. Vette, J. I., Models of the Trapped Radiation Environment, Vol. I: Inner Zone Protons and Electrons, NASA-SP-3024, 1966.
- 3-285. Vette, J. I., The Updating and Dissemination of the Knowledge of Trapped Radiation - Model Environments, in AAS-NASA Symposium on the Physics of Solar Flares, Hess, W. N. (ed.), Goddard Space Flight Center, Greenbelt, Md., Oct. 28-30, NASA-SP-50, 1964, pp. 47-55.
- 3-286. Volynkin, Y. M., Antipov, V. V., Guda, V. A., et al., The Biological Evaluation of Radiation Conditions on the Path Between the Earth and the Moon, presented at XV International Astronautical Congress, Warsaw, Sept. 1964, NASA TT F-279, 1964.
- 3-287. Voyevodina, O. Ye., Effect of Ionizing Radiation on Conditioned Reflex Action, JPRS-43077, Joint Publications Res. Service, Washington, D. C., Oct. 1967. (Translation of selected articles from Russian book "Remote Results of the Effect of Roentgen Rays on the Higher Nervous Activity of Dogs," Voyevodina, O. Ye., Academy of Medical Sciences, USSR, Leningrad, Meditsina Publishing House, 1967).
- 3-288. Wald, N., Thoma, G. E., Jr., Broun, G., Jr., Hematologic Manifestations of Radiation Exposure in Man, in Progress in Hematology, Tocantins, L. M. (ed.), Grune & Stratton, New York, 1962, Vol. III, pp. 1-52.
- 3-289. Wallace, R., Sondhaus, C., Techniques Used in Shielding Calculations for High Energy Accelerators: Applications to Space Shielding, in Proceedings of the Symposium on Protection Against Radiation Hazards in Space, Gatlinburg, Tenn., Nov. 5-7, 1962, TID-7652, Book 2, Atomic Energy Commission, Division of Technical Information, Oak Ridge, Tenn., 1963, pp. 829-851.

- 3-290. Wallace, R., Steward, P. G., Sondhaus, C., Primary- and Secondary-Proton Dose Rates in Spheres and Slabs of Tissue, in Second Symposium on Protection Against Radiation in Space, Gatlinburg, Tenn., Oct. 12-14, 1964, Reetz, A. (ed.), NASA-SP-71, 1965, pp. 301-329.
- 3-291. Wang, R. I. H., Ballantyne, J., Chemical Protection Against Repeated Supralethal Doses of Ionizing Radiation in Mice, Radiation Res., 23: 369-376, 1964.
- 3-292. Warren, S., Bowers, J. Z., The Acute Radiation Syndrome in Man, Ann. Intern. Med., 32: 207-216, Feb. 1950.
- 3-293. Weagent, R. A., Proton Shielding Slide Rule, North American Aviation, Inc., Space and Information System Div., Downey, Calif. 1963.
- 3-294. Webb, P., Combined Stresses, in Bioastronautics Data Book, Webb, P. (ed.), NASA-SP-3006, 1964, pp. 159-165.
- 3-295. Webber, W. R., A Review of Solar Cosmic Ray Events, in AAS-NASA-Symposium on the Physics of Solar Flares, Goddard Space Flight Center, Greenbelt, Md., Oct. 28-30, 1963, Hess, W. N. (ed.), NASA-SP-50, 1964, pp. 215-255.
- 3-296. White, R. S., Synopsis of the Magnetosphere, in Lectures in Aerospace Medicine, Sixth Series, School of Aerospace Medicine, Brooks AFB, Texas, Feb. 6-9, 1967, pp. 401-426.
- 3-297. Woodward, K. T., Michaelson, S. M., Noonan, T. R., et al., The Effect of Dose-Rate on the Acute Lethal Response of Dogs, Int. J. Rad. Biol., 12(3): 265-276, 1967.
- 3-298. Zellmer, R. W., Allen, R. G., Symposium on Aerospace Radiobiology. VIII. Cosmic Radiation - Laboratory Observations, Aerospace Med., 32: 942-946, Oct. 1961.
- 3-299. Zeman, W. H., Curtis, H. J., Baker, C. P., Histopathologic Effect of High-Energy-Particle Microbeams on the Visual Cortex of the Mouse Brain, Radiation Res., 15: 496-514, 1961.
- 3-300. Zeman, W., Curtis, J., Gebhard, E. L., et al., Tolerance of Mouse-Brain Tissue to High-Energy Deuterons, Science, 130: 1760-1761, Dec. 1959.

4. MAGNETIC FIELDS

Prepared by

D. E. Busby, M. D., Lovelace Foundation

TABLE OF CONTENTS

4.	MAGNETIC FIELDS	4-1
	Low Magnetic Fields	4-1
	High Magnetic Fields	4-2
	References	4-5

MAGNETIC FIELDS

In future space operations, astronauts may be exposed to a very wide range of magnetic field intensities and gradients. Figure 4-1 presents magnetic field intensities expected at several points in the solar system. It suggests that field intensities on the lunar surface will be several orders of magnitude less than the geomagnetic field. At a distance of more than 10 Earth radii, the solar wind is expected to have a magnetic field of only 10^{-4} to 10^{-5} gauss (16). Intricacies of the interaction between the solar

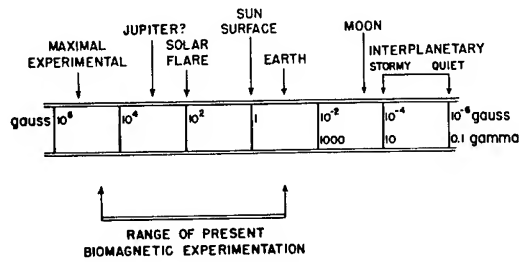


Figure 4-1

Range of Magnetic Field Intensities

(After Beischer⁽⁸⁾)

wind, magnetic fields, and trapped radiation belts around the Earth, are being unraveled (2, 26, 27, 29, 33). A neutral sheet or wedge of low field strength is present on the down-Earth side of magnetosphere. The surface of Venus probably has intensities of less than 0.05 gauss and Mars, even lower values. While the solar photosphere has a field strength of 1 gauss, the center of sunspots have been calculated to range from 1000 to 3500 gauss. The contribution of electronic equipment on board a space vehicle to the total magnetic field experienced by an astronaut both extra- and intra-vehicularily is not clear (15).

The high-gradient magnetic fields with intensities of several tens of thousands gauss suggested for anti-radiation shielding and electric propulsion systems may, in some instances, be involved in human exposure (14, 15, 25).

Relatively little is known about the specific effects of high and low intensity magnetic fields on man (1, 7, 8, 9, 11, 15, 22). Past studies in magneto-biology have been directed mainly at determining the effects of magnetic fields different from that of the geomagnetic field on sub-human species, plants, and simple chemical systems. Several reviews of these background materials are available (1, 3, 5, 7, 8, 9, 11, 15, 19, 22, 31).

Low Magnetic Fields

Very few human exposures to a magnetically quiet environment have been reported. A certain amount of experience has accumulated during ordnance

work inside degaussing coils. A health survey of personnel exposed to an almost magnetically quiet environment during most of their working day over several years revealed no ailment traceable to this unusual environmental exposure (11). A number of physiologic and psychologic studies on two men exposed for 14 days to a magnetic field of about 50 gamma (1 gamma = 10^{-5} gauss) revealed no abnormal responses (9, 11). A similar study of low gauss in which six men were exposed to a magnetic field below 50 gamma revealed significant alterations in scotopic critical flicker fusion and brightness discrimination in five of the six subjects during the period of exposure (10, 13). Such limited observations suggest that some physiologic processes of the human may be altered in the geomagnetic and lunar magnetic fields, but more experimental work is required before the operational significance of these findings is known (15).

The view is generally held that during the millions of years life was evolving in our planet, the general magnitude of the Earth's magnetic field was no different from that measured at the present time (4), though its polarity and strength have detectably changed several times, the last major change occurring about 7×10^5 years ago (20, 28). Accordingly, it is not unreasonable to assume that living creatures have become accustomed to the geomagnetic field as part of their natural habitat, and possibly that some biologic processes have actually become to some degree dependent on the presence of the geomagnetic field (4). It has been pointed out that normal magnetobiologic effects would take place on molecular and atomic levels (8). It is suggested that a turn of the human body in the geomagnetic field imparts a momentary precession, according to the Larmor theorem, of approximately 2000 cps to all hydrogen nuclei in the body. Other magnetic cell constituents should also precess with frequencies according to their mechanical and magnetic moments. One must consider that the near absence of precession movements in very low intensity magnetic fields may deprive living matter of spatial clues, and that very careful long-term physiologic and psychologic observations of man in such fields are necessary before predictions that human performance will be unaltered under such conditions (15).

Few data are available on the magnetic fields encountered within a typical spacecraft cabin. The induced magnetic fields at different distances from specific electronic components and the magnetic characteristics of representative spacecraft materials have been recorded (17). Such data are of value in design of magnetic field experiments in orbit or on the lunar surface.

High Magnetic Fields

What is presently known of the effects of high magnetic fields on man is summarized in Table 4-2. These responses were obtained from personnel of a number of nuclear physics laboratories who are exposed occupationally to high magnetic fields.

This list should not be taken to mean that the performance of man will not be degraded in high magnetic fields. There is every indication from recent studies using spider monkeys as subjects that very high magnetic fields (up to 100,000 gauss for 24 hrs.) may affect neural and cardiac

Table 4-2
Effects of Magnetic Fields on Man
(After Beischer⁽⁹⁾)

<p><u>VISUAL SENSATIONS (PHOSPHENES) IN ALTERNATING FIELD.</u></p> <p><u>NO SENSATION OBSERVED IN PART AND ENTIRE BODY EXPOSURE TO NON-CHANGING FIELDS UP TO 20 kilogauss FOR A DURATION OF 15 MINUTES.</u></p> <p><u>NO AFTER-EFFECTS FOLLOWING EXPOSURE TO FIELDS OF 5 kilogauss FOR LESS THAN 3 DAYS PER YEAR PER MAN.</u></p> <p><u>TASTE AND PAIN SENSATION CAUSED BY INTERACTION WITH FILLINGS OF TEETH SOMETIMES DESCRIBED.</u></p>
--

function (12, 13, 23). These studies demonstrated a shift of the frequency of the EEG to higher values and a considerable increase in intensity of the brain potential. The electrocardiogram showed a decrease in heart rate, an increase in sinus arrhythmia and an augmentation of the amplitude of the T wave. No gross pathology has been seen in these animals. The significance of such alterations to the general health and psychomotor performance of humans remains to be determined.

Exposure of animals, isolated organs, neoplastic and non-neoplastic tissue cultures and simple chemical systems to high magnetic fields has produced a great variety of biologic effects (15). To date, no definite magnetic dose-effect relationship has been established. Effects have been predicated on the basis of field strength alone (9), as well as on the inhomogeneity of the paramagnetic strength of the field (4).

The coupling of magnetic fields with biological systems has been hypothesized as due to (4, 6, 18, 24, 29, 32):

- 1) Generation of electromotive force in moving conductors.
- 2) Force exerted upon moving charge carriers at critical sites (24).
- 3) Torque exerted on permanent magnetic dipoles and non-spherical para- or diamagnetic particles (29).
- 4) Retarding effect on the rotational diffusion of large molecules, leading to a decrease in biochemical reaction rates.
- 5) Alteration of bond angles, which may influence chemical reaction rates (24).
- 6) Alteration of tunneling rate of protons in hydrogen bonds of macromolecular systems.

Any one of these basic factors could possibly alter human performance under very high magnetic fields. Much work is required to classify the mechanisms responsible for behavioral changes in animals exposed to these fields (15, 21).

There is a deficiency of data on electromagnetic fields in which the electro and magnetic components are strongly perturbed. Checklists of sources of different electromagnetic radiations are available (34).

REFERENCES

- 4-1. Alexander, H. S., Biomagnetics - The Biological Effects of Magnetic Fields, Amer. J. Med. Electron., 2: 181-187, July-Sept. 1962.
- 4-2. Axford, W. I., Petschek, H. E., Siscoe, G. L., Tail of the Magnetosphere, J. Geophys. Res., 70: 1231-1236, 1965.
- 4-3. Barnothy, J. M., Biologic Effects of Magnetic Fields, in Medical Physics, Vol. III, Glasser, O., (ed.), The Year Book Publishers, Inc., Chicago, 1960, pp. 61-64.
- 4-4. Barnothy, J. M., Introduction, in Biological Effects of Magnetic Fields, Barnothy, M. F., (ed.), Plenum Press, N. Y., 1964, pp. 3-24.
- 4-5. Barnothy, M. F., (ed.), Biological Effects of Magnetic Fields, Plenum Press, N. Y., 1964.
- 4-6. Barnothy, M. F., A Possible Effect of the Magnetic Field upon the Genetic Code, in Biological Effects of Magnetic Fields, Barnothy, M. F., (ed.), Plenum Press, N. Y., 1964, pp. 80-89.
- 4-7. Becker, R. O., Relationship of Geomagnetic Environment to Human Biology, N. Y. State J. Med., 63(Pt. 2): 2215-2219, Aug. 1963.
- 4-8. Beischer, D. E., Biological Effects of Magnetic Fields in Space Travel, in XIIth International Astronautical Congress, Washington, D. C., 1961, Baker, R. M. L., Jr. and Makemson, M. W., (eds.), Academic Press, N. Y., 1963, pp. 515-525.
- 4-9. Beischer, D. E., Biomagnetics, in Lectures in Aerospace Medicine, School of Aerospace Medicine, Brooks AFB, Texas, Feb. 4-8, 1963, pp. 367-386.
- 4-10. Beischer, D. E., Do Earth and Lunar Magnetic Fields Have an Effect on Man and Does Man Himself Exert Magnetic Forces? Naval Aerospace Medical Inst., Pensacola, Fla., in Preprints of Scientific Program, 37th Annual Meeting, Aerospace Medical Association, Las Vegas, Nev., Apr. 18-21, 1966, pp. 62.

- 4-11. Beischer, D. E., Human Tolerance to Magnetic Fields, Astronautics, 7(3): 24-25, Mar. 1962.
- 4-12. Beischer, D. E., Knepton, J. C., Jr., Influence of Strong Magnetic Fields on the Electrocardiogram of Squirrel Monkeys (Saimiri Sciureus), NAV-SAM-MR005.13-9010-1-8, Naval School of Aviation Medicine, Pensacola, Fla., 1964.
- 4-13. Beischer, D. E., Knepton, J. C., Jr., Kembro, D. V., Exposure of Man to Magnetic Fields as Will be Experienced on the Moon and Mars, Letter Rept. NASA Order No. R-39, Naval Aerospace Medical Inst., Pensacola, Fla., 1967.
- 4-14. Bernert, R. E., Stekly, Z. J. J., Magnetic Radiation Shielding Systems Analysis, AVCO-5278-AMP-134, Avco-Everett Research Lab., Everett, Mass., 1964.
- 4-15. Busby, D. E., Biomagnetics. Considerations Relevant to Manned Space Flight, NASA-CR-889, Sept. 1967.
- 4-16. Cantarano, S., Mariani, F., Magnetic Field Measurements in Interplanetary Space, ESRO-SR-4, European Space Research Organisation, France, 1966.
- 4-17. Fuchs, R. A., Experimenter's Design Handbook for the Manned Lunar Surface Program, HA-SSD-60352R, Hughes Aircraft Co., Culver City, Calif., Jan. 1967, pp. 4-21. (Prepared under NASA Contract NAS 8-20244).
- 4-18. Gross, L., Distortion of the Bond Angle in a Magnetic and Its Possible Magnetobiological Implications, in Biological Effects of Magnetic Fields, Barnothy, M. F., (ed.), Plenum Press, N. Y., 1964, pp. 74-79.
- 4-19. Gualtierotto, T., Effects of a Steady Magnetic Field on Cerebellar Centers for Equilibrium and Orientation, in XIIth International Astronautical Congress, Washington, D. C., 1961, Baker, R. M. L., Jr. and Makemson, M. W., (eds.), Academic Press, N. Y., 1963, pp. 586-604.
- 4-20. Heirtzler, J. R., Hayes, D. E., Magnetic Boundaries in the North Atlantic Ocean, Science, 157: 185-187, Jul. 14, 1967.
- 4-21. Kholodov, Yu. A., The Effect of Electromagnetic and Magnetic Fields on the Central Nervous System, NASA-TT-F-465, June 1967. (Translation of Vliyaniye Elektromagnitnykh i Magnitnykh Poley na Tsentral'nuyu Nervnuyu Sistemu. Academy of Sciences, USSR, Moscow, 1966).

- 4-22. Kholodov, Yu. A., Magnetobiology, JPRS-33321, Joint Publications Research Service, Washington, D. C., Dec. 14, 1965, (Translated from: Priroda, No. 10: 12-21, Oct. 1965).
- 4-23. Knepton, J. C., Jr., Beischer, D. E., Possible Effects of Very High Magnetic Fields on the Electronencephalogram of the Squirrel Monkey (*Saimiri Sciureus*), Naval Aerospace Medical Inst., Pensacola, Fla. (Paper presented at the 37th Annual Meeting of the Aerospace Medical Association, Las Vegas, Nev., Apr. 18-21, 1966).
- 4-24. Kusabayashi, S., Laronge, T. M., Labes, M. M., Mechanisms for the Effects of Electric and Magnetic Fields on Biological Systems, NASA-CR-91523, 1967.
- 4-25. Levy, R. H., Janes, G. S., Plasma Radiation Shielding, AVCO-659-RR-192, Avco-Everett Research Lab., Everett, Mass., Sept. 1964.
- 4-26. Mackin, R. J., Jr., Neugebauer, M., (eds.), The Solar Wind Conference Proceedings, California Institute of Technology, Pasadena, Calif., Apr. 1-4, 1964, sponsored by Jet Propulsion Lab., Pergamon Press, N. Y., 1966.
- 4-27. Ness, N. F., Earth's Magnetic Field: A New Look, Science, 151(3714): 1041-1052, Mar. 1966..
- 4-28. Pitman, W. C., Heirtzler, J. R., Magnetic Anomalies over the Pacific-Antarctic Ridge, Science, 154: 1164-1171, Dec. 1966.
- 4-29. Roth, E. M., Response of Biological Atoms and Molecules to Magnetic Fields, Lovelace Foundation for Medical Education and Research, Albuquerque, N. M., 1967. (Prepared under NASA contract NASr-115, unpublished).
- 4-30. Scarf, F. L., Plasma in the Magnesosphere, NASA-CR-81759, Dec. 1966. (Prepared for Vol. 1 of Advances in Plasma Physics, Thompson, W., Simon, A., (eds.), Interscience Press, N. Y.
- 4-31. University of Illinois, College of Pharmacy, Abstracts of papers of the Third International Biomagnetic Symposium, Univ. of Illinois, Chicago, Mar. 22-23, 1966.
- 4-32. Valentiniuzzi, M., Rotational Diffusion in a Magnetic Field and Its Possible Magnetobiological Implications, in Biological Effects of Magnetic Fields, Barnothy, M. F., (ed.), Plenum Press, N. Y., 1964, pp. 63-73.

-
- 4-33. White, R. S., Synopsis of the Magnetosphere, in Lectures in Aerospace Medicine, Sixth Series, School of Aerospace Medicine, Brooks AFB, Texas, Feb. 6-9, 1967, pp. 401-426.
- 4-34. Zilitinkevich, S. I., Classification of Electromagnetic Wave Sources, JPRS-43874, Joint Publications Research Service, Washington, D. C., Jan. 1968. (Translation of News of Higher Educational Institutions, Leningrad, 10(10): 13-17, 1967).

5. ELECTRIC CURRENT

Prepared by

S. Finkelstein, M. D., Lovelace Foundation

E. M. Roth, M. D., Lovelace Foundation

TABLE OF CONTENTS

5. ELECTRIC CURRENT	5-1
Effect of Electric Currents on Cells and Tissues	5-1
Effect of Electricity on Humans	5-3
Skin and Body Contact Resistance	5-4
Voltage	5-8
Amperage	5-8
Frequency Factors	5-11
Organ Damage by Electric Current	5-12
The Central Nervous System	5-12
The Skin	5-13
The Voluntary Muscles	5-13
The Bones	5-14
The Blood Vessels	5-14
The Eye	5-14
The Heart	5-14
Limits of Tolerance to Electric Currents	5-14
Short Shocks and Discharge Thresholds	5-15
Constant Current Thresholds	5-17
Safety and Emergency Practices	5-20
References	5-21

5.

ELECTRIC CURRENT

Effect of Electric Currents on Cells and Tissues

In the presence of electrical currents, the body behaves like an electro-chemical system. On the other hand, due to anatomical reasons such as the presence of membranes, it generates potential differences between different parts of the body. Therefore, when one considers the possibility of electrical currents acting upon the body, the end result will be the integration of the intrinsic currents plus the externally applied currents.

Physiological systems are assumed to be, from an electrical point of view, a combination of resistors and capacitors (35, 36). When a steady direct current is passed through tissue, the tissue behaves like a simple electrolytic resistance path. Considering organic tissue to be an electrolytic system, the laws of electrolytic conduction can be applied. Suppose a field E exists between two electrodes in an electrolyte. All charges, q , in the solution will experience a force ($f = qE$) causing them to move along the field lines of force. The terminal velocity is equal, specifically, to the product of force f , and the mobility, u , defined as the velocity of the particle when force is acting on it. The total current i , flowing through the electrolyte is equal to the number of charges, N , times their velocity, u :

$$i = Nfu \quad (1)$$

The number of charges will be equal to twice the number of dissociated atoms and the anion and cation will have different mobilities, u_a and u_c , respectively. The number of dissociated molecules in a solution of concentration C can be expressed as δC , so that the current will be:

$$i = q\delta CE(u_a + u_c) \quad (2)$$

where i = current

q = charge

E = field strength

δC = number of dissociated molecules

The conductivity of the solution is defined as the ratio of current to potential difference; potential difference V is related to the field by a relation of the type $E = \frac{V}{d}$ where d is the distance between electrodes, V = potential difference, and E = field strength. In case the electrodes of force are close together so that d is much smaller than the plate size, the lines of force are on the average just d in length. For such a case the conductance (G) of the model electrolytic cell is:

$$G = \frac{1}{R} = \frac{q\delta C}{d} (u_a + u_c) \quad (3)$$

where G = conductance = $\frac{1}{\text{Resistance}}$

The conductivity ρ of the solution in the model cell would be the conductance per unit area normal to the direction of current flow, for unit distance of plate separation, or

$$\rho = q\delta C (u_a + u_c) \quad (4)$$

Since the tissues may be considered as suspensions of cells in the extracellular fluid, the theory of electrical resistivity of suspensions enables one to predict with some accuracy the resistivity of tissues. In general, the cytoplasmic resistivity of cells varies from 30 to 3000 ohm cm, 300 ohm cm being the best representative figure for most mammalian cells. The membrane resistivity varies from 100 to 100,000 ohms cm², with most cells falling in the range of 1000 to 10,000 ohm cm².

In considering alternating currents passing through biological systems, the concept of impedance must be included. For direct currents, impedance and resistance are merely the same, but for A.C. current, impedance is a complex function of resistance and capacitive reactance (see Equation 8). There appears to be no inductive factor present.

Extensive data are available on the electrical characteristics of biological materials (36). Dielectric constant and specific resistance of mammalian tissues are recorded in Figure 1-2 of Microwaves (No. 1). If an alternating potential, V , is applied to a tissue having a conductance, G , the transfer of electrical energy into heat, H , due to the electrical current, i , is given by the equation

$$H = V^2 \cdot F = i^2/G \quad (5)$$

(Joule's law). Similarly, if a small volume ΔV is exposed to a field strength E (in Volt/cm) it develops heat at the rate of

$$H = E^2 \kappa \cdot \Delta V = (j^2/\kappa) \Delta V \text{ watts} \quad (6)$$

where κ is the specific conductance (conductivity) in mho/cm and j is the current density. In the case of a more complex system, where various types of material are exposed to the total available potential, more complex relationships result, which express the heat developed in each type of material as function of its geometry and conductivity κ and also dielectric constant ϵ . (The dielectric constant ϵ is equal to $1/(3.6\pi)$ times the capacitance of a cm-cube, if the capacitance is expressed in units of $\mu\mu$ Farad.) In principle, it is possible to completely characterize the distribution of heat sources from a knowledge of the geometry and electrical properties ϵ and κ .

From Equation (5), it is obvious that the electrical conductance determines predominantly the exchange from electric to heat energy. This constant

characterizes directly the interaction of the electrical charges, which are forced by the electrical field through the material of interest with its molecular structure. The dielectric constant, ϵ , on the other hand, only indirectly participates in the over-all distribution of the heat sources. It characterizes to what extent current can pass as "displacement current" through the material, that is, as a current whose flow does not yield heat. Kirchhoff's law states that the vector sum of real and displacement currents must remain constant through any series arrangement of different layers of matter. Hence, if the displacement current is large, that is when ϵ is large, the resistive current and heat development will be small, and in turn, for small ϵ or high κ , heating will be more pronounced in general.

Several different types of materials are arranged in series in the case when high frequency currents pass from one electrode through skin, subcutaneous fat layer, muscular tissue, etc., and eventually back to the other electrode. The current i delivered from the generator to the total tissue complex is expressed by Ohm's law (V potential)

$$i = V/Z \quad (7)$$

if Z is the over-all impedance of the configuration. Its value is identical with the sum of the individual impedances

$$Z = Z(\text{skin}) + Z(\text{fat}) + Z(\text{muscle}) + \dots$$

of each layer. Each impedance in turn is determined by

$$Z = d / [A(\kappa + j\omega \epsilon \epsilon_r)] \quad (8)$$

where d = tissue layer thickness, A = cross section of tissue passed by current, κ = conductivity in mho/cm, $\omega = 2\pi f$. frequency, ϵ = dielectric constant, $\epsilon_r = 1/(36\pi \cdot 10^{11})$ in farads/cm and $j = \sqrt{-1}$. Hence, heat development in each layer can be obtained, in principle, from a knowledge of the electrical properties of each layer, its thickness, effective cross section, and the generator potential or current by use of the Equations (5 and 6). The ratio of heat development in various layers, obtained in this manner, permits one to predict how much heat is developed in the "deep tissues". (See also Microwaves No. 1.)

Effects of Electricity on Humans

In considering the effects of electricity on a human system, several factors previously mentioned should be taken into account (4, 18, 20, 22, 37).

- Skin and body contact resistance
- The voltage of the circuit
- The amount of current flowing through the body
- The type of circuit, direct or alternating, and the frequency.

Skin and Body Contact Resistance

Resistance of the skin will depend upon many factors (16), namely: size, shape, and nature of the contacting electrodes; individual differences of skin structure and thickness in different areas of the same body; presence or absence of sweat or external moisture contact; and frequency of current. The resistance of skin resides mainly in the epidermis, the thin outer layer of the skin. The epidermis is a layer of stratum corneum and contains no blood capillaries or nerve endings. The scaly, horny layer acts as a poor dielectric, which offers a high impedance (resistance) to the flow of current.

The resistance of the epidermis varies widely on different individuals and also between wide limits on a given individual (17). It is normally lowest on the palms of the hands, the soles of the feet, the central area of the face, the axillae, a belt around the abdomen, and the crotches of the elbows and knees. It is interesting to note that in passing from the palmar side of a finger to the dorsal side, the skin resistance increases in a strip about one-eighth inch wide by a factor of six or sevenfold.

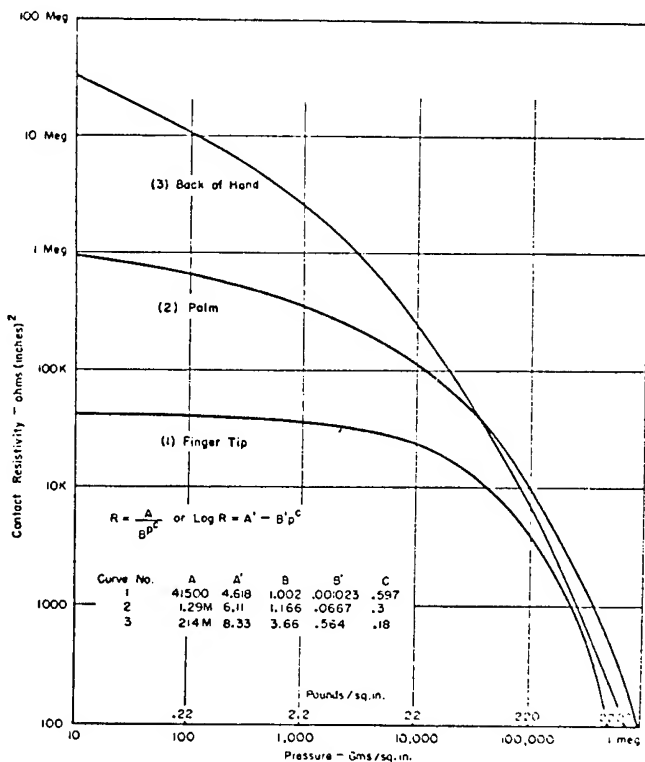
The protection offered by the epidermis is lowered by moisture (it may drop to 1/100th or less of its dry value), by the application of electrode paste (some of these contain finely ground sand particles which pierce the thin epidermis), by heat (blisters), by abrasions, by cuts, by the voltages of the circuit, or by any means that affect the continuity of the epidermis. Thin, moist skin surface may offer 400 ohms resistance or less. Dry skin may present 5000 ohms, and thick, calloused skin, several 100,000 to a million ohms. Once current penetrates epidermis by burning, resistance drops rapidly.

The effect of the level of applied voltage on the resistance of the human body is marked. Many body resistance values reported in medical literature are made at a few volts, or at less than a volt. Under these conditions the values reported are meaningless as far as electric shocks are concerned. There is a critical voltage at which the skin breaks down and its protection is lost. For example, on a fresh cadaver the hand to foot resistance at 50 volts, 60 Hz A.C. was 10,000 ohms; at 500 volts it was 1200 ohms, and at 1000 volts - 1100 ohms (17).

Skin to electrode contacts are very sensitive to pressure, frequency and other factors. Figure 5-1a presents preliminary data on the relationship between pressure and resistivity for the contact of dry human skin to metal. These curves require statistical evaluation for spread of data to be encountered in accidental situations.

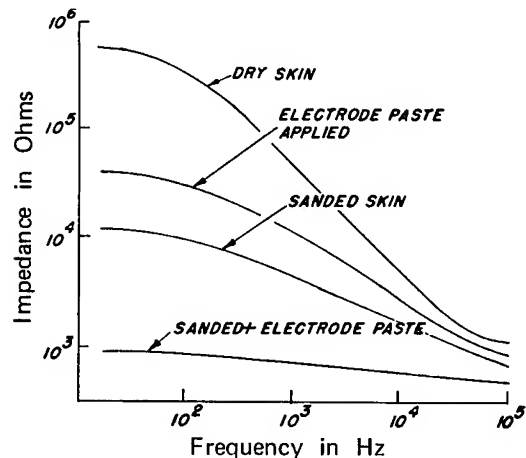
An example of the variation of skin impedance with frequency and marked sensitivity to skin-electrode contact is shown in Figure 5-1b (36). Empirical curves of this type will vary with electrode type, current, and duration of exposure, and should not be used for prediction of accidental conditions. Electrodes of the type recorded in Figure 5-1b are used for electromyographic study of muscle potentials. A flattening of the impedance curve for dry skin at both the high and low frequencies is interpreted as an asymptotic resistive component of the internal tissue structure of the muscle (5). The curve may

Figure 5-1
Variables Controlling Skin to Electrode Contact



- a. Relation Between Pressure and Resistivity for the Contact of Dry Human Skin to Metal.

(After Morse⁽³¹⁾)



- b. An Example of the Variation of Skin Impedance with Frequency and Condition of Electrode-Skin Contact.

Copper-disc electrodes 3/4 in. in diameter were used.(See text)

(After Stacey⁽³⁶⁾ Adapted from Burns⁽⁵⁾)

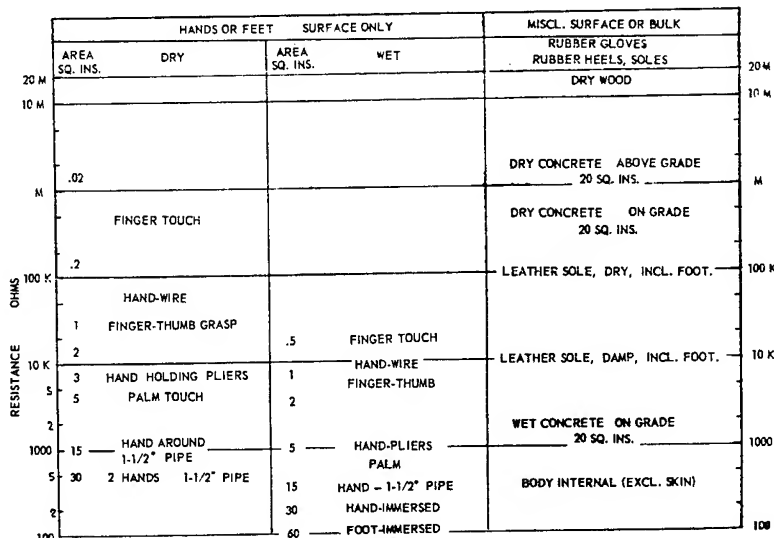
be divided into three major segments and the equivalent circuit, estimated. Complexities of the structure of the subdermal components interfere with exact modeling of the system. Measurements made on electrode separation show no large variation after the separation of two electrodes (3/4-inch diameter) exceeded one-half inch. The effect of electrode size was noticeable by a small increase in impedance with a decrease in electrode size. The diameter-to-spacing ratio is most important in determination of impedance of any one electrode in a linear array of electrodes along the skin.

The measurement of body resistance is highly inexact. Since contact skin area and moisture contact are so highly variable, ranges of 20 to 1 or more for supposedly similar contacts are the rule. The best approach one can take is to pin-point the minimum resistance value for a given condition, and even this approach is far from satisfactory. Some of these are shown in Table 5-2. In the interpretation of this table and Table 5-3, it should be

Table 5-2

Rough Approximation of Typical Lowest Resistances
of Individual Elements of Human Circuits
(See text for details before applying data)

(After Lee⁽²⁶⁾ from the data of Kouwenhoven and Milnor⁽²³⁾
and Dalziel⁽⁹⁾ and Morse⁽³¹⁾)



realized that the skin is punctured when the voltage exceeds 1000 to 2000 volts. This unfortunate circumstance removes a large portion of the total circuit resistance and allows the current to increase many fold. Graphically, this means that the horizontal resistance line is "stepped" at about 2000 volts from the total circuit resistance to the total circuit resistance less the skin resistance. At about this same voltage, or when the current is allowed to reach a few amperes, sparking or arcing may occur across the edges of the soles of shoes, again allowing increase of current. At this level of current, the shock is beyond the fibrillation zone, and serious tissue burning is involved, with the current magnitude limited by only the internal body resistance.

It is obvious that the larger or wetter the contact area, the lower the resistance. Ideally, to find the total resistance to current flow, one can add all the elements of resistance in the path, such as hand-to-wire, body, foot, and floor, or hand, body, hand, since all of these elements are in series. In reality, the variables are so complex as to reduce accuracy of this approach to very much approximation. More detailed data are available on the determination of ground-fault magnitude and human safety from fault-return path impedance (25).

The duration of the contact is of importance when considering electrical injuries. Time of exposure has a direct relationship with the degree of permanent damage observed. Resistance of the skin also decreases during the passage of the current and total body resistance decreases if contact is made with an electric circuit for any length of time. It may decrease within one minute from 260,000 to 380 ohms (16). In animal experiments, it was found that the current increased 5 to 10 percent if the animal was kept in the circuit for any length of time.

Tissue resistance per cc varies; muscle presents 1500 ohms per cc; brain, 2000 ohms per cc; bone, 900 ohms per cc or more; fat (free of muscle), several thousand ohms per cc (17). Total body resistance is a difficult measurement and depends most strongly on the size, location, and distance between electrodes. In electrocuted criminals, it was found to be 218 ohm (16). In these cases, an AC current was passed from the forehead to the feet in four shocks. The strength of the first and third shocks was 2,300 volts and each lasted seven seconds; the strength of the second and fourth shocks was 550 volts for fifty-two seconds. Much higher values are found with less perfect contacts.

If the contact resistance can be eliminated, a tissue resistance of about 100 ohms per cc can be assumed (17). Obviously, the parts of the body where contact is made are of vital importance. One can envision the electric current as spreading radially from the point of entrance to be collected again at the exit point; therefore, the greatest density current can be found at the entrance and exit points. For general purpose, the minimum value of body resistance for hand to foot path is considered to be 500 ohms (17). Most of this resistance resides in the limbs where a large proportion of the total cross section is taken up by the bones. In the trunk, the tissues and organs are considered to act as a conducting gel bathed in saline, and the current spreads out in a fusiform pattern between the points of entrance and exit. In estimating the resistance offered to the flow of current by an electric shock, the resistance of the trunk is considered to be negligible compared to that of the limbs. There is a diurnal variation in an individual's resistance which often confuses experimental data (34).

The anatomical location of vital organs relative to the current path is of great importance (4). In general, current passing through left side of thorax presents greater dangers of ventricular fibrillation and asystole. The cranium presents an excellent shield for the brain since bones are poor conductors. Electrical energy will pass around the cranium in extracranial soft tissues if given the opportunity; and in a longitudinal course (for example, head to ipsilateral upper extremity), scalp and cranium may be severely burned focally with apparently minimal penetration of brain by electricity.

In more transverse courses involving the head (especially where entrance and exit are of opposite sides of the skull) or where the cranial resistance is overcome, more direct cerebral effects occur. Most commonly this results in paralysis of medullary respiratory centers. Spinal cord may also be implicated, commonly in cervical region, by course of electricity from one upper extremity to another.

As seen below, the effects of electric currents are related to the amounts of current which flow and not specifically to the voltages applied. It is fortunate that in most electrical accidents, the contact of the body with the source of voltage is not perfect, and the contact resistance cuts down the amount of current flowing. Paradoxically, it has been shown that a moist skin with low resistance may divert a current to cause only skin burns when it otherwise may have entered the body to damage vital organs (16).

Voltage

The voltage of the circuit is usually the only accurately known factor in electrical shock accidents. The resistance that is offered by the human body depends upon so many parameters that it is difficult to form an estimate of the energy involved in the shock. If, however, the voltage is high enough to break down the contact resistance, and the current path through the individual is from hand to foot, or hand to hand, it is possible to estimate the value of the current on the basis of the resistances of the man's body.

In air at sea level, it requires a potential difference of about 35 KV (crest) for a power source to spark a distance of one inch (17). Therefore, there is only a slight chance that electricity will jump to a man unless he is careless and gets too close to the live circuit. There is, however, the possibility that he may touch a power source and, as he pulls or falls away, an electric arc may be formed between his body and the circuit.

Voltage parameters are divided into two groups, low and high, with 1,000 volts as the borderline (16). The external pathology is much more extensive when a person is exposed to high voltages than when a current at 100 to 200 volts passes through his body. The electric arc which usually leaps from the conductor to the body in high tension currents has a temperature of 2,500 to 3,000°C and melts even bone. The victim is often thrown away from the conductors due to the severe contraction of the muscles. Specific effects of high voltage shocks are related to contact sites and other variables (4). Figure 5-7c presents tentative lethal voltages for ventricular fibrillation as a function of duration of current under accidental wet contacts.

Amperage

The intensity (amperage) of an electric current is the relationship between its tension (voltage) and the resistance of the conductors - in the case of electric shock, the human body. The amperage, therefore, gives a more accurate account of the action of the current in the body than the voltage. In its passage through the body, electrical currents encounter the high resistance of the skin, which is surpassed only by that of the bone. Compared to the skin, the resistance of the internal organs can be neglected. Figure 5-3 shows the interrelations between resistance, 60 Hz voltage, current, and zones for the

various degrees of shock. A resistance of 100,000 ohms, which is about normal dry hand-to-hand touch value, gives a just-perceptile shock of 1.2 ma from a 120 volt system. The sensation produced by an electric shock depends, to a large extent, on the current density at the points of contact with the circuit. If the current density at the point of contact is low, there is no sensation of a shock. It is the value and frequency of the current, its duration, and its pathway through the body that is mainly responsible for the injuries received. If there are no vital organs in its path (two points on same leg or arm, or between the two feet), the injuries are usually limited to burns in those areas. With higher voltages and the same resistance, the currents quickly mount from perceptible to paralytic to fibrillating.

The data of Figure 5-3 are estimates of physiological thresholds taken from several studies (9, 23, 26). They are based on: current flow from arm to arm or arm to leg; one hundred fifty lb subjects - heavier subjects have lighter threshold currents in direct proportion to weight; and fibrillation current for 5 second shock duration.

At the right side of Figure 5-3, the 10 ampere line indicates burning due to overheating and boiling of water. This is the major danger in high voltage shocks. The skin is almost always punctured by the heavy current; 500 ohms is generally the applicable body resistance. Under this condition, voltages above about 2300 are burn-hazardous and are generally less likely to be fatal than voltages from 120 to 2300 v. The danger in the high voltage area is in possible burning damage of vital organs, rather than fibrillation, and statistically is not as dangerous as that of the lower voltage area (26). The range of amperage effects is seen in Table 5-4.

A general estimate of the current value may be made when the victim's reaction to a 60 Hz AC electric shock, his injuries, the current pathway through the body, the shock duration, and the voltage are known (17, 23). A man may be "frozen" to a circuit or he may be thrown away, depending upon whether his flexor muscles, or his extensor muscles, are first stimulated by the shock. If his flexor muscles are paralyzed and he cannot release his hold on the circuit, the amount of current flowing through the muscles of his hand is usually between 12 and 30 milliamperes. When the victim is unconscious but breathing, and has a pulse, the current was probably between 30 and 100 milliamperes. If the shock is at low voltage and the victim is unconscious, not breathing, and pulseless, his heart is probably in ventricular fibrillation, and the current range lies between 60 milliamperes and 4 amperes. If the victim is unconscious, not breathing, but has a pulse, the current through his trunk probably exceeded 10 amperes.

If the current flow through the brain is sufficient, unconsciousness occurs. With currents of 300 to 1200 milliamperes (70 to 150 volts applied across the head through good contact electrodes lasting for 0.1 to 0.5 seconds, such as used in electric shock therapy) unconsciousness is immediate and is followed by convulsive seizures. Coma, stupor, or confusional states are not unusual following electroshock. The current used in therapeutic electro-shock is about 200-1600 milliamperes, 50-60 Hz AC at 70-130 volts for 0.1-0.5 seconds. Clinical reports state the duration of the confusional period as ranging from seconds up to several hours and even days (2, 16). After

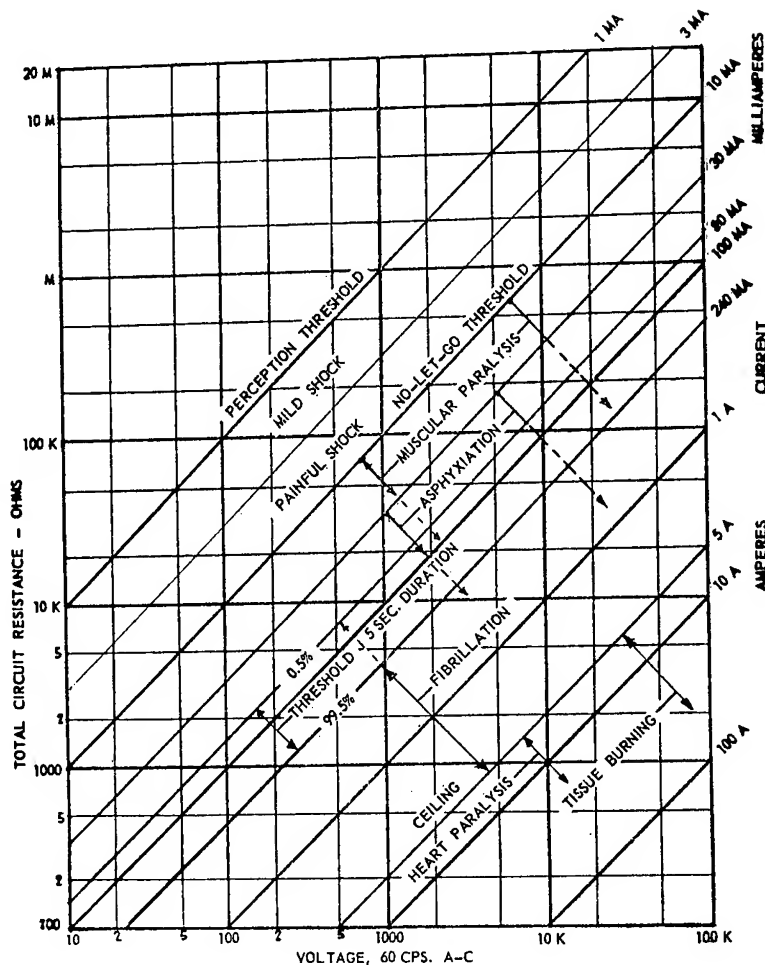


Figure 5-3

Range of Physiological Effects of 60 Hz AC on 150-lb Human

(After Lee⁽²⁶⁾ from the data of Kouwenhoven and Milnor⁽²³⁾
Dalziel⁽⁹⁾, and Morse⁽³¹⁾)

Table 5-4

Range of Current Sensitivity of 150-lb Man at 60 Hz AC

(After Lee⁽²⁶⁾)

Imperceptible	0 - 1 ma
Perceptible, Mild	1 - 3 ma
Annoying, Painful	3 - 10 ma
Paralyzing, "no-let-go"	> 10 ma
Asphyxiation, Unconsciousness	> 30 ma
Fibrillation, Loss of Circulation	80/240 ma - 4a(5 sec.)
Heart Paralysis Threshold	4a approx.
Burning, Heat Damage	> 5a

three to five treatments, EEG alterations are persistent, increasing up to 6 and 12 treatments, reaching a plateau at that level. These changes are diffuse and disappear gradually in weeks after treatments cease, lingering in proportion to the number of treatments given (1).

Frequency Factors

The median threshold of sensation for direct current of over 100 adult men and women is 1.43 milliamperes as compared to 1.0 for 60 Hz AC (17). Other factors equal, alternating current is approximately three times more injurious than direct current (1) (see Table 5-5). Direct current under 220 volts seldom leads to death whereas even 25 volts alternating current may be dangerous (tetanization of respiratory muscles) if the body is well grounded.

Table 5-5

Comparative Effects of AC and DC Currents Given on the Thorax

(Modified from Aita⁽¹⁾)

Direct Current Voltage 110-800	Alternating Current Voltage 110-380, 50-60 cps	Effect
Under 80 millamp.	Under 25 millamp.	Slight contracture of respiratory muscles
80-300 millamp.	25-80 millamp.	Respiratory muscle spasm. ac: If duration over 30 sec., cardiac arrest followed by ventricular fibrillation. dc: Ventricular fibrillation only if precise course through heart.
	80 millamp. to 3 amp.	ac: Ventricular fibrillation if over 1 sec.
300 millamp. to 3 amp.	voltage 3000 and over; over 3 amps.	Respiratory muscle spasm. Cardiac arrest. Serious burns if over few seconds.

Sixty Hz is about the worst possible frequency as far as human safety is concerned. It appears that humans are about five times as sensitive to 60 to 400 Hz as to DC, but more studies are in progress on this point (17). At 10,000 Hz, however, sensitivity is about the same as for DC, and appears to decrease still farther as the frequency is increased, probably due to the skin effect keeping the bulk of the current on the skin, or at least just under the skin. Frequencies above 100,000 Hz do not produce the pricking sensation of low frequency shocks; instead the sensation is one of warmth or heat (17). There, are , however, few data available as to the trauma that may be produced by the continued passage of high frequency current through the body for long periods.

Table 5-6 outlines the relative effect of different frequencies in perception of shock and paralysis normalized to 60 Hz = 1.0.

Table 5-6
 Effect of Frequency (Hz) on Perception and Paralysis
 (fraction of 60 Hz effect)
 (After Lee⁽²⁶⁾)

<u>f(Hz)</u>	<u>effect</u>
0	0.2
10	0.9
60	1.0
300	0.8
1000	0.6
10,000	0.2
RF	0.01

The frequency sensitivity of "let-go" current is seen in Figure 5-10.

Death from electrical injuries is usually due to cardiac or respiratory arrest (4). In most instances, cardiac arrest results from ventricular fibrillation. Respiratory arrest may be due to direct effects of the current on the respiratory center, or secondary to hypoxia of the cells of the center due to inadequate perfusion as a result of the ventricular fibrillation.

Organ Damage by Electric Current

Organs vary greatly in sensitivity and pathological response to electric currents (16, 30). The following summary is far from comprehensive and is intended only as a reference source for planning for emergency procedures after operational accidents:

The Central Nervous System

Organic damage to the nervous system occurs in that portion of the brain or spinal cord where the current passes through. It is not specific and sometimes is similar to that found in other types of cerebral injuries (1, 10, 13, 24).

Post mortem studies indicate that electrical injuries to the nervous system can be summarized as follows:

- mild and severe cellular alterations, from swelling to liquification,
- rupture of the walls of the blood vessels, mainly of the internal elastic membrane,
- shrinkage, thinning, and breaking up of the cerebral parenchyma with the formation of tears, slits or fissures.

Following accidental electroshock, hypoxia and heat damage are likely the causes of permanent neurologic sequelae and pathological changes seen in the occasional patient (1). A diffuse and massive charge of electricity through the brain causes damage by generalized heating. In many instances, the electrical energy dissipates mostly at the scalp and cranium with a burn;

little if any electricity passing through the brain. Many of these patients surviving have no cerebral sequelae; some have a post-concussion syndrome; a small percentage incur burns deep enough to involve dura and brain at a focal site; rarely epidural infection occurs.

Whether isolated cerebrovascular insults may be blamed on electricity is uncertain. Focal thrombosis and hemorrhage have been cited and the problem is much like that seen following direct craniocerebral trauma. One is left to presume that electricity may injure intracranial blood vessels.

Electricity may pass through the spinal cord transversely, obliquely or longitudinally, resulting in many different cord syndromes. Transient deficits are not unusual. Permanent defects may remain, of which syndromes from loss of anterior horn cells are common.

Peripheral nerves likewise may be transiently paralyzed or more permanently damaged by heat-effects from passage of current or by outright burns. Violent tetanic action, falls or blows may also contribute to vertebral and nerve injury.

The Skin

In the skin, with its high resistance, the most marked changes are produced (4, 29, 30). Current effects on the skin are twofold. First, in passing through the skin, the electric energy is transformed into heat which alters the structures along the path of the current. Second, free discharge causes the formation of electric sparks which leads to the formation of third degree burns.

Electrothermal burns have no consistent gross or microscopic characteristics by which they may be distinguished from other hyperthermal injuries (30). Arcing of the current may produce pitlike defects on the surface of hair or epidermis that are rarely, if ever, produced by other forms of heat. Metallic constituents of the external conductor may be deposited in or on the surface of an electrical burn, and their presence may help to establish the kind of an electrode with which the skin was in contact. In the case of alternating current such metallic deposits may be present at both sites of contact. With direct current the deposits will occur only at the site of contact with the negative electrode.

Contact with such a superheated conductor will cause severe and instantaneous burning even though no electricity flows through the skin. Rarely does a current of 110 volts produce a large electrothermal injury of the skin unless the contact is maintained for a considerable period of time. Fern-like markings of pink color are often seen after lightning strikes. The color intensifies post mortem. All severity of burns up to severe charring may be seen after lightning or high voltage arc strikes.

The Voluntary Muscles

In traversing the body, AC currents cause tetanic contractions of the entire musculature. Very often, the body of an electrocuted person is bent

in extreme extension or opisthotonus. The muscular spasm may be so intensive as to cause disruption of muscles, luxation of joints and, rarely, fractures of bones.

The Bones

In high tension accidents in which the current enters the body through the skull, lesions of the bone are common. In some cases the electric arc burns a deep hole in the bone, and the meninges and the brain, too, may be affected. In other cases of less severe types of accidents, the bone is often exposed by the destruction of the soft tissues. The high resistance of the bone, no doubt, gives rise to the formation of an intensive heat (16). When an arc jumps to several small places on a victim's arms or legs, dead sinuses and osteomyelitis may develop (17).

The Blood Vessels

The walls of blood vessels through which long enough to cause necrotic change become brittle endothelial lining of the vessel undergoes changes are attached to the intima. The great vulnerability counts for the severe hemorrhages as complications (16).

The Eye

The changes observed on the eyes are usually late complications of electrical injuries. The so-called electric cataract has been described by several authors and occurs chiefly in lightning cases where the current enters the body through the head (16, 17).

The Heart

Ventricular fibrillation is affected by three factors: a sufficient current density, a low or medium voltage and duration of contact which may very well be short. Currents over 6 amperes (see Figures 5-3 and 5-7; Equations 9 and 10) have a different effect on the myocardium. They do not cause ventricular fibrillation, but cardiac standstill, mostly in systole. Blood pressure falls when these high currents are on, but heart usually resumes beating and reestablishes circulation when the current is turned off (23). Autopsies performed on electrocuted persons usually show no anatomic lesions of the heart (16).

Limits of Tolerance to Electric Currents

Figure 5-3 and Tables 5-4 to 5-6 give a rough estimate of critical thresholds for functional damage caused by electric currents. The following are more refined time-dependent thresholds which can be used for extrapolation in setting safety and design standards for unusual electrical equipment or conditions.

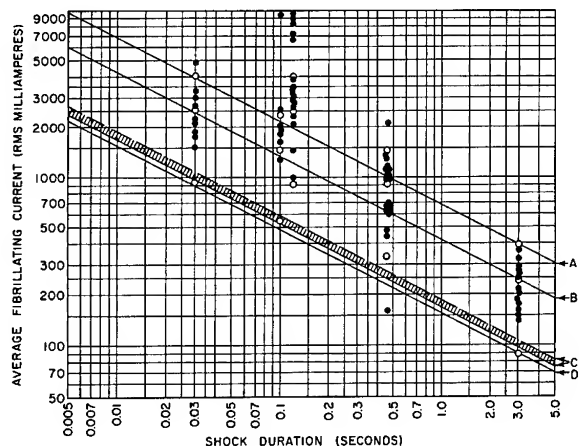
Short Shocks and Discharge Thresholds

Tentative criteria for the hazard from short shocks and impulse discharges are presented in Figure 5-7 (10). The threshold of danger is taken as the minimum shock likely to produce ventricular fibrillation in a large group of normal men (10). One method of extrapolation from animal data is shown in Figure 5-7a. The data points represent results obtained from experiments on sheep using 60 Hz alternating current with shock durations from 0.03 to 3.0 seconds. Several animal species were used to establish the relationship of fibrillating current to body weight, and the cross-hatched areas designated by C represent the probable response for all 70 kilogram animals, including man.

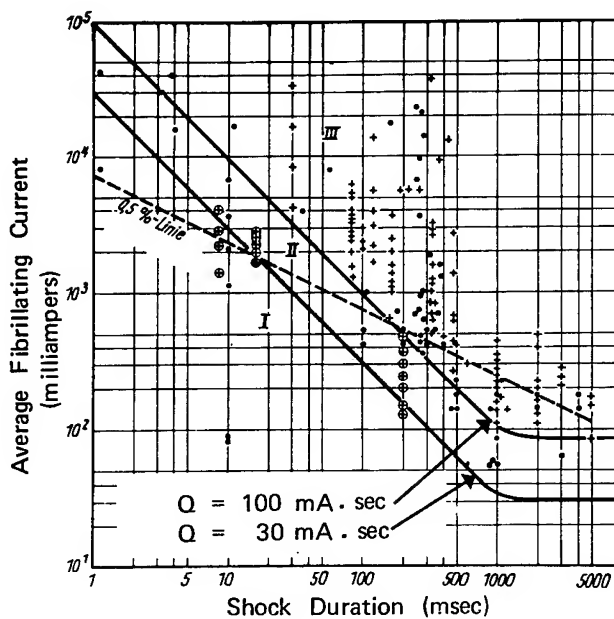
It has been recently pointed out that for AC shocks of one to five seconds' duration, there probably is no significant difference between the threshold values at about 80 millamps as all of these shocks cover an entire heart cycle (19, 33). Figure 5-7b shows a review of animal data from many investigators for 50 and 60 Hz AC as well as condenser discharges. With two exceptions, all tests with fatal shock lie above the 100 mAs (maximum amplitude) value, noted here as the upper boundary of the range ($Q = 100 \text{ mA} \cdot \text{sec}$). The points below the upper boundary represent curarized animals or tests performed under anomalous conditions (from Figure 5-7a) where each animal was given shocks of increasing current strength until ventricular fibrillation resulted, which was then stopped by electric de-fibrillation. After a brief period of recuperation, the animal was again subjected to shock and the resulting ventricular fibrillation was again stopped by electrical counter-shocks. Tests continued until ventricular fibrillation could no longer be stopped. Since some of these test data were disregarded in plotting the 0.5%-fibrillation threshold line of Figure 5-7a, it seemed unwarranted to consider these values in establishing threshold ranges. The 0.5% line in Figure 5-7a (dashed line in Figure 5-7b) resulted from an attempt to establish the probable lower boundary at which lethal fibrillation can still occur. The slope of the straight dashed line of Figure 5-7b appears to be flat, since a large proportion of ventricular fibrillation cases observed with a current passage duration of $> 0.4 \text{ sec}$. are not taken into account. On the other hand, except for the cases mentioned above, all other animal test data found in the literature are compatible with the interpretation that the ventricular fibrillation current threshold is constant beyond 1 second.

Using lower current threshold for range III of Figure 5-7b and the body resistances obtained under the most unfavorable conditions for three different current paths (12), the voltage and time relation can be determined and plotted as Figure 5-7c. The resulting curves represent the boundaries of three current paths for the lethally dangerous voltage as a function of duration under accidental conditions of wet contact over a large area. If the most commonly encountered current path II is used as the criterion of the safe contact voltage, this curve above the 1-sec. duration shows good agreement with the German Electrical Engineering Society's safety voltage of $65 \text{ V}_{\text{eff}}$ (33). The acceptance of these newer curves by any national or international standards group remains for the future.

Figure 5-7
Ventricular Fibrillation Thresholds for Alternating Current



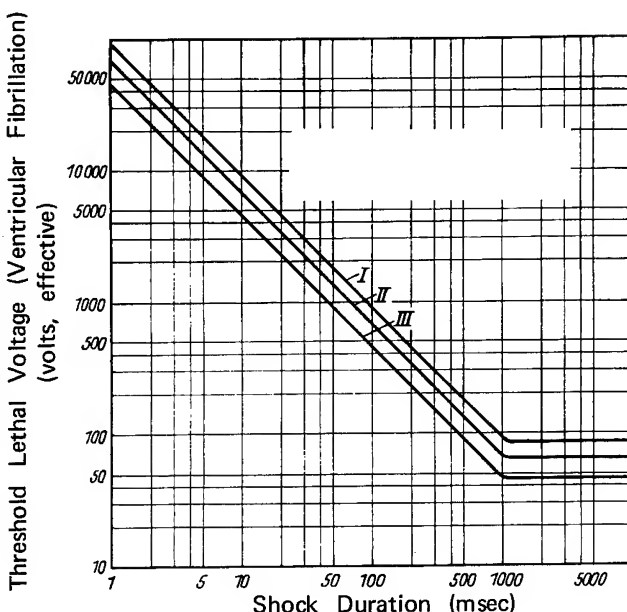
- a. Typical Method of Extrapolation from Animal Data for 60 Hz AC
- Experimental points
 - Calculated points
 - A 99 1/2-per-cent line for 57.4-kg sheep
 - B 50-per-cent line for 57.4-kg sheep
 - C 1/2-per-cent line for all 70-kg animals including man
 - D 1/2-per-cent line for 57.4-kg sheep
- (After Dalziel⁽¹⁰⁾)



- + lethal ventricular fibrillation
 ● nonlethal
 ○ inexact data or animals with heart damage
- b. Comparison of the Fibrillation Current Ranges with Animal Test Data Found in Literature for 50 and 60 Hz AC and Condenser Discharges

The dashed line represents the 0.5% line of Figure 5-7a(C)

(After Osypka⁽³³⁾)



- I current path Hand-trunk-hand (1300 ohms)
 II current path Hand-trunk-feet (970 ohms)
 III current path Hands-trunk-feet (650 ohms)
- c. Lethal Voltages for Ventricular Fibrillation (100 mA·sec) as Function of Duration Under Unfavorable Accidental Conditions of Wet Contact Over Large Body Area (See text)

(After Osypka⁽³³⁾)

Figure 5-8 shows the relationship of theoretical initial current and time constant to the threshold for human accidents resulting from capacitor discharges (8). Short shocks, whose durations are a small fraction of a second, are particularly dangerous if they occur during the T-wave phase of the electrical heart cycle (17). A shock through hand to foot of about one ampere, and of a duration of 0.01 seconds occurring in the T phase, may put a human heart into ventricular fibrillation. The same shock, falling outside of the T phase, will have a transient effect on the heart. Atrial flutter or fibrillation is rare in electric shock cases (17). Small shocks just preceding the refractory phase of the heart cycle may cause atrial fibrillation (3).

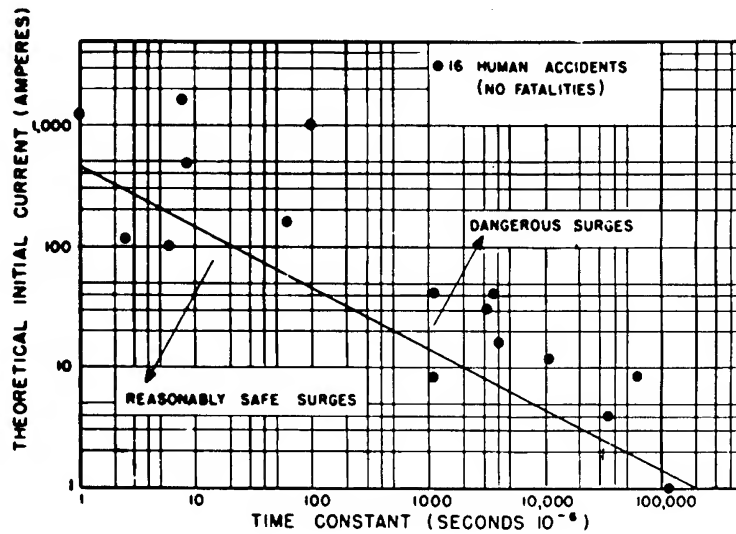


Figure 5-8

Proposed Criterion for Reasonably Safe Surge Currents and Points
Representing 16 Human Capacitor Surge Accidents.
(Based on 50-watt-second discharges)

(After Dalziel⁽⁸⁾)

Constant Current Thresholds

Figure 5-9 shows distribution curves for men and women for effects brought about by exposure to a 60 Hz current (14). The experimental points are defined as the maximal current the subjects are able to tolerate when holding a copper conductor in one hand and yet let go of the conductor by using muscles directly affected by that current, i.e., "let go" current and thresholds.

Figure 5-10 is a plot of frequency in cycles per second versus let-go currents.

From these curves it can be concluded that a reasonably safe electric current for normal healthy adults is the let-go current which 99 1/2 percent of a large group can release by using muscles directly affected by that current.

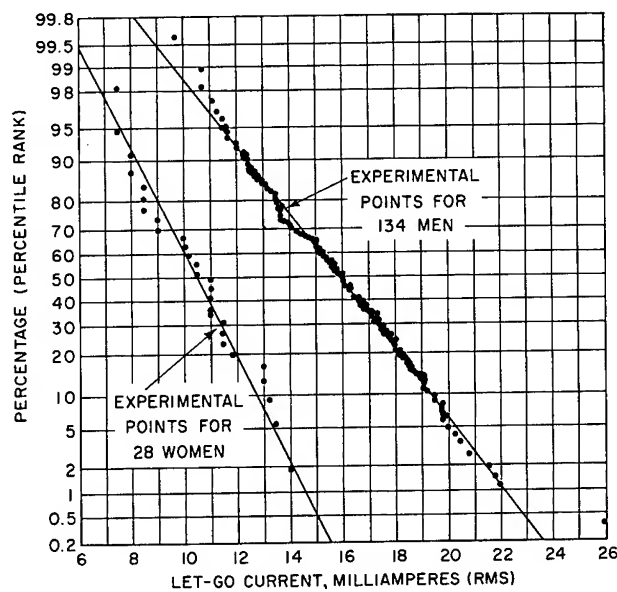


Figure 5-9

Distribution Curves for Men and Women of "Let-go" Current Thresholds at 60 Hz. (See text)

(After Dalziel⁽¹¹⁾)

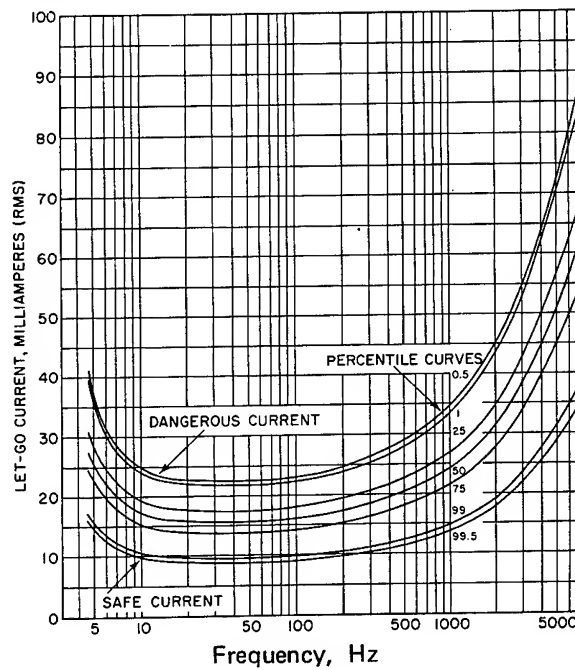


Figure 5-10

Sine-wave "Let-go" Current for Men Versus Frequency

(After Dalziel⁽¹¹⁾)

The reasonably safe 60 Hz AC current for most normal healthy adult men is about nine milliamperes; the reasonably safe 60 Hz current for most normal healthy adult women is about six milliamperes. Let-go currents are affected by frequency. Frequencies of 10-200 Hz appear to be the most dangerous. In interpreting these let-go curves it should be kept in mind that with currents exceeding the no-let-go threshold, the skin at the contacts tends to develop blisters quickly, which reduces the skin resistance, allowing the current to increase. So while the dry skin resistance (Figure 5-2) is applicable up to the "no-let-go" threshold, it should be modified to "wet skin" criteria after that threshold is passed.

The fibrillation threshold for constant current at 60 Hz given arm to leg is seen in Figure 5-3. The data indicating sensitivity to amperage and to shock duration are based on tests on guinea pigs, dogs, sheep, and calves. It was found that the weight relationship held quite well even between animals of different species, as well as for animals of the same species, but of different weights. There are two fibrillation lines, one at which 0.5% of the population is affected and one at which 99.5% is affected. Since there has, as yet, been developed no way to predetermine one's susceptibility, the 0.5% line must be assumed to be the applicable one. Likewise, the 5 second time is generally assumed although the great majority of shocks are of very short duration, muscular reaction throwing the victim free. Experimental data on times over 5 seconds are not available, so it is not known whether extrapolation is justifiable. It has been suggested that a rough evaluation of constant current thresholds may be determined by the equations (26):

$$0.5\% \text{ Probability Current} = \frac{W}{150} \times \frac{165}{\sqrt{t}} \text{ ma} \quad (9)$$

$$99.5\% \text{ Probability Current} = \frac{W}{150} \times \frac{165 \times 3}{\sqrt{t}} \text{ ma} \quad (10)$$

where w = weight, pounds

t = times, seconds (5 sec. max.)

For leg to leg shocks, multiply these currents by 10. Equations 9 and 10 must be used with the appropriate circumspection and knowledge that the human accident does not always fit the equation (17).

The frequency dependence of threshold fibrillating current is not as clearly defined as "let-go" current. It has been suggested that fibrillation threshold current at 0 and 10,000 Hz is 130% of 60 Hz value at and below 0.1 sec. The threshold of 500 ma at 0.1 sec. is conservative for longer times. Between 10 and 1000 Hz, the 60 Hz values should be assumed (26).

Currents of ten or more amperes, flowing from hand to foot, will hold the heart in asystole as long as the current continues to flow. When the circuit is broken the heart will often return to normal sinus rhythm. If, however, the shock was a long one, the heart may remain in standstill.

Safety and Emergency Practices

Safety practices involving electrical equipment have received recent review (6, 10, 26, 37). Electrical safety in hazardous atmospheric environments have also been recently summarized (7, 15, 28, 32).

The emergency treatment following electrical injury include prolonged cardiopulmonary resuscitation; cardiac massage; defibrillation; and hypothermia for severe hypoxia (1, 9, 20, 21, 23, 27). Cerebral edema may be managed by hypertonic urea intravenously or by hypothermia. Closed-chest defibrillation is accomplished by 5-7 amperes at 400-500 volts in 0.1-0.2 second shocks (300 joules or watt-seconds) from manubrium sterni to apex of heart, allowing approximately 1.5 amperes to flow through the heart. Safety precautions must be followed in this procedure (14).

REFERENCES

- 5-1. Aita, J. A., Neurologic Manifestations of Electrical Injury, Nebr. State Med. J., 50: 530-533, Oct. 1965.
- 5-2. Alexander, L., Electrical Injuries to the Central Nervous System, Med. Clin. N. Amer., 22: 663-688, May 1938.
- 5-3. Andrus, E. C., Carter, E. P., The Refractory Period of the Normally-Beating Dog's Auricle; with a Note on the Occurrence of Auricular Fibrillation Following a Single Stimulus, J. Exp. Med., 51(3): 357-367, Mar. 1930.
- 5-4. Brown, K. L., Moritz, A. R., Electrical Injuries, J. Trauma, 4: 608-617, Sept. 1964.
- 5-5. Burns, R. C., Study of Skin Impedance, Electronics, 23: 190-200, Apr. 1950.
- 5-6. Camishion, R. C., Electrical Hazards in the Research Laboratory, J. Surg. Res., 6: 221-227, May 1966.
- 5-7. Corwell-Kulesza, G. G., Intrinsically Safe and Non-Incendive Electrical Installations for Hazardous Environments, Motorola Inc., Phoenix, Arizona, in Environmental Evolution, 13th Annual Technical Meeting of the Institute of Environmental Sciences Proceedings, Apr. 10-12, 1967, Washington, D. C., Vol. I of II, pp. 5-11.
- 5-8. Dalziel, C. F., Deleterious Effects of Electric Shock, University of California, Berkeley, paper presented at the Seminar on Electrical Safety, Univ. of Maine, Orono Campus, Sept. 11, 1962.
- 5-9. Dalziel, C. F., The Effects of Electric Shock on Man, IRE Trans. Med. Electron., PGME-5, May 1956. (Also reprinted as USAEC Safety Bulletin No. 7).
- 5-10. Dalziel, C. F., A Study of the Hazards of Impulse Currents, AIEE Trans., 72: 1032-1043, 1953.
- 5-11. Dalziel, C. F., Ogden, E., Abbott, C. E., Effect of Frequency on Let-Go Currents, AIEE Trans., 62: 745-750, 1943.
- 5-12. Freiberger, H., Der Elektrische Widerstand des Menschlichen Körpers gegen Technischen Gleich und Wechselstrom, Julius Springer Verlag, 1934.

- 5-13. Hassin, G. B., Changes in the Brain in Legal Electrocution, Arch. Neurol. Psychiat., 30: 1046-1060, Nov. 1933.
- 5-14. Hunnicutt, M. D., Jr., Safety Considerations in the Use of DC Defibrillators, American Optical Co., Southbridge, Mass., [1964].
- 5-15. Instrument Society of America, Tentative Recommended Practice, Intrinsically Safe and Non-Incendive Electrical Instruments, ISA-RP-12.2, Pittsburgh, Pa., 1965.
- 5-16. Jaffe, R. H., Electropathology - A Review of the Pathologic Changes Produced by Electric Currents, Arch. Pathol., 5: 837-870, Jan.-Jun. 1928.
- 5-17. Kouwenhoven, W. B., Johns Hopkins University, Baltimore, Md., personal communication on unpublished data, 1968.
- 5-18. Kouwenhoven, W. B., The Effects of Electricity on the Human Body, Bull. Hopkins Hosp., 115: 425-426, Dec. 1964.
- 5-19. Kouwenhoven, W. B., The Gray Area, in 1965 National Safety Congress Trans., 20: 12, 1965.
- 5-20. Kouwenhoven, W. B., The Gray Area, Industr. Med. Surg., 35: 271-274, Apr. 1966.
- 5-21. Kouwenhoven, W. B., Knickerbocker, G. G., Milnor, W. R., et al., Field Treatment in Electric Shock Cases - II, Paper 60-171, presented at the AIEE Winter General Meeting, New York, Jan. 31 - Feb. 5, 1960.
- 5-22. Kouwenhoven, W. B., Langworthy, O. R., Effect of Electric Shock, AIEE Trans., 49: 381-394, 1930.
- 5-23. Kouwenhoven, W. B., Milnor, W. R., Field Treatment of Electric Shock Cases - I, AIEE Trans., Part III, 76: 82-87, Apr. 1957.
- 5-24. Langworthy, O. R., Abnormalities Produced in the Central Nervous System by Electrical Injuries, J. Exper. Med., 51: 943-967, 1930.
- 5-25. Lee, R. H., Ground Fault Magnitude Determination and Human Safety from Fault-Return Path Impedance, E. I. Du Pont De Nemours & Co., Wilmington, Del., paper presented at the IEEE National Industry and General Applications Conf., Pittsburgh, Pa., Oct. 4, 1967, pp. 487-498.

- 5-26. Lee, R. H., Human Electrical Safety, ISA-Mono-110, Instrument Society of America, Pittsburgh, Pa., 1965, p. 35.
- 5-27. Lee, W. R., The Nature and Management of Electric Shock, Brit. J. Anaesth., 36: 572-580, Sept. 1964.
- 5-28. Magison, E. C., Electrical Instruments in Hazardous Locations, Plenum Press, N. Y., 1966.
- 5-29. Mills, W., Jr., Switzer, W. E., Moncrief, J. A., Electrical Injuries, JAMA, 195: 852-854, Mar. 1966.
- 5-30. Moritz, A. R., Davis, J. H., Physical Agents in Causation of Injury and Disease, in Pathology, Anderson, W. A. D., (ed.), C. V. Mosby Co., St. Louis, 1966, Vol. I, Chapt. 5, section on Electrical Injuries, pp. 136-138.
- 5-31. Morse, A. R., Discussion Section of Article by Kouwenhoven and Milnor, See Ref. 23, p. 85.
- 5-32. National Fire Protection Association, National Electrical Code, 1965 Edition, Boston, Mass.
- 5-33. Osypka, P., Quantitative Investigation of Electrocution Accidents Involving Human Beings and Animals, OTS-66-12588, SLA Translation Center, Chicago, Ill., 1966. (Translation of Excerpts from Technische Hochschule Brunswick, Thesis (West Germany), 1963, Sect. 7.1 - 7.2).
- 5-34. Rutenfranz, J., Zur Frage einer Tagesrhythmis des Elektrischen Hautwiderstandes beim Menschen, [Diurnal Rhythm of Man's High Electrical Resistance], Int. Z. Angew Physiol., 16: 152-172, 1955.
- 5-35. Schwan, H. P., Biophysics of Diathermy, in Therapeutic Heat and Cold, Licht, S., (ed.), Waverly Press, Baltimore, 1965.
- 5-36. Stacy, R. W., Williams, D. T., Worden, R. E., et al., Essentials of Biological and Medical Physics, McGraw-Hill, N. Y., 1955.
- 5-37. Wood, J. L., Some Technical Aspects of Electric Shock, Med. Sci. Law, 5: 19-23, Jan. 1965.

6. THERMAL ENVIRONMENT

Prepared by

T. A. Bottomley, Bellcomm, Inc.
E. M. Roth, M. D., Lovelace Foundation

TABLE OF CONTENTS

6.	THERMAL ENVIRONMENT	6-1
	The Biothermal Equation	6-5
	Environmental Comfort and Stress Indices	6-9
	Operative Temperature	6-9
	Environmental Temperature	6-11
	Effective Temperature	6-12
	Reference Operative Temperature	6-16
	Stress Indices	6-16
	Biothermal Properties and Comfort Zones in Space	
	Cabin Atmospheres	6-18
	Radiant Heat Exchange	6-19
	Forced Convective Heat Transfer	6-25
	Free Convective Heat Transfer	6-32
	Evaporative Heat Transfer	6-32
	Respiratory Heat Loss	6-40
	First-Order Estimate of Evaporative Heat Loss in Space Cabins	6-41
	Comfort Zone Predictions in Unusual Gaseous Environments	6-43
	Space Suits and Clothing	6-52
	Radiant Insulation	6-52
	Insulation of "Shirtsleeve" Garments	6-56
	Vapor Resistance	6-57
	Ventilated Suits	6-60
	Liquid-Cooled Suits	6-62
	Conductive Heat Exchange	6-69
	Heat Stress and Tolerance	6-71
	Body Temperature	6-71
	Mean Body Temperature	6-71

Rectal Temperature	6-73
Skin Temperature	6-73
Sweating and Respiratory Water Loss	6-81
Heat Stress Indices	6-81
The Belding-Hatch Heat Stress Index	6-90
The P4SR Index	6-90
Body Storage Index	6-91
Tolerance Time in Heat	
Performance Under Heat Stress	6-95
Acclimatization to Heat	6-103
Skin Pain and Heat Pulses	6-107
Cold Stress	6-107
Cold Stress Tolerance	6-113
Performance in the Cold	6-121
Acclimatization to Cold	6-125
References	6-128

THERMAL ENVIRONMENT

Heat is exchanged between man and the environment through four avenues. (1) Exchanges of radiation may occur with surfaces having higher or lower temperatures than that of the skin or radiation may be absorbed by the skin from high temperature sources such as the sun. (2) The body may exchange heat by convection and this is an important source of heat loss especially if the velocity of currents around the body is high and their temperature, low. (3) Heat may be exchanged by conduction with objects in direct physical contact. (4) Heat may be lost by vaporization from the lungs through respiration and the skin by sweating. Heat may be lost in urine and feces. The body also stores heat in the tissues and body fluids. This stored heat is the currency with which body heat balance is purchased. The various manifestations and ramifications of these basic interactions encompass the field of thermal biophysics.

Because the field of thermal biophysics draws upon many different sciences the problem of consistent units is always present. The following units are those found in the majority of cases but the policy of checking units, when using an equation for the first time, should always be followed (21).

Table 6-1
Nomenclature

<u>Symbol</u>	<u>Definition</u>	<u>BE Units</u>	<u>Metric Units</u>
A	area	ft ²	m ²
A _b	surface area of body	ft ²	m ²
A _g	surface area of garmented body	ft ²	m ²
A _r	radiating area of body	ft ²	m ²
A _w	wetted area of body	ft ²	m ²
B _f	film thickness	in	cm
C'	E _r /E _m		
ΔC	concentration difference	lb/ft ³	gm/cm ³
C _p	unit heat capacity at constant pressure	Btu/lb°F	kcal/Kg°C
C _v	unit heat capacity at constant volume	Btu/ft ³ °F	kcal/m ³ °C
D	diameter or significant dimension	ft	m
D _v	vapor diffusivity -	ft ² /hr	cm ² /sec

<u>Symbol</u>	<u>Definition</u>	<u>BE Units</u>	<u>Metric Units</u>
D_{v0}	diffusivity of water vapor in air at standard pressure	f^2/hr	cm^2/sec
E	energy in general	Btu	kcal
E_r	evaporative water loss	$\text{lbs}/\text{ft}^2/\text{hr}$	$\text{gm}/\text{m}^2/\text{hr}$
E_m	evaporative water loss (maximum)	$\text{lbs}/\text{ft}^2/\text{hr}$	$\text{gm}/\text{m}^2/\text{hr}$
F_{ae}	shape-emissivity factor		dimensionless
F_{12}	shape factor		dimensionless
f_r	radiation area factor		dimensionless
g	fraction of earth gravity		
G	mass velocity	$\text{lb}/\text{ft}^2\text{hr}$	$\text{Kg}/\text{m}^2\text{hr}$
h	overall heat transfer conductance	$\text{Btu}/\text{ft}^2\text{hr}^\circ\text{F}$	$\text{kcal}/\text{m}^2\text{hr}^\circ\text{C}$
h_c	convective conductance	$\text{Btu}/\text{ft}^2\text{hr}^\circ\text{F}$	$\text{kcal}/\text{m}^2\text{hr}^\circ\text{C}$
h_g	clothing conductance	$\text{Btu}/\text{ft}^2\text{hr}^\circ\text{F}$	$\text{kcal}/\text{m}^2\text{hr}^\circ\text{C}$
h_o	operative conductance	$\text{Btu}/\text{ft}^2\text{hr}^\circ\text{F}$	$\text{kcal}/\text{m}^2\text{hr}^\circ\text{C}$
h_r	radiant conductance	$\text{Btu}/\text{ft}^2\text{hr}^\circ\text{F}$	$\text{kcal}/\text{m}^2\text{hr}^\circ\text{C}$
h_{rb}	radiant conductance (black body)	$\text{Btu}/\text{ft}^2\text{hr}^\circ\text{F}$	$\text{kcal}/\text{m}^2\text{hr}^\circ\text{C}$
h_{sr}	solar radiant conductance	$\text{Btu}/\text{ft}^2\text{hr}^\circ\text{F}$	$\text{kcal}/\text{m}^2\text{hr}^\circ\text{C}$
h'	overall evaporative conductance	$\text{Btu}/\text{ft}^2\text{hr}$ in Hg	$\text{kcal}/\text{m}^2\text{hr mmHg}$
h'_c	external, environmental evaporative conductance	$\text{Btu}/\text{ft}^2\text{hr}$ in Hg	$\text{kcal}/\text{m}^2\text{hr mmHg}$
h_D	mass transfer coefficient	ft/hr	m/hr
k	thermal conductivity	$\text{Btu}/\text{ft hr}^\circ\text{F}$	$\text{kcal}/\text{m hr}^\circ\text{C}$
L	thickness	ft	cm
M	molecular weight	lbs/mole	gm/mole
P	barometric pressure	in Hg	mmHg
Pr	Prandtl number ($C_p \mu/k$)		dimensionless
P_o	standard barometric pressure	in Hg	mmHg
p_a	water vapor pressure (absolute humidity)	in Hg	mmHg
p_s	water vapor pressure at the skin	in Hg	mmHg
p_s^*	saturated water vapor pressure at t_s	in Hg	mmHg
q_c	convective heat transfer	$\text{Btu}/\text{ft}^2\text{hr}$	$\text{kcal}/\text{m}^2\text{hr}$

<u>Symbol</u>	<u>Definition</u>	<u>BE Units</u>	<u>Metric Units</u>
q_e	evaporative heat transfer	Btu/ft ² hr	kcal/m ² hr
q_m	metabolism	Btu/ft ² hr	kcal/m ² hr
q_r	radiant heat transfer	Btu/ft ² hr	kcal/m ² hr
q_s	storage rate	Btu/ft ² hr	kcal/m ² hr
q_{sr}	solar heat transfer to man	Btu/ft ² hr	kcal/m ² hr
q_k	conductive heat transfer	Btu/ft ² hr	kcal/m ² hr
q_v	respiratory heat transfer	Btu/ft ² hr	kcal/m ² hr
q_w	energy of work	Btu/ft ² hr	kcal/m ² hr
Q	total heat transfer	Btu/hr	kcal/hr
r	radius	in	cm
$R=1/h$	thermal resistance in general	$\frac{\text{ft}^2 \text{hr}^{\circ}\text{F}}{\text{Btu}}$	$\frac{\text{m}^2 \text{hr}^{\circ}\text{C}}{\text{Kcal}}$
Re	Reynolds number		
$R_g = 1/h_g$	thermal resistance of clothing	$\frac{\text{ft}^2 \text{hr}^{\circ}\text{F}}{\text{Btu}}$	$\frac{\text{m}^2 \text{hr}^{\circ}\text{C}}{\text{Kcal}}$
$R_o = \frac{1}{h_o}$	thermal resistance of the environment	$\frac{\text{ft}^2 \text{hr}^{\circ}\text{F}}{\text{Btu}}$	$\frac{\text{m}^2 \text{hr}^{\circ}\text{C}}{\text{Kcal}}$
R'	vapor resistance in terms of the equivalent thickness of still air	ft still air	cm still air
R'_g	clothing vapor resistance	ft still air	cm still air
R'_e	environment vapor resistance	ft still air	cm still air
t	temperature	°F	°C
t_a	air temperature	°F	°C
t_b	weighted mean body temperature	°F	°C
t_{bm}	midpoint body temperature during exposure	°F	°C
t_E	effective temperature	°F	°C
t_{env}	environmental temperature	°F	°C
t_g	garment surface temperature	°F	°C
t_o	operative temperature	°F	°C
t_{or}	reference operative temperature	°F	°C
t_r	rectal temperature	°F	°C
t_{rm}	midpoint rectal temperature during exposure	°F	°C
t_s	weighted body skin temperature	°F	°C

<u>Symbol</u>	<u>Definition</u>	<u>BE Units</u>	<u>Metric Units</u>
t_{sm}	midpoint skin temperature during exposure	°F	°C
t_{sr}	temperature of the sun	°F	°C
Δt_{osr}	solar operative temperature increment	°F	°C
t_w	average wall temperature	°F	°C
T	absolute temperature	°R	°K
$T_g; T_w$	absolute temperature of garment, wall	°R	°K
T_O	reference or standard temperature	°R	°K
T_f	film temperature	°R	°K
u	internal energy per unit mass	Btu/lb	kcal/kg
U	internal energy	Btu	kcal
\bar{V}	velocity	ft/hr	km/hr
\dot{V}	respiration rate	lbs/hr	liters/min
v	volume per unit mass	ft ³ /lb	cm ³ /gm
w	work per unit mass	ft-lb _f /lb	m-Kg _f /Kg
W_e	work	ft-lb _f	m-Kg _f
W	weight	lb _f	Kg _f
W_p	perspiration rate	lb/ft ² hr	gm/m ² hr

GREEK SYMBOLS

α	Solar absorptivity of skin or garments		
β	coefficient thermal expansion (vol.)		
ϵ	emissivity	dimensionless	
ϵ_g	emissivity of garments	dimensionless	
θ	time of exposure	min or hrs	
θ_m	midpoint time	min or hrs	
θ_t	tolerance time	min or hrs	
λ_e	heat transfer due to evaporation	Btu/lb	kcal/kg
μ	viscosity	lb/ft hr	Kg/m hr
ρ	density	lb/ft ³	Kg/m ³

<u>Symbol</u>	<u>Definition</u>	<u>BE Units</u>	<u>Metric Units</u>
σ	Stefan-Boltzman constant	$\text{Btu}/\text{ft}^2 \text{hr}^\circ \text{R}^4$	$\text{kcal}/\text{m}^2 \text{hr}^\circ \text{K}^4$
τ	Transmission factor for transparent surfaces		
ω	wetted fraction of surface	dimensionless	

DIMENSIONLESS GROUPS OR NUMBERS

$$\text{Nu} = \frac{h_c D}{k} \quad \text{Nusselt number}$$

$$\text{Pr} = \frac{C_p \mu}{k} \quad \text{Prandtl number}$$

$$\text{Re} = \frac{DV\rho}{\mu} \quad \text{Reynold's number}$$

(After Blockley et al., (27))

THE BIOTHERMAL EQUATION

The conditions for thermal equilibrium between the human body and the environment can be examined in terms of the biothermal equation. This equation attempts to balance the normal heat gains and losses and is usually expressed as follows (27):

$$q_{sr} + q_m = q_s \pm q_r \pm q_c + q_v \pm q_k + q_e + q_w \quad (1)$$

Table 6-2 gives the functions or criteria affecting these terms and their effect upon the biothermal equation.

For a state of thermal equilibrium, the heat storage rate is zero ($q_s = 0$). The conductive heat transfer mode is usually quite small and can be assumed, in most instances, to be included in the radiant and/or convective heat transfer terms ($q_k = 0$). Finally, if external heat fluxes are accounted for in terms of induced, environmental parameters, such as internal air and wall temperatures, the term (q_{sr}) can be omitted from the expression.

With comfort as the reference state ($q_s = 0$), the biothermal equation can be expressed as:

$$q_m = \pm q_r \pm q_c + q_e + q_v + q_w \quad (2)$$

and the system can be examined qualitatively in the light of these terms after they have been adequately defined.

Table 6-2
Components of the Biothermal Equation

Term	Function	Effect on System
Metabolism, q_m	f (activity level, body temp.)	Gain at all times
Solar radiation, q_{sr}	$f(h_{sr}, t)$	Gain when present
Infrared radiation, q_r	$f(h_r, t)$	Gain: $t_w > t_g$ Loss: $t_w < t_g$
Convection, q_c	$f(h_c, t)$	Gain: $t_a > t_g$ Loss: $t_a < t_g$
Evaporation, q_e	$f(D_v, \Delta C.P., t)$	Loss in all usual conditions
Resp. heat exch., q_v	f (Resp. mass flow, P, t)	Small gain or loss
Storage, q_s	$f(W, C_p, A_b, dt_b/d\theta)$	Gain: $dt_b/d\theta > 0$ Loss: $dt_b/d\theta < 0$
Work, q_w	nature of activity	Gain: Work done on body; Loss: Work done by body

Heat of metabolism (q_m) is considered to be the sum of the basal metabolic rate (energy required to maintain the body in good health and at equilibrium temperature while at rest) plus an incremental increase in heat energy due to activity and/or stress.

Radiant heat exchange (q_r) is a measure of the heat lost (or gained) as a result of the temperature difference between the skin of the human body and the walls of the surroundings.

Convective heat exchange (q_c) is a measure of the heat lost (or gained) as a result of the temperature difference between the skin and the immediate atmosphere.

Evaporative heat exchange (q_e) is the heat exchange resulting from the vaporization of moisture at the surface of the skin.

Respiratory heat exchange (q_v) is a measure of the heat lost (including vaporization of water) from the lungs due to respiration.

In any environment, all of the above modes of heat transfer may be present. In general, the ambient dry bulb temperature, humidity, air velocity, and ambient pressure determine the partition of mechanisms

actually used by the body. Several computer programs using mathematical models of human thermoregulation have been proposed (37, 38, 188, 194). At the current stage of development, these should be used in close connection with empirical studies in evaluating the effects of unusual thermal environments.

Figure 6-3 represents the changing partition of heat loss mechanisms at rest with increasing dry bulb temperature at a constant relative humidity of 45% and constant gas velocity. The regions of primarily metabolic, vaso-motor and evaporative regulation are noted. High metabolic rate at low temperature is a result of shivering; at temperatures above 90°F metabolic rate may increase due to restlessness and Q₁₀ factors.

Determination of the human body's thermal status in space operations requires analysis of a large number of variables. Many of these variables do not lend themselves to an exact mathematical solution but must be arrived at statistically from experimental data. Even then, the results must be treated with caution when applied to the small population represented by a flight crew. Individual metabolic rates, health variations, tolerances, and motivation can cause wide deviations from predicted states and performances. Diurnal cycles are especially significant.

In general, the variables of interest can be collected under three major classifications. These are environment, body state and clothing. Most of the variables are listed under these major classifications in Table 6-4.

As many of the variables are interdependent, solution of the complete biothermal equation becomes largely a reiterative process modified by heavy reliance on reasonable assumptions and experimental results. As a rule, equipment provided to satisfy a primary functional requirement for biothermal protection and control is integral to the environmental control systems and to the garment assemblies worn by the crew. Maintenance of thermal balance requires the regulation of environmental parameters to maintain man in a state of thermal equilibrium (or compensable quasi-equilibrium) at all anticipated levels of activity to ensure adequate performance and preclude irreversible physiological effects.

Engineering for thermal balance includes the specification of thermal design criteria for all equipment being provided to satisfy, as a primary functional requirement, biothermal protection and control. In addition, it includes identification, quantitatively if possible, of all factors related to

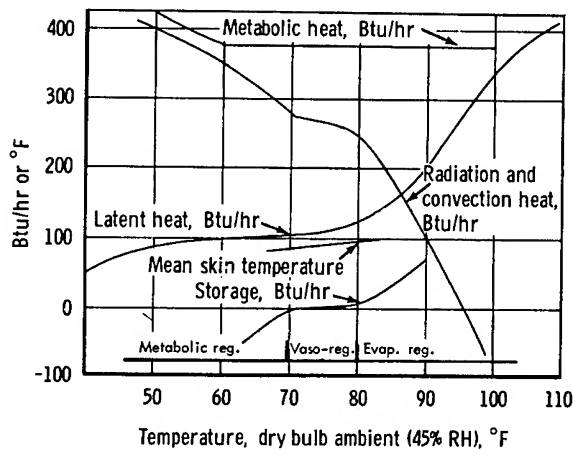


Figure 6-3

Typical Relation Between Human Heat Balance and Temperatures for Lightly Clothed, Resting Subjects in Still Air at Sea Level

(Adapted by Johnson⁽¹¹⁴⁾ from^(81, 102, 225, 226) and others)

Table 6-4
Conditions for Prediction of Body Thermal Status
(After Bottomley⁽³²⁾)

<u>Environment</u>		<u>Body State</u>	<u>Clothing</u>
<u>External (Natural)</u>	<u>Internal (Induced)</u>		
Solar radiation (q_{sr})	Wall temperature (t_w)	Metabolic rate (q_m)	Thermal resistance (R_g)
Earth radiation (q_{er})	Atmospheric temperature (t_a)	Weight (W)	Vapor resistance ($R'g$)
Lunar radiation (q_{lr})	Atmospheric pressure (P)	Posture	Wind permeability
Shadow cones (day/night)	Atmospheric velocity (V)	Area of body (A_b)	Weight
Atmospheric composition	Atmospheric composition	Skin temperature (t_s)	Color (emissivity absorptivity)
Vehicle velocity (if > C/7) (C = vel. of light)	Absolute humidity (p_a)	Rectal temperature (t_r)	Wicking efficiency
Vehicle attitude or orientation	Diffusivity (D_v)	Mean body temperature (t_b)	Effective clothing absorbtance
Vehicle altitude	Specific heats (C_p, C_v)	Respiration rate (V)	
	Surface Area (surroundings) A	Insensible water loss	
	Shape emissivity factor F_{ae}	Sweat rate (sensible (W_e) water loss)	
	Crew operating mode	Wetted area (ω)	
	<u>Stress Factors</u>	Activity/work efficiency	
	System failure	Physical condition	
	G-loads (weightlessness)	Degree of heat stress resistance (acclimatization)	
	Toxicity (CO_2 etc.) effects	Water/electrolyte balance	
	Radiation effects	Radiation area factor (fr)	
	Decompression (emergency)	Radiating area of body (A_r)	
	Hypoxia	Area of body irradiated	
	Psychological (morale, anxiety)	Effective skin absorbtance	
	Vibration		

biothermal control which must be considered in specifications and trade-off studies applicable to other systems and to mission operations, profiles, and constraints. All phases of the mission, including survival on Earth in case of aberrant landing site, must be considered. Data are available on the thermal and related environments to be assumed in the manned lunar surface program (105).

The primary environmental parameters affecting heat exchange between man and his surroundings are:

1. Convective sources or sinks
 - a. Atmospheres (relevant factors include composition, pressure, temperature, absolute humidity, and ventilation rates)
2. Conductive sources or sinks
 - a. Solids (relevant factors include temperature, contact pressure and thermal conductivity)
 - b. Liquids (relevant factors include temperature, film coefficients, flow rates and thermal conductivity)

3. Radiant sources or sinks

- a. External - e.g., solar and planetary radiation, deep space (relevant factors include the solar constant, planetary surface and albedo, mean radiant temperatures, and deep space temperature)
- b. Internal - e.g., wall and equipment surfaces (relevant factors include temperatures and reflectivity, emissivity and absorptivity coefficients)

Once the analysis has entertained all pertinent variables, and a comfort region for thermal equilibrium has been determined, there still remains the establishment of an index which clearly defines the bounds of the region and is translatable into terms which are meaningful to the design engineer.

ENVIRONMENTAL COMFORT AND STRESS INDICES

Comfort zones have been defined in the literature in terms of skin temperature, sweat rates and various indices which relate environmental parameters to subjective impressions of comfort or measured values of selected physiological variables.

For the same conditions and individuals the established boundaries for thermal comfort, performance and tolerance as described by the various design indices may be completely consistent. However, variations in activity, wearing apparel, individual health and acclimatization, and thermal exposure immediately prior to making a determination of comfort will operate to shift the zones and introduce inconsistencies in results (76).

Examples of comfort indices established in the past are the British Comfort Index (67), ASHRAE Effective Temperature (7), and Operative Temperature (212). All but Operative Temperature are psychophysiological determinations which, having been established subjectively, are not as adaptive to quantitative treatment in design and analysis.

For these reasons Operative Temperature is probably the most useful as the primary comfort index for use in biothermal systems design. However, information relating to other indices in general use is provided to permit comparison of new data with old in those cases where an index other than Operative Temperature has been used as a reference. Recent reviews of thermal stress assessment from heat balance data are available (139, 183, 228).

Operative Temperature (t_o)

"Operative Temperature" was first introduced to establish "a generalized environmental temperature scale, that combines as a single measurement certain of the thermal effects of the physical environment, aqueous or atmospheric, and in the latter case for any combination of radiant tempera-

ture, ambient air temperature and air movement" (80). They cover only sea level conditions.

$$(\text{Metric}) \quad t_o = 0.18 t_w + 0.19 \left(\sqrt{\bar{V}} t_a - (\sqrt{\bar{V}} - 1) t_s \right) \quad (3)$$

when $t_a, t_w, t_s = {}^\circ\text{C}$

\bar{V} = atmospheric velocity in cm/sec

$$(\text{English}) \quad t_o = 0.18 t_w + 0.135 \left(\sqrt{\bar{V}} t_a - (\sqrt{\bar{V}} - 1.40) t_s \right) \quad (4)$$

when $t = {}^\circ\text{F}$

\bar{V} = ft/min

Without sacrificing the validity or accuracy of the original definition, operative temperature has been redefined (225) in the following form:

$$t_o = \frac{h_r t_w + h_c t_a}{h_r + h_c} = t_a + \frac{h_r (t_w - t_a)}{h_r + h_c} \quad (5)$$

where

t_w = wall temperature - ${}^\circ\text{F}$. (${}^\circ\text{C}$.)

t_a = atmospheric temperature - ${}^\circ\text{F}$. (${}^\circ\text{C}$.)

h_r = radiant conductance-Btu/ $\text{ft}^2 \text{ hr } {}^\circ\text{F}$. ($\text{kcal}/\text{m}^2 \text{ hr } {}^\circ\text{C}$.)

h_c = convective conductance-Btu/ $\text{ft}^2 \text{ hr } {}^\circ\text{F}$. ($\text{kcal}/\text{m}^2 \text{ hr } {}^\circ\text{C}$.)

The term $h_r(t_w - t_a)$ has been recently called the effective radiant field (ERF) and used as an energy term in calculating total body heat load (77, 78, 79).

Operative temperature is simply the weighted mean of air and wall temperatures and may be determined by use of the nomograph (Figure 6-5) or the values of h_r and h_c for specific atmospheres as computed in accordance with derivations to be covered below. For known values of air and wall temperature, Figure 6-5 may be used.

While operative temperature is derived from the environmental and physiological parameters which determine heat transfer from or to the body in terms of radiation and convection, the design objectives that body storage shall be zero, evaporative heat losses shall be limited to insensible evaporation of moisture produced only by diffusion through the skin without the activity of sweat glands, and that body and skin temperatures shall be maintained near nominal while reflecting the effects of environmental parameters (including humidity, atmospheric pressure) and insensible water loss should be sufficient to bound the design area for thermal control.

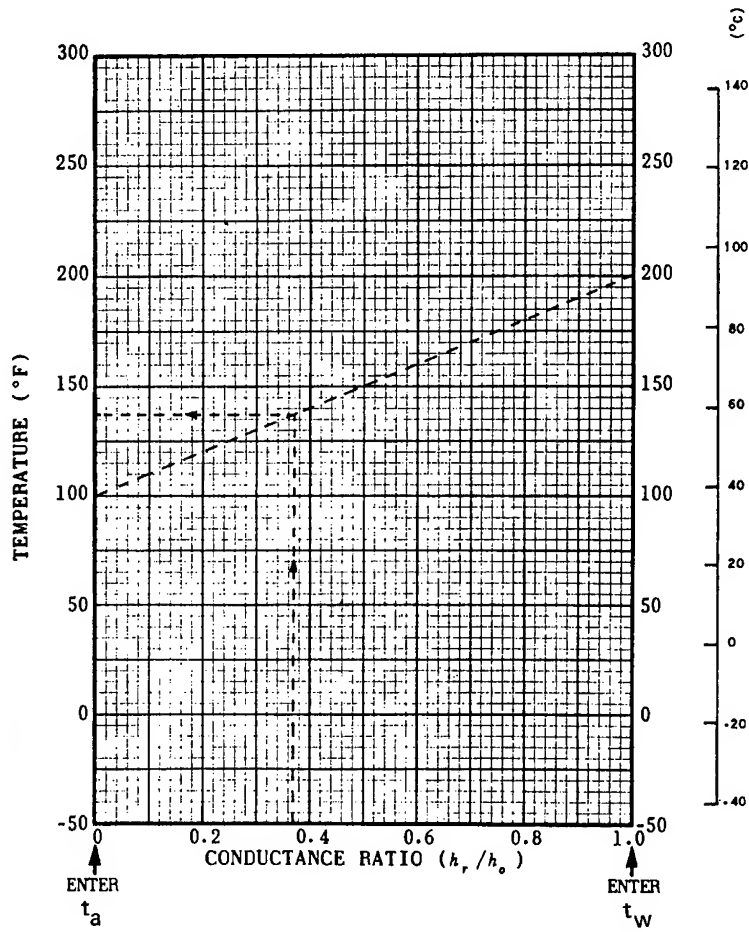


Figure 6-5

Operative Temperature Nomograph

Procedure for graphical solution of:

$$t_o = \frac{t_w h_r + t_a h_c}{h_o}$$

Enter t_a and t_w on indicated ordinates; connect the two points with a straight edge; read t_o at the intersection with the appropriate value of the conductance ratio.

(After Blockley et al (27))

Environmental Temperature ($t_{env.}$)

Environmental temperature is used as a design index when direct solar radiation to the man is a significant heat load not adequately accounted for in terms of induced environmental parameters; otherwise $t_{env} = t_o$ (27).

$$\text{Then } t_{env} = t_o + \Delta t_{o(sr)} \quad (6)$$

$$\text{And } \Delta t_{o(sr)} = \frac{q_{sr}}{h_r + h_c + h_{sr}} \quad (7)$$

$$\text{or } \Delta t_{o(sr)} = \frac{G_t \tau \alpha_1 (A_{sr}/A_b)}{h_r + h_c} \quad (8)$$

where G_t = Total Solar radiation Btu/ft² hr (kcal/m² hr)

τ = Transmission factors for transparent surfaces

α_1 = Solar absorptivity of skin (or clothing)

A_{sr}/A_b = Ratio of area of body directly irradiated by the sun to total area of body

h_r & h_c are as previously defined for t_o

Effective Temperature (t_E) (or E. T.)

The effective temperature index integrates the effects of atmospheric temperature, humidity and ventilation rates based on subjectively reported sensations of warmth, comfort and cold (107, 127, 151). It is acceptable for use when radiant heat exchange is relatively insignificant in comparison with other modes.

Figure 6-6 shows effective temperature indices (i.e., lines of constant thermal sensation in air at sea level) for ventilation flow rates of 15 to 25 feet per minute in air at sea level with effects of seasonal acclimatization.

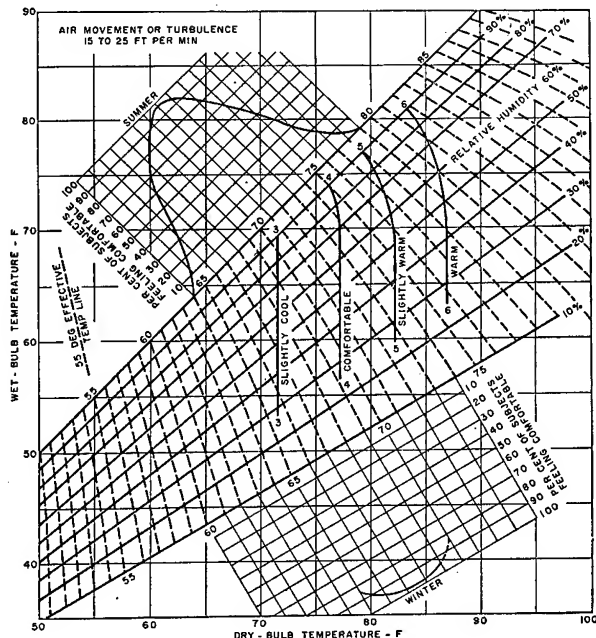
Figure 6-7 is somewhat more appropriate to spacecraft conditions where confined spaces and high ventilation flow rates are likely to be encountered, but covers only air at sea level. It may be of value in consideration of post-landing conditions. Comfort criteria for gaseous variables in sealed cabins will be discussed below.

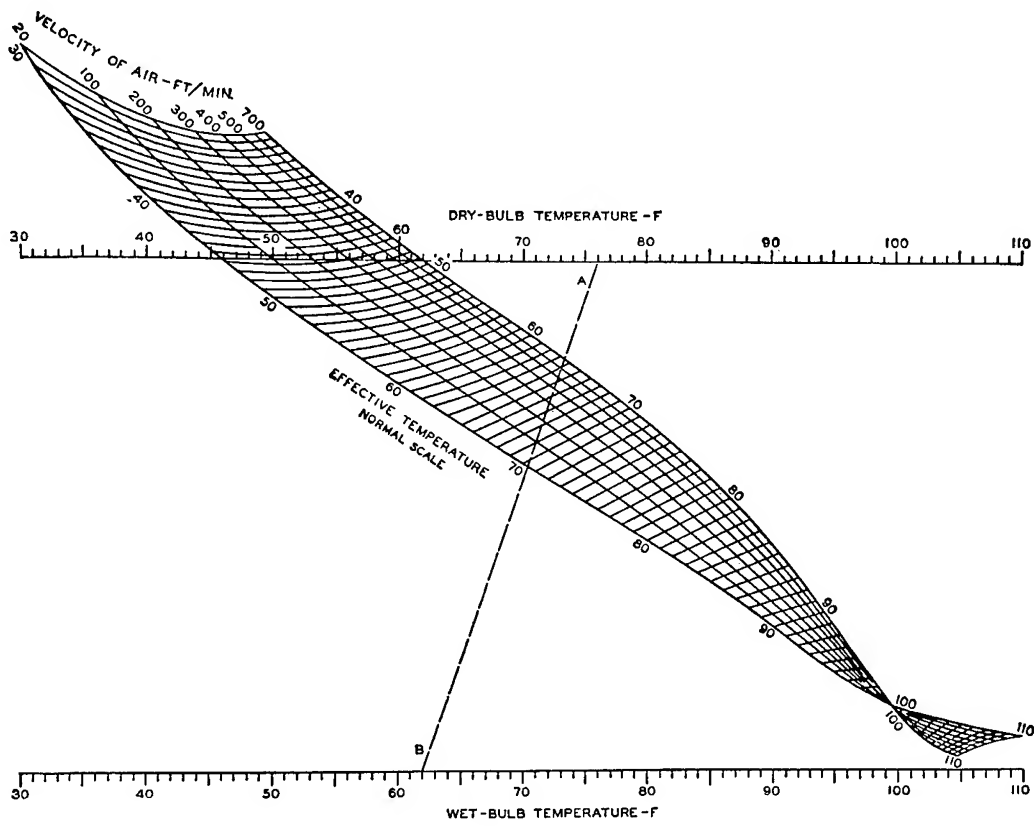
Comfort bands are of value in defining design conditions for office or field laboratory conditions in different climates. In view of the many variables outlined above, the delineation of comfort bands is most difficult. Tables 6-8 and 6-9 present the available data for air at sea level with some

Figure 6-6

Comfort Zones in Summer and Winter.

(After ASHRAE Guide⁽⁷⁾)





Example of the use of the chart: Given dry bulb temperature of 76°F , wet bulb temperature of 62°F , velocity of air 100 fpm; determine: 1) effective temperature (ET) of the condition, 2) ET with still air, 3) cooling produced by the movement of the air, 4) velocity necessary to produce the condition of 66°ET .

Solution: 1) Draw line A-B through given dry and wet bulb temperatures. Its intersection with the 100-fpm curve gives 69° for the ET of the condition. 2) Follow line A-B to the right to its intersection with the 20-fpm velocity line, and read 70.4° for the ET for this velocity or so-called still air. 3) The cooling produced by the movement of the air is $70.4 - 69.0 = 1.4^{\circ}\text{ET}$. 4) Follow line A-B to the left until it crosses the 66° ET line. Interpolate velocity value of 340 fpm to which the movement of the air must be increased for maximum comfort.

Figure 6-7

Thermometric Chart Showing Normal Scale of Effective Temperature. Applicable to Inhabitants of the United States Under the Following Conditions: 1) Clothing: Customary Indoor Clothing; 2) Activity: Sedentary or Light Muscular Work; 3) Heating Methods: Convection Type.

(After ASHRAE Guide⁽⁷⁾)

Table 6-8
Comparison of Comfort Ranges with Zone of Thermal Neutrality
(After ASHRAE Guide⁽⁷⁾)

Investigators	Effective Temperature		Operative Temp Range	Remarks
	Optimum Line	Range		
Comfort Zone				
Houghten and Yaglou	66	63-71	...	Winter nonbasal; at rest, normally clothed. Men and women.
Yaglou and Drinker (237)	71	66-75	...	Summer nonbasal; at rest and normally clothed. Men.
Yaglou (236)	72.5	66-82	...	Entire year; nonbasal; at rest and stripped to waist. Men.
Keeton et al	75	74-76	...	Entire year; basal, nude. Steady state (9 hr exposure). Men and women.
Zone of Thermal Neutrality				
DuBois and Hardy	75 71.8	73.2-76.0 64.8-76.0	...	Basal; nude; men.
Winslow, Herrington, and Gagge (226)	84.0-87.8 74 -84	...	Basal; clothed; men. Nonbasal; at rest; nude; men. Nonbasal; at rest; clothed; men.

Table 6-9
Comfort Bands at Rest in Air at Sea Level

Comfort Level	Physiological Parameter (1)		Environmental Parameter	
	t_s	$E_r / E_m \times 100$	t_a	t_E
Hot	$>95^{\circ}\text{F}$	70-100%	$>87^{\circ}\text{F}$	$>87^{\circ}\text{F}$
Tolerable	$93-94^{\circ}\text{F}$	25-70%	$79-86^{\circ}\text{F}$	82°F
Comfortable	$90-92^{\circ}\text{F}$	10-25%	$68-78^{\circ}\text{F}$	$70-75^{\circ}\text{F}$
Cold	$<89^{\circ}\text{F}$	0-10%	67°F	$<65^{\circ}\text{F}$

Relative humidity 30-70%; air velocity 15-40 ft/min.

physiological correlates. Many field studies have been made to determine the optimum indoor effective temperature for both winter and summer in several metropolitan districts of the United States and Canada, in cooperation with the managements of offices employing large numbers of workers (8). Persons serving in all of these studies were representative of office workers dressed for air-conditioned spaces in the summer season, and engaged in the customary office activity. Some of the results of these studies for the summer season are shown in Figure 6-10. In the warmer areas of the country

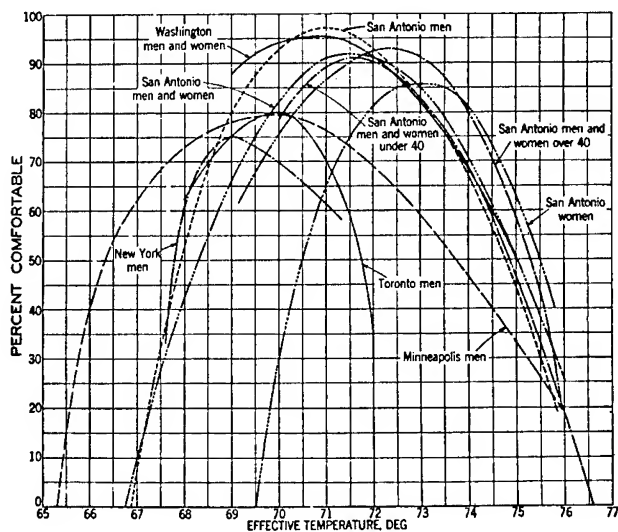


Figure 6-10

Relation Between Effective Temperature and Percentage Observations Indicating Comfort of Office Workers in the Summer Season.

(After ASHRAE Guide⁽⁷⁾)

the optimum effective temperature for summer cooling is approximately 3 degrees higher than in the northern cities. Variations in sensation of comfort among individuals may be greater for any given location than variations due to a difference in geographical location. Available information indicates that changes in weather conditions over a period of a few days do not alter optimum indoor temperature. On the whole, women of all age groups studied prefer an effective temperature for comfort 1.0 degree higher than men. All men and women over 40 years of age prefer a temperature 1 deg ET higher than that desired by persons below this age.

In addition to defining environmental zones of comfort, one must consider indices of graded environmental stress. Indicators of stress may be stated in terms of environmental or physiological variables. In this section, the environmental indices of stress will be covered. Physiological indicators are covered in specific sections on heat and cold stress.

Reference Operative Temperature (t_{or})

Reference Operative Temperature was introduced to permit consideration of the humidity effect as a specific design parameter in assessing the biothermal state under stressful conditions (27). Skin temperature is independent of humidity between zero and about 20 mm Hg vapor pressure. The data in the current literature supports the view that absolute humidity in the range from 0.20 to 0.59 in Hg (5 to 15 mm Hg) is not a significant consideration for biothermal regulation under moderate ambient conditions. For warm humid environments leading to time-limited biothermal states, Reference Operative Temperature can be used as a design index. To determine the equivalent Reference Operative Temperature, Figure 6-11 is entered with values of Operative Temperature and absolute humidity.

"Oxford" or W/D Index

The "Oxford" or W/D Index, is a simple weighting of wet bulb temperature (85%) and dry bulb (air) temperature (15%). It is based on the observation that in non-compensable heat exposures the time to incipient collapse correlated well with this parameter and is used primarily in this context. The presumption is that W/D value is directly related to rate of heat storage, or the imbalance of surface heat exchange. A related index for outdoor use is the wet bulb-globe temperature (WBGT) index. Figure 6-12 can be used for calculation of the Oxford Index. Figure 6-80 presents tolerance times as related to this index.

The following indices of stress are more closely tied to specific physiological endpoint and will be covered in greater detail in the section on heat and cold stress.

The Belding-Hatch Stress Index

This index predicts the ratio for evaporation required for thermal balance in a given environment and compares it to the maximum rate safely attainable for prolonged periods of time. Equation 46 and Figure 6-74 and 6-75 cover this index.

The P4SR Index (Predicted Four Hour Sweat Rate)

The rate of sweating for men in hot environments can be predicted and related to degree of stress. Figure 6-76 presents a nomogram for calculation of the P4SR.

The Body Storage Index

The rate of body heat gain can be correlated with physiological and psychological measurements of heat stress. Tolerance and performance times can be predicted using this index (See Figures 6-77 and 6-78).

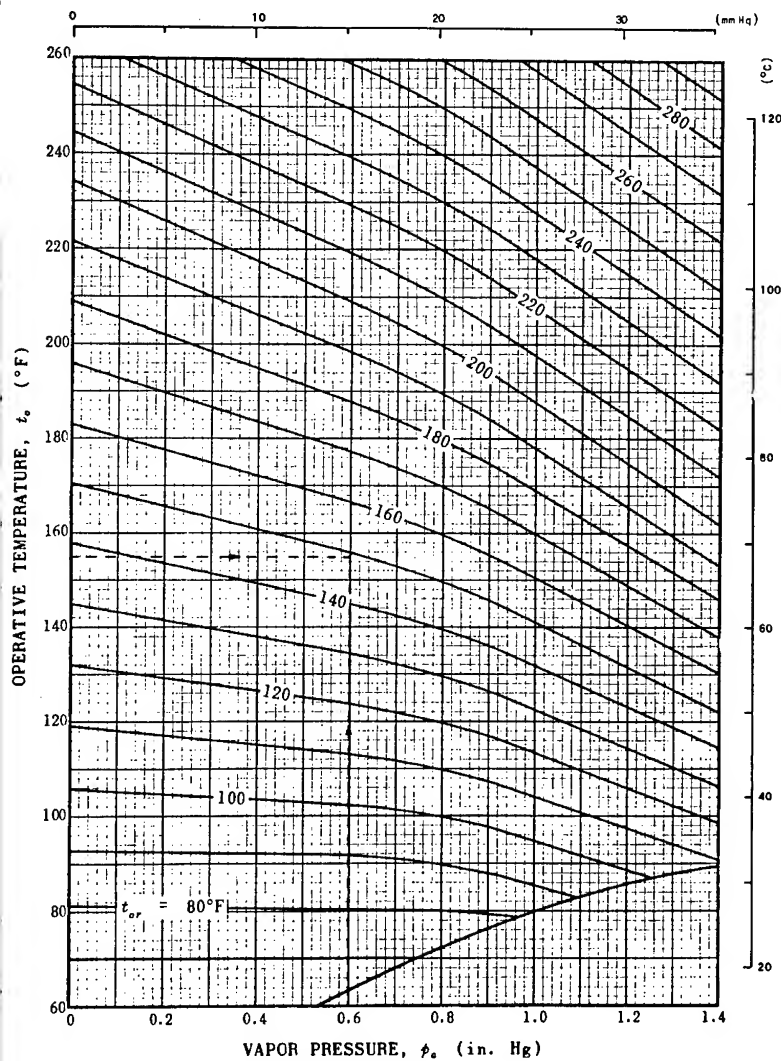


Figure 6-11

Reference Operative Temperature

Display of temperature-humidity equivalences in air according to human thermal effect. Reference operative temperature, t_{or} , is defined as the operative temperature at 0.79 in. Hg vapor pressure.

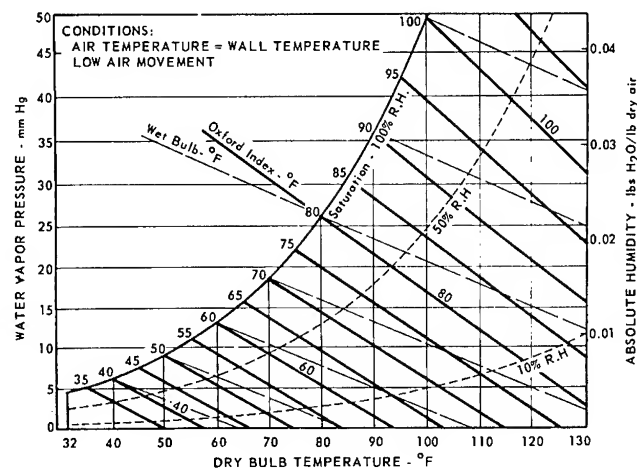
Procedure: Enter with p_a and t_o ; read t_{or} by interpolation in parametric scale.

(After Blockley et al.,⁽²⁷⁾)

Figure 6-12

The Oxford or W/D Index

(After Blockley⁽³⁰⁾ Adapted from Data of Provins, Hellon et al⁽¹⁶²⁾ and Leithead and Lind⁽¹²⁷⁾)



Windchill Index

In severely cold environments, the Windchill Index may be used as a rough measure of cold stress. This is covered in Figure 6-99.

BIO THERMAL PROPERTIES AND COMFORT ZONES IN SPACE CABIN ATMOSPHERES

The determination of human thermal constants in atmospheres other than air is a difficult task (21, 100, 121, 131, 155, 165). Extrapolation of comfort zones to these unusual gaseous environments is also fraught with several uncertainties (174).

The thermal constants of gases and of candidate atmospheres other than air are seen in Table 6-13 representing the properties of the individual gases at 1 atmosphere and Table 6-14, the properties of the mixtures as recommended for space cabins (174). Psychrometric charts are also available for these atmospheres (90, 174, 175).

Table 6-13
Thermal Properties of Component Gases at 80°F (540°R) and Atmospheric Pressures
(After Breeze⁽³⁶⁾)

Gas	Molecular Weight M	Specific Gas Constant R Ft-Lb/Lb-°R	Density Lb/Ft ³	Specific Heat C _p Btu/lb-°F	Dynamic Viscosity X 10 ⁶ μ Lb/Sec-Ft	Thermal Conductivity k Btu/Hr-Ft ² - °F/Ft	Prandtl Number N _{Pr}
Air	29.0	53.3	0.0735	0.240	12.4	0.0152	0.708
CO ₂	44.010	35.1	0.1122	0.208	10.1	0.00958	0.770
H _e	4.002	386	0.0105	1.242	13.5	0.0861	0.740
N _e	20.183	76.6	0.0512	0.246	21.2	0.0280	0.668
N ₂	28.016	55.1	0.0713	0.249	12.0	0.0151	0.713
O ₂	32.000	48.25	0.0812	0.220	13.9	0.0155	0.709
Water Vapor	18.016	85.81	0.0373	0.445	6.6	0.0103	1.03

Table 6-14
Properties of Candidate Systems for Space-Cabin Atmospheres 80°F (540°R)
(After Johnson⁽¹¹⁴⁾)

Atmosphere	Molecular weight, m	k, Btu/ ft-hr-°R	ρ, lb/ft ³	C _p , Btu/ lb-°R	μ, lb/ft-hr	d, ft ² /sec (steam) × 10 ⁻³	α, ft ² /sec × 10 ⁻³	N _{Le} , α/d	N _{Pr} , C _p μ/k
14.7-psia air.....	29	0.0151	0.076	0.24	0.0421	0.264	0.238	0.902	0.67
5-psia O ₂	32	.0154	.0283	.222	.0500	.756	.707	.935	.72
5-psia O ₂ -N ₂	31	.0153	.0268	.23	.0465	.756	.707	.935	.70
5-psia O ₂ -He.....	24	.0267	.0198	.278	.0520	.862	1.355	1.572	.54
7-psia O ₂ -N ₂	30	.0152	.0362	.23	.0470	.540	.500	.926	.71
7-psia O ₂ -He.....	18	.0304	.023	.33	.0512	.705	1.512	2.15	.496

In the determination of comfort zones, heat exchange via conduction will be considered negligible and provided for in heat exchange via convection and/or radiation. Conductive heat exchange, however, is significant in determining garment temperature; assessing the impact of heat shorts and hot or cold surfaces coming in contact with the bare skin; and in analyzing the effectiveness of conduction concepts for thermal regulation. Accordingly, data and equations for calculating conductive heat exchange are included below (Equations 39, 40, 41, Figure 6-56, Tables 6-58, 6-64 and 6-65).

In the comfort state, a man at rest will have a mean skin temperature of $91.4 \pm 1.8^{\circ}\text{F}$ ($33 \pm 1^{\circ}\text{C}$) and a rectal temperature of $98.6 \pm 0.9^{\circ}\text{F}$ ($37 \pm 0.5^{\circ}\text{C}$). There will be no visible sweating and the blood vessels near the surface of the skin will be slightly dilated (36). Any subsequent variation in metabolism or environmental conditions will initiate a change in peripheral blood flow (vascular regulation) of the body (See Figure 6-3).

At nominal ambient temperatures, with light work loads, rectal temperature will be maintained constant at some level above resting value determined by metabolic rate; while skin temperature, respiration rate and, in certain instances, perspiration rate will be varied by regulatory systems of the body to attain thermal balance under the new conditions. Raising the temperature of the environment or increasing metabolic rate by activity or ingestion of food will result in vasodilatation to increase the heat exchange between the core and skin (See Figure 6-3). Sweating or shivering usually occur before the limits of vascular regulation are reached and, in so doing, serve to reduce the load on the vascular system. Experiments indicate that at the limits of vasoregulation, the vasomotor system is capable of exerting a stabilizing effect on rectal and skin temperatures for a finite period (226). The period of stabilization is reduced as the severity of thermal stress is increased.

Radiant Heat Exchange

The analysis of net radiant heat exchange between an astronaut and his surroundings is complicated by the following factors:

- a. Ability of the crew to move around and change position.
- b. Arrangement and surface temperature of the various equipment enclosures.
- c. Localized differences in temperature of the cabin walls due to structural anomalies resulting from variations in thickness, feed-through equipment (e.g., sextant, antennas, etc.) exposed to the space environment, and size and location of windows.

The net radiant exchange of energy between two ideal radiators is

$$q_r = f_r \sigma (T_w^4 - T_s^4) \quad (9)$$

(Stefan-Boltzman)
constant)

$$\sigma = 0.173 \times 10^{-8} \text{ BTU/ft}^2 \text{ hr } ^\circ\text{R}$$

$$\sigma = 4.92 \times 10^{-8} \text{ kcal/m}^2 \text{ hr } ^\circ\text{K}$$

f_r = radiation area factor

T_w , T_s = mean black-body temperature of walls,
and body surface, respectively.

Radiant conductance h_r can be determined directly from Figure 6-15 when the black body temperature of the walls is known. The black body temperature of the skin can be assumed as 92.5°F or 32.5°C. In order to account for variable emissivities and geometric considerations of the human body and environment - a shape-emissivity factor (F_{ae}) and radiation area factor (f_r) must be introduced.

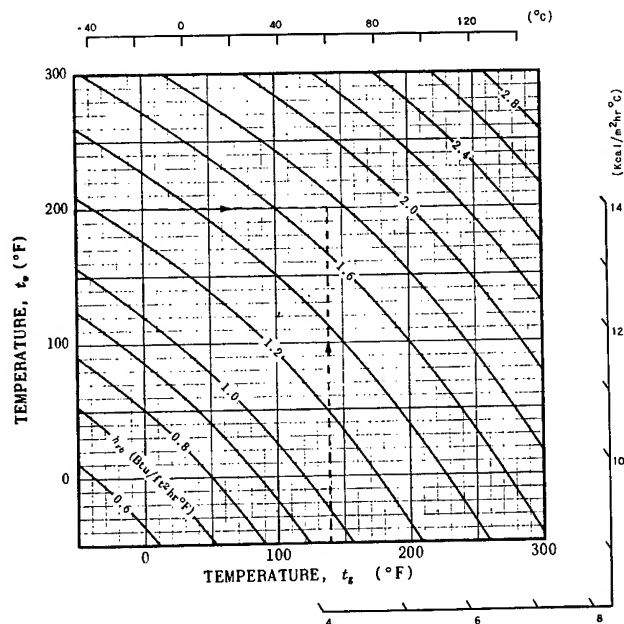


Figure 6-15

Unit Black Body Radiant Conductance

The radiant conduction between black body surfaces of temperature t_w and t_s , is displayed according to the equation:

$$h_{rb} = \sigma(T_w^2 + T_s^2)(T_w + T_s)$$

The average black body temperature of the skin is approximately 92.5°F or 32.5°C.

(After Blockley et al⁽²⁷⁾)

Assuming that source and sink are gray bodies, the following equation which includes the effect of geometric configuration, can be used.

$$F_{ae} = \frac{1}{\frac{1}{F_{12}} + \left(\frac{1}{\epsilon_1} - 1\right) + \frac{A_b}{A_s} \left(\frac{1}{\epsilon_2} - 1\right)} \quad (10)$$

where F_{12} = shape modulus or configuration factor

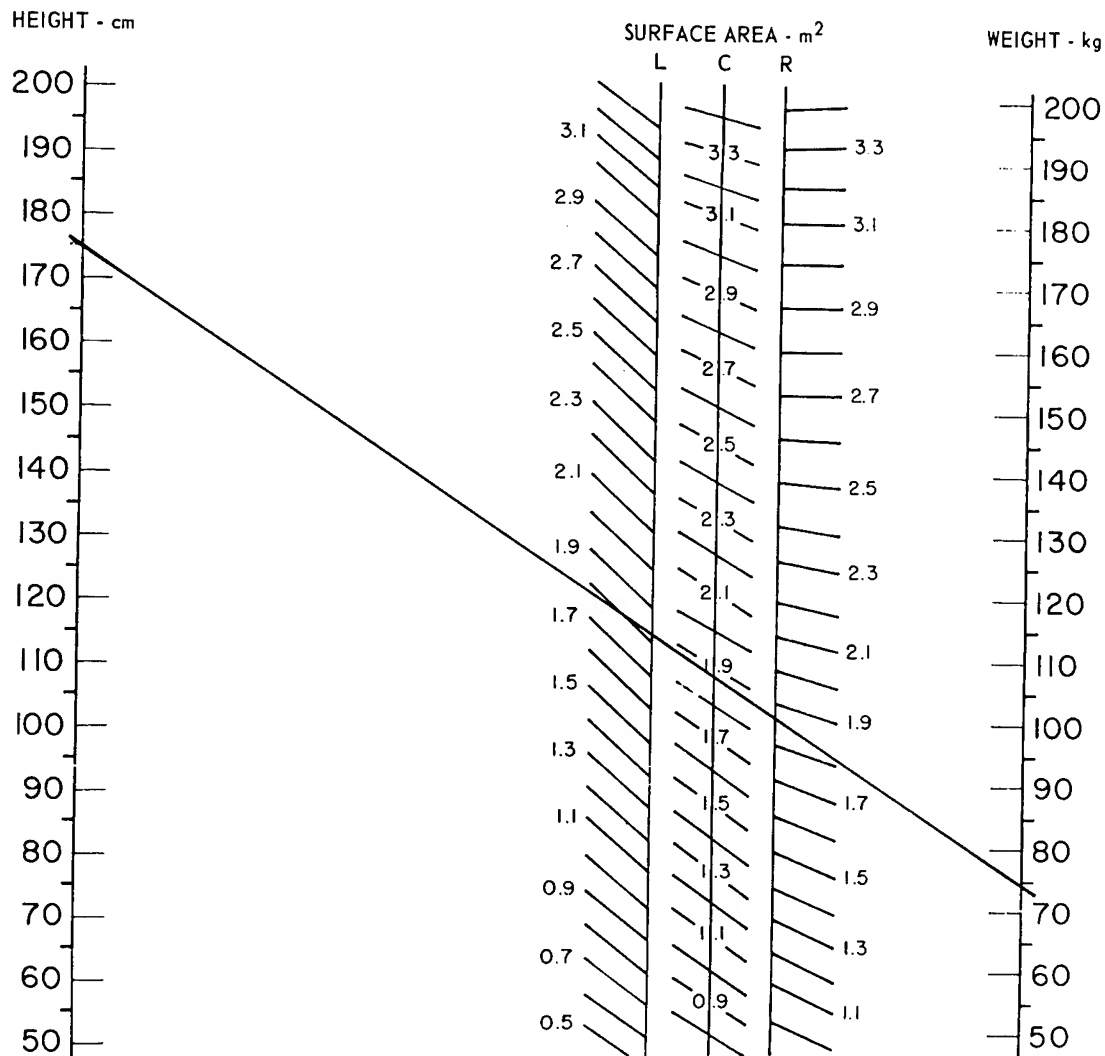
ϵ_1 = emissivity of clothing and skin of astronaut's body

ϵ_2 = emissivity of surroundings (walls, equipment, other astronauts)

A_b = surface area of body - $\text{ft}^2(\text{m}^2)$ (Refer Figure 6-16)

A_s = surface area of surroundings - $\text{ft}^2(\text{m}^2)$

The shape modulus (F_{12}) is 1 for the case of radiation exchange between a completely enclosed body and its enclosure.



Example: To find the surface area of a U.S. Air Force male of mean height and weight (175.5 cm, 74.4 kg), a straight line is drawn between the two appropriate points on the H and W scales. The slope of the line most nearly approximates the slope of the C-scale bar. The surface area of such an individual is approximately 1.9 m^2 .

Figure 6-16

A Nomograph for the Determination of Human Body Surface from Height and Weight,
Based on Data from 252 Subjects.

(Adapted from Sendroy and Collison⁽¹⁸⁰⁾ by Webb⁽²¹²⁾)

The emissivity of human skin in the infrared range is approximately 0.99. The emissivity of clothing and skin (ϵ_1) at body temperature if not known is assumed to be the generally used value, 0.95.

The emissivity of surroundings (ϵ_2) will depend on the proportion of high and low emission surfaces subtended by the body. The range of emissivities will vary from 0.2 (for oxidized aluminum) through 0.9 (for transparent plastics and oil painted surfaces) to 0.95 for an adjacent crew member - also in shirt sleeves.

The radiation area factor (f_r) is required to account for radiation exchange between portions of body.

$$f_r = \frac{A_r}{A_b} \quad (= 0.75 \text{ for sitting man in an average-sized cockpit}) \quad (11)$$

where A_r = equivalent radiating area of the human body
(Figures 6-17 and 6-18)

A_b = total surface area of the body (Figure 6-16)

Then: $q_r = F_{ae} f_r \sigma (T_w^4 - T_s^4)$ (12)

In terms of unit thermal conductances:

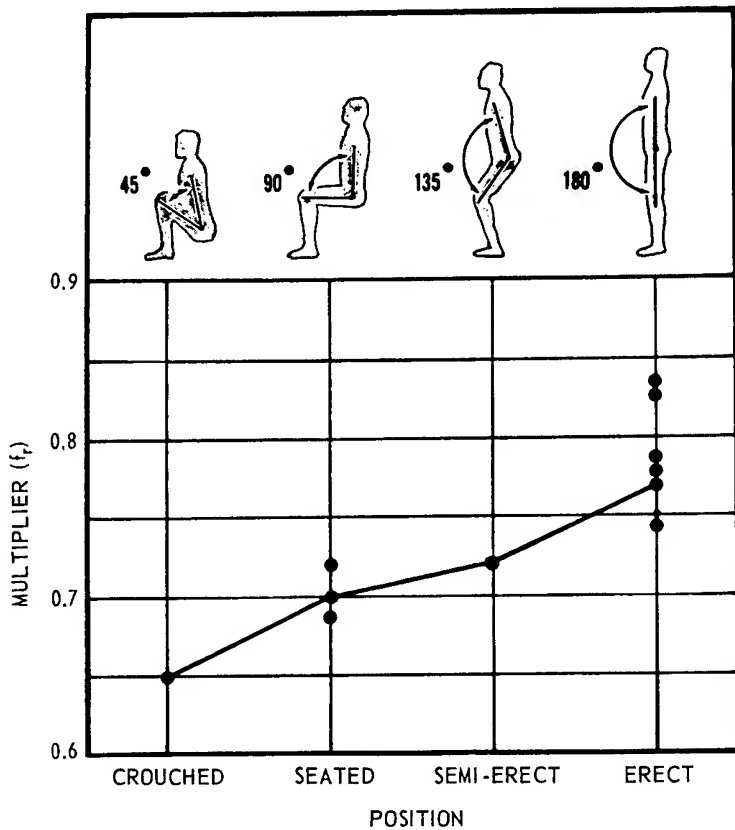
$$q_r = h_r (t_w - t_s) \quad \text{BTU/ft}^2 \text{ hr (kcal/m}^2 \text{ hr)} \quad (13)$$

and $h_r = \frac{\sigma F_{ae} f_r (T_w^4 - T_s^4)}{t_w - t_s} \quad \text{BTU/ft}^2 \text{ hr } ^\circ\text{F (kcal/m}^2 \text{ hr } ^\circ\text{C)}$ (14)

In addition to determining the mean radiant temperature of the surroundings, it is important to locate the external sources and sinks of radiation exchange. A man located between warm and cold surfaces at a neutral atmospheric temperature and apparently comfortable may experience pain and stiffness in the muscles exposed to the cold surface after a prolonged period of time, especially after sleep.

Absorption of radiant energy by the gaseous atmosphere need not be considered in the heat exchange analysis for the following reasons:

1. Gases with symmetrical molecules (e.g., oxygen, nitrogen) do not show absorption or emission bands in the infrared region at the temperatures of interest.



Since the total radiation area of the body varies with position, the diagram shows what multiplier (f_r) to use with total body surface area for each of four common positions. For the nude body the following steps are involved:

- (1) Find the total surface area (S. A.) by:

$$S. A. (\text{in ft}^2) = 0.108 W^{0.425} \times H^{0.725}$$

where W is weight in pounds and H is height in inches; or

$$S. A. (\text{in m}^2) = 0.007184 W^{0.425} \times H^{0.725}$$

where W is weight in kg and H is height in cm

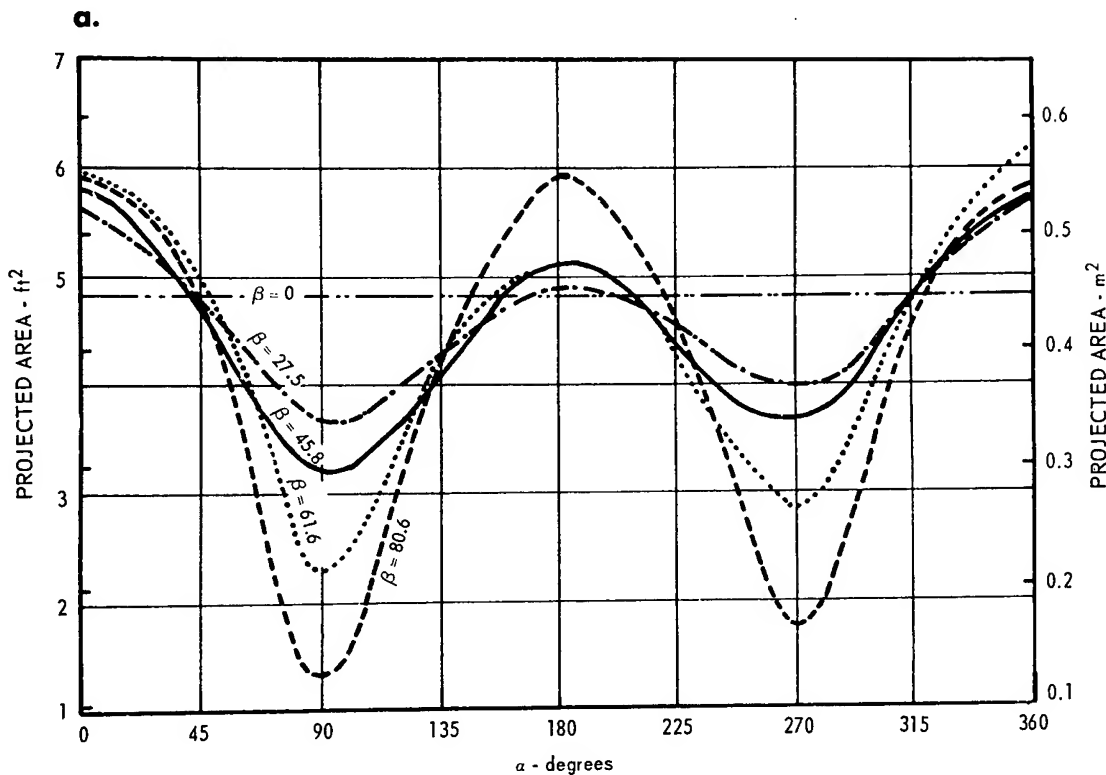
(or use the nomogram, Figure 6-16)

- (2) Then, to find the total radiation area (A_r) for a given position,

$$A_r = S. A. \times f_r.$$

A_r is increased by clothing, but each assembly will add its own increment. A standard set of light street clothing increases A_r by 1.14.

Figure 6-17
Total Radiation Area
(Adapted from Guibert and Taylor⁽⁹²⁾)



Projected areas of the body varying with the angle of view, as shown in the figure at the right. Note that the projected areas apply only to the one position of the body shown. The subject shown is medium-sized (67.8", 159 lb), and lightly clothed in loose-fitting shirt, trousers, socks and low shoes.

Examples of projected surface areas read from the chart:

Given $\alpha = 202.5^\circ$ and $\beta = 45.8^\circ$, the projected surface area is 5.00 ft^2 ;

Given $\alpha = 90^\circ$ and $\beta = 80.6^\circ$, the projected surface area is 1.33 ft^2 .

Similar data are presented (Figure 6-17) for a nude figure in the erect, semi-erect, seated and crouched positions.

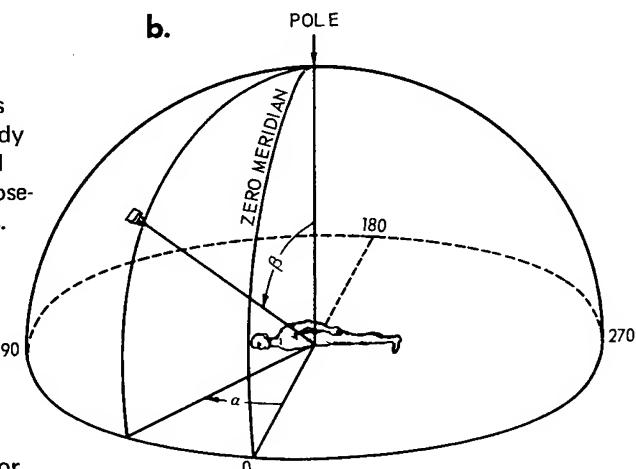


Figure 6-18

Projected Surface Areas

(Adapted from Guibert and Taylor⁽⁹²⁾)

2. The heteropolar gases (such as sulfur dioxide, carbon monoxide, carbon dioxide and water vapor) while having absorption bands in the area of interest will not normally exist in sufficient concentrations in the cabin atmosphere to affect the radiation exchange.

Solar radiation (q_{sr}) and all other external heat fluxes, and all internal heat fluxes from internal equipment and other astronauts are considered to be completely described by wall temperature (t_w).

By assuming a small crewman of 15.6 sq ft body surface area with a uniform clothing surface temperature and an enclosure of greater than 100 sq ft per man, i.e., f_{gs} = area factor of garment = ϵ_g , a simplified radiation cooling equation can be written:

$$q_r = 2.65 \times 10^{-8} \epsilon_g (T_g^4 - T_w^4) \quad (15)$$

A sample graph, assuming $\epsilon_g = 0.9$ is seen in Figure 6-19 where the radiation heat loss to any given environmental temperature is given for several clothing surface temperatures (155). Figure 6-20a represents the radiation heat transfer coefficients (h_r) for different combinations of environmental and clothing temperature desired from the simplified form of equation (15). Figure 6-20b gives h_r for a more severe radiative environment which may be encountered in emergency conditions.

Forced Convective Heat Transfer

The correlation between convective heat transfer processes and mass transfer processes has been used by many investigators to develop analytic models for forced convection heat exchange in man. In the recent analysis of Berenson (19), the following assumptions were made:

1. All sensible heat passes through the clothing by conduction and the clothing heat transfer area is equal to the skin surface area. Since sensible heat loss occurs from non-clothed skin and since the clothing surface may be up to 40% greater than skin surface, these assumptions are conservative. It must be remembered, however, that even though the area increases, the air pockets which are formed act as thermal and mass transfer resistances. Zero gravity will tend to increase resistance by eliminating convection currents in the pockets.
2. The relationship between garment surface temperature (t_g) and skin temperature (t_s) can be determined by the equation:

$$t_g = t_s - \frac{L}{k} \left(\frac{q_c + q_r}{A} \right) \quad (16)$$

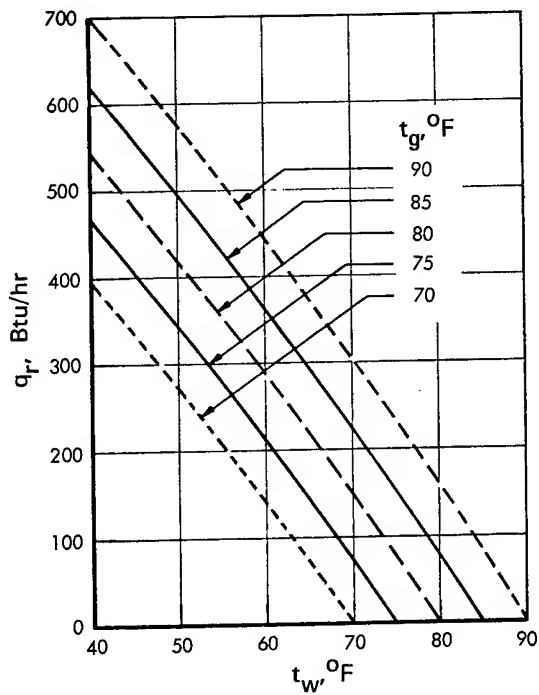


Figure 6-19

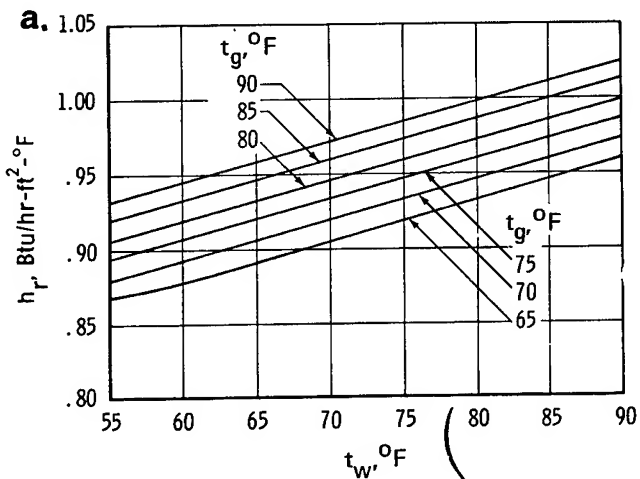
Radiative Heat Loss from Man to His Surroundings

(After Parker et al⁽¹⁵⁵⁾)

Figure 6-20

Radiative Heat Transfer Coefficients

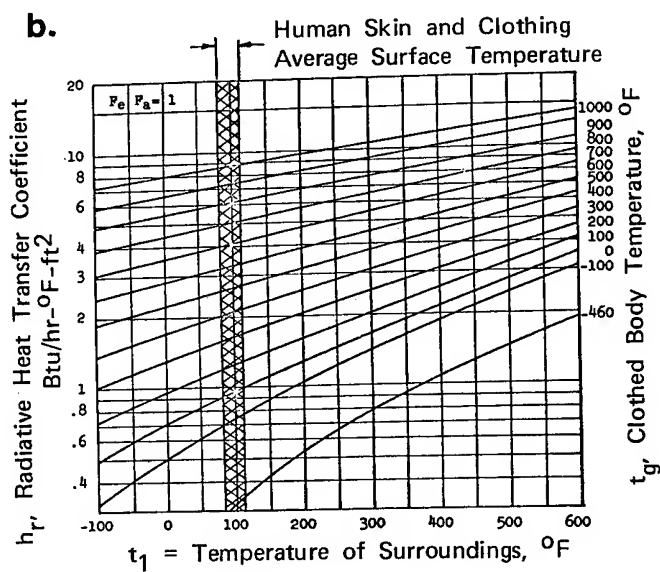
Figure a. represents a narrow band of temperatures in Figure b.



Notes:

1. $h_r' = \epsilon \sigma \left(\frac{T_g^4 - T_w^4}{T_g - T_w} \right)$
2. $\epsilon = 0.9$
3. T_g = Clothing Temperature
4. T_w = Environment Temperature

(After Parker et al⁽¹⁵⁵⁾)



(After Breeze⁽³⁶⁾)

The value of L/k is the useful function of clothing heat transfer resistance, Clo, where $1 \text{ Clo} = .88^\circ\text{F} - \text{ft}^2 - \text{hr}/\text{BTU}$. (See Tables 6-46 and 6-64).

The rate of heat transfer by convection can be written:

$$q_c = h_c A (t_g - t_a) \quad (17)$$

The convective-heat-transfer coefficient is actually a complicated function of fluid flow, thermal properties of the fluid, and the geometry of the body. The value of h_c for convective exchange about the whole human body is a critical coefficient quite sensitive to second-order conditions such as fluid-flow patterns, posture, etc. Unfortunately, there has been some variance between the values used by several different groups in relating the h_c of man to the atmospheric gas velocity. Selection of the appropriate film coefficient or actual heat transfer coefficient is a difficult problem (122). A discussion of the implication of different coefficients used in analysis of forced convection about the human body has been recently published (115).

The early data suggest that for clothed humans sitting in a turbulent air flow the following equation may be used (232):

$$h_c = .153 \bar{V}^{0.5} \left(\frac{\rho}{\rho \text{STD}} \right)^{0.5} \quad (18)$$

This equation is not too different from that derived for rough flat plates (154).

$$h_c = 1.03 k \left(\frac{\rho \bar{V}}{\mu} \right)^{0.5} \quad (18a)$$

Figure 6-21 represents a summary of several approaches to forced convective heat transfer coefficients (convective film coefficients) for man in an environment containing air at 1/2 atmosphere. The first three curves represent the h_c values obtained from data on empirical studies of humans (94, 149, 224). These are compared with four theoretical curves: (1) a cylinder in longitudinal flow, (2) a cylinder ten inches in diameter in cross-flow, (3) a flat plate with flow perpendicular to it, (4) a cylindrical model of man in cross-flow (Figure 6-22). The value of h_c for the cylindrical model of man corresponds closely with those obtained by Nelson (149) and are equivalent to h_c for cross-flow about cylinders five inches in diameter. The specific equation used for the flat plate model in this graph was not stated but appears to differ from the flat plate equation noted above (154) which gives results closer to those of the equation of Winslow et al (224).

For the human body in a semi-reclining position and one atmosphere pressure, loss by convection is proportional to the square root of air velocity for velocities up to 250 cm/sec (493 ft/min).

Figures 6-23 and 6-24 can be used to determine from mass flow rates the unit convective conductance for air (27). Dimensional analysis indicates that pure oxygen at the same absolute pressure as air provides about 0.9 the convective cooling.

Figure 6-25 shows the effect of gas velocity on the convective heat transfer coefficient based on the cylindrical model of man for various helium-oxygen and nitrogen-oxygen atmospheres. The partial pressure of oxygen at 170 mm Hg is near the sea level equivalent and is held constant with the diluent gas ranging from 0 to 400 mm Hg. These curves were generated by taking the heat transfer coefficient as proportional to the various fluid properties as follows:

$$h_c \sim k (Pr)^{0.33} (Re)^{0.5} \sim k (Pr)^{0.33} \left(\frac{\rho \bar{V}}{\mu} \right)^{0.5} \quad (19)$$

The values for neon mixtures will lie between those for helium and nitrogen. It is clear from comparing physical properties of the gases that for different mixtures of oxygen-nitrogen there is little sensitivity of h_c to percent composition of gas (Table 6-13).

The following equation, derived from the heat mass-transfer analog (70) for Prandtl numbers of 0.6 to 15 and Reynolds numbers of 10 to 10^5 , approximates the forced convection cooling rate for all gas mixtures (18, 21).

$$q_c = 0.407 k_c \sqrt{P\bar{V}} (t_g - t_a) \quad (20)$$

where P = psia, \bar{V} = ft/min, and t_g , t_a = °F and

k_c = a factor that depends on the transport properties of the gas mixture. For dry air, $k_c = 1$. For O₂ - N₂ mixtures $k_c = 1$; for other gases,

$$k_c = \frac{k_{mix}}{k_{air}} \left(\frac{M_{mix}}{M_{air}} \times \frac{\mu_{air}}{\mu_{mix}} \right)^{0.5} \left(\frac{Pr_{mix}}{Pr_{air}} \right)^{0.33} \quad (21)$$

For the 70-percent oxygen atmosphere in helium at 5 psia,

$$k_c = \frac{7.37}{4.14} \left(\frac{23.6}{29.0} \times \frac{12.10}{13.49} \right)^{0.5} \left(\frac{0.503}{0.710} \right)^{0.33} = 1.356$$

For the 50-percent oxygen atmosphere in helium at 7 psia,

$$k_c = \frac{10.38}{4.14} \left(\frac{18}{29} \times \frac{12.10}{13.47} \right)^{0.5} \left(\frac{0.437}{0.170} \right)^{0.33} = 1.594$$

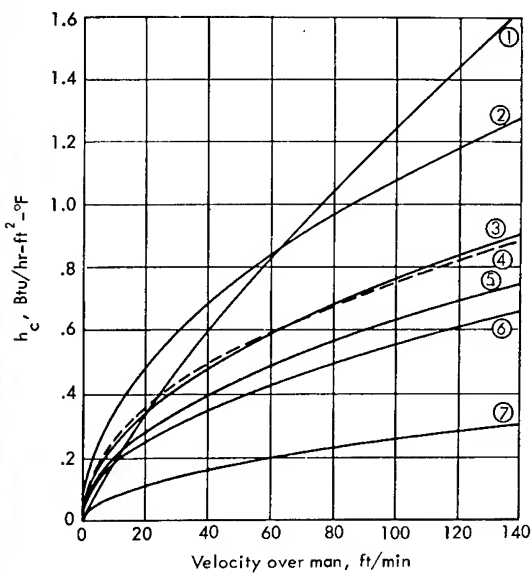
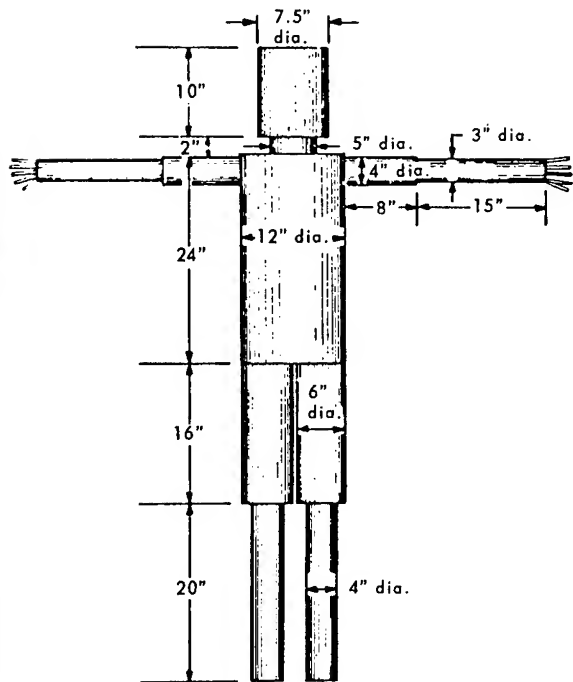


Figure 6-21

Comparison of Forced Convection Film Coefficients
for Standing Man at 1/2 Atmosphere of Air.

- (1) Hall (94)
 - (2) Winslow, Gagge and Herrington (224)
 - (3) Nelson et al (149)
 - (4) Cylindrical Model of Man in Cross-Flow
(Analytical)
 - (5) Flat Plate (Hamilton Standard Curve)
 - (6) 10" Dia. Cylinder in Cross-Flow
 - (7) Longitudinal Flow
- (After Parker et al (155))



Part	Area, ft ² (^a)
Head	1.95
Neck	.22
Trunk	6.18
Upper legs	4.19
Lower legs	3.49
Upper arms	1.40
Lower arms	1.96
Fingers	^b , .67
Total	20.06

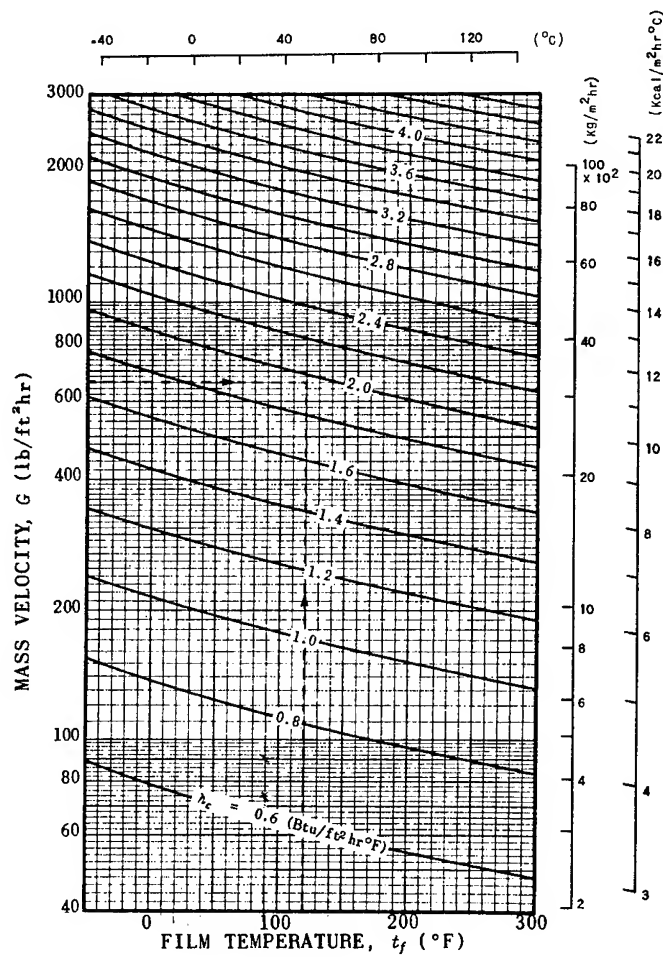
^a 19.5 ft² used to include some factor of safety.

^b Each finger: 3½ inch long by ¼ inch diameter.

Figure 6-22

Cylindrical Model of Man

(After Parker et al (155))



The convective conductance is given in terms of mass velocity and average film temperature according to the equation:

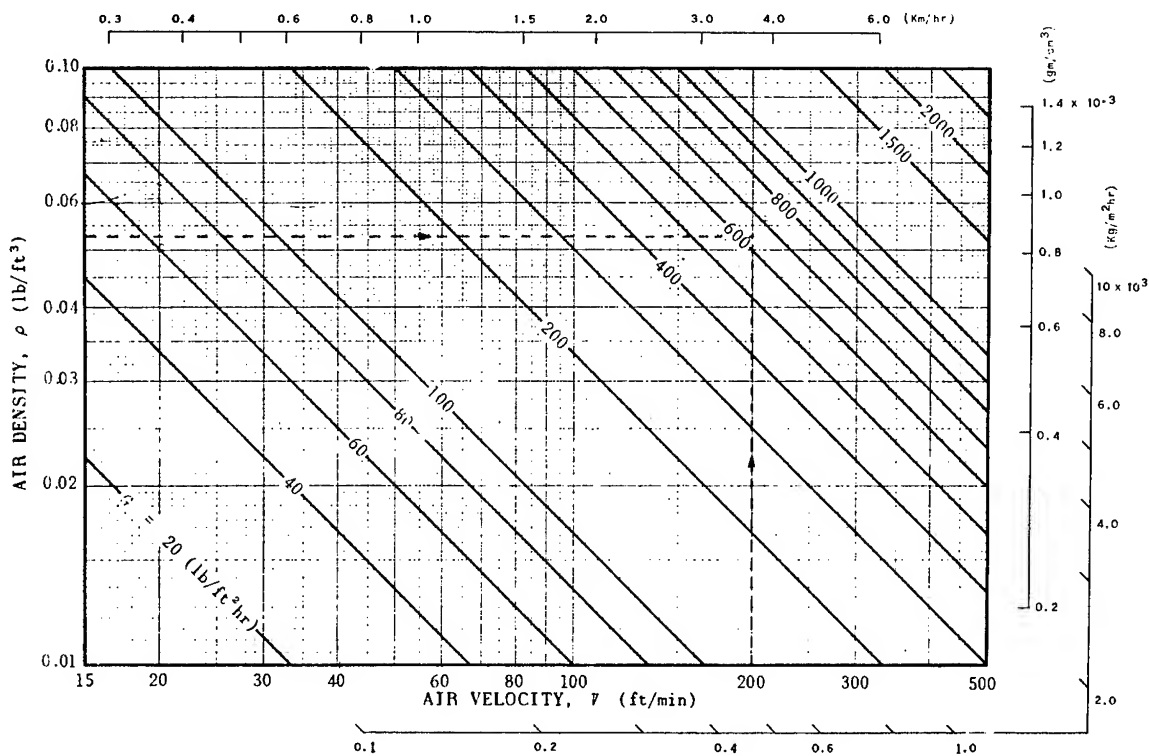
$$h_c = 0.0735 \left(\frac{T_f}{T_o} \right)^{0.5} G^{0.5}$$

where: $T_o = 536^{\circ}\text{R}$ and $T_f = \frac{T_g + T_a}{2}$

Figure 6-23

Unit Convective Conductance in Air

(After Blockley et al⁽²⁷⁾)



The mass velocity is shown as a function of air density and air velocity according to the equation: $G = 607 \rho v$.

Figure 6-24
Mass Velocity

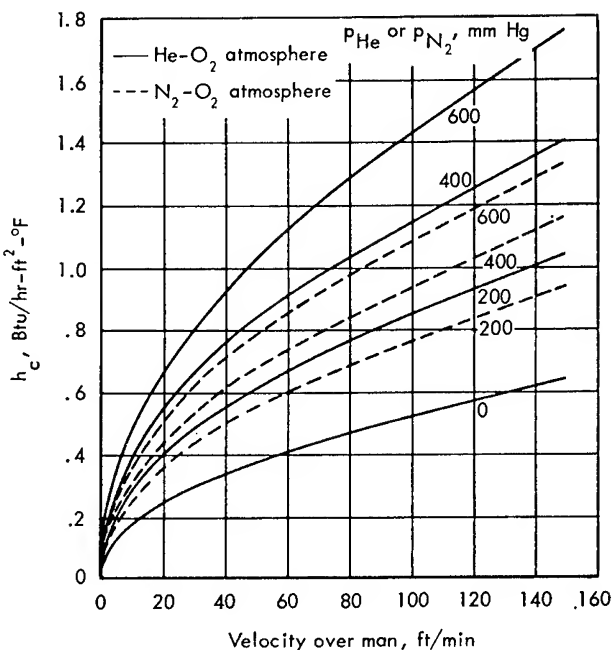
(After Blockley et al⁽²⁷⁾)

Figure 6-25

Heat Transfer Coefficients of Man Standing in O_2 -He and O_2 - N_2 at Different Gas Velocities

- (1) 170 mm Hg of O_2
- (2) p_{He} = Partial Pressure (mm Hg) of He in Atmosphere.
- (3) p_{N_2} = Partial Pressure (mm Hg) of N_2 in Atmosphere.
- (4) Based on Cylindrical Model of Man

(After Parker et al⁽¹⁵⁵⁾)



Free Convective Heat Transfer

In the presence of a gravitational field such as on the Earth, planetary surfaces or rotating space stations, free convection is possible and is the preferred mode of cooling because no additional energy need be expended. One can combine the general free-convection equations with the assumptions regarding clothing effects to yield an equation for free-convective cooling of all nitrogen-oxygen mixtures (19, 20).

$$q_c = 1.17 \left[P^2 g (t_g - t_a) \right]^{0.25} (t_g - t_a)^{1.25} \quad (22)$$

where P = psia, t_g , t_a = °F

The handling of mixed free and forced convection environments can be simplified by the McAdams rule, i.e., both the free and forced convective heat transfer coefficients are calculated and the higher of the two values is used (132). The critical crossover point of the forced convection velocity (V_{crit}) where the forced convection heat transfer coefficient is equal to the free convection coefficient can be calculated for oxygen-nitrogen mixtures by equating equations 20 and 22 and solving for \bar{V} .

Evaporative Heat Transfer (q_e)

The evaporative heat exchange mode (q_e) is limited in this section to sensible and insensible perspiration from the surface of the body. Water loss via respiration is covered under Respiratory Heat Loss.

Low mixing efficiency of ventilating gas and forced convection (i.e., lack of free convection in the weightless state) requires consideration of perspiration rates, sweating thresholds and the order of recruitment of various regions of the body. Stagnant pockets or low ventilation rates in areas of the crew compartment and/or space suits may reduce the effectiveness of evaporative cooling by a significant amount. Because the sweat rate is regulated by the cooling needs of the body, failure to provide sufficient evaporative cooling after initial recruitment of certain regional areas will necessitate recruitment of additional areas in order to bring the bio-thermal system into equilibrium. Mixing efficiencies not greater than 60% have been realized in gas-cooled space suit assemblies.

Insensible water loss is a continuing non-adaptive process and results in loss of body heat under virtually all environmental conditions of interest in space flight. The irreducible insensible water loss from skin and lungs is 0.6 g/kg (body weight)/hr. The lower limit for insensible water loss from the skin alone at one atmosphere and low temperature, $t_a = 68^\circ F$ ($20^\circ C$), is approximately 10 gms/m²hr. At air temperatures above $68^\circ F$ the rate of insensible water loss increases linearly to a value of about 25 gms/m²hr at $t_a = 78.8^\circ F$ ($26^\circ C$). Below the sweating threshold about 40% of the moisture loss is from the palm, sole of the foot, and head (about 13% of the total body

surface). At an operative temperature of 87.8°F (31°C) with air temperatures between 79-93°F (26-34°C), there is a curvilinear increase in water loss as regional areas of the body begin to sweat. The progression of recruitment is generally from the extremities toward the central regions of the body and headward and is subject to effects of training. In this temperature range at rest the onset of sweating for all regions of the body appears at rates of 40-60 gm/m²hr. Above an air temperature of 93°F (34°C) the increment in sweat rate is again linear-increasing at the rate of 18-24 gm/m²hr °C in well trained subjects at rest. With full sweating the trunk and lower limbs provide 70-80% of the total moisture perspired (104).

Tables 6-26, 6-27, and 6-28 summarize the order of recruitment, mean regional evaporative rates, and regional fractions of total evaporation respectively in a still air environment with subject at rest.

Figure 6-29 is a diagrammatic summation of insensible and sensible water loss from regional areas of the body at rest in air at sea level with cooling requirements (16, 116, 154).

The maximum attainable perspiration rate of the human body is in the area of 1.8 liters/hr at rest and 3.9 liters per hour during exercise which could provide an evaporative cooling rate of 572 kcal/m²/hr to 1530 kcal/m²/hr respectively. At these rates, however, even with adequate consumption of water and electrolytes, the sweating mechanism "fatigues" in 6-8 hours and perspiration rates decrease significantly. This fatigue is a function of skin wetness. The maximum effective perspiration rate which can be sustained is extremely variable depending on the individual and his degree of acclimatization.

Evaporative heat loss is a function of volume flow rate, absolute humidity, temperature, and pressure of the atmosphere.

The expression for evaporative heat loss is:

$$q_e = W_e \lambda_e \text{ BTU/ft}^2 \text{ hr kcal/m}^2 \text{ hr} \quad (23)$$

where W_e = weight of water evaporated (gms/lb)

λ_e = latent heat of vaporization - 1800 BTU/lb
(.582 kcal/gm)

under standard conditions. The weight of water evaporated (W_e) is a function of vapor diffusivity, the vapor concentration difference between the body (skin) surface and the atmosphere, and the thickness of the boundary layer

$$W_e = \frac{D_v \Delta C}{R_t} \quad (24)$$

Table 6-26
Recruitment of Sweating
(After Randall and Hertzman⁽¹⁶⁴⁾)

AREA	USUAL (BUT NOT INVARIABLE) ORDER OF RECRUITMENT
Dorsum foot.....	1
Lateral calf.....	2
Medial calf.....	3
Lateral thigh.....	4
Medial thigh.....	5
Abdomen.....	6
Dorsum hand.....	7 or 8
Chest.....	8 or 7
Ulnar forearm.....	9
Radial forearm.....	10
Medial arm.....	11
Lateral arm.....	12

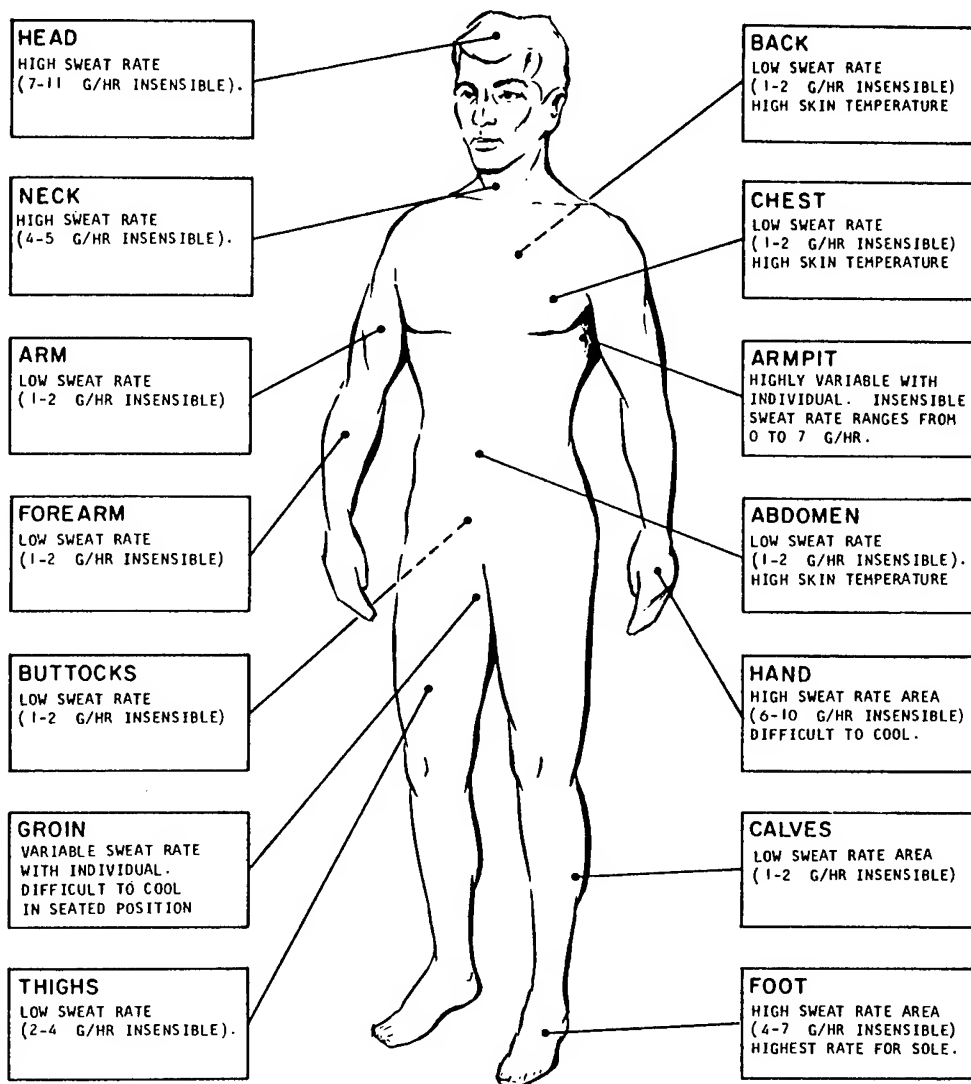
Table 6-27
Increments in Mean Regional Evaporative Rates with Rise in Environmental Temperature

REGION	EVAPORATIVE RATE			INCREMENT IN EVAPORATIVE RATE	
	<i>T A</i> 29°C.	34°C.	38°C.	29-34°C.	34-38°C.
		<i>gm/m²/hr.</i>			<i>gm/m²/hr./°C.</i>
Calf	18.0	86.5	169.0	13.7	20.4
Thigh	14.4	58.7	144.0	8.0	21.3
Abdomen	12.0	60.0	156.0	9.6	24.0
Chest	9.6	37.2	120.0	5.5	20.7
Forearm	12.0	21.6	96.0	1.9	18.6
Arm	10.8	14.4	65.0	0.7	13.0
Cheek	24.0	36.0	108.0	2.4	18.0
Forehead	24.0	60.0	240.0	7.2	45.0

Table 6-28
Regional Fractions of Total Cutaneous Evaporation Expressed as Percentage of Total

REGION	AIR TEMPERATURE							
	24°C.	26°C.	28°C.	30°C.	32°C.	34°C.	36°C.	37°C.
Head	11.8	12.1	11.9	9.7	8.0	7.0	8.5	8.4
Arm	4.6	4.4	4.2	3.4	2.6	2.2	3.1	3.3
Forearm	8.2	7.2	6.0	4.3	3.2	3.1	4.4	4.3
Trunk	22.8	23.0	22.2	22.2	30.0	33.0	43.0	38.2
Thigh	13.6	13.1	17.1	20.2	22.6	23.8	25.5	22.3
Calf	8.5	9.0	11.9	16.0	20.3	22.8	24.1	19.8
Palm	15.6	15.3	13.1	9.6	6.8	4.6	3.5	2.5
Sole	14.7	15.1	13.5	9.9	6.4	3.7	2.3	1.5

(Tables 6-27 and 6-28 After Hertzman et al⁽¹⁰⁴⁾)



Region	Preferred temperature (°F)	Heat loss Btu/hr	Area Ft ²	Skin conductance Btu/Ft ² /hr/°F
Head	94.4	15.9	2.15	1.61
Chest	94.4	32.6	1.83	3.87
Abdomen	94.4	17.9	1.29	3.02
Back	94.4	49.3	2.48	4.31
Buttocks	94.4	35.0	1.94	3.70
Thighs	91.4	47.7	3.55	1.76
Calves	87.5	58.0	2.15	2.35
Feet	83.5	39.7	1.29	1.98
Arms	91.4	33.4	1.07	4.10
Forearms	87.5	34.2	0.86	3.45
Hands	83.5	63.5	0.75	5.45

Figure 6-29

Regional Cooling Requirements of the Human Body in Air at Sea Level at Rest

(After Berenson⁽²¹⁾ from the Data of Kerslake⁽¹¹⁶⁾)

where D_v = vapor diffusivity - ft^2/hr (cm^2/sec)

ΔC = concentration difference - lb/ft^3 (gm/cm^3)

R_t' = thickness of still air layer ft (cm)

The nature of clothing will determine the R_t' factor. This is covered in greater detail in the section on space suits and clothing (see Equation 37 and Tables 6-44 and 6-45).

For air and water vapor under standard conditions (refer to Figure 6-30),

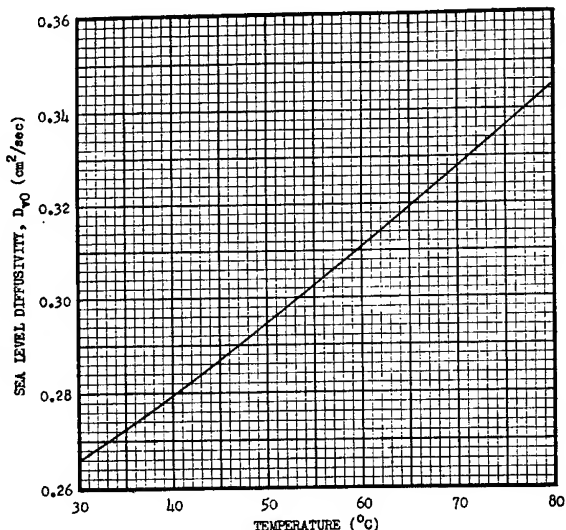


Figure 6-30

Diffusivity of Water Vapor in Air for Standard Sea Level Pressure.

(After Blockley et al⁽²⁷⁾)

$$\text{diffusivity, } D_v = 0.85 \left(\frac{T}{T_0} \right)^{1.75} \frac{P_o}{P} \text{ ft}^2/\text{hr.} \quad (25)$$

$$D_v = 0.220 \left(\frac{T}{T_0} \right)^{1.75} \frac{P_o}{P} \text{ cm}^2/\text{sec} \quad (26)$$

where 0.85 = diffusivity of air and water vapor at standard conditions ft^2/hr (cm^2/sec)

T_0, T = temperature in $^{\circ}\text{R}$ for standard and ambient conditions respectively = 536°R (273°K)

P_o, P = pressure in lbs/ft^2 for standard and ambient conditions respectively.

The diffusivity of oxygen and water vapor under standard conditions is:

$$D_v = 0.81 \left(\frac{T}{T_0} \right)^{1.75} \frac{P_o}{P} \text{ ft}^2/\text{hr} \quad (27)$$

where the terms have the same definitions as covered above.

The concentration difference is related to the amount of water vapor contained in the atmosphere and at the boundary of the skin (153). It is expressed: (Refer to Figures 6-31 and 6-32).

$$\Delta C = 0.825 \left(\frac{P_1}{T_1} - \frac{P_2}{T_2} \right) \text{lb/ft}^3 \quad (28)$$

$$\Delta C = 2.89 \times 10^{-4} \left(\frac{P_1}{T_1} - \frac{P_2}{T_2} \right) \text{gm/cc} \quad (29)$$

where P_1, P_2 = represent partial pressures of water at the two boundaries respectively in Hg (mm Hg)
 T_1, T_2 = temperatures at the two boundaries $^{\circ}\text{R}$ ($^{\circ}\text{K}$).

To determine the diffusivity of other air atmospheres the following expression can be used:

$$D_{v1} = D_{v2} \frac{\rho_2}{\rho_1} \quad (30)$$

where D_{v1}, D_{v2} = diffusivity of the respective atmospheres
 ft^2/hr (cm^2/sec)
 ρ_1, ρ_2 = density of the respective atmospheres
 lb/ft^3 (kg/m^3)

The concentration difference (ΔC) is:

$$\Delta C = C_1 - C_2$$

where $C = \frac{1}{V}$ and V = specific volume ft^3/lb (cc/gm)

$$C = \frac{T_o}{P_o V_o} \cdot \frac{P}{T} \quad (31)$$

where T_o, T = are temperature in $^{\circ}\text{R}$ ($^{\circ}\text{K}$) at standard and ambient conditions respectively
 P_o, P = are pressure in Hg (mm Hg) at standard and ambient conditions respectively
 V_o = volume in ft^3/lb (cc/gm) at standard conditions

The necessity for specifying (and controlling) absolute humidity rather than relative humidity for biothermal control is carefully spelled out (85, 215).

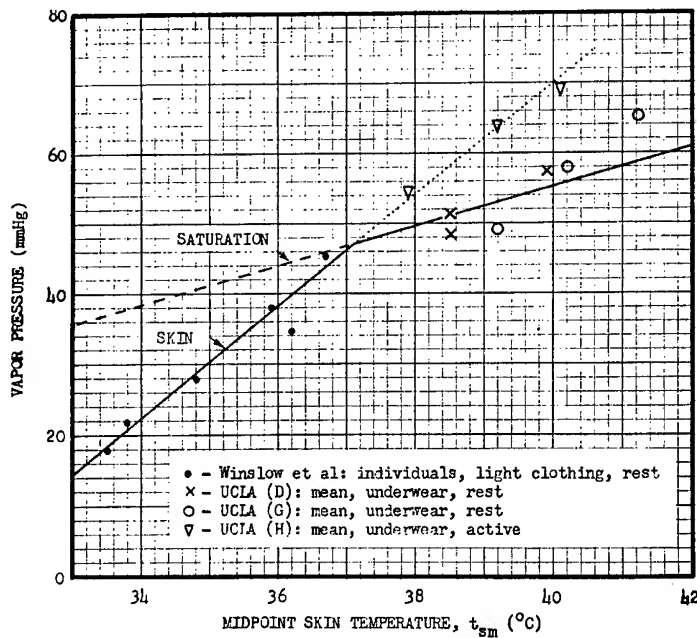


Figure 6-31

Skin Vapor Pressure Prediction Chart for Reference Conditions ($P_a = 20 \text{ mmHg}$).

The solid line is recommended for general prediction purposes. Note that this line follows the saturation curve beyond 37°C , ignoring the possible beneficial effects of wicking associated with activity. The dotted line of relationship is probably valid only in special lightly-clothed conditions where evaporation takes place at the surface of wet clothing.

(After Blockley et al⁽²⁷⁾)

Figure 6-32

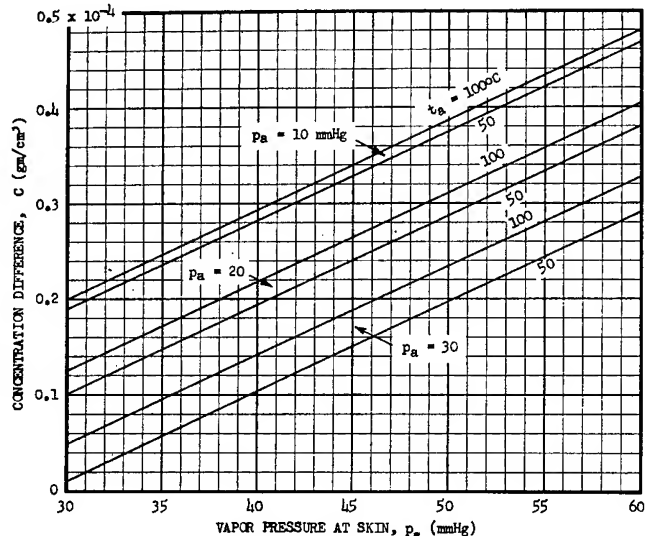
Vapor Concentration Difference for Various Ambient Temperatures and Humidities.

The basic equation is:

$$\Delta C = 2.89 \times 10^{-4} \left(\frac{P_s - P_a}{t_s - t_a} \right);$$

A constant value of 37.5°C has been assumed for t_s in this chart making it applicable only for heat stress situations.

(After Blockley et al⁽²⁷⁾)



The absolute humidity is dependent on the molecular constitution of the gas and this factor must be accounted for in evaporative heat exchange (174). A recent review of water vapor control in space conditions is available (159).

When thermoregulation is completely successful, humidity, as a parameter in evaporative thermal control, is a significant determinant in the fractional area of the skin over which sweating occurs. The wettedness area (ω) varies from 0.1 for comfort conditions (essentially insensible water loss only) to 1.0 for full sweating. Table 6-33 represents the expected comfort level relative to the percent of maximum capacity being used. This concept is quite simplified and may not hold for all values of total sweat output work and atmospheric conditions (27, 115, 183, 215).

It is likely that the body does not become fully wetted with sweat until the sweat rate is about twice the maximum evaporative capacity. Loss of sweat by dripping probably begins when the sweat rate is about 1/3 of the maximum evaporative capacity (115). These figures refer to linear winds only. In turbulent air movements, dripping would be expected to start at relatively higher sweat rates and full wetness be reached at relatively lower ones. It can be assumed that a skin temperature of 36°C marks the onset of the wet skin condition where the zone of evaporative cooling terminates.

Table 6-33

<u>Percent of Maximum Evaporative Capacity</u>	<u>Comfort Level</u>
0 - 10	Cold
10 - 25	Comfortable
25 - 70	Tolerable
70 - 100	Hot
Over 100	Dangerous

The first 10% or so of maximum capability represents basal insensible loss from respiration and diffusion. These losses are, of course, a function of the metabolic output and respiratory rate (vide infra).

The water loss from the nude skin under different atmospheric conditions can be expressed (196):

$$E_r = K_e W (P_s^* - P_a) \quad (32)$$

where E_r = evaporative water loss ($\text{gm}/\text{m}^2\text{hr}$)

K_e = vapor conductance from skin to air ($\text{gm}/\text{m}^2\text{hr mm Hg}$)

P_s^* = saturated water vapor pressure at t_s (mm Hg)

P_a = absolute humidity or water vapor pressure (mm Hg)

W = wetted fraction of skin surface

The value of vapor conductance of body skin in air for the erect man is a function of the convective air movement and pressure by the equation (57, 149, 196, 224):

$$K_e = C \bar{V}^n (P_o/P)^n \quad (32a)$$

where C and n are empirical constants of 0.45 and 0.63 respectively

\bar{V} = air velocity in km/hr

P, P_0 = barometric pressure at altitude and standard sea level (mm Hg)

The perturbing effect of body position and geometry on the constants of these equations cannot be overemphasized. The effect of clothing is also an important factor in determining evaporation rates (27). The vapor conductance from skin to air (R_e) must be modified to include vapor resistance of clothing. This factor is covered in the Section on space suits and clothing. (See Equation 24, 37 and Tables 6-45a and 6-45b.)

Respiratory Heat Loss

Heat loss via respiration varies directly with metabolic rate and is influenced by atmospheric composition (including carbon dioxide and water vapor content) and pressure. Because the respiratory tract is a very efficient saturator of inspired air, heat gain to the body via respiration will not occur until atmospheric temperature approximates 185°F (85°C) (136).

Heat loss via respiration, and insensible water loss from the skin, has been grossly estimated to be equivalent to 25% of the metabolic rate (123). Heat loss from the lungs approximates 10% of the metabolic rate (7-8 kcal/hr) in the neutral zone (97). Definitive data for determining respiratory heat loss for the atmospheric compositions and pressures of interest in space flight environments, especially those of the space suit, are available (39, 136, 214, 215, 232). (See also Figure 6-69.)

After determining the pulmonary ventilation rates corresponding to a specific activity level and stress factors such as hypoxia, hypercapnia, anxiety, etc., the heat loss via respiration can be calculated by determining the sensible heat required to raise the inspired atmosphere to expiration temperature and adding the heat of vaporization increment for the moisture lost to the inspired air from the respiratory tract.

One expression for calculating Respiratory Heat Loss is (232):

$$q_v = V\rho C_p (t_e - t_i) + 0.58 (W_e - W_i) \text{ (Cal/hr)} \quad (33)$$

where V = volume of atmosphere breathed per hour (liters/hr)

ρ = density of the atmosphere (gms/liter)

C_p = specific heat of atmosphere (kcal/Kg °C)

t_e = temperature-expired atmosphere (°C)

t_i = temperature-inspired atmosphere (°C)

0.58 = heat of vaporization H_2O (kcal/gm)

W_e = weight of water in expired atmosphere (gms)

W_i = weight of water in inspired atmosphere (gms)

A more simplified approach is also available (136).

First-Order Estimate of Evaporative Heat Loss in Space Cabins

For the purpose of determining comfort zones and performing tradeoff analyses of space-cabin atmospheres and thermal control systems, a first-order estimate of evaporative heat loss is often required. Many of the concepts presented in Equations 6-23 to 6-33 can be lumped together as a first approximation of evaporative heat loss. The subject and the cabin must therefore be idealized with such factors as body position and clothing neglected. In view of the very light and loose garment assemblies proposed for shirt sleeve operation (Clo values of 0.25 (163), the total intrinsic vapor resistance will probably be low enough to be neglected for this first-order approximation.

The metabolic rate can be estimated for any given level of activity and the difference between the metabolic and sensible heat loss is the required evaporative cooling rate. A simplified equation for latent or evaporative cooling rates neglecting clothing factors (vide supra) can be derived from the heat-mass transfer analogy of Eckert (70) and Equation 19.

A mass-transfer coefficient (h_D) can be defined as

$$\left(\frac{dm}{dt} \right)_{H_2O} = - DA \left(\frac{\partial p}{\partial x} \right)_s = h_D A(p_s - p_a)_{H_2O} \quad (34a)$$

Evaporative heat loss,

$$q_e = h_D \lambda_e AC' \left(\frac{p_s - p_a}{Rt_s} \right) \quad (34b)$$

where h_D = mass transfer coefficient (ft/hr) and $C' = \frac{E_r}{E_m}$

R = gas constant (ft lbs/lb °R)

x = path length

Since the heat-transfer properties of nitrogen-oxygen mixtures are independent of the fraction of each component, the above equation can be reduced for all oxygen-nitrogen mixtures in a forced convection environment to yield (21).

$$q_e = 2.46 C't_a \left(\frac{\bar{V}}{P} \right)^{0.5} (p_s - p_a) \quad (35)$$

It should be pointed out that this equation assumes the exponent of \bar{V} to be 0.5. It can be seen from Equation (32a) that an exponent of 0.63 would probably be a more realistic value for this exponent (57). In view of the other assumptions made regarding clothing and body position, the error introduced by this simplification does not present too great an error. In fact, the values of evaporative loss under conditions of $C' = 1$ give predicted results

only 10% higher than actually measured (57, 174, 215). Since the rate of evaporation and the diffusion coefficient for water vapor are inversely proportional to pressure, it is clear that the latent cooling will increase with decreased (total) pressure (196). Curves illustrating the general magnitude of the predicted pressure, dewpoint, and gas-stream velocity effects at $t_a = 80^{\circ}\text{F}$ and $t_s = 95^{\circ}\text{F}$ are seen in Figure 6-34. These calculated maximum q_e values may be slightly high (174, 215). In the temperature range under consideration for space cabins, the temperature and the dewpoint have relatively little effect as compared to gas stream velocity and ambient pressure.

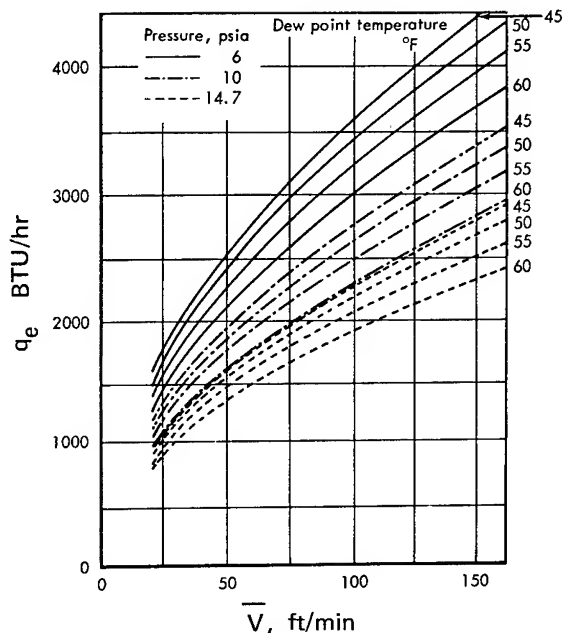


Figure 6-34
Maximum Evaporation Rate at Rest in
Oxygen-Nitrogen Mixtures

$$q_e = 2.46 t_a \sqrt{\bar{V}/P} (p_s - p_a) H_2O$$

$$t_s = 95^{\circ}\text{F}; t_a = 80^{\circ}\text{F}.$$

(After Berenson⁽¹⁹⁾)

For first-order estimates assuming free convection in nitrogen-oxygen mixtures, thermal equations have been developed by combining equations for free convection, transport properties of air, and evaporative cooling to yield (19):

$$q_e = 25.7 \frac{C't_a}{P} (p_s - p_a) \left\{ P_g \left(.005 P (t_g - t_a) + 1.02 (p_s - p_a) \right) \right\}^{0.25} \quad (36)$$

Under forced convection, the following equation holds for nitrogen-oxygen: (18, 20)

$$q_e = 1.98 C't_a^{1.036} k_e \left(\frac{\bar{V}}{P} \right) (p_s - p_a) H_2O \quad (36a)$$

where k_e = a factor that depends upon the diffusivity of water vapor in the gas mixture and on the transport properties of the gas mixture itself. For dry air, $k_e = 1$. For other gases,

$$k_e = (k_D)^{0.67} \left(\frac{M_{mix}}{M_{air}} \times \frac{\mu_{air}}{\mu_{mix}} \right)^{0.17} \quad (36b)$$

The diffusion coefficient for water in helium is 3.5 times that for water in air (166). For the case where the water is diffusing into a mixture of helium and oxygen, diffusivity relative to air is found from

$$k_D = \frac{1}{\frac{\text{MOL FRACT. He}_+}{3.5} + \frac{\text{MOL FRACT. O}_2}{1}} \quad (36c)$$

For the 70-percent oxygen atmosphere in helium at 5 psia,

$$k_D = \frac{1}{\frac{0.298}{3.5} + \frac{0.702}{1}} = 1.271$$

For the 50-percent oxygen atmosphere in helium at 7 psia,

$$k_D = 1.554$$

Therefore, the k_e values can be calculated for the oxygen-helium atmosphere containing 70-percent oxygen,

$$k_e = (1.271)^{0.67} \left(\frac{23.6}{29.0} \times \frac{12.10}{13.49} \right)^{0.17} = 1.113$$

and for the oxygen-helium atmosphere containing 50-percent oxygen,

$$k_e = (1.554)^{0.67} \left(\frac{18}{29} \times \frac{12.10}{13.47} \right)^{0.17} = 1.219$$

Again, it should be emphasized that Equations 34 to 36 are only first-order estimates of the evaporative heat loss.

Comfort Zone Predictions in Unusual Gaseous Environments

In view of the dearth of empirical data on comfort zones in the mixed gas environments, several attempts have been made to predict these values. Figures 6-35, 36 and 37 represent sample predictions of one approach, combining the Equations 15, 20, 22, and 36, to estimate the comfort zone in oxygen-nitrogen mixtures under several different assumptions regarding forced vs. free convection, Clo values, etc. (21). Comfort was estimated from the ratio of predicted to maximum evaporative capacity, C' using the criteria of Table 6-33. For subjects at rest with little clothing, this comfort criterion may not be too fanciful (121, 224). Recent unpublished data from

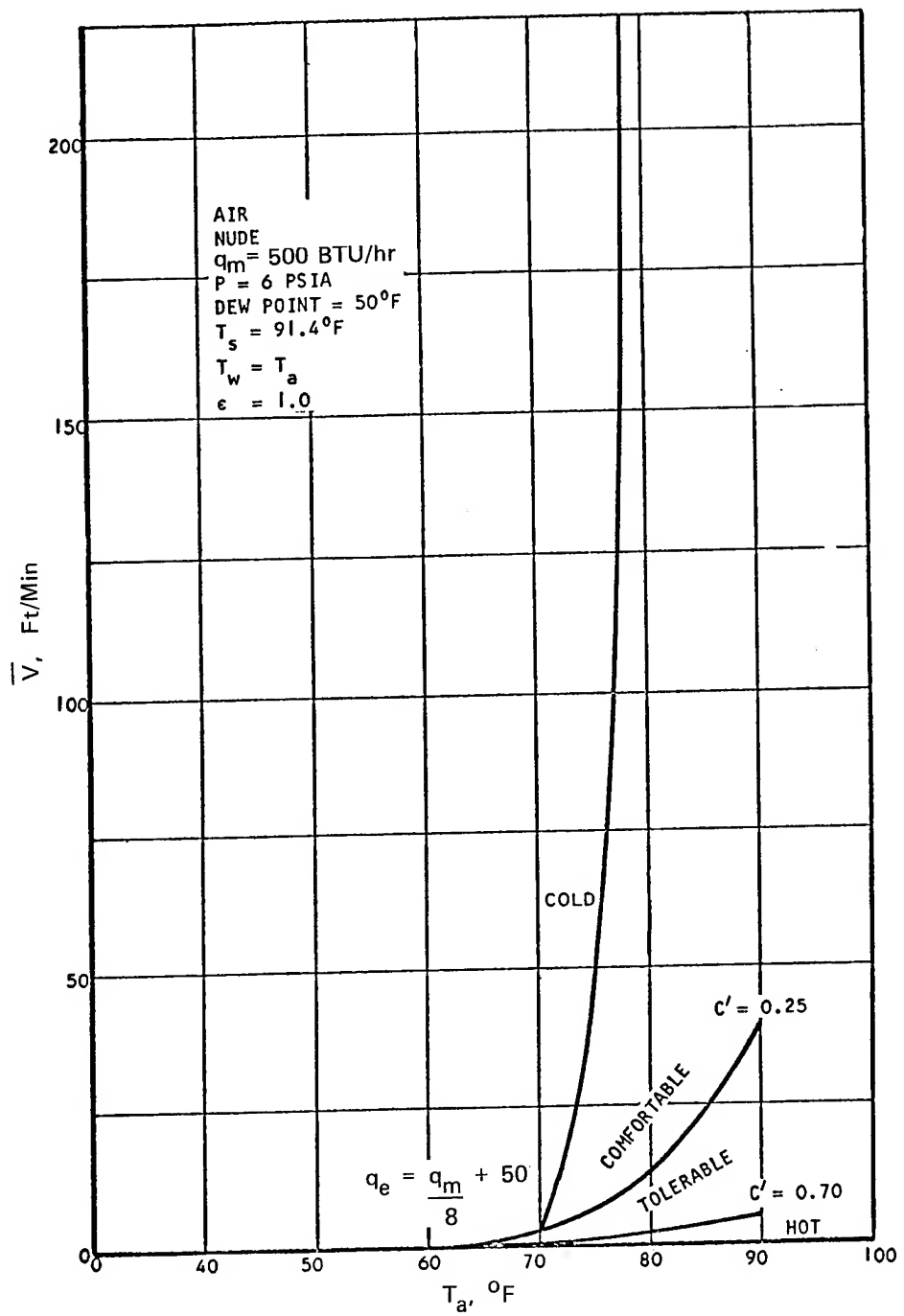


Figure 6-35

Forced-Convection Comfort Zones During Mild Exercise with 1/2 Clo.
(Modified from Berenson⁽²¹⁾)

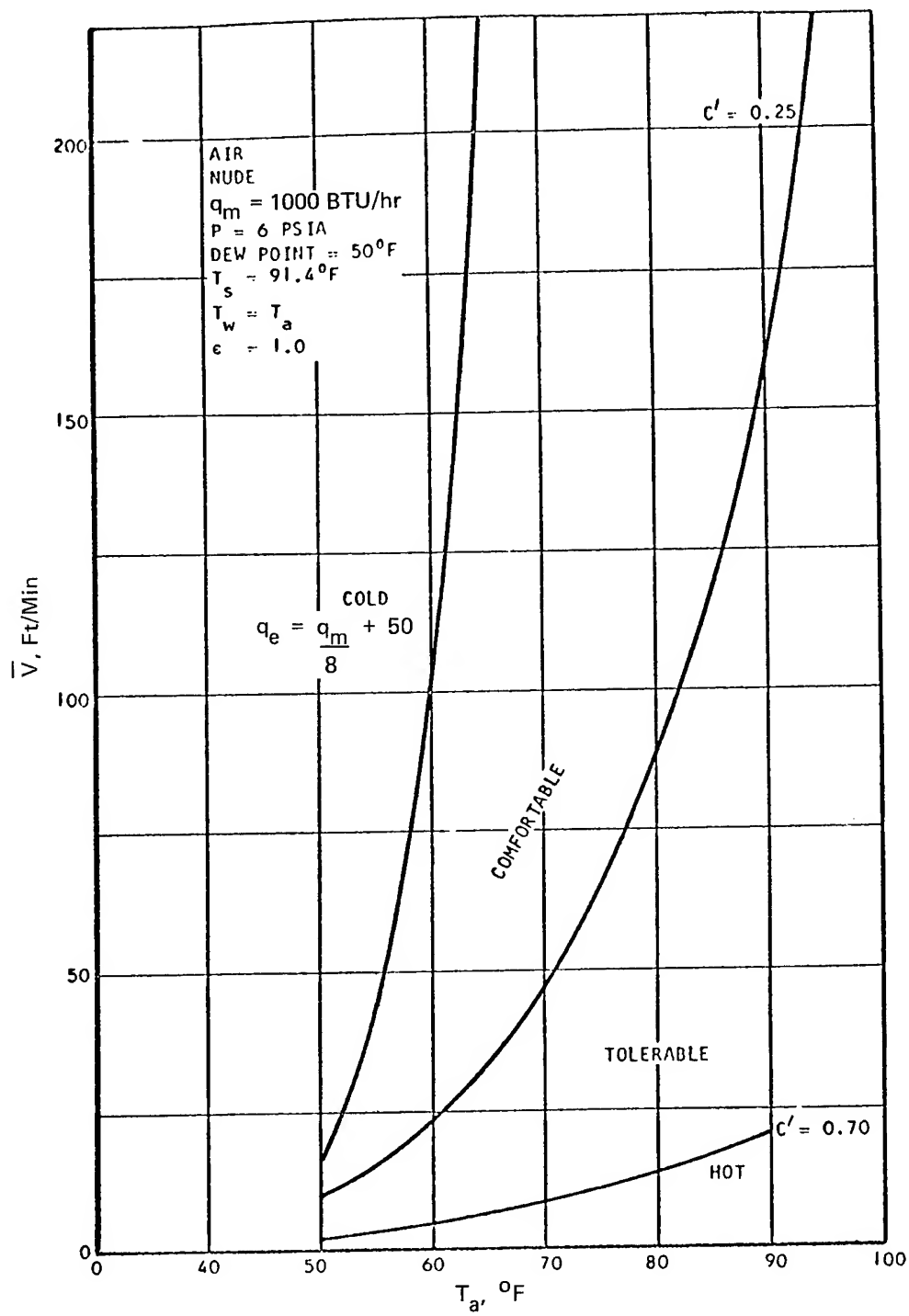


Figure 6-36

Forced-Convection Comfort Zones at Moderate Exercise in the Nude

(Modified from Berenson⁽²¹⁾)

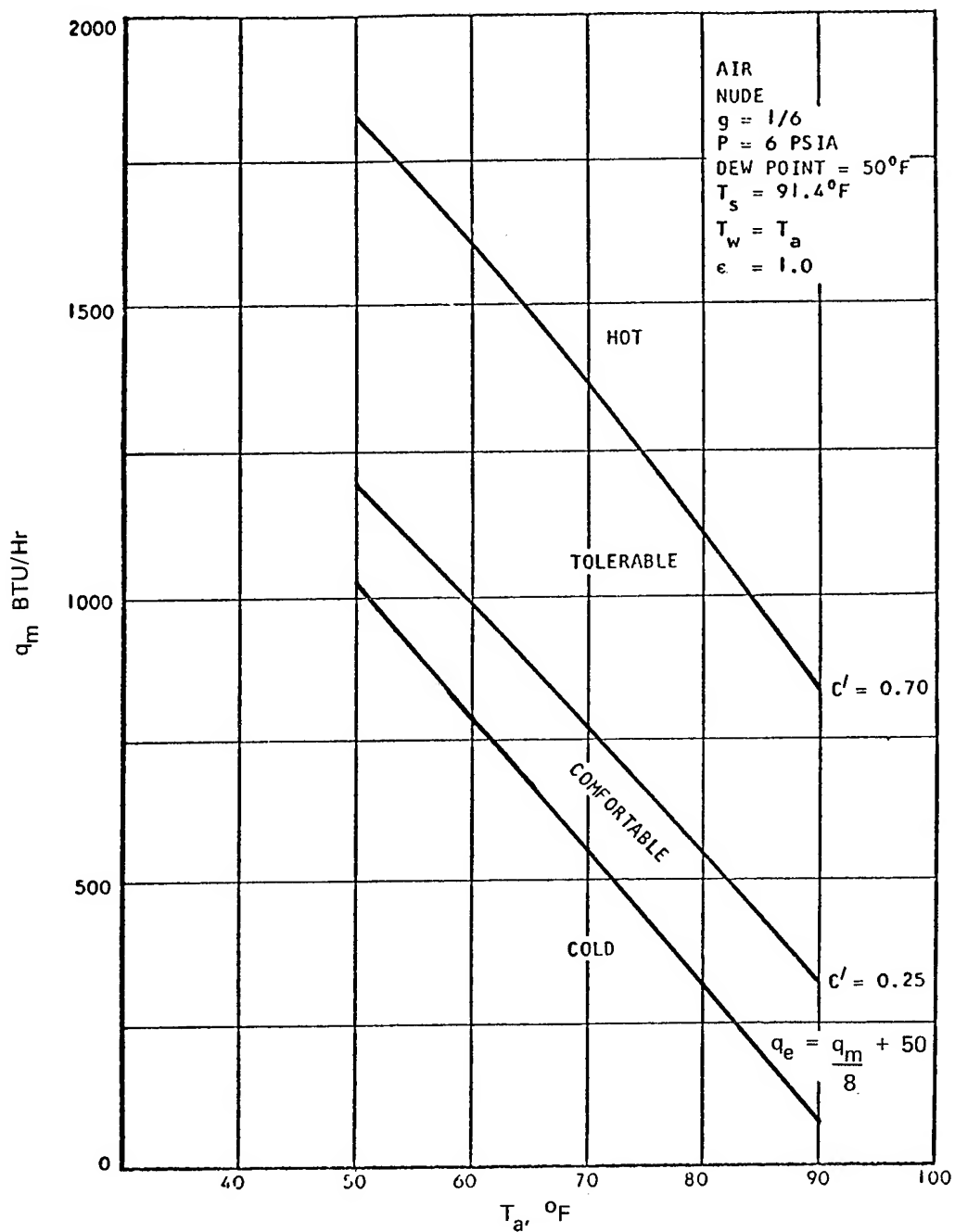


Figure 6-37

Lunar Free-Convection Comfort Zones as Related to Exercise Rate in the Nude
 (Modified from Berenson⁽²¹⁾)

the NASA Manned Spacecraft Center, Houston, suggest that the minimum latent heat loss by evaporation, $q_e \text{ min}$ is given by the following equation:

$$q_e \text{ min} = 0.125 q_m + 50 \text{ (BTU/hr)}$$

This fact alters previous approaches to setting the cold-comfort boundary using $C' = 0.1$ as a criterion (19). The 6 psia pressure is a midpoint of the 5-7 psia range under consideration in the U. S. Space Program (174).

The assumption of a constant skin temperature of 91.4°F and a nude condition represent the most significant errors in these predictive curves. A skin temperature of 90°F should probably be used to evaluate the lower boundary of the comfortable zone, while values of 93° and 95°F should be used to evaluate the boundaries at 25 and 70 percent of maximum evaporative capacity, respectively. This would have the effect of broadening both the comfortable and tolerable zones. Until it has been shown that using a uniform skin temperature leads to a significant error in the results, there is little justification for analyzing the body as a number of separate regions for these predictive curves (20).

The assumption that the mean radiation temperature of the walls and equipment is approximately equal to the atmospheric gas temperature is very useful for general parametric studies, but may be in error. It is necessary in many cases to perform a more rigorous radiation heat-transfer analysis after the enclosure geometry and temperature distribution have been established in some detail (18). The effect of clothing was greatly simplified; the heat-transfer resistance of the clothing was assumed to be uniform over the entire body, and the heat-transfer area and the evaporative-cooling capacity was assumed to be unaffected by the presence of clothing. It is difficult to improve on these assumptions, because of the lack of detailed information pertaining to clothing heat-transfer resistance and area. These assumptions, inherent in Equations 15, 20, 22, and 36 and in Figures 6-35, 6-36, and 6-37, will be modified in future calculations of this type (18). Unfortunately, there are few empirical data to substantiate these curves. Preliminary studies tend to corroborate some of these predictions for different O₂ - N₂ environments (31, 179, 219).

Comfort zone predictions for an oxygen environment at 5 psia with clothing assemblies varying in thermal resistance from 1/4 to 1 Clo have been established by the U.S. Air Force as shown in Figure 6-38 (114). However, the equations and assumptions used in the generation of this figure have not yet been published. The predictions of Figures 6-35 to 6-38 cannot be used for systems other than pure oxygen or oxygen-nitrogen.

For cabins with oxygen-helium mixtures, other heat flow constants must be used to determine comfort zones. (See Equations 21, 36b and 36c.) In order to avoid the movement of papers at one atmosphere in 1-G environments in air, a velocity of 50-60 fpm is stated as the tolerable upper limit of velocity above the 40-50 fpm draft threshold. Since the force of a gas stream is proportional to $\rho \bar{V}^2$, a table of constant force thresholds equivalent

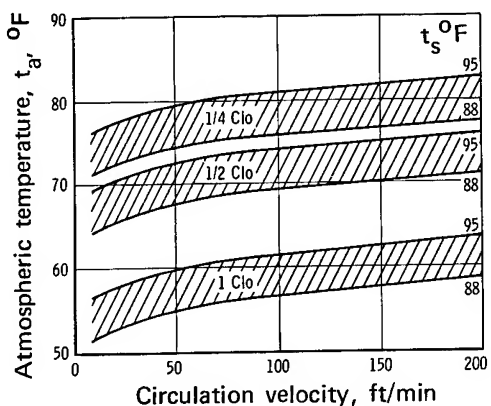


Figure 6-38
Human Comfort Chart at Rest
5.0 psia O₂ (Theoretical)

$$p_{O_2} = 243 \text{ mm Hg}$$

$$p_{H_2O} = 10 \text{ mm Hg}$$

$$p_{CO_2} = 5 \text{ mm Hg}$$

(After Johnson⁽¹¹⁴⁾)

to 50-60 fpm in air can be calculated. Table 6-39 represents this maximum-force velocity along with the corresponding ambient temperature t_a ($^{\circ}\text{F}$) required for maintenance of thermal comfort as measured by average skin temperatures t_s , at 91° and 94°F (116). Fig. 6-40 was used for t_a values.

Predictions of thermal comfort zones of Figure 6-40 a to d for different gas velocities of varied mixtures of oxygen-helium and oxygen-nitrogen in zero g have been made assuming the following conditions:

1. $t_a = t_w$ (Air Temperature = Environment Temperature
= Wall Temperature)
2. No body heat storage
3. $P_{O_2} = 170 \text{ mm Hg}$, in all cases and P_{N_2} or P_{He} increasing from 200 up to 600 mm Hg
4. Zero gravity environment
5. Evaporative heat loss is the same as it is at 1 atmosphere and 1 "g"

Table 6-39

Maximum Velocity over Man

(After Parker et al⁽¹⁵⁵⁾)

$p_{He} \text{ mm Hg}$	$p_{N_2} \text{ mm Hg}$	Maximum velocity over man, ft/min	t _a , °F, required for -	
			$t_s = 91^{\circ}\text{F}$	$t_s = 94^{\circ}\text{F}$
0	0	100 to 120	56.5 to 58.5	66 to 67.5
200	0	94 to 113	65 to 66.5	72 to 73
400	0	88 to 106	68 to 69	74.4 to 75.5
600	0	84 to 100	70 to 71	76.5 to 77.5
0	200	71 to 86	61.5 to 63	69 to 70
0	400	57 to 69	63.5 to 65	70 to 71.5
0	600	50 to 60	64.5 to 65.5	71 to 72

Note: $p_{O_2} = 170 \text{ mm Hg}$; maximum velocity for avoiding movement of papers in 1-G; 1 Clo at rest.

6. Convective heat loss is for cylindrical model of man with $A_g = 19.5 \text{ ft}^2$ in cross-flow (as in Figure 6-22)
7. Metabolic heat generation is for a man seated at rest (400 BTU/hr at 70°F).
8. t_s = skin temperature in the 91°F range
9. $\text{Clo} = 1, \epsilon_2 = 0.9$
10. $A_r = 15.6 \text{ ft}$ and $A_r/A_g = 0.8$
11. Partition of heat loss is similar to that seen in Figure 6-3.
12. The clothing temperature, t_g , is related to atmospheric temperature, t_a , by the relation

$$t_g = t_a + \frac{1.137 (t_s - t_a)}{(0.8 h_r + h_o) \text{Clo} + 1.137}$$

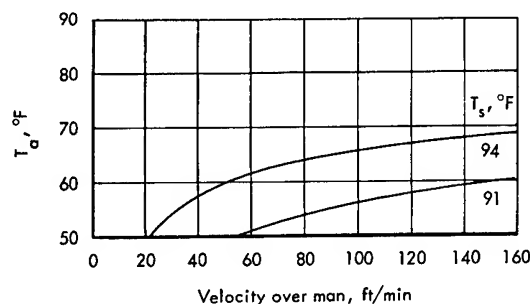
13. The relation of h_r to t_g is the same as that noted in Figure 6-20: $t_w = t_a$

Equations 34, 35, and 36 predict that the rate of evaporation is inversely related to the ambient pressure. However, evaporation probably accounts for less than one-third of the total heat loss at the temperatures in question. The assumption (Figure 6-8) of 1 atmosphere pressure does not present too great an error. In the presence of adequate forced convection, the gravitational factor in Equation 35 would play a minimal role in evaporative heat loss and can be neglected in the solution of comfort zone temperatures. The 1/4th power factor in this equation would in itself reduce the overall weighting of gravity effect.

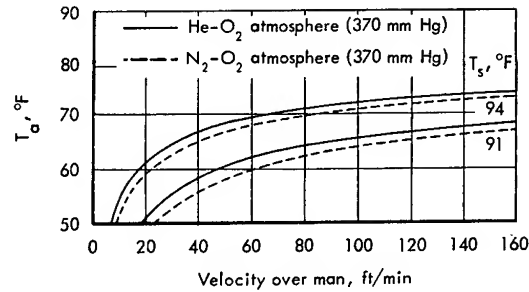
In Figures 6-40a, b, c, and d representing the results of these calculations, the helium-oxygen mixtures show a narrower zone of comfort occurring at higher temperatures especially at lower flow rates than do the nitrogen-oxygen mixtures. This is more marked in the cases of higher fractional content of inert gas (6-40c and d). The temperature values in Table 6-39 indicate the zone of comfort for the maximum gas velocities calculated for each mixture with rustling of papers in 1G as an endpoint.

It should be noted that in these predictions, the one Clo value is as high as one would probably expect to find in a shirt sleeve environment. More typical values would be .25 Clo for the Gemini underwear (163). The effect of helium in reduction of the Clo values of different garments has not been studied. Preliminary studies confirm that Clo values tend to vary inversely with the thermal conductivity of the atmosphere. (See Figure 44b.) The Clo value in 7 psia 50% O₂-50% He would therefore probably be 0.015/0.027 or about 0.56 that of sea level air (174). The expected effect of Clo on the helium-oxygen comfort chart is predicted in Figure 6-41. The 1 Clo prediction is closely parallel to that in Figure 6-40a.

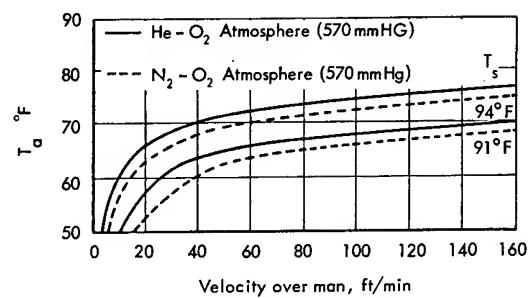
Figure 6-40
Comfort Lines for Man Seated at Rest
(After Parker et al⁽¹⁵⁵⁾)



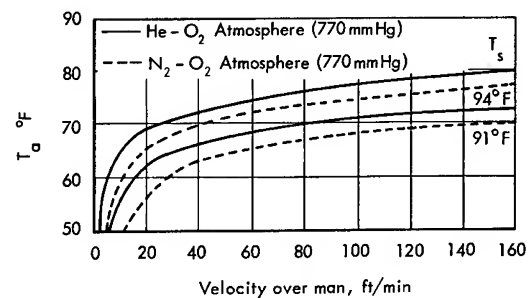
a. With $p_{O_2} = 170 \text{ mm Hg}$ at 1 Clo



b. With $p_{O_2} = 170 \text{ mm Hg}$ and He or
 $p_{N_2} = 200 \text{ mm Hg}$ at 1 Clo



c. With $p_{O_2} = 170 \text{ mm Hg}$ and p_{He} or
 $p_{N_2} = 400 \text{ mm Hg}$ at 1 Clo



d. With $p_{O_2} = 170 \text{ mm Hg}$ and p_{He} or
 $p_{N_2} = 600 \text{ mm Hg}$ at 1 Clo

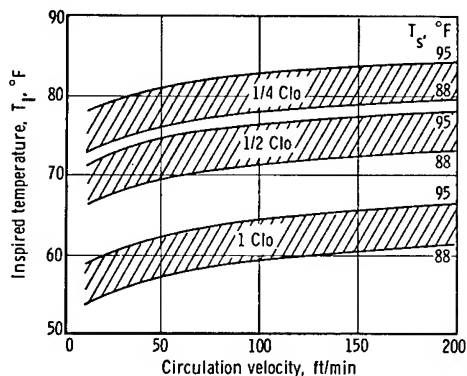


Figure 6-41

Human Comfort Chart
5 psia O₂ - He (Theoretical)

$$p_{O_2} = 173 \text{ mm Hg}$$

$$p_{He} = 75 \text{ mm Hg}$$

$$p_{H_2O} = 10 \text{ mm Hg}$$

$$p_{CO_2} = 5 \text{ mm Hg}$$

(After Johnson⁽¹¹⁴⁾)

Empirical comfort temperatures in different gas mixtures have not been systematically obtained. Comfort temperatures have been recorded only as the average cabin temperature set over periods of several weeks by subjects who had control over the thermostat within the cabins (219). These temperature settings can be seen in Table 6-42 for subjects in surgical clothes which would have about 0.5 Clo in air. These data include varied numbers of different subjects being studied under each gas mixture. No wind speed measurements were made during these studies, however, papers were not rustling and no complaints of wind chill were recorded. No measurements of average skin temperatures were made. The prediction in Figure 6-41 for 1/4 to 1/2 Clo is borne out in these data. Other studies have found comfort temperatures in He-O₂ at higher levels (31, 179). In these studies, the average temperature settings during a varied work-rest cycle with 0.7 Clo were 78°F for nitrogen-oxygen at 7 psia and 85°F for helium-oxygen at 5 psia. Figure 6-41 may therefore have to be altered when more complete data become available. Zero gravity will tend to lower the comfort temperature (31).

Work is in progress to extend the predictive charts of Figures 6-35, 6-36, and 6-37 to He-O₂ mixtures of different composition and pressures and to different values of Clo, exercise rate and skin comfort temperatures (18, 20).

During exercise, the partition of heat loss would be expected to vary with different atmospheres. Figure 6-43 represents the relative modes of heat loss calculated during exercise at 100 watts for 1 hr in ground level air (G. L. air) at 745 mm Hg; ground level He - O₂ (159 mm Hg of O₂ and 579 mm Hg of He) and altitude helium (alt. He-O₂) of 380 mm Hg with 165 mm Hg of O₂ and 206 mm Hg of He. The similarity between G. L. air and alt. He - O₂

Table 6-42

Temperatures Selected by Subjects in Space Cabin Simulators

(After Welch⁽²¹⁹⁾)

	3.7 psia O ₂ -100%	5 psia O ₂ -100%	5 psia P _{O₂} -175 mm Hg pHe- 74 mm Hg	7.3 psia P _{O₂} -150 mm Hg pHe-230 mm Hg	7.3 psia P _{O₂} -165 mm Hg P _{N₂} -206 mm Hg
Selected Temp °F	69.3	70.9	74.7	75.4	72.7

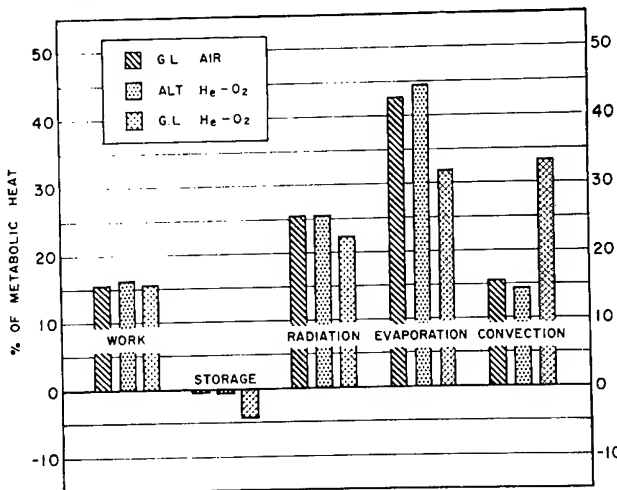


Figure 6-43

Avenues of Heat Exchange as Percentages of Total Metabolic Heat for a 150-Minute Test Period with 1 Hour of Exercise at 26°C.

Dewpoints are:

G.L. Air = 7.4°C

Alt. He - O₂ = 5.0°C

G.L. He - O₂ = 4.0°C

Alt. He - O₂ = O₂ - 165 mm Hg

He - 206 mm Hg

(After Epperson et al⁽⁷³⁾)

is striking as is the difference in convective and evaporative losses produced by the high pHe environment during this exercise load.

SPACE SUITS AND CLOTHING

The thermal physiology of clothing and space suits incorporates many of the principles already covered but requires knowledge of several other factors (27, 30, 48, 151, 173). Clothing must be considered for the shirt-sleeve environment within the cabin, for extravehicular operations in space or on the lunar surface and for survival conditions in remote parts of the Earth.

Radiant Insulation

Radiant input to the astronaut during EVA and on the lunar surface is a major factor in the design of external insulation for space suits. Detailed analyses of radiant input to multicylindrical and hemispherical models of man on the lunar surface (158) and to man in orbit (167, 168) are currently under study.

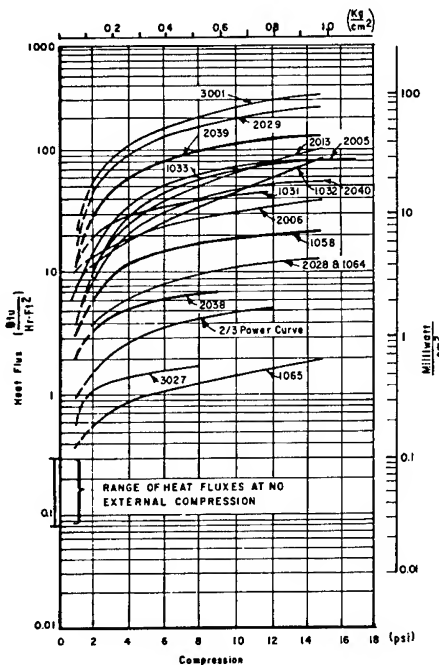
Surface control of the radiant input can be obtained by varying the α/ϵ ratio of the surface materials of the outer coveralls of space suits (167). In noon orbit where the astronaut is out of the umbra and receiving solar input over one-half of his suit, it has been calculated that equilibrium, external temperatures of less than 50°F cannot be maintained by α_o/ϵ_o surface coatings ($\alpha_o/\epsilon_o > 0.2$) when internal heat generation rates are in excess of about 1800 Btu/hr. For an α_o/ϵ_o of 0.2 (the approximate lower limit of α_o/ϵ_o for available space suit coating materials), the range of insulation conductance required for external wall temperatures of 75°F extends from 0.3 Btu/sq ft hr °F at 1000 Btu/hr to 20 Btu/sq ft hr °F at about 2300 Btu/hr. The minimum conductance actually approaches infinity for internal heat generations in excess of 2300 Btu/hr, indicating that the external surface α_o/ϵ_o limits the heat flow.

The α_o/ϵ_o of surface coatings required to maintain the internal wall temperature at 75°F when the insulation conductance is 20 Btu/sq ft hr °F decreases from 0.9 at 1000 Btu/hr to zero for 2500 Btu/hr internal heat generation. Such a range of external surface α_o/ϵ_o ratios is outside the capability of present day spacecraft coating technology. It is concluded that for typical materials ($\epsilon_o = 0.85$ and $\alpha_o/\epsilon_o \geq 0.2$) comfortable skin temperatures cannot be achieved by insulation alone for the highest internal heat generation rate of 2500 Btu/hr. For the lowest internal heat generation rate, 1000 Btu/hr, control is possible by varying α_o/ϵ_o , by varying the insulation conductance or by varying both. Similar calculations have been made for less severe orbital conditions (167). Data are available on the physical properties of various textiles, plastics, and metalized surfaces in current use for thermal control of flexible structures (227) and suits (22, 167, 168). Degradation of the surface with use must be anticipated.

Insulation design for space suits has made use of the newer, multilayer and vacuum insulations (24, 86, 167, 220). The primary requirement for a radiation shield is that it exhibit a low emittance. Silver, aluminum, and gold are low-emittance materials that can be used either as coatings for radiation shields or to form thin foils. Aluminum and aluminum-coated plastic films are most frequently selected for the radiation shields because the emissivity of aluminum is only slightly higher than that of clean silver, whereas silver tarnishes in air, aluminum forms a very thin layer of aluminum oxide which prevents further degradation of the surface. Aluminum is also inexpensive and readily available in various thicknesses of foil and as a coating on a variety of metallic and nonmetallic surfaces. Aluminum vaporizes at a lower temperature than gold, making the aluminum deposition process easier to control. Plastic films with an aluminum deposit have been used for decorative purposes in industry for many years. As a result, aluminum-coated films are less expensive and of a better average quality than gold- or silver-coated films. Data are available on many different metalized film and foam systems for radiant shielding (86).

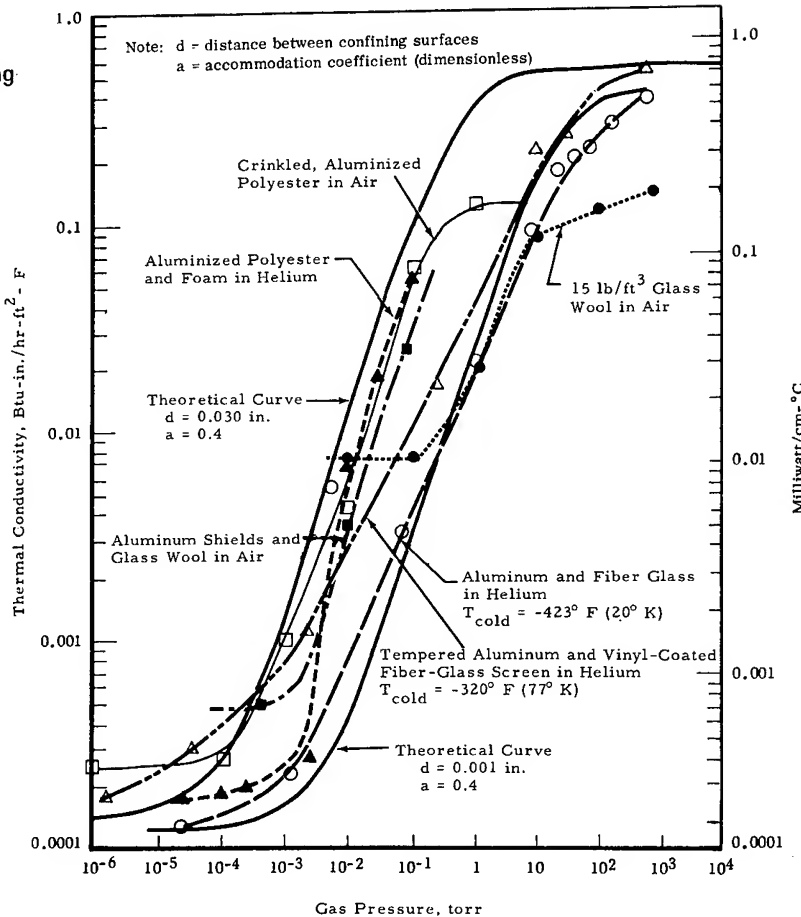
The performance of any given insulation will be greatly affected by the following variables: applied compressive load, number of shields used in the sample, kind of gas filling the insulation and its pressure, size and number of perforations in the insulation to permit outgassing, and temperatures of the warm and cold boundaries. Compressive loads by mechanical contact, by atmospheric pressure when a flexible outer skin is used to contain the insulation and permit evacuation, or those developed during application of multilayer insulations, reduce overall insulating effectiveness (86, 167). Even if the compression by the weight of the upper layers on the lower layers is disregarded, external forces (e.g., tension applied during wrapping of a multilayer insulation around a cylindrical object, thermal expansion or contraction of the insulation components with respect to the object, and localized loads in the vicinity of support points can compress the insulation. These compressive loads may be in the range from 0.01 to 1 psi (0.0048 to 0.48 g/cm²). Figure 6-44a shows the effects of compression on the heat flux through 16 different multilayer insulations used for cryogenic insulation. When compression up to 2 psi (0.96 g/cm²) is applied, the heat flux for the majority of the insulations is about 200 times greater than at the no-load condition. Plots of the heat flux in BTU/hr - ft² (characteristic also of the

Figure 6-44
Insulation Values for Typical Radiant Shielding
(After Glaser, Black et al⁽⁸⁶⁾)



Sample No.	T_{cold} , °F	Number of layers	Description
1031	-320	20	Aluminized polyester film
1032	-423	11	Fiber-glass mesh
1033	-423	10	Tempered aluminum
		11	Perforated fiber-glass mat
1058	-423	10	Aluminized polyester film
		11	Perforated fiber-glass mat
1064	-423	10	Tempered aluminum
		11	CT-448 (0.020 in.)
1065	-423	10	Aluminized polyester film
		11	Polyurethane foam
2005	-320	60	Aluminized polyester film
		61	Polyurethane foam (11 percent support)
2006	-423	20	Aluminized polyester film
		21	Fiber-glass cloth
2013	-423	10	Soft aluminum
		10	Polyester film
2028	-423	10	Tempered aluminum
		11	0.003-inch glass-fiber paper
2029	-423	10	Waffled aluminum
		11	Fiber-glass mat
2038	-423	10	Waffled aluminum
		11	Three-layer fiber-glass cloth
2039	-423	10	Tempered aluminum
		11	CT-449 (11 percent support area, 0.020 in.)
2040	-423	10	Double aluminized polyester film (both sides)
		11	Nylon netting (0.007 in.)
3001	-320	11	Nylon net
3027	-320	60	Tempered aluminum
		6	Crinkled, aluminized polyester film
		7	Aluminized polyester film
			CT-449 (11 percent support area, 0.080 in.)

- a. (top) Effect of Mechanical Loading on the Heat Flux Through Multilayer Insulation.



- b. (right) Effect of Gas Pressure on Thermal Conductivity.

apparent thermal conductivity) versus compressive load in psia on a logarithmic scale fall on straight lines with a slope between 0.5 and 0.67.

In theory, the heat flux passing through an uncompressed sample of the multilayer insulation is inversely proportional to the sample thickness (i.e., number of shields), and, therefore, its thermal conductivity can be evaluated. Experimentally, under 1 g conditions, heat-flux data for a sample with 40 shields are somewhat higher than predicted from the 5-shield sample data (86). This discrepancy may be explained by the compression exerted by the weight of the upper layers on the lower layers of the sample, which may cause the lower layers to perform less efficiently than the upper layers. If an accurate estimate of the heat flux is required, a correction factor for the effect of compression must be applied.

The effects of a gas and its pressure on the performance of insulations have been studied by many investigators (86). The presence of residual gas inside fibrous and powder insulations decreases the thermal performance of a system. Gases of high thermal conductivity (e.g., helium or hydrogen) cause more rapid performance deterioration than gases with low conductivity (e.g., nitrogen or air). These effects are even more pronounced for a multilayer insulation. The effect of gas pressure on the thermal conductivity of several multilayer insulations is shown in Figure 6-44b. For comparison purposes, data for one fibrous insulation (glass wool in air) are plotted in the same figure. The thermal conductivity relates to gas pressure by an S-shaped curve. However, the effect of pressure on performance of multilayer insulations is 2 magnitudes larger than the effect of pressure on powder or fibers (i.e., the performance of a multilayer insulation is 100 times higher than that of a powder, but a pressure 100 times lower is required to reach it). At pressures below 10^{-5} torr, the heat transferred by a gas is directly proportional to the gas pressure. However, the heat conducted by a gas at that pressure is only a small portion of the total heat transferred through the insulation; therefore, the apparent thermal conductivity of the multilayer insulation decreases only slowly at pressures below 10^{-5} torr. At pressures of 10^{-5} to 10^{-4} torr, the mean free path of the gas molecules approaches the distance between the solid particles of the insulation. Beginning at these pressures, the apparent thermal conductivity of the insulation rapidly increases. For this reason the multilayer insulation must be maintained at a pressure below 10^{-4} torr or it will not provide the desired insulation effectiveness. When the gas pressure reaches atmospheric pressure, the heat conducted by the gas becomes the dominant mode of heat transfer. For a warm boundary at room temperature, the radiation component becomes small in comparison to the gas conduction component. Therefore, the apparent thermal conductivity of a multilayer insulation approaches the conductivity of the interstitial gas. After atmospheric pressure has been reached, the conductivity of the gas remains nearly constant and independent of the pressure, as does the apparent thermal conductivity of a multilayer insulation.

Perforations through insulation decrease the efficiency by local compression effects. Perforations have a smaller effect on an insulation with crinkled, aluminized polyester shields than on one with aluminum shields, presumably because the crinkles introduce a more random distribution of holes and improve outgassing (86).

Temperature of the warm and cold boundary layers controls the apparent conductivity of the multilayered insulations (86). For large temperature differentials, heat flux is directly proportional to the fourth power of the warm-boundary temperature through 10 tempered aluminum shields spaced with 11 vinyl-coated fiber-glass-screen spacers. For multilayer insulation with crinkled, aluminized polyester film radiation shields, apparent thermal conductivity is approximately proportional to the third power of the warm-boundary temperature. When the warm-boundary temperature is held constant, a higher thermal conductivity results from increasing the cold-boundary temperature. Data are available on the adequacy of the surface temperature control systems of current Apollo EVA Systems in many different operational conditions (89). Design and effectiveness of the Gemini System are covered under zero gravity of Acceleration, (No. 7), and Pressure, (No. 12).

Insulation of "Shirtsleeve" Garments

In the design of garments for wear within the space cabin it should be recognized that addition of clothing to the body surface reduces the quantity of heat that can be lost by evaporation because of the increased resistance to water vapor diffusion. At the same time, garments reduce the quantity of heat gained or lost by the body through radiation and convection. The addition of clothing may be detrimental, beneficial, or ineffective, depending on the amount of clothing, operative temperature, barometric pressure, and type of fabric used. Two properties of clothing must be evaluated to determine the effect of clothing on thermal balance. These are thermal resistance (R_g), and vapor resistance ($R'g$).

Thermal resistance is the resistance of a particular clothing assembly to flow of heat. It is generally expressed in "Clo" units. It is directly proportional to the sum of the thickness of fabrics plus the thickness and the composition of the gas layers between fabrics (See Equation 16).

The thermal resistance of garments expressed in Clo units is:

$$1 \text{ Clo} = 0.88^{\circ}\text{F ft}^2 \text{ hr/BTU} = 0.18^{\circ}\text{C m}^2 \text{ hr/kCal}$$

Clo values of garment resistance vary from zero (for the nude man) through approximately 5 for pressure garment assemblies to values of 6-7 Clo for fox fur. Insulation values for typical Air Force clothing are recorded (27). The Gemini underwear has an insulation value of 0.25 Clo in sea level air (163).

The total insulation value of a clothing assembly to the man must include the insulation of gas trapped between clothing layers. The best value for still-air insulation at sea level as determined empirically is $0.19 \text{ C/kcal-m}^2 \text{ hr}$ (97). The rate of heat transfer across air space reaches a constant value for thicknesses exceeding 0.3 inches (0.75 cm) at sea level (27). Experimental Clo values for helium-oxygen and nitrogen-oxygen mixtures in fabrics are not yet available. Calculation of the total insulation value of newly designed garments and fabrics requires the knowledge of the thickness of the still air layer (R'_t) which is equal to the sum of the clothing vapor resistance ($R'g$) as a still air equivalent and film resistance of the still air layer, ($R'e$):

$$R'_t = R'_g + R'_e \quad (37)$$

where $R'_e = 0.24$ in (0.6 cm) for air.

Values for R'_g for standard fabrics are shown in Table 6-45a. If fabric thickness is known the relationship

$$\frac{R'_g}{L} = \frac{\text{equivalent air thickness}}{\text{fabric thickness}} \text{ can be used (27).}$$

If thermal resistance in Clo units is known, the relationship

$$\frac{R'_g}{R_g} = \frac{\text{vapor resistance (inches of air)}}{\text{thermal resistance (Clo units)}} = 0.5 \frac{\text{inches of air}}{\text{Clo}} \text{ or } 1.2 \frac{\text{cm of air}}{\text{Clo}}$$

can be used. If the air layer thickness exceeds 0.3 in (0.75 cm) then these latter values should be used for R'_t (27). Techniques are available for measuring insulation values of clothing on working subjects (228).

Vapor Resistance

Vapor resistance (R'_g) depends on vapor diffusion of evaporated water, weave and thickness of the fabric material, the thickness of the air layers between the garments, and the nature of the gaseous environment. While the rate of vapor transfer across near-isothermal air layers is directly proportional to thickness, bellows action and resulting convection suggest use of the same maximum effective thickness for vapor transfer as for heat transfer, i.e., 0.3 inches (0.75 cm). The values of R'/L in Table 6-45a are a convenient estimate of resistance of similar fabrics, even though a more exact relationship of $R' = a(L)^{+b}$ probably is more true to reality (27).

If the resistances to vapor of all the fabrics making up a clothing assembly are known and the thickness of each air layer between successive garments is measured, the total resistance of the assembly can be easily determined (27). The air layer thicknesses can be determined in the following manner (128). Girths are measured first on the nude body at 6 locations (i.e., at two levels on arm, trunk, and leg), and again after each garment is donned. Assuming the body parts to be cylinders, successive radii are computed from the measured girths. The air layer thickness is obtained by subtracting the known garment thickness from the increment in radius produced by each garment.

Strictly speaking, a correction should be applied to the total resistance value obtained by successive addition for each of the three body parts, since the curvature effect reduces the actual resistance below that which would obtain for plane surfaces. However, there is insufficient knowledge at present to permit such a correction, and indeed, the limited accuracy of estimating individual fabric resistances probably does not warrant this

Table 6-45a
 Vapor Resistance of Fabrics
 (After Blockley et al⁽²⁷⁾)

Fabric	Weight (oz/yd ²)	Thickness (L) (cm.)	Resistance (R') (cm air)	R'/L	Ref.
COTTONS					
cotton net	4.4	0.100	0.12	1.2	95
3 x 1 cotton twill	8.2	.097	.19	1.9	94
5 x 1 cotton twill	8.8	.112	.24	2.1	94
2 x 1 cotton twill	4.4	.069	.15	2.2	94
cotton poplin	5.8	.039	.09	2.3	95
cotton oxford	6.7	.081	.19	2.4	94
cotton balloon cloth	2.2	.015.	.04	2.6	95
cotton "jungle cloth" (bedford cord)	13.6	.107	.30	2.9	95
heavy cotton	13.5	.076	.28	3.7	95
close-weave cotton (Shirley L-30)	9.8	.051	.23	4.5	95
WOOLS					
double-face wool pile	22.	1.1	1.1	1.	95
2 x 2 wool twill	10.	.173	.26	1.5	94
worsted serge	6.1	.056	.12	2.1	95
wool serge	10.7	.130	.31	2.4	94
NYLONS					
spun-nylon fabric	4.9	.046	.18	3.9	95
nylon poncho cloth	1.5	.018	.07	3.9	94
5-end nylon sateen	2.3	.016	.08	5.0	94
filament nylon fabric	2.0	.013	.09	6.9	95
plain weave nylon	2.6	.020	.19	9.5	94
RAYONS					
viscose rayon 2 x 2 twill (fil.)	3.6	.025	.13	5.2	94
acetate rayon satin (fil.)	2.7	.018	.14	7.8	94
GLASS					
glass fabric	3.3	.013	.12	9.2	95
plain weave glass fabric	6.6	.030	.32	10.5	94

refinement. Disregard of the curvature effect is a conservative procedure, and may be justified on this basis.

In combining the data for the three areas into an overall resistance value for the body as a whole, some weighting factors for local evaporation rates must be employed. It is appropriate to use as weighting factors the relative proportion of body surface area for the part concerned. In the case of evaporative resistance, however, cognizance should also be taken of the variation in sweat production of these parts (Figure 6-29 and Table 6-45b). Proportionality factors must be used which include both relative surface area and sweat production, measured as evaporation, for various levels of thermal stress (103). Taking data for the upper portion of the environmental range (air temperature 36-37°C), and lumping values for adjacent parts, the relative proportion of trunk, leg, and arm sweat can be obtained (Table 6-45b).

Table 6-45b
Proportions of Evaporative Loss
(After Hertzman et al⁽¹⁰³⁾)

	Proportion of Total Body Surface Sweat	Relative Proportion of Trunk, Leg, Arm Sweat
Arms (forearm & arm)	.07	.08
Legs (calf & thigh)	.42	.48
Trunk	<u>.38</u>	<u>.44</u>
Totals	.87	1.00

The remaining 13% of the body average sweat per unit area is contributed by hands, feet, and head, which are not included in the clothing evaluation under discussion (See Tables 6-26 to 6-28). In a more exact analysis, the gloves, footgear and headgear could be separately evaluated, and their resistances weighted 0.03, 0.02, and 0.08 respectively (103). In a gaseous environment other than air, at sea level, appropriate corrections must be made for R'_g using the factors illustrated by Equations 6-24 to 6-31.

To aid in the first approximation of garment temperature t_g , since both h_c and h_r are functions thereof, Table 6-46 has been prepared for the standard clothing assemblies, showing t_g as a function of $(t_w + t_a)/2$, and the thermal insulation (Clo) value of the garment. Other tables must be prepared for gas mixtures other than air at sea level using Table 6-45a and Equations 17 and 18. For very high radiative temperatures, Figure 6-20b may be used to calculate h_r values.

The relationship between clothing surface temperature (t_g) and skin temperature (t_s) is seen in Equation 16.

When thermal resistance and vapor resistance of the garment assembly have been determined, the boundary for heat exchange with the environment may be shifted from the skin of the body to the surface of the clothing. With clothing as the boundary, t_g is substituted for t_s in all expressions for heat

Table 6-46
Approximate Garment Temperatures
(After Blockley et al⁽²⁷⁾)

$(t_w + t_a)/2$		1 Clo		2.5 Clo		4 Clo	
$^{\circ}\text{F}$	$^{\circ}\text{R}$	$^{\circ}\text{F}$	$^{\circ}\text{R}$	$^{\circ}\text{F}$	$^{\circ}\text{R}$	$^{\circ}\text{F}$	$^{\circ}\text{R}$
100	560	100	560	100	560	100	560
150	610	139	599	145	605	147	607
200	660	178	638	190	650	194	654
250	710	217	677	235	695	241	701
300	760	255	715	280	740	287	747

exchange. The effect of "shirt sleeve" clothing can be considered to increase the effective surface area of the body by a factor of 1.14.

Recent analyses of passive mass transfer of water in space suits are available (159, 167, 168, 182, 209).

Ventilated Suits

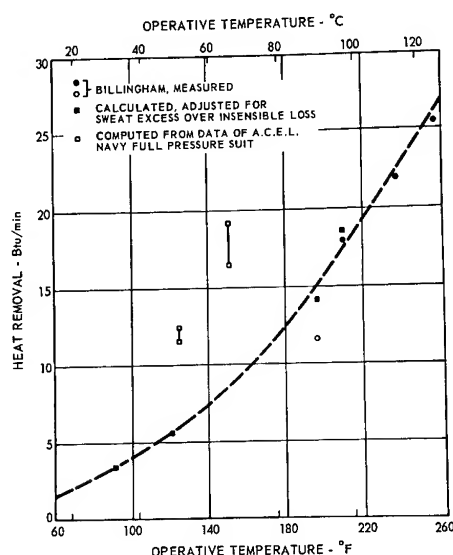
Typical air ventilated garments remove heat convectively (q_v) at a rate shown in Figure 6-47. The graph shows the rate of convective suit cooling

Figure 6-47

Cooling by Ventilated Clothing

The Data Points Marked with Hollow Squares, which are Farthest from the Curve Drawn Through the Other Points, are from Experiments Where There Was Moderate Sweating and Some Heat Storage, Although the Subjects Judged Themselves to be Comfortable. The Adjustments and Corrections for These Cases Could only be approximate.

(After Blockley et al⁽²⁷⁾ Adapted from Data of Billingham and Hughes⁽²³⁾, Greider and Santa Maria⁽⁹¹⁾ and Mauch et al⁽¹⁴¹⁾)



which must be supplied a seated man at rest wearing typical aviation clothing to maintain a comfortable skin temperature of 90°F (32°C) for a range of hot conditions given as operative temperatures (See also Figure 6-5). Suit

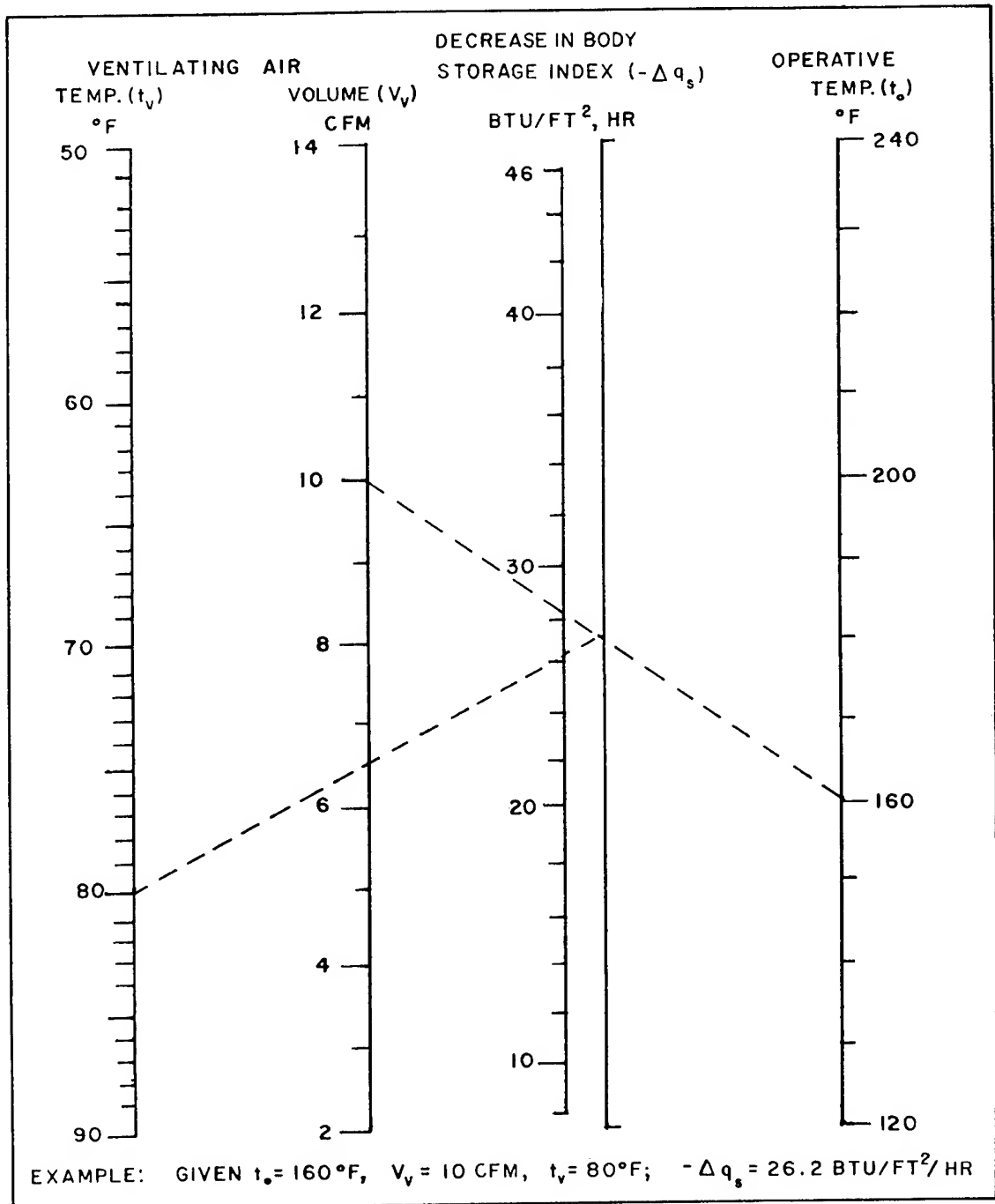


Figure 6-48

Nomograph for Computing Cooling Power of Ventilating Garment
 (After McCutchan and Isherwood⁽¹³⁵⁾)

convective heat removal is computed from the mass flow of ventilating air and the difference between inlet air temperature and the desired surface temperatures (30):

$$q_v = 0.24 (90 - t_v) W_v$$

where q_v = suit convective heat removal in BTU/min

t_v = temperature of ventilating air in $^{\circ}$ F, and

W_v = mass flow of ventilating air in lbs/min.

When a ventilating garment is worn, the effective body heat storage index ($q_s \text{ eff}$) is found by the following equation:

$$q_s \text{ eff} = q_s - \Delta q_s$$

where

q_s = heat storage index (BTU/ $\text{ft}^2 \text{ hr}$)

Δq_s = decrease in heat storage index

Figure 6-48 presents a nomograph for computing the cooling power of a typical ventilating garment ($-\Delta q_s$) from the ventilating air temperature (t_v), the volume flow (V_v), and operative temperature (t_o) (135). Each garment will present somewhat different parameters. Figure 6-48 should therefore be used only as a general example for first-order engineering estimates.

The cooling capacity of Apollo prototype ventilated suits as a function of gas flow at several internal suit pressures is seen in Figure 6-49. The partition of cooling into sensible and latent loads is shown. Figure 6-53 compares the efficacy of ventilated and liquid cooled suits under different metabolic loads.

The capacity of Apollo prototype ventilated suits to handle different metabolic loads is seen in Figure 6-50.

Liquid Cooled Suits

The inadequacy of ventilated suits in handling large metabolic loads is clear in Figure 6-50 (45, 173). For work loads above 600 BTU/hr, liquid cooling must be added. The dotted line in Figure 6-49 represents projected capacity for liquid-cooling cascade addition to ventilated suits (44).

Total liquid loop suits have been used to extract heat in a warm environment and heat the body in a cool environment (49, 113, 119, 125). The thermodynamics of suit performance for current designs have been studied (45, 49, 51, 113, 119, 125). Analytic studies of skin to liquid loop conduction for other liquid-cooled systems are also available (9, 60, 168).

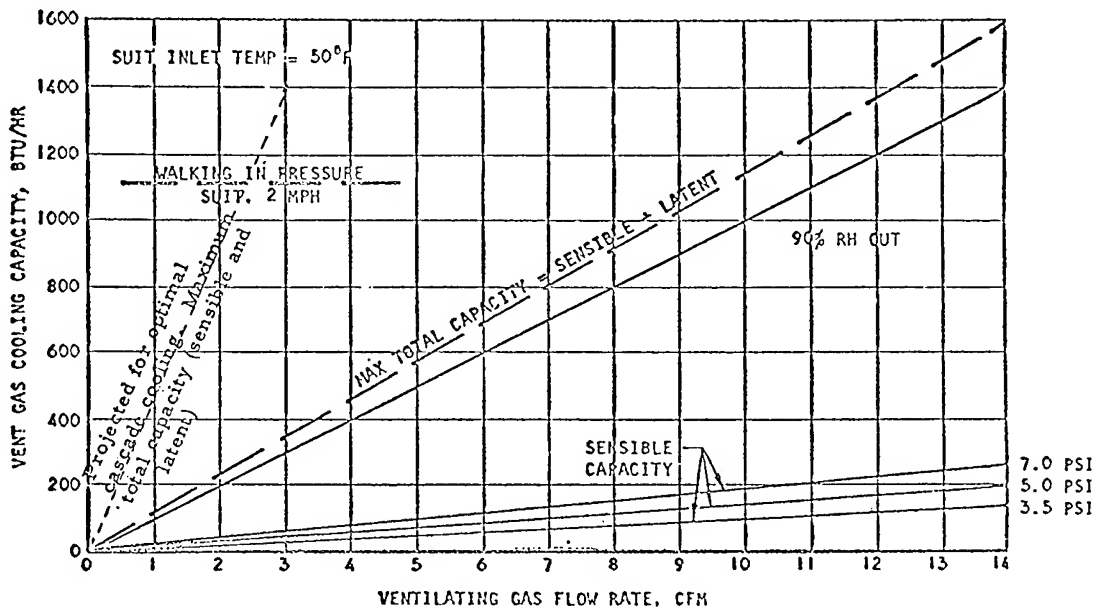


Figure 6-49

Pressure Suit Ventilating Gas Cooling

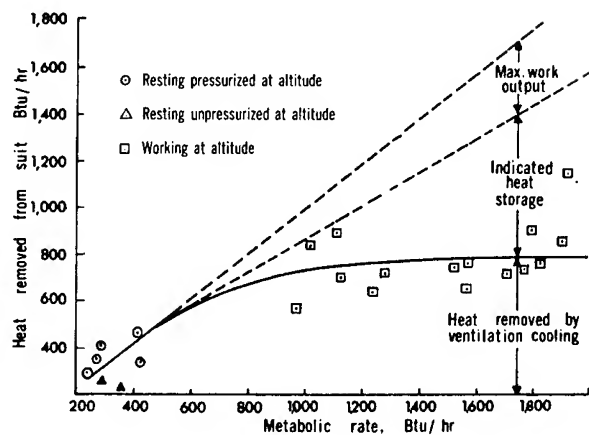
The dashed line represents the addition to cooling capacity of the ventilating suit theoretically possible by optimum function of a cascade cooling system proposed for the Apollo system.

(Adapted from Burris et al⁽⁴⁴⁾)

Figure 6-50

Heat Removed from an International Latex Prototype Apollo Suit Pressurized at 3.5 psia Above Ambient with Air Flow at 15 ft³/min.

(After Roth⁽¹⁷³⁾) Adapted from Air Research Corp.⁽⁶⁾



For an early prototype suit system, Figure 6-51a plots the suit performance equation as suit mass flow rate vs inlet temperature according to the equation:

$$t_{in} = 91.5 - \frac{q}{m C_p} [1 - \exp(-AU/m C_p)] \quad (38)$$

where \dot{m} = total mass flow of air in suit (lb/hr)

q = the cooling requirement (BTU/hr)

AU = the thermal conductance of the clothing
and its associated air film (BTU/hr °F)

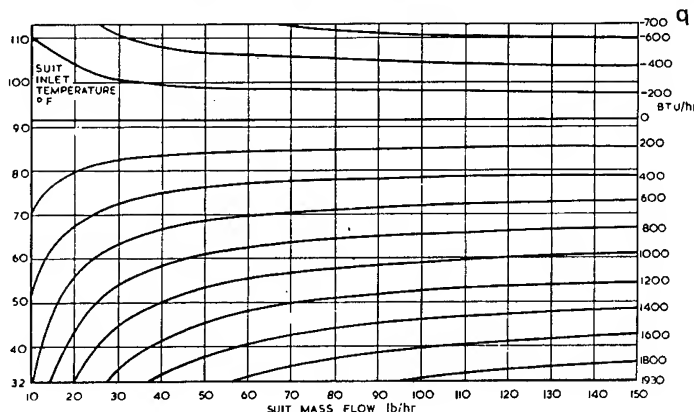
t_{in} = temperature of inlet fluid (°F)

91.5 = the assumed mean skin temperature of
a comfortable subject (°F)

C_p = specific heat of liquid at constant pressure
(BTU/lb °C)

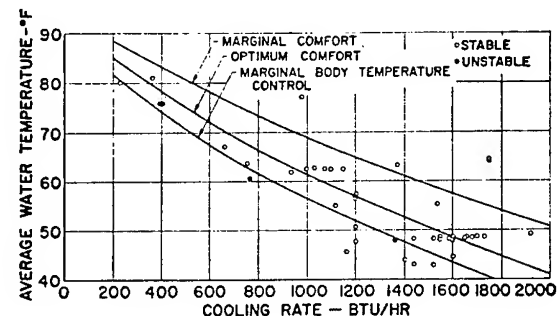
Figure 6-51

Effect of Water Temperature on the Performance of Prototype Liquid-Cooled Suits



a. Suit Performance for an Early Prototype Liquid-Cooled Suit.

(After Burton⁽⁵⁰⁾)



b. Cooling Garment Operating Limitations of Average Water Temperature and Cooling Rate for Several Prototype Apollo Suits.

(After Jennings⁽¹¹³⁾)

If the cooling requirement for a given thermal situation is accurately known, the appropriate line on Figure 6-51a gives a family of suitable inlet temperature and flow combinations to meet the requirement. The inlet temperature coordinate has a lower limit of 32°F because for all practical purposes pure water can only exist in liquid form above this temperature and because of the possibility of causing local frostbite. The upper limit of inlet temperature has been set at 113°F because it has been found that temperatures above this are liable to burn the skin. Mass flow coordinates extend up to 150 lb/hr because this is about the maximum flow of which this specific suit is capable. It is seen that the suit should be capable of absolute maximum cooling rates of 1930 BTU/hr, and heating rates up to 700 BTU/hr at a flow of 150 lb/hr. The heat transfer range is not very much reduced if the flow is cut by half to 75 lb/hr because of the compensating increase of effectiveness. If the

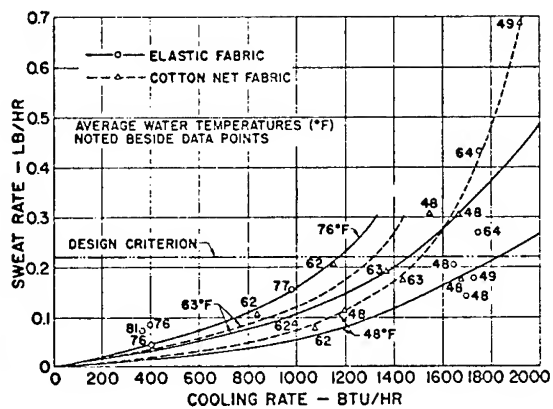
cooling requirement is accurately known the performance equation of Figure 6-51a should specify inlet temperatures to about 2°C ($\sigma = 1.81^{\circ}\text{C}$) or 32°F . The optimum mass flow will be determined not only by metabolic factors but also by tradeoffs on battery vs. cooling sublimator weight (125).

Figure 6-51b gives the average water temperature vs. cooling rate for all test runs of several Apollo prototype suits (113). The boundary envelope follows approximately the limits of comfort, since tests were not run beyond the edge of serious discomfort. The points marked unstable were those runs in which the rectal temperature did not approach a constant value for some reason, usually because of excessive cooling.

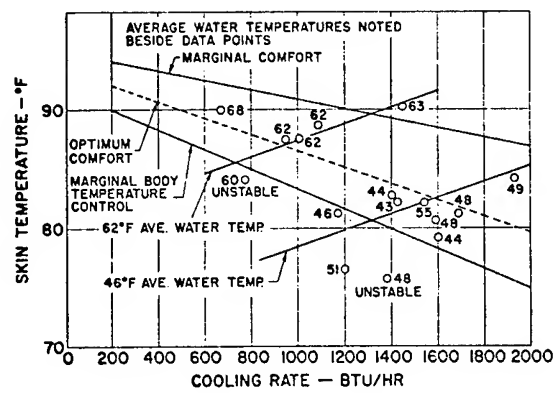
Other methods of evaluating suit function are the sweat rate, skin temperature and rectal temperature responses. Figure 6-52a shows that sweat

Figure 6-52

Physiological Response to Several Apollo Prototype Liquid-Cooled Garments
(After Jennings⁽¹¹³⁾)



a. Sweat Rate as a Function of Cooling Rate at Constant Average Water Temperature.



b. Skin Temperature as a Function of Cooling Rate at Constant Average Water Temperature. Subjective Comfort Zone Boundaries are Superimposed.

rates for the Apollo prototype elastic fabric garments (solid curves, CG7, CG6, CG10) are lower than for the cotton net fabric garments (dashed curves, CG3, CG3A) because of better skin contact with the former. Subjective reaction to elastic garments was that the apparent temperature distribution was more uniform. The horizontal line at 0.22 lb/hr sweat rate represents a design objective. Water inlet temperatures were recorded at 45° , 60° and 75°F for the elastic garments, and at 45° and 60°F for the cotton net.

Measurements of skin temperatures at 6 to 9 positions on the body were weighted according to local body areas and averaged. Figure 6-52b depicts mean skin temperature vs cooling rate for 46 and 62°F average water temperatures. Two additional solid curves define approximate boundaries at which various test subjects complained of excessive cold or warmth. An estimated optimum comfort line (dashed) starts from a skin temperature of 92°F and 200 Btu/hr cooling rate corresponding to 400 Btu/hr metabolic.

Figure 6-53 compares the equilibrium rectal temperatures attainable for different suit systems at various metabolic rates.

The recommended distribution of tubing in a typical water-conditioned suit (for use at rest) required to give no local overcooling is seen in Figure 6-54a (51). Unfortunately, requirements brought about by severe exercise conditions may alter this distribution (113, 213). Distributions used in the early prototype Apollo suits are shown in Figure 6-54b. The rationale for this approach was as follows: "Cooling tubes were connected to supply and return manifolds. By designing for low water velocity, the system losses were mainly from wall friction (losses at bends, entrances, and exits were small). The use of equal manifold-to-manifold tube lengths insured uniformity of flow distribution throughout the garment. Local tube length distribution of Table 6-54b was made proportional to body mass distribution, on the assumption that regional heat generation during work would be nearly proportional to the regional mass of muscle tissue. Coolant was supplied at the garment extremities and returned from the waist in accordance with observed conditions of comfort at rest, in which extremities are maintained cooler than the mid-region of the body. Water temperature rise along the cooling tubes was intended to be limited to comfortable ranges by control of the water flow rate, and by the layout of the tube patterns on the garment, including on the torso where necessary reversals of direction were kept small. The tubes were not extended over the hands, feet, or head. Internal cooling by means of blood circulation was relied upon for the cooling of these parts, which, fortunately, do not generate large quantities of heat as do the massively muscled parts of the body."

Open mesh fabric was used as the garment structure to which the tubes were attached. This choice was made to permit compatible operation in a pressurized space suit supplied with ventilation gas but no circulating water by a cabin life support system. Body cooling by evaporation of sweat would be enhanced by gas circulation through the mesh. The stretch characteristic of the net fabric further afforded snugness of fit. The tubes generally were laid out in patterns following the 45° slope of the net strands, or in meandering paths between parallel boundaries, so that the garment's two-way stretch with body displacement was not impaired. The later garment, CG7, of one-way stretch elastic fabric, had tubes laid out in straight lines along the grain of the material.

The tube wall thicknesses were selected to reduce the likelihood of collapse from external loads or sharp bends. Transparent 0.063-in. i.d. x 0.031-in. wall polyvinylchloride (PVC) tubing was chosen for its flexibility and durability and to permit visual inspection of joint bonds and gas bubbles; supply and return tubes (0.188-in. i.d. x 0.063-in. wall) were of stiffer PVC to increase wall support.

Tubing was fastened to the garment by stitching while the garment was distended over a flat form having dimensions corresponding to body semi-circumferences. Tack stitches were taken through mesh cross strands on each side of tube with the thread crossing over the tube. The tube thereby followed the strand centerline and had no noticeable effect upon garment flexibility. For CG1, each cooling tube was 74 in. long, and ten started at

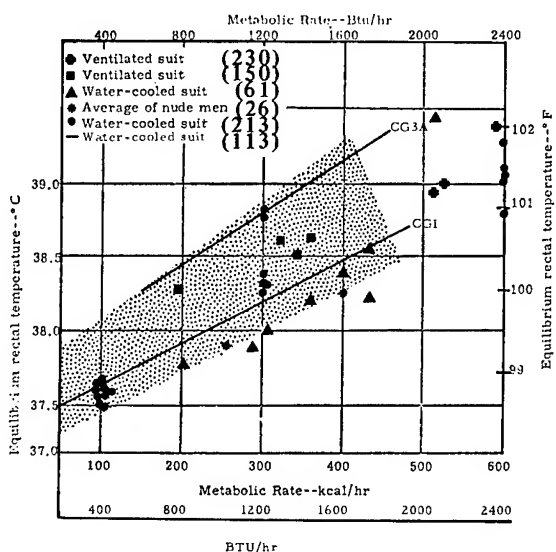


Figure 6-53

A Plot of Rectal Temperatures at Equilibrium (thermal balance) Versus Work Level, Incorporating Data from Many Sources. The shaded area is an envelope of data from 5 sources (212). The solid lines represent the range of prototype Apollo suit systems, CG1 and CG3A (113).

(Adapted from Webb and Annis (213) and Jennings (113)).

Table 6-54
Distribution of Tubing and Cooling in Liquid-Cooled Suits

a. Recommended Distribution of Tubing in Water-Conditioned Suit at Rest.

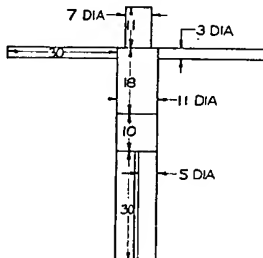
Region	Percentage of Tubing	
1/2 Head	0	
Hand	0	
Foot	0	
Forearm	9.3	
Arm	16.9	
1/2 Back	10.0	
1/2 Chest	8.8	
Calf	18.1	
Thigh	25.6	
Buttock	4.5	
1/2 Abdomen	6.8	
		(After Burton and Collier (51))

b. Tube Distribution Calculation Based on Body Mass Distribution Used in Apollo Prototype Liquid-Cooled Garments (CG1)

Vol., in. ³	Wt., lb	Area, ft ²	Distributed volume and area ^b						
			Vol. fraction	Area fraction	Height, in.	Vol. fraction	Area fraction	Tube length, in.	Tube length fraction
Arm, each	212	7.6	0.045	0.104	...	0.049	0.114	15.4	0.052
Upper torso ^a	855	30.8	0.182	0.115	18	0.201	0.126	58.6	0.198
Lower torso ^a	475	17.1	0.102	0.084	10	0.111	0.070	33.4	0.113
Leg, each	589	21.2	0.126	0.173	30	0.130	0.190	40.6	0.137
Total	4685	168.8	1.000	1.000	69

* Left or right half, each.

^a Includes distributed portion for head.



(After Jennings (113))

each wrist and ankle. Other suits had 232 ft of tubing in contact with the skin. Of the total 247 ft of tubing, 232 ft made contact with the skin. Tubes were attached to a two-piece, medium-size, net fabric undergarment of about 7/16-in. mesh. Supply and return tubes followed zigzag patterns from waist to ankles and elbows for flexibility. They were attached to the cooling tubes by cementing to molded PVC connectors." In addition to the liquid cooling, heat transfer by conduction through gas at the surface of tubes and adjacent skin is available in these garments. For example, for a 0.12-in. heat-transfer distance through O₂ at 3.5 psia and 85°F and adjacent surfaces 0.12 in. wide on the skin and the tube at each side, the heat transfer over 300 ft of tubing with 50°F water will be 334 Btu/hr, or about 19% of the 1800 Btu/hr desired.

Other reviews of the efficacy of liquid-loop suit designs are available (61, 125, 177, 207, 210, 213, 231). Data on the latency of cooling after exercise loads have recently been gathered and are most useful for design of thermal regulators for liquid-cooled suits (213).

Liquid cooled suits create the unusual condition of sweating with a cool skin (12, 16). The effect of skin cooling on expected sweating response to high body core temperatures may be seen in Figure 6-70. Figures 6-52b and 6-55 give shivering and sweating thresholds for subjects in Apollo prototype liquid-cooled suits. Extravehicular suits for lunar operations must be designed to remove at least 2000 BTU/hr (500 kcal/hr) of heat and remain within these thresholds of sweating and shivering (125, 173). Automatic temperature control for liquid-cooled suits is now under study (142, 213).

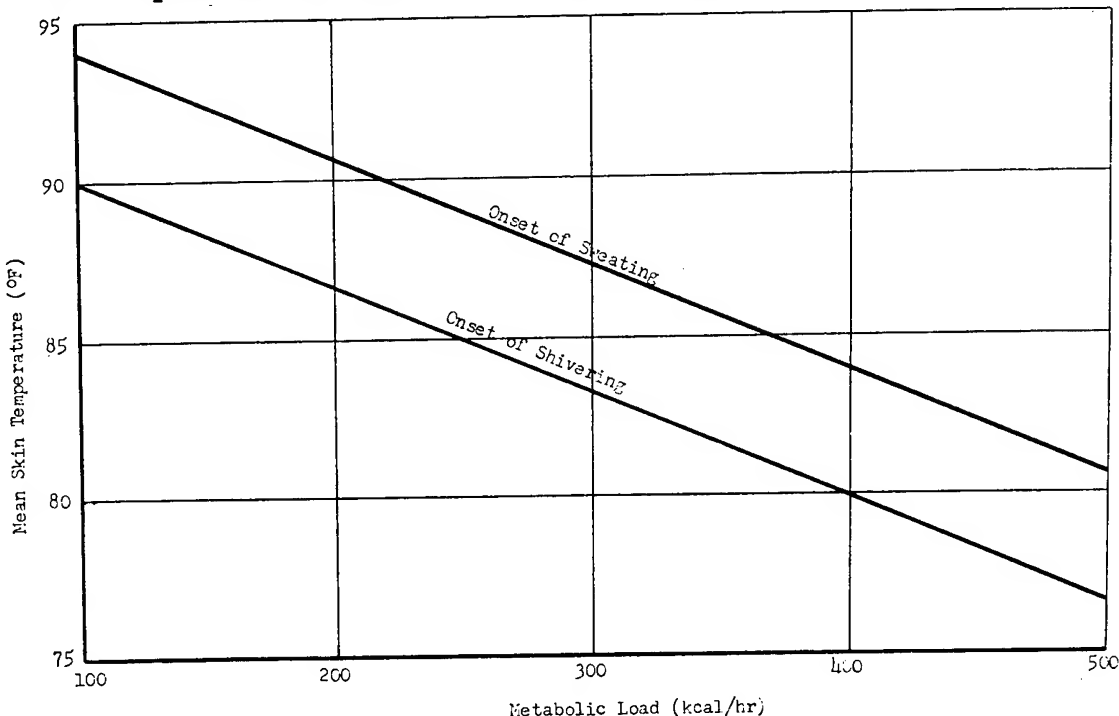


Figure 6-55
Comfort Thresholds of Sweating and Shivering in a Prototype Liquid-Cooled Apollo Suit
(After Lang and Syversen⁽¹²⁵⁾)

Another approach to the cooling of space suits is the passive control system. Concepts including passive heat sinks, semi-permeable membranes, and wicking systems involving the pressure-retaining structures of the suits are being considered (159, 167, 168, 181, 182, 209).

Conductive Heat Exchange (q_k)

In the thermal analysis of man in an open environment, conductive heat exchange can, in many instances, be assumed to be included in the computations for radiation and convective heat exchange. This is justified, for the latter cannot exist if conduction is occurring over a given area. In addition, body heat lost by conduction will usually be transferred to the environment by radiation or convection modes. Liquid cooling garments, require that physiological constraints to conductive cooling modes be quantifiably identified. These constraints include sensitivity to thermal and pressure gradients on the skin surface, tube-to-skin contact resistance, skin resistance, temperature ranges (for comfort) of the body parts, and the effects of hair and perspiration on conductive exchange.

Unfortunately, the liquid-cooled space suit is worn under exercise conditions where skin comfort temperatures, thermal conductances to deeper subcutaneous structures, and similar factors are quite different from the resting condition (113, 213). The characteristics of the skin in thermal comfort as represented by Figure 6-29 and Tables 6-57, 6-58, 6-64, and 6-65 cannot be used under the unusual environmental condition of exercise in a liquid-cooled suit. Specific data are needed on the determinants of skin comfort under such conditions (113). Figure 6-55 is a good example of the type of data needed.

In the determination of heat conduction in the steady state, the following equation may be used for conditions other than space suits (39).

$$q_k = h_k (t_1 - t_2) \quad (39)$$

and

$$h_k = \frac{k}{L}$$

where q_k = conductive heat transfer - BTU/ft² hr (kcal/m² hr)

$$h_k = \text{thermal conductance} - \frac{\text{BTU-inch}}{\text{ft}^2 \cdot \text{hr} \cdot {}^\circ\text{F}} \quad \frac{\text{kcal-cm}}{\text{m}^2 \cdot \text{hr} \cdot {}^\circ\text{C}}$$

t_1, t_2 = temperature of surfaces - ${}^\circ\text{F}$ (${}^\circ\text{C}$)

k = thermal conductivity BTU/in sec ${}^\circ\text{F}$ (kcal/cm sec ${}^\circ\text{C}$)

L = thickness of the conducting medium inches (cm)

In the resting condition, the thermal conductivity constant, k , for conducting heat from the interior of the body to the skin (tissue conductance only) is:

$$k = 1.5 \pm 0.3 \times 10^{-3} \text{ kcal/cm sec}^{\circ}\text{C} \text{ (at } 23\text{-}25^{\circ}\text{C ambient)}$$

At full vasoconstriction, when tissue conductance is $9\text{-}10 \text{ kcal/m}^2/\text{hr}^{\circ}\text{C}$ the value for conductance corresponds to a tissue layer 1.8-2.2 cm thick. At the limit of vasodilation, thermal conductance is increased to values of 28-30 $\text{kcal/m}^2 \text{ hr}^{\circ}\text{C}$. Values above and below these limits have been reported in the literature. However, many of the subjects may have become acclimated by the tests and accordingly, their values of conductance would exceed the norm. As a rule of thumb, a change from full vasoconstriction to full vasodilation lowers thermal resistance of the body approximately 1 Clo unit.

Figure 6-29 represents typical local skin conductances of local body areas at rest in still air at sea level. Tables 6-58, 6-64, and 6-65 present thermal conductivity and inertia data of body parts which may be of value in evaluating conductive heat loss and discomfort thresholds at rest. Equivalent thermal conductance between adjacent radial layers of head, trunk, and extremities has recently been suggested. Assuming the specific conductivity of tissue of $36 \text{ kcal cm/m}^2 \text{ hr}^{\circ}\text{C}$ (194) physiologically effective masses and heat capacitance of different body compartments have also been calculated. Measure of the effectiveness of vascular convective heat transport can be made quantitatively by deriving values of thermal conductance for the peripheral tissues of the body (194). Cardiovascular changes such as shunting during exercise considerably complicate such calculations and are, unfortunately, key factors in operational situations where such data are sorely needed (168).

The commonly used expression for conductance is:

$$K = \frac{q_m - q_s - q_v}{t_r - t_s} \text{ BTU/hr ft}^2 {}^{\circ}\text{F} \text{ (kcal/hr m}^2 {}^{\circ}\text{C)} \quad (40)$$

where the terms on the right side of the equation are as previously defined.

Values of thermal conductance as a function of operative temperature are shown in Figure 6-56 (80).

The large difference in the two cases between the rate of rise in peripheral circulation with increasing operative temperature indicates the relative economy in vascular effort provided by the process of evaporation in air. An expression for nude human conductance, h_o , in air is:

$$h_o = 7.0 (0.48 + 0.52 \sqrt{\frac{\bar{V}}{7.6}}) \text{ kcal/m}^2 \text{ hr}^{\circ}\text{C} \quad (41)$$

\bar{V} = atmospheric velocity in cm/sec

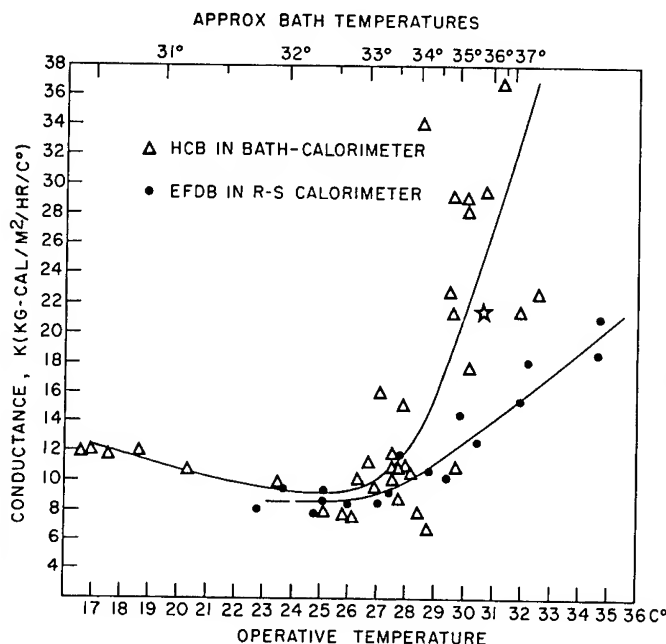


Figure 6-56

The Relation Between Conductance (A Measure of Peripheral Blood Flow) and Operative Temperature for a Subject (EFDB) in the Dubois-Hardy Calorimeter, and Another (HCB) in the Burton-Bazett Water Bath Calorimeter.

(After Gagge⁽⁸⁰⁾)

HEAT STRESS AND TOLERANCE

To establish indices of thermal stress and tolerance in space operations, data are required beyond those for basic comfort limits such as presented in Section 2. Such variables as body temperature, sweating response to thermal loads, pain and discomfort thresholds for heat and cold, body stress indices, and performance under thermal stress must be evaluated. The role of dehydration in thermal tolerance has been covered in Water (No. 15).

Body Temperature

The body temperatures of interest in biothermal analyses are mean body temperature (t_b), rectal temperature (t_r), and skin temperature (t_s).

Mean Body Temperature (t_b)

Mean body temperature is the weighted average of rectal and skin temperature. The weighting varies with ambient temperature (194). In accordance with the Burton expression, (for $t_a < 30^\circ\text{C}$):

$$t_b = 0.67 t_r + 0.33 t_s \quad ^\circ\text{F} \quad (\text{°C}) \quad (42)$$

In the heat ($t_a > 30^\circ\text{C}$), the weighting is 1:9 for $t_r:t_s$. Mean body temperature is used primarily as a parameter in determining heat storage as seen in Equation 47.

Table 6-57

Mean Surface Temperature at Various Stations on a Supine Human Subject
at Rest in Still Air at Sea Level

(After Iberall and Cardon⁽¹¹¹⁾)

Station No. & Name	Mean Ambient Temperature (°C) of:						
	1			2		3	
	21.0±.2	20.0±.1	20.5±.3	29.0±.2	29.0±.1	35.0±.3	34.0±.2
1 Forehead	33.8±.4	32.4±.3	---	35.2±.2	35.7±.3	35.5±.3	36.1±.6
2 Left Shoulder	31.8±.3	30.1±.7	32.7±1.6	34.2±.1	35.8±.5	35.6±.4	36.7±.4
3 Left Bicep	31.0±.2	30.5±.4	34.0±.4	33.9±.1	35.7±.1	36.2±.2	36.7±.2
4 Left Forearm	30.1±.3	28.9±.5	31.2±1.1	33.5±.2	36.0±.1	37.0±.3	36.1±.4
5 Index Finger	22.6→20.3 22→19.6	22.6±1.0	26.6±1.0	33→28.2	36.5±.2	35.0→30	37.6±.2
6 Upper Chest	---	35.5±.2	29.9±.8	34.6±.2	35.7±.1	36.0±.8	42.6→35.2
7 Sternum	32.4±.2	31.6±.2	32.8±.5	34.9±.1	36.1±.2	39.3±.2	36.7±.2
8 Mid-Abdomen	30.8±.1	30.1±.3	33.2±.4	34.4±.1	38.7±.3	35.4±.1	33.6±.2
9 Left Thigh (Anterior)	---	27.0±.3	29.3±.4	33.8±.1	34.9±.1	35.5±.2	36.2±.4
10 Left Leg (Anterior)	27.9±.3	27.1±.6	28.3±1.3	32.7±.4	34.0±.1	35.2±.1	35.9±.2
11 Toe	19.5→20.3 21.5→19	21.5±.8	31.5→28	35.4±.3	36.3±.1	37.1±.1	
12 Neck (2-3 Cervical Vert.)	32.2±.4	32.2±.8	29.9±.8	34.1±.2	35.3±.3	36.1±.3	36.8±.1
13 Upper Back (2-3 Thoracic Vert.)	33.0±.2	32.4±.5	31.3±.4	34.8±.3	35.4±.1	35.7±.3	35.5±.4
14 Mid-Back (6-7 Thoracic Vert.)	33.0±.2	30.2±.3	31.9±.2	34.7±.2	34.5±.2	35.8±.1	34.7±.2
15 Lower Back (Lumbar Region)	33.4±.1	31.4±.2	27.9±.5	34.6±.4	33.3±.5	38.3±.2.4 35.0±.3	
16 Right Buttock	30.6±.1	32.1±.3	29.6±.5	31.7±.3	33.6±.2	35.8±.2	36.1±.3
17 Right Thigh (Posterior)	31.2±.2	28.5±.2	29.9±.5	33.8±.1	35.5±.5	35.8±.2	37.3±.4
18 Right Leg (Posterior)	28.3±.3	25.8±.5	28.2±1.0	32.5±.3	34.5±.3	35.9±.1	36.7±.3
19 Right Heel	21.4→19	23.5→20	22.1±.6	31.4→28	34.4±.3	35.7→34	36.2±.2
Mean (Gross)	29.6±.3	28.9±.4	29.7±.7	33.3±.2	35.3±.3	36.0±.4	36.3±.3
Mean (Weighted)	30.4±.3	29.6±.4	30.1±.7	33.7±.2	35.2±.3	36.1±.4	36.2±.3

Rectal Temperature (t_r)

Rectal (or core) temperature varies as a function of activity level and is environment independent for ambient conditions extending well above the comfort zone. A complete discussion of rectal temperature variations with activity and environmental conditions follows below. Diurnal sensitivity must always be considered along with effects of leg experience (72).

Skin Temperature (t_s)

Figure 6-29 represents the preferred skin temperatures at different body sites at rest in still air under sea level pressures. Table 6-57 shows variations in skin temperature at various locations on the human body for a range of ambient temperatures between 68 and 95°F (20 and 35°C) at rest in air at sea level pressure.

An expression weighting the various stations of the human body for use in determining mean skin temperature for Apollo design purposes is as follows (148):

$$t_s \text{ (mean)} = \frac{12t_{\text{back}} + 12t_{\text{chest}} + 12t_{\text{abdomen}} + 14t_{\text{arm}} + 19t_{\text{thigh}} + 13t_{\text{leg}} + 5t_{\text{hand}} + 7t_{\text{head}} + 6t_{\text{foot}}}{100} \quad (43)$$

Table 6-58 gives thermal properties of the skin which may be used in evaluation of tolerance thresholds.

Below 23°C ambient air temperature, only a fraction of the area of the body is regulated in accordance with the expression (111).

$$f = \frac{A_r}{A_b} = \frac{9}{33 - t_a} \quad (44)$$

where A_r = area of body regulated

A_b = total surface area of the body

t_a = ambient air temperature (°C)

Figures 6-59a, 6-59b, 6-60a, b, c, 6-61, 6-62, and 6-63 represent the response of body core (rectal) and skin temperature to heat stress produced by ambient conditions and metabolic loads. Corresponding curves for atmospheres other than air at sea level are under study (73). Response of body temperatures to various thermal and metabolic conditions in ventilated and liquid-cooled suits is summarized in Figures 6-52, 53, 55, and Reference (149).

Figures 6-100, 6-102c, and 6-107 represent response of various body temperatures to the cold. Skin temperature responses of different populations

Table 6-58

Properties of the Skin

(After Blockley⁽³⁰⁾ from Data Compiled by Buettner⁽⁴⁰⁾ and Stoll⁽¹⁹³⁾)

Approximate values of the physical dimensions of whole skin for the "average man": 154 lb, 5'7"

Weight	8.8 lb	4 kg
Surface area	20 sq ft	1.8 m ²
Volume	3.7 qt	3.6 liters
Water content	70 - 75%	
Specific gravity	1.1	
Thickness	0.02 - 0.2 in.	0.5 - 5.0 mm

Approximate values for thermal properties of skin:

Heat production	240 kcal/day
Conductance	9 to 30 kcal/m ² hr °C
Thermal conductivity (k)	(1.5 ± 0.3) × 10 ⁻³ cal/cm sec °C, at 23 - 25°C ambient
Diffusivity (k/pc)	7 × 10 ⁻⁴ cm ² /sec (surface layer 0.26 mm thick)
Thermal inertia (kpc)	90 to 400 × 10 ⁻⁵ cal ² /cm ⁴ sec (°C) ²
Heat capacity	~0.8 cal/gm

Skin temperature and thermal sensation:

Pain threshold for any area of skin	113°F (45°C)	The typical sensation is:
When mean weighted skin temperature is:		
above 95°F (35°C)		unpleasantly warm
93°F (34°C)		comfortably warm
below 88°F (31°C)		uncomfortably cold
86°F (30°C)		shivering cold
84°F (29°C)		extremely cold
When the hands reach:	When the feet reach:	They feel:
68°F (20°C)	73.5°F (23°C)	uncomfortably cold
59°F (15°C)	64.5°F (18°C)	extremely cold
50°F (10°C)	55.5°F (13°C)	painful and numb

Approximate optical properties of skin:

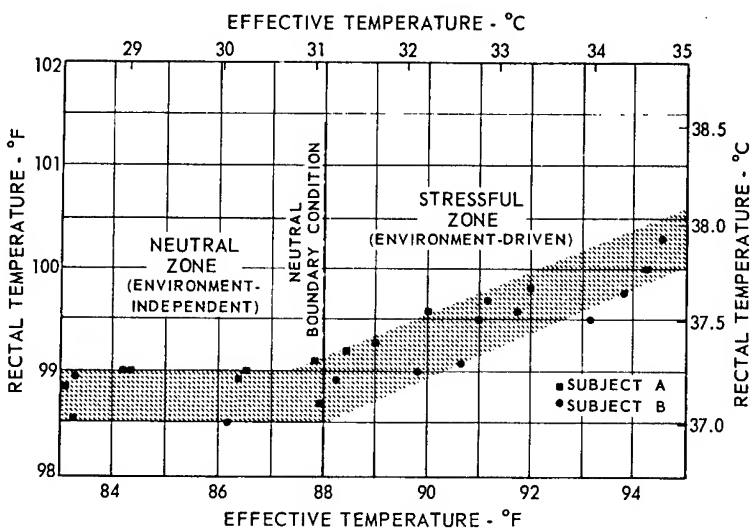
Emissivity (infrared)	~0.99
Reflectance (wave-length dependent)	Maximum 0.6 to 1.1μ Minima <0.3 and >1.2μ
Transmittance (wave-length dependent)	Maxima 1.2, 1.7, 2.2, 6, 11μ Minima 0.5, 1.4, 1.9, 3, 7, 12μ
Solar reflectivity of surface	
Very white skin	42%
5 "white" subjects	28 - 40%, average 34%
6 "colored" subjects	19 - 24%, average 21%
Very black skin	10%
Solar penetration--very white skin	45.5% passes 0.1 mm depth 39.6% passes 0.2 mm depth 32.0% passes 0.4 mm depth 19.0% passes 1.0 mm depth 10.2% passes 2.0 mm depth
Solar penetration--very dark skin	75% passes 0.1 mm depth 40% absorbed in the melanin layer 35% passes 0.2 mm depth

Figure 6-59
Body Temperatures at Rest

a. Body Temperature as a Function of Effective Temperature in Heat

(After Blockley⁽³⁰⁾ Adapted from Macpherson⁽¹⁴⁰⁾)

This graph relates the final rectal (core) temperature of resting men to a range of environmental heat stress. Each data point shows the level of rectal temperature observed in two men wearing coveralls and seated while exposed to dry bulb temperatures from 90 to 120°F and wet bulb temperatures from 83 to 88°F (E. T.'s from below 84 to above 94°F). In the region labeled "neutral zone," which extends well above the comfort zone, while other parameters such as skin temperature, heart rate, and sweat rate are increased with each successive increase in stress, core temperature remains independent of the environmental heat stress. Further increases in heat stress index beyond the "Neutral Boundary Condition" for the activity, clothing, and state of training concerned produce progressively higher core temperatures. This state of affairs characterizes the "stressful zone," where rectal temperature is environment-driven, and the probability of breakdown, or failure to compensate, becomes progressively higher, particularly for untrained or unacclimatized men.



b. Midpoint Rectal and Skin Temperatures as a Function of Reference Operative Temperature at Rest.

Mean values for the collected series are shown by characteristic symbols. Least Square regression lines have the following equations:

$$t_r = 37.8$$

$$t_s = 34.8 + 0.056(t_{or})$$

(After Blockley et al⁽²⁷⁾)

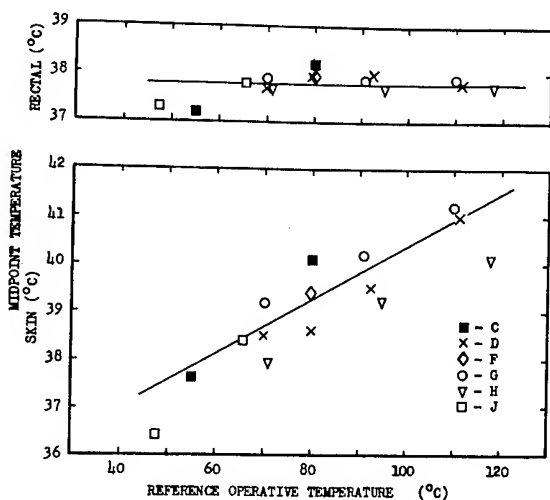


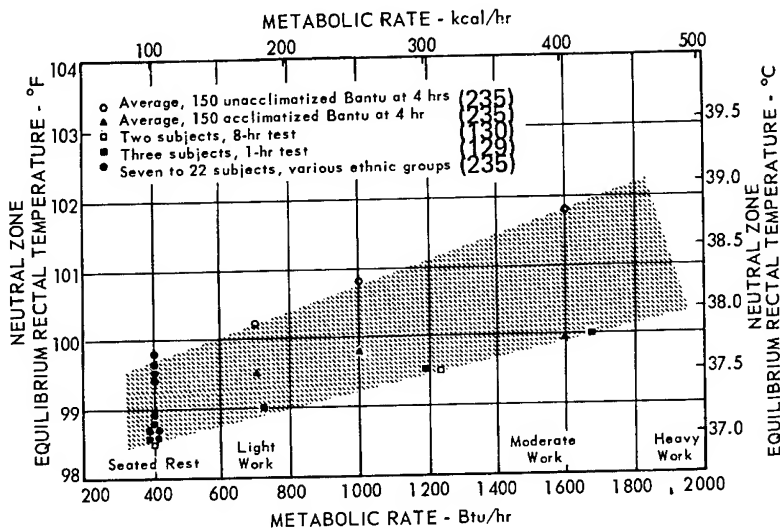
Figure 6-60
Body Temperature at Work in Heat

a. Variations in Rectal Temperature at Sea Level as a Function of Activity

(After Blockley⁽³⁰⁾ Adapted from Hanifan et al⁽⁹⁶⁾. Based on Data from Lind^(129, 130), Strydom and Wyndham⁽¹⁹⁵⁾, and Wyndham et al⁽²³⁵⁾)

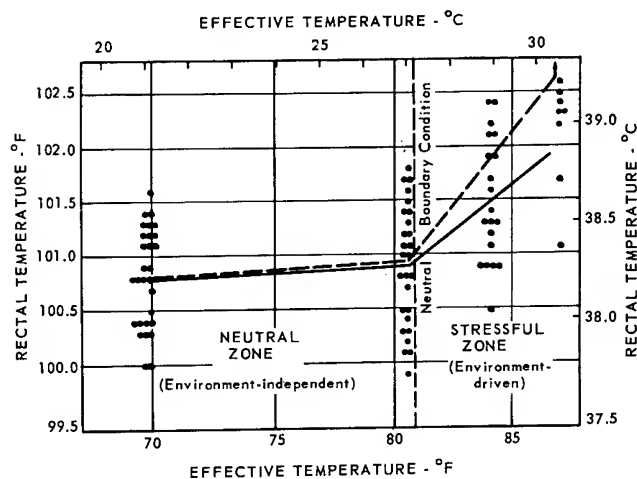
For each level of work, there appears to be a characteristic internal or core temperature at equilibrium which is unaffected by the environment so long as the neutral boundary condition (Figure 6-59a) is not exceeded. As shown here, the characteristic internal (i.e., rectal) temperature for a particular work load varies between groups; both physical training and training for work in the heat (acclimatization) produce lower values. Superficial differences between ethnic groups appear to be due to habit patterns and experience relative to working under hot conditions.

Note that persons completely untrained for a particular activity or exercise would probably show rectal temperatures considerably higher than those indicated in this chart for African natives recruited for mine labor.



b. Rectal Temperatures and Stress Zones for Work in the Heat at Sea Level.

(From Blockley⁽³⁰⁾ Adapted from Leithead and Lind⁽¹²⁷⁾)

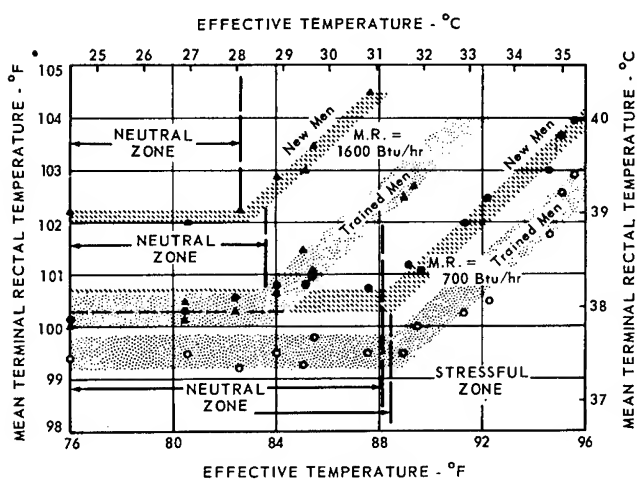


Final rectal temperatures are shown as a function of environmental heat stress for working men in figure b. Each point represents a single exposure of a different man--approximately 30 men in each environment, or a total of 128 untrained subjects. The task was three hours of treadmill marching at 3.5 mph wearing shorts; the metabolic rate was 300 kcal/hr. Only in the two environments that lie in the Neutral Zone did all subjects complete the task. In the two hotter climates, 25% and 57% of the subjects had to be removed before the end of the period because of excessive heart rates or rectal temperature, to prevent collapse or damage. The dashed line on the graph connects the median values of final rectal temperature for all subjects, while the solid line connects the means for those subjects completing the full three hours.

Figure 6-60 (continued)

c. Rectal Temperatures and Stress Zones for Work in the Heat at Sea Level.

(After Blockley⁽³⁰⁾ Drawn from Data of Wyndham et al⁽²³⁵⁾)



In figure C, each point is the average of a group of ten men; the chart thus summarizes data from approximately 460 individuals, 2 work rates, and 15 different humid environments. The vertical lines delineate the boundary conditions separating the "Neutral" (environment-independent) and "Stressful" (environment-driven) zones before and after training.

Clearly illustrated is the effect of heat training (acclimatization) on the equilibrium rectal temperature, and the small, probably insignificant effect of training on the location of the Neutral Boundary. Note that in the "Neutral" zone, heat-trained men working at 1600 Btu/hr maintain body temperatures as low as or lower than novice workers working at 700 Btu/hr; however, when both groups are in the "Stress Zones" for their respective work levels, the difference between their mean body temperatures is 1.5°F. For comparison, new men working at 1600 Btu/hr have temperatures 1.5°F higher than similar men working at 700 Btu/hr, when both are in their neutral zone of environments.

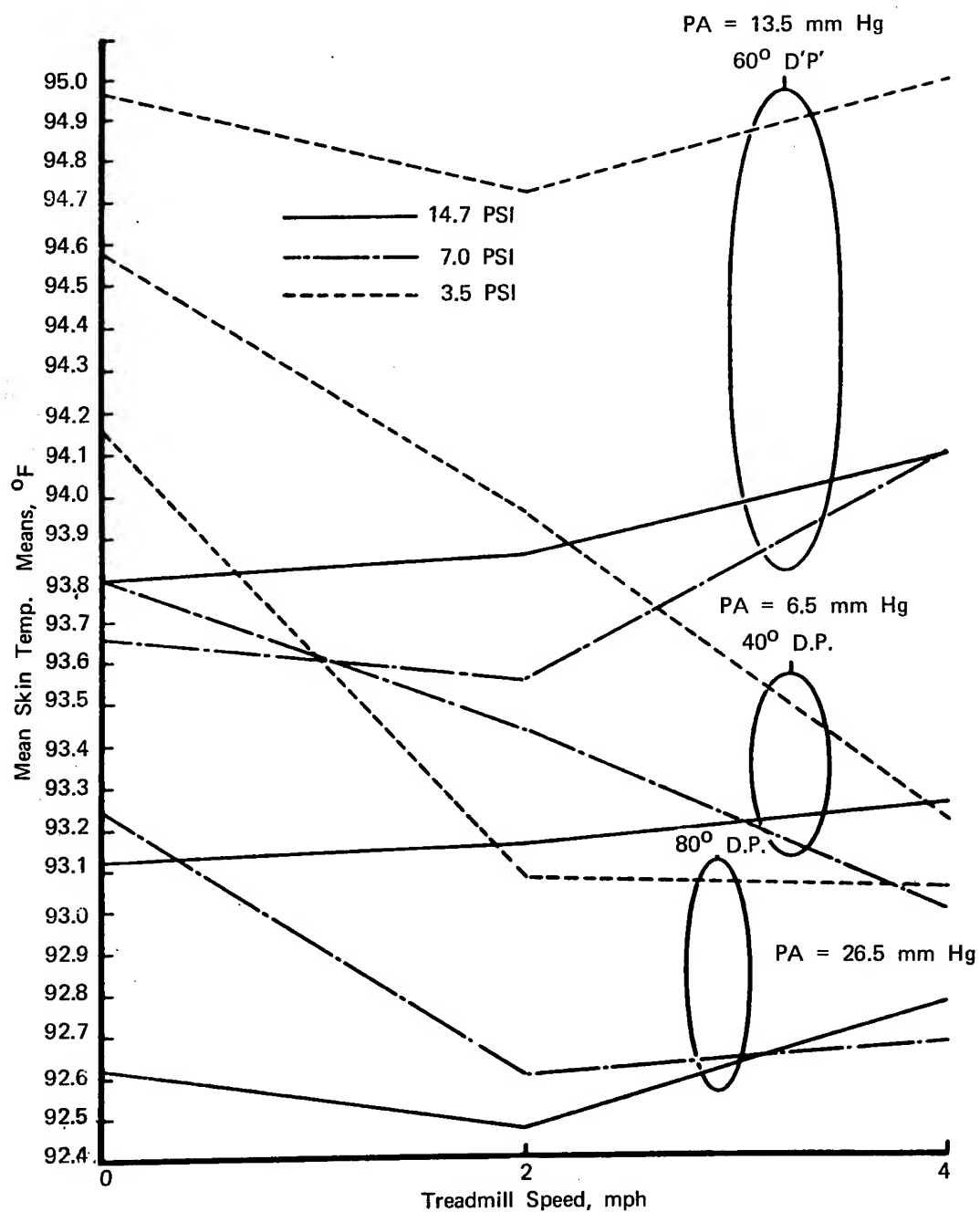


Figure 6-61

Mean Skin Temperature, °F, as a Function of Treadmill Speed, Miles Per Hour, at 95°F
Dry Bulb in Shirt-Sleeve Environment

(After Wortz⁽²³²⁾)

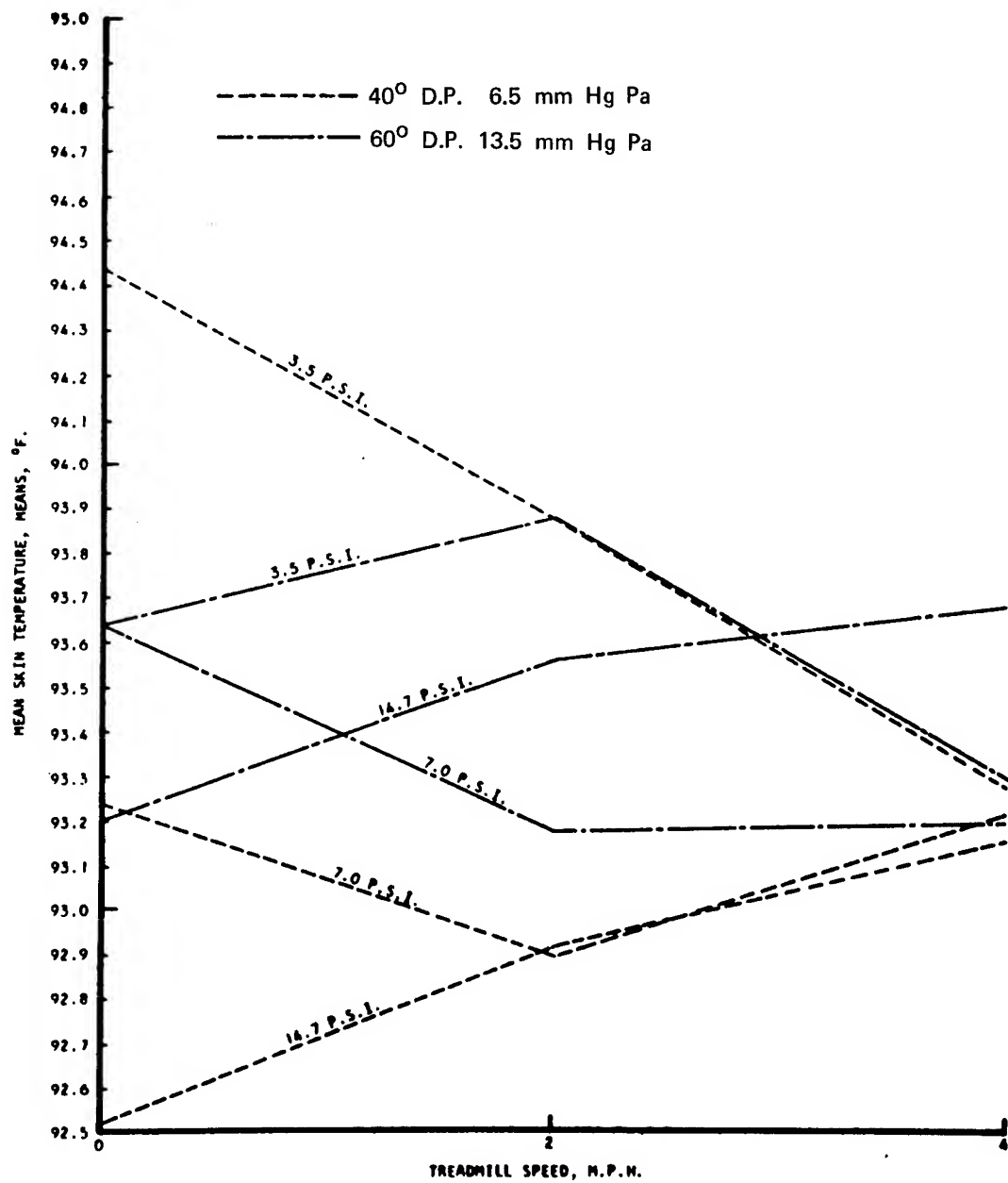


Figure 6-62

Mean Skin Temperature, °F, as a Function of Treadmill Speed, Miles Per Hour, at 75°F Dry Bulb in Shirt-Sleeve Environment.

(After Wortz⁽²³²⁾)

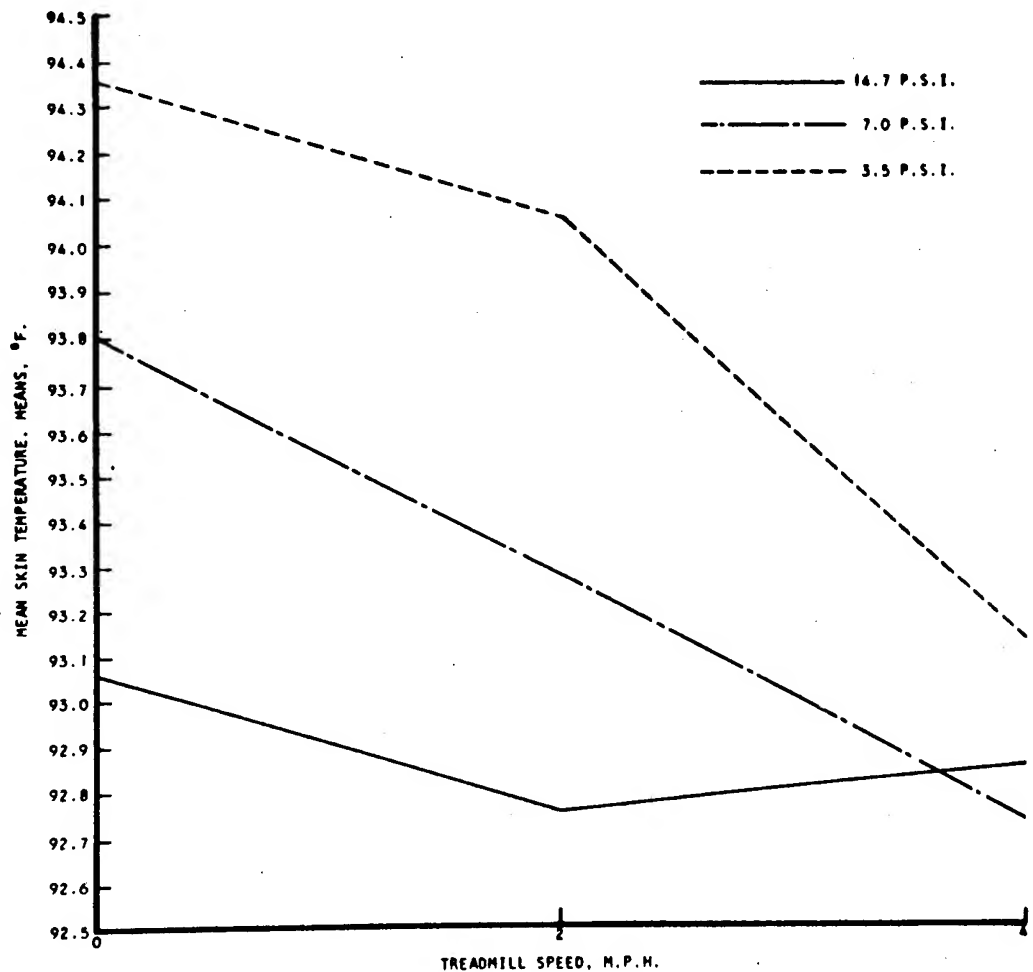


Figure 6-63

Mean Skin Temperature, °F, as a Function of Treadmill Speed, Miles Per Hour, at 55°F
Dry Bulb in Shirt-Sleeve Environment.

(After Wortz⁽²³²⁾)

to sleep under varied environmental temperature are available (72). The general increase in Clo value required for comfort in a cool environment during sleep must always be considered.

Figure 6-29 and Tables 6-64 and 6-65 represent odd aspects of the thermal characteristics of "the average man" at rest which can be used in the analysis of local thermal effects and tolerances in air at sea level.

Sweating and Respiratory Water Loss

Heat stress may be measured by the rate of water loss by the body. Analysis of the evaporative heat exchange mode in unusual atmospheres has been presented above. Tables 6-26 to 6-33, Equations 23-26, and Figures 6-29 to 6-34, and 6-50 may be used to obtain appropriate data for design and operational analysis under the specific limitations noted.

In addition to these data for space operations, Figures 6-66 to 6-69 represent the sweat production rates to be expected under survival conditions on Earth. Additional data on sweating are available in Water (No. 15) and Reference 215.

Inside a liquid-cooled suit, a heavily working man may have a high core temperature but a low skin temperature. The expected sweat response may thus be altered as seen in Figure 6-70. Retention of CO₂ may also alter the set point of sweating. The sweating rate in 6% CO₂ at sea level air may be 100% greater than in normal air (42).

Figure 6-71 represents the sensitivity of water loss through respiration to metabolic rate, ambient pressure and dewpoint (115). Rates of nonthermal sweating are about 80-220 gms/hr from covered areas and 20-40 gms/hr from the rest of the skin (26, 34, 215). This can be increased by psychogenic stimuli of many types (2, 215).

Heat Stress Indices

In the non-compensable zones of thermal control, performance and tolerance have an inverse exponential relationship with exposure time. Figure 6-72 reflects the general time-tolerance relationship for extremes of ambient air temperature under sea level conditions.

Figure 6-73 shows the physiological impairment which may be anticipated due to extremes of body temperature. The tolerance limits reflect the borders of physiological collapse to be used for rough evaluation of situations.

Under conditions of heat stress, the mode of evaporative heat loss cannot completely compensate for the difference between total heat load and heat losses via other modes. This lack may be attributable to failure to achieve a sufficiently high perspiration rate or by failure to achieve a sufficiently high evaporation rate. Even though the perspiration rate is adequate to maintain thermal balance, conditions of high humidity and/or low ventilation

Table 6-64
 Physiological and Thermal Characteristics of the "Average" Man
 (After Breeze⁽³⁶⁾)

<u>CHARACTERISTIC</u>	<u>METRIC UNITS</u>	<u>ENGLISH UNITS</u>	<u>REFERENCE NO.</u>
Weight	68-72 kg	150-160 lbs.	66
Height	170 cm.	68-69 inches	66
Total Body Surface Area	1.8 sq. meters	19.5 ft ²	66
Volume	0.07 meters ³	2.5 ft ³	66
Specific heat	0.8 cal/gm-°C	0.8 Btu/lb-°F	66
Heat Capacity (using 160 lb. man)	57.6 cal/°C	128 Btu/°F	66
Body temperature (rectal)	37°C	98.6 0.5°F	66
Body surface temp.	33-34°C	91-93°F	65
Body and clothing Surface temperature (ave. - 1 Clo)	28°C	82.2°F	108
Body temperature ($\frac{2}{3} t_r + \frac{1}{3} t_s$)	35.6°C	96.1°F	98
Body percent water	70%	70%	65

HUMAN SKIN

Weight	4.0 kg	8.8 lbs.	192, 193
Surface Area	1.8 meters ²	19.5 ft ²	192, 193
Volume	3.6 liters	3.7 Quarts	192, 193
Water Content	70-75%	70-75%	192, 193
Specific Gravity	1.1	1.1	192, 193
Thickness	0.5 mm (Eyelids) to 5 mm (back)	0.02 to 0.2 inches	192, 193
Heat production	13% (Body's Metabolic Heat Prod.)	13%	192, 193

Table 6-64 (continued)

<u>CHARACTERISTIC</u>	<u>METRIC UNITS</u>	<u>ENGLISH UNITS</u>	<u>REFERENCE NO.</u>
Conductance	$9 \rightarrow 30 \text{ kgCal/m}^2\text{-hr. -}^\circ\text{C}$		192, 193
Thermal Conductivity (k)	$1.5 \pm 0.3 \times 10^{-3}$ Cal/cm-sec- $^\circ\text{C}$ at 23-25 $^\circ\text{C}$ Ambient		192, 193
Diffusivity ($k/\rho C_p$)	$7 \times 10^{-4} \text{ cm}^2/\text{sec}$ (Surface Layer 0.26 mm Thick)		192, 193
Thermal Inertia ($k/\rho C_p$)	$90-400 \times 10^{-5}$ cal $^2/\text{cm}^4\text{-sec-}^\circ\text{C}^2$		192, 193
Heat Capacity (Cp)	0.8 cal/gm- $^\circ\text{C}$	0.8 Btu/lb- $^\circ\text{F}$	192, 193
Emissivity (Infrared) Skin and Clothing	- 0.99 - 0.94		192, 193
Reflectance (Wave Length Dependent)	MAX. 0.5-1.1 μ MIN. 0.3 and 1.2 μ		
Transmittance (Wave Length Dependent)	MAX. 1.2, 1.7, 2.2, 6, 11 μ MIN. 0.5, 1.4, 1.9, 3, 7, 12 μ		192, 193

TERM

DEFINITION

Clo Insulation value of that quantity of clothing that will maintain comfortable thermal equilibrium in a man sitting at rest in an environment of: (a) 70 $^\circ\text{F}$ air and wall temperature, (b) less than 50% rel. humidity, and (c) 20 ft/min air movement.

$$1 \text{ Clo} = \frac{0.18 \text{ Deg. F}}{\text{kg-cal/Hr}}$$

$$1 \text{ Clo} = \frac{0.04536 \text{ Deg. F.}}{\text{Btu/Hr}}$$

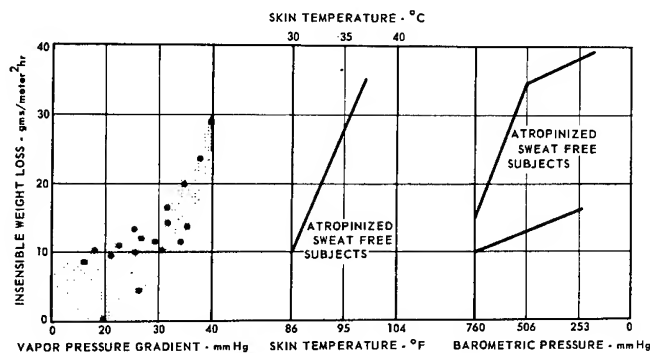
{In combined units
{For 1.8 m 2 Surface Area
{1 kg-cal = 3.968 Btu

Heat Capacity of Body Periphery 40 Btu/ $^\circ\text{F}$ Outer layer to skin as opposed to body core.
Approximately 1.0 inches thick.

Resistance of Periphery Function of body activity and is equivalent to 0.16 to 0.70 Clo

Table 6-65
K ρ C of Various Body Tissues
(After Breeze⁽³⁶⁾)

Tissue	VALUES FROM DIRECT MEASUREMENT (LITERATURE)					
	K (Thermal Conductivity) gm. cals/cm sec °C $\times 10^{-5}$	ρ (density) gms/cm ³	C (Thermal Capacity) gms. cals/gm °C	K ρ C (Thermal Inertia) Cals ² /cm ⁴ °C ² sec $\times 10^{-5}$	Computed	Measured
Fat	43 ± 10	0.92	0.55	22 ± 7	26	
Muscle	83 ± 30	1.27	0.91	96 ± 34	113 (moist) 56 (dry)	
Skin, Dead	70	1.20	0.81	70	66	
Skin, Living					90 (no blood flow) 125 (normal)	
Bone					50	



Loss of water through the skin by diffusion is influenced by the vapor pressure gradient, the skin temperature, and the barometric pressure. On the left, water loss in grams per square meter of body surface per hour is plotted against the difference in vapor pressure in the air and vapor pressure at the skin, as reported by four different authors (34, 93, 216, 239). In the center, a high skin temperature is seen to be related to a high diffusion loss. Warm skin free of sweat was produced by high atropine dosage (216). On the right, the graph shows an increase in diffusion as the barometric pressure is lowered (93, 216).

Figure 6-66
Insensible Water Loss from the Skin as a Function of Absolute Humidity, Skin Temperature, and Barometric Pressure.
(After Blockley⁽³⁰⁾ Drawn from Data of Brebner et al⁽³⁴⁾, Hale et al⁽⁹³⁾, Webb et al⁽²¹⁶⁾ and Zollner et al⁽²³⁹⁾)

Figure 6-67

Water Loss by Sweating Under Different Environmental Conditions
 (After Blockley⁽³⁰⁾ Adapted from a, Adolph⁽³⁾; b, MacPherson⁽¹⁴⁰⁾
 Robinson et al⁽¹⁷⁰⁾, Taylor and Buettner⁽¹⁹⁶⁾, and Webb et al⁽²¹⁶⁾;
 c, Adolph⁽³⁾; d, Thompson Ramo Wooldridge, Inc.⁽²⁰³⁾)

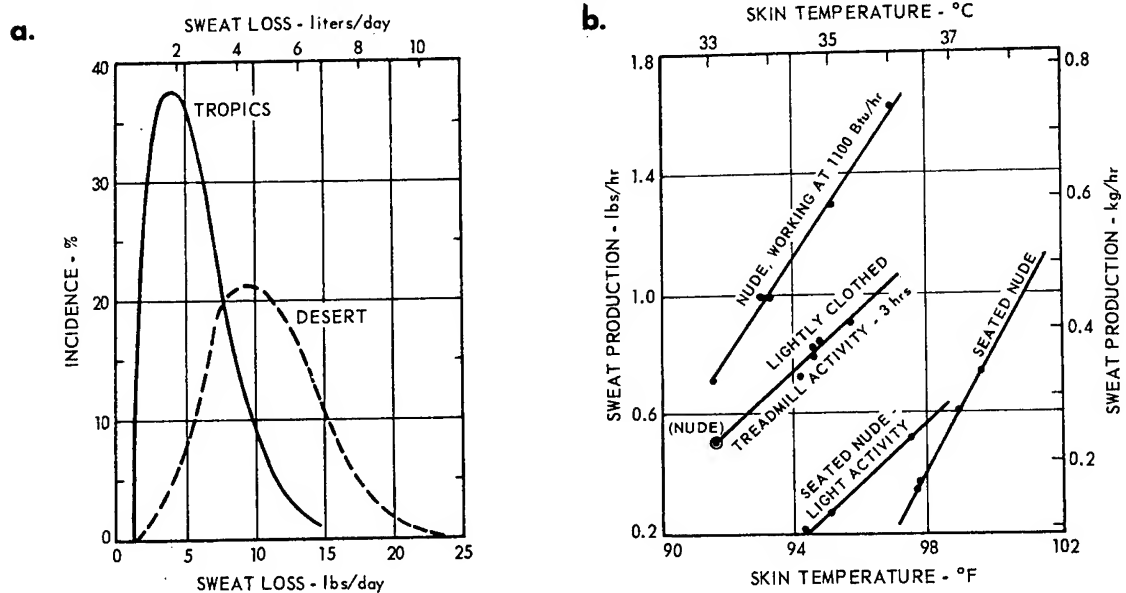


Figure a shows the frequency distribution of daily sweat production for 26 men in the tropics and 97 men in the desert. In figure b, various sweat rates during various laboratory procedures are plotted as a function of skin temperature, to show how variable this relationship is. Air temperature influences sweating in men sitting still in the desert sun, as shown in figure c. Figure d shows sweating and evaporative heat loss varying with air temperature and activity level.

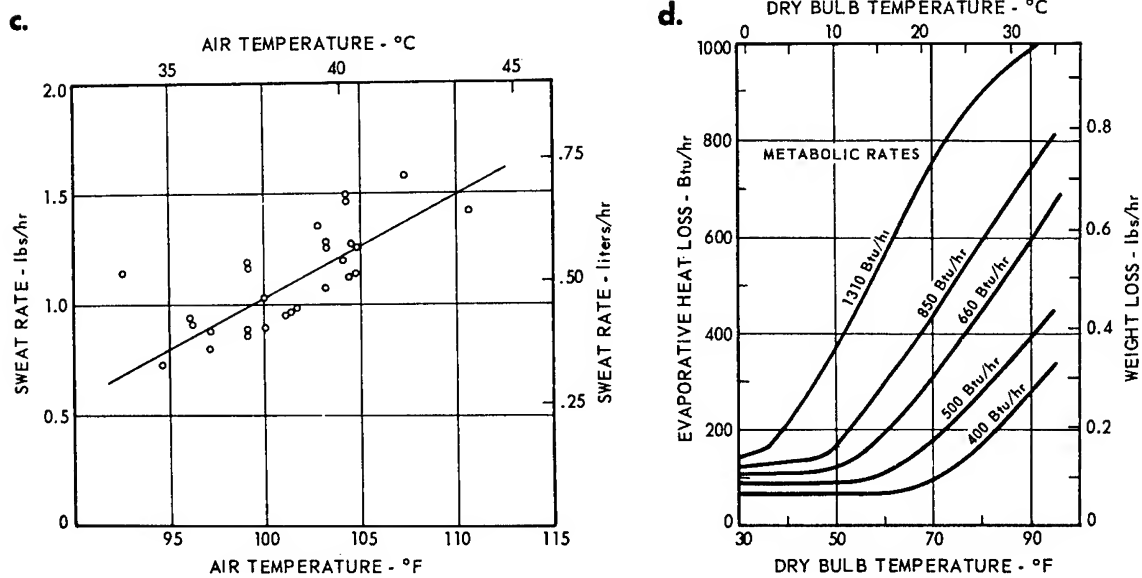


Figure 6-68
Sweating Rates; Water Replacement

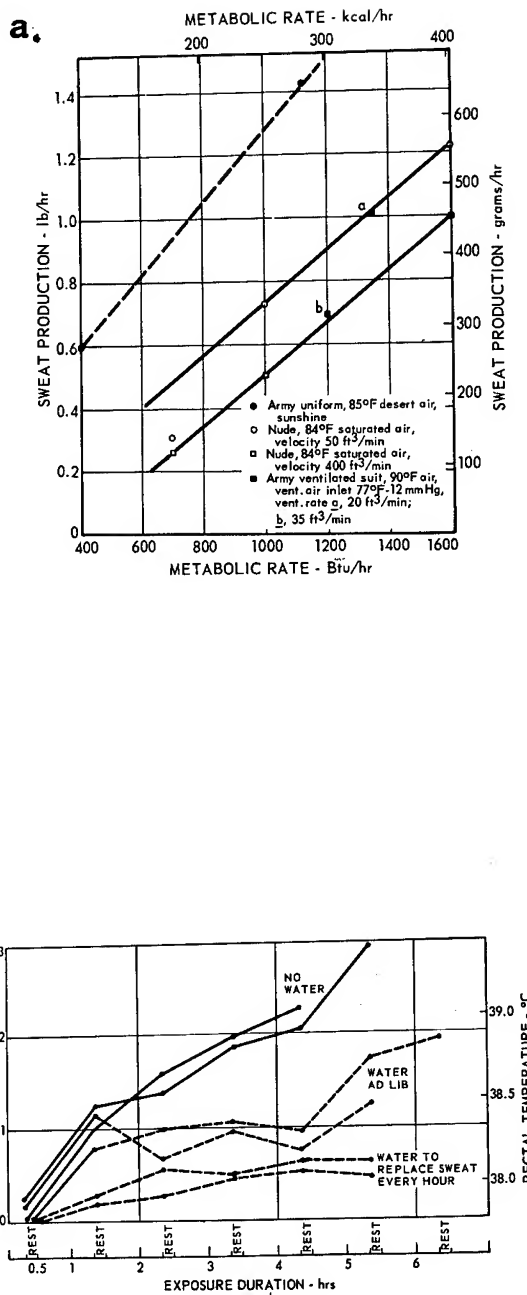
Sweat production is a highly variable quantity both within and between individuals. This chart is intended merely to indicate orders of magnitude and some of the sources of variability. Missing entirely from this picture is the question of the physiological cost of producing sweat, which is a function of the body temperatures and work rates at which a given sweat rate is achieved. Rates as high as 2 lbs/hr can be maintained for many hours if sufficient water is ingested, but rates between 3 and 4 lbs/hr cannot be sustained for 6 hours. When the skin is totally wet, the maximum achievable sweat rate is drastically reduced.

(After Blockley⁽³⁰⁾ from data of Adolph⁽³⁾, Craig⁽⁵⁹⁾, Gerking and Robinson⁽⁸⁴⁾, and Wyndham et al⁽²³⁵⁾)

Data are plotted here from six experiments on one subject, "fully acclimatized," of "better than average stamina," marching at 3.5 mph up a 2.5% grade, at 100°F and 20 mm Hg, with a 10-minute rest every hour. The more water drunk, the lower was the rectal temperature. Experiments with nude subjects resting at 110°F and vapor pressure of 25 mm Hg showed that they were able to maintain equilibrium only if they replaced water continuously. It may be concluded that failure to replace completely the water lost in sweat, hour by hour, leads to elevation of body temperature and excessive physiological strain. Thirst or the desire to drink is unreliable as an indication of the requirement for water intake to make up for heavy sweating.

Other work by the same authors has shown that replacement of salt at regular meal times is adequate, in contrast to the situation illustrated here for water.

(After Blockley⁽³⁰⁾ adapted from Pitts et al⁽¹⁶¹⁾)



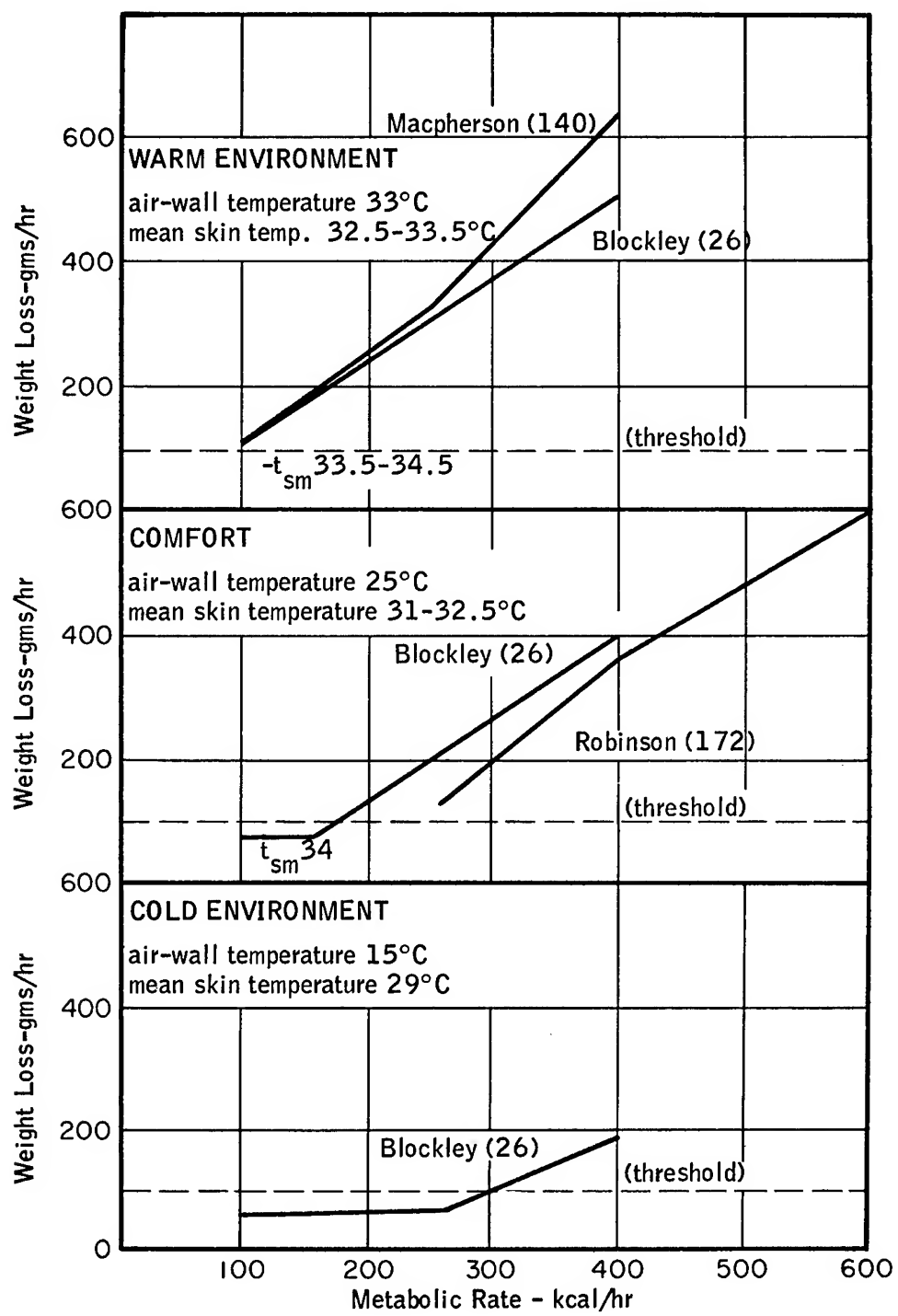


Figure 6-69

Sweat Rates as Functions of Metabolic Rate in Warm, Comfortable, and Cold Environments for Men in Shorts. The Threshold for Sweating is Taken to be a Rate of Weight Loss of 100 gm/hr.

(After Webb⁽²¹⁵⁾)

Figure 6-70

Intensity of Thermoregulatory Sweating of a Metabolically Active Man During Cold Reception at the Skin. Sweating Rates Were Plotted Against Internal Cranial Temperatures. Measurements Obtained at Similar Skin Temperatures Were Connected with "Best Lines." At Given Cranial Internal Temperature, Sweating Rates are Seen to be Diminished by Approximately 40 cal/sec for Every Degree C Decrease in Level of Skin Temperature.

(After Benzinger et al⁽¹⁷⁾)

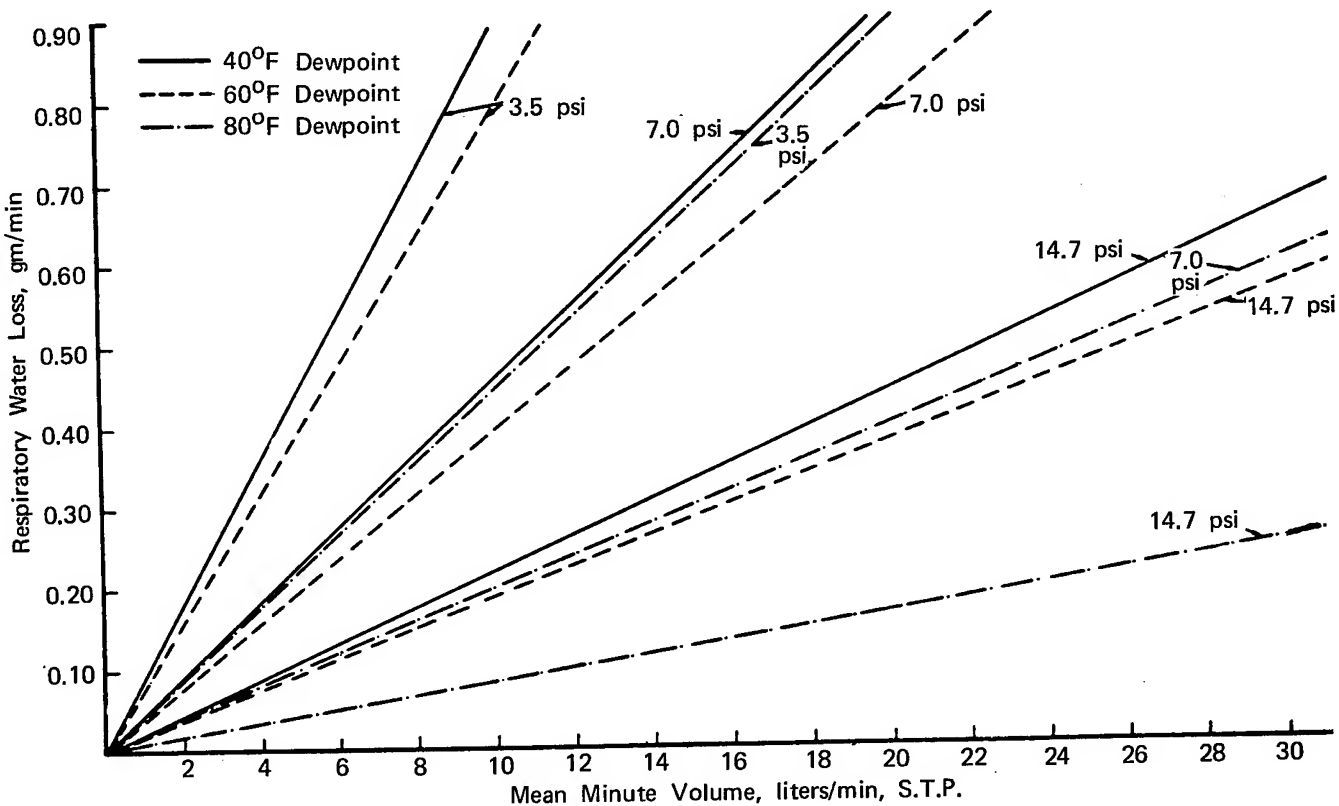
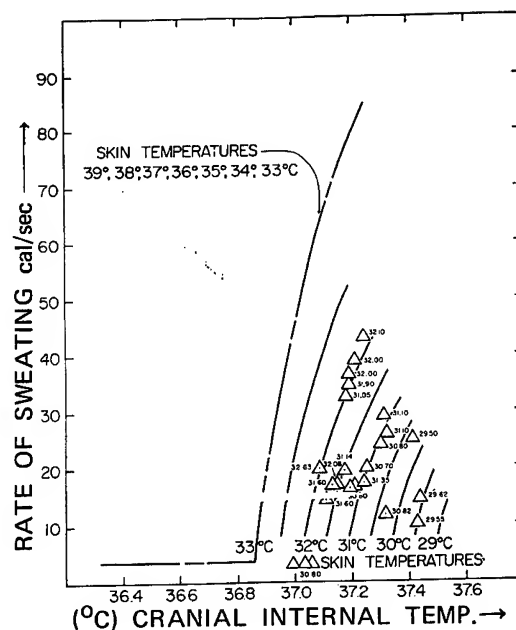


Figure 6-71

Respiratory Water Loss, Grams Per Minute, as a Function of Minute Volume, Liters Per Minute at STP, for All Work Rates and Drybulb Temperatures.

(After Wortz et al⁽²³²⁾)

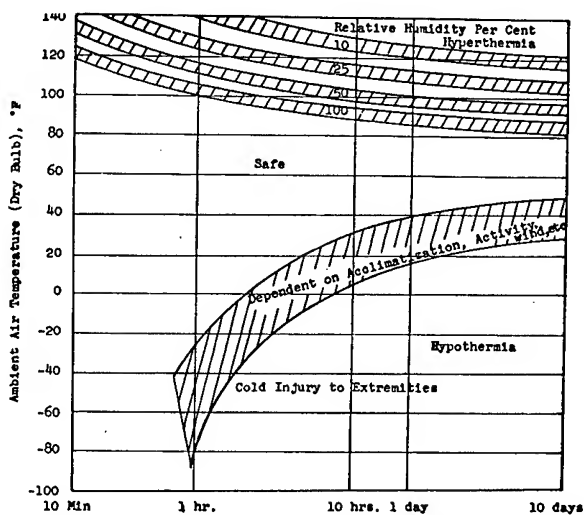


Figure 6-72

Approximate Human Time-Tolerance Temperature with Optimum Clothing
(After Breeze⁽³⁶⁾)

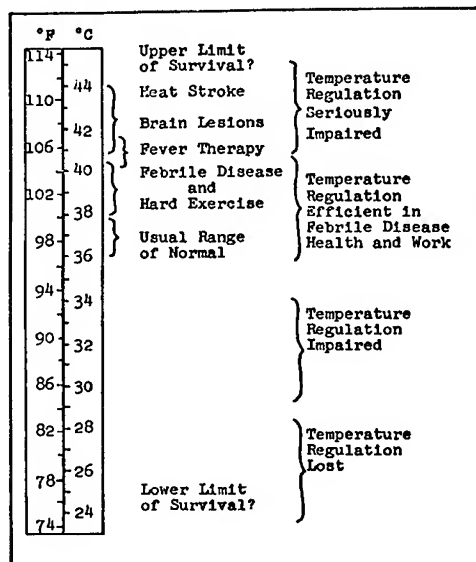


Figure 6-73

Human Body Temperature Extremes Defining Zones of Temperature Regulations
(After Breeze⁽³⁶⁾)

rates may limit evaporation rate to values below that required for adequate cooling.

The following equation can be used to determine the maximum conditions under which thermal balance can be maintained at rest, in air at S. L. (97).

$$q_m + 22(t_w - t_s) + 2\sqrt{\bar{V}}(t_w - t_s) = 10\bar{V} \cdot 0.4(p_s - p_a) \quad (45)$$

where q_m = energy of metabolism

t_w = mean radiant temperature of the walls ($^{\circ}$ F)

t_s = mean skin temperature ($^{\circ}$ F)

\bar{V} = effective air velocity (ft/min)

p_s = vapor pressure of water at skin temperature (mm Hg)

p_a = vapor pressure of water in the atmosphere

Some environmental correlates of comfort and stress have already been covered in Section 2. The more physiologically determined indices will now be reviewed. A more detailed critique of the physically and physiologically determined heat stress indices is available (139).

The Belding-Hatch Heat Stress Index (HSI) (15)

This heat stress index is defined as the ratio of evaporation rate required for thermal balance to maximum perspiration rate safely attainable for prolonged periods -- both expressed in liters (of sweat) per hour, or:

$$HSI = \frac{E_r}{E_m} \times 100 \quad (46)$$

The criteria on which heat stress index is based are:

- 1) body heat storage will not exceed the limit represented by a mean skin temperature of 95°F, and
- 2) E_m will not exceed 1 liter per hour-equivalent to 2400 BTU/hr (400 kcal/hr).

Figure 6-74 and Table 6-75 can be used as indicated to estimate the physiological and general function impairment of an 8 hr exposure at sea level to several stressful thermodynamic parameters.

The P4SR Index

The sweat rate can be used as a predictor of thermal stress in another way. The predicted four-hour sweat rate (P4SR) uses only the rate of sweating as a criterion of heat stress in environments that are hot enough to cause sweating (234). On the basis of British experimental work, empirical nomograms have been developed for predicting the probable amount of sweat in liters that would be secreted over a 4-hour period by fit, acclimatized men under different environmental conditions (67, 140, 186). A P4SR nomogram is seen in Figure 6-76.

The group of curves S1 and S2 in the center of the nomogram, running downwards from right to left, is the scale from which the basic 4 hr sweat rate (B4SR) is read. If the predicted 4 hr sweat rate (P4SR) is required for men sitting in shorts, the calculation is very easy as the P4SR is the same as the B4SR. All that is necessary is to join the appropriate point on the drybulb scale to the wetbulb temperature on the wetbulb scale corresponding to the air movement. The P4SR is given by the point where this line intersects the curve on Scales S1 and S2 corresponding with the air movement. Otherwise the P4SR is calculated in three stages.

In the first stage W. B. may require modification depending on the amount of radiation, the metabolic rate or the character of clothing. In the second stage the nomogram is used to obtain the B4SR and in the third stage the P4SR is obtained by adding certain constants to the B4SR depending on the metabolic rate (see wet bulb equivalent of metabolic rate in inset) and clothing. A P4SR of 4.5 liters was provisionally adapted as the upper limit of tolerance for physically fit men. Details regarding the 3 stage modification are available (140).

The P4SR, although derived under rather different conditions than expected in space flight, offers some hope if suitably extended (215). It was originally based on several types of experimental data taken on heat-acclimatized young men in Singapore and in environmental chambers. However, it is unsafe to use it as a means of predicting sweat rate unless all the conditions are similar to those originally used. Used with care, it does allow prediction of thermal effect in a number of different situations (26). The limitations are chiefly those of a narrow range of activity (up to 250 kcal/m²hr), limited clothing combinations, and the fact that all the subjects were heat acclimatized.

It is recommended that the P4SR not be used for predicting sweat rate, but for comparing environments in terms of thermal stress, to be followed by experimental evaluation of the environments, with sweat production being taken as one dependent variable (85). The data of Blockley which are shown in Figure 6-69 are examples of such usage of the index. More such usage could lead to useful extension of the P4SR scale to cover the environmental and physiological conditions of flight.

Body Storage Index (27)

The body storage index (q_s) is defined as the steady state rate of heat loss or gain to the body which results from imbalance in the biothermal equation. The body storage equation is:

$$q_s = \frac{WC_p}{A_b} \cdot \frac{dt_b}{d\theta} \text{ BTU/ft}^2\text{hr} \quad (47)$$

where W = body weight (lb)

C_p = 0.83 = spec. ht. of body (BTU/lb°F)

A_b = body surface area (ft²)

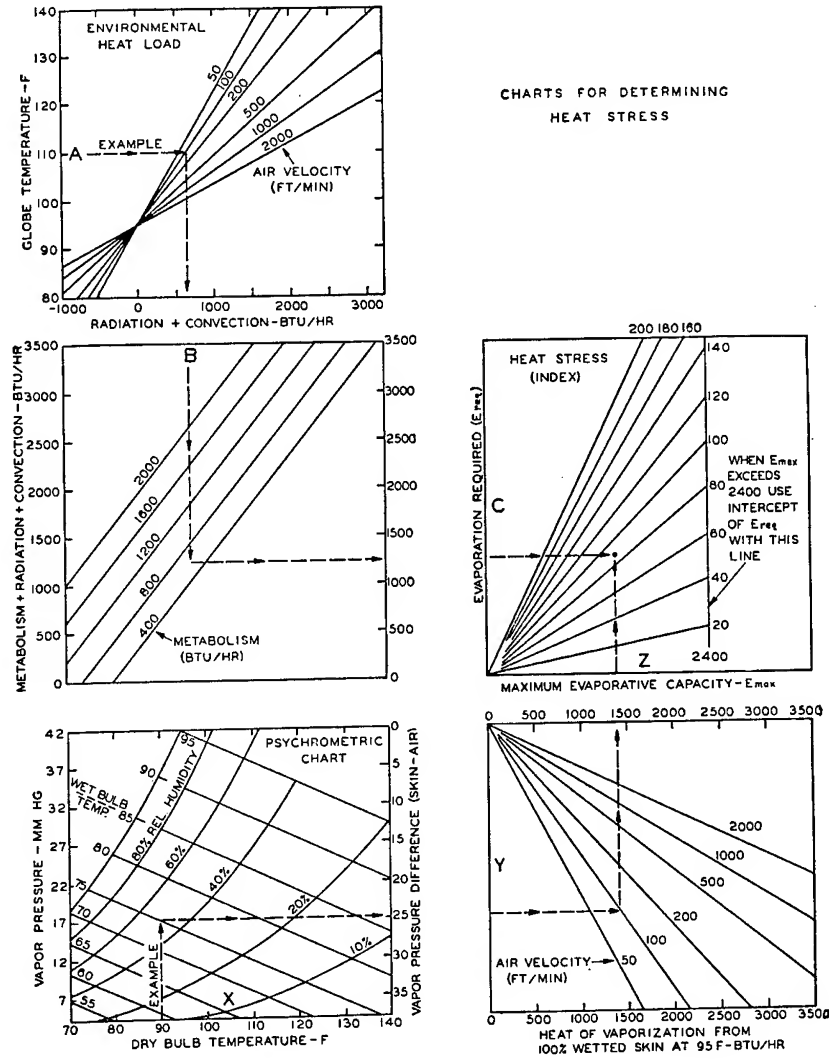
$\frac{dt_b}{d\theta}$ = rate of body temperature change (°F/hr)

and where $t_b = 0.33 t_s + 0.67 t_r$

Tolerance Time in Heat

The maximum tolerance time (θ_t) for heat gain which represents an emergency maximum for thermal stress is inversely proportional to the heat storage index:

$$\theta_t = 3300/q_s \text{ (minutes)} \text{ or } 55/q_s \text{ hrs.}$$



Example: Determine Heat Stress Index for worker doing light arm work while standing at a bench.

Metabolism

600 Btuh

Environmental conditions:

Globe thermometer temperature

110 deg

Dry-bulb temperature

90 F

Wet-bulb temperature

75 F

Air velocity

100 fpm

Solution: Follow the broken lines from the globe thermometer temperature and from dry-bulb temperature to their intersection on above diagram C to read a heat stress index of 90.

Figure 6-74

Flow Charts for Determining Heat Stress Index Values at Sea Level Conditions.

(After ASHRAE⁽⁷⁾)

Table 6-75
Evaluation of Index of Heat Stress
(After ASHRAE⁽⁷⁾)

Index of Heat Stress OF	Physiological and Hygienic Implications of 8-Hr Exposures to Various Heat Stresses
-20	Mild cold strain. This condition frequently exists in areas where men recover from exposure to heat.
-10	
0	No thermal strain.
+10	Mild to moderate heat strain. Where a job involves higher intellectual functions, dexterity, or alertness, subtle to substantial decrements in performance may be expected. In performance of heavy physical work, little decrement expected unless ability of individuals to perform such work under no thermal stress is marginal.
20	
30	
40	Severe heat strain, involving a threat to health unless men are physically fit. Break-in period required for men not previously acclimatized. Some decrement in performance of physical work is to be expected. Medical selection of personnel desirable because these conditions are unsuitable for those with cardiovascular or respiratory impairment or with chronic dermatitis. These working conditions are also unsuitable for activities requiring sustained mental effort.
50	
60	
70	Very severe heat strain. Only a small percentage of the population may be expected to qualify for this work.
80	Personnel should be selected (a) by medical examination and (b) by trial on the job (after acclimatization). Special measures are needed to assure adequate water and salt intake. Amelioration of working conditions by any feasible means is highly desirable, and may be expected to decrease the health hazard while increasing efficiency on the job.
90	Slight "indisposition" which in most jobs would be insufficient to affect performance may render workers unfit for this exposure.
100	The maximum strain tolerated daily by fit, acclimatized young men.

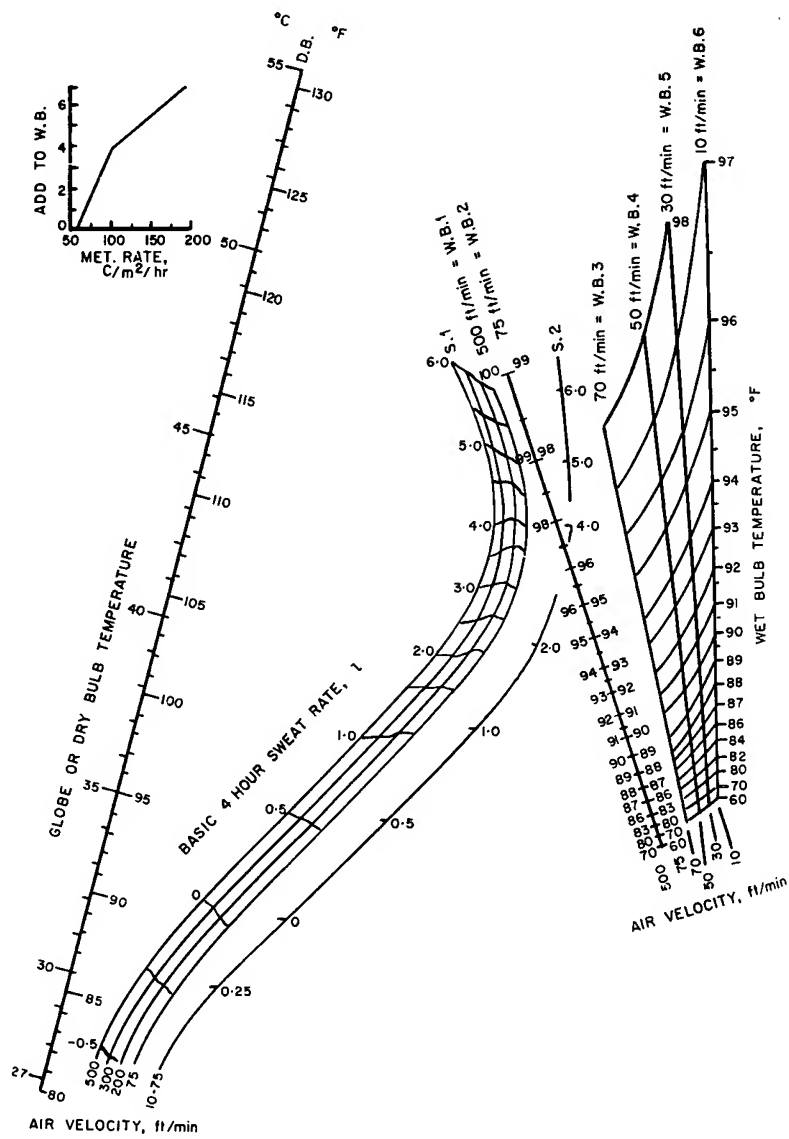


Figure 6-76

Nomograph for the Prediction of 4-Hr Sweat Loss (P4SR)
(After MacPherson⁽¹⁴⁰⁾)

The tolerance and general performance limits as a function of time and body heat storage are seen in Figure 6-77 (29). The heat storage at tolerance is inversely related to the rate of heat storage (88). There is recent evidence that men actively exercising in space suits can store up to 1000 BTU's in actively working muscle (233). This storage must be kept in mind during analysis of tolerance times in exercising subjects.

Figure 6-78 allows performance to be predicted through the heat storage index by following the dotted line and instructions. It should be remembered that these curves are for pilots undergoing normal resting activity in aircraft cabins. This fact must be considered in applying heat storage indices to predictive performance curves. Tolerance time can also be related to other heat stress indices (88, 139, 228).

Figure 6-79 indicates the conservative nature of earlier tolerance limits. The dashed lines represent the tolerance time levels more recently established (117) and reconfirmed(88). It will be noted that these are nearly double the solid-line limits established by earlier papers. It suggests that engineers, designing in terms of earlier tables, have been more restricted than necessary or have enjoyed a wide margin of safety even in the response of the most sensitive occupants. The ranges represented by these tables also reflect individual differences between subjects as well as differences in motivation. The dashed lines probably represent the capabilities of highly motivated space crews in top physical condition, and free of immediately prior physiological stresses.

The W/D index has often been used as a measure of tolerance time. Figure 6-80 represents the roles of exercise and W/D index in determining the time to collapse. Figure 6-81 uses the reference operative temperature. There are high correlations between the final skin temperature, rate of rectal temperature rise, rate of heart rate increase as linear functions of the W/D index (88). Comparison of the tolerance time for the heat stress using the Craig, effective temperature, P4SR and WGBT (aspirated) indices is available (88). These indices of heat stress tolerance can be used in limited sea level conditions related to post-landing emergencies and remote field-station operations.

Performance Under Heat Stress

As a general "rule-of-thumb" performance begins to deteriorate in any given condition at about 75% of the physiological tolerance limit. This is seen in Figures 6-77 and 6-81. Highly motivated individuals may prove capable of exceeding normally established performance and tolerance limits (202). However, excessive penalties in recovery time may be required if normal limits are exceeded. Even though no other stresses are anticipated or evident, it is suggested that the 75% of the average tolerance limit level not be exceeded until the significance of deconditioning which occurs during space flight is better understood. The synergism between prior dehydration by the diuresis of weightlessness and heat tolerance is discussed in Water (No. 15).

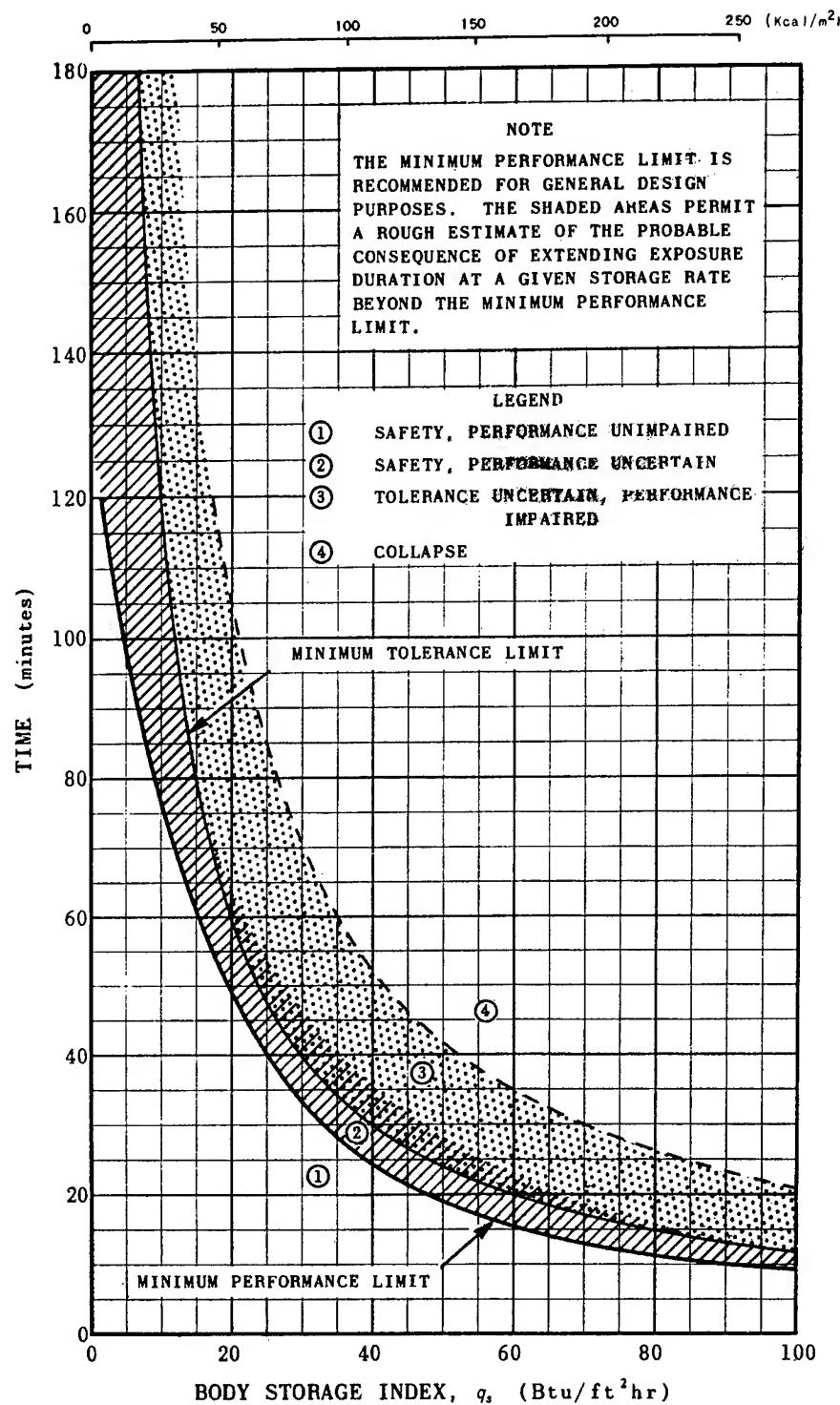


Figure 6-77

Performance and Tolerance Limits: Transient Zone

(After Blockley et al⁽²⁷⁾)

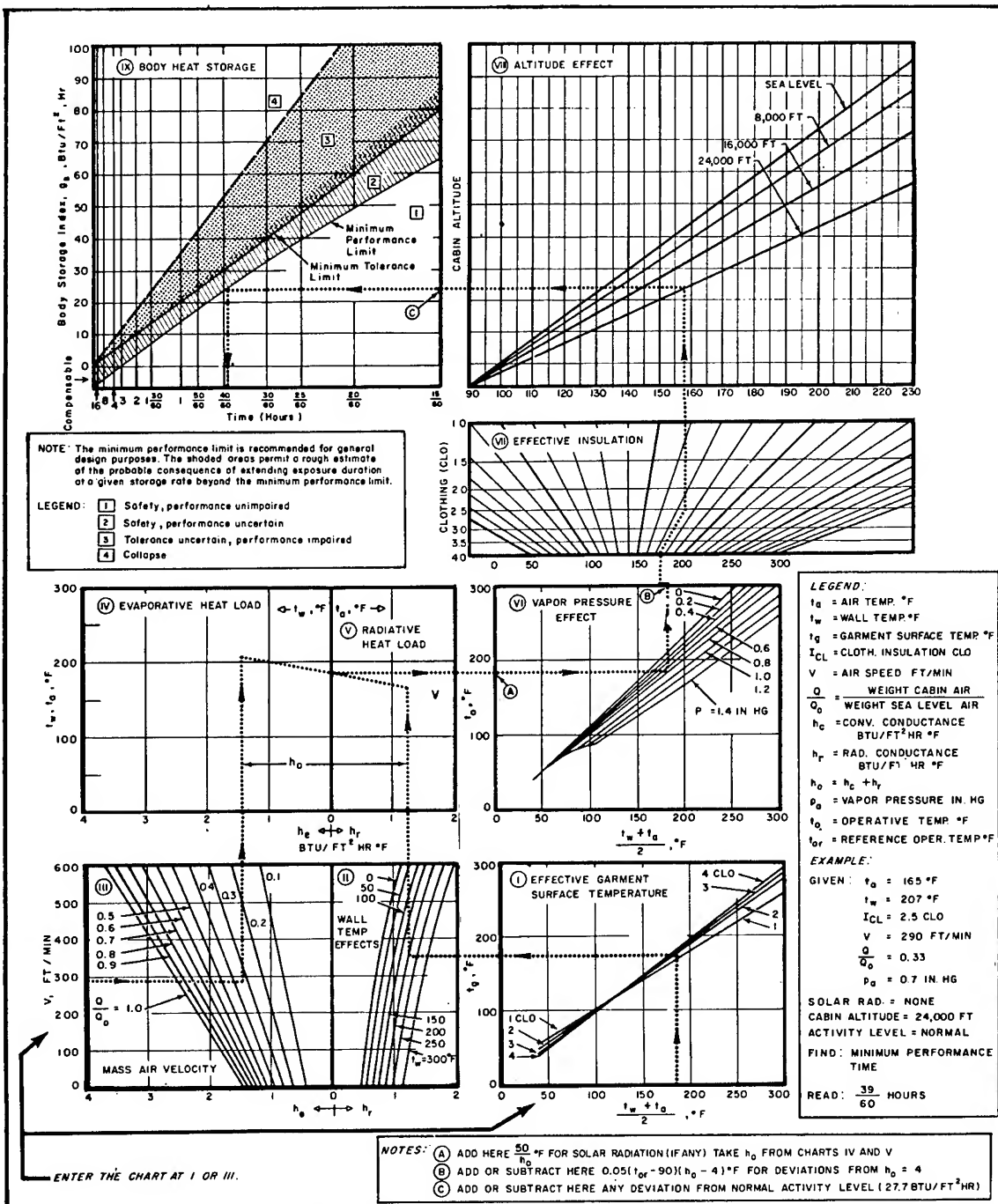


Figure 6-78

Exposure Limits for Crew Members in a Space Cabin with an Air Atmosphere at 1 g.

(After AFSCM 80-3⁽⁴⁾)

Exercise performance decreases during hyperthermia (169). When mean body temperature was raised from control values of 35.5°C up to 38.1°C , the average treadmill times to exhaustion were reduced from control values of 4.63 minutes down to 3.31 minutes. Average reduction of 50% in $\dot{V}\text{O}_{2\text{ max}}$ and 10% in O_2 debt (associated with a 15% decrease in blood lactate) were noted, though the oxygen requirement per minute of running time was unchanged from control values. Changes were attributed to conflicting demands between cutaneous and muscular circulation.

Figures 6-81 to 6-88 reflect performance decrements as a function of ambient and effective temperature. Figure 6-88 reviews the previous data related to effective temperature for fine mental work. There are, of course, certain limitations in the resulting performance curve. First, there are limits on the generality of the curve. It most adequately represents the performance threshold of artificially-acclimatized, military personnel during learning or re-acquisition of highly stress-sensitive mental tasks. As such, the curve properly represents the lower-limit of an "impairment zone." The threshold for some mental tasks, or for subjects highly practiced on tasks, or for naturally-acclimatized subjects may lie somewhat higher (i.e., in the zone between the present curve and the recommended physiological limit). Secondly, because the curve is plotted in terms of effective temperature, there is the danger of assuming that all the combinations of temperature, humidity and air speed which yield a given effective temperature also produce the same degree of performance decrement. This is undoubtedly not the case. Eventually performance decrements should be separately determined for a large number of combinations of temperature, humidity and air movement and reported in a tri-dimensional chart. However, such voluminous data are not yet available, and it is fortunate that the effective temperature scale could be used for establishing a tentative threshold for unimpaired mental performance. A recent review of this problem is available (157).

Table 6-89 summarizes the physiological response to heat. The debilitating effects of heat have received much attention (80, 127, 131, 221). Figure 6-73, and 6-74 set gross symptoms for different temperatures. Table 6-90 represents a classification of the symptoms to be expected.

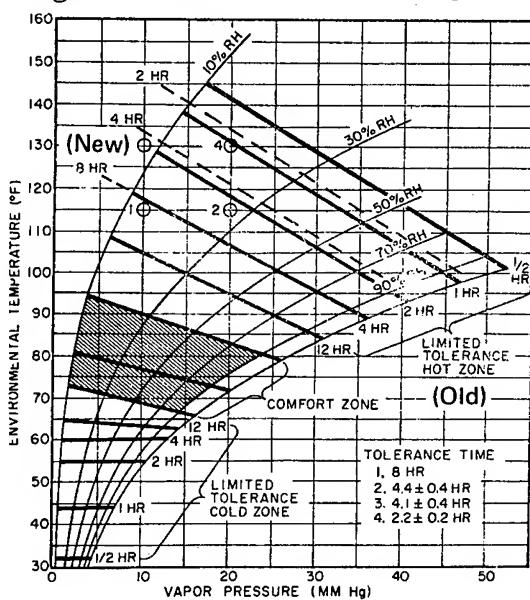
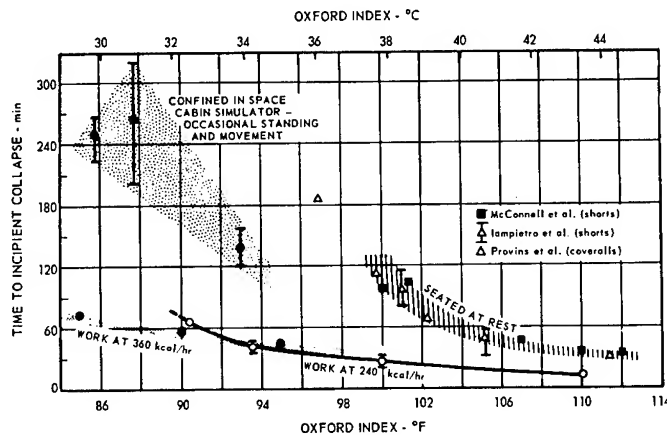


Figure 6-79

Maximum Tolerable Environments According to Duration of Exposure for Sitting, Clothed Subjects Under Sea Level Conditions in Aircraft Design. (See Text)

The tolerance limit at high temperature is based on faintness, dyspnea, nausea, and restlessness as an endpoint. Points 1, 2, 3, and 4 and the dashed lines for tolerance time represent more recent data and point out the conservative nature of previous design limits.

(After Trumbull⁽²⁰⁴⁾ from data of Kaufman⁽¹¹⁷⁾, Winslow et al⁽²²⁵⁾, Taylor⁽¹⁹⁷⁾, and others.

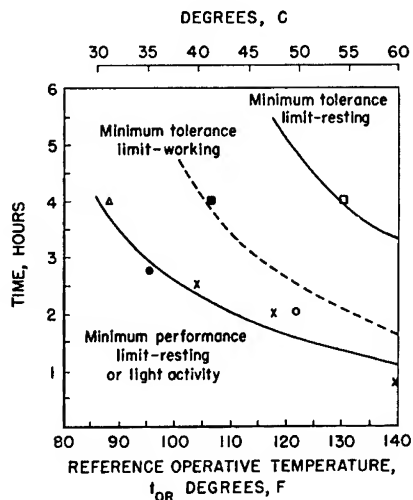


The effect of activity on tolerance time for untrained men at sea level is shown for a wide range of heat stress conditions. Vertical bars indicate the range of times to incipient collapse. The dramatic influence of metabolic rate on endurance time in hot environments is emphasized here. The use of the "Oxford Index" (Fig. 6-12) permits intercomparison of environments ranging from very hot and dry to very humid and warm (vapor pressures as low as 7 mm Hg and as high as 70 mm Hg). Note the increase in variability at the milder conditions; it is in this same environmental stress zone that the effects of training for work in the heat ("acclimatization") are most striking, endurance times for trained men being several times as high as those of the same men when they are unused to heat stress.

Figure 6-80

Activity Level and Heat Tolerance

(After Blockley⁽³⁰⁾ from Data of Blockley⁽²⁵⁾, Provins et al⁽¹⁶²⁾, Lampietro et al⁽¹¹⁰⁾, Kaufman⁽¹¹⁷⁾, Leithead and Lind⁽¹²⁷⁾, and McConnell and Yaglou⁽¹³⁴⁾)



t_{OR} = Operative temperature of 0.79 in Hg vapor pressure

- Heavy pursuitmeter test
- △ Mixed test battery
- Working men
- ×
- Wireless telegraphy test
- Visual vigilance test
- Resting men

Figure 6-81

Performance and Tolerance Limits in the Quasi-compensable Zone for Lightly Dressed Men.

(After Blockley et al⁽²⁷⁾)

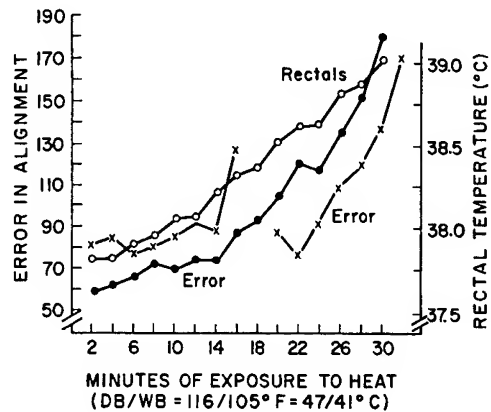


Figure 6-82

Continuous Error and Rectal Temperature Curves are the Means of Six Subjects. Interrupted Error Curve Based on One Subject. The Break Represents an Insertion of a Two-Minute Rest Period During Which Time the Subject Remained in the Environment.

(After Teichner⁽²⁰²⁾ Adapted from Pepler⁽¹⁵⁶⁾)

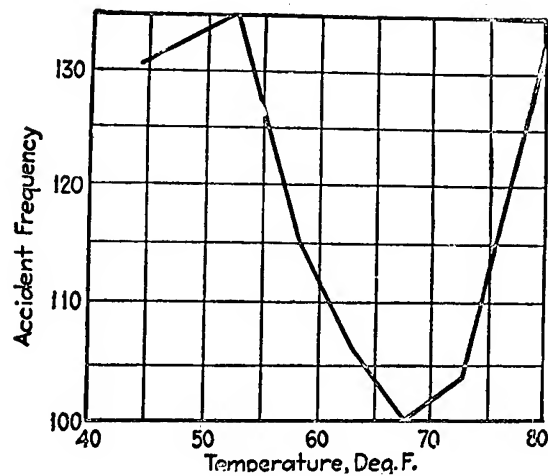


Figure 6-83

Frequency of Accidents in Relation to Cabin Air-Temperatures.

(After Breeze⁽³⁶⁾)

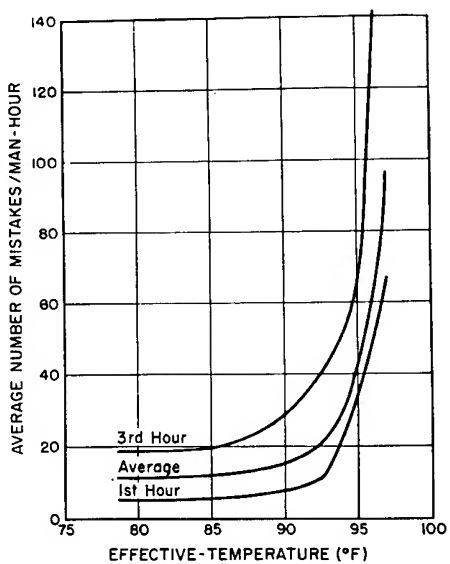


Figure 6-84

Combined Performance Averages for 11 Wireless Telegraph Operators Under Conditions of Extreme Heat.

(After Mackworth⁽¹³⁷⁾)

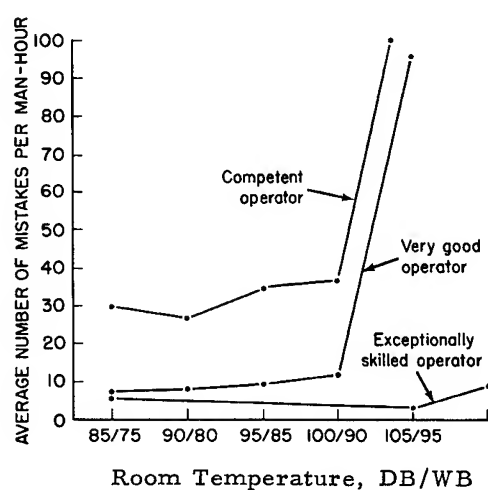


Figure 6-85

Room Temperature and Frequency of Error in Memory-Coordination Task.

(After Mackworth⁽¹³⁷⁾)

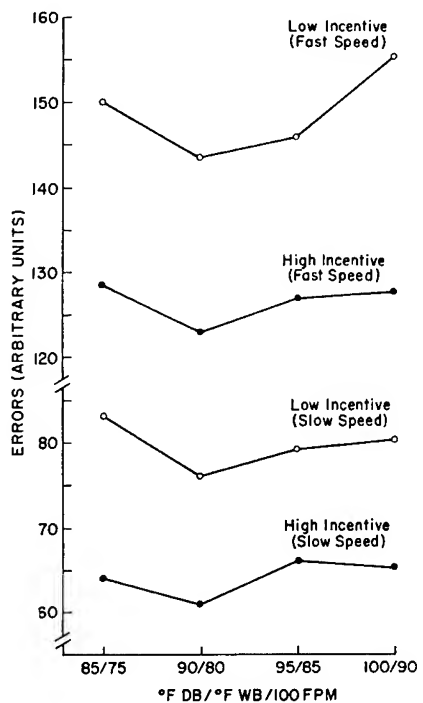


Figure 6-86

Effects of Incentives, Target Speed and Environmental Warmth on the Accuracy of Manual Tracking.

(After Teichner⁽²⁰²⁾ Adapted from Pepler⁽¹⁵⁶⁾)

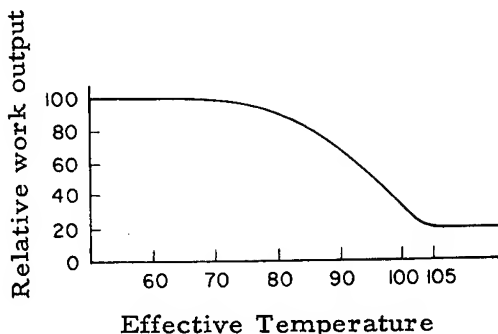


Figure 6-87

Relative Output of Hard Physical Labor (as % of Maximum ft-lbs/hr) at Various Effective Temperatures.

(After Yaglou⁽²³⁸⁾)

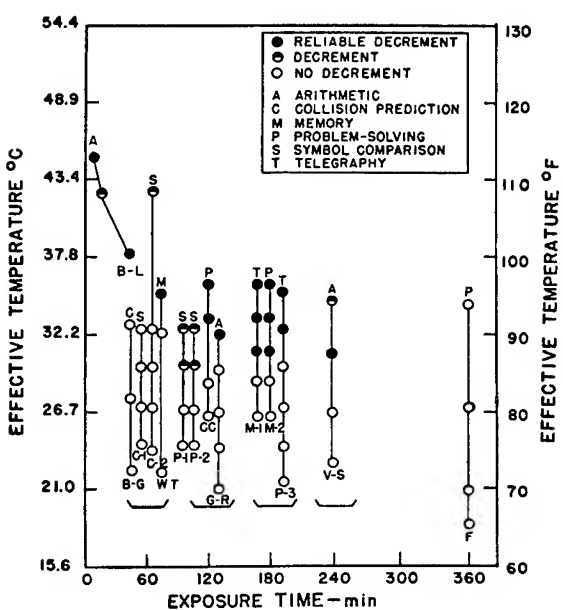


Figure 6-88

Summary Characteristics for the 14 Experiments on Performance Degradation at High Temperatures. Each Experiment is Represented by a Vertical Line with Initials of the Investigator(s) Beneath It. The Circles on a Line Are Test Temperatures. Solid Circles Indicate Statistically-Reliable Impairment in Performance; Half-Filled Circles Indicate Decrements Which Were Not Evaluated (or Were Improperly Evaluated) Statistically; and Open Circles Indicate No Decrement. Alphabetic Symbols Beneath the Vertical Lines Initials of Authors Quoted in Source Reference.

(After Wing⁽²²³⁾)

Table 6-89

Effects of Environmental Temperature Change:
Values are for Resting State

(After Spector⁽¹⁸⁹⁾)

Animal	Variable	Increase of Environmental Temperature			Decrease of Environmental Temperature		
		Single Exposure Response		Repeated or Continued Exposure	Single Exposure Response		Repeated or Continued Exposure
		General	15-20°C Inc.		General	15-20°C Dec.	
Man	Blood volume	Increase		Increase	Decrease		Decrease
	Cardiac output	Increase		Return toward normal	Variable		Return toward normal
	Food intake	Decrease		Decrease	-5/min		Increase
	Heart rate	Increase		Return toward normal	50 to 100 Cal ²		Return toward normal
	Heat production	0 or slight + 1		Some decrease	2 to 3%		Increase
	Manual skill	Deteriorates		Return toward normal	-1 to 2°C		Return toward normal
	Packed cell volume	Slight decrease	-2 to 3%	Decrease	-10 to 15°C		Increase
	Rectal temperature	Increase	0.5 to 1°C	Return toward normal	200 to 500 ³		Return toward normal
	Skin temperature	Increase	10 to 15°C	Return toward normal			Return toward normal
	Output of urine	Decrease	-200 to 500 ³	Sustain low level			Sustain high level
	Blood flow ⁴	Decrease	400 ³	Return toward normal			Return toward normal
	Water intake	Increase		Sustain high level	-400 ³		Sustain low level

/1/ No change or slight increase

/2/ Per sq m/hr.

/3/ ml/da.

/4/ Visceral

Table 6-90

Classification of Debilitating Effects of Heat

(After Buskirk and Bass⁽⁵³⁾)

<u>Disorder</u>	<u>Cause</u>	<u>Symptoms</u>	<u>Prevention/First Aid</u>
Heat Cramps	Excessive loss of salt in sweating with inadequate replacement	Pain and muscle spasm; pupillary constriction with each spasm. Body temperature normal or below normal	Normal diet and fluid intake. Rest, administer salt and water
Heat Exhaustion	Cardiovascular inadequacy; dehydration	Giddiness; headache; fainting; rapid and weak pulse; vomiting; cold, pale, clammy skin; small rise in body temperature	Frequent and early replacement of water, frequent pauses. Rest in shade in recumbent position. Administer fluids.
Heat Stroke	Failure of temperature regulatory center, due to excessively high body temperature	High body temperature; irritability, prostration, delirium; hot, dry, flushed skin. Sweating diminished or absent	Adequate pacing of activity, avoidance of severe effort by unacclimatized men in hot environment. Alcohol spray bath or immersion in cold water. Medical emergency requiring a physician.

Figure 6-91 represents the humidity and temperature maxima for cases of total heat stroke. Treatment of thermal emergencies in space has been reviewed (52).

Acclimatization to Heat

Acclimatization can alter the response of humans to heat loads (11, 35, 71, 74, 75, 96, 112, 124, 127, 129, 171, 235, 236). Figures 6-92 and 6-93 represent examples of the improvement in function which is possible through heat acclimatization. The major physiological adaptations in heat acclimatization have been summarized (71): "Deep tissue temperature is returned to the normal level set by the metabolic rate of the task in a cool environment, but neither total body temperature nor mean skin temperature are returned to their levels in the cool environment. Mean skin temperature is adjusted to a level which permits thermal equilibrium between the body and the environment on the one hand, and on the other, maintains an internal thermal gradient which permits the transport of the deep heat to the surface without overtaxing the circulation . . ." These conditions are attained almost wholly as a result of the increased evaporative cooling in which the efficiency, rate, and total volume of sweating are favorably improved by acclimatization.

Acclimatization is well retained for 1 to 2 weeks, after which it is lost at a variable rate. Most men lose the major portion of their acclimatization in 1 month -- a few are able to retain it for 2 months. Men who remain in good physical condition retain their acclimatization best. Repeated exposures to heat are required at intervals not exceeding 1 month, if a high degree of acclimatization is to be maintained for long periods of time. Newer techniques, pioneered by Fox in England concentrate on raising core temperature to the same fixed level each day, so that thermal strain, rather than the stress, remains constant throughout the acclimatization process (74). Improvement continues for longer periods and to greater levels than the standard exposure techniques. Heat acclimatization may not be as important in hot, wet environments where increased evaporative cooling cannot be produced even if there is an increased sweat secretion, since no increase in the internal thermal gradient between "core" and skin can be achieved (88). However, techniques for acclimatization en route to hot-wet climatic conditions are under study (165).

The practical value of heat acclimatization in space operations is still a controversial issue (52, 173). Current NASA opinion is centered on the concept that excellent physical conditioning of the astronaut will be adequate to cover anticipated thermal emergencies and not impose further on the already overburdened training schedule of the astronauts. The issue of interference with resistance to acceleration by the vasodilatory effects of heat acclimatization has been raised (see Acceleration, No. 7). Simultaneous heat and cold acclimatization is also a problem in future lunar and planetary operations (see discussion of this under cold acclimatization). More work in this area is necessary before formal recommendations can be stated.

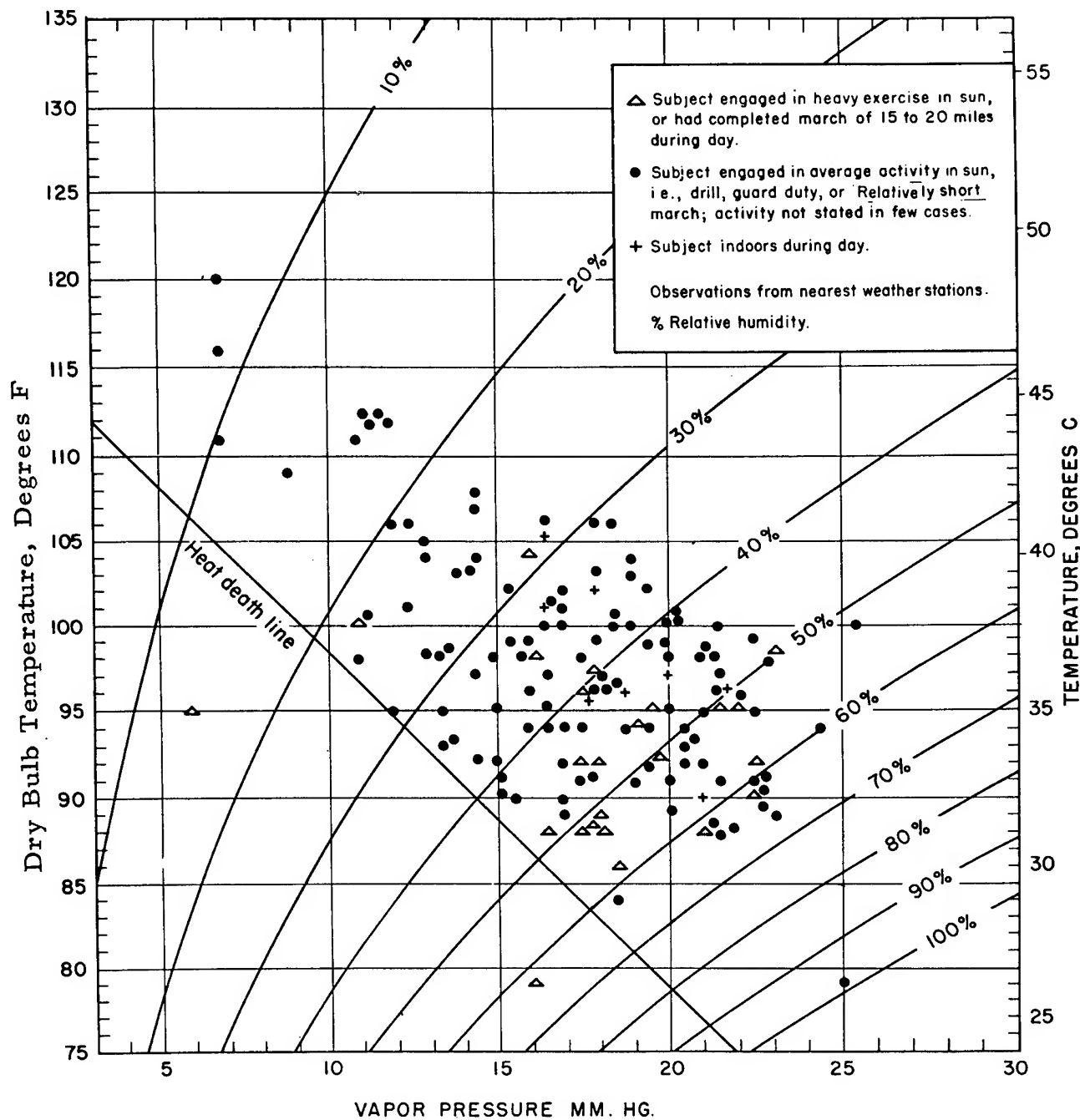


Figure 6-91

Humidity and Maximum Temperature on Day of Onset of 157 Cases of Fatal Heat Stroke in the U.S. Army, 1942-44.

(After Schickele⁽¹⁷⁸⁾)

Figure 6-92
Acclimatization to Heat

(After Blockley⁽³⁰⁾, Adapted from a Wyndham et al⁽²³⁵⁾, b Lind and Bass⁽¹²⁹⁾)

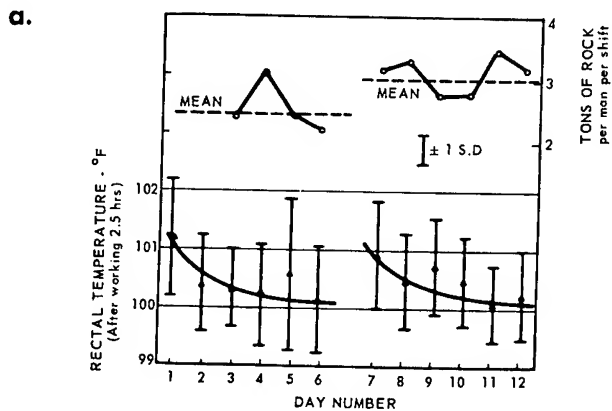


Figure a shows the results obtained with the standard acclimatization procedure used in South African gold mines to prepare laborers recruited from remote villages for work in saturated environments underground. The duration of the daily work period is five hours, and the work is shoveling rock under close supervision. For the first six days the Effective Temperature was 84°F; the next six days the E.T. was 89.5°F and the amount of rock shoveled was increased. Note the fall in rectal temperature--the curves are means for over 100 men, the bar shows ± 1 S.D. --during each of the six-day work periods.

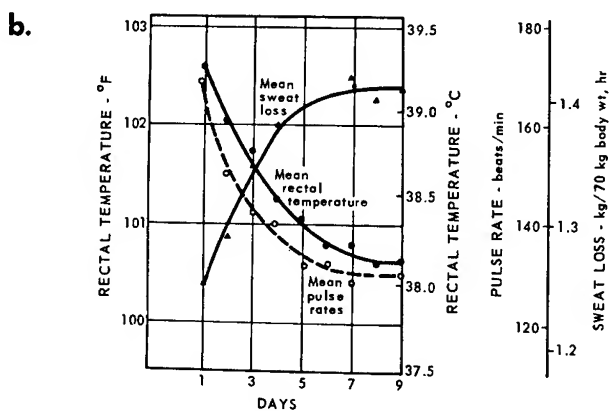


Figure b illustrates the results of a technique used at the U.S. Army laboratories at Natick, where men marched at 3.5 mph for 100 minutes each day in an environment of 120°F dry bulb, 80°F wet bulb, 200 ft/min air velocity (E.T. 89°F, vapor pressure 15 mm Hg). The value of the shorter exposure period technique in preparing men to work for long periods such as five hours or more in the heat is the subject of considerable controversy.

Newer techniques, pioneered by Fox in England, concentrate on raising core temperature to the same fixed level each day, so that thermal strain, rather than the stress, remains constant throughout the acclimatization process. (74)

Figure 6-93
Improvement in Function from Heat Acclimatization

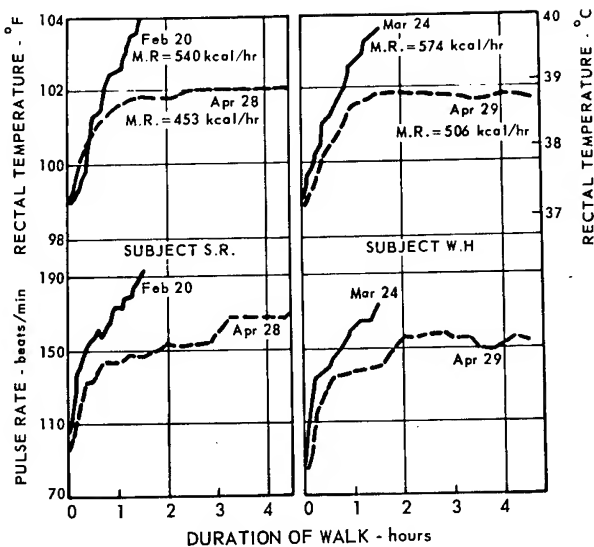
a.

These data dramatically illustrate acclimatization to heat as shown by the lowering of body temperatures and heart rates of two men walking at 3.5 mph on a 5.6% grade in room temperature of 104° F., vapor pressure 13 mm Hg (E. T. 84° F.).

(1) Subject S. R. was acclimatized by 23 exposures to these conditions between February 20 and March 20. After March 20 his only exposures were on April 16 and 28.

(2) Subject W. H. was acclimatized by 11 exposures between March 24 and April 8. After April 8 his only exposures were on April 22 and 29.

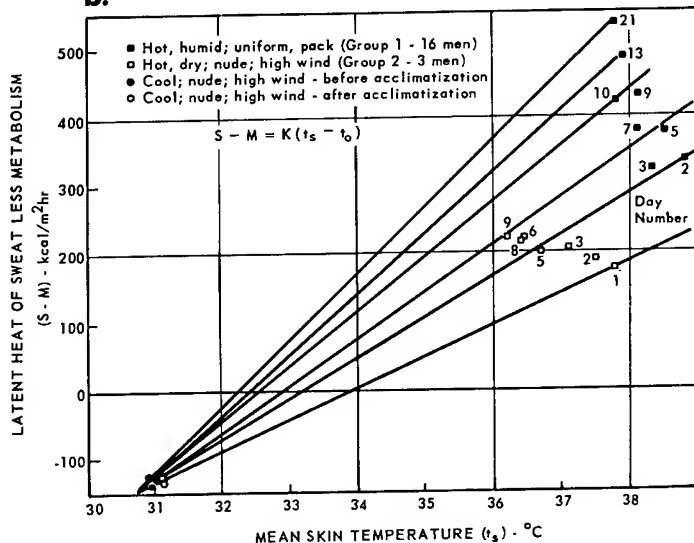
On the first exposure, the experiment was terminated by the collapse of the subjects at 90 minutes. After acclimatization, the men were still maintaining equilibrium with ease after 4.5 hours.



(After Blockley⁽³⁰⁾, Adapted from Robinson et al⁽¹⁷¹⁾)

Figure b is a diagrammatic presentation of mean results from two studies of the heat acclimatization phenomenon. Subjects in both groups were drawn from the same Army population at Fort Knox, Kentucky. The two studies are related by means of a parameter combining the sweat rate (expressed as its caloric value if evaporated) and metabolic rate. The slope of the straight lines in the diagram represents an estimate of the sensitivity of the sweat response to increases in temperature of the peripheral tissues or blood (expressed as a function of surface temperature and metabolic heat output). It can be seen that when men are unclothed and the air is dry, sweat rate changes but little, but the skin temperature needed to produce that amount of sweat becomes steadily lower in successive exposures; when the climate is humid, and evaporation is impeded by clothing, the skin temperature does not change much on successive days, but the quantity of sweat produced at that temperature is enormously increased as acclimatization progresses.

b.



(After Blockley⁽³⁰⁾, Adapted from Hanifan et al⁽⁹⁶⁾, Eichna et al⁽⁷¹⁾, and Horvath and Shelly⁽¹⁰⁵⁾)

Skin Pain and Heat Pulses

Tables 6-64, 6-65, 6-94, and Figure 6-95 cover the pain thresholds for the skin from conductive, radiant and convective heating. In general, the pain threshold is reached when the skin attains a temperature of 45°C. Figure 6-96 shows the influence of skin temperature on the thresholds of three sensations, pain from heat, warmth, and cold (69). The average value of the cold thresholds between 16°C and 24°C air temperature is -0.25, ± 0.061 millical/cm²/sec., and increased (absolute energy change) to -0.67, ± 0.073 millical/cm²/sec. between 35°C and 40°C. There was no change in the warmth thresholds, which were +0.32, ± 0.081 millical/cm²/sec and +0.32, ± 0.075 millical/cm²/sec., respectively, for the above air temperatures. Indirect evidence is offered that the rise in the cold thresholds in the higher environmental temperatures is associated with vasodilation of the blood vessels in the skin. The face and the neck are most sensitive to thermal stimuli and the backs of the hands are next (99).

The ability of the body to withstand high heat pulses is shown in Figure 6-97. A computer program is available for evaluation of time-temperature histories of the skin at different depths following heat pulses (211).

COLD STRESS

Exposures to cold stress are not as likely to occur during space flight as heat stress. This is due primarily to man's capability for generating heat and the relative ease with which he can be insulated against heat loss to the space environment by provision of adequate clothing. Except for nocturnal operations on the lunar surface, the likelihood of cold exposure after return to Earth is much greater and must be considered in the design of survival gear and plans for recovery (173).

A simplified heat loss equation can be obtained from Equation 1 indicating that the total heat lost from the body surface to the environment, \bar{H} , is (54):

$$\bar{H} = q_s + q_m = K(t_s - t_a) + q_e \quad (48)$$

where \bar{H} = total heat loss

K = a constant which depends on humidity, ventilation, and clothing

t_s = average skin temperature

t_a = ambient air temperature

q_e = evaporative heat loss

If evaporative heat loss is ignored, as it can be in the cold, the equation becomes:

$$\bar{H} = K(t_s - t_a) \quad (49)$$

Heat loss from the interior of the body to the surface is similar:

$$\bar{H} = K' (t_b - t_s) \quad (50)$$

Table 6-94
Pain from Conductive Heating
(After Blockley⁽³⁰⁾, Adapted from North American Aviation⁽¹⁵²⁾)

Body Area	Clothing Worn	Metal Surface Temperature	Average
			Tolerance Time seconds
Hand	Bare skin	120	10-15
Kneecap	Bare skin	117	34
	Bare skin	120	5
Fingertip	AF/B-3A leather gloves	150	12.6
	AF/B-3A leather gloves	160	7.3
Hand - palm	AF/B-3A leather gloves	150	25.2
	AF/B-3A leather gloves	175	9.7
	AF/B-3A leather gloves	185	8.0
Forearm	SAC alert suit	150	20.6
	SAC alert suit	175	8.0
Upper arm	K-2B light AF flight coverall	150	7.5
	SAC alert suit	150	31.3
	Alert suit plus Brynje net string underwear	300	7.2
	K-2B suit	150	18.1
	K-2B suit plus Brynje underwear	150	61.9
Buttocks	SAC alert suit	150	70.3
	Alert suit plus Brynje underwear	300	21.7
	K-2B suit	150	32.5
	K-2B suit plus Brynje underwear	150	+90
Mid-thigh	SAC alert suit	150	35.6
	Alert suit plus Brynje underwear	300	13.1
	K-2B suit	150	13.6
	K-2B suit plus Brynje underwear	150	+90
Kneecap flexed	SAC alert suit	150	14.4
	Alert suit plus Brynje underwear	175	9.5
	K-2B suit	150	7.3
Calf muscle	SAC alert suit	150	14.4
	Alert suit plus Brynje underwear	300	11.4
	K-2B suit	150	13.2
	K-2B suit plus Brynje underwear	150	66.1
Upper arm	MD-3A wool-nylon anti-exposure suit	300	12.0
	MD-3ABB-nylon anti-exposure suit	400	10.2
Forearm	MD-3A suit	250	15.9
Palm of hand	Aluminized asbestos glove	250	13.5
Back of hand	Aluminized asbestos glove	250	5.2
Palm of hand	Arctic mitten	300	18.7
	Arctic mitten plus B-3A glove	300	37.0
	Arctic mitten plus B-3A glove	400	27.6
	Pigskin '800°F' heat glove	300	30.7
	Pigskin '800°F' heat glove	400	21.0
	Pigskin '800°F' heat glove	500	18.5

Notes: Light touch pressure (less than 1 psi) applied to heated metal surface. The elbow and knee sometimes received second degree burns without pain.

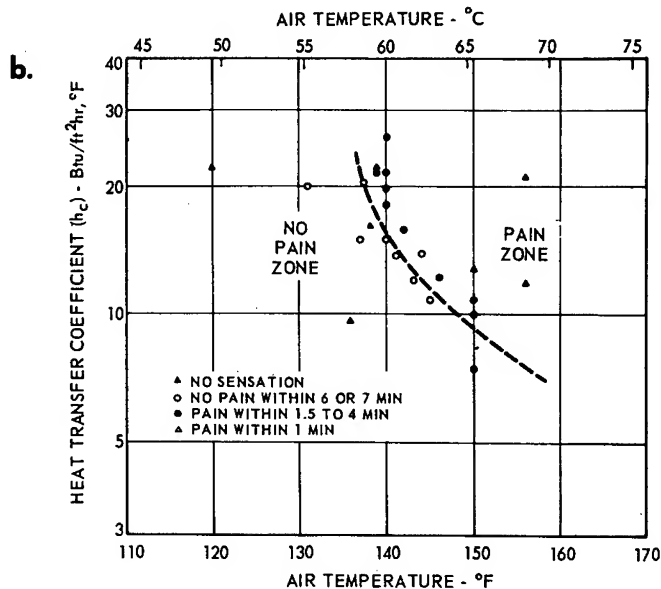
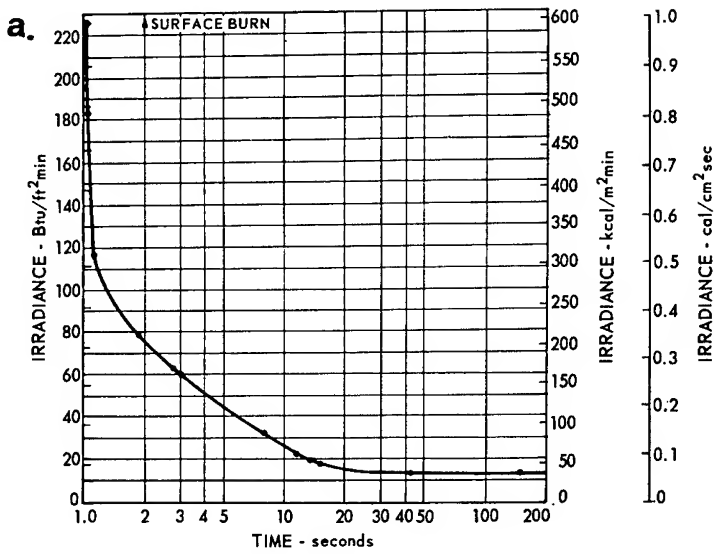
Figure 6-95
Pain from Radiant and Convective Heating

Figure a shows the time to reach strong skin pain from radiant heating, with radiation sources ranging from the simulated intense thermal flash of a nuclear weapon (approximately 100 Btu/ft²min) to the slow heat pulse associated with re-entry heating, where the heating is partly convective as well. The curve is derived from experiments involving heating of single small areas of forehead or forearm or exposed areas of skin of a subject in flight clothing, and of the whole body surface. The pain threshold is reached when the skin temperature comes to 45°C, and a skin temperature of 46°C is intolerably painful.

For small skin areas the curve becomes asymptotic at about 18 Btu/ft²min, which means that at this level and below, the blood supply to the skin is carrying off the heat as fast as it arrives, and heat is stored in the body; how long this can go on with the total body exposed is not established.

(After Blockley⁽³⁰⁾, Adapted from Buettner⁽⁴⁰⁾, Hardy⁽¹⁰¹⁾, Kaufman et al⁽¹¹⁸⁾, Stoll and Greene⁽¹⁹¹⁾, and Webb⁽²¹⁷⁾)

These data indicate the dividing line between painful and non-painful heating for air at various temperatures, versus the heat transfer coefficient, which depends on air density, air velocity, and surface areas and shape. The data were obtained by exposing a small segment of the cheek to a flowing air stream through a padded hole in the wall of a cylindrical tube. h_c was computed from air velocity and duct geometry.



(After Blockley⁽³⁰⁾, Adapted from North American Aviation⁽¹⁵²⁾)

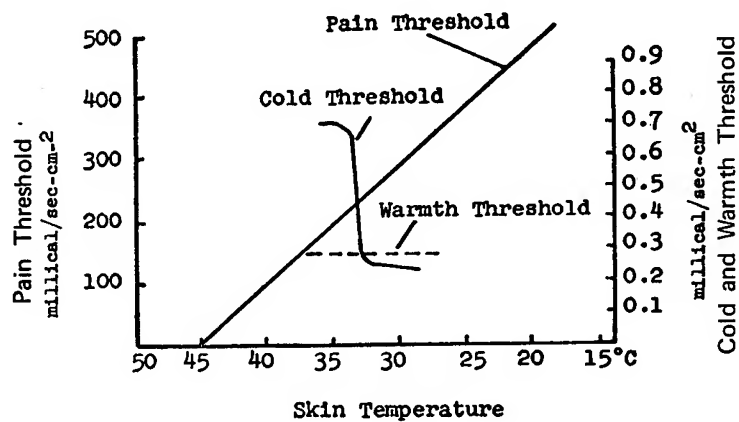
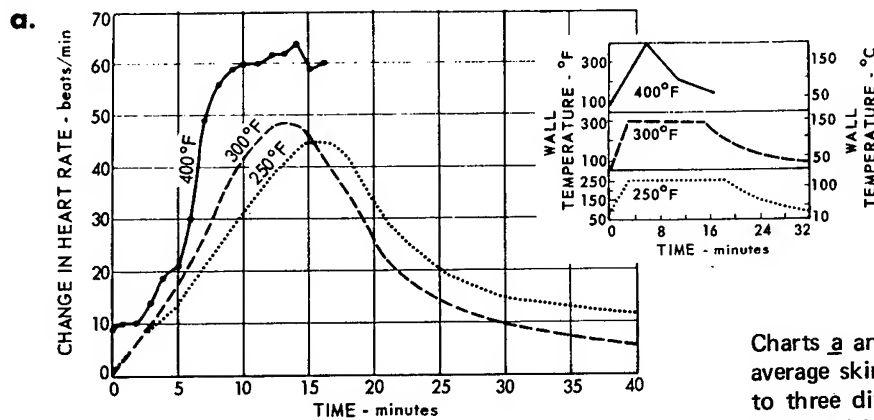


Figure 6-96

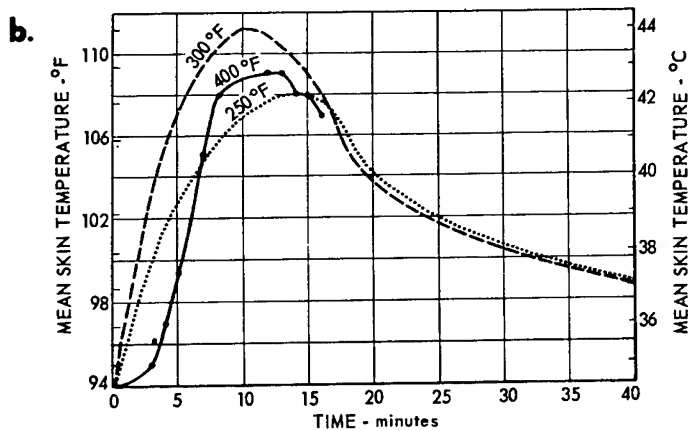
Influence of Skin Temperature
Upon Thresholds of Warmth,
Cold, and Pain.
(After Breeze⁽³⁶⁾)

Figure 6-97

Tolerable Heat Pulses



Charts a and b show the pulse responses and average skin temperatures of subjects exposed to three different severe heat exposure transients which come close to both pain limit and the heat storage limit. Each curve represents the average data from five or six subjects. Clothing consisted of a standard flying coverall over long underwear with an insulation value of 1 clo.



(After Blockley⁽³⁰⁾, Adapted from Kissen and Hall⁽¹²⁰⁾, Kaufman⁽¹¹⁷⁾, and Webb⁽²¹⁷⁾)

Figure 6-97 (continued)

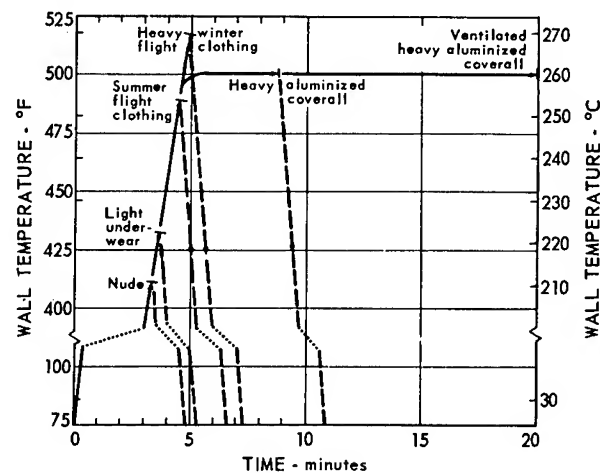
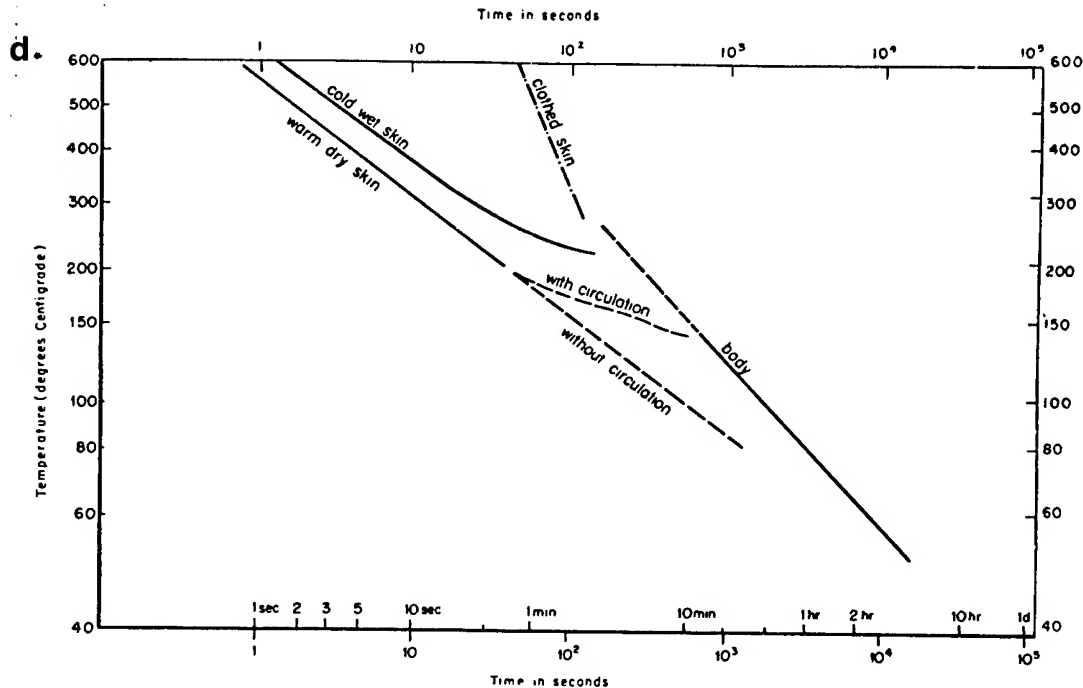


Chart c shows the increase in tolerance times (voluntary limit when surface pain becomes unbearable) for subjects exposed to a heat pulse where wall temperature was increased at $100^{\circ}\text{F}/\text{min}$, and the subjects wore clothing affording various degrees of protection. Each limit represents average data for from 3 to 10 subjects. When an aluminized surface was used with a heavy coverall, the protection increased again; exposures were changed in form — the increase in wall temperature was stopped at 500°F and that temperature held until tolerance was reached. Adding ventilation with air at about 85°F allowed these exposures to last beyond 20 minutes.

(After Blockley⁽³⁰⁾, adapted from Kissen and Hall⁽¹²⁰⁾, Kaufman⁽¹¹⁷⁾, and Webb⁽²¹⁷⁾)



Tolerance time for man in a hot environment. The time scale indicates pre-pain time for exposure of the skin to radiant heat, and escape time for curve marked body. The latter refers to a lightly clad man with face exposed. The temperature scale denotes room temperature for the body curve and radiation temperatures for curves referable to the skin. The curve marked warm dry refers to experiments with an initially dry skin, and a skin temperature initially of about 30°C . A tourniquet was applied to obtain the data marked without circulation. The cold wet curve utilized skin exposed wet at an initial skin temperature of about 15°C . The clothed skin curve was obtained using skin covered with 1 cm insulating cloth with an initial skin temperature near 30°C .

(After Buettner⁽⁴¹⁾ from the data of Blockley and Taylor⁽²⁸⁾, Pfleiderer and Buettner⁽¹⁶⁰⁾)

where K' = a constant which depends on tissue conditions

t_b = internal body or core temperature

Since heat loss (\bar{H}) is the same in both equations, then:

$$K' (t_b - t_s) = K (t_s - t_a) \quad (51)$$

and

$$K'/K = (t_b - t_s) / (t_s - t_a) \quad (52)$$

which is called a "thermal circulation index" because if humidity, ventilation and clothing are held constant, then K'/K will depend largely on circulation (197). This ratio may be used as an index of the physiological state of the tissue or of physiological stress in the cold. From it may also be derived the heat loss of circulatory convection (54).

Inspection of K'/K shows that the most important quantities are air, body, and skin temperatures. As discussed under Heat Stress, body temperature is usually estimated with rectal temperature; skin temperature is taken as an average of selected points on the body surface each appropriately weighted by the surface area it represents. The value of q_s depends upon t_b , t_s , the mass changing temperature and specific heat of the tissue. This highly simplified equation 48 hides a number of complexities and does not isolate the specific contributions of radiative, convective, conductive, and evaporative heat losses (See Figure 6-56 and Equations 39, 40, 41). More detail is available (48, 54, 151).

Shivering ensues when heat losses to the environment exceed the metabolic energy being produced by the body. The shivering reaction increases skeletal muscle activity (without doing measurable work) and results in an increase in metabolic heat production. A two-fold increase in metabolism due to shivering has been observed after exposure to an ambient temperature of 41°F (5°C) for more than one hour. A five-fold increase in metabolism due to shivering is considered to be the maximum attainable (43). While shivering may add enough to metabolic heat production to prevent further heat loss it is never sufficient to replace heat already lost. The shivering response may be triggered by the rate of temperature fall of the body and not the temperature per se (47).

The body does not similarly respond to warm environments by reducing metabolic heat production. Instead, as body temperature increases, metabolic heat production increases in accordance with Van't Hoff's law (i.e., a 10°C rise in temperature will increase the velocity of a chemical reaction by a factor K , where $2 < K < 3$).

For a body at rest the temperature coefficient of metabolism can be expressed mathematically:

$$q_m = a_{(BMR)} (1 + 0.12\Delta t_b) \quad (53)$$

where Δt_b = rise in body temperature above 37°C - ($^\circ\text{C}$).

Figure 6-55 covers shivering thresholds of skin temperature during several metabolic loads.

Cold Stress Tolerance

The effective loss of about 80 kcal/m^2 or 31 BTU/ft^2 has been taken as the maximum heat loss a person can tolerate with severe discomfort (189). The heat available for loss can therefore be taken as $0.75 q_m + 80 \text{ kcal/m}^2$ where q_m is the metabolic rate in $\text{kcal/m}^2/\text{hr}$. Sleep of unacclimatized Caucasians will be disturbed by restlessness at 50% of this loss rate. The lowest ambient temperature at sea level which can be tolerated for prolonged thermal equilibrium is a function of the exercise rate, insulation, wind speed, and several other variables. A rough estimate of this critical temperature at very low wind velocities may be obtained by the equation (189):

$$\frac{t_a = 5.56 t_s - (I \times H)}{5.56} \quad (54)$$

t_s = mean skin temperature in $^\circ\text{C}$ assumed to be 32°C in the cold.

I = total insulation against convective and conductive loss in Clo units where 1 Clo = insulation maintaining a temperature difference of $.18^\circ\text{C}$ for a flow of $1 \text{ kcal/m}^2/\text{hr}$.

H = total heat available for convective and radiative loss or 0.75 times the metabolic rate (q_m) in $\text{kcal/m}^2/\text{hr}$ under equilibrium conditions.

Figure 6-98 may be used as a rough estimate of relative comfort levels at different metabolic rates and under different ambient temperature and insulation conditions. It is invalid for wind speeds above 20 ft/min.

An empirical expression for the total cooling power of the environment, disregarding evaporation, is called Windchill (109):

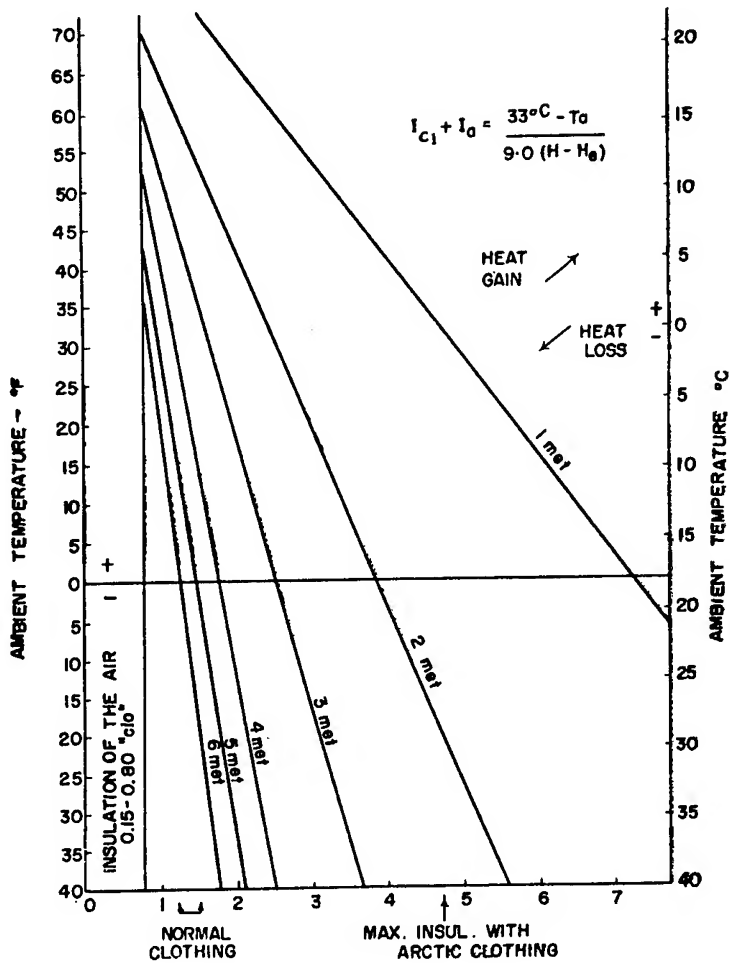
$$K_c = (\sqrt{\bar{V} \times 100} + 10.5 - \bar{V}) (33 - t_a) \quad (55)$$

where K_c = windchill, i.e., total cooling in kilogram calories per square meter per hour

\bar{V} = wind velocity in meters per second

t_a = air temperature in $^\circ\text{C}$

While K_c is not representative of human cooling, and is probably not very closely representative of physical cooling either, windchill has come into common use as a single-valued index of the severity of the temperature-wind combinations. As such it provides a descriptive quantity against which human cooling phenomena can be evaluated. A nomogram, giving rapid approximations of windchill is provided as Figure 6-99. When the



$$1 \text{ met} = 50 \text{ kcal/hr}\cdot\text{m}^2$$

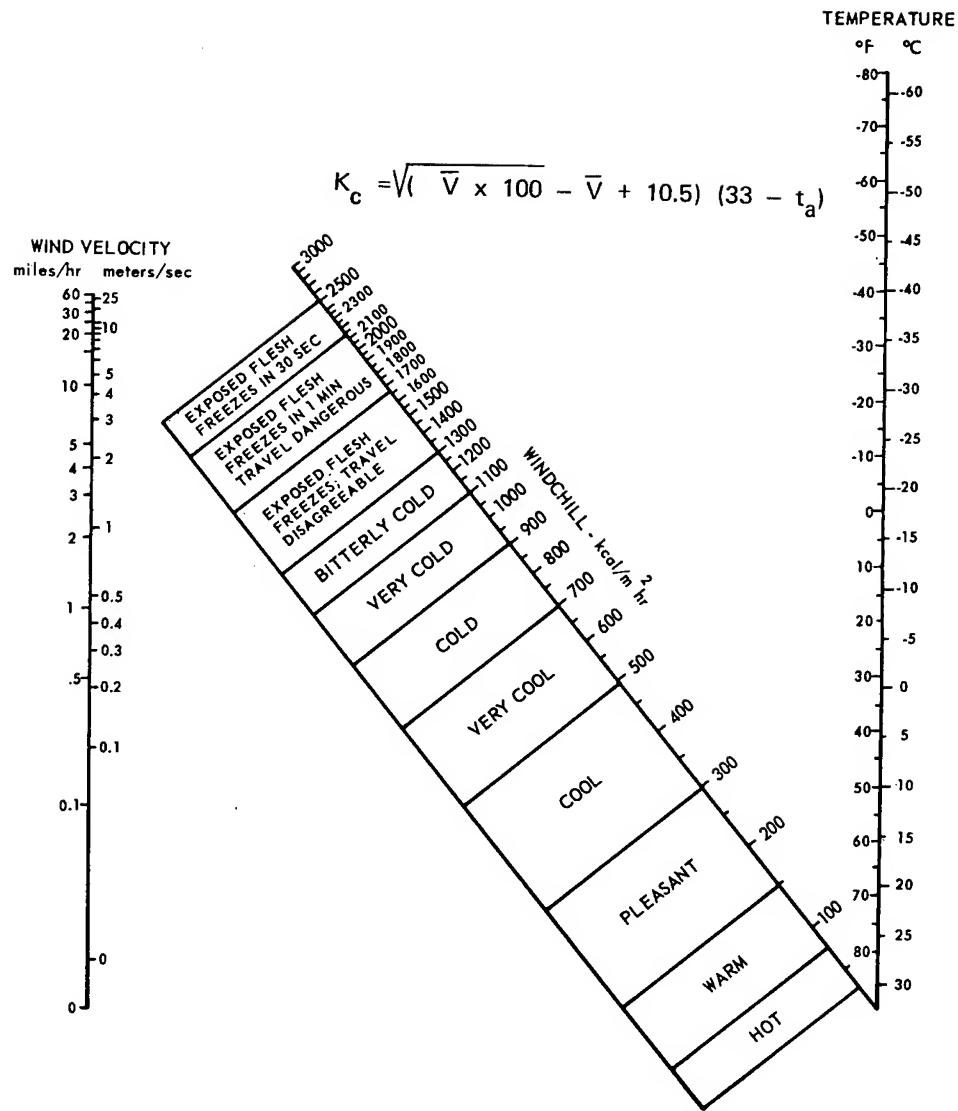
$$1 \text{ Clo} = 0.18^\circ\text{C}/\text{kcal}\cdot\text{m}^2\cdot\text{hr}$$

This chart shows the approximate relationship between ambient temperature and the units of insulation (expressed as "Clo") required to maintain thermal comfort. It will, in addition, indicate the varying degrees of heat loss (or gain) and levels of thermal equilibrium under varying degrees of heat production and exercise. No estimates can be made with this diagram to include the effects of wind velocity greater than 20 ft/min.

Figure 6-98

Comfort Levels at Various Ambient Temperatures with Different Levels of Heat Production

(After Adams⁽¹⁾)



In outdoor cold weather, the wind velocity has a profound, sometimes decisive, effect on the hazard to men who are exposed. The windchill concept dramatizes this well known fact by providing a means for quantitative comparison of various combinations of temperature and wind speed. Note for example that -50°F with an air movement of 0.1 mph has the same windchill value, and therefore is predicted to produce the same sensation on exposed skin, as -15°F with a wind of only 1 mph or $+14^{\circ}\text{F}$ with a wind of 5 mph. The windchill index does not account for physiological adaptations or adjustments and should not be used in a rigorous manner. It is based on field measurements by Paul Siple during World War II of the rate of cooling of a container of water.

Figure 6-99

Windchill Nomogram

(After Blockley⁽³⁰⁾, Adapted from Consolazio et al⁽⁵⁸⁾ and Siple and Passell⁽¹⁸⁴⁾)

rate of body heat production is greater than the windchill, excess heat is removed by evaporation; under bright, sunny conditions, the nomogram values should be reduced approximately 200 kg. cal. Figure 6-100 represents the heat lost by men under different windchill conditions in the nude.

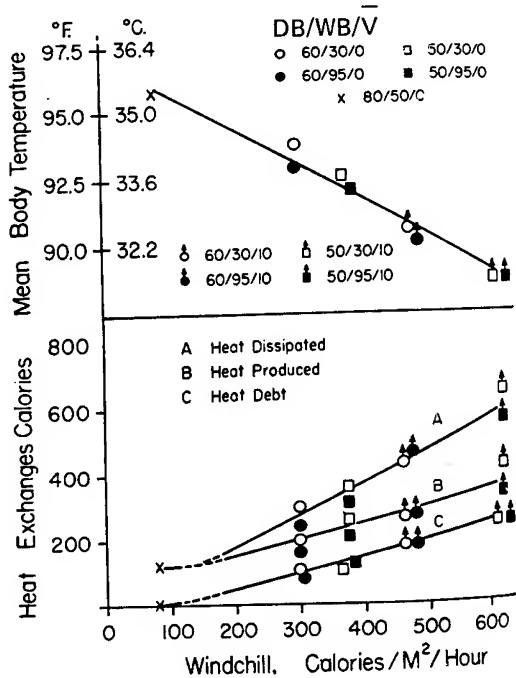


Figure 6-100

The Relationship of Mean Body Temperature and Heat Exchanges of Six Men to Windchill, after 100 Minutes of Exposure in the Nude.

The conditions are coded as dry bulb temp ($^{\circ}$ F)/relative humidity (%)/ windspeed (mph).

(After Lampietro, Bass, and Buskirk⁽¹⁰⁹⁾)

In military operations or when the wetting of feet is a problem, the freezing of flesh begins at variable levels lower than 1400 windchill. Well-trained and acclimatized men can tolerate a higher windchill index (222). The windchill index has often been criticized because it is not feasible to express the effect of wind on heat loss without references to the amount of clothing being worn. The same wind speed will increase the heat loss of a lightly clad man very greatly, but increases only slightly the heat loss of a heavily clothed man. These objections can be avoided by using the windchill values as index numbers on a relative scale and not expressing them in actual amounts of heat loss in $\text{kcal} \times \text{m}^{-2} \times \text{hr}^{-1}$. Used in this manner it has been found to provide an index corresponding quite well with the discomfort and tolerance of man in the cold. This is because the tolerance will be determined by the parts of the body which are usually unprotected, such as the face and hands. The windchill then applies to the naked face or the bare hands, where the pathological effect of cooling first will appear.

Figures 6-101 and 6-102 indicate the insulation required in cold air at sea level for comfort and thermal equilibrium. Table 6-89 represents the physiological response to cold air.

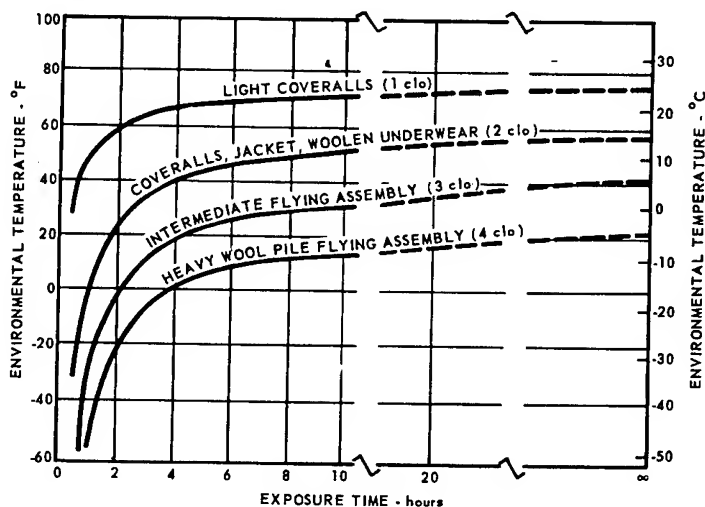
For ocean recovery in winter months, the rate of cooling in water is of importance. Figure 6-103 is a nomogram for estimating tolerance time to cold water immersion (187). Figure 6-104 is a graphic presentation of

Figure 6-101

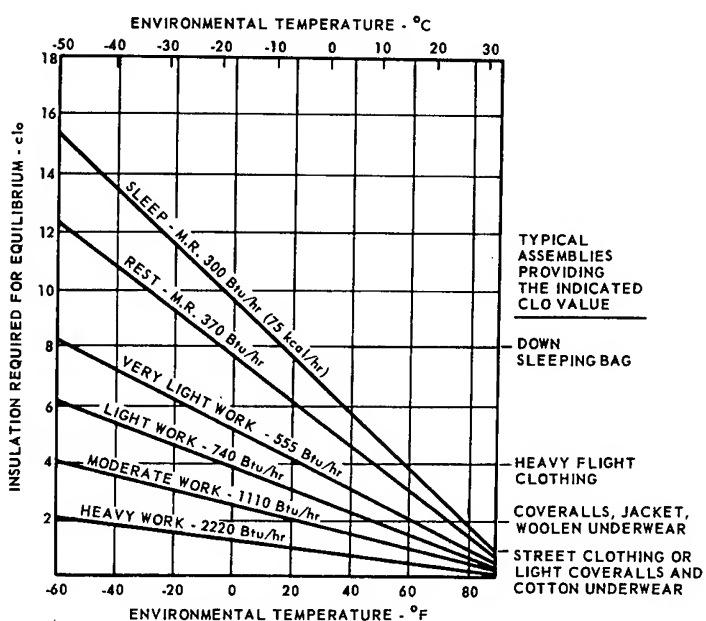
Insulation Required in Cold Air at Sea Level

(After Blockley⁽³⁰⁾, Adapted from Burton and Edholm⁽⁴⁸⁾, and Taylor⁽¹⁹⁷⁾)

a.



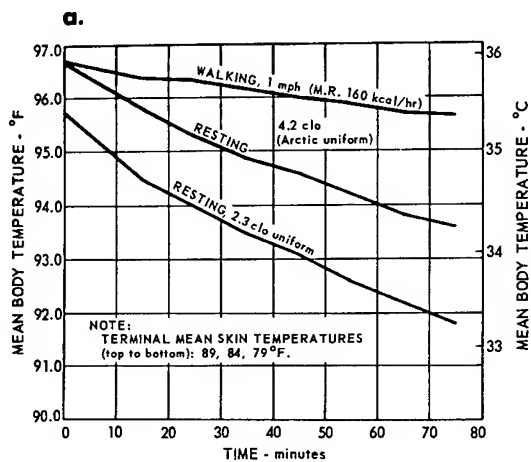
b.



The amount of clothing insulation that is adequate for a particular cold environment depends on the length of time one is to be exposed and the activity level, or metabolic heat production rate. Chart a shows the influence of exposure time for low activity, sitting (pilot activity), while chart b illustrates the effect of metabolic rate on the insulation required for continuous exposure which requires maintaining heat balance indefinitely. Both charts are slightly unrealistic--the first because of the uncertainty as to appropriate criteria for tolerance limits, and the second because no activity, even sitting, is continued indefinitely. Note also that clothing insulation of more than 4.5 clo at one atmosphere becomes almost impossibly bulky, and even this amount of insulation is unattainable in ordinary footgear and handgear; thus the predictions of this diagram cannot be achieved in practice without taking special precautions to protect hands and feet (e.g., by electrical heating) or by using non-anthropomorphic protective enclosures.

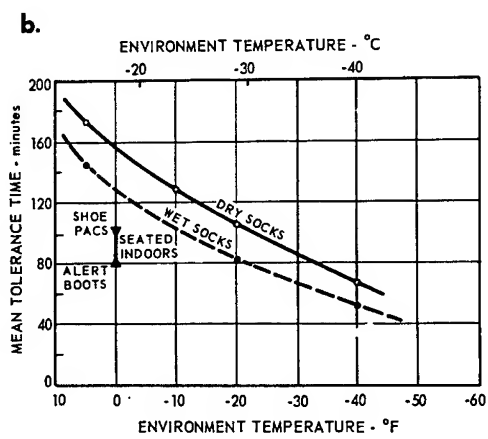
Figure 6-102

Cold Tolerance of Active Clothed Subjects



(After Blockley⁽³⁰⁾, Adapted from data of Veghte and Clogston⁽²⁰⁸⁾)

Tolerance to cold wearing inadequate body insulation is shown in figure a, which illustrates the principles underlying estimation of tolerance time in severe cold stress situations. The data are averages for four subjects studied outdoors in Alaska. Temperatures were all within a few degrees of the average, -32°C (-26°F), and wind velocity ranged from zero for the 2.3 clo tests to 65 ft/min for the resting experiments with the 4.2 clo uniform. The rate of fall of the body temperature ($0.67 \times \text{rectal} + 0.33 \times \text{skin}$) is a measure of the rate of negative storage, reflecting the imbalance between heat production and heat loss by the body. It has been estimated that serious discomfort results from a total heat debt of 150 kcal. The survivable limit of heat debt is uncertain; it would in any case be heavily dependent on the procedures and facilities for rewarming. Most practical experiments are necessarily terminated at the point of incipient tissue damage—temperature of 4°C (39°F) or less at some local surface. It may be that death from hopelessness is a more frequent sequel of real exposures beyond this point than the incurring of an intolerable heat debt.



Cold tolerance at rest wearing adequate body insulation is shown in figure b for increasingly cold environments. The prime limiting factor in voluntary tolerance of cold distress is the development of painfully cold feet. (The hands are more easily protected inside the clothing.) Even when the total body insulation is an impractical 5.9 clo (close to wearing a sleeping bag), ordinary footgear limits tolerance time at 0°F (shown by the vertical bar) to 77-104 minutes, which are average times for five men. The chart shows that the improvement so far achieved with insulated boots is not impressive, particularly if the socks become wet. There is a distinct risk of tissue damage when any part of the skin reaches 39°F (4°C). Most men refuse to continue before this point is reached.

(After Blockley⁽³⁰⁾, Adapted from Carlson⁽⁵⁴⁾, and Skrettingland et al⁽¹⁸⁵⁾)

Figure 6-102 (continued)

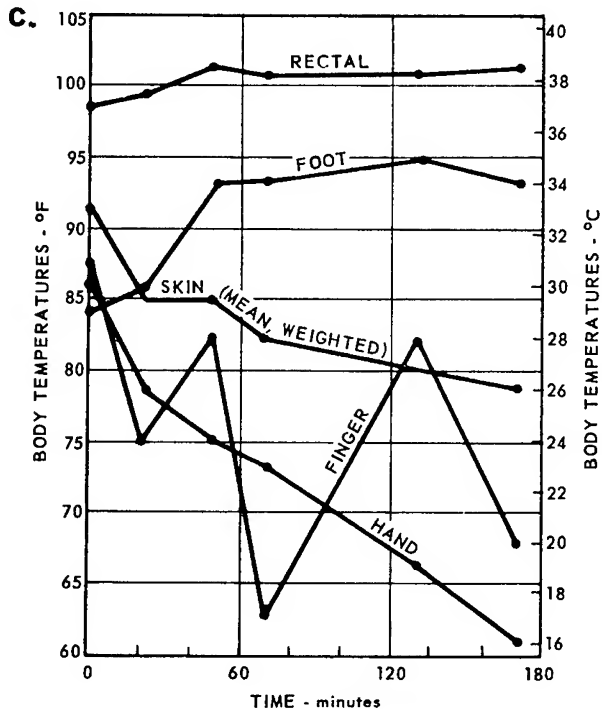
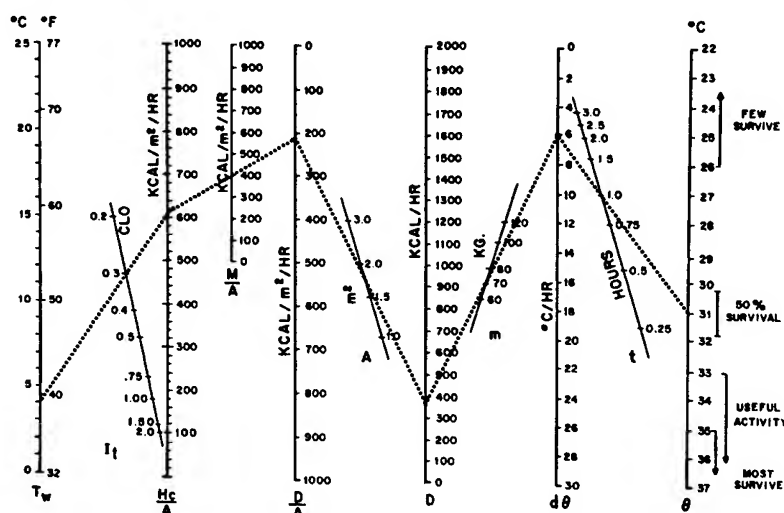


Figure c is a record of body temperatures while marching at -38°F (-39°C) for one subject who was dressed in long underwear, wool shirt and sweater, army field jacket and trousers with liner, arctic felt boots, two pairs of socks, mittens and wool gloves. He walked six miles on hard-packed snow, with his metabolic rate averaging $220 \text{ kcal/m}^2\text{ hr}$. The wind velocity was 8 mph, so that the windchill index was 1850 ("travel dangerous, flesh freezes 1 min").

These data illustrate the fact that rectal temperature can be maintained at its customary level during work in severe cold, provided sufficient clothing is worn. In such situations, the constant dangers are of freezing of under-protected areas and sweating of over-protected parts of the body. As soon as the activity is reduced or stopped, excessive heat loss occurs from the area wetted by sweat during work, and a precipitous drop in body temperature may result.

(After Blockley⁽³⁰⁾, Adapted from Milan⁽¹⁴⁴⁾)



To relate the many factors involved in estimating tolerance in cold water, the nomogram below has been devised where one knows or can assume: water temperature (T_w); insulation of clothing and tissue (I_t); metabolic heat production per unit surface area (M/A); the immersed surface area (A); body mass (m); and exposure time (t). As shown by the dotted example line (for a nude man in water at 4°C , a metabolic rate of $400 \text{ kcal/m}^2\text{ hr}$, an immersed surface area of 1.75 m^2 , a body mass of 75 kg , and an exposure time of one hour) the nomogram predicts: heat loss to the environment H_e/A ; heat debt per unit surface area (D/A); heat debt (D); change in mean body temperature ($d\theta$); and mean body temperature (θ).

Figure 6-103

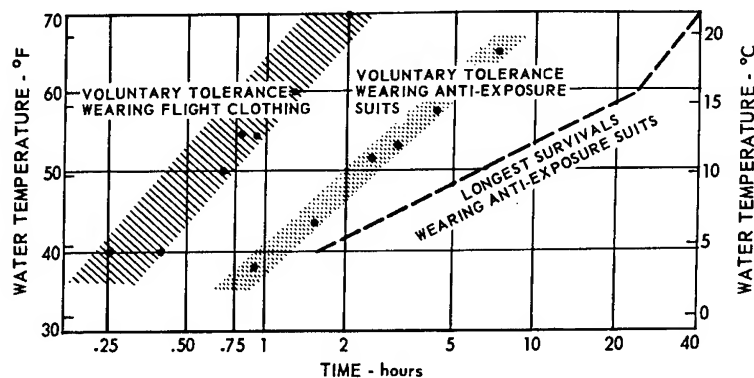
Nomograph for Estimation of Tolerance Times to Cold Water Immersion. (See text for use)

(Adapted from Smith and Hames⁽¹⁸⁷⁾ by Gillies⁽⁸⁵⁾ and Blockley⁽³⁰⁾)

Figure 6-104
Survival in Cold Water

(After Blockley⁽³⁰⁾, Adapted from Beckman and Reeves⁽¹³⁾, Damato and Radliff⁽⁶²⁾, Hall et al⁽⁹⁵⁾, McCance et al⁽¹³³⁾, Molnar⁽¹⁴⁷⁾, U.S. Navy⁽²⁰⁵⁾, and Barnett⁽¹⁰⁾)

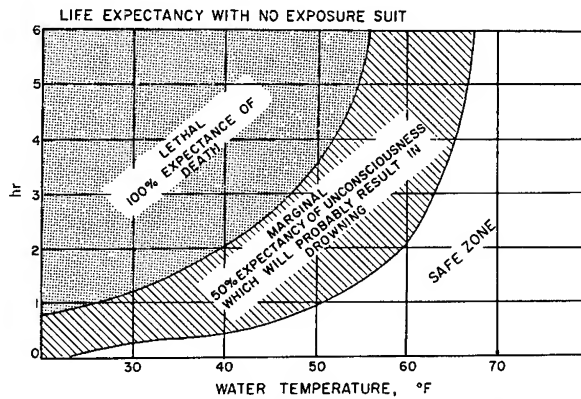
a. Voluntary Tolerance to Cold Water



The "voluntary tolerance, flight clothing" zone in figure a shows the average results from numerous experimental studies, including a recent one using a diver's "wet suit" in conjunction with a flight suit and long underwear. Such experiments are typically terminated when the subject declines to accept the discomfort any longer, or reaches a skin temperature below 50°F. The second limit shown, pertaining to men protected by potentially waterproof garments, reflects the fact that hands and feet cannot be adequately insulated and remain functional. Nude men in 75°F water reach within 12 hours one or another tolerance limit (rectal temperature below 95°F, blood sugar below 60 mg/100 ml, or muscle cramps).

The extent to which real survival time would exceed this limit is difficult to predict, due to the importance of injury, equipment available, and such psychological factors as belief in the possibility of rescue. An analysis of over 25,000 personnel on ships lost at sea during 1940-44 showed that of those who reached life rafts, half died by the sixth day if the air temperature was below 41°F (5°C); survival time increased with increasing air temperature.

b. Life Expectancy in Cold Water with No Exposure Suit



The expectation of life following cold water immersion. The data is that of Molnar.

practical experience in cold water tolerance with routine flight clothing and anti-exposure suits. Figure 6-105 represents the time to reach critical core and skin temperatures after exposure to cold water in several types of exposure suits. Recent developments in isotopic heating devices make practical the use of exposure garments heated for long periods of time (176).

In cold air, injury to the extremities is often a limiting factor in human performance (42). Figure 6-106 represents the power required to attain given skin temperatures of hand and foot in electrically heated gloves and socks with subjects in air temperature of -40°F in a 10 mph wind. Performance is severely hindered if temperature of fifth finger falls below 55°F (55).

Figure 6-107 represents a typical physiological response of a body immersed in cold water and rewarmed. The pathophysiology and treatment of hypothermia and cold injury in space operations have been recently reviewed (52).

Performance in the Cold

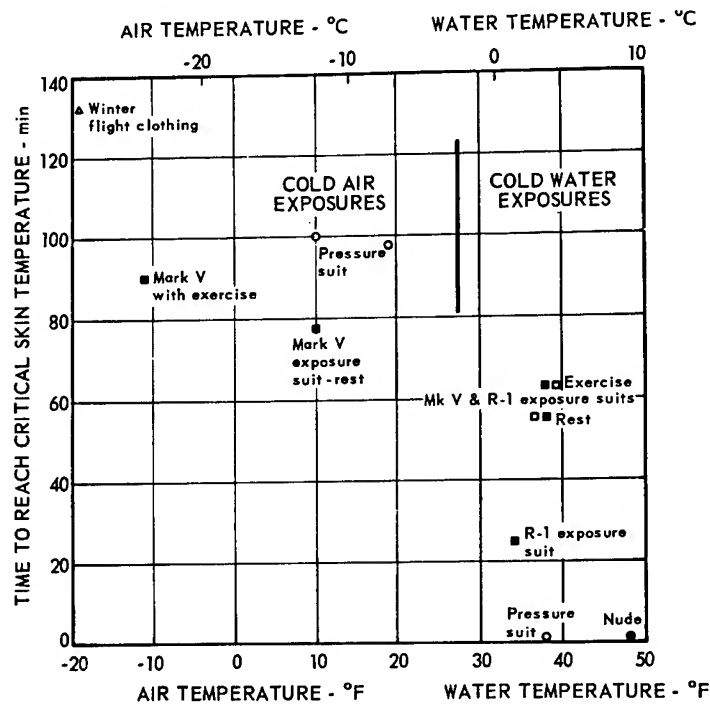
Exercise performance decreases during hypothermia (169). When the mean body temperature is decreased from a control value of 35.5°C to 33.3°C, and thermal gradients from core to skin increased from 2.7°C to 10.1°C, mean treadmill times to exhaustion decreased from 4.6 minutes to 4.1 minutes. The VO₂ max decreased 5%, O₂ requirement per minute of running increased 6%. There was no significant difference in average values of O₂ debt and lactate values from controls. The decreased efficiency in the cold is attributed to increased tension and viscosity in cold muscles and from the fact that in the cold, a greater proportion of the energy appeared to come from anaerobic sources than in the control runs.

Skilled motor performance shows a progressive loss with continued cold exposure (202). The sensitivity of skin to cold stress is seen in Figure 6-96 and Tables 6-58, 6-64 and 6-65.

Tactual sensitivity is markedly affected by lowered skin temperature. A numbness index has been developed based upon the individual's ability to discriminate the separateness in space of two straight edges upon which the finger is placed (V-test or two-edge limen) (138). Figure 6-108 shows the great difference in the size of gap required to detect the presence of the gap under varying conditions of air temperature and wind speed. Exposure was for approximately three min. The numbness index is the difference in just detectable gap between control data obtained before exposure, at the end of exposure, and at varying intervals following exposure. The data are clear in showing a great loss in tactual sensitivity under the more extreme conditions and a slower recovery following them. Figure 6-109 shows data using both the V-test and the classical two-point (aesthesiometer) test to describe the relationship between tactual acuity and digital temperature (145, 146). It is clear that there is no difference between the two types of stimulation. The minimum detectable gap appears to be approaching infinity at skin temperatures slightly greater than freezing. In the case of individual subjects, gaps of 14 millimeters could not be discriminated at skin temperatures slightly above the freezing point.

Figure 6-105
Clothing Tests in Cold Air and Water

a. Time to Reach Critical Skin Temperature in Cold Air and Water



The relative protection of various types of aircrew clothing in water immersion and exposure to cold air is illustrated in this graph, which shows the time required to reach a critical mean skin temperature of 76°F in each assembly. The criterion of 76°F is based on the general observation of extreme discomfort when this point is passed; in most of the experiments summarized here, some subjects requested termination of the exposure at or near the time when the group average reached this point. The clothing assemblies were: winter flight clothing--the group average reached this point. The clothing assemblies were: winter flight clothing--the assembly specified by the Alaskan Air Command, USAF; the Navy anti-exposure suit assembly, Mark V; the (obsolete) Air Force anti-exposure suit assembly, R-1; and an Air Force pressure suit with bladders in torso, arms, and legs, designated CSU 4/P. Note for comparison the data point for nude exposure to water at 48°F. The value of exercising in cold air, and the lack of an advantage in cold water, is evident.

(After Blockley⁽³⁰⁾, Adapted from Barnett⁽¹⁰⁾)

b. Estimated Survival Times in Cold Water with Latest Survival Clothing*

Suit	Water Temp.	Air Temp.	Time *
R1-A	1.9°C	-18°C	5 hrs
R1-A	0°C	1°C	18 hrs
CWU-12/P	12°C	15°C	15 hrs
CWU-3/P	7°C	12°C	10 hrs

* Estimated time (in hours) required for subjects' rectal temperatures to reach 31°C.
Rapid rewarming of hypothermic subject in 42°C water required for resuscitation.

(After Milan⁽¹⁴³⁾)

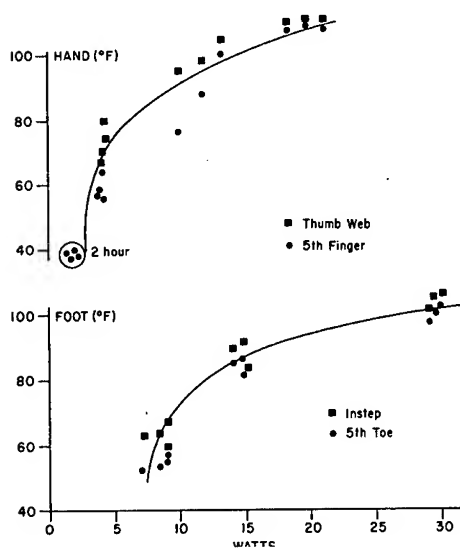


Figure 6-106

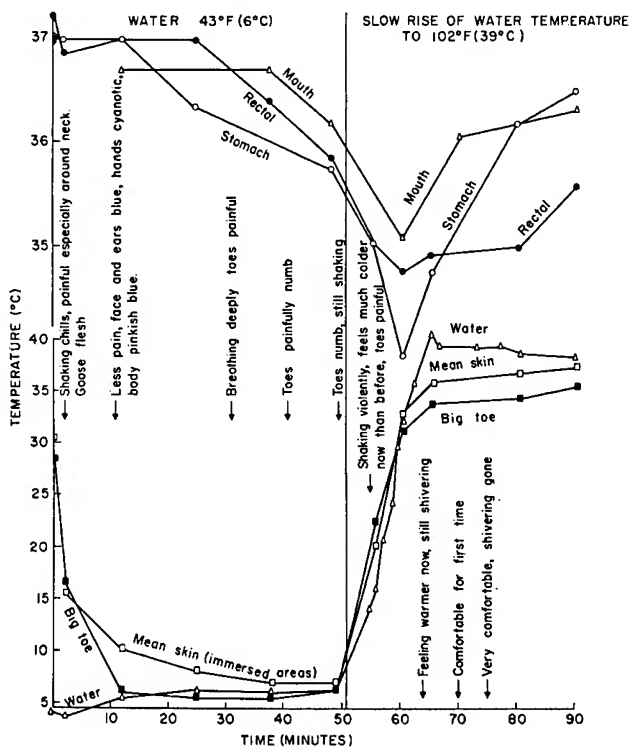
The Hand and Foot Temperatures Maintained as a Function of the Power Used for Auxiliary Heated Gloves and Socks. Air Temperature is -40°F with a 10 mph Wind. Body Core was wound in a U.S Army Quartermaster 4.3 Clo Cold-Dry Standard Clothing Ensemble.

(After Goldman⁽⁸⁷⁾)

Figure 6-107

Changes in Body and Skin Temperature of Subject Immersed in Water at 6°C (43°F) for 52 Minutes. The Water Was then Warmed to 39°C . Note the Sharp Fall of Gastric, Oral, and Rectal Temperatures Initially on Warming.

(After Behnke and Yaglou⁽¹⁴⁾)



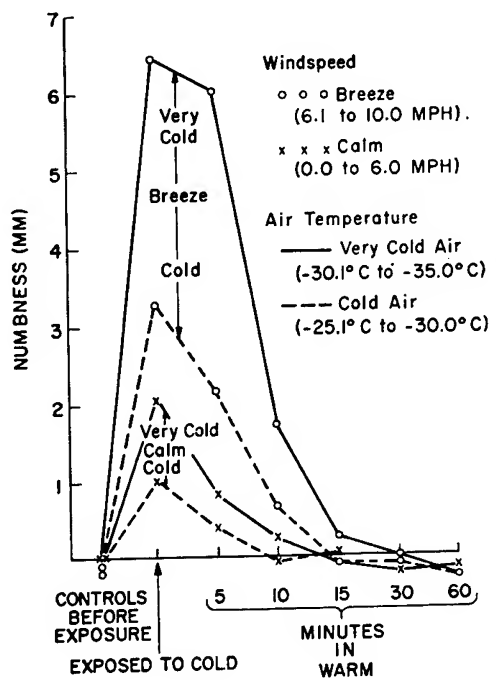


Figure 6-108

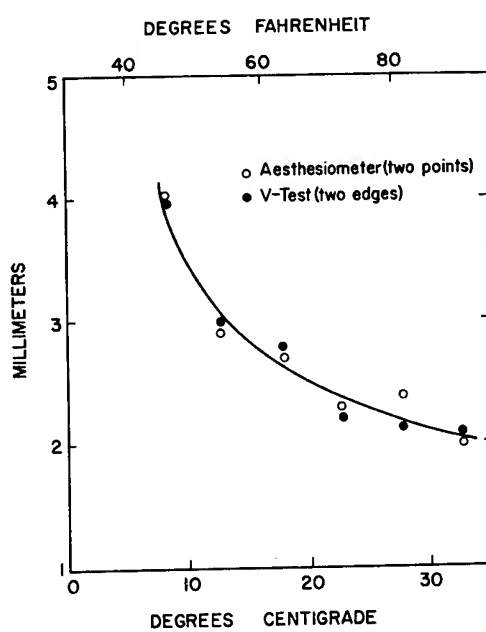
Comparison of the Effects of Windspeed and Air Temperatures on the Numbness Index in Air at Sea Level

(After Macworth⁽¹³⁸⁾)

Figure 6-109

Comparison of the Two-Edge and Two-Point Thresholds as a Function of the Skin Temperature in Air at Sea Level.

(After Mills⁽¹⁴⁶⁾)



The minimum pressure on the skin required for detection is inversely proportional to skin temperature (146). Threshold amplitude of vibration of the skin depends on relatively small changes in skin temperature, the greatest sensitivity to vibration occurring when the skin temperature (of the wrist) was increased about 4°C above normal; above and below this optimum, sensitivity decreased (218).

General performance is also altered by cold in a complex way. Figure 6-110 shows the effects of various combinations of air temperature and velocity (and thus windchill) on the manual dexterity of soldiers. Complete arctic uniforms were worn except as indicated. During the test trials the subjects removed the heavy arctic gauntlet and performed with only the wool trigger-finger insert. The results are based upon a total of 530 soldiers sorted into the various subgroups of the experiment. It may be seen that performance time increased in direct proportion to the windchill and that mean skin temperature and digital temperature were roughly inversely proportional to windchill. The rate of cooling is an important factor (56, 82, 83). There is clearly a relationship between performance and the skin temperatures. However, analysis of these data and those of Figure 6-111 indicates that the direct dependence of performance on finger and skin temperatures may be relatively small; that other factors of a psychological or physiological nature may be of equal or possibly greater importance. Total body cooling is not as significant a factor as finger temperature in dexterity tests (82, 83). It has been shown that cooling of the hand decreases finger flexibility(126).

The speed of reaction of men to simple visual signals is also affected by the cold (201). The relative loss is not as great as that of tactual sensitivity, but it is greater than that of manual dexterity. Figure 6-112 shows a comparison of these three phenomena for appropriately dressed, but unacclimatized men in terms of the percentage loss relative to optimum thermal conditions. Figure 6-113 shows degradation of pursuit performance at low temperature.

It is thus reasonable to expect losses in the cold for all types of performance which depend upon any of these functions, as well as tasks of eye-hand coordination (199) and intellectual tasks requiring fast reactions such as the code test (106). So far there has been nothing reported to indicate that intellectual tasks not requiring fast reaction times, motor skills or tactual sensitivity are affected by cold exposure, at least short of the accumulation of a serious heat debt.

Acclimatization to Cold

Recent evidence is contrary to the older view that under cold conditions increased voluntary caloric intakes and other compensatory processes result from low temperature as such; rather, they may result from the increased energy expenditures associated with field activities (8, 33, 54, 63, 206). Whatever the direct cause, the result contributes to a beneficial increase in heat production, vasomotor, and renal control. The major known physiological changes, both short and long term, which are produced in the cold are shown in Table 6-89. Inspection of this table shows that acclimatization

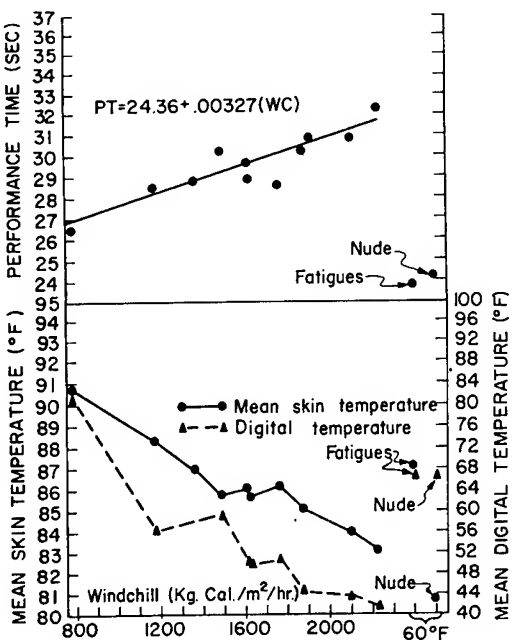


Figure 6-110

Performance Time, Skin and Digital Temperature as a Function of Windchill. Arctic Clothing Worn Except Where Indicated. Hand Exposed During Performance Only. Follows Approximately 35 Minutes of Exposure.

(After Teichner⁽²⁰⁰⁾)

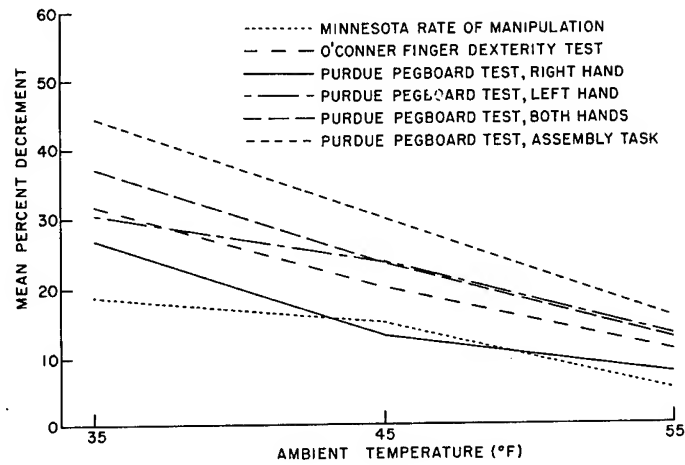


Figure 6-111

Percent Decrement in Performance as a Function of Ambient Temperature at Sea Level

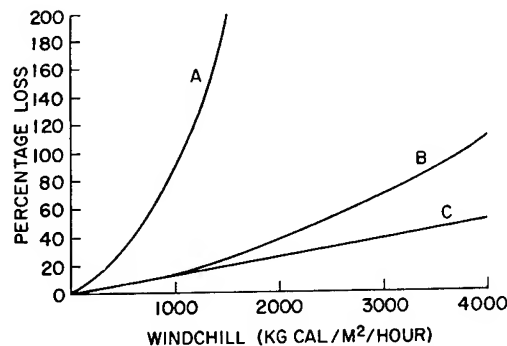
(After Dusek⁽⁶⁸⁾)

Figure 6-112

Minimum Effects of the Cold on Selected Functions. Each Curve is an Estimated Percentage Loss of the Indicated Type of Performance for Appropriately Dressed but Unacclimatized Men.

- A) Tactual Sensitivity of the Bare Hand
- B) Simple Visual Reaction Time
- C) Manual Skill

(After Teichner⁽²⁰¹⁾)



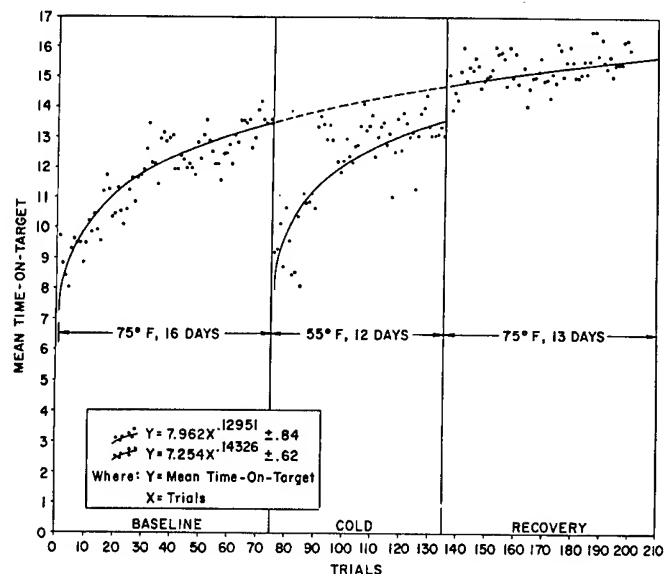


Figure 6-113

Rotor Pursuit Performance as a Function of Practice Under Different Conditions of Temperature

(After Teichner and Kobrick (198))

takes the form of increased levels of some functions and the return to normal of others. Data have been obtained on the cold acclimatization of skills (138, 198, 202) as shown in Figure 6-113. Discussions of the problems of acclimatizing astronauts to cold are available (52, 173). The value of such an approach to increasing the performance and survival capabilities of astronauts during emergencies in such missions as lunar night operations has not as yet been established.

As to the question of conflicts in the simultaneous acclimatization to heat and cold, it has been found that fully acclimatized men retain acclimatization to heat during 14 days of severe cold exposure (5-1/2 hours per day at -20°F). (190). Conversely, it has been suggested that artificially or seasonally acquired "cold acclimatization" is unaffected by a 21-day heat exposure (64). These findings do not conclusively prove but only suggest that heat and cold acclimatization are not mutually exclusive; they can coexist in an individual, and the loss of one usually occurs not as a result of the other, but as a result of the absence of an adequate acclimatizing stimulus. No serious conflicts between cold acclimatization and acclimatization to other stress parameters of lunar flight are apparent, though studies on these combined adaptations are distinctly limited. Much remains to be done in this area.

REFERENCES

- 6-1. Adams, T., Environmental Factors Influencing Thermal Exchange, AAL-TR-59-22, Arctic Aeromedical Lab., Ladd AFB, Alaska, Sept. 1960.
- 6-2. Adams, T., Funkhouser, G. E., Kendall, W. W., A Method for the Measurement of Physiological Evaporative Water Loss, FAA-63-25, Federal Aviation Agency, Oklahoma City, Okla., 1963.
- 6-3. Adolph, E. F. and Associates, Physiology of Man in the Desert, Interscience Publishers, N. Y., 1947.
- 6-4. Air Force Systems Command, Headquarters, Handbook of Instructions for Aerospace Personnel Subsystems Design, AFSCM-80-3, Andrews AFB, Washington, D. C., 1966.
- 6-5. Air Technical Service Command Engineering Division, Aerospace Medical Labs., Wright-Patterson AFB, Ohio, MR-TSEAL-3-695-55, 1945.
- 6-6. AiResearch Manufacturing Co., Division of Garrett Corp., Extravehicular Suit Thermal and Atmospheric Control, SS-3056, Los Angeles, Calif., 1964.
- 6-7. American Society of Heating, Refrigerating and Air-Conditioning Engineers, ASHRAE Guide and Data Book for 1965-66, New York, 1965.
- 6-8. Andersen, K. L., Interaction of Chronic Cold Exposure and Physical Training upon Human Bodily Tolerance to Cold, Inst. of Work Physiology, Oslo, Norway. (Arctic Aeromedical Lab. contract no. AF61(052)-758, Aug. 1964).
- 6-9. Bader, F., Considerations for Temperature Control of Air-crewman through Water Cooled Garments, SLS-121-65, Johns Hopkins Applied Physics Lab., Silver Spring, Md., 1965, p. 6.
- 6-10. Barnett, P., Field Tests of Two Anti-exposure Assemblies, AAL-TDR-61-56, Arctic Aeromedical Lab., Fort Wainwright, Alaska, 1962.

- 6-11. Bass, D. E., Kleeman, C. R., Quinn, M., et al., Mechanisms, of Acclimatization to Heat in Man, Medicine, 34: 323-380, 1955.
- 6-12. Beaumont, W. van, Bullard, R. W., Sweating: Direct Influence of Skin Temperature, Science, 147: 1465-1467, Mar. 1965.
- 6-13. Beckman, E. L., Reeves, E., Physiological Implications as to Survival from Immersion in 75° Water, Aerospace Med., 37: 1136-1142, 1966.
- 6-14. Behnke, A. R., Yaglou, C. P., Physiological Responses of Men to Chilling in Ice Water and to Slow and Fast Rewarming, J. Appl. Physiol., 3: 591-602, Apr. 1951.
- 6-15. Belding, H. S., Hatch, T. F., Index for Evaluating Heat Stress in Terms of Resulting Physiologic Strains, Heating, Piping and Air Conditioning, 27: 129-136, Aug. 1955.
- 6-16. Benzinger, T. H., The Diminution of Thermoregulatory Sweating during Cold-Reception at the Skin, Proc. Nat. Acad. Sci., 47: 1683-1688, 1961.
- 6-17. Benzinger, T. H., Kitzinger, C., Pratt, A. W., The Human Thermostat, in Temperature, Its Measurement and Control in Science and Industry, Vol. 3, Pt. 3, Biology and Medicine, Hardy, J. D., (ed.), Reinhold Publishing Corp., N. Y., 1963, pp. 637-665.
- 6-18. Berenson, P. J., AiResearch Mfg., Co., 9851-9951 Sepulveda Blvd., Los Angeles, Calif., personal communication, 1967.
- 6-19. Berenson, P. J., General Analysis of Human Thermal Comfort, Rep. SS-3245, AiResearch Mfg. Co., Div. of Garrett Corp., Los Angeles, Calif., Jan. 1965.
- 6-20. Berenson, P. J., Green, F. H., Human Thermal Comfort in Helium-Oxygen Atmospheres, Rep. LS-149, AiResearch Mfg. Co., Div. of Garrett Corp., Los Angeles, Calif., May 12, 1965.
- 6-21. Berenson, P. J., Prediction of Human Thermal Comfort in Oxygen-Nitrogen Atmospheres, in Physiological and Performance Determinants in Manned Space Systems, Horowitz, P., (ed.), American Astronautical Society, Baltimore, Md., 1965, Vol. 5, pp. 1-29.
- 6-22. Bevans, J. T., The Thermal Properties of Selected Space Suit Materials, NASA-CR-65678, Oct. 1965.

- 6-23. Billingham, J., Hughes, T. L., Protection of Aircrew against the High Cabin Temperatures Which May Occur in Prolonged Supersonic Flight After Failure of the Cabin Cooling System, FPRC 1109, RAF Flying Personnel Res. Comm. Farnborough, England, 1960.
- 6-24. Black, I. A., et al., Basic Investigation of Multi-Layer Insulation Systems, NASA-CR-54191, Oct. 1964.
- 6-25. Blockley, W. V., Changes in the Boundary between Neutral and Stressful Thermal Conditions Caused by Respiratory Protective Equipment, Final Report, Webb Associates, Yellow Springs, Ohio, 1964. (Subcontract A-815-3 to Prime Contract DA-18-108-CML-6611(A) with Mine Safety Appliances).
- 6-26. Blockley, W. V., Human Sweat Response to Activity and Environment in the Compensable Zone of Thermal Stress: A Systematic Study, NASA-CR-65260, 1965.
- 6-27. Blockley, W. V., McCutchan, J. W., Taylor, C. L., Prediction of Human Tolerance for Heat in Aircraft: A Design Guide, WADC-TR-53-346, May 1954. (AD-47084).
- 6-28. Blockley, W. V., Taylor, C. L., Studies of Human Tolerance for Extreme Heat, First Summary Report, Memo Rep. No. 696-113A, Air Materiel Command, Wright-Patterson AFB, Ohio, 1948.
- 6-29. Blockley, W. V., Taylor, C. L., Studies of Human Tolerance for Extreme Heat, Second Summary Rep., AF-TR-5831, Air Materiel Command, Wright-Patterson AFB, Ohio, 1950.
- 6-30. Blockley, W. V., Temperature, in Bioastronautics Data Book, Webb, P., (ed.), NASA-SP-3006, 1964, pp. 103-131.
- 6-31. Bonura, M. S., Nelson, W. G., Engineering Criteria for Spacecraft Cabin Atmosphere Selection, NASA-CR-891, Sept. 1967.
- 6-32. Bottomley, T., Bellcomm, Inc., 1100 Seventeenth St., Washington, D. C., personal communication, 1966.
- 6-33. Brauer, R. W., Behnke, A. R., Hypothermia, in Principles of Internal Medicine, Harrison, T. R., Adams, R. D., Bennett, I. L., Jr., et al., McGraw-Hill (Blakiston Div.), N. Y., 4th Ed., 1962, pp. 835-841.

- 6-34. Brebner, D. F., Kerslake, D. Mck., Waddell, J. L., Diffusion of Water Vapor through Human Skin, J. Physiol., 132: 225-231, 1956.
- 6-35. Brebner, D. F., Rapid Acclimatization to Heat in Man, FPRC-Memo-177, RAF Flying Personnel Research Comm., Farnborough, England, July 1961.
- 6-36. Breeze, R. K., Space Vehicle Environmental Control Requirements Based on Equipment and Physiological Criteria, ASD-TR-61-161(Pt. 1), Aeronautical Systems Div., Wright-Patterson AFB, Ohio, 1961.
- 6-37. Brown, A. C., Analog Computer Simulation of Temperature Regulation in Man, AMRL-TDR-63-116, Aerospace Medical Research Labs., Wright-Patterson AFB, Ohio, 1963.
- 6-38. Brown, A. C., Further Development of the Biothermal Analog Computer, AMRL-TR-66-197, Aerospace Medical Research Labs., Wright-Patterson AFB, Ohio, 1966.
- 6-39. Bryan, A. C., Breathing, in Bioastronautics Data Book, Webb, P., (ed.), NASA-SP-3006, 1964, pp. 273-290.
- 6-40. Buettner, K., Effects of Extreme Heat and Cold on Human Skin. III. Penetrating Flash, J. Appl. Physiol., 5: 207-220, 1952.
- 6-41. Buettner, K., Thermal Aspects of Travel in the Aeropause Problems of Thermal Radiation, in Physics and Medicine of the Upper Atmosphere, White, C. S., Benson, O. O., Jr., (eds.), University of New Mexico Press, Albuquerque, 1952, pp. 88-98.
- 6-42. Bullard, R. W., Sweating: Its Rapid Response to Muscular Work, Science, 141: 643-646, 1963.
- 6-43. Bullard, R. W., Temperature Regulation, in Physiology, Selkurt, E. E., (ed.), Little, Brown and Co., Boston, Mass., 1963.
- 6-44. Burris, W. L., Wortz, E. C., Belton, N. J., et al., Internal Thermal Environment Management Program, SS-847, Rev. 2, AiResearch Mfg. Co., Div. of Garrett Corp., Los Angeles, Calif., Sept. 1963.
- 6-45. Burriss, W. L., Lin, S. H., Berenson, P. J., Study of the Thermal Processes for Man-in-Space, NASA-CR-216, Apr. 1965.

- 6-46. Burton, A. C., The Application of the Theory of Heat Flow to the Study of Energy Metabolism, J. Nutr., 7: 497-533, 1934.
- 6-47. Burton, A. C., Clothing and Heat Exchanges, Fed. Proc., 5: 344-351, 1946.
- 6-48. Burton, A. C., Edholm, O. G., Man in a Cold Environment: Physiological and Pathological Effects of Exposure to Low Temperatures, Edward Arnold, Ltd., London, 1955.
- 6-49. Burton, D. R., Collier, L., The Development of Water Conditioned Suits, RAE-ME-TN-400, Royal Aircraft Establishment, Farnborough, England, 1964.
- 6-50. Burton, D. R., Performance of Water Conditioned Suits, Aerospace Med., 37: 500-504, 1966.
- 6-51. Burton, D. R., Collier, L., Performance of Water Conditioned Suits, RAE-TR-65004, Royal Aircraft Establishment, Farnborough, England, 1965.
- 6-52. Busby, D. E., Clinical Space Medicine: A Prospective Look at Medical Problems from Hazards of Space Operations, NASA-CR-856, Jul. 1967.
- 6-53. Buskirk, E. R., Bass, D. E., Climate and Exercise, QREC-EP-61, Quartermaster Res. & Engin. Center, Natick, Mass., 1957.
- 6-54. Carlson, L. D., Man in Cold Environment. A Study in Physiology, Univ. of Washington, School of Medicine, Seattle, Wash., Aug. 1954.
- 6-55. Clark, R. E., The Limiting Hand Skin Temperature for Unaffected Manual Performance in the Cold, J. Appl. Psychol., 45: 193-194, 1961.
- 6-56. Clark, R. E., Cohen, A., Manual Performance as a Function of Rate of Change in Hand Skin Temperature, J. Appl. Physiol., 15: 496-498, 1960.
- 6-57. Clifford, J., Kerslake, D. McK., Waddell, J. L., The Effect of Wind Speed on Maximum Evaporative Capacity in Man, J. Physiol., 147: 253-259, 1959.
- 6-58. Consolazio, C. F., Johnson, R. E., Marek, E., Metabolic Methods, C. V. Mosby Co., St. Louis, 1951.

- 6-59. Craig, F. N., Ventilation Requirements of an Impermeable Protective Suit, Medical Division Research Rep. 5, Chemical Corps., Army Chemical Center, Md., Apr. 1950.
- 6-60. Cramer, K. R., Irvine, T. F., Jr., Attenuation of Nonuniform Suit Temperatures for Space Suits in Orbit, AMRL-TDR-63-80, Aerospace Medical Research Labs., Wright-Patterson AFB, Ohio, Sept. 1963. (AD-296343).
- 6-61. Crocker, J. F., Webb, P., Jennings, D. C., Metabolic Heat Balances in Men Wearing Liquid-Cooled Sealed Clothing, AIAA-CP-10, AIAA-NASA Third Manned Spaceflight Meeting, Houston, Texas, Nov. 4-6, 1964, pp. 111-117.
- 6-62. Damato, M. J., Radliff, M. H., Evaluation of the Divers' Wet Suit as Considered for Use by Pilots of Helicopters and Fixed-wing Aircraft, Naval Air Engineering Center, Air Crew Equipment Lab., Philadelphia, Pa., paper presented at the 35th Annual Meeting, Aerospace Medical Association, Miami Beach, Fla., May 11-14, 1964.
- 6-63. Davis, T. R. A., Acclimatization to Cold in Man, in Temperature: Its Measurement and Control in Science and Industry, Hardy, J. D. (ed.), Reinhold, New York, 1963, Vol. 3, Pt. 3, pp. 443-452.
- 6-64. Davis, T. R. A., Effect of Heat Acclimatization on Artificial and Natural Cold Acclimatization in Man, J. Appl. Physiol., 17: 751-753, 1962.
- 6-65. Dryden, C. E., Han, L., Hitchcock, F. A., et al., Artificial Cabin Atmosphere Systems for High Altitude Aircraft, WADC-TR-55-353, 1956.
- 6-66. Dubois, E. F., Mechanisms of Heat Loss and Temperature Regulation, Trans. Ass. Amer. Phys., 51: 252-299, 1936.
- 6-67. Dunham, W., Holling, H. E., Ladell, W. S., et al., The Effects of Air Movement in Severe Heat, RNP-46/316, Royal Naval Personnel Research Committee, Medical Research Council, London, 1946.
- 6-68. Dusek, E. R., Effect of Temperature on Manual Performance, in Protection and Functioning of the Hands in Cold Climates, Fisher, F. R., (ed.), National Academy of Sciences, National Research Council, Washington, D. C., 1957, pp. 63-76.

- 6-69. Ebaugh, F. C., Jr., Thauer, R., Influence of Various Environmental Temperatures on the Cold and Warmth Thresholds, J. Appl. Physiol., 3: 173-182, 1950.
- 6-70. Eckert, E. R. G., Drake, R. M., Jr., Heat and Mass Transfer, McGraw-Hill, N. Y., 1959.
- 6-71. Eichna, L. W., Park, C. R., Nelson, N., et al., Thermal Regulation during Acclimatization in a Hot, Dry (Desert Type) Environment, Am. J. Physiol., 163: 585-597, 1950.
- 6-72. Elsner, R. W., Bolstad, A., Thermal and Metabolic Responses to Cold of Peruvian Indians Native to High Altitude, AAL-TDR-62-64, Arctic Aeromedical Lab., Fort Wainwright, Alaska, 1963.
- 6-73. Epperson, W. L., Quigley, D. G., Robertson, W. G., Observations on Man in an Oxygen-Helium Environment at 380 mm Hg Total Pressure. III. Heat Exchange, Aerospace Med., 37: 457-462, 1966.
- 6-74. Fox, R. H., Goldsmith, R., Hampton, I. F. G., et al., The Nature of the Increase in Sweating Capacity Produced by Heat Acclimatization, J. Physiol., 171: 368-376, 1964.
- 6-75. Fuchs, R. A., Experimenter's Design Handbook for the Manned Lunar Surface Program, HA-SSD-60352R, Hughes Aircraft Co., Culver City, Calif., NASA Contract No. NAS-8-20244, Jan. 1967.
- 6-76. Gagge, A. P., Comfort: New Concepts and Applications, Building Research, 3: July-Aug. 1966.
- 6-77. Gagge, A. P., Rapp, G. M., Hardy, J. D., The Effective Radiant Field and Operative Temperature Necessary for Comfort With Radiant Heating, for Inclusion in ASHRAE Transactions, 1967, No. 2013.
- 6-78. Gagge, A. P., Hardy, J. D., Rapp, G. M., Exploratory Study on Comfort for High Temperature Sources of Radiant Heat, prepared for presentation at the ASHRAE 72nd Annual Meeting, Portland, Oregon, July 5, 1965.
- 6-79. Gagge, A. P., Rapp, G. M., Hardy, J. D., Mean Radiant and Operative Temperature for High-Temperature Sources of Radiant Heat, presented at the ASHRAE 71st Annual Meeting, Cleveland, Ohio, June 29, 1964.
- 6-80. Gagge, A. P., Standard Operative Temperature, A Generalized Temperature Scale, Applicable to Direct and Partitional Calorimetry, Amer. J. Physiol., 131: 92-102, 1940.

- 6-81. Gagge, A. P., Herrington, L. P., Winslow, C. -E. A., Thermal Interchanges between the Human Body and Its Atmospheric Environment, Amer. J. Hyg., 26: 84-102, 1937.
- 6-82. Gaydos, H. F., Effect on Complex Manual Performance of Cooling the Body While Maintaining the Hands at Normal Temperatures, J. Appl. Physiol., 12: 373-376, 1958.
- 6-83. Gaydos, H. F., Dusek, E. R., Effects of Localized Hand Cooling Versus Total Body Cooling on Manual Performance, J. Appl. Physiol., 12: 377-380, 1958.
- 6-84. Gerking, S. D., Robinson, S., Decline in Rates of Sweating of Men Working in Severe Heat, Am. J. Physiol., 147: 370-378, 1946.
- 6-85. Gillies, J. A., (ed.), A Textbook of Aviation Physiology, Pergamon Press, Edinburgh, Scotland, 1965.
- 6-86. Glaser, P. E., Black, I. A., Lindstrom, R. S., et al., Thermal Insulation Systems, NASA-SP-5027, 1967.
- 6-87. Goldman, R. F., The Arctic Soldier: Possible Research Solutions for His Protection, U. S. Army Research Inst. of Environmental Medicine, Natick, Mass., 1965. (AD-613189).
- 6-88. Goldman, R. F., Green, E. B., Iampietro, P. F., Tolerance of Hot, Wet Environments by Resting Men, J. Appl. Physiol., 20: 271-277, 1965.
- 6-89. Goodnight, F. H., Pearson, R. O., Copeland, R. J., Thermal Performance Tests of the A-2H Apollo Extravehicular Mobility Unit, Rep. No. 00.638, Vol. 2, NASA-CR-65856, Mar. 1965.
- 6-90. Green, F. H., Psychrometric Data, ARMC-66-537, AiResearch Mfg. Co., Division of the Garrett Corp., Los Angeles, Calif., 1966.
- 6-91. Greider, H. R., Santa Maria, L. J., Subjective Thermal Comfort Zones of Ventilated Full Pressure Suit at Altitude, J. Aviat. Med., 28: 272-276, 1957.
- 6-92. Guibert, A., Taylor, C. L., The Radiation Area of the Human Body, AF-TR-6706, Wright Air Development Center, Wright-Patterson AFB, Ohio, 1951. (AD-136760). (Also in J. Appl. Physiol., 5(1): 24-37, July 1952).

- 6-93. Hale, F. C., Westland, R. A., Taylor, C. L., Barometric and Vapor Pressure Influences on Insensible Weight Loss, J. Appl. Physiol., 12(1): 20-28, 1958.
- 6-94. Hall, J. F., Jr., Copper Manikin Regional Loss and Cooling Constants, WADC-AML-MR-696-105P, Aero-Medical Lab., Wright-Patterson AFB, Ohio, Oct. 1950.
- 6-95. Hall, J. F., Jr., Polte, J. W., Kelley, R. L., et al., Cooling of Clothed Subjects Immersed in Cold Water, WADC-TR-53-323, Wright Air Development Center, Wright-Patterson AFB, Ohio, Apr. 1953.
- 6-96. Hanifan, D. T., Blockley, W. V., Mitchell, M. B., et al., Physiological and Psychological Effects of Overloading Fall-out Shelters, Dunlap Associates, Inc., Santa Monica, Calif., Apr. 1963. (AD-420449).
- 6-97. Hardy, J. D., (ed.), Physiological Problems in Space Exploration, Charles C. Thomas, Springfield, Ill., 1964, p. 42.
- 6-98. Hardy, J. D., The Physiology of Temperature Regulation, NADC-MA-6015, Naval Air Development Center, Johnsville, Pa., June 1960.
- 6-99. Hardy, J. D., Summary Review of the Influence of Thermal Radiation on Human Skin, NADC-MA-5415, Naval Air Development Center, Johnsville, Pa., Nov. 1954.
- 6-100. Hardy, J. D., (ed.), Temperature. Its Measurement and Control in Science and Industry, Vol. 3, Part 3: Biology and Medicine, Reinhold Publishing Corp., N. Y., 1963.
- 6-101. Hardy, J. D., Thresholds of Pain and Reflex Contraction as Related to Noxious Stimulation, J. Appl. Physiol., 5(12): 725-739, June 1953.
- 6-102. Herrington, L. P., Winslow, C. -E. A., Gagge, A. P., The Relative Influence of Radiation and Convection upon Vasomotor Temperature Regulation, Amer. J. Physiol., 120: 133-143, 1937.
- 6-103. Hertzman, A. B., Randall, W. C., Peis, C. N., et al., The Regional Rates of Evaporation from the Skin, AF-TR-6680, Part 2, Aero-Medical Lab., Wright-Patterson AFB, Ohio, 1951.
- 6-104. Hertzman, A. B., Randall, W. C., Peis, C. N., et al., The Regional Rates of Evaporation from Skin at Various Environmental Temperatures, J. Appl. Physiol., 5(4): 153-161, 1952.

- 6-105. Horvath, S. M., Shelley, W. B., Acclimatization to Extreme Heat and Its Effect on Ability to Work in Less Severe Environments, Am. J. Physiol., 146: 336-343, 1946.
- 6-106. Horvath, S. M., Freedman, A., The Influence of Cold upon the Efficiency of Man, J. Aviat. Med., 18: 158-164, 1947.
- 6-107. Houghten, F. C., Yaglou, C. P., Determination of the Comfort Zone, J. Amer. Soc. Heat. and Vent. Engrs., 29: 515, 1923.
- 6-108. Houghton, F. C., Teague, W. W., Miller, W. E., et al., Thermal Exchange between the Bodies of Men Working and the Atmospheric Environment, Amer. J. Hyg., 13: 415-431, Mar. 1931.
- 6-109. Iampietro, P. F., Bass, D. E., Buskirk, E. R., Heat Exchanges of Nude Men in the Cold: Effect of Humidity, Temperature and Windspeed, J. Appl. Physiol., 12: 351-356, 1958.
- 6-110. Iampietro, P. F., Mager, M., Green, E. B., Some Physiological Changes Accompanying Tetany Induced by Exposure to Hot Wet Conditions, J. Appl. Physiol., 16: 409-412, 1961.
- 6-111. Iberall, A. S., Cardon, S. Z., Analysis of Dynamic Systems Response of Some Internal Human Systems, NASA-CR-141, 1965.
- 6-112. Iosel'son, S. A., Physiological Bases for Increased Endurance of People under Intense Thermal Conditions, FTD-MT-65-493, Foreign Technology Division, Wright-Patterson AFB, Ohio, Mar. 1967. (AD-652475).
- 6-113. Jennings, D. C., Water-Cooled Space Suit, J. Spacecraft, 3: 1251-1256, 1966.
- 6-114. Johnson, A. L., Aerospace Corp., Manager, Life Support Section, Los Angeles, Calif., unpublished data. To be published in the Diluent Selection Study for the MOL Program, 1966.
- 6-115. Kerslake, D. McK., Errors Arising from the Use of Mean Heat Exchange Coefficients in the Calculation of the Heat Exchanges of a Cylindrical Body in a Transverse Wind, in Temperature, Vol. 3, Part 3, Biology and Medicine, Hardy J. D., (ed.), Reinhold Publishing Corp., N. Y., 1963, pp. 183-190.

- 6-116. Kerslake, D. Mck., An Estimate of the Preferred Skin Temperature Distribution in Man, FPRC-Memo-213, RAF Flying Personnel Res. Comm., Farnborough, England, 1964.
- 6-117. Kaufman, W. C., Human Tolerance Limits for Some Thermal Environments of Aerospace, Aerospace Med., 34: 889-896, Oct. 1963.
- 6-118. Kaufman, W. C., Swan, A. G., Davis, H. T., Skin Temperature Responses to Simulated Thermonuclear Flash, ASD-TR-61-510, Aeronaautical Systems Division, Wright-Patterson AFB, Ohio, 1961.
- 6-119. Kincaide, W. C., Apollo Portable Life-Support System - Development Status, Paper 65-AV-45, paper presented at the American Society of Mechanical Engineers, Aviation and Space Conference, Los Angeles, Calif., Mar. 14-18, 1965.
- 6-120. Kissen, A. T., Hall, J. F., Physiologic Response to Transient Heat Stress in Reflective Versus Non-Reflective Clothing, AMRL-TDR-63-79, Aerospace Medical Research Labs., Wright-Patterson AFB, Ohio, Aug. 1963.
- 6-121. Krantz, P., Calculating Human Comfort, ASHRAE J., 6: 68-77, Sept. 1964.
- 6-122. Kreith, F., Principles of Heat Transfer, International Textbook Company, Scranton, Pa., 1962.
- 6-123. Kuno, Y., Human Perspiration, Charles C. Thomas, Springfield, Mass., 1956.
- 6-124. Ladell, W. S. S., Thermal Sweating, Brit. Med. Bull., 3: 175-179, 1945.
- 6-125. Lang, R., Syversen, R. G., Factors Affecting the Thermal Equilibrium of a Subject in the Apollo Extra-Vehicular Mobility Unit, (TP-65-11), Hamilton Standard Division, United Aircraft Corp., Windsor Locks, Conn., in Proceedings of the Second Space Congress, Apr. 5-7, 1965, Cocoa Beach, Fla., pp. 269-280.
- 6-126. LeBlanc, J. S., Impairment of Manual Dexterity in the Cold, J. Appl. Physiol., 9: 62-64, 1956.
- 6-127. Leithead, C. S., Lind, A. R., Heat Stress and Heat Disorders, F. A. Davis, Philadelphia, Pa., 1964.

- 6-128. Libet, B., Estimation of the Thermal Insulation of Clothing by Measuring Increases in Girth of the Wearer, TSEAL-5H-5-241, Air Technical Service Command, Wright-Patterson AFB, Ohio, 1945.
- 6-129. Lind, A. R., Bass, D. E., Optimal Exposure Time for Development of Acclimatization to Heat, Fed. Proc., 22(3): 704-708, 1963.
- 6-130. Lind, A. R., Physiological Effects of Continuous or Intermittent Work in the Heat, J. Appl. Physiol., 18(1): 57-60, 1963.
- 6-131. Lind, A. R., Tolerable Limits for Prolonged and Intermittent Exposures to Heat, in Temperature, Its Measurement and Control in Science and Industry, Vol. 3, Part 3, Biology and Medicine, Hardy, J. D., (ed.), Reinhold Publishing Co., N. Y., 1963, pp. 337-345.
- 6-132. McAdams, W. H., Heat Transmission, McGraw-Hill, N. Y., 1954.
- 6-133. McCance, R. A., Ungleay, C. C., Crosfill, J. W. L., et al., The Hazards to Men in Ships Lost at Sea, 1940-44, MRC-SR-291, Medical Research Council, Her Majesty's Stationery Office, London, 1956.
- 6-134. McConnell, W. J., Yaglou, C. P., Work Tests Conducted in Atmosphere of High Temperature and Various Humidities in Still and Moving Air, ASHVE J., 30: 35, 1925.
- 6-135. McCutchan, J. W., Isherwood, J. D., Prediction of Thermal Tolerance When Using an MA-2 Ventilating Garment with a Modified MK-IV Anti-Exposure Suit, WADC-TR-59-326, 1959.
- 6-136. McCutchan, J. W., Taylor, C. L., Respiratory Heat Exchange with Varying Temperature and Humidity of Inspired Air, J. Appl. Physiol., 4: 121-135, 1951.
- 6-137. Mackworth, N. H., Effects of Heat on Wireless Telegraphy Operators Hearing and Recording Morse Messages, Brit. J. Industr. Med., 3: 143-158, 1946.
- 6-138. Mackworth, N. H., Finger Numbness in Very Cold Winds, J. Appl. Physiol., 5: 533-543, 1953.
- 6-139. MacPherson, R. K., The Assessment of the Thermal Environment. A Review, Brit. J. Industr. Med., 19: 151-164, 1962.

- 6-140. MacPherson, R. K., Physiological Responses to Hot Environments, MRC-SRS-298, Medical Research Council, Her Majesty's Stationery Office, London, 1960.
- 6-141. Mauch, H. A., Hall, J. F., Lemm, F. K., A Ventilating System for Clothing, WADC-TR-55-152, Wright Air Development Command, Wright-Patterson AFB, Ohio, 1955.
- 6-142. Merrill, G. L., Starr, J. B., Automatic Temperature Control for Liquid-Cooled Flight Suits, NADC-AC-6702, Naval Air Development Center, Johnsville, Warminster, Pa., Aug. 1967.
- 6-143. Milan, F. A., Cold Water Tests of USAF Anti-Exposure Suits, AAL-TR-64-31, Arctic Aeromedical Lab., Fort Wainwright, Alaska, 1965.
- 6-144. Milan, F. A., Thermal Stress in the Antarctic, AAL-TR-60-10, Arctic Aeromedical Lab., Fort Wainwright, Alaska, 1961.
- 6-145. Mills, A. W., Finger Numbness and Skin Temperature, J. Appl. Physiol., 9: 447-450, 1956.
- 6-146. Mills, A. W., Tactile Sensitivity in the Cold, in Protection and Functioning of the Hands in Cold Climates, Fisher, F. R., (ed.), National Academy of Sciences - National Research Council, Washington, D. C., 1957, pp. 76-86.
- 6-147. Molnar, G. W., Survival of Hypothermia by Men Immersed in the Ocean, JAMA, 131: 1046-1050, 1946.
- 6-148. National Aeronautics and Space Administration, Performance/Design and Product Configuration Requirements, Extravehicular Mobility Unit for Apollo Block II Missions, EMU-CSD-A-096, Sect. 3.1.1.2.1.1.4, Apollo Spaceflight Program Office, Houston, Texas, Jan. 1966, p. 17.
- 6-149. Nelson, N., Eichna, L. W., Horvath, S. M., et al., Thermal Exchanges of Man at High Temperatures, Amer. J. Physiol., 151: 627-652, 1947.
- 6-150. Nelson, W. G., Brown, L., Krumland, L. R., Preliminary Results of the Gemini Extravehicular Suit Pressurization--Ventilated Test Series, SS-55-3135, AiResearch Mfg. Co., Div. of Garrett Corp., Los Angeles, Calif., 1964.
- 6-151. Newburgh, L. H., (ed.), Physiology of Heat Regulation and the Science of Clothing, W. B. Saunders, Philadelphia, Pa., 1949.

- 6-152. North American Aviation, unpublished data, 1959.
- 6-153. Ohara, K., Ono, T., Regional Relationship of Water Vapor Pressure on Human Body Surface, J. Appl. Physiol., 18: 1019-1022, 1963.
- 6-154. Olsen, R., Moir, R. K., Richards, W., et al., Engineering Tradeoffs of Different Gas Systems Pertaining to the Selection of Space Cabin Atmospheres, Boeing Aircraft Corp., 1965. (unpublished data).
- 6-155. Parker, F. A., Ekberg, D. A., Withey, D. J., et al., Atmosphere Selection and Control for Manned Space Stations, General Electric Co., Missile and Space Div., Valley Forge, Pa., presented at the International Symposium for Manned Space Stations in Munich, Sept. 1965.
- 6-156. Pepler, R. D., Extreme Warmth and Sensorimotor Coordination, J. Appl. Physiol., 14: 383-386, 1959.
- 6-157. Pepler, R. D., Performance and Well-Being in Heat, in Temperature, Its Measurement and Control in Science and Industry, Vol. 3, Part 3, Biology and Medicine, Hardy, J. D., (ed.), Reinhold Publishing Company, N. Y., 1963, pp. 319-336.
- 6-158. Perel, D. H., Chapman, A. J., An Evaluation of the Thermally Radiant Environs of a Man on the Lunar Surface, NASA-TN-D-4243, Nov. 1967.
- 6-159. Peterson, J. A., Cafaro, C., Shlosinger, A. P., et al., Analytical Review of Passive Mass Transfer of Water Vapor in a Space Suit, NASA-CR-63144, 1965.
- 6-160. Pfleiderer, H., Buettner, K., Bioklimatologie, Lehrbuch d. Baeder und Klimaheilkunde, Berlin: Julius, Springs, 1940, pp. 609-949.
- 6-161. Pitts, G. C., Johnson, R. E., Consolazio, F. C., Work in Heat as Affected by Intake of Water, Salt, and Glucose, Amer. J. Physiol., 142(2): 253-259, 1944.
- 6-162. Provins, K. A., Hellon, R. F., Bell, C. R., et al., Tolerance to Heat of Subjects Engaged in Sedentary Work, Ergonomics, 5(1): 93-97, 1962.
- 6-163. Radnofsky, M. I., National Aeronautics and Space Administration, Apollo Spacecraft Office, Crew Systems Div., Houston, Texas, personal communication, Feb. 1966.

- 6-164. Randall, W. C., Hertzman, A. B., Dermaternal Recruitment of Sweating, J. Appl. Physiol., 5: 399-409, 1953.
- 6-165. Rasch, P. J., Boyers, J. H., Hamby, J. W., et al., Evaluation of a Method of Acclimatizing Marines en Route to a Hot-Wet Climate, MF022.03.04-8002.6, Naval Medical Field, Research Lab., Camp LeJeune, N. C., Mar. 1967.
- 6-166. Reid, R. C., Sherwood, T. K., The Properties of Gases and Liquids, McGraw-Hill, N. Y., 1958.
- 6-167. Richardson, D. L., Study and Development of Materials and Techniques for Passive Thermal Control of Flexible Extravehicular Space Garments, AMRL-TR-65-156, Aerospace Medical Research Labs., Wright-Patterson AFB, Ohio, 1965.
- 6-168. Richardson, D. L., Techniques and Materials for Passive Thermal Control of Rigid and Flexible Extravehicular Space Enclosures, AMRL-TR-67-128, Aerospace Medical Research Labs., Wright-Patterson AFB, Ohio, Dec. 1967.
- 6-169. Robinson, S., Sadowski, B., Newton, J. L., The Effects of Thermal Stresses on the Aerobic and Anaerobic Work Capacities of Man, Part 3, NASA-CR-83929, Dec. 1966.
- 6-170. Robinson, S., Turrell, E. S., Gerking, S. D., Physiologically Equivalent Conditions of Air Temperature and Humidity, Am. J. Physiol., 143: 21-32, 1945.
- 6-171. Robinson, S., Turrell, E. S., Belding, H., et al., Rapid Acclimatization to Work in Hot Climates, Am. J. Physiol., 140: 168-176, 1943.
- 6-172. Robinson, S., Meyer, F. R., Newton, J. L., et al., Relations between Sweating, Cutaneous Blood Flow, and Body Temperature in Work, J. Appl. Physiol., 20(4): 575-582, July 1965.
- 6-173. Roth, E. M., Bioenergetics of Space Suits for Lunar Exploration, NASA-SP-84, 1966.
- 6-174. Roth, E. M., Space-Cabin Atmospheres, Part IV. Engineering Trade-Offs of One-Versus-Two Gas Systems, NASA-SP-118, 1967.
- 6-175. Rousseau, J., Atmospheric Control Systems for Space Vehicles, ASD-TDR-62-527, Pt. 1, Aeronautical Systems Div., Wright-Patterson AFB, Ohio, 1963.

- 6-176. Sanders Nuclear Corp., Technical Proposal for a Radioisotope Fueled Diving Suit Heating System (U), Sanders-Prop-86 HX, Nashua, New Hampshire, 1966.
- 6-177. Santa Maria, L. J., Burgess, M. B., Dery, D. D., Physiological Effects of Water-Cooling and Oxygen Ventilation in Different Space Flight Conditions (Abstract), Aerospace Med., 37: 300, 1966.
- 6-178. Schickele, E., Environment and Fatal Heat Stroke. An Analysis of 157 Cases Occurring in the Army in the U. S. during World War II, Milit. Surg., 100: 235-256, 1947.
- 6-179. Secord, T. C., Bonura, M. S., Life Support Systems Data from Sixty-Two Days of Testing in a Manned Space Laboratory Simulator, in AIAA Fourth Manned Space Flight Meeting, Oct. 11-13, 1965, St. Louis, Mo., American Institute of Aeronautics and Astronautics, N. Y., 1965, pp. 306-317.
- 6-180. Sendroy, J., Jr., Collison, H. A., Nomogram for the Determination of Human Body Surface Area from Height and Weight, NMRI-Rept. No. 2, MR 005.12-3001.01, Naval Medical Research Inst., Bethesda, Md., 1960. (Also in: J. Appl. Physiol., 15: 958-959, 1960).
- 6-181. Shlosinger, A. P., Woo, W., Feasibility Study of Integral Heat Sink Space Suit Concepts, NASA-CR-63399, 1965.
- 6-182. Shlosinger, A. P., Study of Passive Temperature and Humidity Control Systems for Advanced Space Suits, NASA-CR-73168, Sept. 1967.
- 6-183. Sibbons, J. L. H., Assessment of Thermal Stress from Energy Balance Considerations, J. Appl. Physiol., 21: 1207-1217, 1966.
- 6-184. Siple, P. A., Passel, C. F., Measurements of Dry Atmospheric Cooling in Subfreezing Temperatures, Proc. Amer. Phil. Soc., 89: 177-199, 1945.
- 6-185. Skrettingland, K. R., Clogston, J., Veghte, J. H., Evaluation of Various Types of Boots in Cold Environments, AAL-TN-61-7, Arctic Aeromedical Lab., Fort Wainwright, Alaska, Oct. 1961.
- 6-186. Smith, F. E., Indices of Heat Stress, MRC-Memo-29, Medical Research Council, Her Majesty's Stationery's House, London, 1955.

- 6-187. Smith, G. B., Jr., Hames, E. F., Estimation of Tolerance Times for Cold Water Immersion, Aerospace Med., 33(7): 834-840, 1962.
- 6-188. Smith, P. E., Jr., James, E. W., II, Human Responses to Heat Stress: Simulation by Analog Computer, Arch. Environ. Health, 9: 332-342, 1964.
- 6-189. Spector, W. S., (ed.), Handbook of Biological Data, WADC-TR-56-273, Wright Air Development Center, Wright-Patterson AFB, Ohio, 1956.
- 6-190. Stein, H. J., Eliot, J. W., Bodner, R. A., Physiological Reactions to Cold and Their Effects on Retention of Acclimatization to Heat, J. Appl. Physiol., 1: 575-585, Feb. 1949.
- 6-191. Stoll, A. M., Greene, L. C., Relationship between Pain and Tissue Damage Due to Thermal Radiation, J. Appl. Physiol., 14(3): 373-382, May 1959.
- 6-192. Stoll, A. M., The Role of Skin in Heat Transfer, NADC-MA-5918, Naval Air Development Center, Johnsville, Pa., Oct. 1959.
- 6-193. Stoll, A. M., The Role of the Skin in Heat Transfer, ASME Paper 59-A-138, J. of Heat Transfer, ASME Trans. Sect. C, 82: 239-241, 1960.
- 6-194. Stolwijk, J. A. J., Hardy, J. D., Temperature Regulation in Man - A Theoretical Study, Pflügers Arch., 291: 129-162, 1966.
- 6-195. Strydom, N. B., Wyndham, C. H., Natural State of Heat Acclimatization of Different Ethnic Groups, Fed. Proc., 22(3): Part 1, 801-809, 1963.
- 6-196. Taylor, C. L., Buettner, K., The Evaporative Effect on Human Perspiration, WADC-TR-53-345, Wright Air Development Center, Wright-Patterson AFB, Ohio, 1953.
- 6-197. Taylor, C. L., Human Tolerance for Temperature Extremes, in Physics and Medicine of the Upper Atmospheres, White, C. S., (ed.), University of New Mexico Press, Albuquerque, 1952.
- 6-198. Teichner, W. H., Kobrick, J. L., Effects of Prolonged Exposure to Low Temperature on Visual Motor Performance, J. Exp. Psychol., 49: 122-126, 1955.

- 6-199. Teichner, W. H., Kobrick, J. L., Effects of Prolonged Exposure to Low Temperature on Visual Motor Performance, Flicker Fusion, and Pain Sensitivity, Tech. Rep. EPD 230, Quartermaster Res. and Development Center, Natick, Mass., 1954.
- 6-200. Teichner, W. H., Manual Dexterity in the Cold, J. Appl. Physiol., 11: 333-338, 1957.
- 6-201. Teichner, W. H., Reaction Time in the Cold, J. Appl. Psychol., 42: 54-59, 1958.
- 6-202. Teichner, W. H., Temperature, Humidity, and Ventilation, (Preliminary Draft), Guggenheim Center for Aviation Health and Safety, Harvard School of Public Health, Boston, Mass., 1961.
- 6-203. Thompson Ramo Wooldridge, Inc., Propellant-Atmosphere System Study, WADD-TR-60-622, Mar. 1961. (AD-268768).
- 6-204. Trumbull, R., Environmental Modification for Human Performance, ONR-ACR-105, Office of Naval Research, Washington, D. C., 1965.
- 6-205. United States Navy, Medical News Letter 31: 12, 1958.
- 6-206. Vaughan, L., (ed.), Nutritional Requirements for Survival in the Cold and at Altitude, Proceedings of the Fifth Symposium on Arctic Biology and Medicine, Arctic Aeromedical Lab., Fort Wainwright, Alaska, Mar. 23-24, 1965.
- 6-207. Veghte, J. H., Efficacy of Air Cooling Systems in Pressure Suits in Hot Environments, Aerospace Medical Research Labs., Wright-Patterson AFB, Ohio, in Preprints, 36th Annual Scientific Meeting, Aerospace Medical Association New York, Apr. 26-29, 1965.
- 6-208. Veghte, J. H., Clogston, J. R., A New Heavy Winter Flying Clothing Assembly, AAL-TN-61-4, Arctic Aeromedical Lab., Fort Wainwright, Alaska, 1961.
- 6-209. Votta, F., Jr., Experimental Study of a Passive Thermal Control System for Space Suits, Status Rep. 9, NASA-CR-88546, Jul. 1967.
- 6-210. Waligora, J. M., Michel, E. L., Application of Conductive Cooling for Working Men in a Thermally Isolated Environment, (Abstract), Aerospace Med., 37: 306, 1966.

- 6-211. Weaver, J. A., Calculation of Time-Temperature Histories and Prediction of Injury to Skin Exposed to Thermal Radiation, NADC-MR-6623, Naval Air Development Center, Johnsville, Warminster, Pa., June 1967.
- 6-212. Webb, P., (ed.), Bioastronautics Data Book, NASA-SP-3006, 1964.
- 6-213. Webb, P., Annis, J. F., Bio-Thermal Responses to Varied Work Programs in Men Kept Thermally Neutral by Water Cooled Clothing, NASA-CR-739, 1966.
- 6-214. Webb, P., Heat Loss from the Respiratory Tract in Cold, Project No. 7-7951, Rep. No. 3, Arctic Aeromedical Lab., Ladd AFB, Alaska, Apr. 1955.
- 6-215. Webb, P., Human Water Exchange in Space Suits and Capsules, NASA-CR-804, 1967.
- 6-216. Webb, P., Garlington, L. N., Schwarz, M. J., Insensible Weight Loss at High Skin Temperatures, J. Appl. Physiol., 11: 41-44, 1957.
- 6-217. Webb, P., Pain Limited Heat Exposures, in Temperature, Its Measurement and Control in Science and Industry, Vol. 3, Pt. 3, Biology and Medicine, Hardy, J. D., (ed.), Reinhold Publishing Co., N. Y., 1963, pp. 245-250.
- 6-218. Weitz, J., Vibratory Sensitivity as a Function of Skin Temperature, J. Exp. Psychol., 28: 21-36, 1941.
- 6-219. Welch, B. E., Chief, Environmental Systems Branch, USAF School of Aerospace Medicine, Aerospace Medical Div., Air Force Systems Command, Brooks AFB, Texas, personal communication, Mar. 1966.
- 6-220. Whisenhunt, G. B., Knezek, R. A., A Thermal Protection System for Extra-Vehicular Space Suits, Vought Astronautics Div., Chance Vought Corp., Dallas, Texas, ARS-Paper 2472-62, presented at American Rocket Society Lunar Missions Meeting, July 17-19, 1962, Cleveland, Ohio.
- 6-221. Wilkinson, R. T., Fox, R. H., Goldsmith, R., et al., Psychological and Physiological Responses to Raised Body Temperature, J. Appl. Physiol., 19: 287-291, 1964.

- 6-222. Wilson, O. V., Atmospheric Cooling and the Occurrence of Frostbite in Exposed Skin, in Proceedings of the 4th Symposium on Arctic Medicine and Biology, Frostbite, Viereck, E., (ed.), Arctic Aeromedical Lab., Fort Wainwright, Alaska, 1964.
- 6-223. Wing, J. F., Upper Thermal Tolerance Limits for Unimpaired Mental Performance, Aerospace Med., 36(10): 960-964, 1965. (Also AMRL-TR-65-71, Oct. 1965).
- 6-224. Winslow, C. -E. A., Gagge, A. P., Herrington, L. P., The Influence of Air Movement upon Heat Losses from the Clothed Human Body, Amer. J. Physiol., 127: 505-518, 1939.
- 6-225. Winslow, C. -E. A., Herrington, L. P., Gagge, A. P., Physiological Reactions of the Human Body to Varying Environmental Temperatures, Amer. J. Physiol., 120: 1-22, 1937.
- 6-226. Winslow, C. -E. A., Herrington, L. P., Gagge, A. P., Relations between Atmospheric Conditions, Physiological Reactions and Sensation of Pleasantness, Amer. J. Hyg., 26: 103-115, 1937.
- 6-227. Withey, D. J., Glanfield, E. J., Dohner, C. V., Application of Permselective Composite Techniques for Atmosphere-Thermal Control of Emergency and Extravehicular Manned Space Assemblies, AMRL-TR-66-224, Aerospace Medical Research Labs., Wright-Patterson AFB, Ohio, Apr. 1967.
- 2-228. Woodcock, A. H., Breckenridge, J. R., A Model Description of Thermal Exchange for the Nude Man in Hot Environments, Ergonomics, 8: 223-235, 1965.
- 2-229. Woodcock, A. H., Goldman, R. F., A Technique for Measuring Clothing Insulation under Dynamic Conditions, QREC-EP-137, Quartermaster Research and Engineering Center, Environmental Protection Research Div., Natick, Mass., 1960.
- 6-230. Wortz, E. C., Full Pressure Suit Heat Balance Studies, LS-140, AiResearch Mfg. Co., Division of Garrett Corp., Los Angeles, Calif., 1965.
- 6-231. Wortz, E. C., Edwards, D. K., Harrington, T. J., New Techniques in Pressure Suit Cooling, Aerospace Med., 35: 987-984, 1964.

- 6-232. Wortz, E. C., Diaz, R. A., Green, F. H., et al., Reduced Barometric Pressure and Respiratory Water Loss, SAM-TR-66-4, School of Aerospace Medicine, Brooks AFB, Texas, 1966.
- 6-233. Wortz, E. C., Edwards, D. K., III, Diaz, R. A., et al., Study of Heat Balance in Full Pressure Suits, Aerospace Med., 38: 181-188, 1967.
- 6-234. Wyndham, C. H., Bouwer, W., Devine, M. G., et al., Examination of Use of Heat Exchange Equations for Determining Changes in Body Temperature, J. Appl. Physiol., 5: 299-307, 1952.
- 6-235. Wyndham, C. H., Strydom, N. B., Morrison, J. F., et al., Responses of Unacclimatized Men under Stress of Heat and Work, J. Appl. Physiol., 6: 681-686, 1954.
- 6-236. Yaglou, C. P., Indices of Comfort, in Physiology of Heat Regulation and Science of Clothing, Newburg, L. H., (ed.), W. B. Saunders, Philadelphia, Pa., 1949, Chapter 9.
- 6-237. Yaglou, C. P., Drinker, P., The Summer Comfort Zone Climate and Clothing, ASHVE Trans., 35: 269, 1929.
- 6-238. Yaglou, C. P., Temperature, Humidity, and Air Movement in Industries: The Effective Temperature Index, J. Industr. Hyg. Toxicol., 9: 297-309, 1927.
- 6-239. Zollner, G., Thauer, R., Kaufmann, W., Der Insensible Gewichtsverlust als Funktion der Umweltbedingungen. Die Abhangigkeit der Hautwasserabgabe von der Hauttemperatur bei Verschiedenen Temperaturen und Wasserdampfdrucken der umgebenden Luft, Arch. Ges. Physiol., 260: 261-273, 1955.